

Development of Regioselective Nitrene-Transfer [5+1] Cycloadditions as a Strategy for  
the Synthesis of Nitrogen Heterocycles

Julie Ellen Laudenschlager  
West Islip, New York

B.S. Biochemistry and Molecular Biology, Gettysburg College, 2016

A Dissertation presented to the Graduate Faculty of the University of Virginia in  
Candidacy for the Degree of Doctor of Philosophy

Department of Chemistry  
University of Virginia  
December 2022

## Copyright Information

The following chapters contain data and experiments that have been previously published works.

**Chapter 3:** Combee, L. A.; Johnson, S. L.; Laudenschlager, J. E.; Hilinski, M. K. "Rh(II)-Catalyzed Nitrene-Transfer [5+1] Cycloadditions of Aryl-Substituted Vinylcyclopropanes." *Org. Lett.* **2019**, 21, 2307-2311.

**Chapter 4:** Laudenschlager, J. E.; Combee, L. A.; Hilinski, M. K. "Intermolecular Scandium-Triflate Promoted Nitrene Transfer [5+1] Cycloadditions of Vinylcyclopropanes." *Org. Biomol. Chem.* **2019**, 17, 9413-9417.

## Abstract

Nitrogen heterocycles appear in a majority of FDA-approved drugs with piperidine being the most prevalent. As such, synthetic chemists are searching for methods that would allow for the facile synthesis of these motifs since many current methods are limited to certain substitution patterns in the product. This potential area of study to address this problem is using nitrenes and metallonitrenes in nitrene-transfer catalysis. However, known examples of nitrene precursors in intermolecular cyclizations are restricted in the literature to only five-membered rings through [4+1] or [2+2+1] cycloadditions. Herein, in this dissertation, we present the first syntheses of six-membered rings via nitrene-transfer cycloaddition in a [5+1] fashion, using vinylcyclopropanes (VCPs) as the aliphatic backbone.

Rh(II) catalysts have long been used for both intra- and intermolecular amination and aziridination. As such, we have shown that  $\text{Rh}_2(\text{esp})_2$  – the DuBois catalyst – was effective for nitrene transfer of *N*-tosyloxycarbamates to biaryl VCPs, resulting in the formation of 2,5-tetrahydropyridine products – a substitution pattern that was previously non-existent in the literature. Furthermore, we were able to demonstrate the additional synthetic utility of these compounds through hydrogenation and selective epoxidation. We later investigated the use of a  $\text{Rh}_2^{\text{II,III}}$  dimer catalyst to not only improve the method in terms of time but also introduce pyridine rings as a viable substituent to VCPs. In addition, we explored how pyridine substituents could be amenable to using  $\text{Rh}_2(\text{esp})_2$  as a catalyst.

Through our initial investigations, we found that our substrate scope was quite limited. Thus, we explored other sources for nitrogen transfer for mono-arylated VCPs.

Brønsted and Lewis acids were both found to be effective with this substrate class with  $\text{Sc}(\text{OTf})_3$ . In addition, cyclopropyl-substitution patterns not tolerable to the Rh-conditions were used in the Sc-conditions to provide the desired cycloadducts. The complementarity of both methods indicated that their respective mechanisms are different. Using the radical scavenger TEMPO, we were able to show that the acid-promoter method is undergoing a radical – not cationic – pathway. The development of this strategy further expanded the synthetic library of the [5+1] reaction.

## Acknowledgments

To my advisor Prof. Michael Hilinski – I thought that after our initial conversation about coffee mugs you may have had reservations about me, but I am so thankful you allowed me to join your lab. You have always supported me not just professionally but personally as well. My path to completing this degree has been non-conventional, but you were always there to help me, guide me, and allow me to make my way to this point. I truly couldn't think of a better mentor to have on this journey.

To my fellow incoming labmates of 2016 – Shea “Freddie” Johnson, Robert Dyer, and Philip Hahn. It has been a journey to get to this point, but I am so happy that I was able to learn from you all and challenge each other to think more critically about our work. Freddie, thank you for being the person I always went to with interesting proposals for projects, or for certain lab techniques that I should have known about but never judged me that I did not. Our random pKa and bond length trivia rounds is a tale I still tell. Rob, thank you for being a great residential lab technician as well as giving me advice and so much help as I wrapped up my dissertation. Philip, thank you for being such a supportive labmate as well as a great friend outside of lab. Your openness to me when we lived at Eagles and during those classes we took during our first year together made my transition to Charlottesville so much easier.

Will Shuler and Logan Combee, I am grateful to you both for your patience. Will always answered my silly questions and helped me acclimate into the lab while making it fun along the way. Logan was my mentor when it came to the initial [5+1] reactions. He constantly challenged me on my chemical knowledge and taught me how to approach synthetic problems. I am grateful for this guidance and the lessons that he taught me. It was tough love in the beginning, but it has only made me a better chemist.

Anna Davis – a fellow labmate when you joined our group, but you quickly became a close friend. Your love for scientific curiosity but also wanting to have fun along the way always inspired me as a senior student. I am so happy that we are an epitome of opposites attract. Thank you so much for providing homemade grilled cheese and tomato soup nights whenever I needed to vent.

To my other labmates during this journey – Teresa Jones, Han Kim, Yubo Xu, Kevin Burns, Balaram Raya, Johnathon Dooley, and Jared Lowe – thank you for not only our research discussions but also people that I could confide in about other non-chemistry related matters.

Profs. W. Dean Harman, Lin Pu, Ken Hsu, and Rachel A. Letteri – thank you for taking the time to serve as members of my committee.

For the friends I made in the department and in Charlottesville at large – thank you for letting me to be a part of this community and helping me along the way. Whether it was making dinner, after-Friday seminar outings, or going on hours long walks, I appreciate all those conversations and I'm so happy to have met so many great people. I cannot wait to see what you all accomplish in your careers.

To Chemistry L.E.A.D., thank you for allowing me to participate in your group and, at one point, serving as President. Being involved in this organization has opened how I can use my knowledge of science communication to students of all ages. I was able to meet new people and strengthen bonds with peers. I hope to be able to deliver the message of this group beyond UVA to enhance science outreach.

For my friends – Becca Duffy, Jess Ball, and Kate Ball – that always picked up the phone if I needed a moment of stress relief. During different stages of this PhD journey, they would always re-affirm me that I was able to fulfill this goal. Thank you for supporting me not only during this time, but in high school, college, and out on the cross-country course or track.

To my aunts, uncles, and cousins near and far – thank you all for your love and support through these past years. Whether it is a call or text out of the blue, visits to Charlottesville, or spending the holidays together, you all always allowed me to switch off the brain and have some much-needed fun.

I think my Grandpa and Connie were more excited than I was when I was accepted to UVA. I thank them both for those dinners to clear my head of lab work and listening to me when I've been happy, stressed, confused, and all the emotions in between. I am so happy we have been able to become closer during my time in Virginia.

My Nana always joked with me about how much time I was spending in lab during my graduate school experience. I am so thankful for that when I went through rough times, Nana always gave me the love and assertion that I needed.

I would be reluctant not to mention our family pup Bella. While she did not understand what was going on when I was studying or prepping for my defense, she never failed me on providing me cuddles when they were much needed.

For my brothers, Jeff and Devin – thank you for your continuous check-in's when I get lost in my work. You have both been such a backbone during this journey and somehow, either of you called or texted at the right moment when I needed you. We have made our siblingship even stronger through these years and I am so grateful for that.

To my Dad, thank you for supporting me through this crazy adventure. I remember telling you in Gettysburg that I wanted to go on this path of graduate school to study chemistry. From that day, you have supported me in this path that I did not even fully

understand either. You are always so excited to watch me draw my reactions on napkins and explain my research to you – even it may seem gibberish. I love you and am forever thankful for your support of me.

And to Taylor Smart - we met on the first day of TA training and the cards seemed to fall into place. Whenever I had a hard day or week in lab, you may not have had the answers to my project struggles, but you always encouraged me to persist when an ending did not seem in sight in my eyes. Thank you for being my rock through my personal tough times and being that hug that I could always rely on being there. I could not have imagined this journey without you. I love you so much.

---

I dedicate this dissertation to my Papa, Connell McGee, and my Mom, Marian Laudenschlager.

My Papa instilled in me how to work hard but also have fun along the way. While he always yelled at me when I was in lab when he called me, he would always say how proud of me he was. I only hope to be as kind and humorous as he was.

“That’s my baby!” is what my Mom would have screamed after I fulfilled this PhD journey. She always supported whatever crazy dreams and aspirations I had, including her buying a pound of calf’s liver for my high school science research experiment without her even questioning it. Mom, thank you for being my protective Mama Bear and always pushing me to pursue whatever I wanted to do. I truly would have never ended up here if it was not for your love. I hope that I have made you proud.

## Table of Contents

<b>Copyright Information</b>	<b>I</b>
<b>Abstract</b>	<b>II</b>
<b>Acknowledgements</b>	<b>IV</b>
<b>Table of Contents</b>	<b>VII</b>
<b>List of Figures</b>	<b>XIII</b>
<b>List of Schemes</b>	<b>XVI</b>
<b>List of Tables</b>	<b>XXIII</b>
<b>List of Abbreviations</b>	<b>XXIV</b>
<b>1. Synthesis of Cycloadducts using Nitrenes as a Single Atom Component</b>	<b>1</b>
1.1. Introduction	1
1.2. [3+1] Cycloadditions Using Nitrenes	2
1.2.1. [3+1] Cycloadditions with Thiazolones	2
1.2.2. [3+1] Cycloadditions with Oxaziridines	3
1.3. [4+1] Cycloadditions with Nitrenes	4
1.3.1. [4+1] Cycloadditions using Dienes and Azides	4
1.3.2. [4+1] Cycloadditions using Dienes and Iminoiodinanes	8
1.4. [2+2+1] Cycloadditions	11
1.4.1. Ti-catalyzed [2+2+1] Cycloadditions with Alkynes and Diazines	11
1.4.2. V-catalyzed [2+2+1] Cycloadditions with Diazines	20

1.4.3.	Ti-catalyzed [2+2+1] Reaction with Alkynes and Azides	23
1.4.4.	Ru-[2+2+1] Cycloadditions with Alkynes and Sulfoximines	26
1.5.	Conclusions	29
1.6.	References	30
<b>2.</b>	<b>The Use of Vinylcyclopropanes in Ring-Forming Reactions</b>	<b>33</b>
2.1.	Introduction	33
2.2.	Vinylcyclopropane Rearrangements	34
2.2.1.	VCPs into cyclopentenenes	34
2.2.2.	Other VCP rearrangements	42
2.3.	VCPs in [5+1] Cycloadditions	43
2.4.	VCPs in [5+2] Cycloadditions	47
2.4.1.	Intramolecular [5+2] cycloaddition with alkynes	47
2.4.2.	Intermolecular [5+2] cycloaddition with alkynes	60
2.4.3.	[5+2] cycloaddition with alkenes	70
2.4.4.	[5+2] cycloaddition with allenes	72
2.5.	Multi-component and Cascade Cycloadditions with VCPs	75
2.6.	Total Syntheses using VCPs	83
2.6.1.	VCP rearrangements	83
2.6.2.	[5+2] cycloadditions	89
2.6.3.	Rh(I)-[5+2+1] cycloaddition	90
2.6.4.	Radical cascade cyclization	93

2.7.	Conclusions	94
2.8.	References	94
<b>3.</b>	<b>Rh(II)-Catalyzed [5+1] Cycloaddition of VCPs</b>	<b>104</b>
3.1.	Introduction	104
3.2.	Overview of Rh(II) as a Nitrene Transfer Catalyst	104
3.2.1.	Intramolecular C-H amination	104
3.2.2.	Intermolecular C-H amination	108
3.2.3.	Intramolecular olefin aziridination	110
3.2.4.	Intermolecular olefin aziridination	113
3.3.	Investigations with 2,4-diarylvinylcyclopropanes	116
3.3.1.	Screening of Rh(II) catalysts	116
3.3.2.	Nitrogen sources	117
3.3.3.	Further optimization	119
3.3.4.	Assessment of the scope	121
3.3.5.	Functionalization of the tetrahydropyridine products	123
3.3.6.	Mechanism of the Rh(II)-catalyzed method	124
3.4.	Expanding the Use of the Aza-[5+1] Cycloaddition	127
3.4.1.	Berry's novel Rh <sub>2</sub> <sup>II,III</sup> dimer catalyst	127
3.4.2.	Investigation of aza-[5+1] cycloaddition with Rh <sub>2</sub> <sup>II,III</sup> dimer catalyst	129
3.4.3.	The effect of 2-substitution on the pyridine VCP	131
3.5.	Conclusions	133

3.6. References	134
<b>4. Sc(OTf)<sub>3</sub>-Promoted Aza-[5+1] Cycloaddition of Vinylcyclopropanes</b>	<b>138</b>
4.1. Introduction	138
4.2. Cyclopropylcarbiny l Radicals	138
4.2.1. Introduction of cyclopropyl radical clocks	138
4.2.2. Effect of substitution on cyclopropyl radicals	139
4.2.3. Kinetic and thermodynamics of cyclopropyl vs cyclobutyl ring opening	141
4.3. Cyclopropylcarbiny l Cations	143
4.3.1. Seminal work with cyclopropylmethlium	143
4.3.2. Effect of substitution on cyclopropylcarbiny l cations	144
4.3.3. VCP rearrangements through protonation	145
4.4. Investigations with 2-arylvinylcyclopropanes	149
4.4.1. Screening of Brønsted and Lewis acids	149
4.4.2. Optimization of Sc(OTf) <sub>3</sub> -promoted conditions	150
4.4.3. Scope of Sc(OTf) <sub>3</sub> -promoted [5+1] cycloaddition	154
4.4.4. Complementarity of Rh(II) and Sc(OTf) <sub>3</sub> methods	157
4.4.5. Mechanistic insight into the Sc(III)-promoted reaction	160
4.5. Conclusions	161
4.6. References	162

<b>A1. Appendix 1 – Chapter 3 Experimental and Characterization</b>	<b>164</b>
1.1. General Methods	164
1.2. General procedure for synthesis of 2,4-disubstituted vinylcyclopropanes	165
1.3. Characterization of new 2,4-disubstituted vinylcyclopropanes	167
1.4. General procedure for Rh(II)-catalyzed [5+1] reaction	210
1.5. Characterization of products from Rh(II)-method	211
1.6. Scale-up reaction of Rh(II)-aza-[5+1] reaction	271
1.7. Hydrogenation of <b>3.70</b>	272
1.8. Epoxidation of <b>3.70</b>	274
1.9. NMR Study of Rh <sub>2</sub> (esp) <sub>2</sub> catalyzed [5+1] reaction	276
1.10. References	277
 <b>A2. Appendix 2 – Chapter 4 Experimental and Characterization</b>	 <b>278</b>
2.1. General Methods	278
2.2. General procedure for synthesis of 2-substituted vinylcyclopropanes	279
2.3. Characterization of new 2-substituted vinylcyclopropanes	280
2.4. Synthesis of (1-((1 <i>R</i> ,2 <i>R</i> )-2-butylcyclopropyl)vinyl)benzene ( <b>SM 4.96</b> )	294
2.5. Synthesis of (1-(1-phenylcyclopropyl)vinyl)benzene ( <b>SM 4.97</b> )	297
2.6. Synthesis of (1-(1-methylcyclopropyl)vinyl)benzene ( <b>SM 4.98</b> )	300
2.7. Synthesis of N-Tosylphenylimidoiodinane (PhINTs, <b>4.66</b> )	302
2.8. General procedure for Sc(III)-promoted aza-[5+1] reaction	303

2.9. Previously reported products of the Sc(III)-[5+1] method	304
2.10. Characterization of new products of Sc(OTf) <sub>3</sub> -promoted method	311
2.11. TEMPO radical trapping experiment	336
2.12. References	339

## List of Figures

<b>Figure 1.1.</b>	Examples of FDA-approved medications containing a nitrogen heterocycle	1
<b>Figure 1.2.</b>	Ring expansion of aziridines to form larger heterocycles	2
<b>Figure 1.3.</b>	Pearson's seminal intramolecular [4+1] cycloaddition of dienes and azides	5
<b>Figure 1.4.</b>	Plausible mechanistic pathways for the [4+1] reaction	10
<b>Figure 1.5.</b>	Proposed mechanistic models for stereoselectivity of the [4+1] reaction	11
<b>Figure 1.6.</b>	Preliminary mechanistic proposal for Tonks' [2+2+1] cycloaddition	13
<b>Figure 1.7a.</b>	[2+2] addition step in Tonks' [2+2+1] cycloaddition	17
<b>Figure 1.7b.</b>	Migratory insertion step of TMS-phenylacetylene in [2+2+1] cycloaddition	17
<b>Figure 1.8.</b>	Electronically-controlled ( <b>1.82</b> ) vs directed 2 <sup>nd</sup> insertion ( <b>1.83</b> )	18
<b>Figure 1.9.</b>	Proposed mechanistic cycle for vanadium-catalyzed cycloaddition	22
<b>Figure 1.10.</b>	Mechanism of [2+2+1] with Ru-catalysis	29
<b>Figure 2.1.</b>	Mechanism of Louie's Ni(0)-NHC-catalyzed VCP isomerization	39
<b>Figure 2.2a.</b>	Tang's Rh(I)-catalyzed preparation of cycloheptadienes	42
<b>Figure 2.2b.</b>	Allene intermediate formation	43
<b>Figure 2.3.</b>	[5+1] cycloaddition of VCPs and vinylidenes	46
<b>Figure 2.4.</b>	Reaction mechanism of Rh(I)-catalyzed intramolecular [5+2] cycloaddition	51
<b>Figure 2.5.</b>	Asymmetric Rh(I)-catalyzed intramolecular [5+2] cycloaddition	53

<b>Figure 2.6.</b>	Rationale for enhanced regioselectivity of <i>cis</i> cyclopropyl substrates in Ru(II)-method	57
<b>Figure 2.7.</b>	Diastereoselectivity of selected substrates in Ru(II)-catalyzed reaction	58
<b>Figure 2.8.</b>	Mechanism of Ni(0)-catalyzed intramolecular [5+2] reaction	60
<b>Figure 2.9.</b>	Intermolecular [5+2] with un-activated VCPs	63
<b>Figure 2.10a.</b>	Comparison of Rh(I) catalysts in regioselectivity and efficiency of intermolecular [5+2] cycloaddition	67
<b>Figure 2.10b.</b>	Rh(I) catalysts	68
<b>Figure 2.11.</b>	Regioselectivity rationale of the Rh(I)-catalyzed reaction	69
<b>Figure 2.12.</b>	Intermediates of the asymmetric intramolecular [5+2] reaction with alkenes	71
<b>Figure 2.13.</b>	Transition states of Rh(I)-catalyzed [5+2] cycloaddition	75
<b>Figure 2.14.</b>	Intermolecular [5+1+2+1] with VCP, alkynes, and CO	78
<b>Figure 2.15.</b>	Mechanism of nucleophilic-promoted tandem domino reaction	81
<b>Figure 2.16.</b>	Hudlicky's synthesis of natural products and their epimers	86
<b>Figure 2.17.</b>	Structures of compounds synthesized via Rh(I)-catalyzed [5+2] cycloaddition with alkynes	90
<b>Figure 2.18.</b>	Tandem [5+2+1]/aldol reaction in synthesis of (±)-hirsutene and (±)-1-desoxyhypnophilin	91
<b>Figure 2.19.</b>	Structure of (±)-asterisca-3(15),6-diene	92
<b>Figure 2.20.</b>	Pattenden's synthesis of (±)-estrone via radical initiation	93
<b>Figure 3.1.</b>	Du Bois' intramolecular C-H amination with carbamates	105
<b>Figure 3.2.</b>	Intramolecular C-H insertion using Rh <sub>2</sub> (esp) <sub>2</sub>	107
<b>Figure 3.3.</b>	Du Bois' intermolecular C-H insertion with sulfamates	109

<b>Figure 3.4.</b>	Diastereoselective intermolecular C-H amination with chiral sulfimidamide	109
<b>Figure 3.5.</b>	Kürti's synthesis of unprotected aziridines	116
<b>Figure 3.6.</b>	NMR mechanistic study of Rh(II)-[5+1] reaction	125
<b>Figure 3.7.</b>	Proposed mechanism for the Rh(II)-catalyzed [5+1] reaction	126
<b>Figure 3.8.</b>	Pyridine-appended VCPs in Rh(II) aza-[5+1] reaction	127
<b>Figure 3.9.</b>	Berry's Rh <sub>2</sub> <sup>II,III</sup> dimer catalyst	128
<b>Figure 3.10.</b>	Simplified structure of dimer catalyst	131
<b>Figure 3.11.</b>	Modifications to pyridine ring	132
<b>Figure 4.1.</b>	Conformations for cyclopropyl system	143
<b>Figure 4.2.</b>	Methyl-stabilization of cyclopropylcarbinyl cation	145
<b>Figure 4.3.</b>	Investigation of metal-ligand triflate complexes	153
<b>Figure 4.4.</b>	Incompatible substrates with the Sc(III)-promoted conditions	156
<b>Figure 4.5.</b>	Proposed mechanism in Sc(OTf) <sub>3</sub> aza-[5+1] cycloaddition	161

## List of Schemes

<b>Scheme 1.1.</b>	Sheradsky's [3+1] cycloaddition of mesoionic thiazolones	3
<b>Scheme 1.2.</b>	Scope of [3+1] cycloaddition of cyclopropanes and oxaziridines	4
<b>Scheme 1.3.</b>	Partial scope of intramolecular [4+1] reaction	6
<b>Scheme 1.4.</b>	Diastereoselective intramolecular [4+1] cycloaddition	7
<b>Scheme 1.5.</b>	Hudlicky's mechanistic proposal for the [4+1] cycloaddition using azides	8
<b>Scheme 1.6.</b>	Scope of Zhou's [4+1] cyclization between dienes and iminoiodinanes	9
<b>Scheme 1.7.</b>	Isomerization of a dimethyl-substituted aziridine in the presence of diphenylbutadiene	10
<b>Scheme 1.8.</b>	Scope of Tonk's initial [2+2+1] cyclization using alkynes and azobenzene	12
<b>Scheme 1.9.</b>	Scope of [2+2+1] cycloaddition using TMS-alkynes, 1-phenylpropyne and azobenzene	15
<b>Scheme 1.10.</b>	Scope of [2+2+1] cycloaddition using TMS-alkynes, di-substituted alkynes and azobenzene	16
<b>Scheme 1.11.</b>	Scope of [2+2+1] cycloaddition using dative directing groups	19
<b>Scheme 1.12.</b>	One-pot subsequent [2+2+1] cycloaddition and cross-coupling reaction	20
<b>Scheme 1.13.</b>	V-catalyzed [2+2+1] reaction scope	21
<b>Scheme 1.14.</b>	V-catalyzed synthesis of azadiphospholes reaction scope	23
<b>Scheme 1.15.</b>	Scope of azides with Tonks' [2+2+1] cycloaddition	25
<b>Scheme 1.16.</b>	Scope of mono-substituted alkynes with [2+2+1] cycloaddition	26
<b>Scheme 1.17a.</b>	Scope of Yamamoto's Ru-catalyzed [2+2+1] cycloaddition	27

<b>Scheme 1.17b.</b>	Further diversification of propargyl pyrrole product	27
<b>Scheme 2.1.</b>	Initial discoveries of VCP rearrangement	35
<b>Scheme 2.2.</b>	Trost's work with 1-substituted VCPs.	36
<b>Scheme 2.3.</b>	Flash vacuum pyrolysis of VCPs	37
<b>Scheme 2.4.</b>	Paquette's synthesis of cis-bicyclo[3.3.0]octenones	38
<b>Scheme 2.5.</b>	Williamson's Rh(I)-complex synthesis and thermolysis	38
<b>Scheme 2.6.</b>	Oshima's Pd-catalyzed method for VCP rearrangement	40
<b>Scheme 2.7.</b>	Danheiser's <sup>n</sup> BuLi-promoted rearrangement	40
<b>Scheme 2.8.</b>	Lewis acid-promoted VCP rearrangement	41
<b>Scheme 2.9.</b>	Photocatalytic transformation of bi-aryl VCPs	41
<b>Scheme 2.10.</b>	Synthesis of tetrahydrooxepinone ring	43
<b>Scheme 2.11.</b>	Radical cascade cycloaddition of VCP and selenyl ester	44
<b>Scheme 2.12.</b>	Photo-irradiated CO insertion	44
<b>Scheme 2.13.</b>	Schulze's iron-mediated CO insertion	45
<b>Scheme 2.14.</b>	Catalytic [5+1] reaction of VCP and CO	46
<b>Scheme 2.15.</b>	Synthesis of 4-aryl-substituted silacyclohexanes	47
<b>Scheme 2.16.</b>	Wender's intramolecular [5+2] cycloaddition between VCPs and alkynes	48
<b>Scheme 2.17.</b>	Reversal of regioselectivity with different Rh(I) catalysts	49
<b>Scheme 2.18.</b>	Wender's greener method for intramolecular [5+2] cycloaddition	52
<b>Scheme 2.19.</b>	Chung's Rh(I)-NHC catalyst system for intramolecular [5+2] reaction	52
<b>Scheme 2.20.</b>	Trost's Ru(II)-catalyzed intramolecular [5+2] cycloaddition with alkynes	54

<b>Scheme 2.21.</b>	Diastereoselectivity of Trost's [5+2] method	55
<b>Scheme 2.22.</b>	Mechanism of Ru(II)-catalyzed intramolecular [5+2] cycloaddition	56
<b>Scheme 2.23.</b>	Fürstner's iron-catalyzed intramolecular [5+2] method	59
<b>Scheme 2.24.</b>	Louie's Ni(0)-catalyzed [5+2] intramolecular cycloaddition	59
<b>Scheme 2.25.</b>	Wender's first report of intermolecular [5+2] cycloaddition with alkynes	61
<b>Scheme 2.26.</b>	Employing VCP <b>2.153</b> in intermolecular [5+2]	62
<b>Scheme 2.27.</b>	Mechanistic pathways for the Rh(I)-catalyzed intermolecular reaction	64
<b>Scheme 2.28a.</b>	Effect of internal alkene substitution on regioselectivity	65
<b>Scheme 2.28b.</b>	Effect of terminal alkene substitution on regioselectivity	65
<b>Scheme 2.28c.</b>	Effect of 1,2-substitution on VCP on regioselectivity	65
<b>Scheme 2.29.</b>	Cationic Rh(I) complex for intermolecular [5+2] cycloaddition	66
<b>Scheme 2.30a.</b>	Intermolecular [5+2] reaction with allene equivalents	66
<b>Scheme 2.30b.</b>	Intermolecular [5+2] reaction with ketene equivalents	67
<b>Scheme 2.31.</b>	Ir-catalyzed intermolecular [5+2] cycloaddition reaction	70
<b>Scheme 2.32.</b>	Wender's intramolecular cycloaddition with alkenes	70
<b>Scheme 2.33.</b>	Wender's intramolecular cycloaddition with allenes	72
<b>Scheme 2.34.</b>	Intermolecular [5+2] cycloaddition with allene	73
<b>Scheme 2.35a.</b>	Wender's [5+2+1] cycloaddition with VCP, alkynes, and CO	76
<b>Scheme 2.35b.</b>	Wender's [5+2+1] cycloaddition with VCP, allenes, and CO	76
<b>Scheme 2.36a.</b>	Intramolecular [5+2+1] cycloaddition with alkenes	77
<b>Scheme 2.36b.</b>	Synthesis of tricyclic systems with [5+2+1] cycloaddition	77

<b>Scheme 2.37.</b>	Yu's [5+1]/[2+2+1] cycloaddition with VCPs, alkynes, and CO	79
<b>Scheme 2.38.</b>	Wender's serial [5+2]/[4+2] cycloaddition	80
<b>Scheme 2.39.</b>	Tandem [5+2]/Nazarov cycloaddition	80
<b>Scheme 2.40.</b>	Serial [5+2]/1,4-Peterson elimination/[4+2] reaction	82
<b>Scheme 2.41.</b>	Pattenden's radical-initiated [5+4] cycloaddition	83
<b>Scheme 2.42.</b>	Synthesis of steroid skeletons via radical cascade cyclizations	83
<b>Scheme 2.43.</b>	Trost's synthesis of aphidicolin	84
<b>Scheme 2.44.</b>	Synthesis of (±)-zizane using VCP rearrangement	84
<b>Scheme 2.45.</b>	Corey's total synthesis of hirsutene	85
<b>Scheme 2.46.</b>	Lewis acid-promoted rearrangement in synthesis of (±)-A <sub>An</sub>	85
<b>Scheme 2.47.</b>	VCP rearrangement in the synthesis of (-)-retigeranic acid	87
<b>Scheme 2.48.</b>	Hudlicky's total synthesis of (-)-specionin	87
<b>Scheme 2.49.</b>	Synthesis of (±)-vetispiene through thermal VCP rearrangement	87
<b>Scheme 2.50a.</b>	Sonawane's total synthesis of (-)-Δ <sup>9(12)</sup> -Capnellene	88
<b>Scheme 2.50b.</b>	Synthesis of (+)-grandisol	88
<b>Scheme 2.51.</b>	VCP rearrangement in the synthesis of (+)-longifolene	89
<b>Scheme 2.52a.</b>	Total synthesis of (+)-dictamnol through VCP cycloaddition	89
<b>Scheme 2.52b.</b>	Intramolecular [5+2] cycloaddition with allenes in (+)-aphanamol synthesis	89
<b>Scheme 2.53.</b>	Total synthesis of (+)-frondosin A with Ru(II)-[5+2] method	90
<b>Scheme 2.54.</b>	[5+2+1] cycloaddition used in racemic and asymmetric synthesis of hirustene	91
<b>Scheme 2.55.</b>	Preparation of (±)-hirsutic acid via tandem [5+2+1]/aldol reaction	92

<b>Scheme 2.56.</b>	Preparation of (+)-asteriscanolide	93
<b>Scheme 3.1.</b>	Intramolecular C-H insertion with imidoiodobenzene derivative <b>3.1</b>	105
<b>Scheme 3.2.</b>	Intramolecular C-H insertion with sulfamate esters	106
<b>Scheme 3.3.</b>	Enantioselective intramolecular C-H insertion with sulfamate esters	108
<b>Scheme 3.4a.</b>	Intermolecular C-H insertion with <i>N</i> -tosyloxycarbamates	110
<b>Scheme 3.4b.</b>	Stereoselective C-H amination of alkenes with chiral <i>N</i> -tosyloxycarbamate	110
<b>Scheme 3.5.</b>	Che's intramolecular aziridination	111
<b>Scheme 3.6a.</b>	Allylic <i>N</i> -tosyloxycarbamates in intramolecular aziridination	112
<b>Scheme 3.6b.</b>	Attempt to synthesize six-membered ring through aziridination	112
<b>Scheme 3.7.</b>	Aziridination of allene followed by [4+3] cycloaddition	113
<b>Scheme 3.8a.</b>	Müller's intermolecular olefin aziridination	114
<b>Scheme 3.8b.</b>	Du Bois' improved Rh(II)-catalyzed aziridination	114
<b>Scheme 3.9.</b>	Stereoselective Rh(II)-catalyzed aziridnation	115
<b>Scheme 3.10.</b>	Screening of Rh(II) catalysts	117
<b>Scheme 3.11a.</b>	Investigations of the nitrene precursor	118
<b>Scheme 3.11b.</b>	Leaving group on the benzyloxycarbamate	118
<b>Scheme 3.11c.</b>	Equivalents of nitrene precursor	118
<b>Scheme 3.12a.</b>	Screening of inorganic and organic bases	119
<b>Scheme 3.12b.</b>	Equivalents of NaOAc	120
<b>Scheme 3.13.</b>	Effect of concentration of substrate in reaction	120
<b>Scheme 3.14.</b>	Solvent screening	121

<b>Scheme 3.15.</b>	Further functionalization of [5+1] products	124
<b>Scheme 3.16.</b>	Pyridine-appended VCPs in Rh(II) aza-[5+1] reaction	127
<b>Scheme 3.17.</b>	Intramolecular amination with Berry's Rh <sub>2</sub> <sup>II,III</sup> dimer catalyst	129
<b>Scheme 3.18a.</b>	Screening Rh <sub>2</sub> (espn) <sub>2</sub> Cl for the aza-[5+1] cycloaddition	130
<b>Scheme 3.18b.</b>	<i>In situ</i> iminoiodinane formation with Berry's catalyst	130
<b>Scheme 3.19.</b>	Aza-[5+1] reaction with pyridine-appended VCP	131
<b>Scheme 3.20.</b>	Effect of pyridine substitution on aza-[5+1] reaction	133
<b>Scheme 4.1.</b>	Phenyl-substitution on cyclopropyl ring systems	141
<b>Scheme 4.2.</b>	Initial reports of the "non-classical" carbocation	144
<b>Scheme 4.3.</b>	Initial discoveries of VCP rearrangement	144
<b>Scheme 4.4.</b>	Silver-initiated cyclopropyl-cyclobutyl arrangement	146
<b>Scheme 4.5.</b>	Hydrolysis of 4-halogenated VCP <b>4.49</b>	147
<b>Scheme 4.6a.</b>	VCP rearrangement with Brønsted acid	148
<b>Scheme 4.6b.</b>	Lewis acid-promoted VCP rearrangement	148
<b>Scheme 4.6c.</b>	Silyl ether appended-VCP rearrangement	148
<b>Scheme 4.7.</b>	Screening of Brønsted and Lewis acids for [5+1] reaction	149
<b>Scheme 4.8.</b>	Metal triflates screening	150
<b>Scheme 4.9a.</b>	Screening of iminoiodinanes	151
<b>Scheme 4.9b.</b>	Equivalents of nitrogen source	151
<b>Scheme 4.10.</b>	Solvent screening	152
<b>Scheme 4.11.</b>	Employing diphenyl substrate in Sc(III)-[5+1] reaction	152
<b>Scheme 4.12.</b>	Pre-mixing time with Sc(OTf) <sub>3</sub> and <b>4.77</b>	154
<b>Scheme 4.13.</b>	Employing diphenyl substrate in Sc(III)-[5+1] reaction	156

<b>Scheme 4.14.</b>	Substrate dependency of Rh-catalyzed and Sc-promoted conditions	158
<b>Scheme 4.15.</b>	Role of the nitrene precursor	159
<b>Scheme 4.16.</b>	Radical trapping experiment with TEMPO	161

### List of Tables

<b>Table 3.1.</b>	Scope of the Rh(II)-catalyzed aza-[5+1] cycloaddition	122
<b>Table 4.1.</b>	Kinetic and thermodynamic data for rearrangement of cyclopropyl rings and 5-hexenyl	139
<b>Table 4.2.</b>	Comparison of rate constants for differing substituted radicals	140
<b>Table 4.3.</b>	Kinetic and thermodynamic data for rearrangement of $\alpha$ -substituted vs 2-substituted cyclopropyl rings	141
<b>Table 4.4.</b>	Data for rearrangement of cyclopropyl and cyclobutyl rings	142
<b>Table 4.5.</b>	Isolated products from the Sc(OTf) <sub>3</sub> aza-[5+1] reaction	155

## List of Abbreviations

acac	Acetylacetone
Ad	Adamantyl
AcOH	Acetic acid
AIBN	Azobisisobutyronitrile
Alk	Alkyl
Ar	Aryl
9-BBN	9-Borabicyclo(3.3.1)nonane
BINAP	2,2'-bis(diphenylphosphino)-1,1'-binaphthyl
Bn	Benzyl
Boc	<i>Tert</i> -Butyloxycarbonyl
br	Broad
CAN	Ceric ammonium nitrate
Cbz	Benzyloxycarbonyl
COD	Cyclooctadiene
Cp	Cyclopentadienyl
CSA	Camphorsulfonic acid
Cy	Cyclohexyl
d	Doublet
DABCO	1,4-diazabicyclo[2.2.2]octane
dbcot	Dibenzo[ <i>a,e</i> ]cyclooctatetraene
DCE	Dichloroethane

DCM	Dichloromethane
DFT	Density Functional Theory
DMA	Dimethylacetamide
DME	Dimethoxyethane
DMF	Dimethylformamide
DMSO	Dimethyl sulfoxide
dnCOT	Dinaphthocyclooctatetraene
dppp	1,3-Bis(diphenylphosphino)propane
dr	Diastomeric ratio
EDG	Electron-donating group
ee	Enantiomeric excess
esp	$\alpha,\alpha,\alpha',\alpha'$ -tetramethyl-1,3-benzenedipropionic acid
Et	Ethyl
EWG	Electron-withdrawing group
hfacac	Hexafluoroacetylacetone
HFIP	Hexafluoroisopropanol
HMDS	Hexamethyldisilazane
HOSA	Hydroxylamine-O-sulfonic acid
<sup>i</sup> Pr	Isopropyl
L <sub>n</sub>	Ligand
m	Multiplet
<i>m</i> -CPBA	Meta-Chloroperoxybenzoic acid
Me	Methyl

MeCN	Acetonitrile
Mes	Mesityl
MOM	Methoxymethyl
naph	Naphthalene
NBD	Norbornadiene
<sup>n</sup> Bu	n-Butyl
n-dec	n-Decyl
NHC	N-Heterocyclic Carbene
<sup>n</sup> Pr	n-Propyl
Ns	Nosyl
nttl	N-(1,2-Naphthaloyl)-(S)- <i>tert</i> -Lucine
OAc	Acetate
OMe	Methoxy
OPiv	Pivolate
OTf	Triflate
OTs	Tosylate
Ph	Phenyl
PMB	p-Methoxybenzyl
py	Pyrrole
q	Quartet
RDS	Rate determining step
s	Singlet
t	Triplet

TBDMS	<i>tert</i> -Butyldimethylsilyl
TBS	<i>tert</i> -Butyldimethylsilyl
<sup>t</sup> Bu	<i>tert</i> -Butyl
TCE	Trichloroethane
Tces	Trichloroethylsulfamate
tfacam	2,2,2-Trifluoroacetamide
TFE	2,2,2-Trifluoroethanol
TfOH	Trifluoromethanesulfonic acid
THF	Tetrahydrofuran
TIPS	Triisopropyl silane
TLC	Thin-layer chromatography
TMS	Trimethylsilyl
tol	Tolyl
tpa	Tris(2-pyridylmethyl)amine
Troc	2,2,2-Trichloroethoxycarbonyl
Ts	Tosyl
TTMSS	Tris(trimethylsilyl)silane
VCP	Vinylcyclopropane

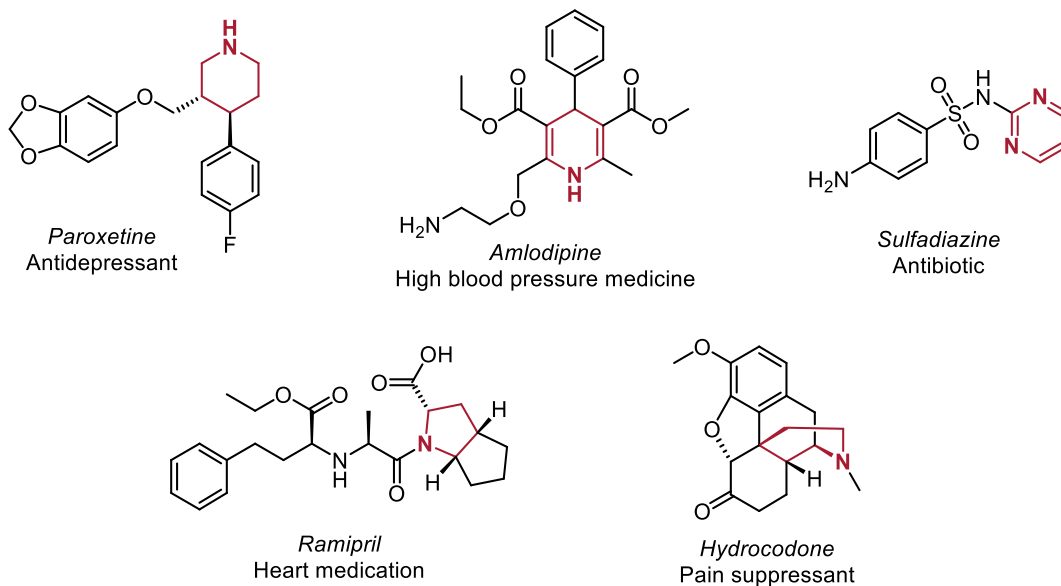
## Chapter 1

### *Synthesis of Cycloadducts using Nitrenes as a Single Atom Component*

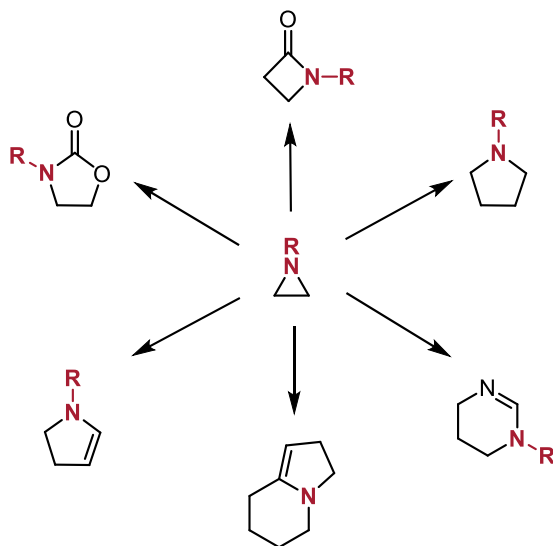
#### 1.1. Introduction

Nitrogen heterocycles are prevalent in FDA-approved pharmaceutical drugs. According to a recent review, 59% of current small molecule drugs contain at least one (Figure 1.1).<sup>1</sup> As such, synthetic chemists are searching for methods that would allow for the facile synthesis of these motifs. Investigation into the use of nitrenes or nitrenoids as one-atom components in heterocycle synthesis has previously been focused on the synthesis of aziridines from alkenes, which can be considered a [2+1] cycloaddition.<sup>2</sup> These products can then be utilized as building blocks to form an array of different ring systems, including indolizidines,<sup>3</sup> imidazoles,<sup>4</sup>  $\beta$ -lactams,<sup>4</sup> di-hydropyrroles,<sup>5</sup> and tetrahydropyrimidines<sup>6</sup> (Figure 1.2).

**Figure 1.1.** Examples of FDA-approved medications containing a nitrogen heterocycle



**Figure 1.2.** Ring expansion of aziridines to form larger heterocycles



To streamline the formation of nitrogen heterocycles, researchers are now investigating the use of nitrenes in multicomponent cycloaddition reactions. This would expand the types of substitution patterns in nitrogen heterocycles, such as pyrroles, that are otherwise difficult to access. In this chapter, these novel strategies will be explored.

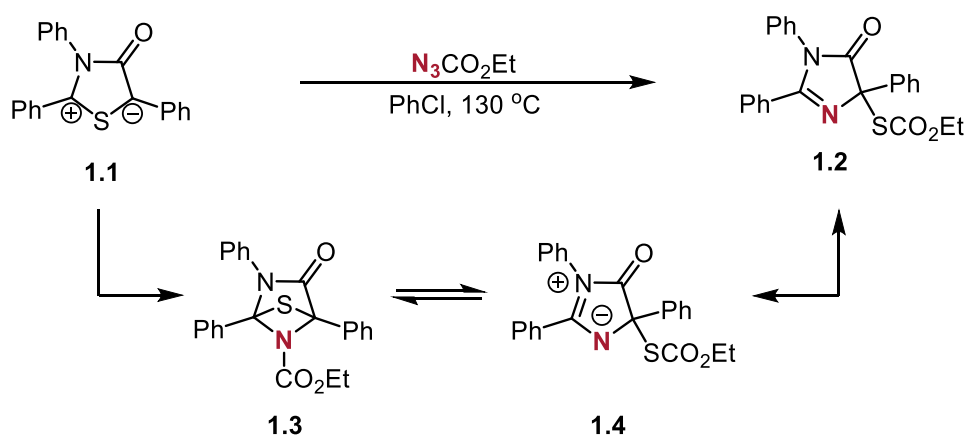
## 1.2. [3+1] Cycloadditions

### 1.2.1. [3+1] Cycloadditions with Thiazolones

Sheradsky and co-workers reported an early example of a probable (3+1) cycloaddition between thiazolone **1.1** and ethyl azidoformate to form thio-imidazolinone **1.2** in 45% yield (**Scheme 1.1**).<sup>7</sup> It was hypothesized that dipole species **1.1** undergoes a (3+1) cycloaddition to form adduct **1.3** with the simultaneous release of diatomic nitrogen. **1.3** exists in equilibrium with species **1.4** which is a resonance structure of thio-imidazolinone **1.2**. This mechanism was simply deemed the most plausible path and

intermediate **1.3** was not isolated. It was reported that this reaction is tolerant of electron-withdrawing phenyl substituents (4-Cl, 2-Cl, and 2,4-Cl) on the thiazolone ring, although no yields or characterization data apart from elemental analysis were provided. Thioimidazolinone **1.2**'s structure was confirmed using x-ray crystallography.

**Scheme 1.1.** Sheradsky's [3+1] cycloaddition of mesoionic thiazolones

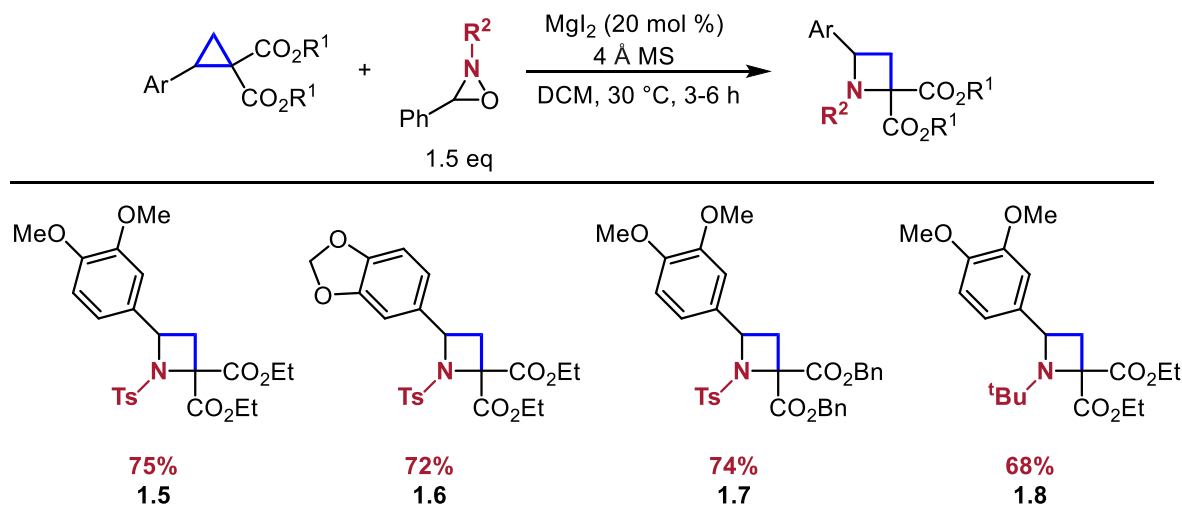


### 1.2.2. [3+1] Cycloadditions with Oxaziridines

In 2016, Chattaraj and Banerjee demonstrated a [3+1] cycloaddition using oxaziridines as the nitrogen source in the presence of  $\text{MgI}_2$  to synthesize azetidines (**Scheme 1.2**).<sup>8</sup>  $\text{MgI}_2$  acted as a Lewis acid to facilitate the cleavage of the N-O bond. For this reaction, only donor-acceptor cyclopropanes substituted with an aryl group were amenable. In addition, only electron-donating aryl groups provided the desired heterocycle (**1.5** – **1.8**). Changing the esters on the cyclopropane had little effect on the yield of the cycloadduct (**1.7**). Furthermore, a range of nitrogen substitution was also

tolerated. While the majority of them were sulfonamides, at least one alkyl-substituted compound, bearing a <sup>t</sup>Bu group, was tolerated (**1.8**).

**Scheme 1.2.** Scope of [3+1] cycloaddition of cyclopropanes and oxaziridines

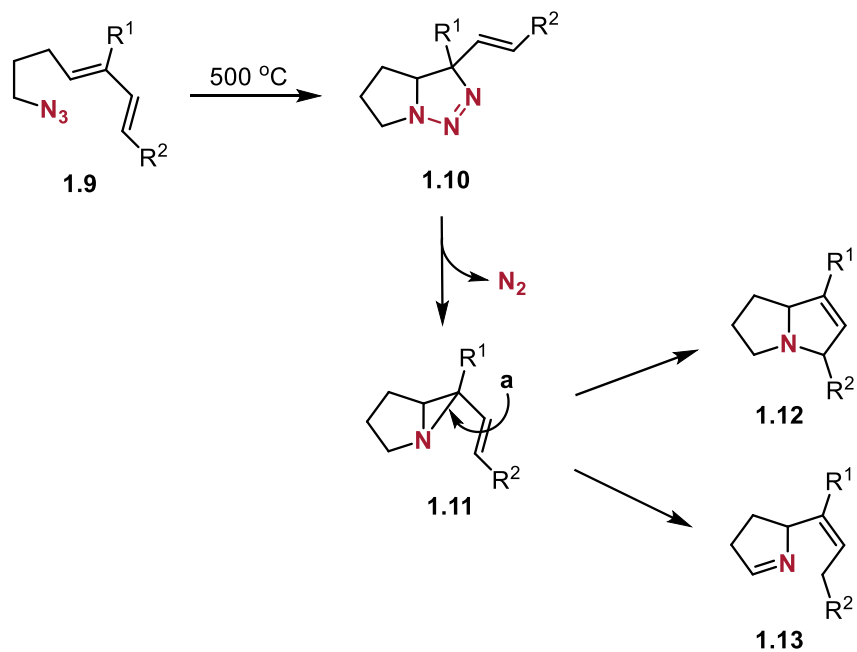


### 1.3. [4+1] Cycloadditions

#### 1.3.1. [4+1] Cycloadditions using Dienes and Azides

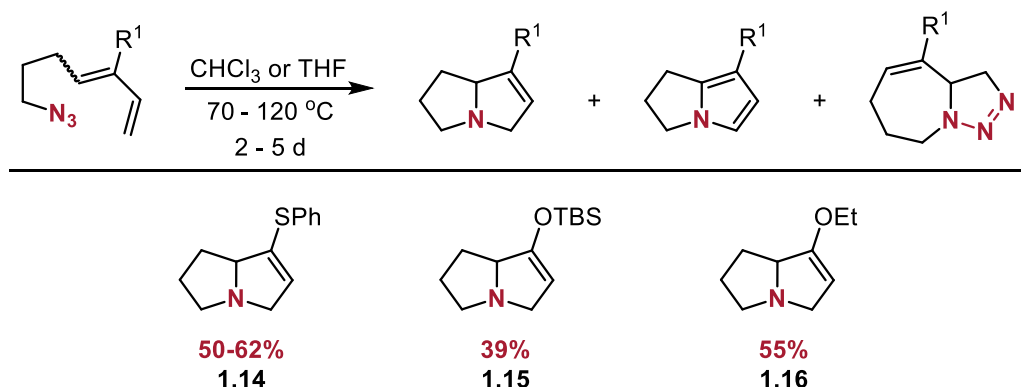
The Pearson group published an early example of a [4+1] cycloaddition using dienes and azides for the synthesis of bicyclic 3-pyrrolines (**Figure 1.3**).<sup>9</sup> Initially, at an elevated temperature, two products were observed (**1.12** and **1.13**), with **1.12** being favored. It was postulated that the cleavage of the aziridine bond (labelled **a**) was the rate determining step that would lead to the formation of either product. The cleavage of this bond is favored due to its ketal-like state as well as its allylic nature and three-membered ring strain. The 1,5-homodienyl shift to form **1.13** was suppressed using heterosubstituted dienes that would weaken the C-N bond in species **1.11**. Thus, bicyclic product **1.12** would be favored.

**Figure 1.3.** Pearson's seminal intramolecular [4+1] cycloaddition of dienes and azides

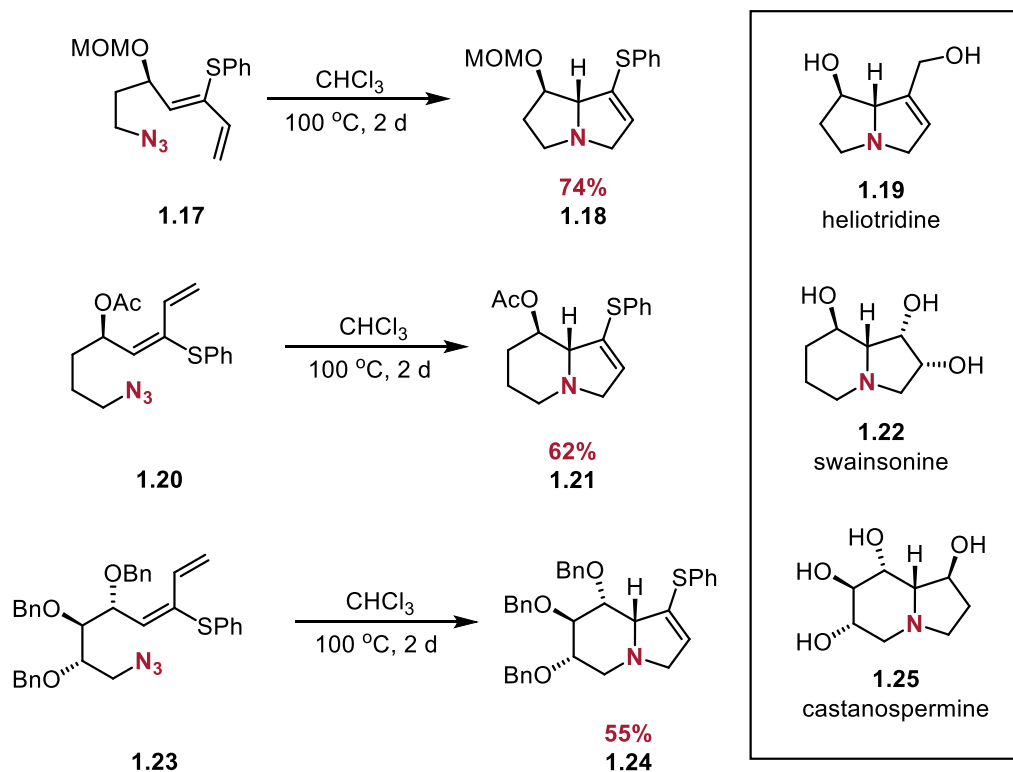


This was observed through the formation of dihydropyrrolizines **1.14** – **1.16** (**Scheme 1.3**). When exposed to higher temperatures, the 3-pyrroline ring was oxidized to a pyrrole. Upon extended reaction times, a fused [5,7] triazole ring product was isolated due to its favored geometry. Lastly, the use of a non-polar solvent (THF) favored the formation of the triazole isomer.

**Scheme 1.3.** Partial scope of intramolecular [4+1] reaction



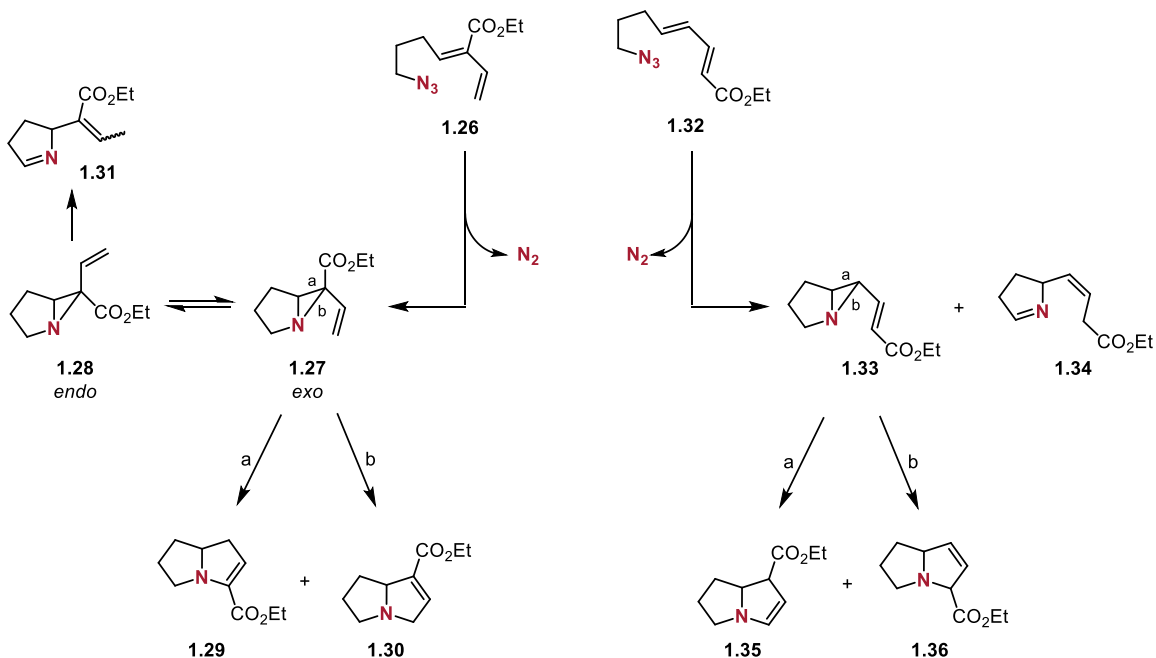
Pearson later demonstrated performing the azide-diene cyclization diastereoselectively to synthesize the core structure of some natural products.<sup>10</sup> The frameworks of heliotridine, swainsonine, and castanospermine were synthesized using related conditions in refluxing chloroform (**Scheme 1.4**). In all cases, only one product was isolated (**1.18**, **1.21**, **1.24**). The selectivity of this reaction was rationalized by the allylic strain between the SPh or vinyl group (depending on alkene geometry) and the allylic ether that exists in one transition state (TS) conformation and not the other.

**Scheme 1.4.** Diastereoselective intramolecular [4+1] cycloaddition


Hudlicky studied the mechanism of this intramolecular reaction in order to preferentially synthesize regioisomers (**Scheme 1.5**).<sup>11</sup> Pearson's hypothesis of an aziridine as a key intermediate was confirmed as well as the fact that its formation is dependent on the placement of the ester group. Then, ring opening of the aziridine dictates which regioisomer is formed. When using **1.26**, the *exo* and *endo* aziridines can form and, in the case of the former, the aziridine opens and leads to a 4:1 mixture of pyrrolizines **1.30** and **1.29**, which is attributed to the favored cleavage of the  $\alpha$ -amino ester bond. In the case of **1.28**, the intermediate rapidly isomerizes to imine **1.31**. For substrate **1.32**, aziridine **1.33** was isolated as well as a minimal amount of imine **1.34**.

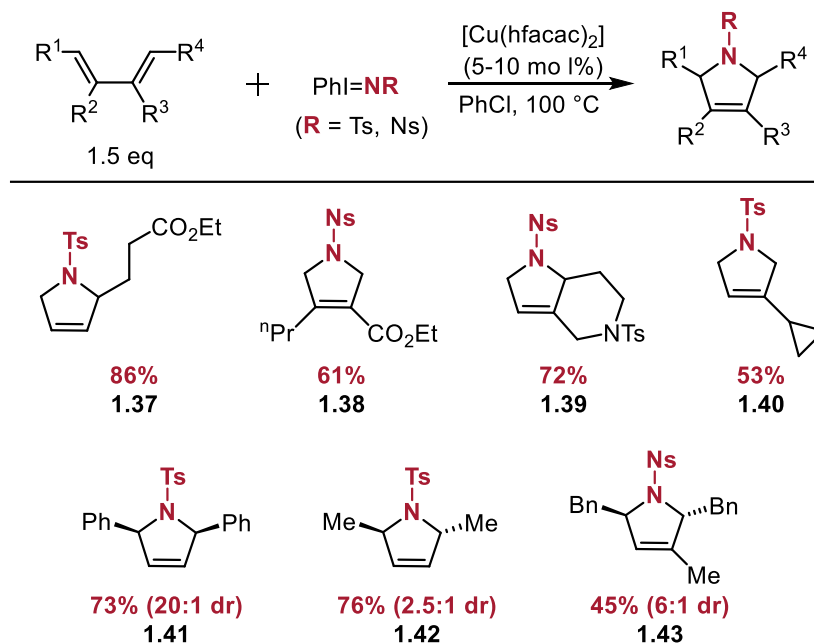
After subjecting **1.33** to flash pyrolysis, dihydropyrrolizine **1.35** was exclusively formed; however, the enamine would rapidly isomerize to form the more substituted alkene.

**Scheme 1.5.** Hudlicky's mechanistic proposal for the [4+1] cycloaddition using azides

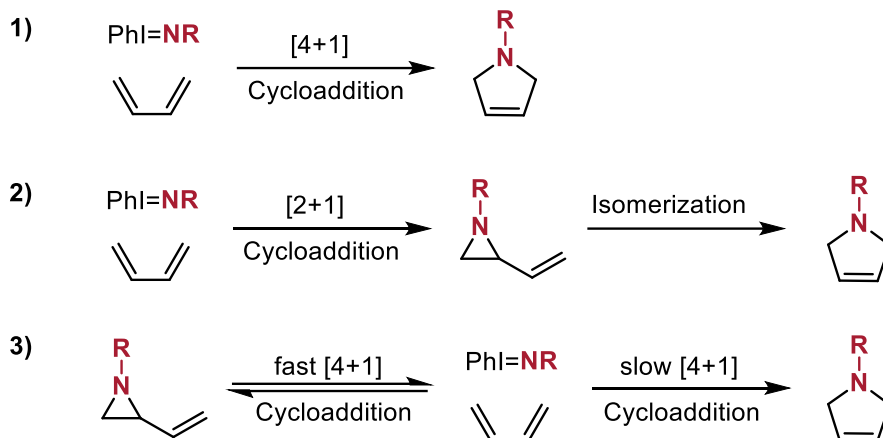
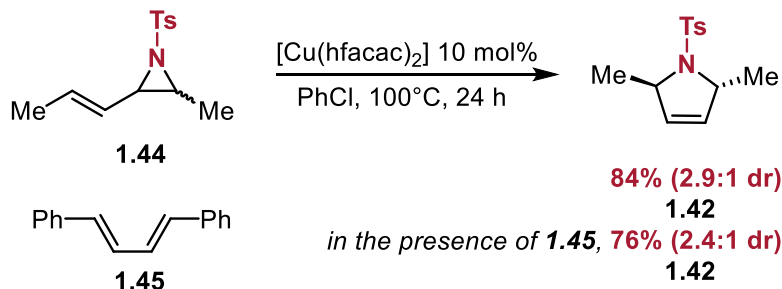


### 1.3.2. [4+1] Cycloadditions using Dienes and Iminoiodinanes

Zhou and co-workers reported the first examples of an overall [4+1] reaction using dienes and iminoiodinanes as the nitrene precursor.<sup>12</sup> For this strategy, [Cu(hfacac)<sub>2</sub>] served as the catalyst to synthesize dihydropyrroles in up to 93% yield with a moderate to excellent diastereoselectivity. (**Scheme 1.6**). 3-pyrrolines bearing multiple substitution patterns were isolated, and a range of different functional groups, including esters and sulfonamides, were tolerated. (**1.37 – 1.43**) 1,4-Dialkyl substituted dienes (e.g., **1.42**) exhibited lower diastereoselectivity compared to 1,4-diphenyl substituted dienes (e.g., **1.41**), which was explored later in mechanistic experiments.

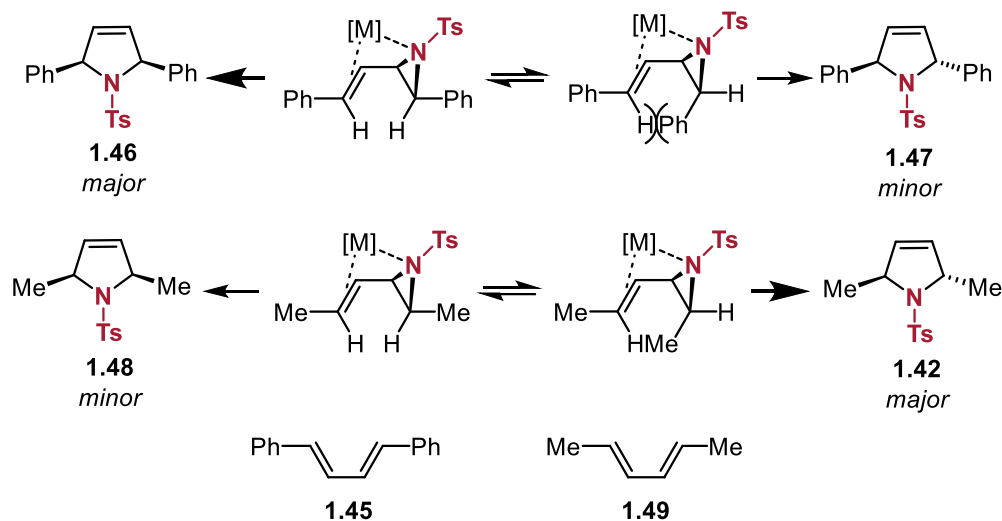
**Scheme 1.6.** Scope of Zhou's [4+1] cyclization between dienes and iminoiodinanes

Three mechanisms were considered for the formation of the cycloadducts: 1) a concerted [4+1] cycloaddition between the diene and metal-nitrene species; 2) a formal [2+1] reaction to form a vinyl aziridine species, followed by isomerization; and, 3) a fast, reversible aziridination occurring in conjugation with a slow, irreversible [4+1] cycloaddition (**Figure 1.4**). Following subsequent experiments, pathway 2 was seen as most plausible. First, increasing the temperature of the reaction from 100°C to 150°C resulted in a change of product distribution from vinylaziridines to dihydropyrroles, which has been previously reported by Njardarson and co-workers.<sup>13</sup> Furthermore, in the presence of **1.45**, isomerization of **1.44** still occurred in a 76% yield, indicating no crossover vinylaziridines or 3-pyrrolines and confirming pathway 3 as not plausible (**Scheme 1.7**).

**Figure 1.4.** Plausible mechanistic pathways for the [4+1] reaction**Scheme 1.7.** Isomerization of a di-methyl substituted aziridine in the presence of diphenylbutadiene

The stereoselectivity of this reaction was further explored using differently substituted butadienes – **1.45** and **1.49** (**Figure 1.5**). The observed dr for the former can be attributed to the steric repulsion between the phenyl group and the nearby H-atom, leading to the formation of **1.46**. However, when a bulkier substituent is an alkyl group, the steric interaction is minimized by single-bond rotation, so **1.42** is more favorable.

**Figure 1.5.** Proposed mechanistic models for stereoselectivity of the [4+1] reaction



([M] = [Cu(hfacac)<sub>2</sub>]<sup>+</sup>)

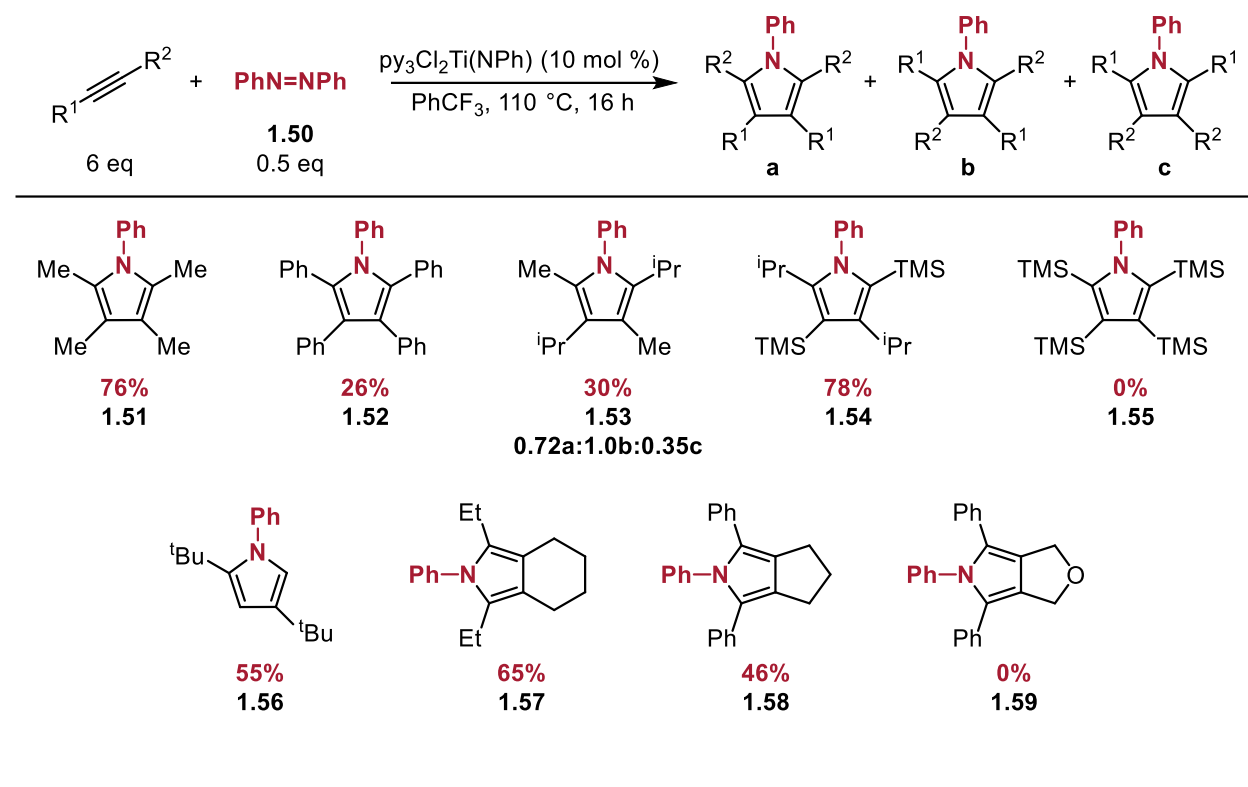
## 1.4. [2+2+1] Cycloadditions

### 1.4.1 Ti-catalyzed [2+2+1] Cycloadditions with Alkynes and Diazines

In their seminal work for this reaction class, Tonks and co-workers presented a new catalytic strategy for the synthesis of pyrroles through a formal [2+2+1] oxidative coupling of alkynes and diazines (**Scheme 1.8**).<sup>14</sup> Homo alkyl-disubstituted alkynes provided exceptional yields (**1.51**) while the use of diphenylacetylene greatly decreased cyclization (**1.52**). The use of hetero-substituted alkynes showed little regioselectivity (**1.53**); however, when a hetero-substituted silyl alkyne was employed, only a single regioisomer was observed (**1.54**). Interestingly, the use of bis(trimethylsilyl)acetylene showed no reactivity under the optimized conditions (**1.55**). Mono-substituted alkynes with an alkyl or phenyl group were compatible with this reaction, with *tert*-butylacetylene

exclusively forming one product (**1.56**). Tethered alkynes with alkyl and aryl groups were well tolerated (**1.57** and **1.58**), but tethered alkyl ethers did not react (**1.59**).

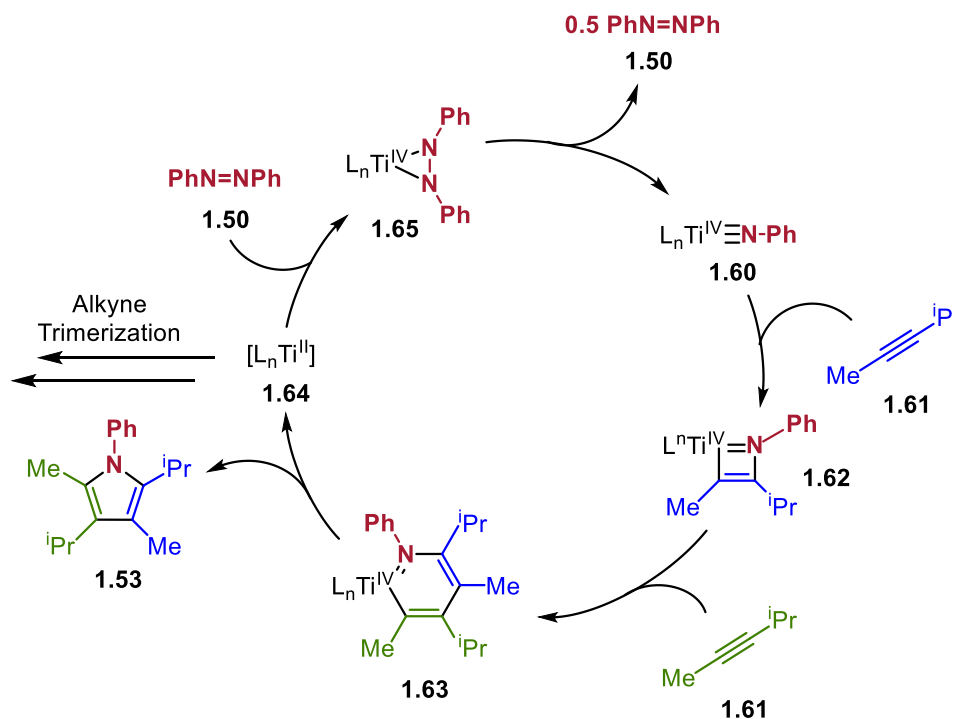
**Scheme 1.8.** Scope of Tonks' initial [2+2+1] cyclization using alkynes and azobenzene



A proposed mechanism is presented in **Figure 1.6**.  $\text{Ti}^{\text{IV}}$  imido complex **1.60** initially undergoes a [2+2] insertion with **1.61** to form a four-membered metallacycle (**1.62**), which has been seen in previous studies about Ti-catalyzed hydroamination.<sup>15-17</sup> Subsequently, a second alkyne molecule inserts into the Ti metallacycle to form azatitanacyclohexadiene **1.63**. While this step is quite rare, it has been seen by both Mountford<sup>18</sup> and Odom.<sup>19</sup> Reductive elimination results in the pyrrole product (**1.52**) as well as reforming  $\text{Ti}^{\text{II}}$  catalyst **1.64**. Alkyne trimerization is known to occur competitively in the presence of  $\text{Ti}^{\text{II}}$  intermediates.<sup>20</sup> A diazene molecule then forms three-membered Ti

complex **1.65** which, after Ti dimerization and a retro-[2+2+2], reforms **1.60**, which restarts the catalytic cycle.

**Figure 1.6.** Preliminary mechanistic proposal for Tonks' [2+2+1] cycloaddition

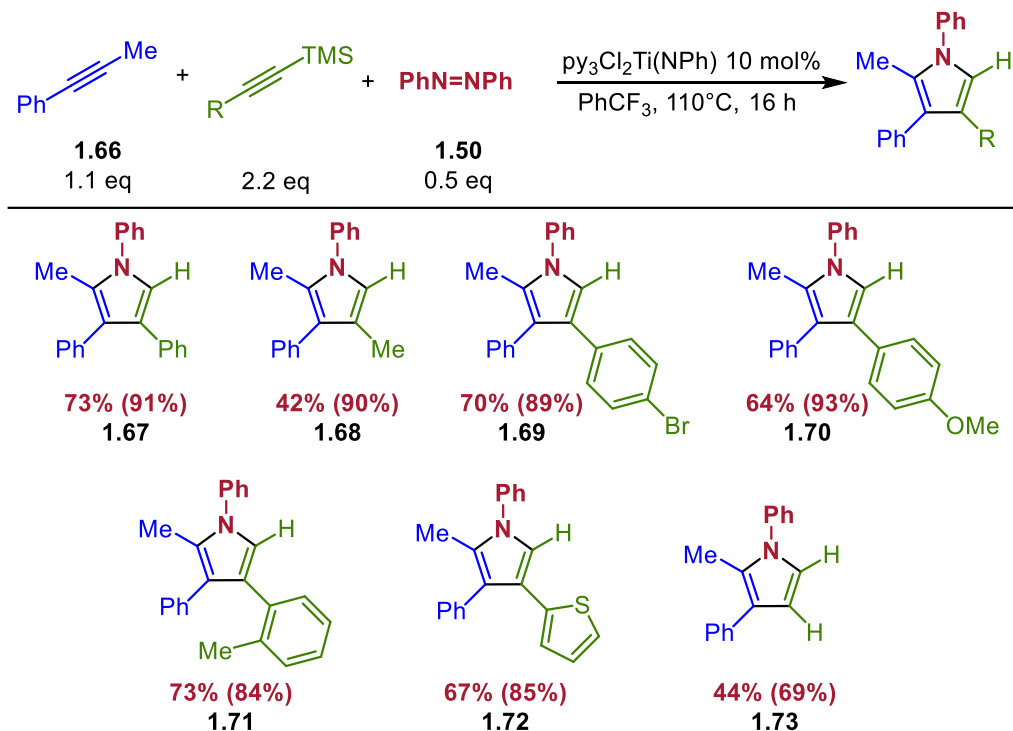


Computational and kinetic studies were conducted in a collaboration between Goodpaster and Tonks following these publications to further understand the mechanism of the Ti-redox catalyzed [2+2+1] reaction.<sup>21</sup> Kinetics revealed that between second alkyne insertion or the reductive elimination of **1.53**, the latter was determined to be the rate-determining step. In addition, it was confirmed that the alkynes are inserting into the Ti complex in two different manners, allowing for the possibility of using other unsaturated systems that may be able to undergo the second insertion step, expanding the reaction scope for this method. Furthermore, it was revealed that the low valent  $Ti^{II}$  intermediates are stabilized by both solvent effects as well as  $\pi^*$  backdonation into the reaction product.

Computations and kinetics also revealed that in terms of regioselectivity of the pyrrole adduct, steric effects play a role for terminal alkynes while inductive effects control that for internal alkynes.

The Tonks group followed up the study by exploring TMS-protected alkynes as selective cross-coupling partners.<sup>22</sup> In almost all cases, one regioisomer was isolated after hydrolysis of the TMS group. The reaction scope with respect to the TMS-acetylene substrates was first investigated (**Scheme 1.9**). The reaction was amenable for the use of both alkyl and phenyl groups on the silyl alkyne (**1.67** and **1.68**), with the exception of *tert*-butylacetylene. Electron-withdrawing and-donating groups had no effect on selectivity (**1.69** and **1.70**) and *ortho*-substituted aryl rings also lead to the pyrrole product (**1.71**). In addition, some Lewis basic groups were also tolerated (**1.72**). Lastly, using TMS-acetylene resulted in a moderate yield of the cycloadduct (**1.73**).

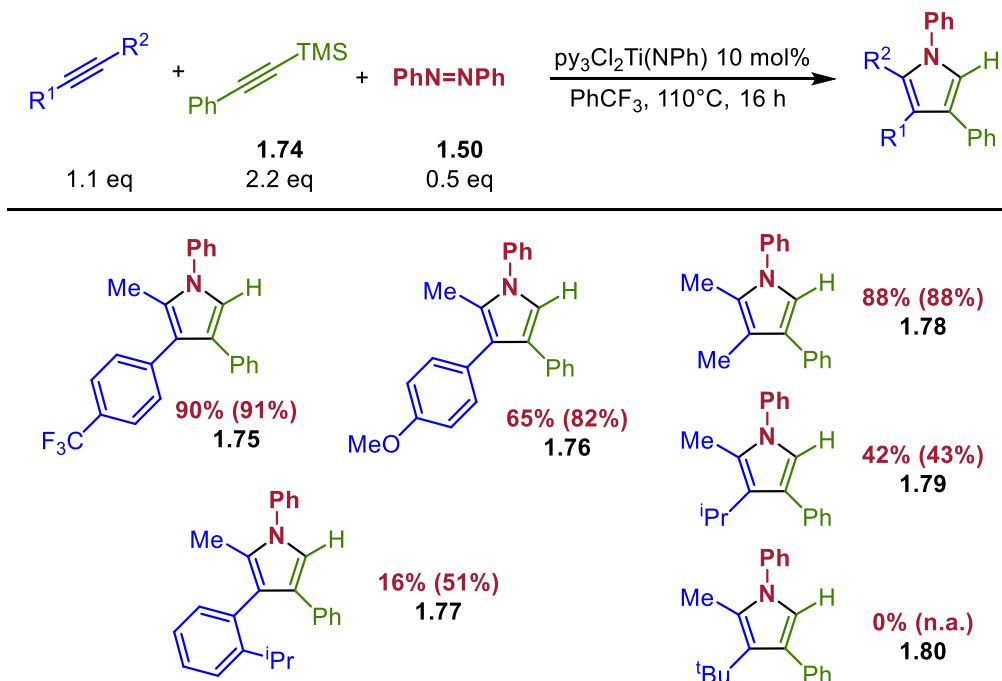
**Scheme 1.9.** Scope of [2+2+1] cycloaddition using TMS-alkynes, 1-phenylpropyne and azobenzene



Selectivity of shown pyrrole adducts in parentheses

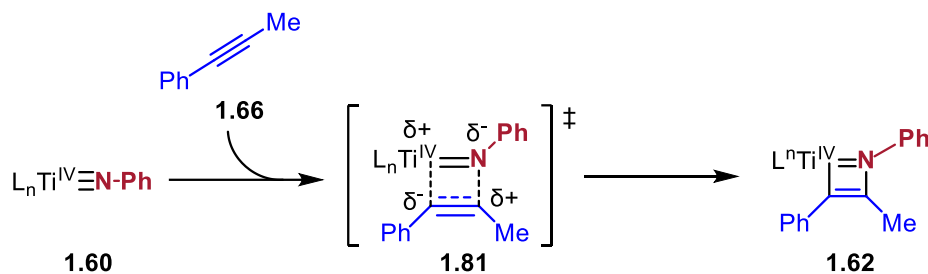
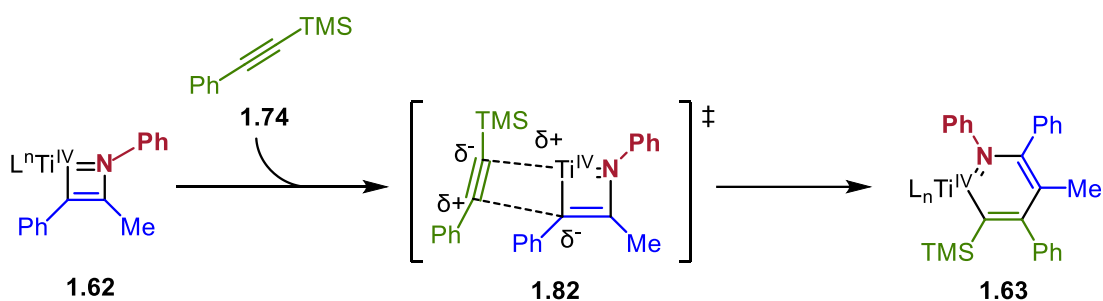
Subsequently, the scope of the cycloaddition was then studied with respect to the internal alkyne using phenylacetylene (**Scheme 1.10**). While *para* electron-donating and electron-withdrawing aryl substitution was well tolerated (**1.75** and **1.76**), yields and selectivity were found to be very sensitive to steric effects for *ortho*-substituted arenes (**1.77**). Furthermore, some dialkyl alkynes were amenable (**1.78**); however, the yield and product selectivity greatly decreased as the steric bulk of the substituents increased (**1.79** and **1.80**).

**Scheme 1.10.** Scope of [2+2+1] cycloaddition using TMS-alkynes, di-substituted alkynes and azobenzene



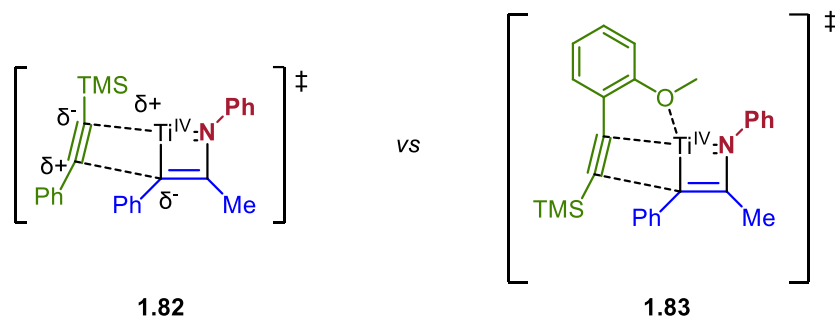
Selectivity of shown pyrrole adducts in parentheses

The degree of regioselectivity was determined to be driven by the electronic nature of transition state **1.81** leading to the formation of metallocycle **1.62** (**Figure 1.7a**). It was proposed that the  $\delta^+$  charge is better stabilized by the methyl group rather than a hydrogen atom. Furthermore, the chemoselectivity of alkyne insertion into the Ti-C bond is driven by the alkyne coordination to the Ti center (**1.82**) (**Figure 1.7b**). Because electron-rich alkynes are better stabilizers for  $\text{Ti}^{\text{IV}}$  Lewis acids, TMS alkynes out compete other alkynes for insertion, leading to **1.63**.

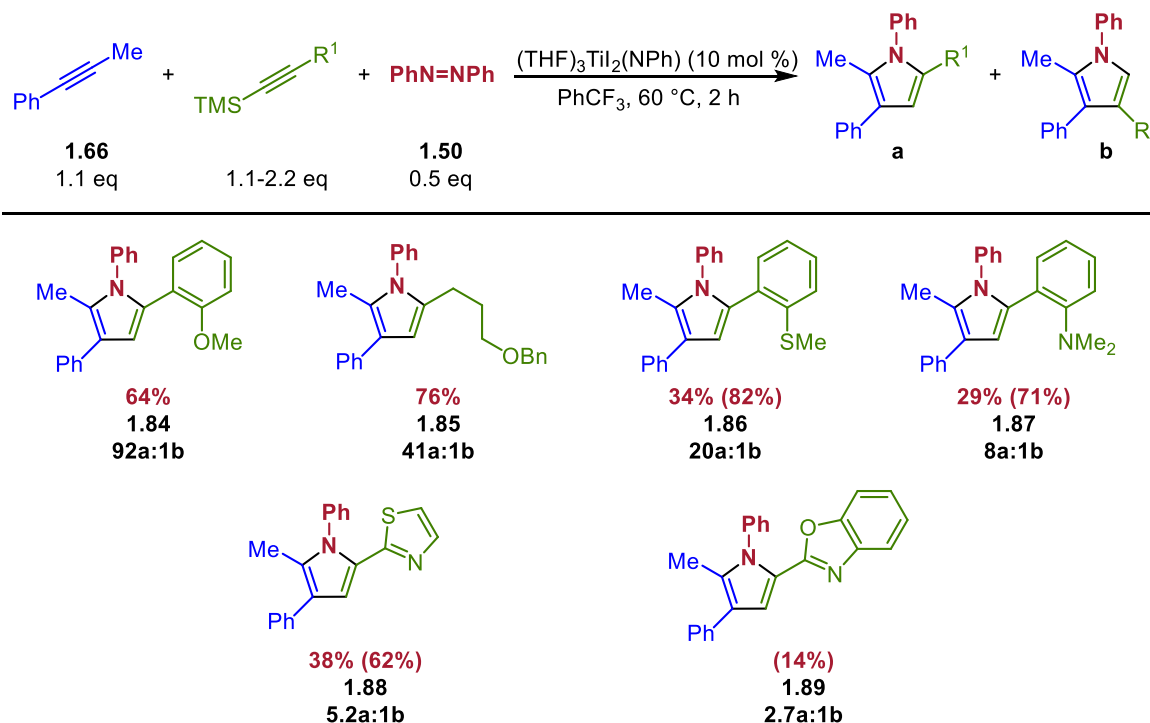
**Figure 1.7a.** [2+2] addition step in Tonks' [2+2+1] cycloaddition**Figure 1.7b.** Migratory insertion step of TMS-phenylacetylene in [2+2+1] cycloaddition

In order to control the regioselectivity of TMS-protected alkyne insertion, the Tonks group used Lewis basic groups to cause a directing-group effect between the substrate and the Ti center.<sup>23</sup> A more Lewis acidic catalyst  $((THF)_3TiI_2(NPh))$  was used to coordinate more strongly to the donor substituents. In addition, lowering the temperature further improved selectivity, most likely due to the slower dissociation of the donor substituent, resulting in the kinetically preferred metallacycle arising from TS **1.83** rather than **1.82** (Figure 1.8).

**Figure 1.8.** Electronically-controlled (**1.82**) vs directed 2<sup>nd</sup> insertion (**1.83**)



This directing group effect can be seen in **Scheme 1.11**. Methoxy and benzyloxy groups were found to have a strong directing effect, providing highly regioselective access to the desired adducts (**1.84** and **1.85**). In addition, aryl groups substituted with other heteroatoms also displayed this effect (**1.86** and **1.87**). Lastly, depending on the Lewis basicity, some heterocycles also acted as great directing groups (**1.88** and **1.89**). If stronger basic heterocycles were used, such as pyridine, catalysis was inhibited. On the other hand, weakly basic systems, such as furan, were not strong enough to serve as a directing group and thus, the reaction proceeds via TS **1.82**.

**Scheme 1.11.** Scope of [2+2+1] cycloaddition using dative directing groups

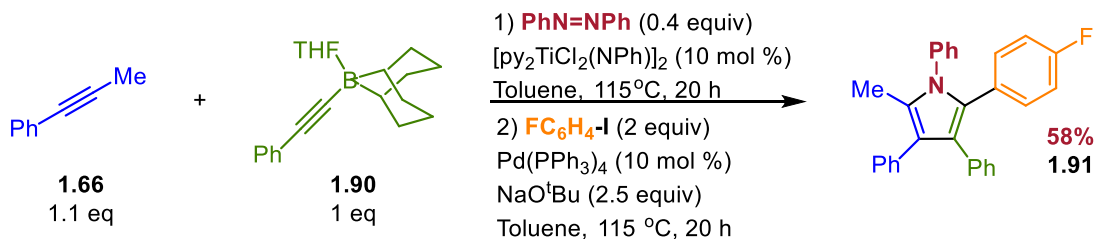
NMR yields in parentheses

In a subsequent collaborative study with Tsurugi and Mashima, Tonks and co-workers further developed this work in to make this synthetic strategy benchtop-compatible.<sup>24</sup> To accomplish this, several reductants were evaluated to be able to activate the air-stable  $\text{TiCl}_4(\text{THF})_2$  into the active  $\text{Ti}^{\text{IV}}$  species *in situ* and enter the catalytic cycle (see **Figure 1.6**). After extensive screening,  $\text{Zn}^0$  was determined to be the most efficient reductant. Using this method, the yield of the pyrrole adducts in air conditions ranged from 40 to 95% yield.

The [2+2+1] cycloaddition between azobenzene and alkynes was later used by Tonks and co-workers to develop a one pot sequential cycloaddition and cross-coupling reaction.<sup>25</sup> 9-BBN alkynes were used with methylphenylacetylene and azobenzene to

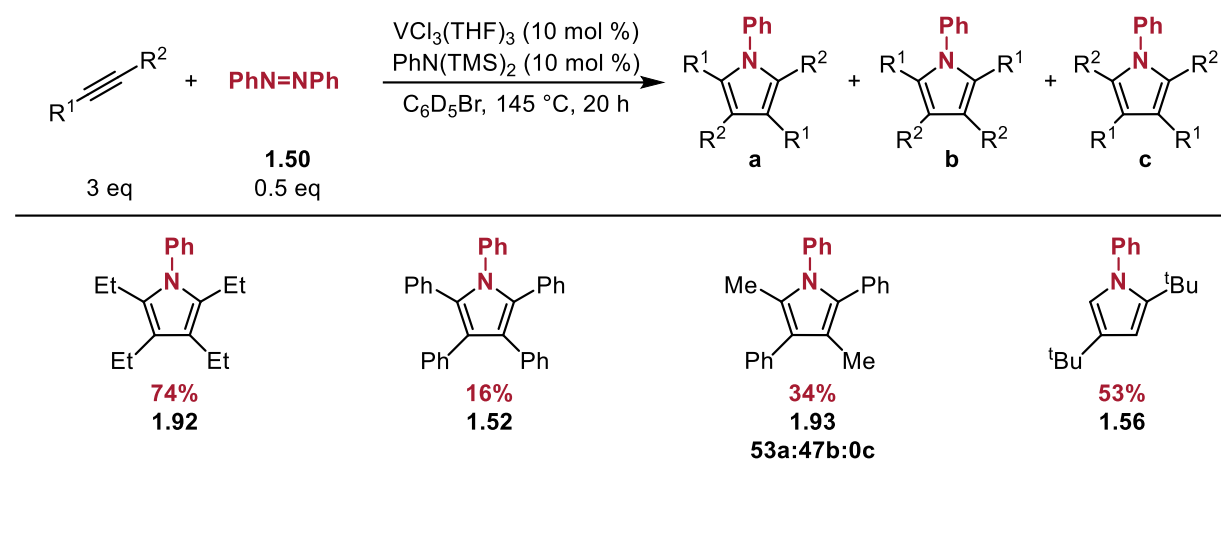
form the pyrrole ring, which was then exposed to  $\text{Pd}(\text{PPh}_3)_4$  and an aryl iodide to synthesize a wide array of differently substituted cycloadducts, as shown in **Scheme 1.12**.

**Scheme 1.12.** One-pot subsequent [2+2+1] cycloaddition and cross-coupling reaction



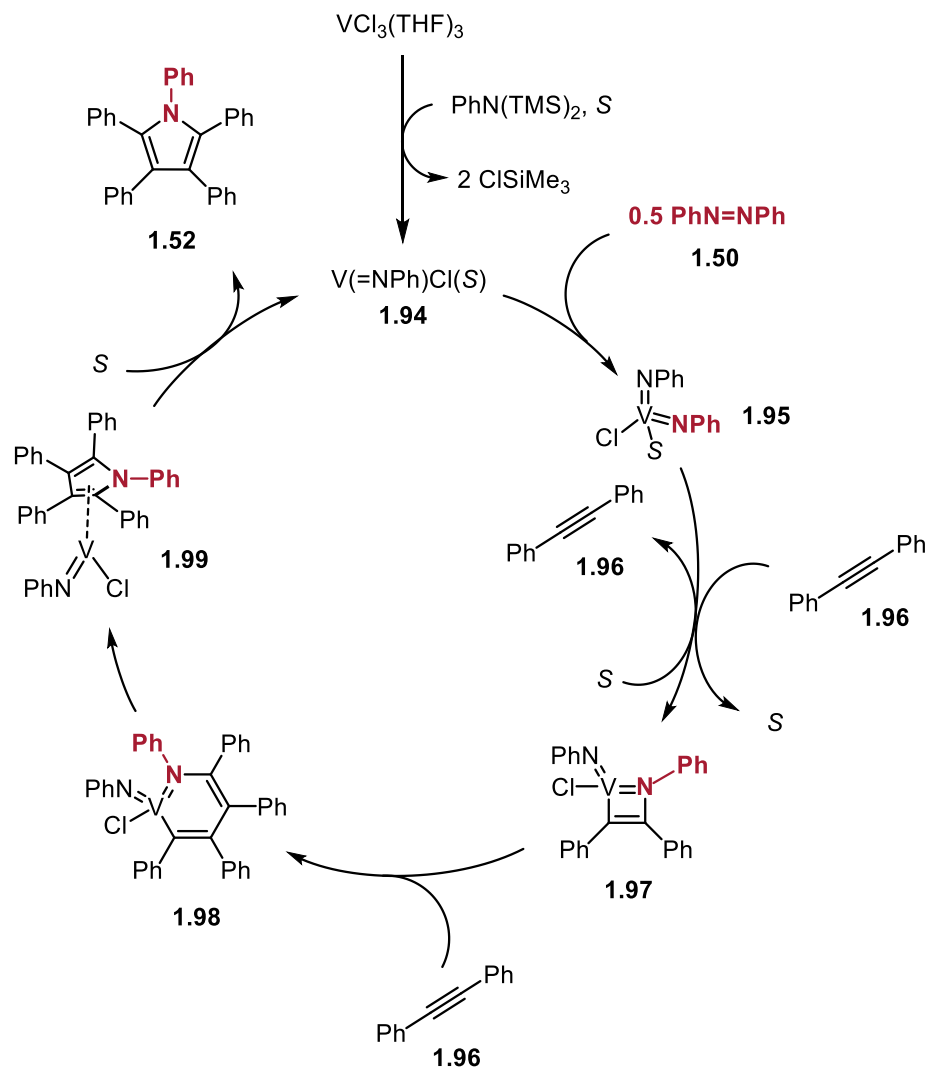
#### 1.4.2. V-catalyzed [2+2+1] Cycloadditions with Diazines

Tonks expanded the capabilities of this strategy through another collaboration with Tsurugi and Mashima in which they used a vanadium complex to catalyze the [2+2+1] cycloaddition between alkynes and using azobenzene. This expanded the diversity of catalysts, scaffolds, and oxidation states that could play a role in these transformations.<sup>26</sup> Using  $\text{VCl}_3(\text{THF})_3$  as the catalyst and  $\text{PhN}(\text{SiMe}_3)_2$  as an additive, these modifications were able to show a moderate selectivity in pyrrole ring formation (**Scheme 1.13**). Dialkyl-substituted alkynes provided a great yield (**1.92**) while diphenylacetylene led to a decrease in adduct product but retained selectivity (**1.52**). The use of 1-phenyl-1-propyne strongly decreased yields as well as almost providing a 1:1 distribution of pyrrole products (**1.93**). Lastly, a mono-substituted alkyne resulted in a moderate yield of a single regioisomer (**1.56**).

**Scheme 1.13.** V-catalyzed [2+2+1] reaction scope

The mechanism of this reaction, seen in **Figure 1.9**, was proposed to be very similar to that of Tonks' (See **Figure 1.6**). The reported vanadium catalyst reacts with  $PhN(TMS)_2$  to form the  $V^{III}$  species **1.94** which undergoes a reductive cleavage with diazene **1.50** to form a bisimido species (**1.95**). It is postulated that the formation of **1.95** undergoes the same Ti dimerization process postulated in previous work. This complex then undergoes a [2+2] addition via one of the vanadium imino moieties to form V-metallacycle **1.97**. Subsequently, an additional alkyne inserts into the V-C bond to form a six-membered intermediate. Following reductive elimination, pyrrole **1.52** was released and active species **1.94** undergoes the catalytic cycle again.

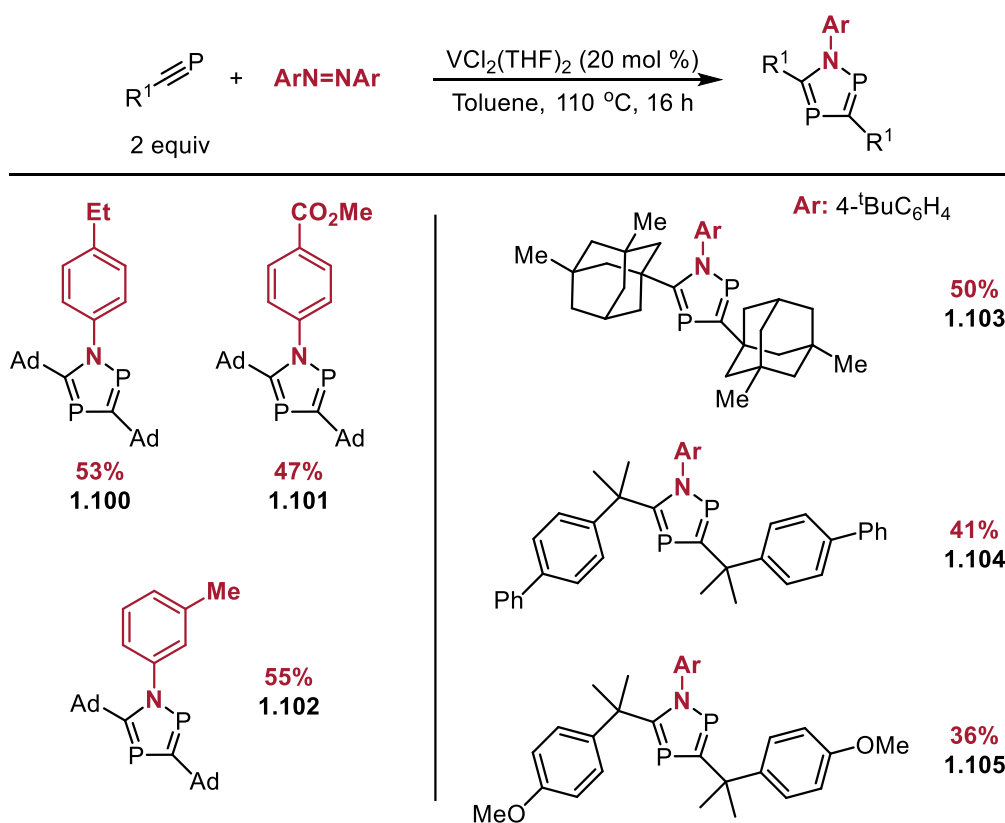
**Figure 1.9.** Proposed mechanistic cycle for vanadium-catalyzed cycloaddition



Inspired by the vanadium catalysis study, Nishibayashi and co-workers developed a [2+2+1] reaction using phosphalkynes as the two-atom component and azobenzenes as the nitrogen source (**Scheme 1.14**).<sup>27</sup> Numerous azobenzenes were employed and tolerated for this cycloaddition, including an ester substituent that could undergo further transformations (**1.100 – 1.102**). Unfortunately, using diazenes without an aryl substituent resulted in no formation of the azadiphosphole product. When changing the

phosphaalkynes, adamanyl and benzyl derivatives provided the five-membered ring in modest yields (**1.103** – **1.105**). While the reaction scope of this method is quite limited, it shows an opportunity to utilize these multicomponent reactions outside of purely alkyl sources.

**Scheme 1.14.** V-catalyzed synthesis of azadiphospholes reaction scope



#### 1.4.3. Ti-catalyzed [2+2+1] Cycloadditions with Alkynes and Azides

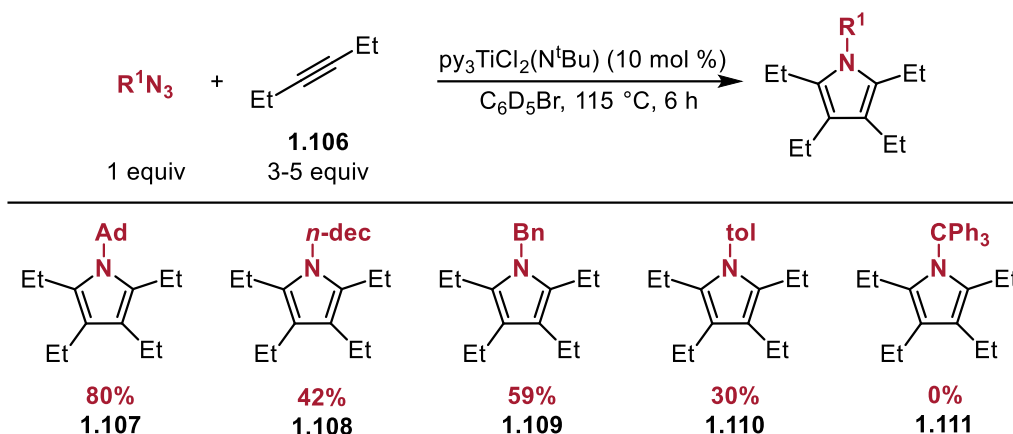
The Tonks group expanded the utility of the [2+2+1] Ti-redox catalyzed reaction to include azides as their nitrene source.<sup>28</sup> Azides are seen as a desired source due to their ease of synthesis,<sup>29-32</sup> their thermal stability<sup>33,34</sup> and their atom economy. In addition,

diazenes are synthesized from azides, so their direct use would streamline precursor synthesis.<sup>35,36</sup>

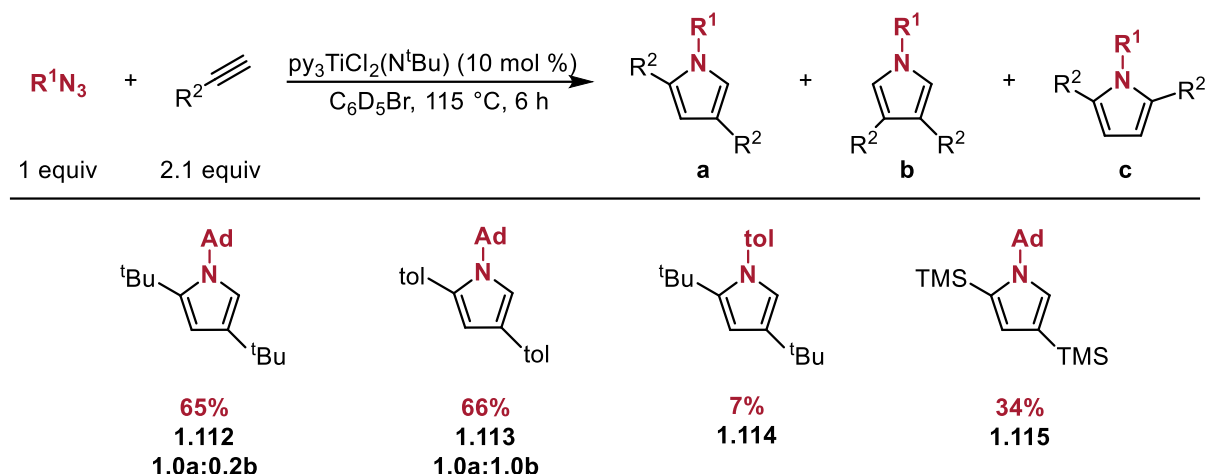
When using their previously reported catalyst<sup>14</sup> with *p*-tolN<sub>3</sub> and adamantyl azide, there was a very low conversion to the pyrrole product. In an attempt to increase yields, the catalyst was modified to be more Lewis acidic in order to increase ligand binding. As a result, (THF)<sub>3</sub>TiI<sub>2</sub>(Ntol) afforded the desired pyrrole in 80% yield with no detectable side products from azide decomposition.

It was shown through kinetic studies that the mechanism for pyrrole synthesis from azides proceeds similarly to that of using azobenzene that was previously reported. However, the oxidation of Ti<sup>II</sup> to Ti<sup>IV</sup> was faster in the use of AdN<sub>3</sub> vs azobenzene. The differing rate orders of [Ti] between the azide and azobenzene reactions (1<sup>st</sup> vs 0.5 order) showed that Ti dimerization is not kinetically relevant in the former, resulting in a faster oxidation of Ti<sup>II</sup>.

The scope of this reaction was investigated using different azide sources as well as different alkynes (**Scheme 1.15**). Adamantyl azide was compatible with alkynes substituted with at least one alkyl group (**1.107**) while using diphenylacetylene resulted in trace amounts of the pyrrole product. The use of *n*-decyl, benzyl, and tolyl azides resulted in moderate yields of the cycloadduct using 3-hexyne as the alkyne source (**1.108** – **1.110**). Ph<sub>3</sub>CN<sub>3</sub> resulted in no formation of cyclized product **1.111** most likely due to its electron-withdrawing nature and its steric bulkiness.

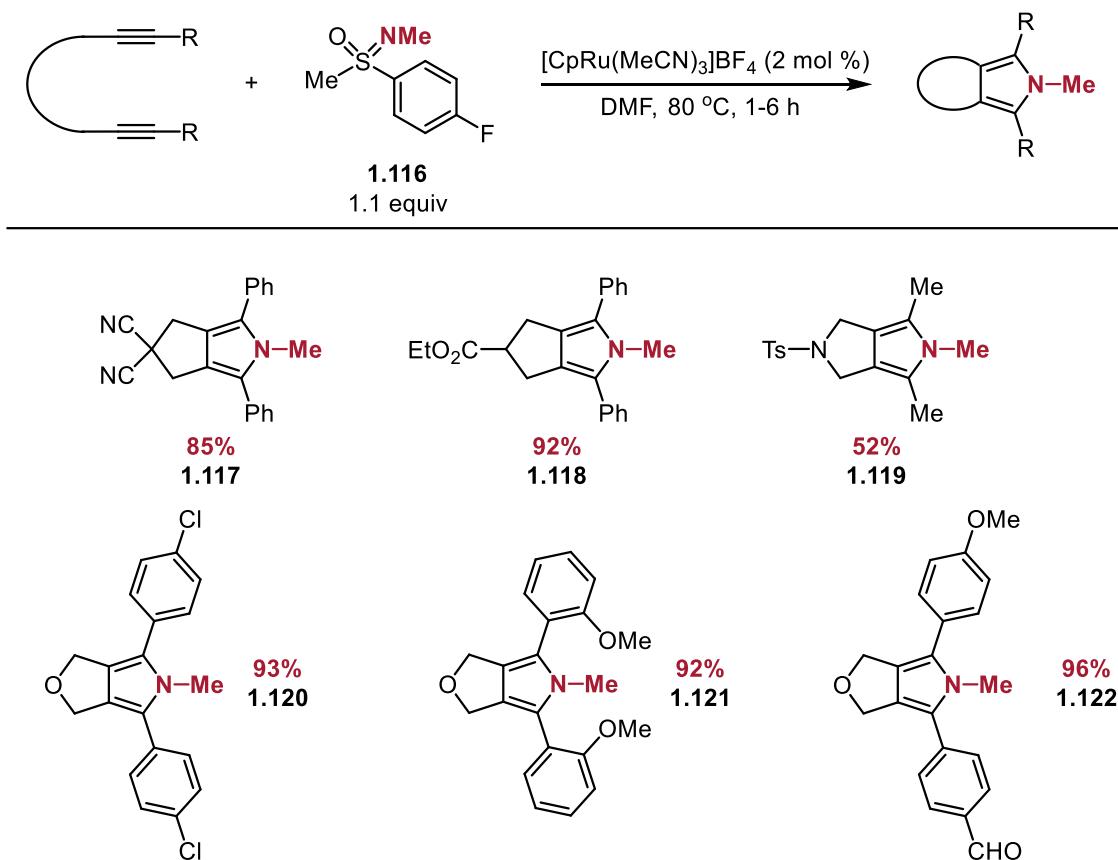
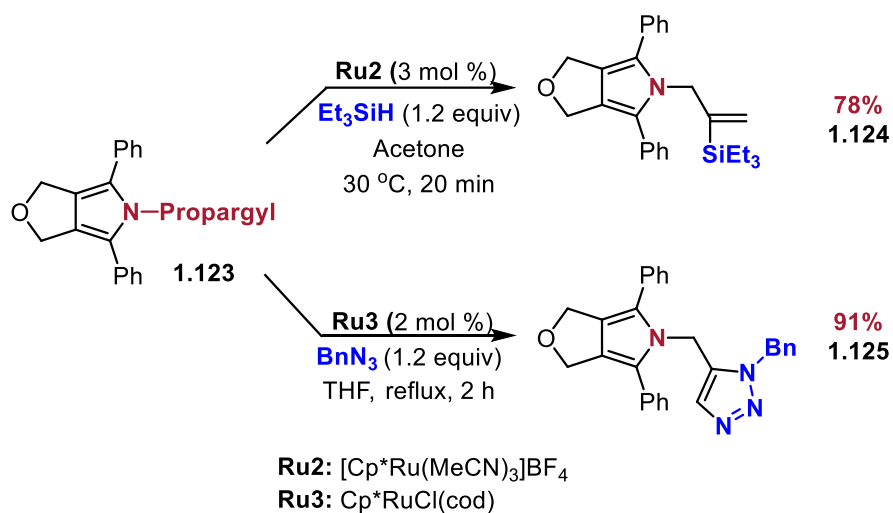
**Scheme 1.15.** Scope of azides with Tonks' [2+2+1] cycloaddition


Because  $(THF)_3TiI_2(Ntol)$  rapidly cyclotrimerizes terminal alkynes,  $py_3TiCl_2(N^tBu)$  was used to study the [2+2+1] reaction between azides and terminal alkynes (**Scheme 1.16**). Using  $AdN_3$  with simple alkyl or aryl acetylenes gave moderate yields with the former showing a high degree of selectivity (**1.112**); however, using *p*-tolylacetylene resulted in a 1:1 mixture of **1.113** and its regioisomer. Using the less-bulky *p*-tolyl azide provided the **1.114** in a lower yield with a significant amount of nitrene decomposition products. Lastly, using the bulkier TMS alkyne resulted in a decrease of desired pyrrole product **1.115** due to the more favorable [3+2] cycloaddition and cyclotrimerization.

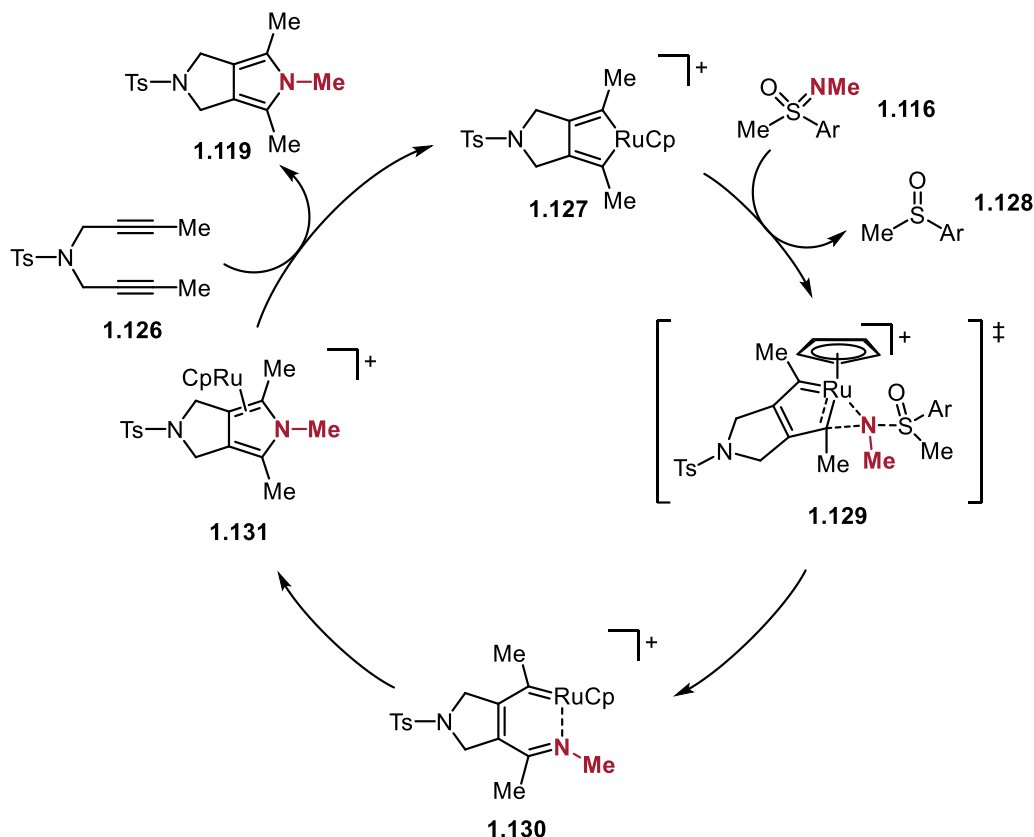
**Scheme 1.16.** Scope of mono-substituted alkynes with [2+2+1] cycloaddition

#### 1.4.4. Ru-catalyzed [2+2+1] Cycloadditions with Alkynes and Sulfoximines

In 2018, Yamamoto and co-workers reported a ruthenium-catalyzed [2+2+1] cycloaddition using sulfoximines.<sup>37</sup> Due to their stable nature, the loss of nitrogen from sulfoximines is very rare<sup>38,39</sup> and has never been shown to be involved in nitrogen transfer. Using tethered alkynes, ethers, and amines, a wide array of cyclic systems containing a pyrrole ring were synthesized (**Scheme 1.17a**). Tethered alkynes containing different functional groups were tolerated, allowing for further functionalization (**1.117** – **1.118**). In addition, tethered ethers substituted with electron-donating and withdrawing groups showed the same synthetic efficiency (**1.120** – **1.122**). Alkynes substituted with alkyl groups showed a decrease in yields while hetero-substituted alkynes cyclized in high yields. Lastly, further transformations of N-propargyl pyrroles were reported, showing the capability for further diversification (**Scheme 1.17b**).

**Scheme 1.17a.** Scope of Yamamoto's Ru-catalyzed [2+2+1] cycloaddition

**Scheme 1.17b.** Further diversification of propargyl pyrrole product


The mechanism for this strategy was investigated using enantiopure sulfoximine (*R*)-**1.116**. After 6 h, (*R*)-methyl phenyl sulfoxide was isolated in 68% yield with 98% ee, indicating that nitrogen transfer from sulfoximines occurs with retention of stereochemistry of the sulfur center. In addition, a stoichiometric reaction of a ruthenacycle formed by a tethered ether with sulfoximine **1.116** provided the desired pyrrole in 58% yield. With these results in hand, the mechanism in **Figure 1.10**. was proposed. The Ru catalyst interacts with a diyne in order to form metallacycle **1.127**. Subsequently, nitrogen transfer from sulfoximine occurs via **1.129** to form complex **1.130**. Cycloisomerization then affords  $\eta^5$ -pyrrole complex **1.131** which, after oxidative cyclization, results in the formation of the desired cycloadduct as well as reforming the metallocycle.

**Figure 1.10.** Mechanism of [2+2+1] with Ru-catalysis

## 1.5. Conclusions

Using nitrenes in cyclization strategies is an attractive avenue towards the assembly of nitrogen-containing rings. While there have been numerous published works on the use of nitrenes in different cycloadditions, the field is underdeveloped. The methods described here lead to the formation of solely five-membered nitrogen heterocycles with a majority focused on [2+2+1] reactions pioneered mainly by the Tonks group. In addition, which the exception of Nishibayashi, these methods only use alkyl sources as cycloaddition components. As such, expanding the synthetic toolbox of this

methodology to include different ring sizes as well as including additional heteroatoms is essential in to further develop this area of study.

## 1.6. References

- (1) Vitaku, E.; Smith, D. T.; Njardarson, J. T. *J. Med. Chem.* **2014**, *57*, 10257.
- (2) Degennaro, L.; Trinchera, P.; Luisi, R. *Chem. Rev.* **2014**, *114*, 7881.
- (3) Zhu, W.; Cai, Guorong, C.; Ma, D. *Org. Lett.* **2005**, *7*, 5545.
- (4) Padwa, A.; Murphree, S. S. *ARKIVOC* **2006**, *3*, 6.
- (5) Wender, P. A.; Strand, D. *J. Am. Chem. Soc.* **2009**, *131*, 7528.
- (6) Bhattacharyya, A.; Shahi, C. K.; Pradhan, S.; Ghorai, M. K. *Org. Lett.* **2018**, *20*, 2925
- (7) Sheradskey, T.; Zbaida, D. *Tet. Lett.* **1981**, *22*, 1639.
- (8) Ghosh, A.; Mandal, S.; Chattaraj, P. K.; Banerjee, P. *Org. Lett.* **2016**, *18*, 4940.
- (9) Pearson, W. H.; Celebuski, J. E.; Poon, Y.-F. *Tet. Lett.* **1986**, *27*, 6301.
- (10) Pearson, W. H.; Bergmeier, S. C.; Degan, S.; Lin, K. C.; Poon, Y. F.; Schkeryantz, J. M.; Williams, J. P. *J. Org. Chem.* **1990**, *55*, 5719.
- (11) Hudlicky, T.; Frazier, J. O.; Seoane, G.; Tiedje, M.; Seoane, A.; Kwart, L. D.; Beal, C. *J. Am. Chem. Soc.* **1986**, *108*, 3755.
- (12) Wu, Q.; Hu, J.; Ren, X.; Zhou, J. *Chem. Eur. J.* **2011**, *17*, 11553.
- (13) Brichacek, M.; Lee, D.; Njardarson, J. T. *Org. Lett.* **2008**, *10*, 5023.
- (14) Gilbert, Z. W.; Hue, R. J.; Tonks, I. A. *Nat. Chem.* **2016**, *8*, 63.
- (15) Müller, T. E.; Hultsch, K. C.; Yus, M.; Foubelo, F.; Tada, M. *Chem. Rev.* **2008**, *108*, 3795.

- (16) Straub, B. F.; Bergman, R. G. *Angew. Chem. Int. Ed.* **2001**, *40*, 4632.
- (17) Weitershaus, K.; Ward, B. D.; Kubiak, R.; Müller, C.; Wadepohl, H.; Doye, S.; Gade, L. H. *Dalton Trans.* **2009**, 4586.
- (18) Vujkovic, N.; Fillol, J. L.; Ward, B. D.; Wadepohl, H.; Mountford, P.; Gade, L. H. *Organometallics* **2008**, *27*, 2518.
- (19) Barnea, E.; Majumder, S.; Staples, R. J.; Odom, A. L. *Organometallics* **2009**, *28*, 3876.
- (20) Ozerov, O. V.; Patrick, B. O.; Lapido, F. T. *J. Am. Chem. Soc.* **2000**, *122*, 6423.
- (21) Davis-Gilbert, Z. W.; Wen, X.; Goodpaster, J. D.; Tonks, I. A. *J. Am. Chem. Soc.* **2018**, *140*, 7267.
- (22) Chiu, H.-C.; Tonks, I. A. *Angew. Chem.* **2018**, *130*, 6198.
- (23) Chiu, H.-C.; See, X. Y.; Tonks, I. A. *ACS Catal.* **2019**, *9*, 216.
- (24) Davis-Gilbert, Z. W.; Kawakita, K.; Blechschmidt, D. R.; Tsurugi, H.; Mashima, K.; Tonks, I. A. *Organometallics* **2018**, *37*, 4439.
- (25) Cheng, Y.; Klein, C. K.; Tonks, I. A. *Chem. Sci.* **2020**, *11*, 10236.
- (26) Kawakita, K.; Beaumier, E. P.; Kakiuchi, Y.; Tsurugi, H.; Tonks, I. A.; Mashima, K. *J. Am. Chem. Soc.* **2019**, *141*, 4194.
- (27) Liang, W.; Nakajima, K.; Nishibayashi, Y. *RSC Adv.* **2020**, *10*, 12730.
- (28) Pearce, A. J.; See, X. Y.; Tonks, I. A. *Chem. Commun.* **2018**, *54*, 6891.
- (29) Heyduk, A. F.; Zarkesh, R. A.; Nguyen, A. I. *Inorg. Chem.* **2011**, *50*, 9849.
- (30) Harman, W. H.; Lichterman, M. F.; Piro, N. A.; Chang, C. J. *Inorg. Chem.* **2012**, *51*, 10037.
- (31) Mankad, N. P.; Müller, P.; Peters, J. C. *J. Am. Chem. Soc.* **2010**, *132*, 4083.

- (32) Powers, I. G.; Andjaba, J. M.; Luo, X.; Mei, J.; Uyeda, C. *J. Am. Chem. Soc.* **2018**, *140*, 4110.
- (33) Engel, P. S. *Chem. Rev.* **1980**, *80*, 99.
- (34) L'Abbe, G. *Chem. Rev.* **1969**, *69*, 345.
- (35) Ju, Y.; Kumar, D.; Varma, R. S. *J. Org. Chem.* **2006**, *71*, 6697.
- (36) Kitamura, M.; Koga, T.; Yano, M.; Okauchi, T. *Synlett*, **2012**, *23*, 1335.
- (37) Matsui, K.; Shibuya, M.; Yamamoto, Y. *Communications Chemistry* **2018**, *1*, 1.
- (38) Cram, D. J.; Day, J.; Rayner, D. R.; von Schriltz, D. M.; Duchamp, D. J.; Garwood, D. C. *J. Am. Chem. Soc.* **1970**, *92*, 7369.
- (39) Li, Z.; Yu, H.; Bolm, C. *Angew. Chem. Int. Ed.* **2017**, *56*, 9532.

## Chapter 2

### *The Use of Vinylcyclopropanes In Ring-Forming Reactions*

#### 2.1. Introduction

Since the first reported studies on their thermal rearrangements,<sup>1</sup> vinylcyclopropanes (VCPs) have been used synthetically in numerous ways. Synthetic chemists have exploited the ring strain released upon ring opening of the cyclopropane to build more complex molecules.

Long chains and polymers have been synthesized using VCPs. Dienes can be obtained through E2 elimination upon opening of the cyclopropyl ring.<sup>2</sup> Polymers of different molecular weights can be selectively synthesized using a metal catalyst as well as a nucleophilic initiator.<sup>3</sup> VCPs have been coupled with alkynes,<sup>4</sup> arenes,<sup>5</sup> aliphatic C-H bonds,<sup>6</sup> and aldehydes<sup>7</sup> to form highly functionalized linear molecules. Furthermore, nucleophilic<sup>8</sup> and electrophilic additions<sup>9</sup> expand the ability obtain diverse structures.

The 1,3-dipolar synthon has also been utilized in intramolecular [3+2] cycloadditions with alkenes<sup>10</sup> and alkynes,<sup>11</sup> as well as carbonyl-containing compounds,<sup>12-13</sup> to assemble five-membered ring systems. This class was then expanded for intermolecular reactions, with alkenes as the first examples using Pd(0) to form cyclopentanes.<sup>14</sup> Recent studies employ iminium/enamine organocatalysis in conjunction with Pd(0) catalysis to perform formal [3+2] cycloadditions between VCPs and enals.<sup>15</sup>

This strategy has been further developed to perform cycloadditions intermolecularly with a wide range of two-atom partners, including imines,<sup>16</sup> nitriles,<sup>17</sup> nitrosos,<sup>18</sup> isocyanates,<sup>19</sup> ketenes,<sup>20</sup> aldehydes,<sup>21</sup> and ketones.<sup>21</sup> In addition, employing five-membered ring systems, such as azlactone alkylidenes,<sup>22</sup> isatins,<sup>23</sup> and diazooxindoles<sup>24</sup> have been used to synthesize bi- and tricyclic spiro compounds.

VCPs have been viewed as a homolog of butadiene since given that the ease of cyclopropane C–C bond cleavage, allows for their use as five-atom, rather than four-atom, components in cycloadditions. With this, synthetic chemists have utilized this synthon to build more complex molecules. These have been demonstrated in both intramolecular and intermolecular contexts with a variety of cycloaddition partners, such as alkynes, alkenes, and CO. This field has further been expanded to use these reactions in a variety of total syntheses to form fused ring systems. This chapter will summarize how these rearrangements and cycloadditions have been developed and their applications in complex molecule syntheses.

## 2.2. Vinylcyclopropane rearrangements

### 2.2.1. VCPs into cyclopentenes

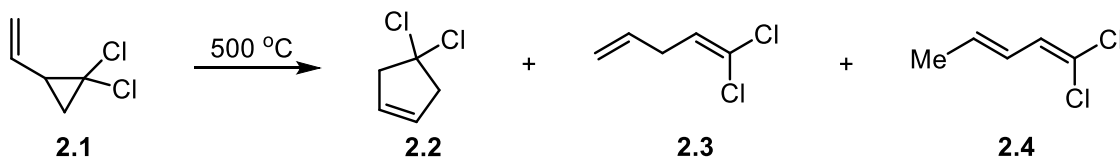
Neureiter reported the first example of VCP rearrangement in 1959 when he discovered that upon heating VCP **2.1** at 500 °C, product **2.2** was isolated.<sup>1</sup> Two dichloropentadiene isomers (**2.3** and **2.4**) were identified as side products, suggesting a mechanism in which the cyclopropane opens to a resonance-stabilized diradical species, which itself goes on to form either the cyclic or diene products. Overberger followed up a

year later showing that refluxing VCP **2.5** in acetic acid leads to its to cyclopentane **2.6** (**Scheme 2.1**).<sup>25</sup>

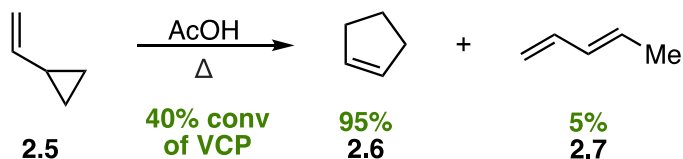
---

**Scheme 2.1.** Initial discoveries of VCP rearrangement

*Neureiter:*



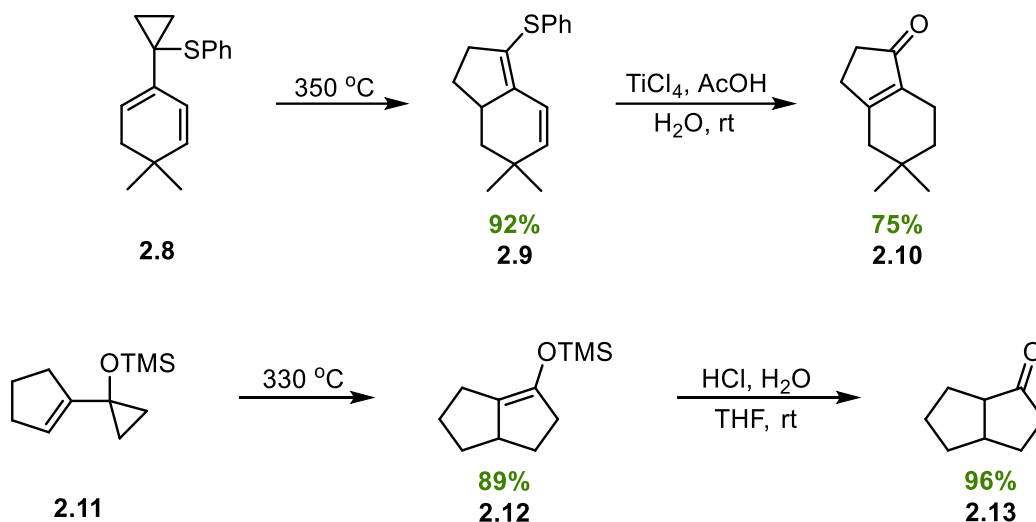
*Overberger:*




---

Trost<sup>26</sup> and Miller<sup>27</sup> showed that thermal rearrangement of 1-(phenylsulfanyl)VCPs led to the corresponding enol thioethers, which were hydrolyzed to form cyclopentanones in moderate to good yields (**Scheme 2.2**). Subsequently, Trost found that incorporating a siloxy-group at the 1-position greatly increased the reaction rate, forming enolsilane **2.12** in quantitative yield within four seconds at 330 °C.<sup>28</sup> This observation was explained by invoking a stabilizing effect of an oxygen  $\alpha$  to the radical, which is analogous to the oxy-Cope rearrangement.<sup>29</sup> A follow-up kinetics experiment by Trost showed that compared to its hydrocarbon counterpart, silyl ether substitution at that position significantly decreases the  $E_a$  of rearrangement, accounting for the accelerated cyclization rate.<sup>30</sup>

**Scheme 2.2.** Trost's work with 1-substituted VCPs.



Simpson and co-workers performed kinetics studies on the effect of 2-substitution on the thermal rearrangement of VCPs. It was reported that having phenyl and methoxy substituents at the 2-position reduces the activation energy for the rearrangement by 9 and 11 kcal/mol, respectively, compared to 1-methoxy which lowers the  $E_a$  by 5 kcal/mol. In addition, a trans stereochemical relationship between the vinyl group and substituent was found to be preferable to the cis due to acyclic transition states. A cis configuration around the interior allylic bond is required for the terminal carbons to form the five-membered ring, which requires rotation around the partial double bonds. Compared to the cis-configuration, the trans-configuration would require less energy to do so because of reduced steric interactions.<sup>31</sup>

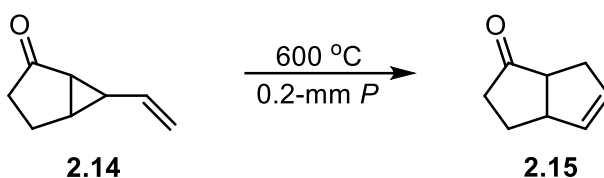
Corey and co-workers used flash vacuum pyrolysis to convert VCP **2.14** into ketone product **2.15** (**Scheme 2.3**).<sup>32</sup> De Meijere also used this method to synthesize triquinane **2.17** as a mix of stereoisomers from donor-substituted VCP **2.16**.<sup>33</sup> Further

studies from this group allowed for preparation of cyclopentenenes without the need for electronic modulation of cyclopropyl substituents.<sup>34,35</sup> In one report, de Meijere reported the synthesis of cyclopentene-annellated nitrogen heterocycles from the heterocyclic VCP.<sup>36</sup>

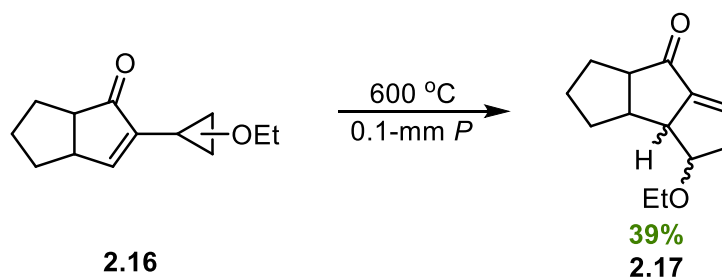
---

**Scheme 2.3.** Flash vacuum pyrolysis of VCPs

*Corey:*



*de Meijere:*

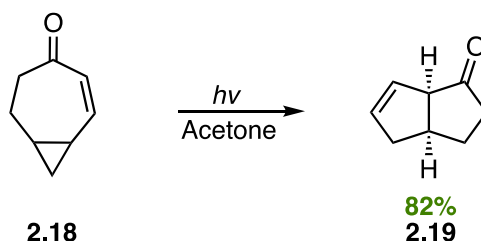



---

Paquette disclosed the photochemical rearrangement of cis-bicyclo[5.1.0]octenones to cis-bicyclo[3.3.0]octenones in up to 82% yield (**Scheme 2.4**). This rearrangement was explained by invoking the bent nature of the internal bond of the cyclopropane, enabling continuous overlap with the carbonyl group and the alkene. In addition, this allow for a strain-free cyclic pathway for bond reformation upon cyclopropyl ring opening.<sup>37</sup> In a follow-up study, this method was applied to the methylene analogs. Dreiding models of the ketone and methylene VCPs indicate that the ketone substrates react from the respective triplet states whereas the methylene VCPs proceed in its singlet state due to the differing  $\pi$ -bonding overlap in the transoid  $T_1$  states.<sup>38</sup> Sonawane later

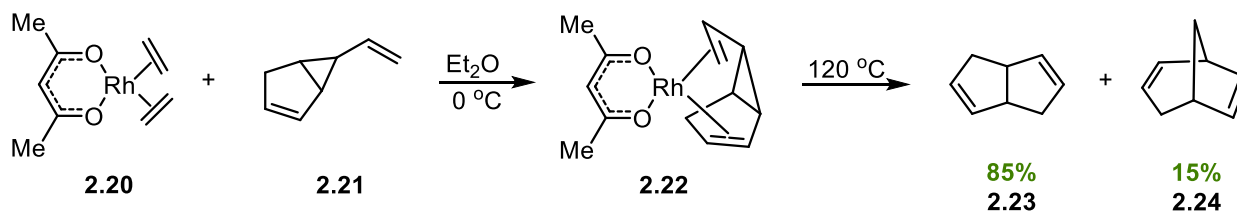
used  $\Delta^2$ -Carene derivatives to photochemically prepare 7-substituted bicyclo[3.2.0]heptenes with some diastereomeric control.<sup>39</sup>

**Scheme 2.4.** Paquette's synthesis of cis-bicyclo[3.3.0]ocetenones



Metal catalysts and complexes have been investigated as tools to promote this transformation. Williamson and co-workers reported the synthesis of Rh(I)-complex **2.22** from the coordination of **2.20** and **2.21** which, when subjected to thermal conditions, leads to the formation of products **2.23** and **2.24** (**Scheme 2.5**).<sup>40</sup> Hudlicky used a stoichiometric amount of  $(C_2H_4)_2Rh(acac)$  under reflux conditions to prepare bicyclooctanes up to 75% yield.<sup>41</sup>

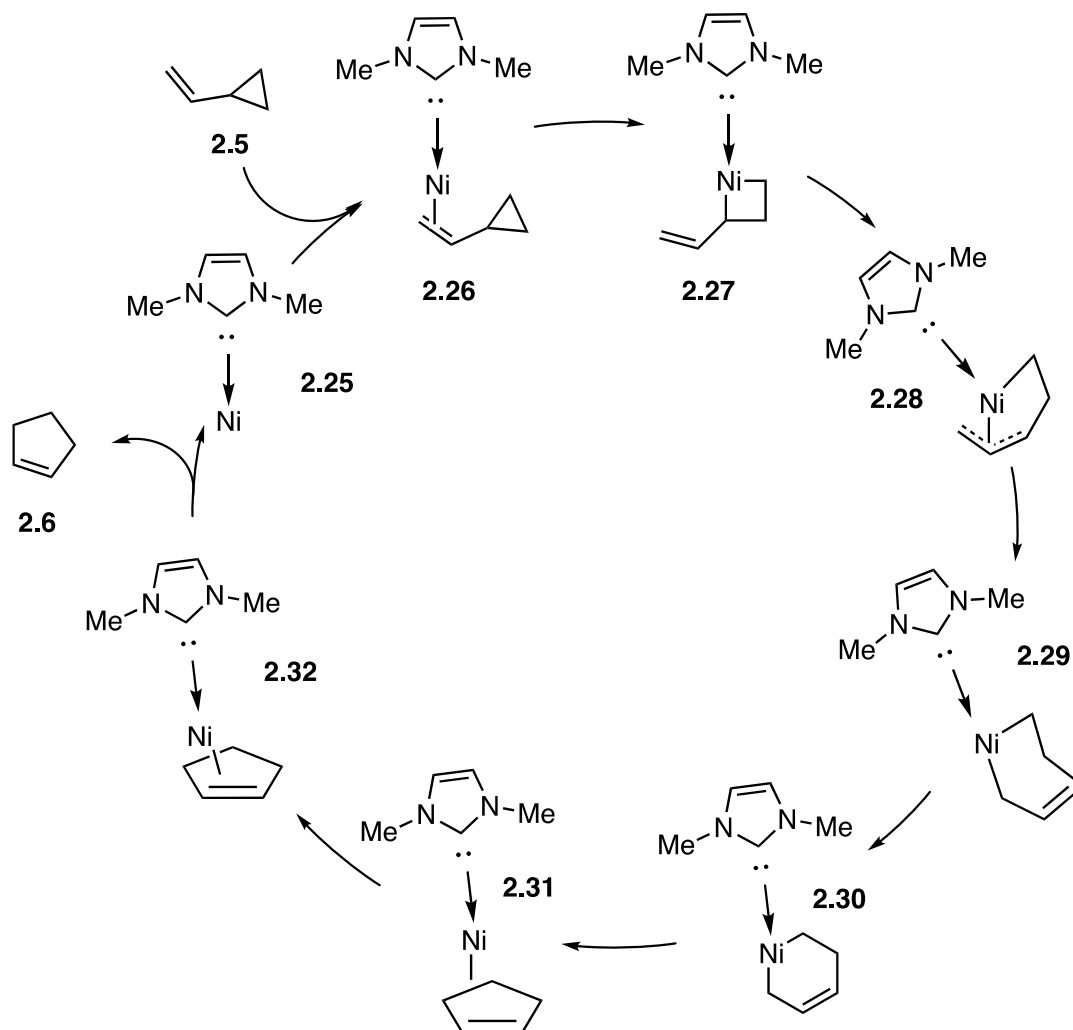
**Scheme 2.5.** Williamson's Rh(I)-complex synthesis and thermolysis



Murakami developed the first metal-catalyzed VCP rearrangement using  $Ni(COD)_2 \cdot PBu_3$  under reflux to synthesize cyclopentenones up to 93% yield.<sup>42</sup> Louie and co-workers later built upon this work by using a NHC-ligated Ni catalyst to perform this

isomerization at 1 mol% catalyst loading.<sup>43</sup> In a follow-up study, Louie and Tantillo developed a mechanistic model for this Ni(0)-NHC-catalyzed rearrangement (**Figure 2.1**).

**Figure 2.1.** Mechanism of Louie's Ni(0)-NHC-catalyzed VCP isomerization

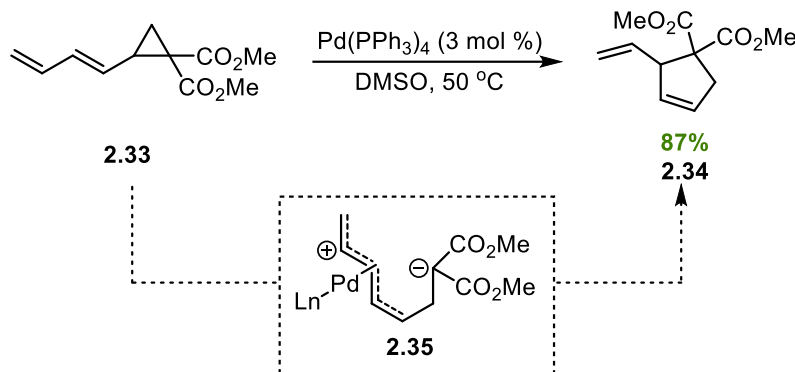


In addition, it was found that bulkier NHCs better promote rearrangement by favoring dissociation of one of the NHC to allow Ni-coordination to the vinyl group. They also proposed that COD facilitates this process.<sup>44</sup>

Oshima and co-workers were able to perform the VCP-cyclopentene rearrangement using  $\text{Pd}(\text{PPh}_3)_4$  as the catalyst under milder conditions in up to 96% yield

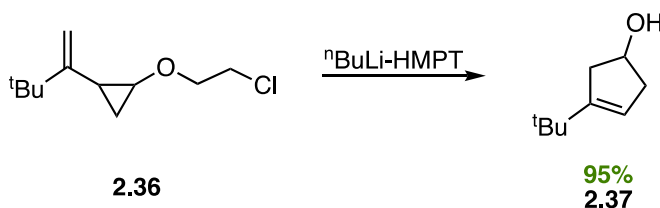
(**Scheme 2.6**). It was proposed that a nucleophilic attack of Pd(0) to the dienic group promotes cyclopropyl ring opening to form zwitterion **2.35**, which collapses to form **2.34** exclusively.<sup>45</sup>

**Scheme 2.6.** Oshima's Pd-catalyzed method for VCP rearrangement



Common and readily available organic reagents have been used for this isomerization. Danheiser reported that in the presence of excess *n*-BuLi, 2-vinylcyclopropyl ethers rearrange to cyclopentenols at room temperature in up to 95% yield (**Scheme 2.7**).<sup>46</sup> In a subsequent study, they found that when using a mixture of 2-vinylcyclopropyl ethers, only one stereoisomer was formed.<sup>47</sup>

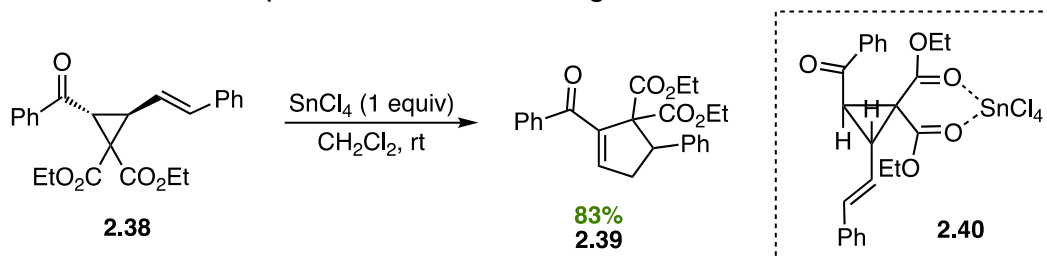
**Scheme 2.7.** Danheiser's *n*BuLi-promoted rearrangement



Suzukamo reported the use of Lewis acids ( $\text{BBr}_3$ ,  $\text{AlCl}_3$  and  $\text{BCl}_3$ ) to promote the ring expansion of donor acceptor VCPs.<sup>48</sup> This methodology was further explored by

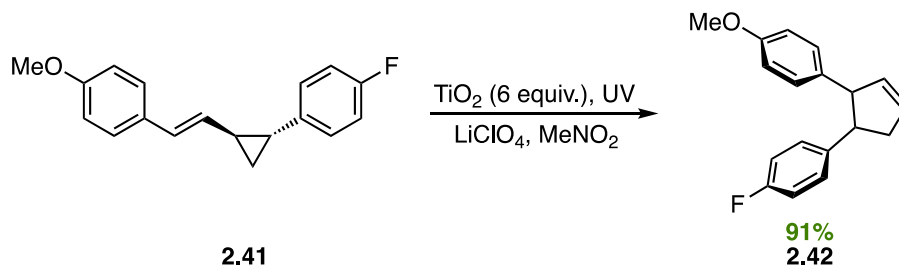
Srinivasan who employed  $\text{SnCl}_4$  to perform this rearrangement preferentially over proton elimination to synthesize 1,3-dienes (**Scheme 2.8**). The Lewis acid species coordinates to the carbonyl group (**2.40**), allowing for the cyclopropyl ring to open into a zwitterionic species that cyclizes to form cyclopentene **2.39**.<sup>49</sup>

**Scheme 2.8.** Lewis acid-promoted VCP rearrangement



Most recently, Okada and co-workers disclosed the rearrangement of bi-aryl VCPs by  $\text{TiO}_2$  photocatalysis (**Scheme 2.9**). Through DFT calculations and mechanistic experiments, it was postulated that the reaction is going through a stepwise mechanism via distonic radical cations triggered by oxidative single electron transfer (SET).<sup>50</sup>

**Scheme 2.9.** Photocatalytic transformation of bi-aryl VCPs

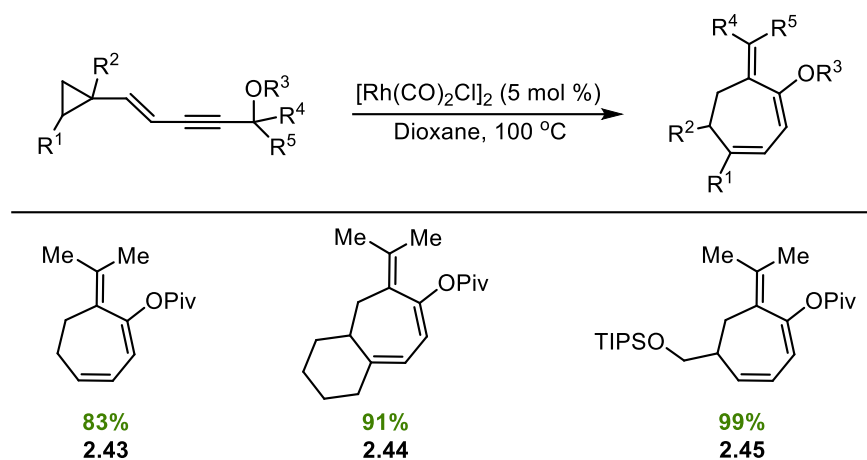


### 2.2.2. Other VCP rearrangements

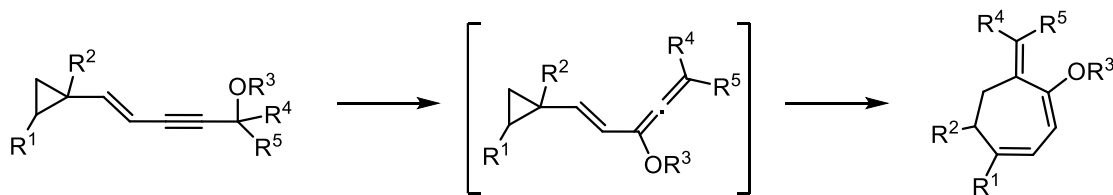
Tang reported a  $\text{Rh(I)}$ -catalyzed method to prepare cycloheptadienes (**2.43** – **2.45**) intramolecularly using VCPs tethered to propargyl esters. The reaction occurs through a

1,5 C,C-migration (**Figure 2.2a**). Through a 1,3 acyloxy migration, a key allene intermediate is generated that subsequently coordinates with Rh to form an alkylidene metallacyclopentene. Following cleavage of the cyclopropane ring and reductive elimination, the seven-membered ring is formed (**Figure 2.2b**).<sup>51</sup>

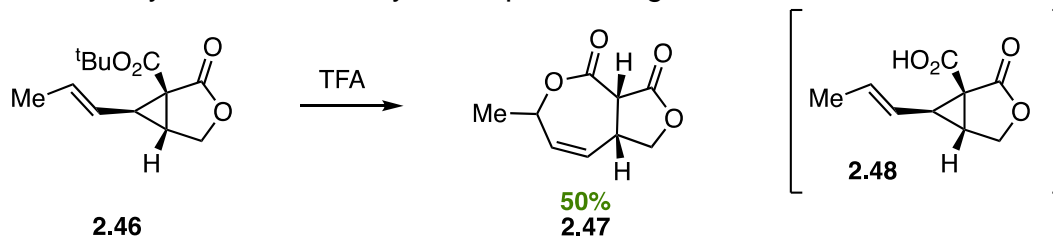
**Figure 2.2a.** Tang's Rh(I)-catalyzed preparation of cycloheptadienes



**Figure 2.2b.** Allene intermediate formation

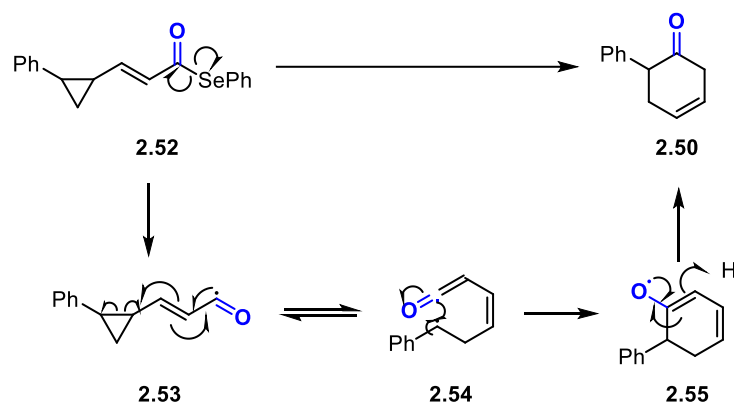
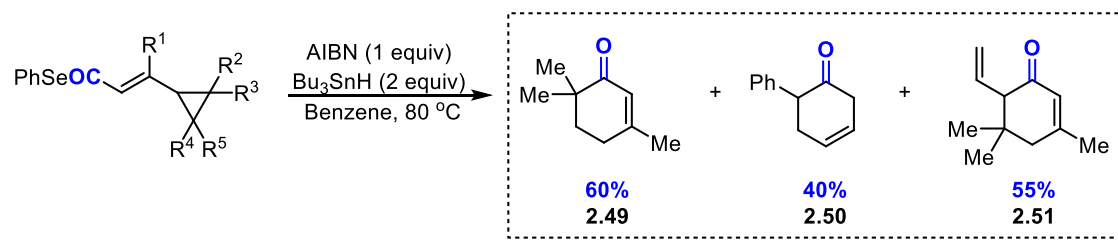


Koskinen and Rissanen disclosed an acid-promoted rearrangement of VCP **2.46** to form bicyclic product **2.47** at room temperature in 50% yield (**Scheme 2.10**). TFA first cleaves the ester to form intermediate **2.48**, which then rearranges and tautomerizes to form the isolated product.<sup>52</sup>

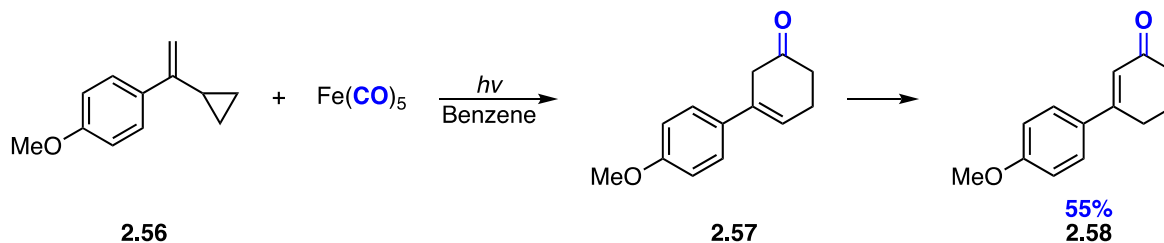
**Scheme 2.10.** Synthesis of tetrahydrooxepinone ring

### 2.3. VCPs in [5+1] cycloadditions

VCPs have been used recently in multicomponent cycloaddition strategies to build more complex structures aside from cyclopentenones. The synthesis of 2,3-cyclohexanones from vinylcyclopropyl selenyl esters was reported by Pattenden to offer products **2.49** – **2.51** in moderate yields (**Scheme 2.11**). The cascade cyclization is initiated using  $\text{Bu}_3\text{SnH}$ -AIBN to form ketene intermediate **2.54**, which serves as a one atom CO component to engage in an intramolecular [5+1] reaction.<sup>53</sup>

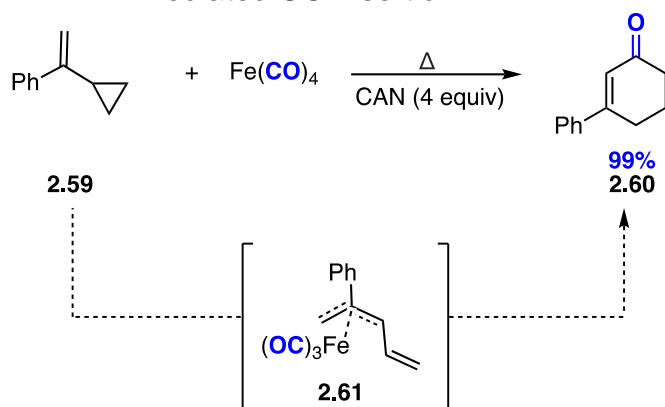
**Scheme 2.11.** Radical cascade cycloaddition of VCP and selenyl ester

CO insertion with VCPs results in the preparation of differently substituted cyclohexenones. This method was first presented by Sarel and co-workers in which they employed  $\text{Fe}(\text{CO})_5$  and VCPs under photoirradiation to synthesize  $\alpha,\beta$ -substituted cyclohexanones up to 55% yield (**Scheme 2.12**).<sup>54</sup> Taber further developed an enantioselective<sup>55</sup> variant and also improved functional group tolerance.<sup>56</sup>

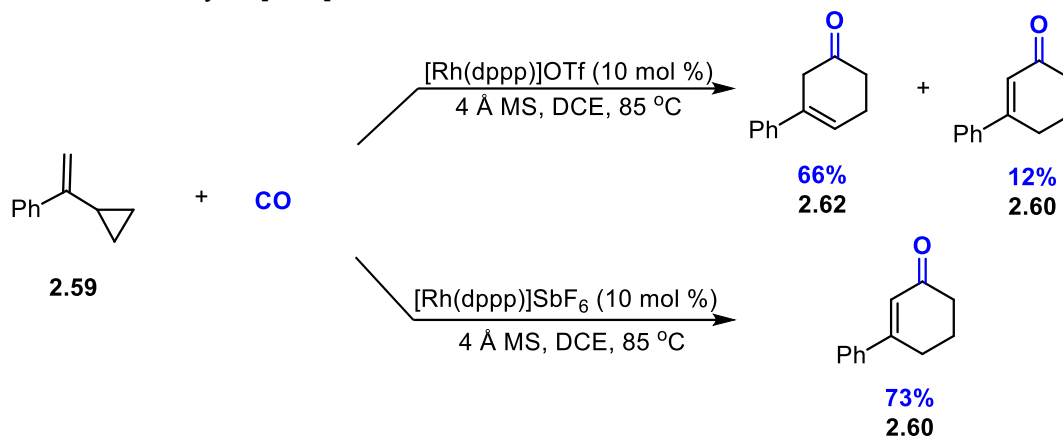
**Scheme 2.12.** Photo-irradiated CO insertion

To avoid photoirradiation, Schulze performed this reaction with ceric ammonium nitrate to assemble cyclohexenone **2.60** in quantitative yield (**Scheme 2.13**).<sup>57</sup> Deuterium-labeling experiments revealed that intermediate **2.61** is being generated followed by CO insertion.<sup>58</sup> Yu and co-workers later replaced the iron-mediator with  $\text{Fe}_2(\text{CO})_9$  – a cheaper complex – to prepare **2.60** up to 80% yield.<sup>59</sup>

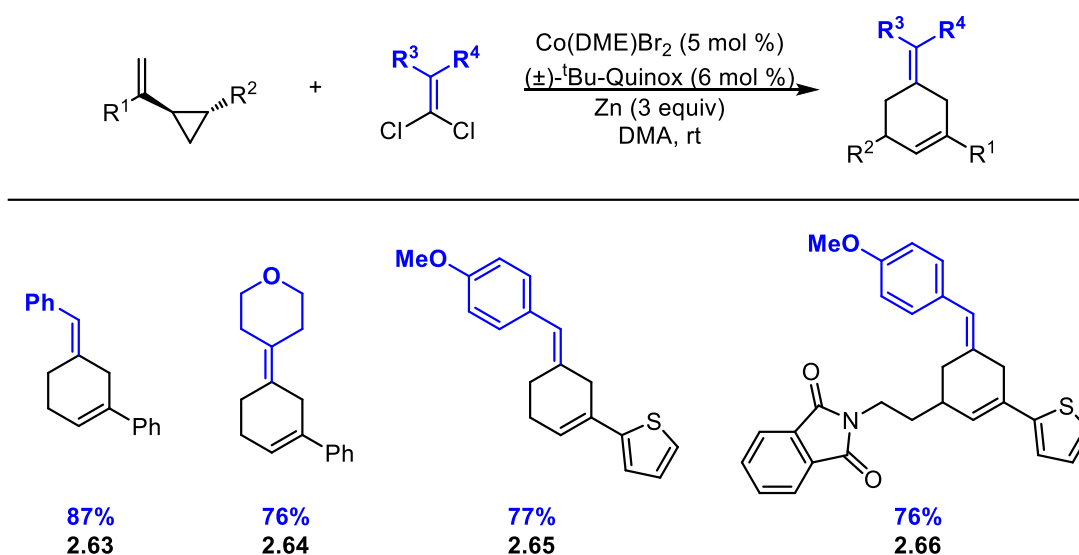
**Scheme 2.13.** Schulze's iron-mediated CO insertion



Other metal sources have been investigated for catalytic [5+1] transformations. De Meijere disclosed methods using  $\text{Co}_2(\text{CO})_8$  or  $[\text{Rh}(\text{CO})_2\text{Cl}]_2$  under a CO atmosphere to assemble  $\beta$ - $\gamma$ -substituted cyclohexanones.<sup>60</sup> Yu and co-workers developed two different procedures to selectively synthesize either  $\alpha,\beta$  and  $\beta,\gamma$ -substituted cyclohexanones exclusively (**Scheme 2.14**).<sup>61</sup>

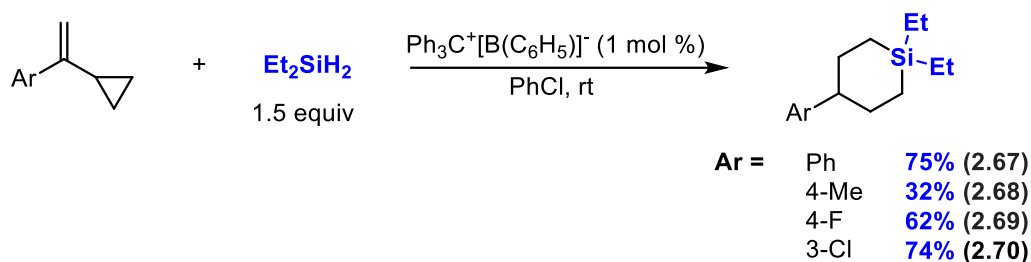
**Scheme 2.14.** Catalytic [5+1] reaction of VCP and CO

Expanding this class of cycloadditions beyond CO insertion has only recently been garnering attention. The Uyeda group out of Purdue University demonstrated a cobalt-catalyzed [5+1] reaction between VCPs and vinylidenes to prepare methylenecyclohexenes **2.63** – **2.66** exclusively (**Figure 2.3**).<sup>62</sup>

**Figure 2.3.** [5+1] cycloaddition of VCPs and vinylidenes

Oestreich and co-workers recently reported a [5+1] cycloaddition of VCPs with hydrosilanes to synthesize silacyclohexanes involving a [1,2]-migration of an aryl group to provide 4-aryl-substituted silacyclohexanes **2.67** – **2.70** as the major products (**Scheme 2.15**).<sup>63</sup>

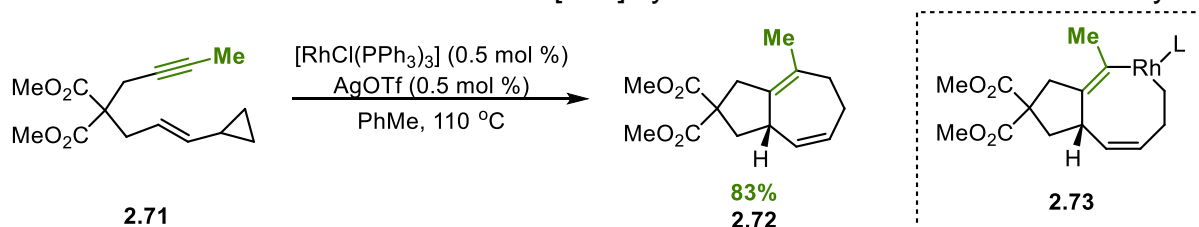
**Scheme 2.15.** Synthesis of 4-aryl-substituted silacyclohexanes



## 2.4. VCPs in [5+2] Cycloadditions

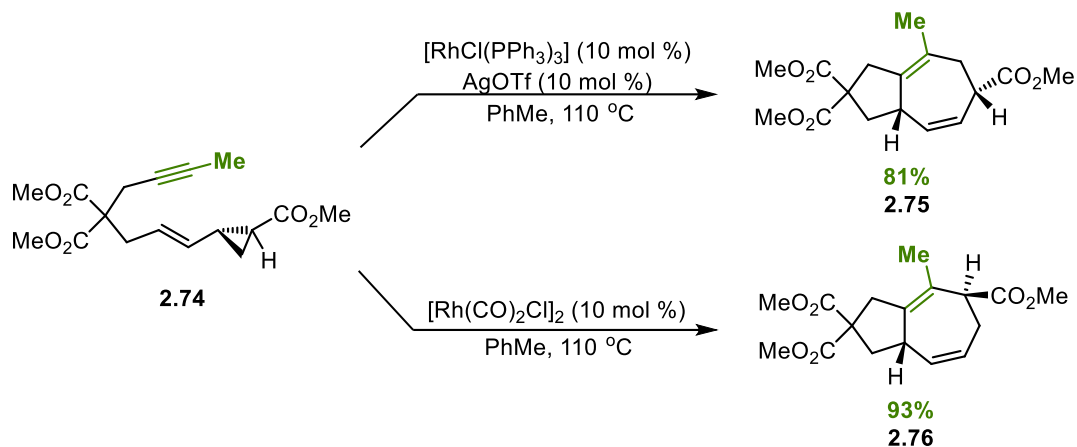
### 2.4.1. Intramolecular [5+2] cycloaddition with alkynes

In 1995, Wender disclosed the first example of using VCPs as a five-atom component in [5+2] cycloadditions by cyclizing a VCP and alkyne intramolecularly using Wilkinson's catalyst along with a AgOTf additive (**Scheme 2.16**). This reaction was conceived based on a mechanistic hypothesis in which a metal catalyst would oxidatively add to the vinyl group and the addition of the alkyne would cause cleavage of the cyclopropane ring, forming metallacycle **2.73**. After reductive elimination, the desired product is obtained.<sup>64</sup>

**Scheme 2.16.** Wender's intramolecular [5+2] cycloaddition between VCPs and alkynes

Wender and co-workers continued to develop this reaction paradigm by employing  $[\text{Rh}(\text{CO})_2\text{Cl}]_2$  as the Rh(I) species due to its less demanding steric environment as well as its ability to catalyze the formation of dienes and cyclopentenes from VCPs.<sup>65</sup> This catalyst was able to complete the transformation using as low as 1 mol % catalyst loading, with shorter reaction times. In addition, the reaction could be conducted at a concentration up to 2 M without any significant polymerization, which was an issue when using Wilkinson's catalyst.<sup>66</sup>

With both systems in hand, the Wender group sought to investigate the stereo- and regioselectivity of these reactions using 2-substituted VCPs, including how substituent modification and/or the catalyst system affects this selectivity (**Scheme 2.17**). Interestingly, in some examples, there were observations of regioselectivity reversal when employing a different catalyst system. Using substrate **2.74**, the use of Wilkinson's catalyst favored the synthesis of product **2.75** in a 20:1 selectivity compared to product **2.76**. In the case of the rhodium dimer, product **2.76** was instead favored in a ratio of 11:1. When using the *cis* diastereomer of substrate **2.74**, there was no reversal of regioselectivity when different Rh(I) catalysts were used, suggesting bond cleavage of the cyclopropane is affected by competing steric and electronic factors.<sup>67</sup>

**Scheme 2.17.** Reversal of regioselectivity with different Rh(I) catalysts

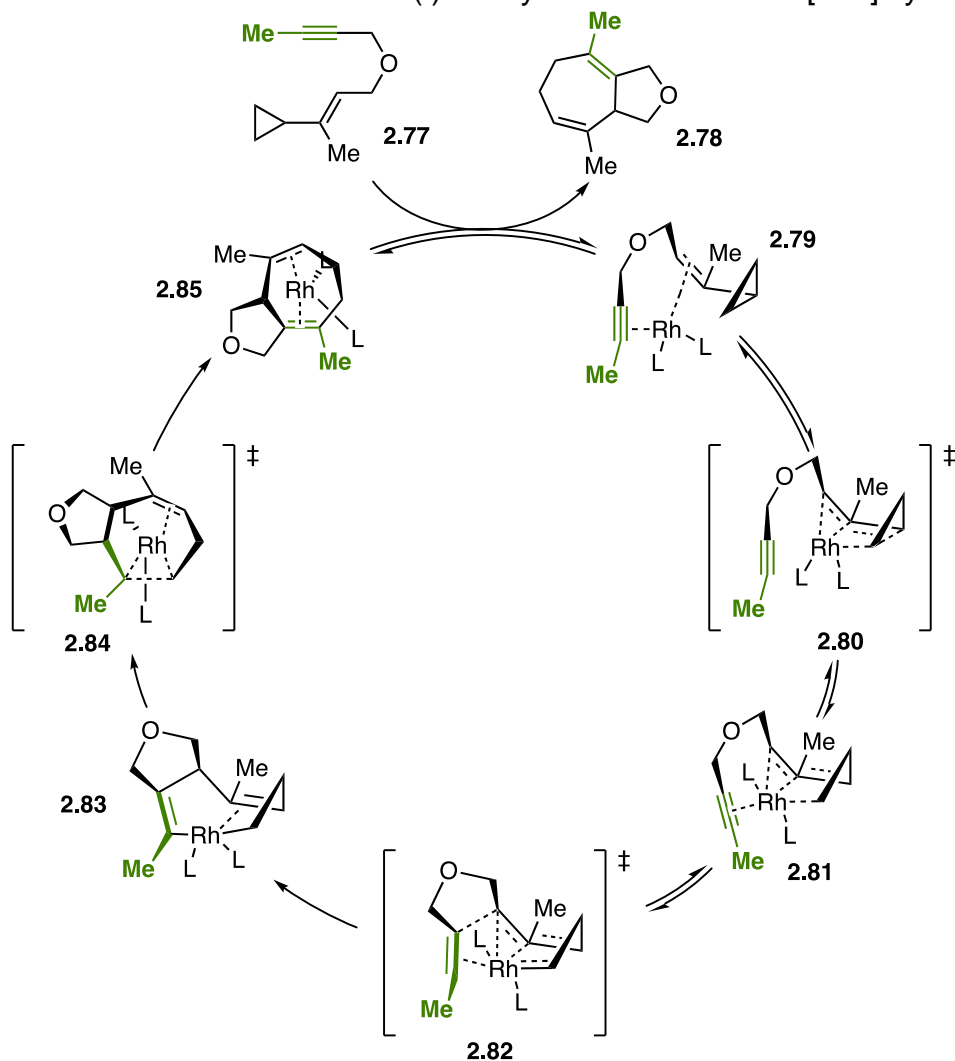
Wender further developed this Rh(I)-catalyst approach with exploring  $[(\text{arene})\text{Rh}(\text{cod})]^+$  as it was shown by Chung and co-workers that these species can catalyze an intermolecular [4+2] cycloaddition between 1,3-dienes and nonactivated acetylenes.<sup>68</sup> Compared to the previously explored catalysts,  $[(\text{C}_{10}\text{H}_8)\text{Rh}(\text{cod})]\text{SbF}_6$  resulted in higher yields in a shorter reaction time. This system was also able to perform comparably when the reaction was scaled up to 1g of substrate.<sup>69</sup>

Following this study, Wender and co-workers investigated using NHC-metal complexes to catalyze this [5+2] cycloaddition. A Rh(I) carbene complex was prepared using  $[\text{Rh}(\text{cod})\text{Cl}]_2$  and an alkoxyimidazol-2-ylidinium salt. Using substrate **2.71**, the [5+2] reaction proceeded to form product **2.72** in 93% yield.<sup>70</sup>

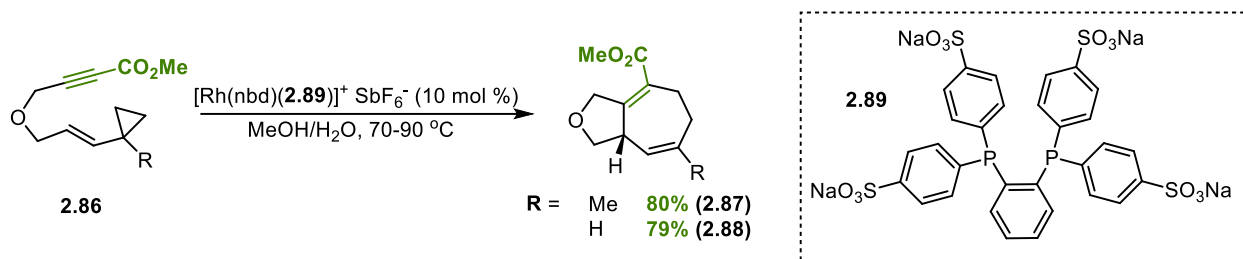
The differing reactivities of these catalysts were studied through DFT calculations. The key steps of the reaction mechanism involve the  $2\pi$ -insertion (the rate-determining step) (**2.82**) and reductive elimination (**2.84**) (**Figure 2.4**).<sup>71</sup> The transition state geometries of these steps are indistinguishable when using any of the catalysts, suggesting that the efficiency of these catalysts relies on the catalyst's ability to mitigate

the electronic and steric effects of the TS geometry. The productivity of these Rh(I)-catalysts was measured through the computed free energy span (FES), which correlated with previously observed efficiencies with RhNHC-IPr having the lowest FES at 19.5 kcal/mol. . In addition, TS models of the key steps as well as the computed reaction coordinate also further demonstrate the higher efficacy of the RhNHC-IPr catalyst with three key features:

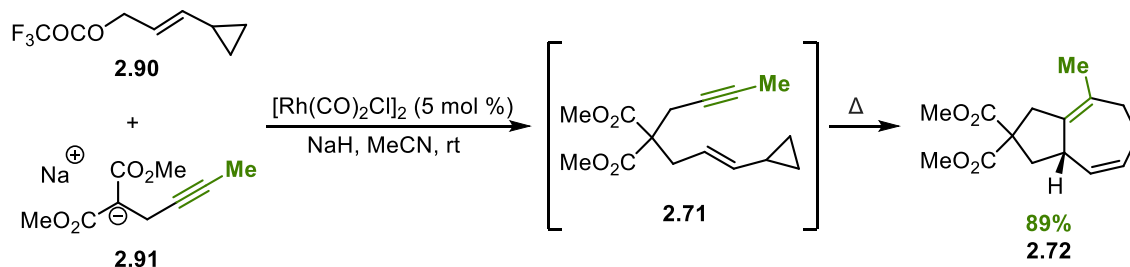
- 1) The electronic stabilization of the ring-opening and breaking step through agostic interactions between the Rh and the hydrogens of the diisopropyl groups on the NHC;
- 2) The lower energy barrier of the RDS; and
- 3) Lack of product inhibition during the transfer of catalyst to the next substrate.

**Figure 2.4.** Reaction mechanism of Rh(I)-catalyzed intramolecular [5+2] cycloaddition

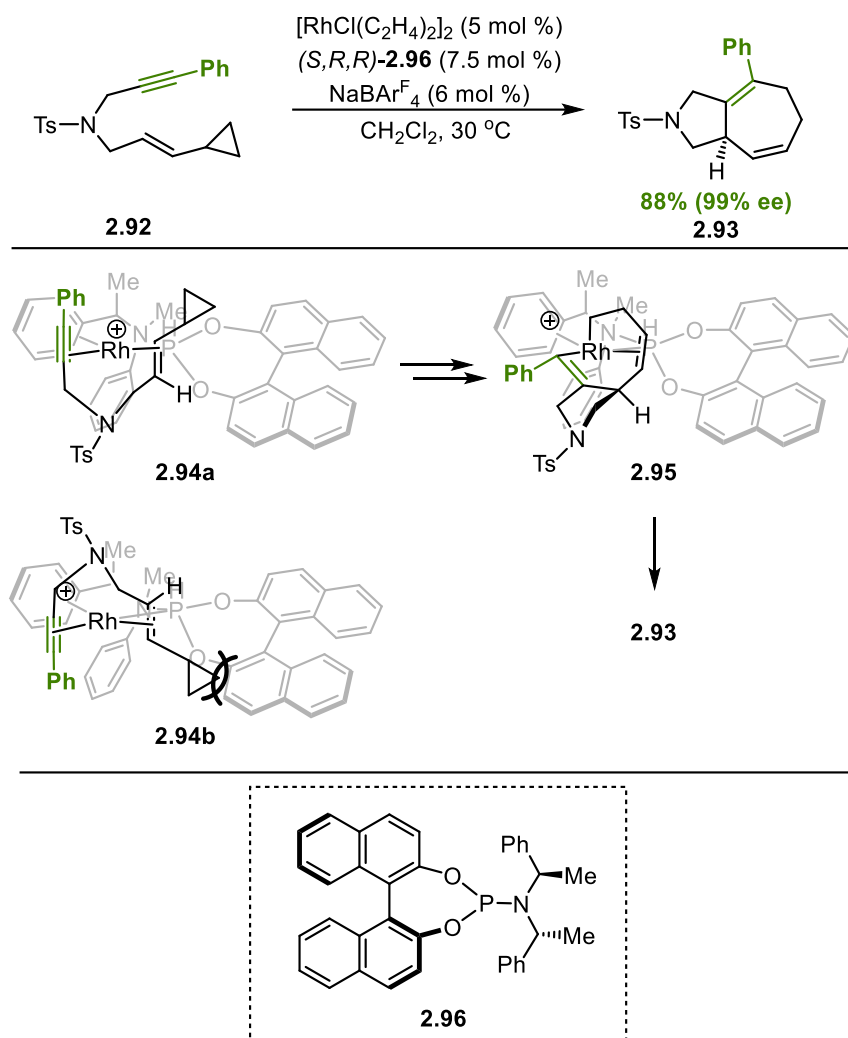
The Wender group developed a greener method to perform this [5+2] reaction using  $[\text{Rh}(\text{nbd})]\text{SbF}_6$ , and bidentate phosphine ligand **2.89** to form a catalyst *in situ* that was able to be recycled with high efficiency. Products **2.87** and **2.88** were obtained in high yields (**Scheme 2.18**).<sup>72</sup>

**Scheme 2.18.** Wender's greener method for intramolecular [5+2] cycloaddition


Inspired by Wender's work, Chung used a new Rh(I)-NHC catalyst system –  $[\text{Rh}(\text{IPMeS})(\text{cod})\text{Cl}]/\text{AgSbF}_6$  – to execute the cycloaddition in almost quantitative yield in less than ten minutes.<sup>73</sup> Martin and co-workers disclosed a tandem allylic alkylation/[5+2] cycloaddition between malonate **2.91** and trifluoroacetate VCP **2.90** using  $[\text{Rh}(\text{CO})_2\text{Cl}]_2$  to synthesize **2.72** in 89% yield through intermediate **2.71** (**Scheme 2.19**).

**Scheme 2.19.** Chung's Rh(I)-NHC catalyst system for intramolecular [5+2] reaction


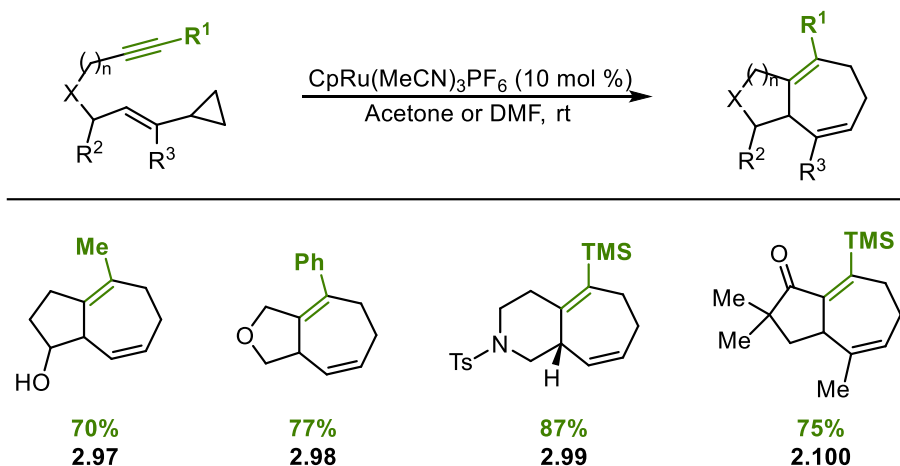
Hayashi and co-workers developed an asymmetric Rh(I)-catalyzed procedure using chiral phosphoramidite ligand **2.96** to form the cycloadducts with high stereoselectivity. The naphthyl rings creates a chiral environment around the Rh atom leading to coordination of **2.92** as seen in **2.94a** rather than **2.94b**. This minimizes the steric interactions between the cyclopropyl ring and the naphthyl moieties (**Figure 2.5**).<sup>75</sup>

**Figure 2.5.** Asymmetric Rh(I)-catalyzed intramolecular [5+2] cycloaddition

Trost and co-workers investigated Ru(II)-catalysis as cheaper, alternative catalysts to drive this intramolecular [5+2] reaction. Using their previously reported  $\text{CpRu}(\text{CH}_3\text{CN})_3\text{PF}_6$  catalyst,<sup>76</sup> the group was able to enable this transformation, forming products **2.97** – **2.100** in good to excellent yields with a high tolerance for functional groups, including ketones, amides, and alcohols. Most interesting, this method was extended to synthesize [6.7] ring systems as well (**Scheme 2.20**).<sup>77</sup> In a subsequent study, this Ru-catalyzed method was used to prepare a library of tricyclic compounds in

good to excellent yields with a high functional group tolerance to show the applicability of this system for total synthesis strategies of natural products.<sup>78</sup>

**Scheme 2.20.** Trost's Ru(II)-catalyzed intramolecular [5+2] cycloaddition with alkynes

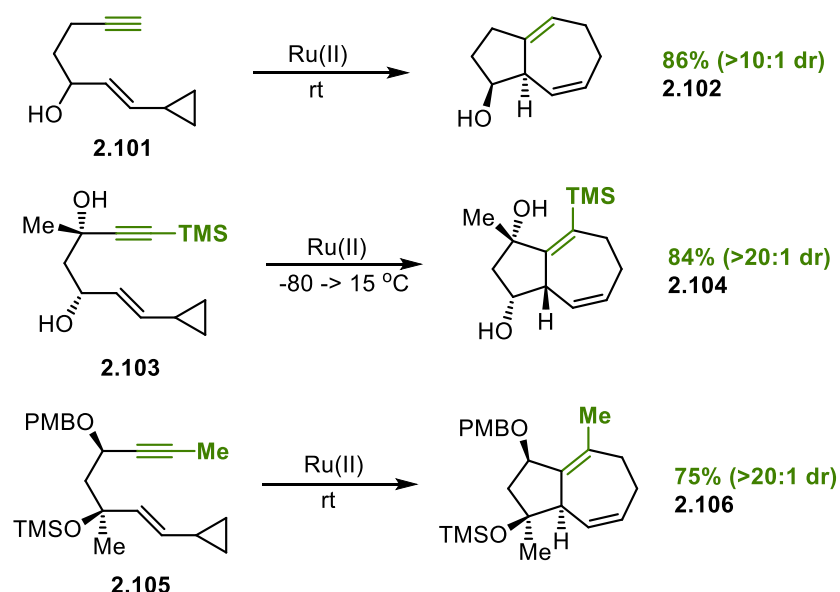


The regioselectivity of this Ru-catalyzed method was investigated regarding the steric and electronic influence of substituents on the regioselectivity of cyclopropyl bond cleavage in *cis* and *trans* cyclopropyl substrates. For the *trans* substrates, the more substituted cyclopropyl bond is broken, identifying cyclopropyl bond strength as the major contributor in product distribution. In contrast, the less substituted carbon breaks during cycloisomerization, suggesting that sterics is the significant factor in this group of substrates. Interestingly, the aldehyde substrates showed differences from the rest of the entries in the series, indicating that steric and electronic effects are both involved. In addition, the *cis* substrates showed a dramatically higher level of regioselectivity compared to the *trans* substrates.<sup>79</sup>

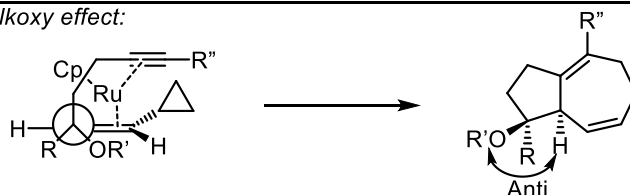
The diastereoselectivity of this method was investigated through strategic substrate design (**Scheme 2.21**). Protected and unprotected allylic hydroxyl groups would result in a *trans* relationship between the hydroxyl group and the bridgehead hydrogen

atom (**2.102**). In addition, a quaternary propargylic carbon with an allylic substituent exhibited complete diastereoselectivity (**2.104**). This was also seen with a quaternary allylic carbon atom and a propargylic PMB ether (**2.106**). The observed *anti*-relationship of the bridgehead hydrogen and the homoallylic OR' substituent agrees with the Stork/Houk-Jäger "inside alkoxy" model. The  $\sigma^*_{CO}$  orbital is orthogonal to the alkene  $\pi$  orbital, so the overlap of these orbitals is minimized. In addition, electron donation from the  $\sigma_{CH}$  and/or  $\sigma_{CR}$  further stabilizes the transition state.<sup>80</sup>

**Scheme 2.21.** Diastereoselectivity of Trost's [5+2] method



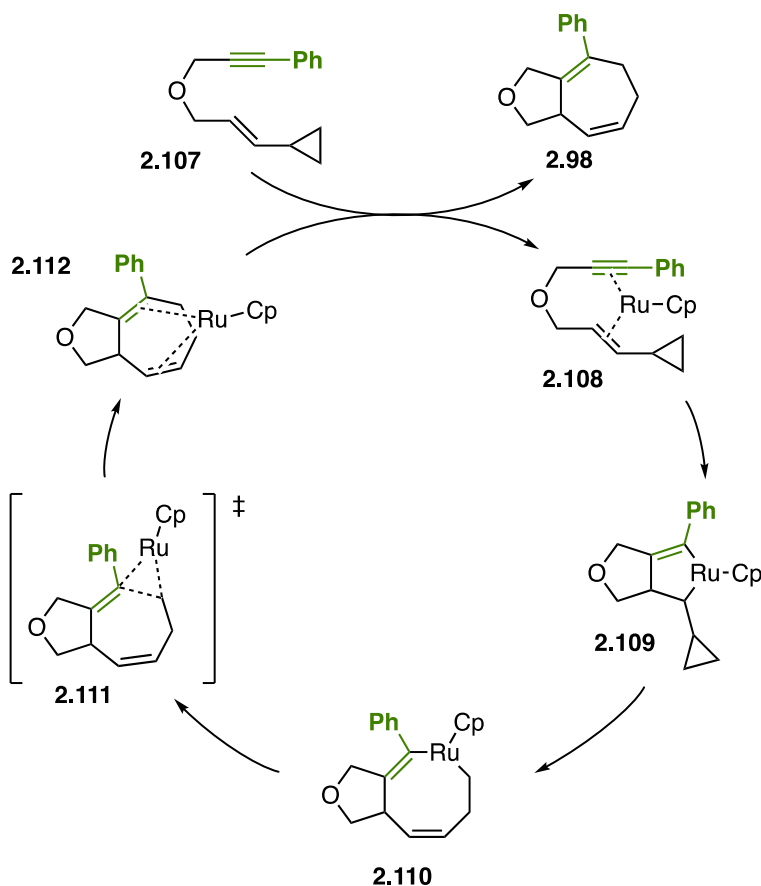
*Inside alkoxy effect:*



The mechanism, regioselectivity and diastereoselectivity, of the Ru(II)-catalyzed reaction was investigated through DFT calculations. Contrary to the Rh(I) pathway, this cycloaddition undergoes a metallacyclopentene mechanism due to the lower barrier of

the oxidative cyclization step (**2.108** to **2.109**) (**Scheme 2.22**). This was explained through the difference of the redox potentials of the two metals, since the oxidation state of the metal increases in the metallacycle formation.<sup>81</sup>

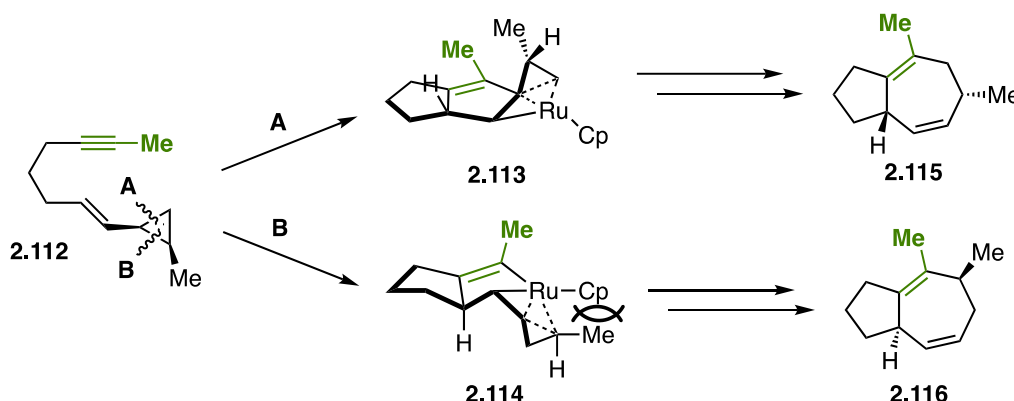
**Scheme 2.22.** Mechanism of Ru(II)-catalyzed intramolecular [5+2] cycloaddition



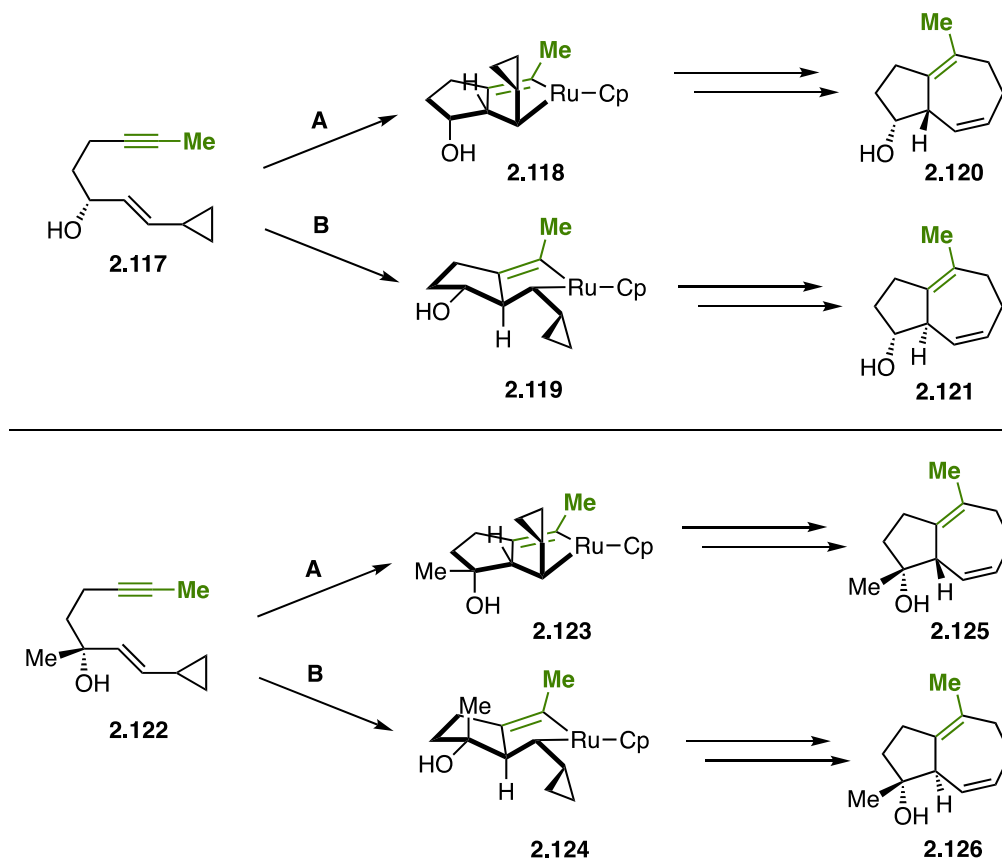
The enhanced regioselectivity seen in the *cis* substrates versus the *trans* substrates was rationalized using Gibbs free energies of the cyclopropyl group cleavage step. In the case of the *trans* substrates, the breaking of either the more (16.8 kcal/mol) or less (17.4 kcal/mol) substituted cyclopropyl bond has a small energy difference and results in a lower regioselectivity. In contrast, the cleavage of the more (22.2 kcal/mol) substituted (**2.114**) has a higher energy cost due to the methyl position being in a more

sterically hindered side compared to intermediate **2.113** (**Figure 2.6**). Because of this, this steric repulsion allows for the higher regioselectivity seen for the *cis* substrates (**2.115**).<sup>81</sup>

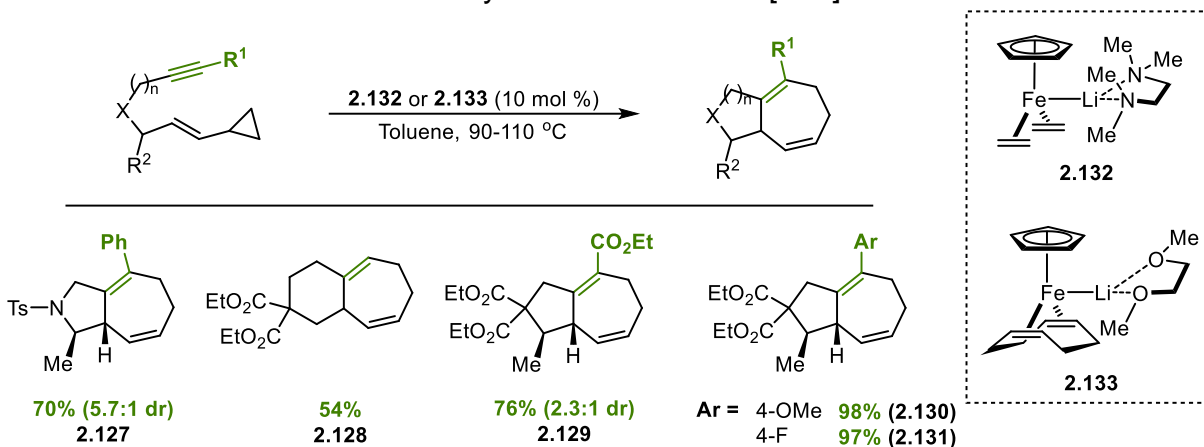
**Figure 2.6.** Rationale for enhanced regioselectivity of *cis* cyclopropyl substrates in Ru(II)-method



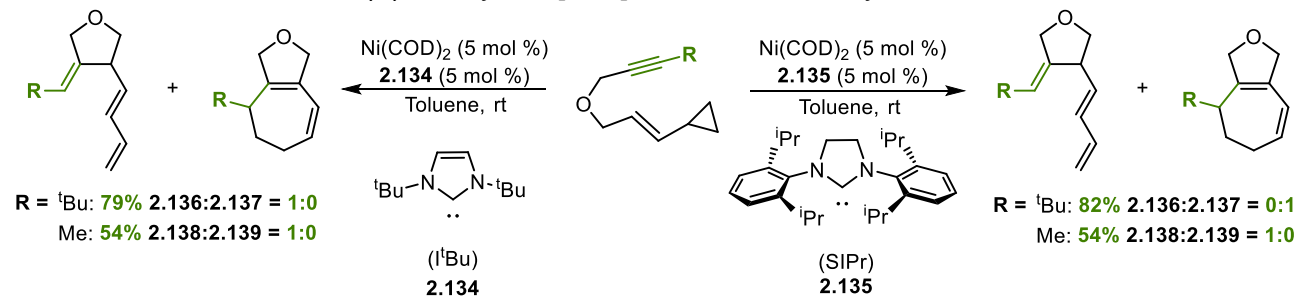
The observed diastereoselectivity seen previously was also investigated (**Figure 2.7**). When the allylic position is substituted with a hydroxyl group, intermediate **2.118** was calculated to be more stable than intermediate **2.119**, which was attributed to the fact that the oxygen atom in **2.118** is closer to the cationic metal center, allowing for the lone pairs to stabilize the reaction center through electrostatic interactions. Due to this, the *trans* cycloadduct **2.120** is favored. Furthermore, in the case where that position is disubstituted with a methyl and hydroxyl group, intermediate **2.124** is less favorable due to the steric repulsions of the methyl substituent and the  $\beta$ -hydrogen from the double bond. Thus, in favored cycloadduct product **2.125**, the methyl group and the adjacent hydrogen appear *cis* to each other.<sup>81</sup>

**Figure 2.7.** Diastereoselectivity of selected substrates in Ru(II)-catalyzed reaction

To avoid the use of noble metal catalysis, Fürstner reported using low-valent iron complexes **2.132** and **2.133** to catalyze the [5+2] cycloaddition to exclusively synthesize the major isomers **2.127** – **2.131** in moderate to great yields (**Scheme 2.23**). In addition, complex **2.133** afforded product **2.128**, expanding this chemistry to generate bicyclic [5.4.0] scaffolds without the need of a nitrogen-containing group.<sup>82</sup>

**Scheme 2.23.** Fürstner's iron-catalyzed intramolecular [5+2] method

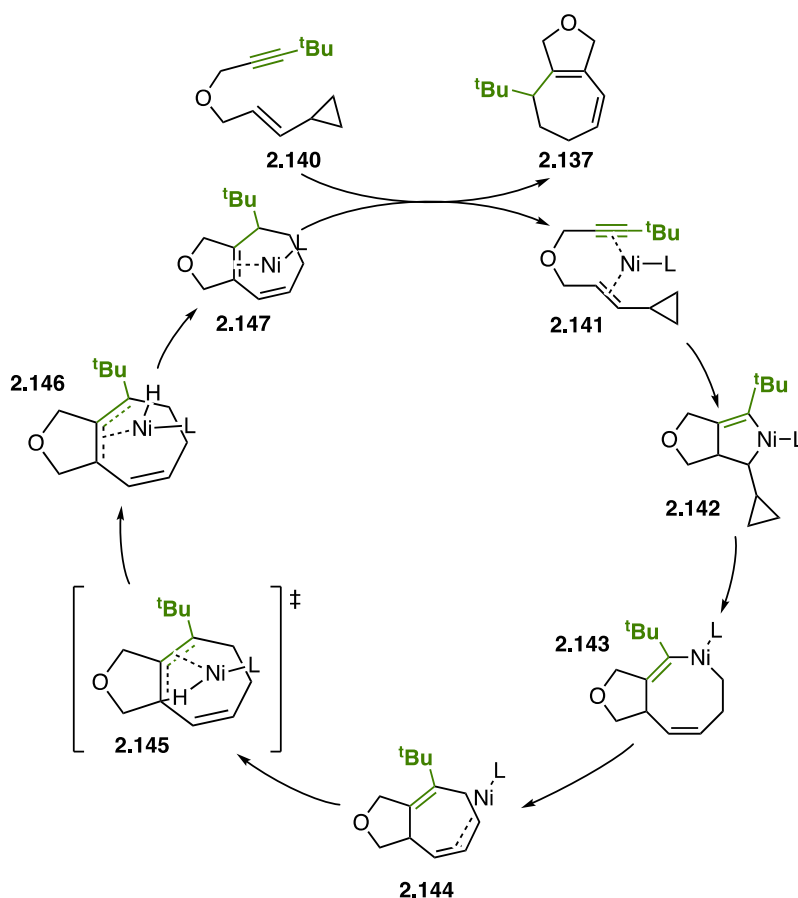
Louie and co-workers demonstrated with their Ni(0) catalysis that the rearrangement of the tethered ether VCPs to either tetrahydrofurans or bicyclic structures can be controlled by the NHC ligand used and the substituent on the alkene (**Scheme 2.24**). In the case of the bulkier ligand **2.135** and a larger R group (i.e. <sup>t</sup>Bu), **2.137** is exclusively formed whereas, when R is smaller (i.e. Me), **2.138** is preferentially formed. Furthermore, in the case of using ligand **2.134**, **2.136** and **2.138** are observed.<sup>83</sup>

**Scheme 2.24.** Louie's Ni(0)-catalyzed [5+2] intramolecular cycloaddition

This distribution of products can be explained through the reaction mechanism (**Figure 2.8**). When ligand **2.134** is used, intermediate **2.143** undergoes β-hydride elimination and reductive elimination to form **2.136**. However, if ligand **2.135** is instead

employed,  $\beta$ -hydride elimination cannot occur due to sterics so reductive elimination occurs, leading to intermediate **2.144**. After diene isomerization, allyl nickel (II) hydrate **2.146** undergoes reductive elimination to form complex **2.147**. Lastly, product **2.137** is released and the Ni-reactant complex **2.141** is regenerated.<sup>84</sup>

**Figure 2.8.** Mechanism of Ni(0)-catalyzed intramolecular [5+2] reaction

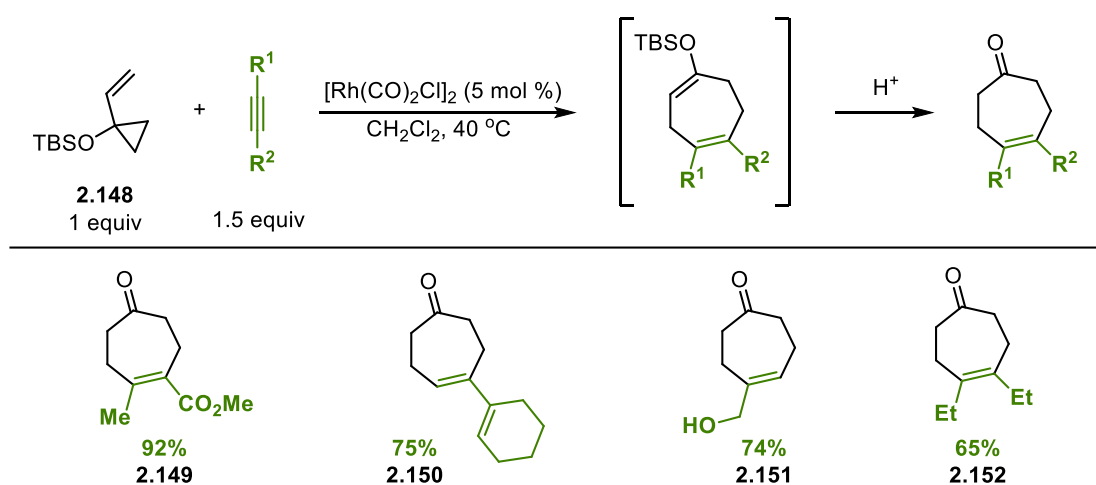


#### 2.4.2. Intermolecular [5+2] cycloaddition with alkynes

Following their initial reports of the [5+2] intramolecular cycloaddition, Wender and co-workers disclosed the first example of a metal-catalyzed intermolecular [5+2] cycloaddition between VCPs and alkynes – the homologue to the classic Diels-Alder

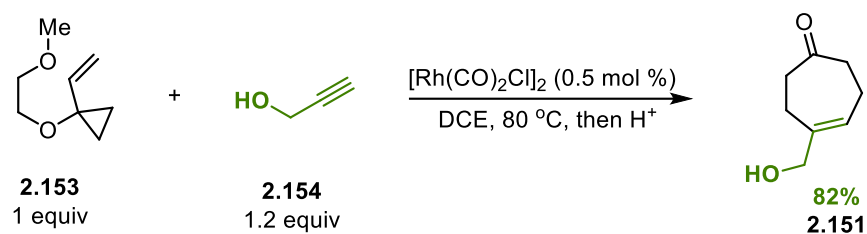
cycloaddition (**Scheme 2.25**). In the initial report, siloxy-VCP **2.148** was used to facilitate ring-opening of the cyclopropane ring for the cyclization to occur. Using  $[\text{Rh}(\text{CO})_2\text{Cl}]_2$ , the [5+2] between VCP **2.148** and a wide range of alkynes occurred to provide the cycloadducts in good to excellent yields. The silylenol ethers were hydrolyzed to provide the corresponding cycloheptenones **2.149** – **2.152**.<sup>85</sup>

**Scheme 2.25.** Wender's first report of intermolecular [5+2] cycloaddition with alkynes

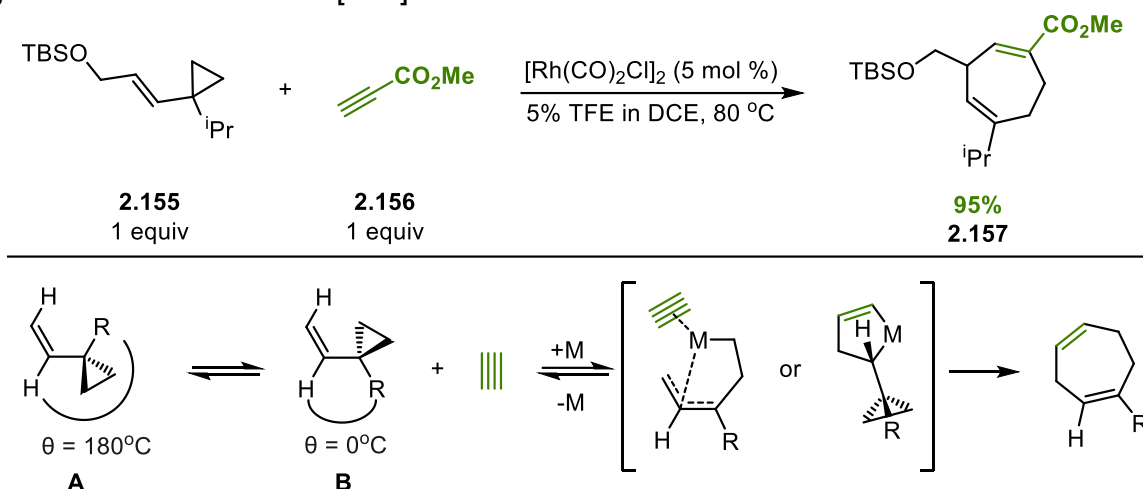


In a follow-up study, VCP **2.153** was prepared in fewer steps with inexpensive reagents as a substitute for VCP **2.148**. With this new iteration, the cycloadducts were obtained with a 6-fold increase in reaction rate while also using a 10-fold decrease in catalyst loading (**Scheme 2.26**). In addition, this method was able to be scaled up to 100 mmol.<sup>86</sup>

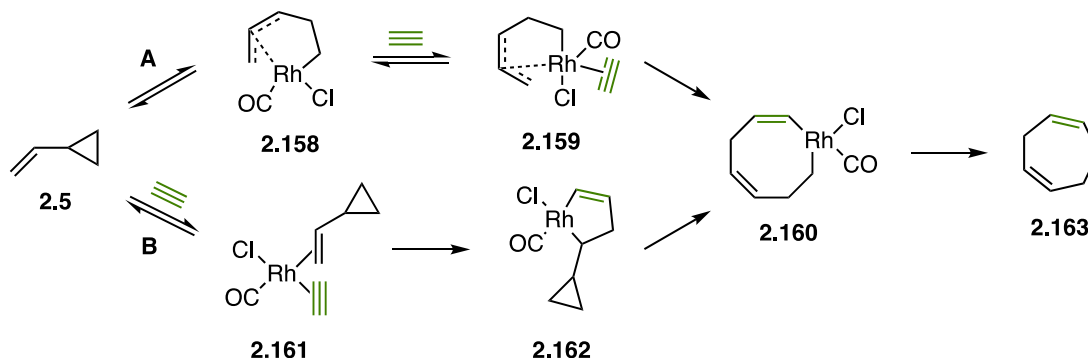
**Scheme 2.26.** Employing VCP **2.153** in intermolecular [5+2] reaction



To expand the substrate scope of this reaction, the Wender group published the following year a method using simple, un-activated VCPs to afford cycloheptadiene products (**Figure 2.9**). While VCPs **2.148** and **2.153** have higher reactivity from the electronic contribution of the heteroatom substituent, it was hypothesized that it could also be due to an influence from the conformation of intermediates being formed. Based on the proposed mechanistic hypothesis, having a substituent at the 1-position reduces the energetic difference between species **A** and **B**, leading to an increased distribution towards **B** which, due to it having the appropriate dihedral angle of 0 °C, can form the desired cis-alkene of the cycloadduct product. A range of alkynes and VCPs were able to undergo this cycloaddition in either DCE or 5% TFE in DCE if the reaction was sluggish.<sup>87</sup>

**Figure 2.9.** Intermolecular [5+2] with un-activated VCPs

Wender and colleagues had proposed two reaction mechanisms for how the Rh species is catalyzing this cycloaddition (**Scheme 2.27**). In Pathway **A**, the Rh catalyst coordinates with the vinyl group, which favors cyclopropyl ring opening to generate intermediate **2.158**. Coordination of an alkyne generates 18 e<sup>-</sup> complex **2.159**, which is then inserted into the five-carbon moiety to form metallacycle **2.160**. Finally, reductive elimination then provides the desired cycloadduct **2.163**. In Pathway **B**, it was hypothesized that instead five-membered metallacycle **2.162** is formed by the oxidative coupling of the alkyne and the vinyl group of the VCP, leaving the cyclopropyl ring intact. Through DFT calculations, however, it was found that there is a substantial energetic cost (26.9 kcal/mol) to have these components in a planar conformation for the coupling to occur compared to the alkyne insertion step (21.9 kcal/mol) of Pathway **A**. With this, as well as coordination of solvents to stabilize intermediates, Pathway **A** was deemed as the more plausible mechanism for this reaction.<sup>88</sup>

**Scheme 2.27.** Mechanistic pathways for the Rh(I)-catalyzed intermolecular reaction

With a mechanism in hand, Wender, Houk, and Yu sought to quantitatively explain the differing reactivities of 1-substituted VCPs when R=H, M, 1-isopropyl, 1-alkoxy, and 1-siloxy as previously mentioned through DFT calculations. For these calculations, four VCPs were used: **1a**, R=H; **1b**, R=Me; **1c**, R=<sup>i</sup>Pr; **1d**, R=OMe. The activation barriers for each of the VCPs were computed based on three factors:

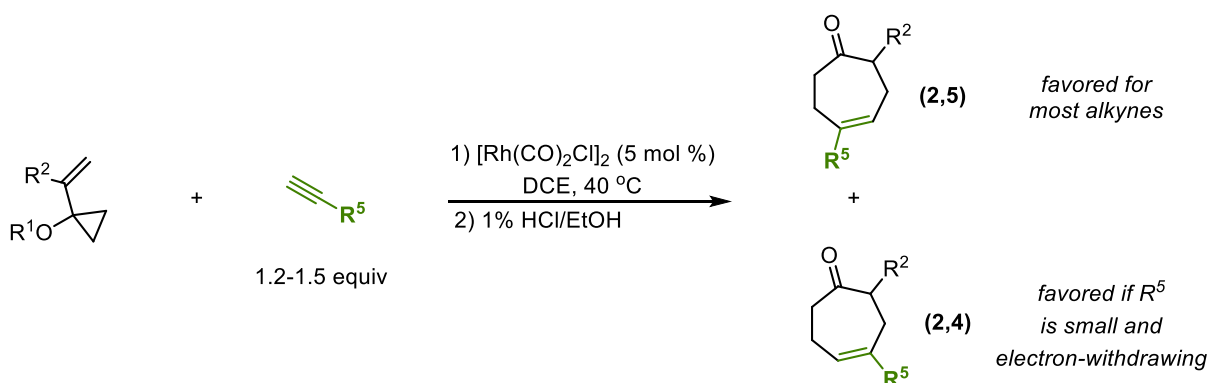
- 1) the electronic stabilization transition state of the alkyne insertion step;
  - 2) the steric effects of the preorganization energy and the free energy of exchange;
- and
- 3) the free energy of transfer from product complex.

Based on these factors, the reaction free energy barriers were determined as 27.7, 24.7, 22.8, and 20.4 kcal/mol for **1a**, **1b**, **1c**, and **1d**, respectively. This trend aligns with previous experimental data of how bulky substituents and heteroatom substituents at the 1-position greatly increase the reaction rate.<sup>89</sup>

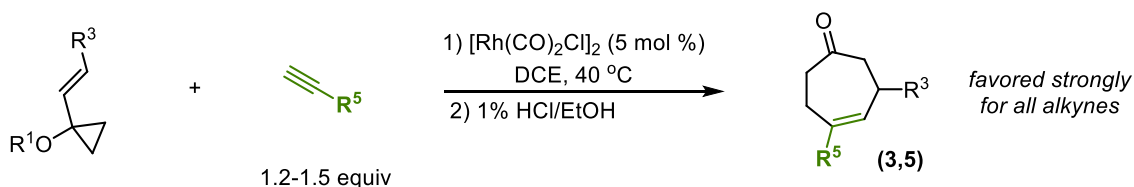
The electronic and steric control of regioselectivities of the Rh(I)-catalyzed [5+2] with VCPs and alkynes were studied both experimentally and computationally. In cases

where the VCP has substitution at the internal position, 2,5-regioselectivity is generally favored; however, if the alkyne substituent is smaller and electron-withdrawing, the 2,4-regioisomer is preferred (**Scheme 2.28a**). VCPs that had terminal substitution on the alkene exhibited a high degree of regioselectivity due to a steric preference of the bulky alkyne substituents to be distal to the forming C-C bond between the open cyclopropyl chain and the alkyne (**Scheme 2.28b**). Lastly, if the substituent on the alkyne is large and not strongly electron withdrawing, the 2,4-regioisomer is favored (**Scheme 2.28c**). However, a mixture of the other regioisomers can result due to the competing sterics and the strong back-bonding donation from the rhodium to the  $\pi^*$ -orbital of the alkyne.<sup>90</sup>

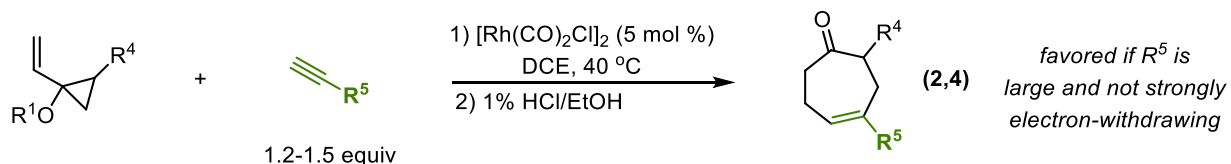
**Scheme 2.28a.** Effect of internal alkene substitution on regioselectivity



**Scheme 2.28b.** Effect of terminal alkene substitution on regioselectivity

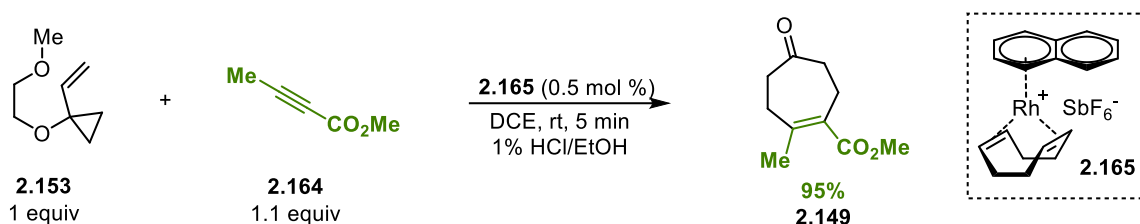


**Scheme 2.28c.** Effect of 1,2-substitution on VCP on regioselectivity



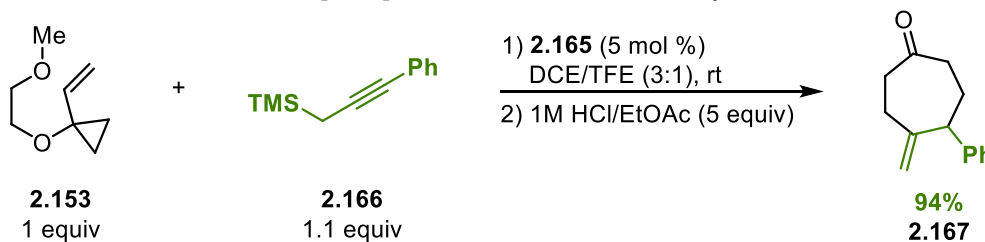
Wender has disclosed cationic Rh(I) complex **2.165** ( $[(C_{10}H_8)Rh(cod)]SbF_6$ ) that can catalyze the [5+2] intermolecular reaction within fifteen minutes to provide cycloheptenones in excellent yields with a high functional group tolerance in respect to the alkyne (**Scheme 2.29**).<sup>91</sup>

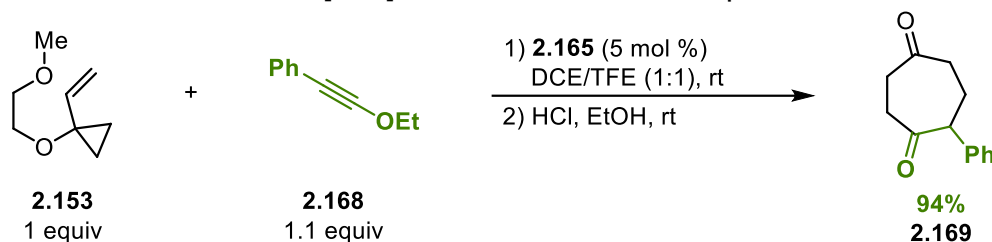
**Scheme 2.29.** Cationic Rh(I) complex for intermolecular [5+2] cycloaddition



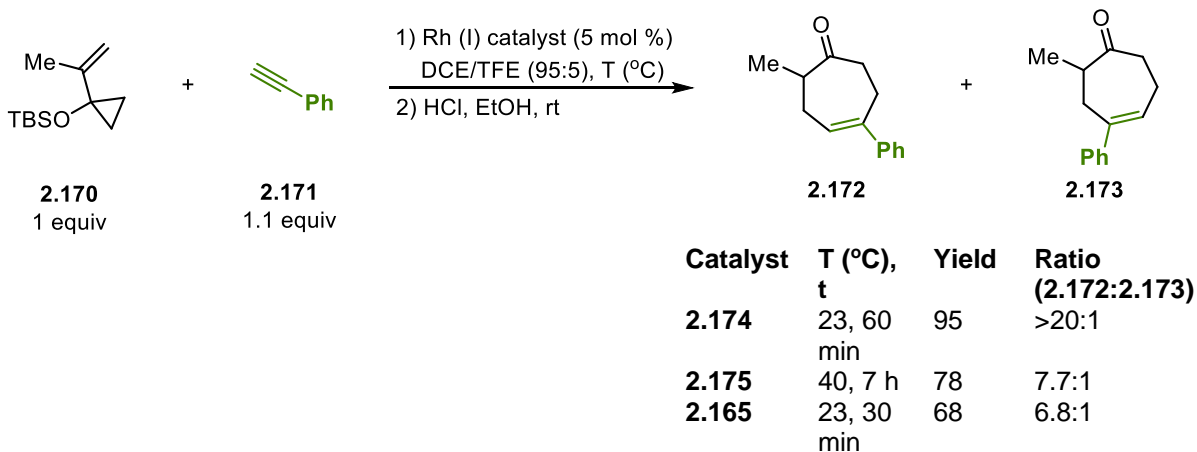
With Rh catalyst **2.165**, Wender and co-workers have used alkynes as equivalents to provide functionality that are more difficult to achieve in a cycloaddition strategy. Propargyltrimethylsilanes were employed as allene equivalents to synthesize formal allene cycloadducts upon protodesilylation (**Scheme 2.30a**).<sup>92</sup> Most recently, ynol ethers were used as ketene equivalents to form cycloheptadiones – a common scaffold in natural products and intermediates towards non-natural products (**Scheme 2.30b**).<sup>93</sup>

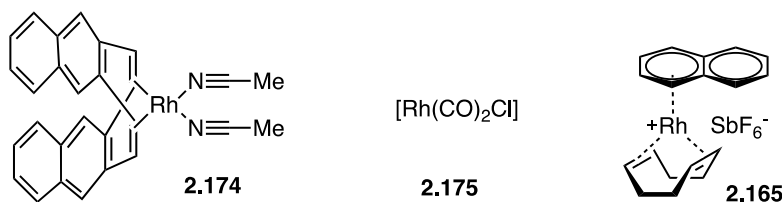
**Scheme 2.30a.** Intermolecular [5+2] reaction with allene equivalents



**Scheme 2.30b.** Intermolecular [5+2] reaction with ketene equivalents

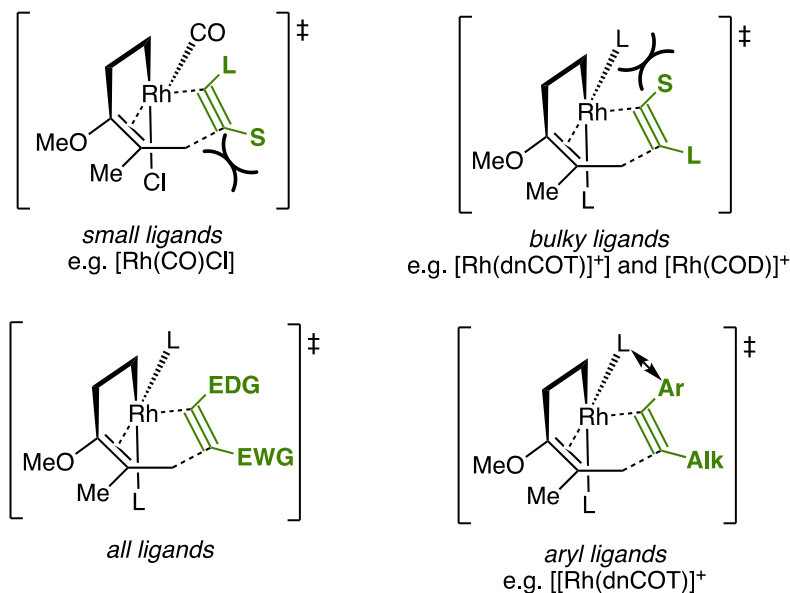
To further develop this intermolecular transformation, Wender looked at different scaffolds for control of the regioselectivity of the cycloaddition. Rh catalyst **2.174** ( $[\text{Rh}(\text{dnCOT})(\text{MeCN})_2]\text{SbF}_6$ ) was prepared, since modifications to COT complexes have been shown to enhance their ability to bind to transition metals.<sup>94</sup> Compared to the previously reported catalysts (**Figure 2.10a**), **2.174** exhibited improvements in both reaction rates and efficiency (**Figure 2.10b**). In addition, it enabled an enhancement in regioselectivity and, in some instances, produced only one regioisomer. Furthermore, it was also able to catalyze the intramolecular [5+2] reaction with VCPs and either alkynes or alkenes.<sup>95</sup>

**Figure 2.10a.** Comparison of Rh(I) catalysts in regioselectivity and efficiency of intermolecular [5+2] cycloaddition

**Figure 2.10b.** Rh(I) catalysts

The effect of ligands on the rates and regioselectivities of this Rh(I)-catalyzed method were investigated computationally. In this study,  $[\text{Rh}(\text{dnCOT})]^+$ ,  $[\text{Rh}(\text{COD})]^+$ , and  $[\text{Rh}(\text{CO})\text{Cl}]$  were used. As seen previously, the rate and regioselectivity controlling step is the alkyne insertion step. The higher reactivities of the cationic catalysts were found to be due to the steric and dispersion effects of the COD and dnCOT ligands. The steric repulsions of the bulky ligand and the product in the Rh-product complex allow for ease of product liberation and the ligands do not significantly affect the alkyne insertion step.<sup>96</sup>

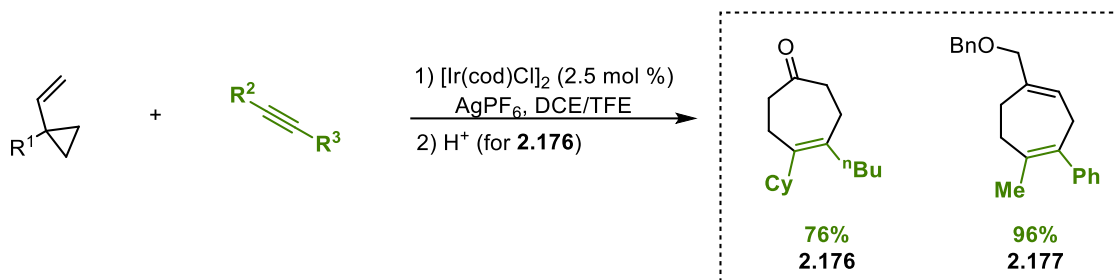
The regioselectivity of these catalysts are affected by substrate-substrate and ligand-substrate steric repulsions, electronic effects, and ligand-substrate  $\pi/\pi$  and C-H/ $\pi$  interactions (**Figure 2.11**). Smaller ligands prefer distal products while bulkier ones prefer proximal products when the alkynes are alkyl or TMS-substituted. Electronic effects are more prominent when the alkyne substituent is small and strongly electron-withdrawing, such as acyl or formyl. In this scenario, these substituents prefer the proximal pathway and enhance the proximal steric control by bulky ligands or reverse if the ligand is smaller. Lastly, aryl substituents on the alkyne have strong directing effects to favor the distal products when using cationic Rh(I) catalysts due to the stabilizing ligand-substrate  $\pi/\pi$  and C-H/ $\pi$  interactions between the ligand and the aryl group.<sup>96</sup>

**Figure 2.11.** Regioselectivity rationale of the Rh(I)-catalyzed reaction

Expanding this concept beyond rhodium catalysis, Strand reported using Ir(I) catalysis coupled with Ag(I)-mediation as a cheaper method to form the desired cycloadducts. A cationic Ir catalyst –  $[\text{Ir}(\text{cod})\text{Cl}]_2\text{PF}_6$  – generated *in situ* catalyzed the formation of a diverse set of cycloheptenones and cycloheptdienes in good to excellent yields (**Scheme 2.31**). This method was also successful in enabling intramolecular [5+2] cycloadditions. The mechanism of this method was analyzed through DFT calculations comparing the energy profiles of the Rh and Ir-catalyzed processes. Both methods share the same principal elements of the overall mechanism. However, while there are differences in energy barriers for certain transition states, of most notable is that the turnover frequency determining TS is not the same in both cycles and as a result, the free energy span is 16.03 kcal/mol for Ir(I) and 28.22 kcal/mol for Rh(I), suggesting that using a cationic Ir catalyst is faster than the Rh catalyst. This was further confirmed through a

comparative kinetics study in which the TOF of  $[\text{Ir}(\text{dbcot})\text{Cl}]_2\text{PF}_6$  ( $10.0 \text{ min}^{-1}$ ) was 50 times higher than that of  $[\text{Rh}(\text{dbcot})\text{Cl}]_2\text{PF}_6$  ( $0.2 \text{ min}^{-1}$ ).<sup>97</sup>

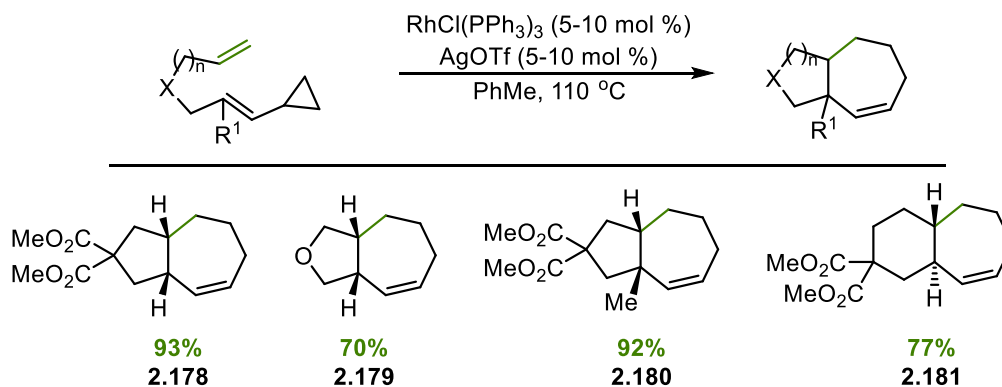
**Scheme 2.31.** Ir-catalyzed intermolecular [5+2] cycloaddition reaction



**2.4.3. [5+2] cycloaddition with alkenes**

This cycloaddition strategy was further extended to include alkenes as the two-atom component with Wender's first report in 1998 when ene-VCP, in the presence of a Rh(I) catalyst and Ag(I) additive under thermal conditions, cyclizes to form the desired cycloadducts **2.178** – **2.181** (**Scheme 2.32**). The substrate scope also included bicyclo[5.4.0]decenes (**2.180**), which are naturally occurring and often difficult to synthesize with the quaternary center formation.<sup>98</sup>

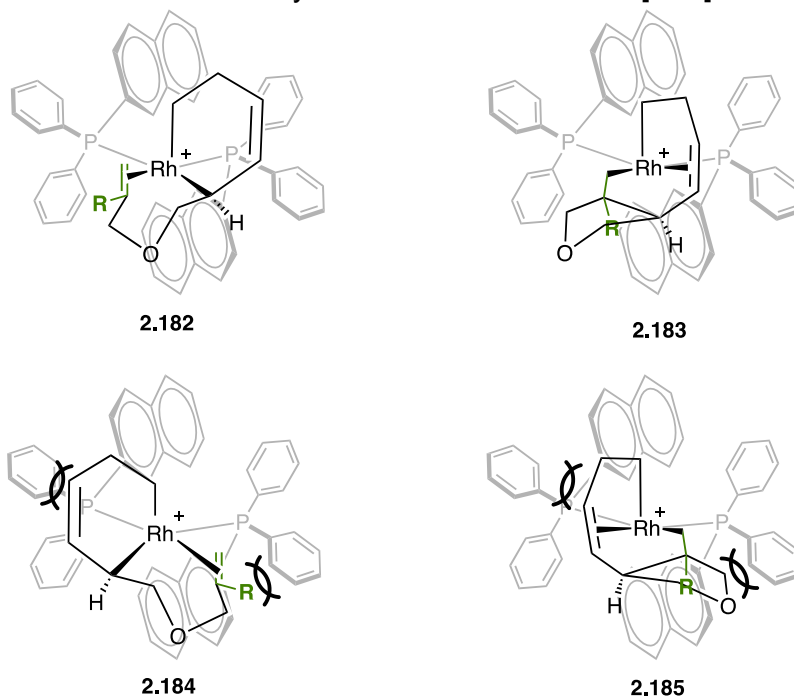
**Scheme 2.32.** Wender's intramolecular [5+2] reaction with alkenes



Wender's previously reported greener method for [5+2] cycloadditions was also successful in forming these bicyclic structures in up to 85% yield.<sup>72</sup>

An asymmetric version of this method was later developed with the use of (*R*)-BINAP ligands to achieve excellent enantioselectivity, up to 99% ee (**Figure 2.12**). The stereocenter is formed during the oxidative coupling of the alkene and the cyclopropyl ring, which was determined to be the RDS during DFT calculations in a previous study.<sup>88</sup> In this step, the growing chain is aligned so the forward phenyl groups of the BINAP-ligand are not engaging in destabilizing interactions with the cyclopropyl and alkenyl groups (**2.182** and **2.183**). This is also confirmed by the increase in ee if there is a substituent, like methyl, on the alkene or the cyclopropane.<sup>99</sup>

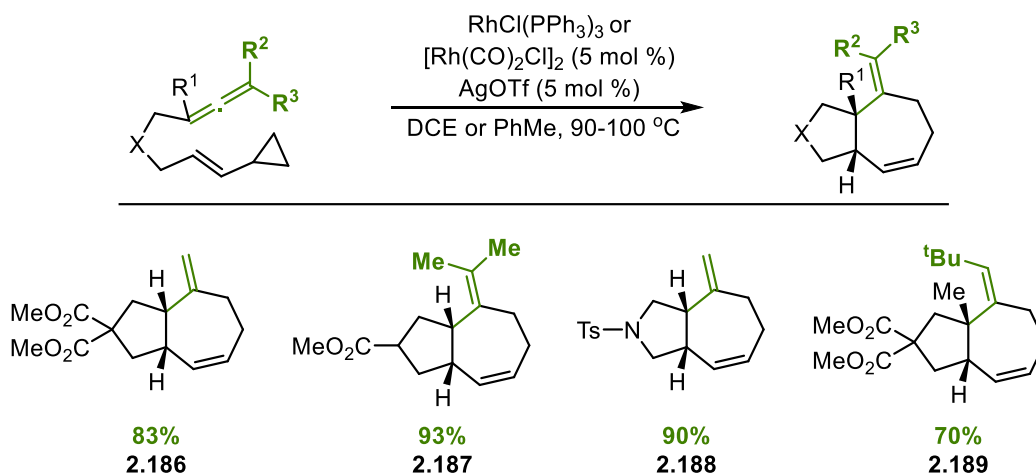
**Figure 2.12.** Intermediates of the asymmetric intramolecular [5+2] reaction with alkenes



#### 2.4.4. [5+2] cycloaddition with allenes

A hindrance in the advancement of the [5+2] reaction was the inability to perform the cycloaddition when using 1,2-disubstituted alkenes to access carbocyclic cores that are found very common in natural product families, such as guaianes and tiglanes. To address this limitation, Wender and co-workers employed allenes to serve as the two-atom component in this intramolecular reaction using either  $\text{RhCl}(\text{PPh}_3)_3$  or  $[\text{Rh}(\text{CO})_2\text{Cl}]_2$  (**Scheme 2.33**). The cyclization occurred at the internal alkene favorably due to entropic considerations. The distribution of the cis and trans products was found to be controlled by the catalyst system with  $[\text{Rh}(\text{CO})_2\text{Cl}]_2$  showing a strong preferential for the formation of the cis-fused ring system. In addition, this method was also able to successfully synthesize cycloadduct **2.189**, which contains a quaternary carbon center.<sup>100</sup>

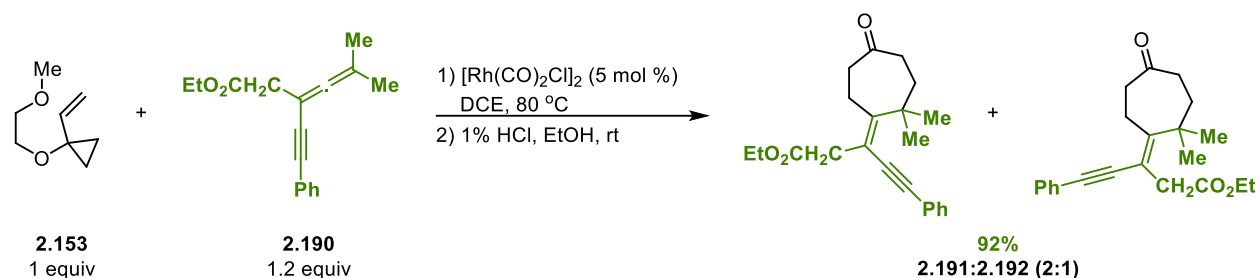
**Scheme 2.33.** Wender's intramolecular cycloaddition with allene



Following this discovery, de Meijere and Wender in collaboration disclosed the first examples of using this strategy in an intermolecular fashion (**Scheme 2.34**). For this

reaction to occur, the allenes had to have an additional coordinating group, such as an alkyne, to interact with the Rh(I)-center.<sup>101</sup>

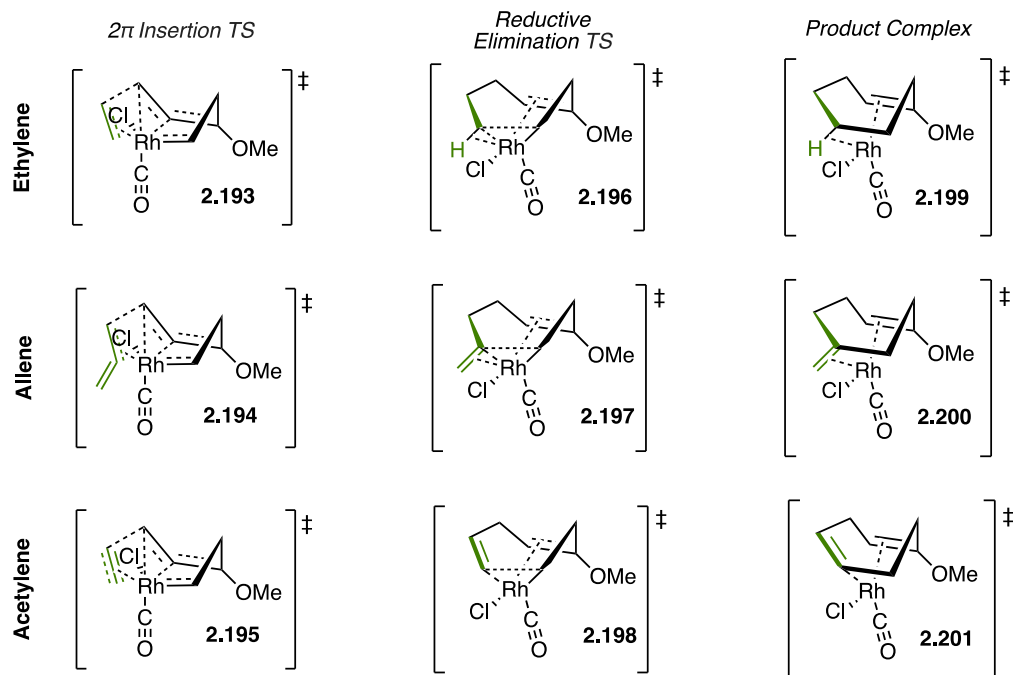
**Scheme 2.34.** Intermolecular [5+2] cycloaddition with allene



The reactivity and chemoselectivity of the intermolecular [5+2] cycloaddition with allenes were studied computationally, as well as the competing formation of allene dimerization with rhodium. The  $2\pi$  insertion is the rate-determining step for the [5+2] cycloaddition. For terminally unsubstituted allenes, the barrier of allene dimerization is only 1.3 kcal/mol higher than the [5+2] cycloaddition, so these pathways are competitive. Due to this, this dimerization “poisons” the rhodium catalyst, leading to a decrease in reactivity and, therefore, yields. However, in the case of di-substituted allenes, the free energy of the dimerization is 4.0 kcal/mol higher than the cycloaddition due to sterics, making the former pathway less competitive. The exclusive chemoselectivity for the terminal allene-yne double bond in the is due to the lower energy barrier of the  $2\pi$  insertion step. The insertion of the terminal double bond has a stronger  $d-\pi^*$  interaction between the rhodium and the enyne from allene-yne, so the energetic cost is lower.<sup>102</sup>

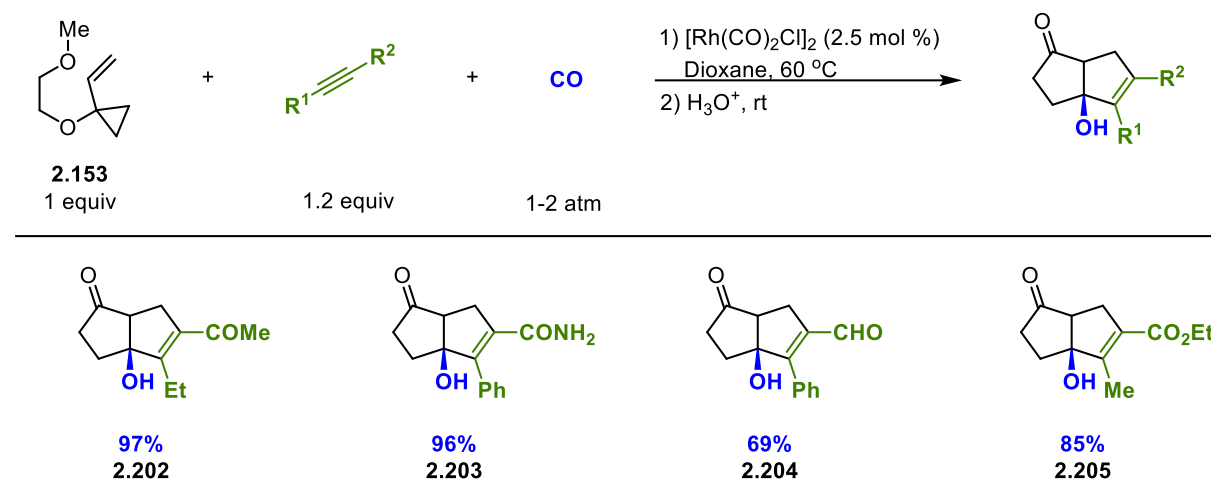
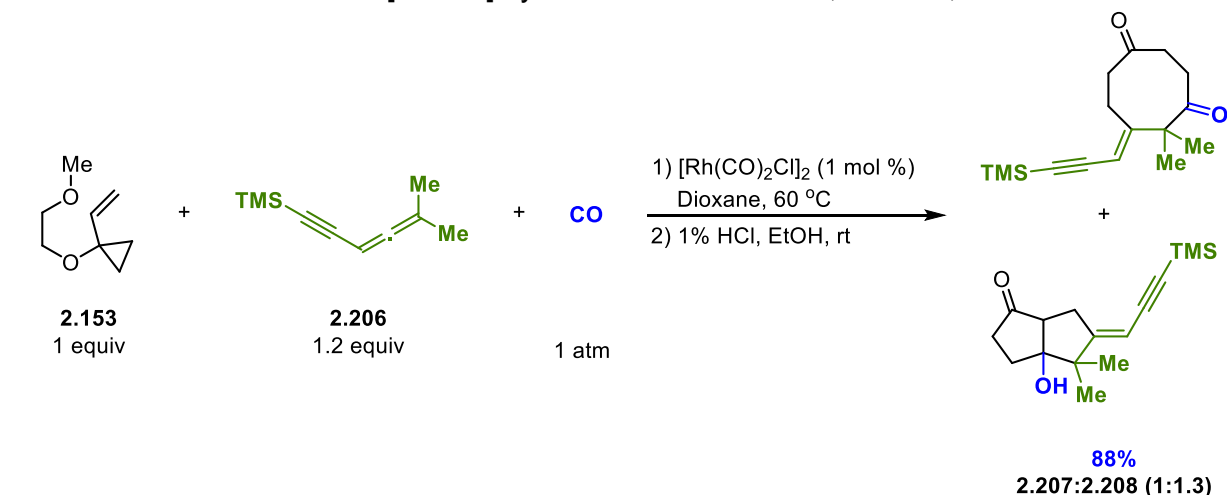
The differing reactivities of alkenes, alkynes, and allenes were investigated computationally using ethylene, acetylene, and allene (**Figure 2.13**). The energy differences of the  $2\pi$  insertion step among the three species are minimal (**2.193** – **2.195**).

The reductive step is much faster for allene and acetylene with a free energy barrier of 20.0 and 14.5 kcal/mol, respectively, than for ethylene (29.3 kcal/mol). The large difference is mainly due to the ability of each substrate to facilitate the reductive elimination (RE) by the residual  $\pi$ -bond. For allene and acetylene, this step is a migratory RE, which involves the assistance of a conventional RE by the developing  $\pi$ -Rh coordination (**2.197** and **2.198**). Therefore, the Rh-C bond can easily become into a Rh-C  $\pi$ -bond. This, however, is not evident for ethylene, leading to a higher energy barrier (**2.196**). In addition, the product complexes for allene and acetylene are coordinated by two  $\pi$ -bonds (**2.200** and **2.201**). For that of ethylene, it is coordinated by a single  $\pi$ -bond and a weaker C-H agostic interaction (**2.199**). Because of this, the liberation of the products from the [5+2] with allenes and alkynes are more exergonic.<sup>103</sup>

**Figure 2.13.** Transition states of Rh(I)-catalyzed [5+2] cycloaddition

## 2.5. Multi-component and cascade cycloadditions with VCPs

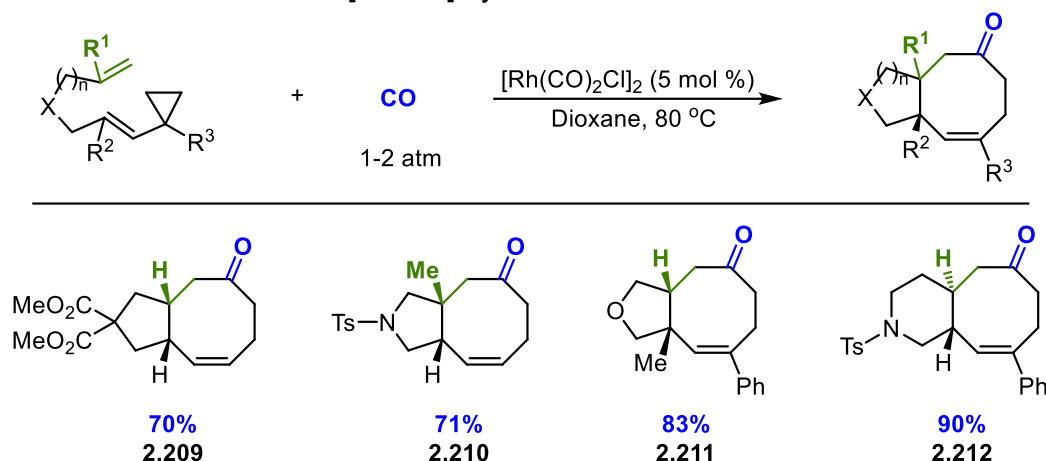
To further improve the synthetic utility of VCPs, Wender and co-workers investigated their use in three-component cycloaddition reactions. In 2002, this group reported the first examples of [5+2+1] cycloadditions of VCPs, alkynes, and CO to assemble bicyclo[3.3.0]octenone skeletons (**Scheme 2.35a**). In this seminal work, the reaction partners were limited to VCP **2.153** and alkynes with carbonyl activated alkynes. However, in all cases, only one regioisomer was formed.<sup>104</sup> This concept was further extended to allenes, resulting in a mixture of products **2.207** and **2.208** (**Scheme 2.35b**).<sup>105</sup>

**Scheme 2.35a.** Wender's [5+2+1] cycloaddition with VCP, alkynes, and CO

**Scheme 2.35b.** Wender's [5+2+1] cycloaddition with VCP, allenes, and CO


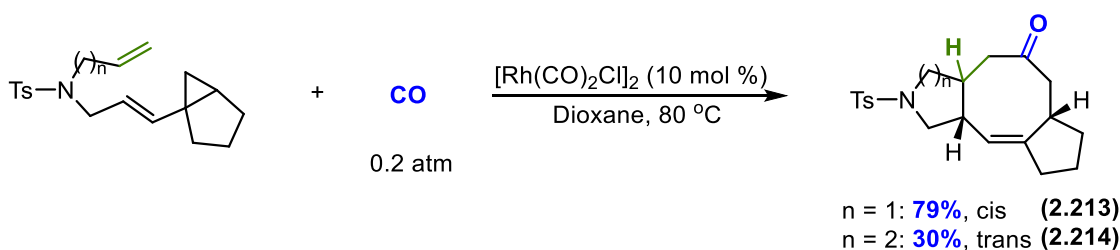
In an intramolecular fashion, this reaction paradigm was expanded to include alkenes as the two-atom component (**Scheme 2.36a**). It was initially hypothesized that the migratory reductive elimination (MRE) step that would occur after CO insertion to form a  $(\text{sp}^2)\text{C}-\text{C}(\text{sp}^3)$  bond would be favorable over the reductive elimination (RE) step to form the [5+2] product. This was confirmed through computational methods in which the activation energy of the RE step was determined to be about 25-30 kcal/mol and the CO

insertion and MRE steps were computed to be 13-14 and 23-24 kcal/mol, respectively, further confirming that the [5+2+1] products would be favored over the [5+2] products. This was experimentally confirmed through the use of  $[\text{Rh}(\text{CO})_2\text{Cl}]_2$  and 1 atm of CO. Using this method, fused 5/8 and 6/8 ring systems were synthesized as well as examples of a quaternary center being formed.<sup>106</sup> Yu and co-workers later expanded on this to assemble [5-8-5] and [6-8-5] ring cyclooctenones (**Scheme 2.36b**).<sup>107</sup>

**Scheme 2.36a.** Intramolecular [5+2+1] cycloaddition with alkenes



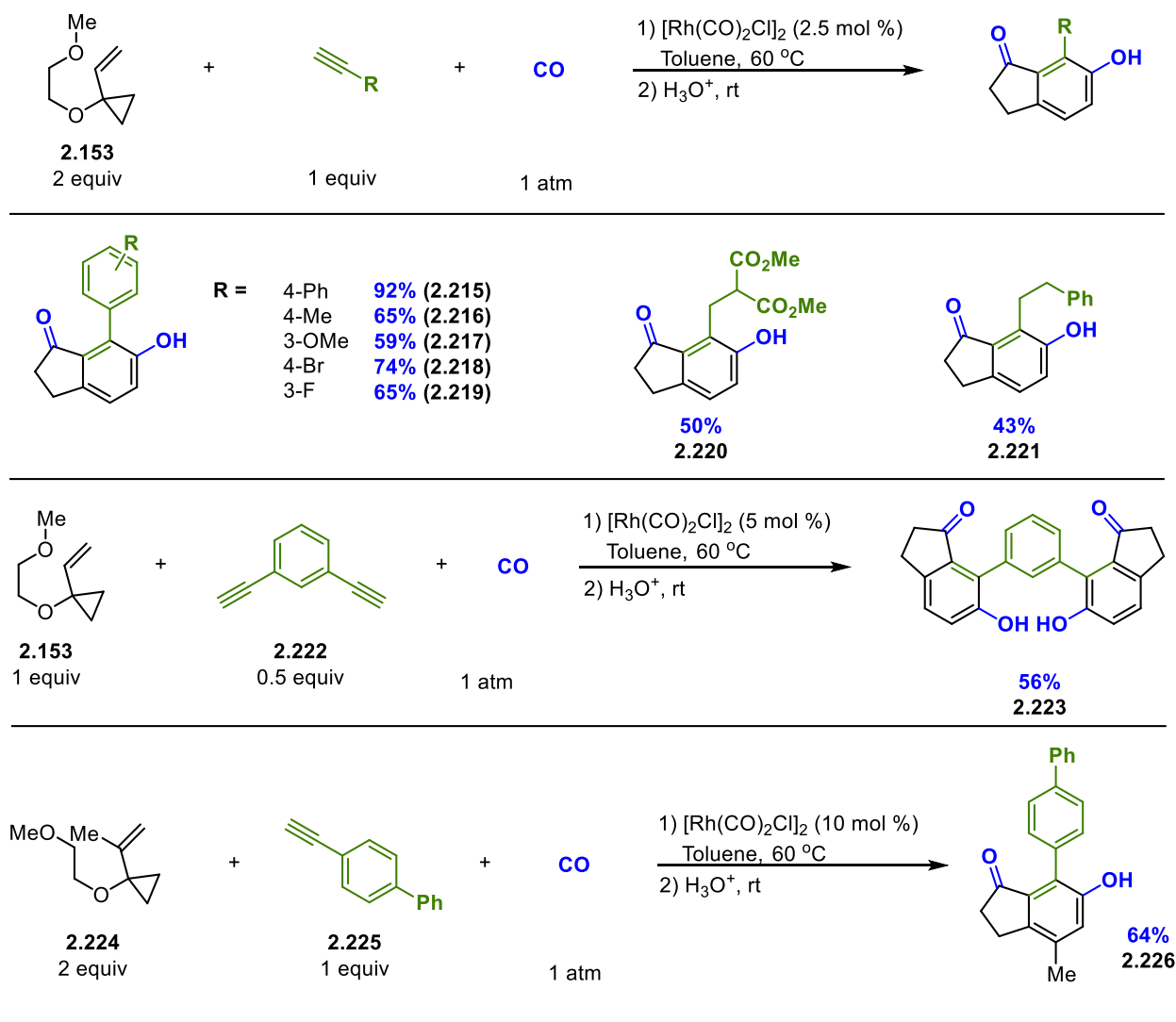
**Scheme 2.36b.** Synthesis of tricyclic systems with [5+2+1] cycloaddition



Wender further developed these multicomponent reactions including a [5+1+2+1] reaction to incorporate two CO units (**Figure 2.14**). In their initial reaction, they observed the formation of three different products. Using excess VCP and a solvent system to precipitate out the desired products allowed them to isolate **2.215** – **2.221** up to 92% yield.

In addition, they were able to have this cycloaddition occur twice in one pot with the use of 1,3-diethynylbenzene to form **2.223** in 56% yield. VCP **2.224** was employed to synthesize more substituted cycloadducts, such as **2.226**, in 64% yield.<sup>108</sup>

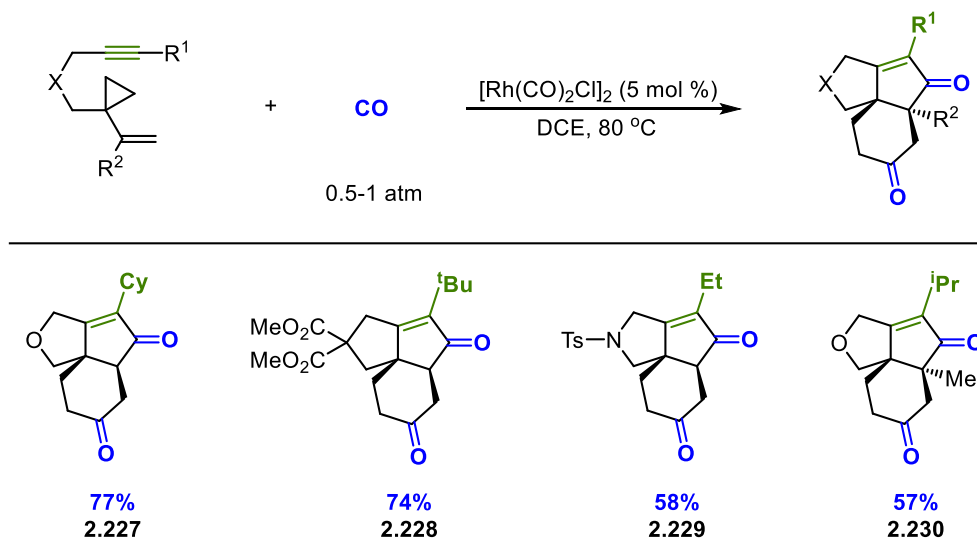
**Figure 2.14.** Intermolecular [5+1+2+1] with VCP, alkynes, and CO



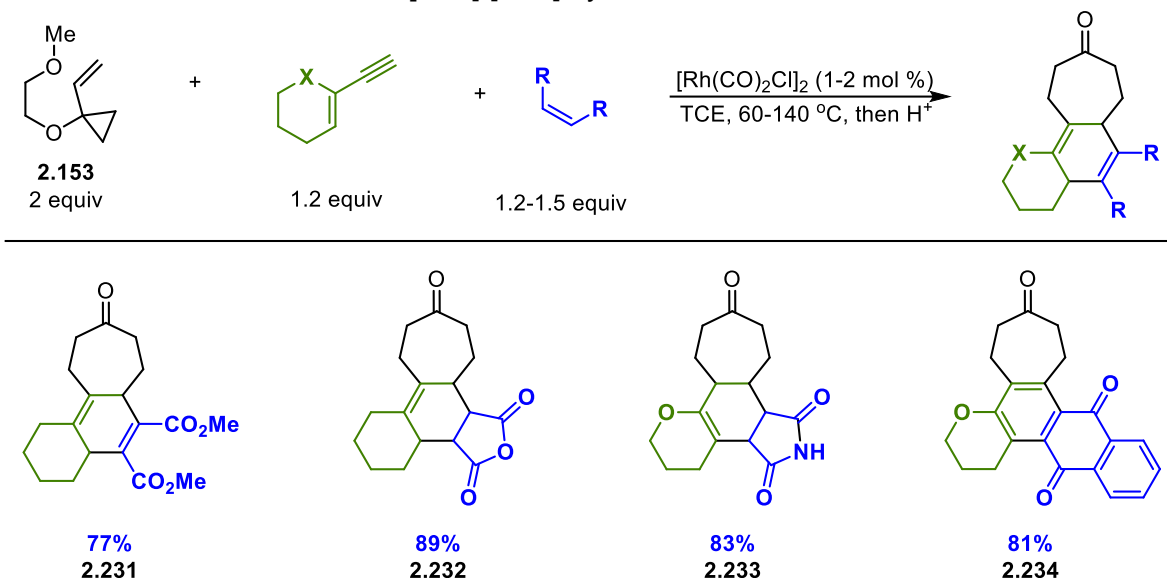
Yu and co-workers reported a formal [5+1]/[2+2+1] cycloaddition of 1-yne-VCPs and two CO units to synthesize [5-5-6] structures using Rh(I) catalysis (**Scheme 2.37**). The reaction provided major products **2.227** – **2.230**. This method allowed for the ability to form heterocycles as well as two adjacent quaternary all-carbon stereocenters. The

reaction was found to not be going through a cascade mechanism when the [5+1] intermediate did not form the desired tricyclic product.<sup>109</sup>

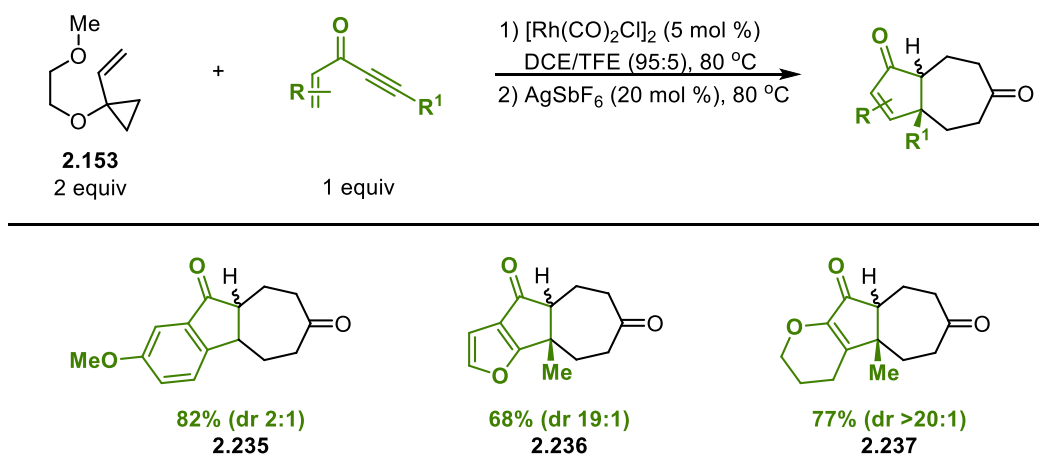
**Scheme 2.37.** Yu's [5+1]/[2+2+1] cycloaddition with VCPs, alkynes, and CO



Tandem cycloadditions have been investigated to form even more complex fused ring systems. Wender disclosed the first method of performing this transformation through a serial [5+2]/[4+2] cycloaddition using VCP **2.153** and commercially available dienophiles and terminal enynes to assemble tri-, tetra-, and pentacyclic structures in excellent yields (**Scheme 2.38**). This method was also scaled up to a 100 mmol scale and provided a 91% yield of the desired cycloadduct.<sup>110</sup>

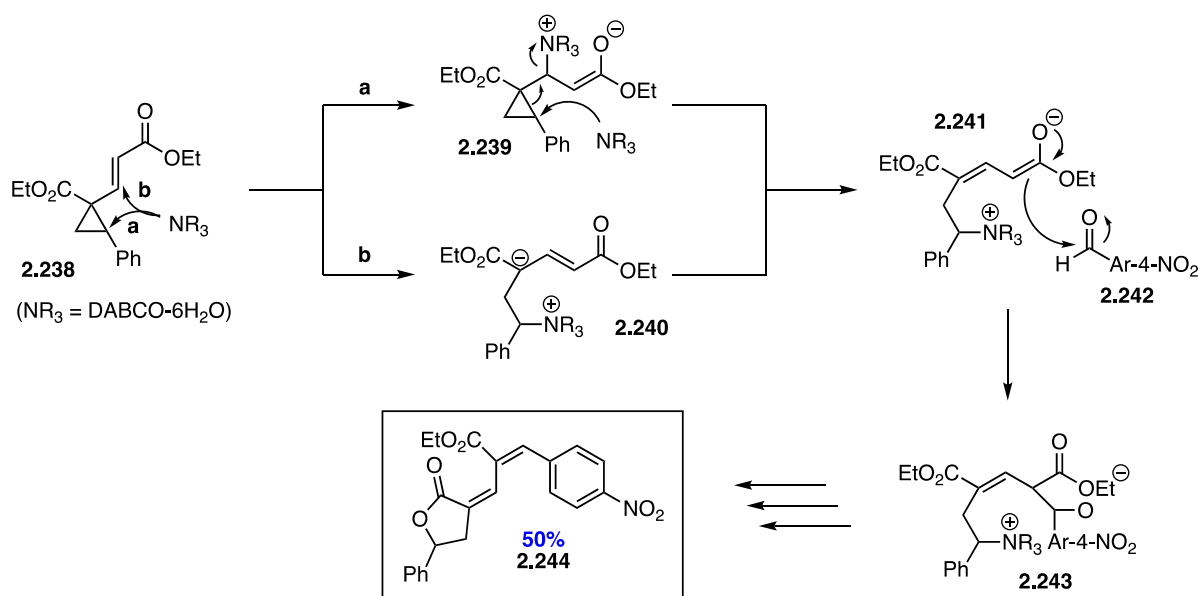
**Scheme 2.38.** Wender's serial [5+2]/[4+2] cycloaddition

Wender and co-workers followed up with the development of a tandem [5+2]/Nazarov cycloaddition to synthesize **2.235** – **2.237** in good yields (**Scheme 2.39**). This process was able to be completed in one pot using Rh(I) and  $\text{AgSbF}_6$ . In some cases, showed a very high degree of diastereoselectivity.<sup>111</sup>

**Scheme 2.39.** Tandem [5+2]/Nazarov cycloaddition

Wang reported a nucleophilic-promoted tandem domino process using activated VCPs and benzaldehydes in the presence of DABCO-6H<sub>2</sub>O to synthesize  $\alpha$ -methylene  $\gamma$ -butyrolactones in aqueous media (**Figure 2.15**). It was proposed that the base promotes ring-opening of the cyclopropane by either: 1) the formation of the Baylis-Hillman intermediate **2.239** and another equivalent of base attacking the cyclopropane or 2) nucleophilic attack of the cyclopropyl ring by the base (**2.240**). Both pathways lead to the formation of zwitterionic species **2.241**, which attacks **2.242** and, following dehydration, ring closing, and release of ethanol, provides **2.244** in 50% yield.<sup>112</sup>

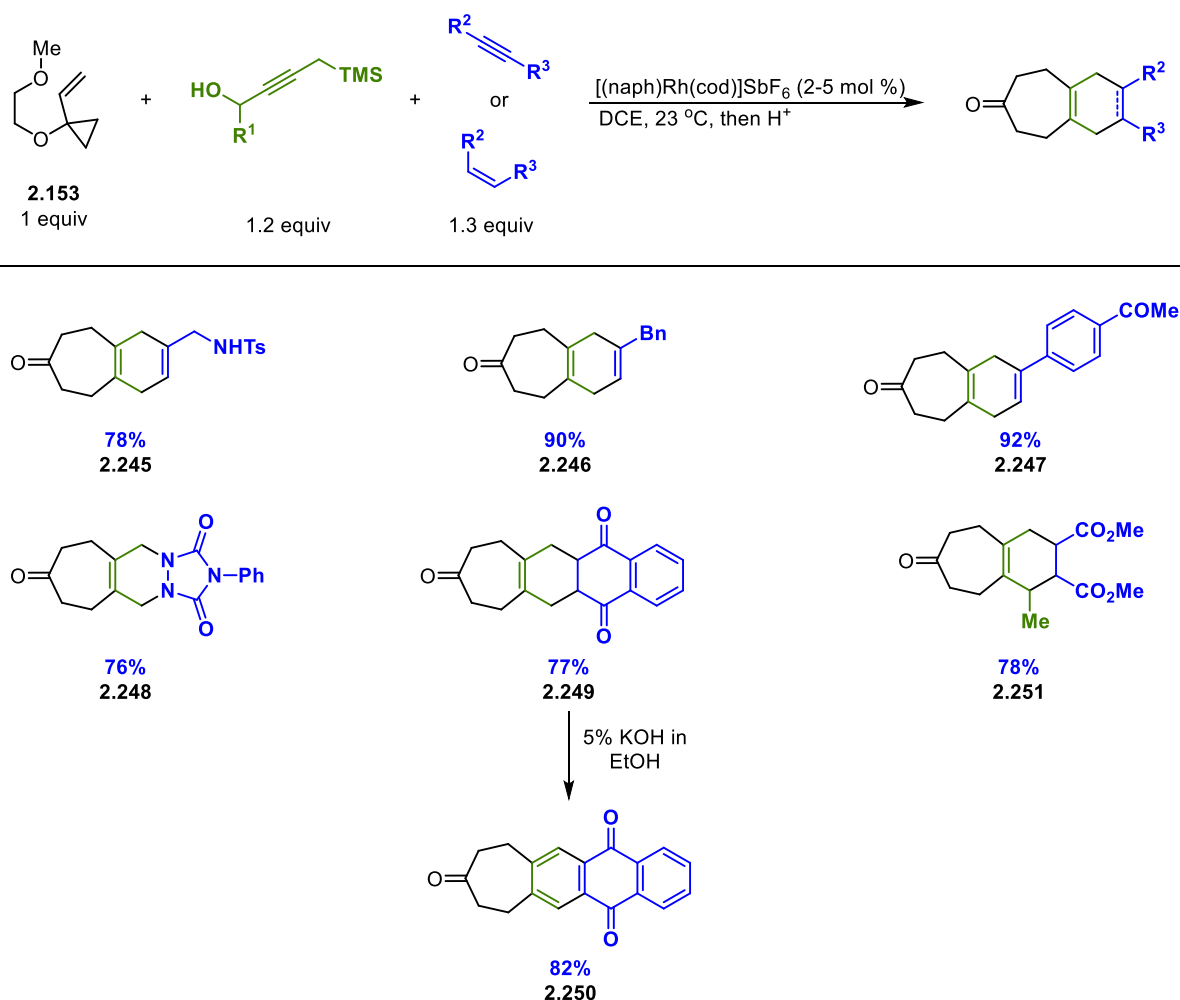
**Figure 2.15.** Mechanism of nucleophilic-promoted tandem domino reaction



Most recently, Wender reported a three-step tandem reaction in one pot to synthesize an array of polycyclic skeletons (**Scheme 2.40**). The initial step involves a [5+2] reaction with a VCP and a 1,2,3-butatriene equivalent to form the seven-membered cycloadduct. A diene is formed through a 1,4-Peterson elimination, then subsequently engages in a metal-catalyzed or thermal [4+2] cycloaddition. A variety of alkene and

alkyne dienophiles were able to be used as well as more substituted alkynes to build a library full of cycloheptanone-fused scaffolds (**2.245** – **2.251**). In addition, to extend this method as a way to synthesize a new family of kinase inhibitors, the cyclohexadienyl rings can undergo oxidation aromatization to form the core arenyl system, such as in **2.250**.<sup>113</sup>

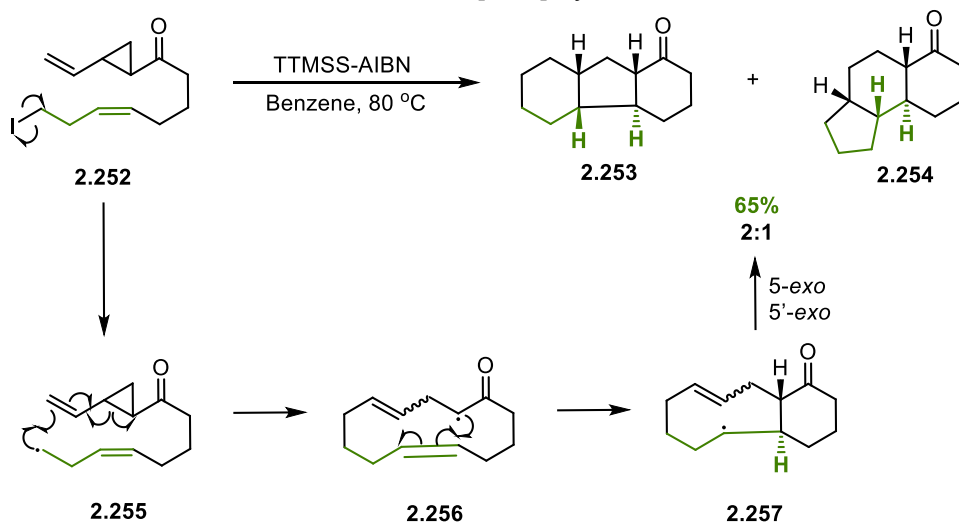
**Scheme 2.40.** Serial [5+2]/1,4-Peterson elimination/[4+2] reaction



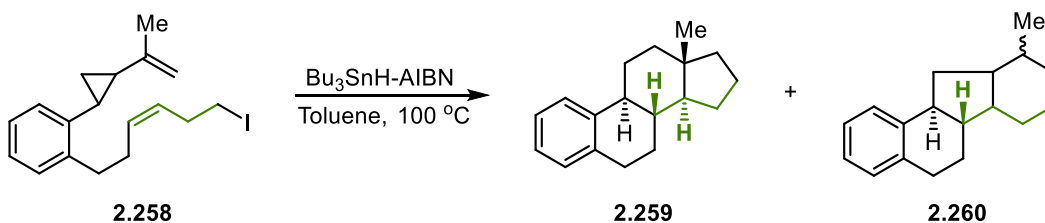
Pattenden and co-workers used their radical chemistry to develop a [5+4] cycloaddition with VCP **2.252** for the synthesis of tricyclic ketone products **2.253** and **2.254** (Scheme 2.41). The cyclization is initiated with TTMSS and AIBN to release iodide,

which then goes on to promote ring-opening of the cyclopropyl group to further go on and cyclize.<sup>114</sup> This strategy was also further developed as a radical cascade cyclization method for the synthesis of steroid frameworks (**Scheme 2.42**).<sup>115</sup>

**Scheme 2.41.** Pattenden's radical-initiated [5+4] cycloaddition



**Scheme 2.42.** Synthesis of steroid skeletons via radical cascade cyclizations



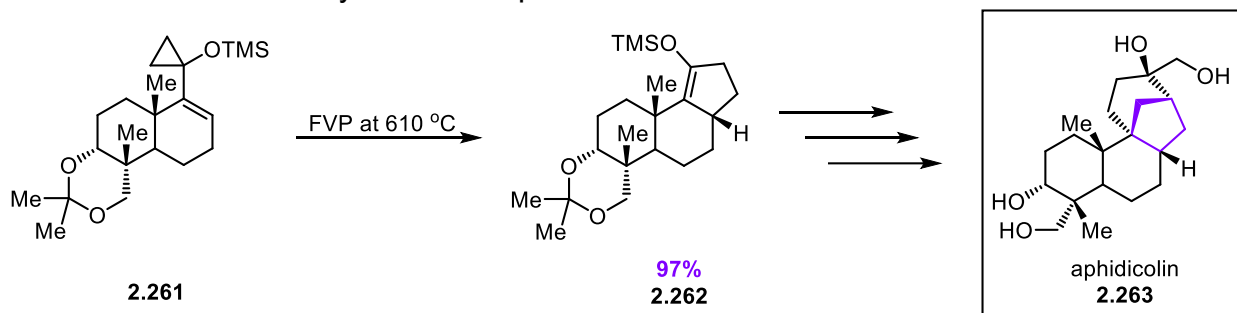
## 2.6. Total Syntheses using VCPs

### 2.6.1. VCP Rearrangements

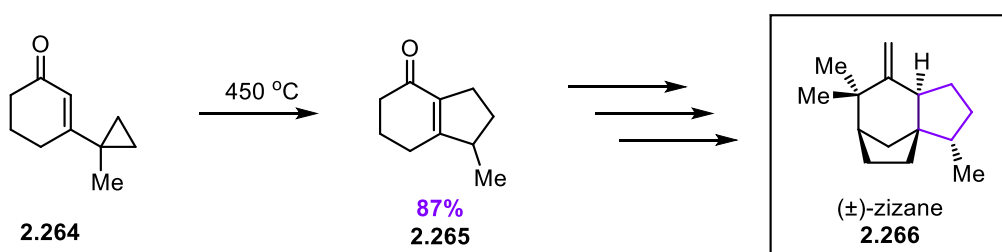
The use of the VCP rearrangement was utilized in initial steps for a total synthesis route. Trost and co-workers disclosed the first method toward their synthesis of aphidicolin in which, through a FVP strategy, they were able to assemble the

cyclopentene ring that would later be diversified to assemble the core cyclic structure (**Scheme 2.43**).<sup>116</sup> Piers also used this strategy as the initial step of his synthesis of (±)-zizane (**Scheme 2.44**).<sup>117</sup>

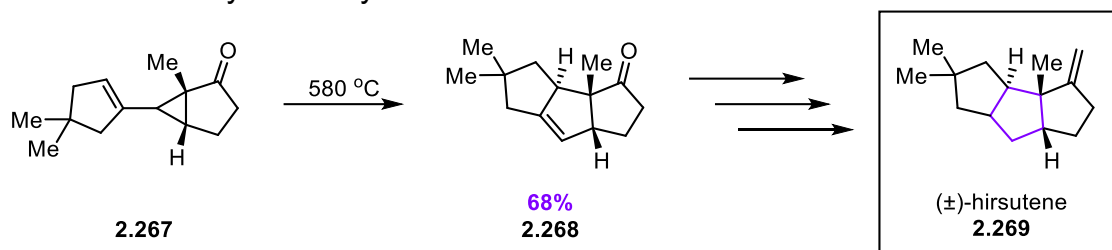
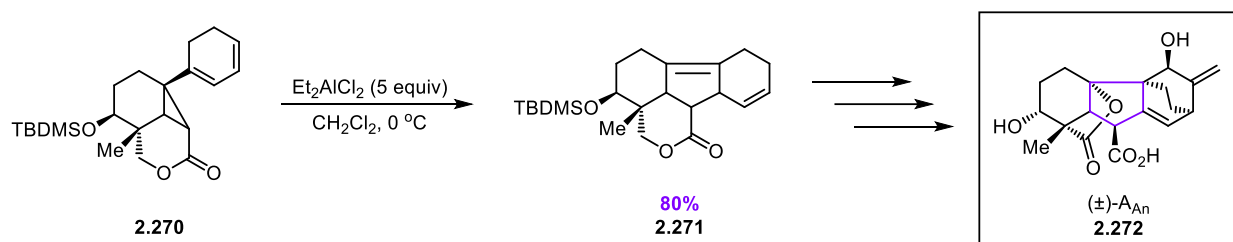
**Scheme 2.43.** Trost's synthesis of aphidicolin



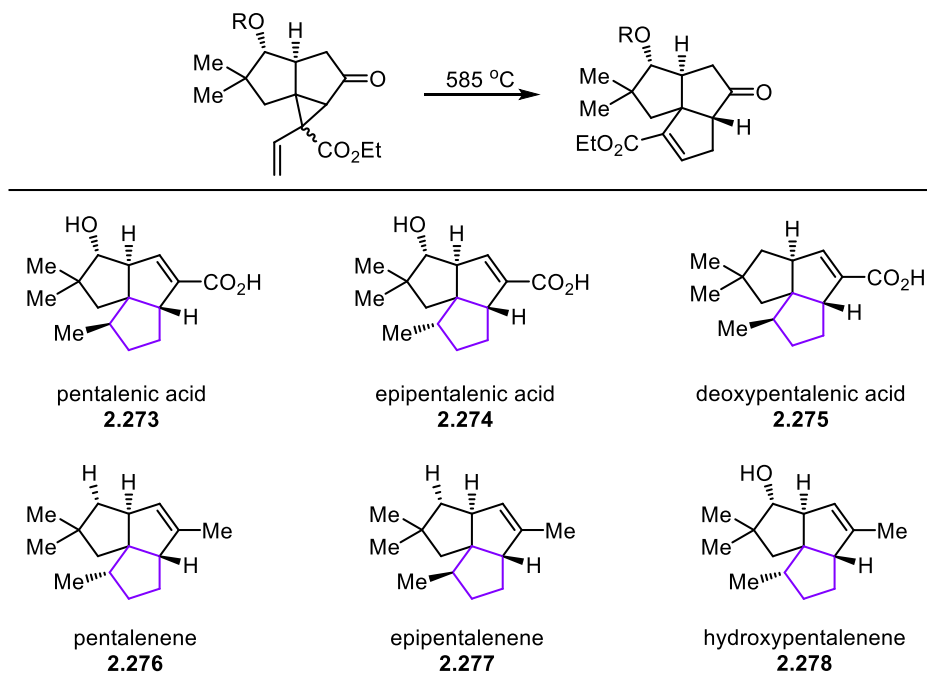
**Scheme 2.44.** Synthesis of (±)-zizane using VCP rearrangement



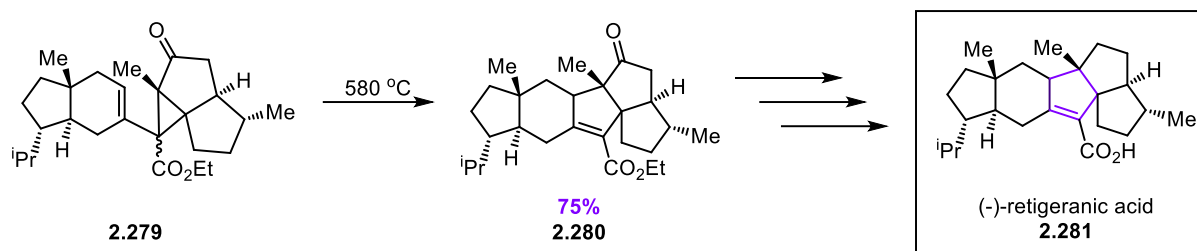
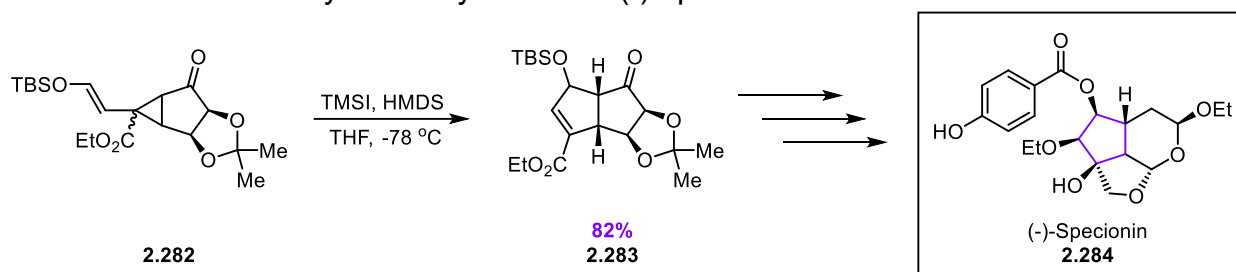
In other reports, the rearrangement of a VCP was essential to build the core scaffold of natural products. The first disclosed example from the Hudlicky group utilized the FVP method to form the tricyclic system in the synthesis of hirsutene in one step in 68% yield (**Scheme 2.45**).<sup>118</sup> Corey and co-workers followed up on this strategy in their formal synthesis of an antheridiogen growth factor ((±)-A<sub>AN</sub>) to construct a tetracyclic structure in 80% yield using Et<sub>2</sub>AlCl<sub>2</sub> (**Scheme 2.46**).<sup>119</sup>

**Scheme 2.45.** Corey's total synthesis of hirsutene**Scheme 2.46.** Lewis acid-promoted rearrangement in synthesis of (±)-A<sub>An</sub>

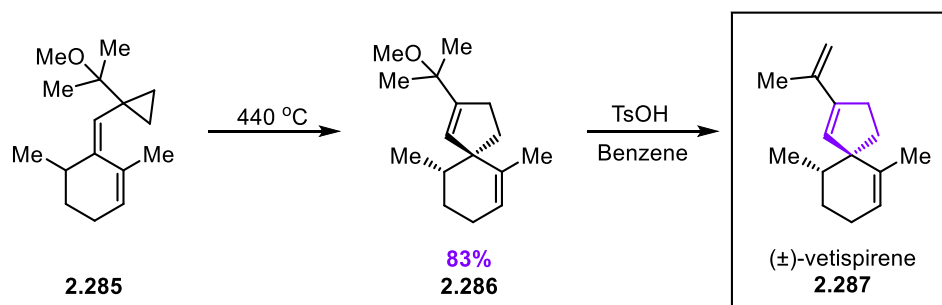
Hudlicky and co-workers later used the FVP of VCPs in order to form a tricyclic backbone from a 1-ester substituted VCP in moderate to good yields (**Figure 2.16**). This scaffold was then later diversified to form an array of natural products and their epimers (**2.273 – 2.278**).<sup>120</sup>

**Figure 2.16.** Hudlicky's synthesis of natural products and their epimers

Hudlicky disclosed a total synthesis of (-)-retigeranic acid in which VCP rearrangement was used in order to assemble the pentacyclic structure in 75% yield (**Scheme 2.47**).<sup>121</sup> Fleming and co-workers used this method a year later in their synthesis of **2.281**.<sup>122</sup> In addition, Hudlicky and co-workers reported a synthetic route to (-)-specionin to prepare the tricyclic core in 82% yield with the use of TMSI or  $t\text{BuNH}_4\text{F}$  at  $-78^{\circ}\text{C}$  (**Scheme 2.48**).<sup>123</sup>

**Scheme 2.47.** VCP rearrangement in the synthesis of (-)-retigeranic acid**Scheme 2.48.** Hudlicky's total synthesis of (-)-specionin

Paquette synthesized *spiro* compounds with the use of VCP thermal rearrangement of **2.285** in the total synthesis of ( $\pm$ )-vetispirene, which was completed in the subsequent acid-promoted elimination step (**Scheme 2.49**).<sup>124</sup>

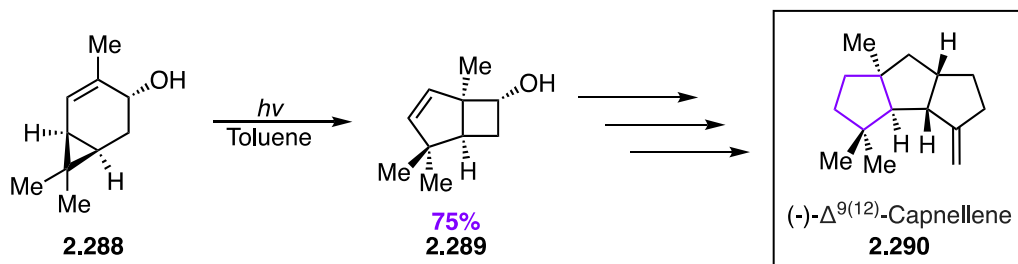
**Scheme 2.49.** Synthesis of ( $\pm$ )-vetispirene through thermal VCP rearrangement

The photochemical rearrangement of **2.288** leads to a [5,4] bicyclic structure in the first step of the total synthesis of (-)- $\Delta^{9(12)}$ -Capnellene by Sonawane (**Scheme 2.50a**).<sup>125</sup>

To prepare (+)-grandisol, the strained cyclobutane ring was synthesized using an endocyclic VCP rearrangement rather than having to employ the [2+2] photocycloaddition of ethylene to enones (**Scheme 2.50b**).<sup>125</sup>

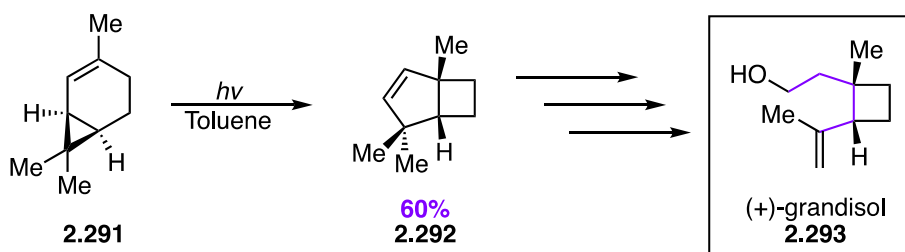
---

**Scheme 2.50a.** Sonawane's total synthesis of (-)- $\Delta^{9(12)}$ -Capnellene



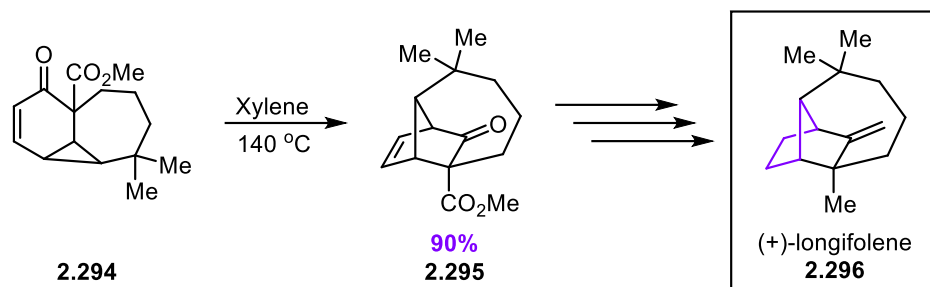

---

**Scheme 2.50b.** Synthesis of (+)-grandisol



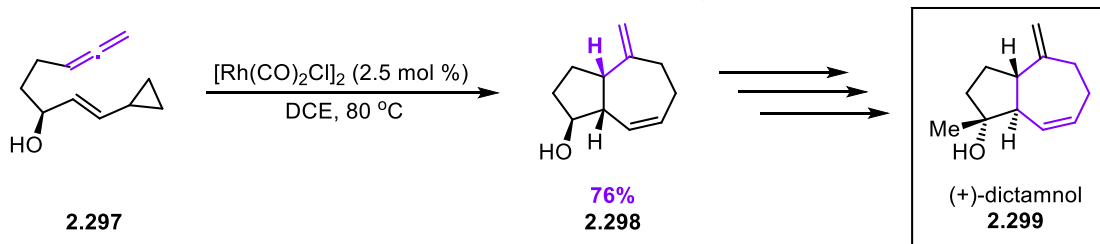
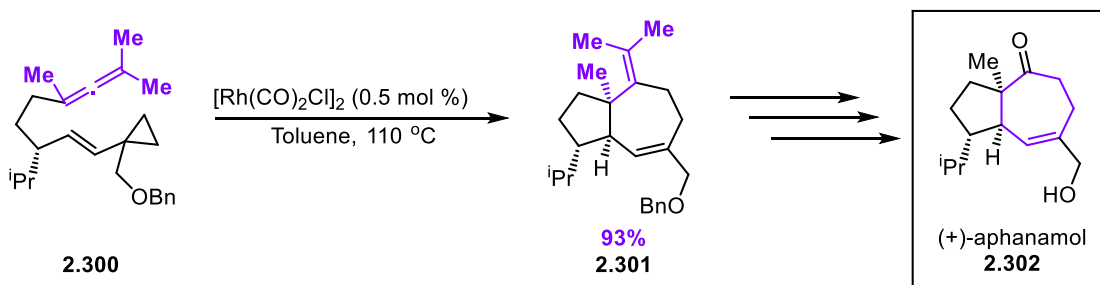

---

In an interesting transformation, refluxing VCP in xylene formed a complex framework in **2.295** in the total synthesis of tricyclic sesquiterpene (+)-longifolene (**Scheme 2.51**).<sup>126</sup>

**Scheme 2.51.** VCP rearrangement in the synthesis of (+)-longifolene


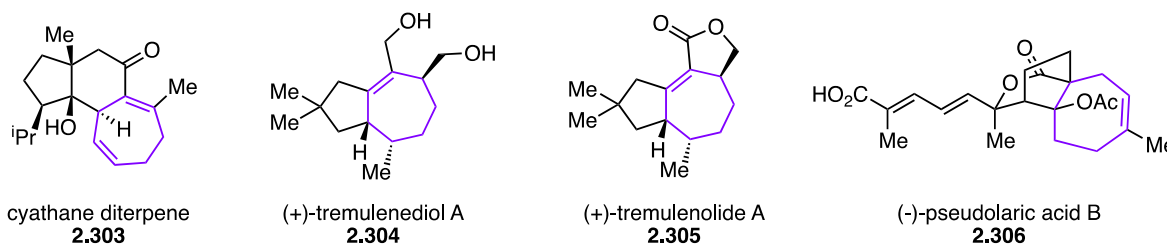
## 2.6.2. [5+2] Cycloadditions

Wender and co-workers used their Rh(I)-catalyzed intramolecular [5+2] cycloaddition between VCPs and allenes in the syntheses of (+)-dictamnol<sup>127</sup> and (+)-aphanamol<sup>128</sup> to assemble the [5,7] bicyclic systems (**Scheme 2.52a and b**).

**Scheme 2.52a.** Total synthesis of (+)-dictamnol through VCP cycloaddition

**Scheme 2.52b.** Intramolecular [5+2] cycloaddition with allenes in (+)-aphanamol synthesis


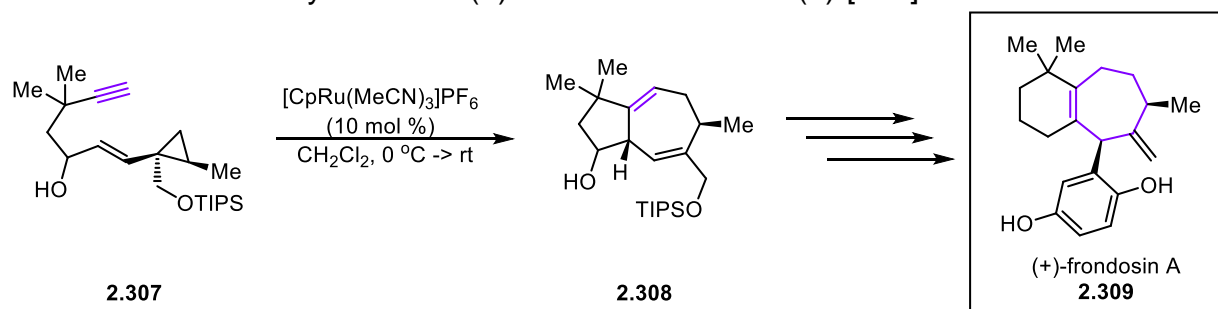
This approach with the use of alkynes as the two-atom component in this Rh(I)-catalyzed intramolecular cycloaddition was also used by Wender, Martin, and Trost in their syntheses of cyathane diterpenes,<sup>129</sup> (+)-tremulenediol A,<sup>130</sup> (+)-tremulenolide A,<sup>130</sup> and (-)-pseudolaric acid B,<sup>131</sup> respectively (**Figure 2.17**).

**Figure 2.17.** Structures of compounds synthesized via Rh(I)-catalyzed [5+2] cycloaddition with alkynes



Trost and co-workers were also able to use their previously reported Ru-catalyzed [5+2] cycloaddition in the total synthesis of (+)-frondosin A (**Scheme 2.53**).<sup>132</sup>

**Scheme 2.53.** Total synthesis of (+)-frondosin A with Ru(II)-[5+2] method

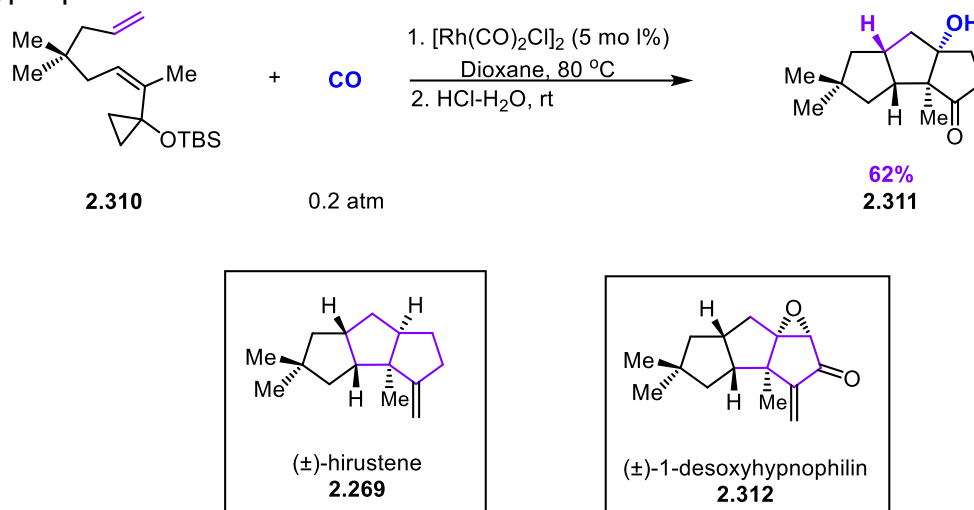


### 2.6.3. Rh(I)-[5+2+1] Cycloaddition

Yu and co-workers have done extensive work on the application of the Rh(I)-catalyzed [5+2+1] reaction in different ways. In their first report, the group disclosed using

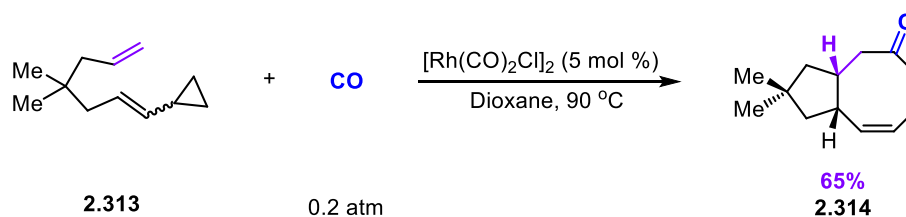
this method in a tandem aldol to form a tricyclic core in the preparation of (±)-hirsutene and (±)-1-desoxyhypnophilin (**Figure 2.18**).<sup>133</sup>

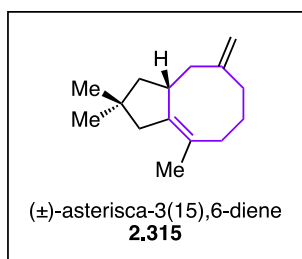
**Figure 2.18.** Tandem [5+2+1]/aldol reaction in synthesis of (±)-hirsutene and (±)-1-desoxyhypnophilin



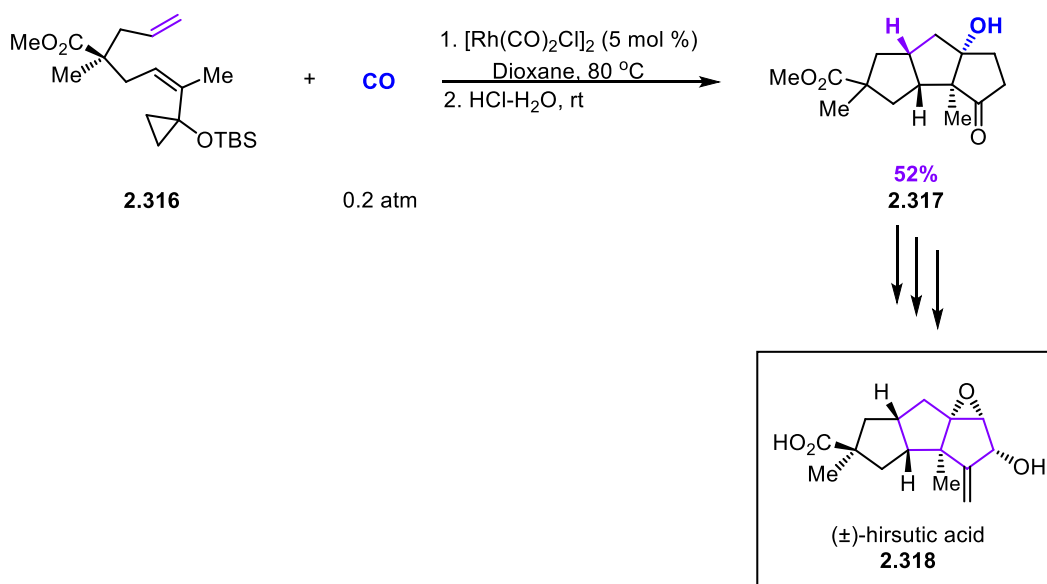
In a follow-up study, (+)- and (-)-hirsutene were prepared through an alternative [5+2+1] reaction to cyclooctene intermediate **2.314** (**Scheme 2.54**), which was later used for the racemic and asymmetric syntheses of hirsutene.<sup>134</sup> In addition, the group reported methods using this strategy for the total syntheses of pentalenene (**2.276**) and (±)-asterisca-3(15),6-diene (**2.315**).<sup>135</sup>

**Scheme 2.54.** [5+2+1] cycloaddition used in racemic and asymmetric synthesis of hirsutene



**Figure 2.19.** Structure of (±)-asterisca-3(15),6-diene

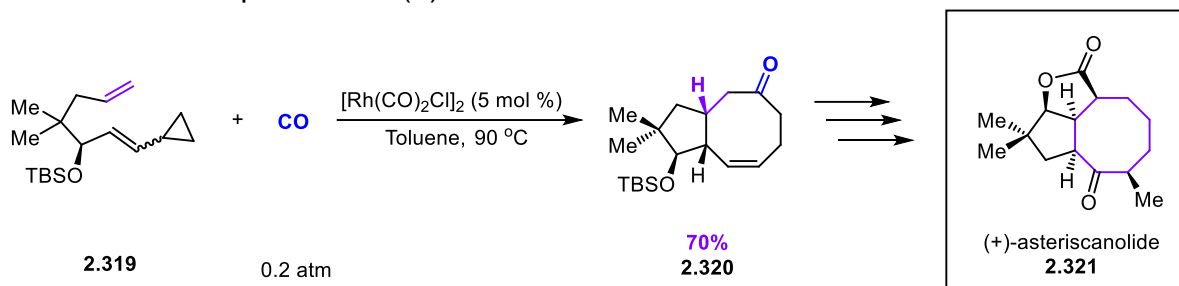
In the synthesis of (±)-hirsutic acid (**2.318**), **2.316** was subjected to the Rh-catalyzed [5+2+1] and acid-promoted aldol reaction to form **2.317** as a racemic mixture in 52% yield to form the tricyclic framework in one step (**Scheme 2.55**).<sup>136</sup>

**Scheme 2.55.** Preparation of (±)-hirsutic acid via tandem [5+2+1]/aldol reaction

Most recently, the [6.3.0] core structure of (+)-asteriscanolide was prepared through the Rh-catalyzed [5+2+1] intramolecular cycloaddition (**Scheme 2.56**). The

bridging butyrolactone ring in **2.321** was later constructed with the radical cyclization of a selenocarbonate in the presence of AIBN and  $n\text{Bu}_3\text{SnH}$ .<sup>137</sup>

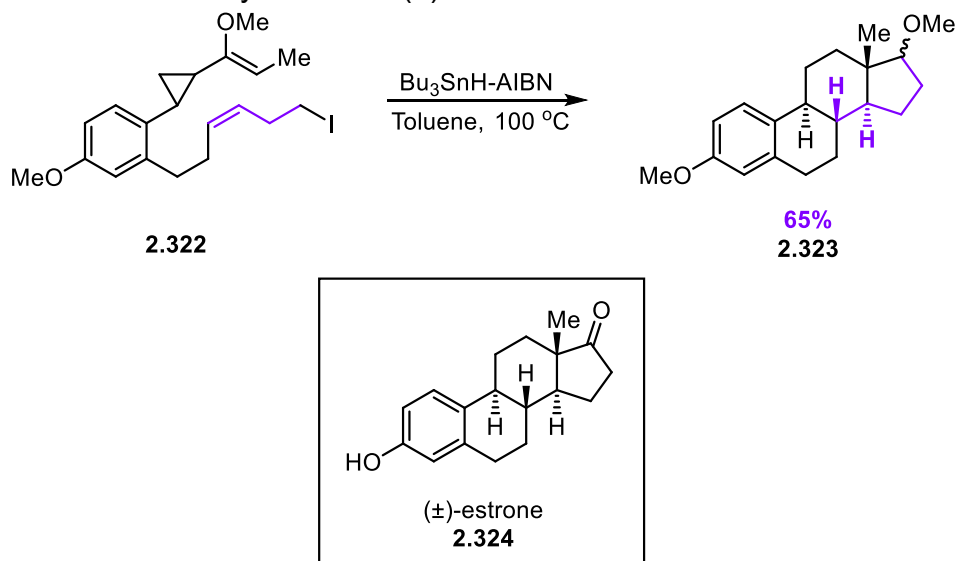
**Scheme 2.56.** Preparation of (+)-asteriscanolide



#### 2.6.4. Radical cascade cyclization

Pattenden successfully constructed the tetracyclic framework of ( $\pm$ )-estrone in one step through a radical cascade cyclization initiated with  $\text{Bu}_3\text{SnH}$  and AIBN to synthesize estrone methyl ester **2.323** in 65% yield (**Figure 2.32**).<sup>115</sup>

**Figure 2.20.** Pattenden's synthesis of ( $\pm$ )-estrone via radical initiation



## 2.7. Conclusions

While VCPs have long been used for rearrangements, they also have been studied as a unique synthon to engage in multi-component cycloadditions both intra- and intermolecularly. Using alkynes, alkenes, allenes, and CO as coupling partners, complex structures have been synthesized with VCPs. These strategies have also been shown to be successful in the total synthesis of both natural products and bioactive compounds. While this field has progressed in the past few decades, using a different one-atom component from CO remains relatively unexplored aside from two studies. This inspired our interest in developing this field further to include nitrogen heterocycles in the library of structural motifs that can be accessed through VCPs.

## 2.8. References

- (1) Neureiter, N. P. *J. Org. Chem.*, **1959**, *24*, 2044.
- (2) Schulze, M. M.; Gockel, U. *Tetrahedron Lett.* **1996**, *37*, 357.
- (3) Suzuki, M.; Sawada, S.; Yoshida, S.; Eberhardt, A.; Saegusa, T. *Macromolecules* **1993**, *26*, 4748.
- (4) Mori, T.; Nakamura, T.; Kimura, M. *Org. Lett.* **2011**, *13*, 2266.
- (5) Wu, J.-Q.; Qiu, Z.-P.; Zhang, S.-S.; Liu, J.-G.; Lao, Y.-X.; Gu, L.-Q.; Huang, Z.-S.; Li, J.; Wang, H. *Chem. Commun.* **2015**, *51*, 77.
- (6) Dieskau, A. P.; Holzwarth, M. S.; Plietker, B. *J. Am. Chem. Soc.* **2012**, *134*, 5048.
- (7) Ieki, R.; Kani, Y.; Tsunoi, S.; Shibata, I. *Chem. Eur. J.* **2015**, *21*, 6295.
- (8) Hirata, G.; Onodera, G.; Kimura, M. *Synlett* **2014**, *25*, 2306.

- (9) Ganesh, V.; Kundu, T.; Chandrasekaran, S. *Tetrahedron* **2014**, 70, 7268.
- (10) Jiao, L.; Ye, S.; Yu, Z.-X. *J. Am. Chem. Soc.* **2008**, 130, 7178.
- (11) Lin, M.; Kang, G.-Y.; Guo, Y.-A.; Yu, Z.-X. *J. Am. Chem. Soc.* **2012**, 134, 398.
- (12) Bowman, R. K.; Johnson, J. S. *Org. Lett.* **2006**, 8, 573.
- (13) Morizawa, Y.; Hiyama, T.; Nozaki, H. *Tetrahedron Lett.* **1981**, 22, 2297.
- (14) Shimizu, I.; Ohashi, Y.; Tsuji, J. *Tetrahedron Lett.* **1985**, 26, 3825.
- (15) Laugeois, M.; Ponra, S.; Ratovelomanana-Vidal, V.; Michelet, V.; Vitale, M. R. *Chem. Commun.* **2016**, 52, 5332.
- (16) Pursely, D.; Plietker, B. *Synlett* **2014**, 25, 2316.
- (17) Cui B, Ren J, Wang Z. *J. Org. Chem.* **2014**, 79, 790.
- (18) Chakrabarty, S.; Chatterjee, I.; Wibbeling, B.; Daniliuc, C. G.; Studer, A. *Angew. Chem., Int. Ed.* **2014**, 53, 5964.
- (19) Yamamoto, K.; Ishida, T.; Tsuji, J. *Chem. Lett.* **1987**, 16, 1157.
- (20) Mondal, M.; Panda, M.; McKee, V.; Kerrigan, N. J. *J. Org. Chem.* **2019**, 84, 11983.
- (21) Pohlhaus, P. D.; Sanders, S. D.; Parsons, A. T.; Li, W.; Johnson, J. S. *J. Am. Chem. Soc.* **2008**, 130, 8642.
- (22) Trost, B. M.; Morris, P. J. *Angew. Chem., Int. Ed.* **2011**, 50, 6167.
- (23) Mei, L.-Y.; Wei, Y.; Xu, Q.; Shi, M. *Organometallics*, **2013**, 32, 3544.
- (24) Cao, B.; Mei, L.-Y.; Li, X.-G.; Shi, M. *RSC Adv.* **2015**, 5, 92545.
- (25) Overberger, C. G.; Borchert, A. E. *J. Am. Chem. Soc.* **1960**, 82, 1007.
- (26) Trost, B. M.; Keeley, D. E. *J. Am. Chem. Soc.* **1976**, 98, 248.
- (27) Miller, R. D. *J. Chem. Soc., Chem. Commun.* **1976**, 277.

- (28) Trost, B. M.; Bogdanowicz, M. J. *J. Am. Chem. Soc.* **1973**, *95*, 5311.
- (29) Thies, R. W. *J. Chem. Soc. D*, **1971**, 237.
- (30) Trost, B. M.; Scudder, P. H. *J. Org. Chem.* **1981**, *46*, 506.
- (31) Simpson, J. M.; Richey, H. G. *Tetrahedron Lett.* **1973**, *27*, 2545.
- (32) Corey, E. J.; Wollenberg, R. H. *J. Org. Chem.* **1975**, *40*, 2265.
- (33) Keyaniyan, S.; Apel, M.; Richmond, J. P.; de Meijere, A. *Angew. Chem., Int. Ed.* **1985**, *97*, 763.
- (34) Binger, P.; Wedemann, P.; Kozhushkov, S. I.; de Meijere, A. *Eur. J. Org. Chem.* **1998**, 113.
- (35) de Meijere, A.; Kozhushkov, S. I.; Faber, D.; Bagutskii, V.; Boese, R.; Haumann, T.; Walsh, R. *Eur. J. Org. Chem.* **2001**, 3607.
- (36) Brandi, A.; Cicchi, S.; Brandl, M.; Kozhushkov, S. I.; de Meijere, A. *Synlett* **2001**, 433.
- (37) Paquette, L. A.; Meehan, G. V.; Eisember, R. F. *Tetrahedron. Lett.*, **1969**, *10*, 995.
- (38) Paquette, L. A.; Meehan, G. V.; Henzel, R. P.; Eizember, R. F. *J. Org. Chem.* **1973**, *38*, 3250.
- (39) Sonawane, H. R.; Bellur, N. S.; Kulkarni, D. G.; Ahuja, J. R. *Synlett* **1993**, 875.
- (40) N. W. Alcock; J. M. Brown; J. A. Conneely; D. H. Williamson, *J. Chem. Soc. Perkin Trans 2*, **1979**, 962.
- (41) Hudlicky, T.; Koszyk, F. F.; Kutchan, T. M.; Sheth, J. P. *J. Org. Chem.* **1980**, *45*, 5020.
- (42) Murakami, M.; Nishida, S. *Chem. Lett.* **1979**, 927.

- (43) Zuo, G.; Louie, J. *Angew. Chem., Int. Ed.*, **2004**, 43, 2277.
- (44) Wang, S. C.; Troast, D. M.; Conda-Sheridan, M.; Zuo, G.; LaGarde, D.; Louie, J.; Tantillo, D. J. *J. Org. Chem.* **2009**, 74, 7822.
- (45) Morizawa, Y.; Oshima, K.; Nozaki, H. *Tetrahedron Lett.* **1982**, 23, 2871.
- (46) Danheiser, R. L.; Martinez-Davila, C.; Morin, Jr, J. M. *J. Org. Chem.* **1980**, 45, 1340.
- (47) Danheiser, R. L.; Martinez-Davila, C.; Auchus, R. J.; Kadonga, J. T. *J. Am. Chem. Soc.* **1981**, 103, 2443.
- (48) Sakito, Y.; Suzukamo, G. *Chem. Lett.* **1986**, 15, 621.
- (49) Thangamani, M.; Srinivasan, K. *J. Org. Chem.* **2018**, 83, 571.
- (50) Maeta, N.; Kamiya, H.; Okada, Y. *J. Org. Chem.* **2020**, 85, 6551.
- (51) Li, X.; Zhang, M.; Shu, D.; Robichaux, P. J.; Huang, S.; Tang, W. *Angew. Chem., Int. Ed.* **2011**, 50, 10421.
- (52) Koskinen, A. M. P.; Muñoz, L.; Rissanen, K. *J. Chem. Soc., Chem. Commun.* **1993**, 491.
- (53) Herbert, N.; Pattenden, G. *Synlett* **1997**, 1, 69.
- (54) Victor, R.; Ben-Shoshan, R.; Sarel, S. *Tetrahedron Lett.* **1970**, 4253.
- (55) Taber, D. F.; Kanai, K.; Jiang, Q.; Bui, G. *J. Am. Chem. Soc.* **2000**, 122, 6807.
- (56) Taber, D. F.; Joshi, P. V.; Kanai, K. *J. Org. Chem.* **2004**, 69, 2268.
- (57) Schulze, M. M.; Gockel, U. *Tetrahedron Lett.* **1996**, 37, 357.
- (58) Schulze, M. M.; Gockel, U. *J. Organomet. Chem.* **1996**, 525, 155.
- (59) Liu, C. H.; Zhuang, Z.; Bose, S.; Yu, Z. X. *Tetrahedron* **2016**, 72, 2752.
- (60) Kurahashi, T.; de Meijere, A. *Synlett.*, **2005**, 15, 2619.

- (61) Jiang, G.-J.; Fu, X.-F.; Li, Q.; Yu, Z.-Z. *Org. Lett.*, **2012**, *14*, 692.
- (62) Farley, C. M.; Sasakura, K.; Zhou, Y.-Y.; Kanale, V. V.; Uyeda, C. *J. Am. Chem. Soc.* **2020**, *142*, 4598.
- (63) Silylium-ion promoted (5+1) cycloaddition of aryl-substituted VCPs and hydrosilanes involving aryl migration. *Angew Chem Int Ed* **2020**
- (64) Wender, P. A.; Takahashi, H.; Witulski, B. *J. Am. Chem. Soc.* **1995**, *117*, 4720.
- (65) Khusnutdinov, R. I.; Dzhemiley, U. M. *J. Organomet. Chem.* **1994**, *471*, 1.
- (66) Wender, P. A.; Sperandio, D. *J. Org. Chem.* **1998**, *63*, 4164.
- (67) Wender, P. A.; Dyckman, A. J. *Org. Lett.*, **1999**, *1*, 2089.
- (68) Paik, S.-J.; Son, S. U.; Chung, Y. K. *Org. Lett.* **1999**, *1*, 2045.
- (69) Wender, P. A.; Williams, T. J. *Angew. Chem. Int. Ed.* **2002**, *41*, 4550.
- (70) Gómez, F. J.; Kamber, N. E.; Deschamps, N. M.; Cole, A. P.; Wender, P. A.; Waymouth, R. M. *Organometallics* **2007**, *26*, 4541.
- (71) Mustard, T. J. L.; Wender, P. A.; Cheong, P. H.-Y. *ACS Catal.* **2015**, *5*, 1758.
- (72) Wender, P. A.; Love, J. A.; Williams, T. J. *Synlett*, **2003**, 1295.
- (73) Lee, S. I.; Park, S. Y.; Park, J. H.; Jung, I. G.; Choi, S. Y.; Chung, Y. K.; Lee, B. Y. *J. Org. Chem.*, **2006**, *71*, 91.
- (74) Ashfeld, B. L.; Miller, K. A.; Smith, A. J.; Tran, K.; Martin, S. F. *J. Org. Chem.* **2007**, *72*, 9018.
- (75) Shintani, R.; Nakatsu, H.; Takatsu, K.; Hayashi, T. *Chem. Eur. J.* **2009**, *15*, 8692.
- (76) Trost, B. M.; Toste, F. D. *Tetrahedron Lett.* **1999**, *40*, 7739.
- (77) Trost, B. M.; Toste, F. D.; Shen, H. *J. Am. Chem. Soc.* **2000**, *122*, 2379.

- (78) Trost, B. M.; Shen, H. C. *Angew. Chem., Int. Ed.* **2001**, 40, 2313.
- (79) Trost, B. M.; Shen, H. C. *Org. Lett.* **2000**, 2, 2523.
- (80) Trost, B. M.; Shen, H. C.; Schulz, T.; Koradin, C.; Schirok, H. *Org. Lett.* **2003**, 5, 4149.
- (81) Hong, X.; Trost, B. M.; Houk, K. N. *J. Am. Chem. Soc.* **2013**, 135, 6588.
- (82) Fürstner, A.; Majima, K.; Martín, R.; Krause, H.; Kattnig, E.; Goddard, R.; Lehmann, C. W. *J. Am. Chem. Soc.* **2008**, 130, 1992.
- (83) Zuo, G.; Louie, J. *J. Am. Chem. Soc.*, **2005**, 127, 5798.
- (84) Hong, X.; Liu, P.; Houk, K. N. *J. Am. Chem. Soc.*, **2013**, 135, 1456.
- (85) Wender, P. A.; Rieck, H.; Fujii, M. *J. Am. Chem. Soc.* **1998**, 120, 10976.
- (86) Wender, P. A.; Dyckman, A. J.; Husfeld, C. O.; Scanio, M. J. C. *Org. Lett.*, **2000**, 2, 1609.
- (87) Wender, P. A.; Barzilay, C. M.; Dyckman, A. J. *J. Am. Chem. Soc.* **2001**, 123, 179.
- (88) Yu, Z.-X.; Wender, P. A.; Houk, K. N. *J. Am. Chem. Soc.* **2004**, 126, 9154.
- (89) Liu, P.; Cheong, P. H.-Y.; Yu, Z.-X.; Wender, P. A.; Houk, K. N. *Angew. Chem., Int. Ed.*, **2008**, 47, 3939.
- (90) Liu, P.; Sirois, L. E.; Cheong, P. H.-Y.; Yu, Z.-X.; Hartung, I. V.; Rieck, H.; Wender, P. A.; Houk, K. N. *J. Am. Chem. Soc.*, **2010**, 132, 10127.
- (91) Wender, P. A.; Sirois, L. E.; Stemmler, R. T.; Williams, T. J. *Org. Lett.* **2010**, 12, 1604.
- (92) Wender, P. A.; Inagaki, F.; Pfaffenbach, M.; Stevens, M. C. *Org. Lett.* **2014**, 16, 2923.

- (93) Wender, P. A.; Ebner, C.; Fennell, B. D.; Inagaki, F.; Schröder, B. *Org. Lett.* **2017**, *19*, 5810.
- (94) Singh, A.; Sharp, P. R. *Organometallics* **2006**, *25*, 678.
- (95) Wender, P. A.; Lesser, A. B.; Sirois, L. E. *Angew. Chem., Int. Ed.*, **2012**, *51*, 2736.
- (96) Xu, X.; Liu, P.; Lesser, A.; Sirois, L. E.; Wender, P. A.; Houk, K. N. *J. Am. Chem. Soc.*, **2012**, *134*, 11012.
- (97) Melcher, M.-C.; von Wachenfeldt, H.; Sundin, A.; Strand, D. *Chem. Eur. J.*, **2015**, *21*, 531.
- (98) Wender, P. A.; Husfeld, C. O.; Langkopf, E.; Love, J. A. *J. Am. Chem. Soc.* **1998**, *120*, 1940.
- (99) Wender, P. A.; Haustedt, L. O.; Lim, J.; Love, J. A.; Williams, T. J.; Yoon, J.-Y. *J. Am. Chem. Soc.* **2006**, *128*, 6302.
- (100) Wender, P. A.; Glorius, F.; Husfeld, C. O.; Langkopf, E.; Love, J. A. *J. Am. Chem. Soc.*, **1999**, *121*, 5348.
- (101) Wegner, H. A.; de Meijere, A.; Wender, P. A. *J. Am. Chem. Soc.* **2005**, *127*, 6530.
- (102) Hong, X.; Stevens, M. C.; Liu, P.; Wender, P. A.; Houk, K. N. *J. Am. Chem. Soc.*, **2014**, *136*, 17273–17283.
- (103) Z.-X. Yu, P. H.-Y. Cheong, P. Liu, C. Y. Legault, P. A. Wender and K. N. Houk, *J. Am. Chem. Soc.*, **2008**, *130*, 2378–2379.
- (104) Wender, P. A.; Gamber, G. G.; Hubbard, R. D.; Zhang, L. *J. Am. Chem. Soc.* **2002**, *124*, 2876.

- (105) Wegner, H. A.; de Meijere, A.; Wender, P. A. *J. Am. Chem. Soc.* **2005**, *127*, 6530.
- (106) Wang, Y.; Wang, J.; Su, J.; Huang, F.; Jiao, L.; Liang, Y.; Yang, D.; Zhang, S.; Wender, P. A.; Yu, Z.-X. *J. Am. Chem. Soc.* **2007**, *129*, 10060.
- (107) Huang, F.; Yao, Z.-K.; Wang, Y.; Wang, Y.; Zhang, J.; Yu, Z.-X. *Chem. Asian J.* **2010**, *5*, 1555.
- (108) Wender, P. A.; Gamber, G. G.; Hubbard, R. D.; Pham, S. M.; Zhang, L. *J. Am. Chem. Soc.* **2005**, *127*, 2836.
- (109) Lin, M.; Li, F.; Jiao, L.; Yu, Z.-X. *J. Am. Chem. Soc.* **2011**, *133*, 1690.
- (110) Wender, P. A.; Gamber, G. G.; Scanio, M. J. C. *Angew. Chem. Int. Ed.* **2001**, *40*, 3895.
- (111) P. A. Wender, P. A.; R. T. Stemmler, R. T.; and L. E. Sirois, *J. Am. Chem. Soc.*, **2010**, *132*, 2532.
- (112) Du, D.; Wang, Z. *Tetrahedron Lett.* **2008**, *49*, 956.
- (113) Wender, P. A.; Fournogerakis, D. N.; Jeffreys, M. S.; Quiroz, R. V.; Inagaki, F.; Pfaffenbach, M. *Nat. Chem.* **2014**, *6*, 448.
- (114) Pattenden, G.; Wiedenau, P. *Tetrahedron Lett.* **1997**, *38*, 3647-3650
- (115) Pattenden, G.; Gonzalez, M. A.; McCulloch, S.; Walter, A.; Woodhead, S. J. *PNAS* **2004**, *101*, 12024.
- (116) Trost, B. M.; Nishimura, Y.; Yamamoto, K.; McElvain, S. S. *J. Am. Chem. Soc.* **1979**, *101*, 1328.
- (117) Piers, E.; Banville, J. *J. Chem. Soc. Chem. Commun.* **1979**, 1138.

- (118) Hudlicky, T.; Kutchan, T. M.; Wilson, S. R.; Mao, D. T. *J. Am. Chem. Soc.* **1980**, *102*, 6351.
- (119) Corey, E. J.; Myers, A. G. *J. Am. Chem. Soc.* **1985**, *107*, 5574.
- (120) Hudlicky, T.; Sinai-Zingde, G.; Natchus, M. G.; Ranu, B. C.; Papadopoulos, P. *Tetrahedron* **1987**, *43*, 5685.
- (121) Hudlicky, T.; Radesca-Kwart, L.; Li, L.; Bryant, T. *Tetrahedron Lett.* **1988**, *29*, 3283.
- (122) Fleming, A.; Radesca, L. *J. Am. Chem. Soc.* **1989**, *111*, 6691.
- (123) Hudlicky, T.; Natchus, M. G. *J. Org. Chem.* **1992**, *57*, 4740.
- (124) Yan, T.-H.; Paquette, L. A. *Tetrahedron Lett.* **1982**, *23*, 3227.
- (125) Sonawane, H. R.; Naik, V. G.; Bellur, N. S.; Shah, V. G.; Purohit, P. C.; Kumar, M. U.; Kulltarni, D. G.; Ahuja, J. R. *Tetrahedron* **1991**, *47*, 8259.
- (126) Schultz, A. G.; Puig, S. *J. Org. Chem.* **1985**, *50*, 915.
- (127) Wender, P. A.; Fuji, M.; Husfeld, C. O.; Love, J. A. *Org. Lett.* **1999**, *1*, 137.
- (128) Wender, P. A.; Zhang, L. *Org. Lett.* **2000**, *2*, 2323.
- (129) Wender, P. A.; Bi, F. C.; Brodney, M. A.; Gosselin, F. *Org. Lett.* **2001**, *3*, 2105.
- (130) Ashfeld, B. L.; Martin, S. F. *Org. Lett.* **2005**, *7*, 4535.
- (131) Trost, B. M.; Waser, J.; Meyer, A. *J. Am. Chem. Soc.* **2007**, *129*, 14556.
- (132) Trost, B. M.; Hu, Y.; Horne, D. B. *J. Am. Chem. Soc.* **2007**, *129*, 11781.
- (133) Jiao, L.; Yuan, C.; Yu, Z.-X. *J. Am. Chem. Soc.* **2008**, *130*, 4421.
- (134) Fan, X.; Tang, M.-X.; Zhuo, L.-G.; Tu, Y. Q.; Yu, Z.-X. *Tetrahedron Lett.* **2009**, *50*, 155.
- (135) Fan, X.; Zhuo, L.-G.; Tu, Y. Q.; Yu, Z.-X. *Tetrahedron* **2009**, *65*, 4709.

- (136) Yuan, C.; Jiao, L.; Yu, Z.-X. *Tetrahedron Lett.* **2010**, 51, 5674.
- (137) Liang, Y.; Jiang, X.; Yu, Z.-X. *Chem. Commun.* **2011**, 47, 6659.

## Chapter 3

### *Rh(II)-Catalyzed Nitrene-Transfer [5+1] Cycloadditions of Vinylcyclopropanes*

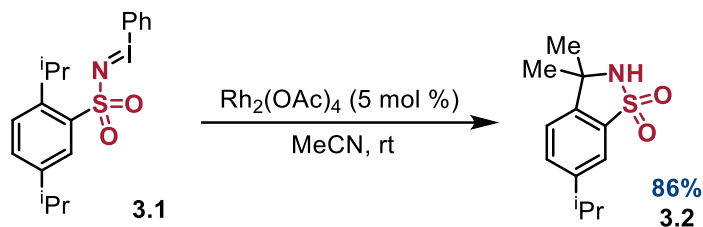
#### 3.1. Introduction

Nitrogen-containing heterocycles appear in the majority of FDA-approved drugs, piperidine being the most abundant.<sup>1</sup> Even so, the diversity of substitution patterns that are available via practical synthetic methods is still quite limited, so new methods for N-heterocycle synthesis are sought.<sup>2</sup> A potential area of study to address this problem is through the use of nitrenes and metallonitrenes as one-atom components in nitrene-transfer cycloaddition reactions. Prior to our work, literature examples of the use of nitrene precursors in intermolecular cycloadditions were restricted to five membered ring synthesis through [4+1] or [2+2+1] cycloadditions.<sup>3-6</sup> Herein, we report the first synthesis of six membered heterocycles via a [5+1] cycloaddition. Vinylcyclopropanes (VCPs) were used as five-atom components in combination with nitrene precursors. In this initial work, we were able to use 2,4-diaryl vinylcyclopropanes to synthesize 2,5-substituted tetrahydropyridines using  $\text{Rh}_2(\text{esp})_2$  as the nitrene transfer catalyst.

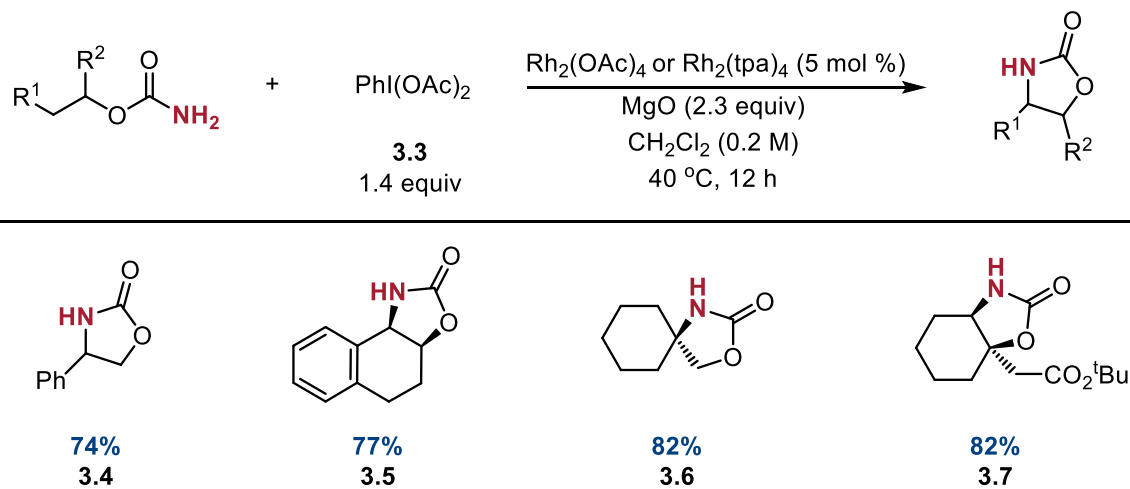
#### 3.2. Overview of Rh(II) as a Nitrene Transfer Catalyst

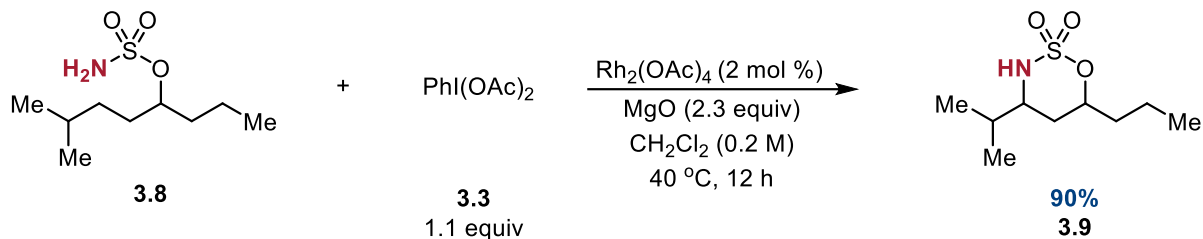
##### *3.2.1 Intramolecular C-H amination*

The first example of Rh(II) species being used as a catalyst for intramolecular nitrene transfer was reported by Breslow and Gellman in 1983 (**Scheme 3.1**). In this seminal work, an imidoiodobenzene derivative in the presence of  $\text{Rh}_2(\text{OAc})_4$  underwent C-H insertion to form bicyclic product **3.2** in 86% yield.<sup>7</sup>

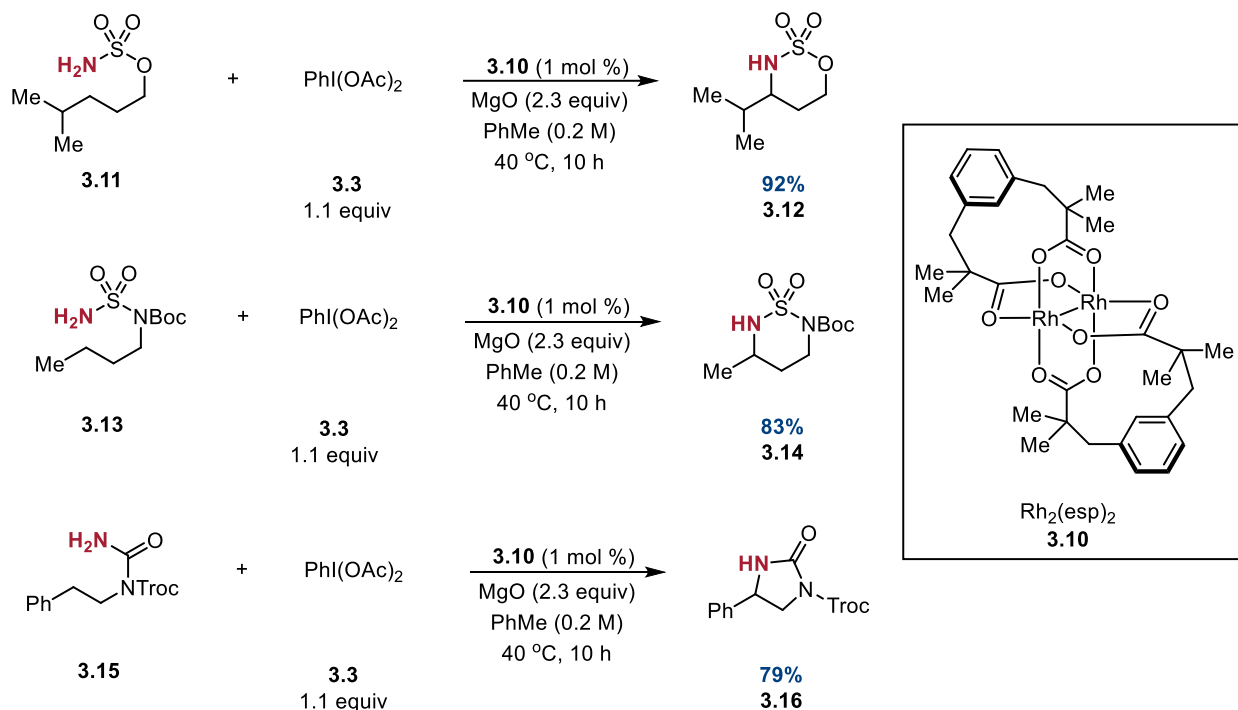
**Scheme 3.1.** Intramolecular C-H insertion with imidoiodobenzene derivative **3.1**


This intramolecular C-H amination was advanced significantly when Espino and Du Bois disclosed an oxidative cyclization of carbamates through Rh(II)-nitrenoid chemistry (**Figure 3.1**).<sup>8</sup> With this method, the nitrene precursors were generated *in situ* with the use of an iodine oxidant to synthesize oxazolidinones. In a subsequent study, this reaction paradigm was extended to sulfamate esters, which showed selectivity for the formation of six-membered rings over five-membered rings (**Scheme 3.2**).<sup>9</sup>

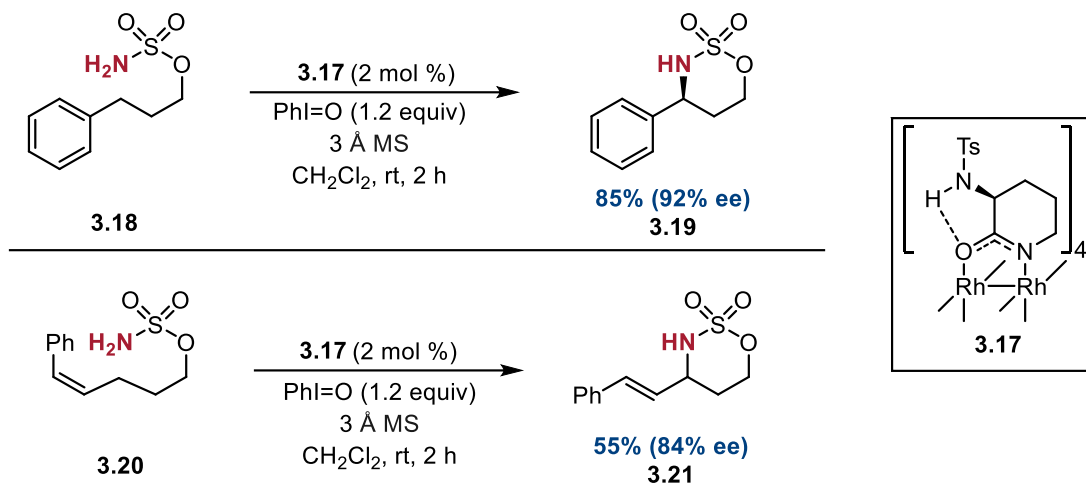
**Figure 3.1.** Du Bois' intramolecular C-H amination with carbamates


**Scheme 3.2.** Intramolecular C-H insertion with sulfamate esters


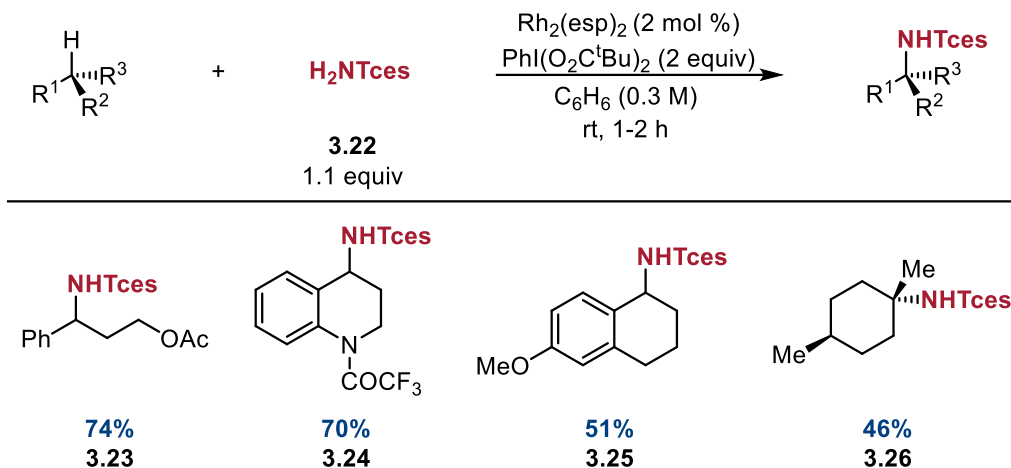
To further expand and improve this reaction, Du Bois and co-workers developed a new Rh(II) catalyst –  $\text{Rh}_2(\text{esp})_2$  (**3.10**). It was previously reported that tetracarboxylate Rh dimers engage in ligand exchange reactions<sup>10</sup> and, when the carboxylate fully detaches from the Rh center, catalyst degradation occurs. They hypothesized that tethering of the two carboxylates would add stability via the chelate effect,<sup>11</sup> which would disfavor complete ligand dissociation and preserve the Rh(II) catalyst structure.<sup>12</sup> *m*-Benzenedipropionic acid was substituted with methyl groups in order to provide some preorganization to an otherwise conformationally unconstrained ligand. Using this catalyst, intramolecular amination was achieved with sulfamate, urea, and sulfamide substrates in excellent yields (**Figure 3.2**).<sup>13</sup>

**Figure 3.2.** Intramolecular C-H insertion using  $\text{Rh}_2(\text{esp})_2$ 

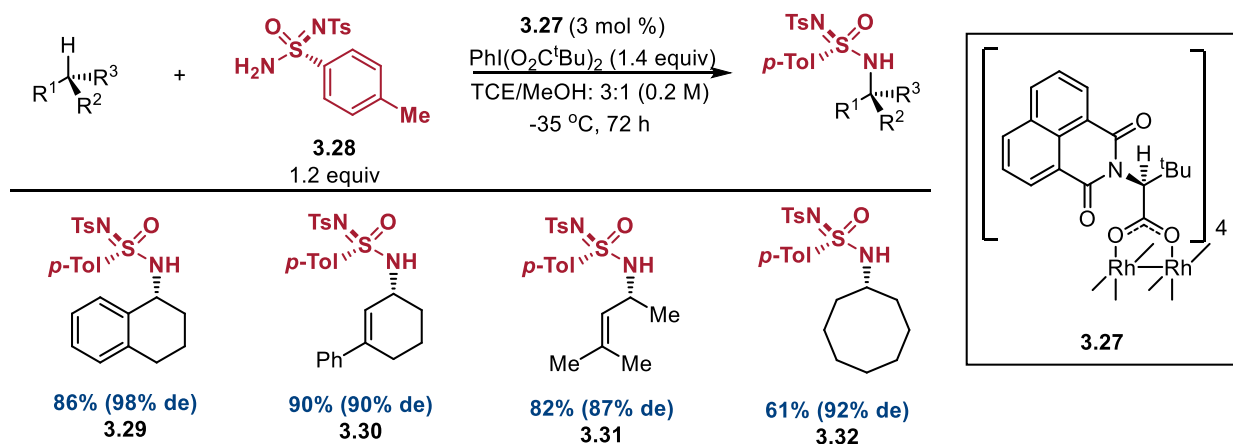
DuBois later accomplished this reaction enantioselectively through the design of  $\text{Rh}_2[(S)\text{-nap}]_4$  (**3.17**) (**Scheme 3.3**). It was hypothesized that the 2° sulfonamide on the ligand allows for intramolecular hydrogen bonding between the N-H group and the carbonyl oxygen of the amide, allowing for a higher redox potential and making it more efficient for this oxidative process. In addition to forming cyclic sulfamates with high ee, this catalyst was also chemoselective for C-H bond insertion over aziridination in the presence of olefins.<sup>14</sup>

**Scheme 3.3.** Enantioselective intramolecular C-H insertion with sulfamate esters**3.2.2. Intermolecular C-H amination**

Du Bois and co-workers applied their  $\text{Rh}_2(\text{esp})_2$  catalyst for intermolecular C-H amination using sulfamates in the presence of a hypervalent iodine oxidant (**Figure 3.3**).<sup>15</sup> For this method, benzylic and 3° C-H bonds were preferentially aminated (**3.23 – 3.26**). Through Hammett analysis and a radical clock experiment, it was postulated that there is a concerted two-electron asynchronous transition state for Rh-mediation nitrene insertion reaction and that the intra- and intermolecular C-H amination reactions are mechanistically analogous. The data also suggests that there is a common nitrene-like oxidant in this transformation.

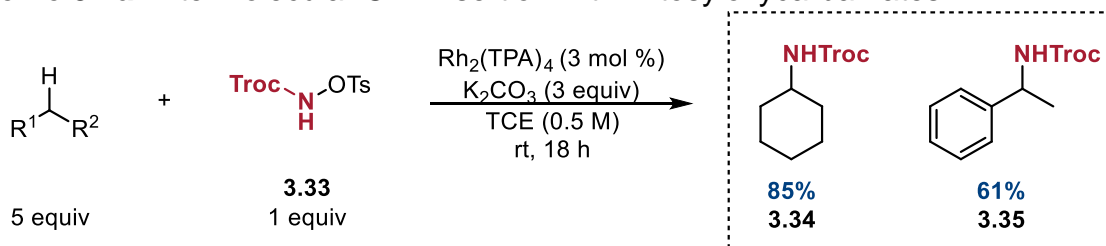
**Figure 3.3.** Du Bois' intermolecular C-H insertion with sulfamates

Dauban and co-workers reported a diastereoselective method with chiral Rh(II) catalyst **3.27** ( $\text{Rh}[(S)\text{-nttl}]_4$ ) and chiral sulfimidamide **3.28** to aminate benzylic, allylic, and aliphatic C-H bonds in good to excellent yields with high diastereoselectivity (**Figure 3.4**). When using a racemic mixture of the sulfonimidamide, there is a chiral resolution of the reaction mixture due to chiral match/mismatch with the Rh(II) catalyst.<sup>16</sup>

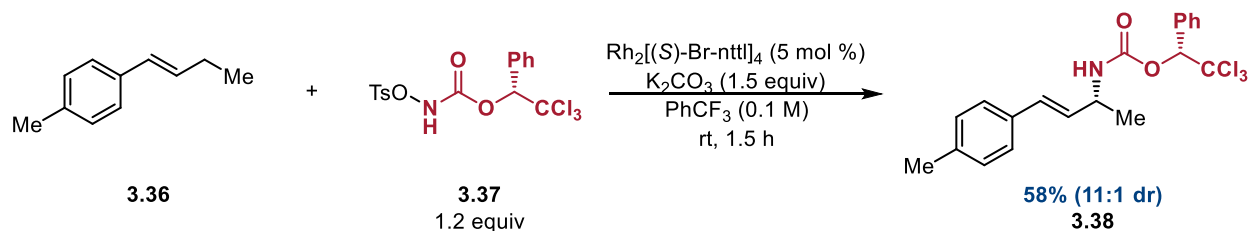
**Figure 3.4.** Diastereoselective intermolecular C-H amination with chiral sulfimidamide

Lebel employed *N*-tosyloxycarbamates as the nitrene precursor for intermolecular C-H amination of both aliphatic and benzylic C-H bonds using  $\text{Rh}_2(\text{TPA})_4$  (**Scheme 3.4a**).<sup>17,18</sup> This was seen as an attractive method due to the ease of N-deprotection following C-H insertion. While sulfonyl groups need to be removed with excess Zn/Cu<sup>19</sup>, the carbamate can be decarboxylated with hydrogenation. The use of these nitrene precursors with a chiral Rh(II) catalyst was extended to stereoselectively aminate allylic C-H bonds in up to 11:1 dr (**Scheme 3.4b**).<sup>20</sup>

**Scheme 3.4a.** Intermolecular C-H insertion with *N*-tosyloxycarbamates



**Scheme 3.4b.** Stereoselective C-H amination of alkenes with chiral *N*-tosyloxycarbamate

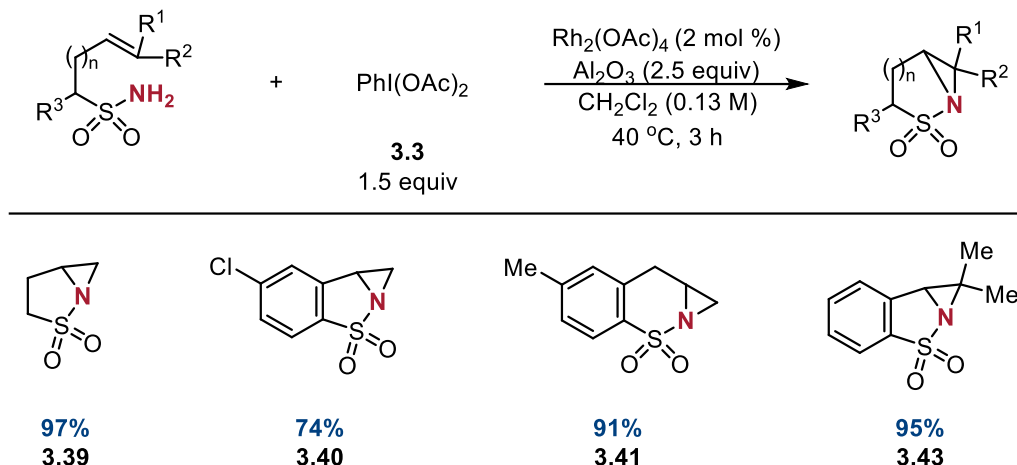


### 3.2.3. Intramolecular olefin aziridination

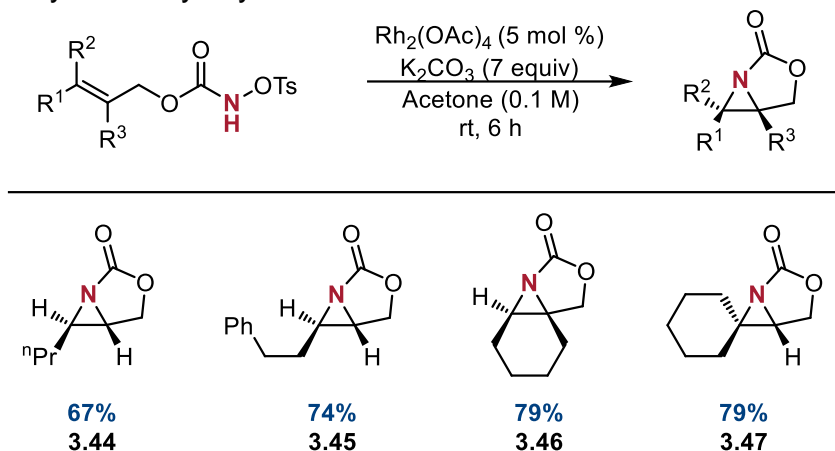
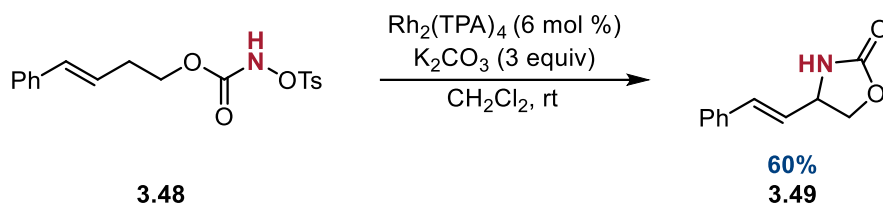
Che and co-workers reported the first Rh-catalyzed intramolecular aziridination through the use of unsaturated sulfonamides and  $\text{PhI}(\text{OAc})_2$  using  $\text{Rh}_2(\text{OAc})_4$  as the catalyst. Using these conditions, they were able to synthesize bicyclic aziridines (**3.39 – 3.43**) in excellent yields (**Scheme 3.5**).<sup>21</sup> They later expanded this work to complete this

transformation enantioselectively with both sulfonamides and carbamates using the Doyle dirhodium catalyst.<sup>22</sup>

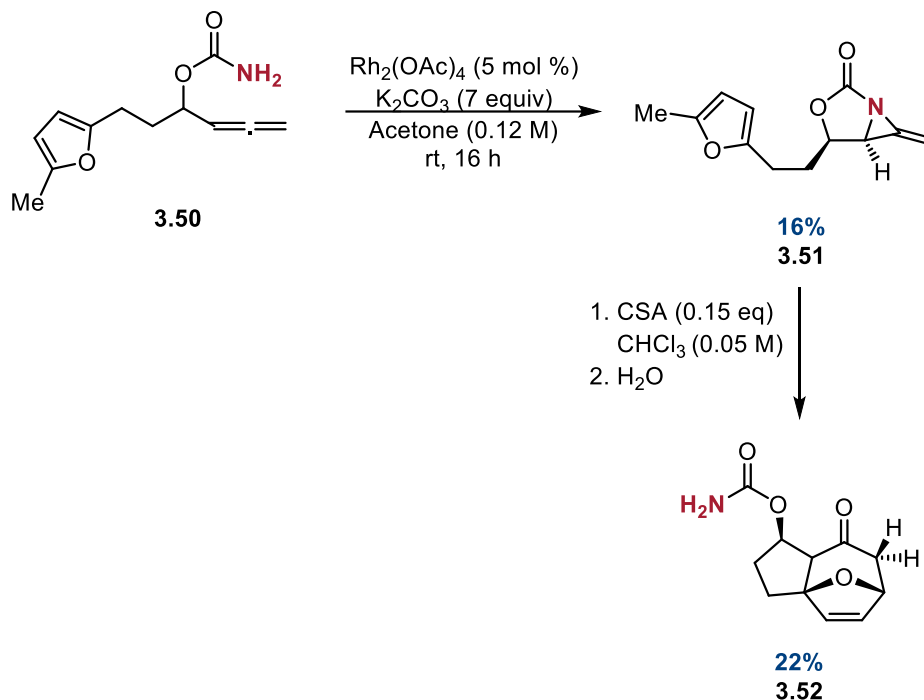
**Scheme 3.5.** Che's intramolecular aziridination



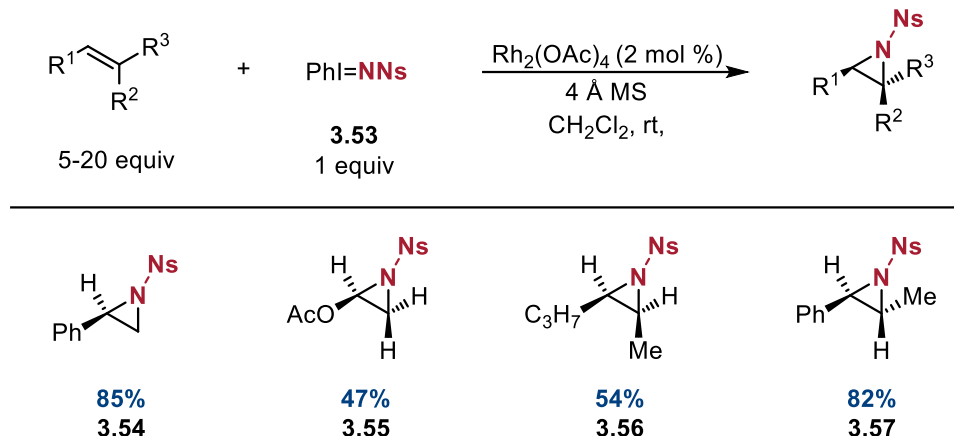
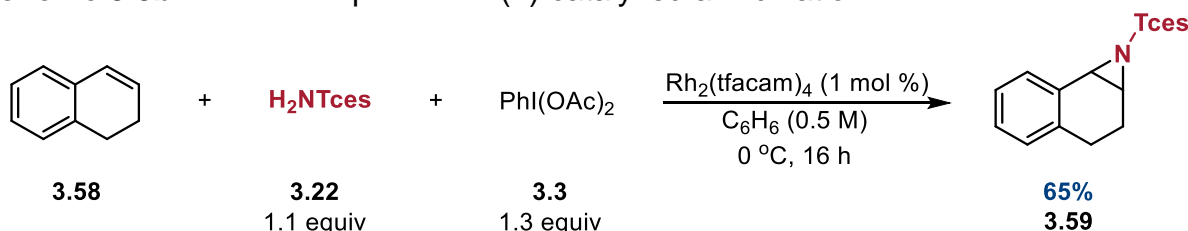
Lebel disclosed an intramolecular aziridination strategy to synthesize a variety of bi- and tricyclic systems using allylic *N*-tosyloxycarbamates using catalytic Rh<sub>2</sub>(OAc)<sub>4</sub> (**Scheme 3.6a**). This approach, however, could not be extended to prepare the six-membered ring using homoallylic alcohol-derived substrates. Instead, only the corresponding oxazolidinone formed via C-H insertion was isolated (**Scheme 3.6b**).<sup>23</sup>

**Scheme 3.6a.** Allylic *N*-tosyloxycarbamates in intramolecular aziridination**Scheme 3.6b.** Attempt to synthesize six-membered ring through aziridination

In an interesting example, Robertson and co-workers were able to aziridinate allenes at the internal position to synthesize methylene aziridines (**Scheme 3.7**).<sup>24</sup> With the use of a Brønsted or a Lewis acids, these derivatives undergo isomerization and, in the presence of furan, engages in a [4+3] cycloaddition to form tricycle **3.52**. Schomaker<sup>25-27</sup> and Blakey<sup>28-30</sup> have also disclosed similar tandem aziridination/rearrangements with Rh(II)-catalysis and acid promoters.

**Scheme 3.7.** Aziridination of allene followed by [4+3] cycloaddition**3.2.4. Intermolecular olefin aziridination**

Müller and co-workers reported the first examples of intermolecular olefin aziridination by using PhINNs with  $\text{Rh}_2(\text{OAc})_4$  as the nitrogen transfer catalyst (**Scheme 3.8a.**).<sup>31</sup> With the observed partial loss of stereospecificity, they hypothesized that, similar to Cu-catalyzed aziridination<sup>32</sup>, this reaction undergoes a two-step mechanism with the formation of a dipolar species that then collapses to form the three-membered ring. Following this work, Guthikonda and DuBois published their intermolecular aziridination with  $\text{Rh}_2(\text{tfacam})_4$ .<sup>33</sup> In contrast to Müller's report, this method called for the *in situ* formation of the iminoiodinane as well as the olefin as the limiting reagent (**Scheme 3.8b**).

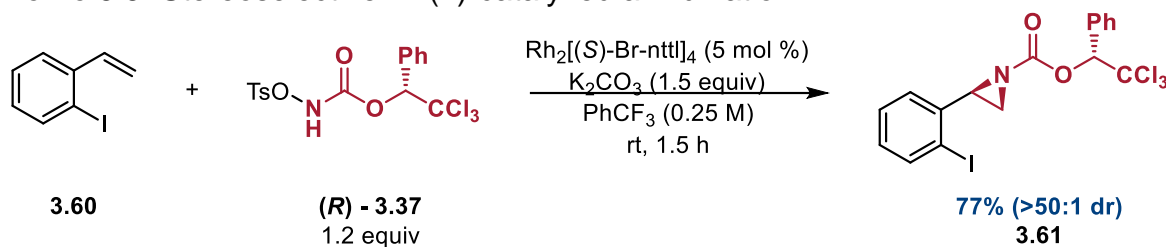
**Scheme 3.8a.** Müller's intermolecular olefin aziridination**Scheme 3.8b.** Du Bois' improved Rh(II)-catalyzed aziridination

With the use of a chiral sulfonimidamide **3.28** and a hypervalent iodine oxidant to form an iminoiodinane in situ, Müller and co-workers were able to synthesize chiral aziridines with up to 80% diastereoselectivity.<sup>34</sup> This method was seen as complementary to the Cu(II)-catalyzed asymmetric procedure.<sup>35</sup> While the Cu(II) salts gave the best results with  $\alpha,\beta$ -unsaturated carbonyl compounds, the Rh(II) complexes are able to catalyze the aziridination of styrenes.

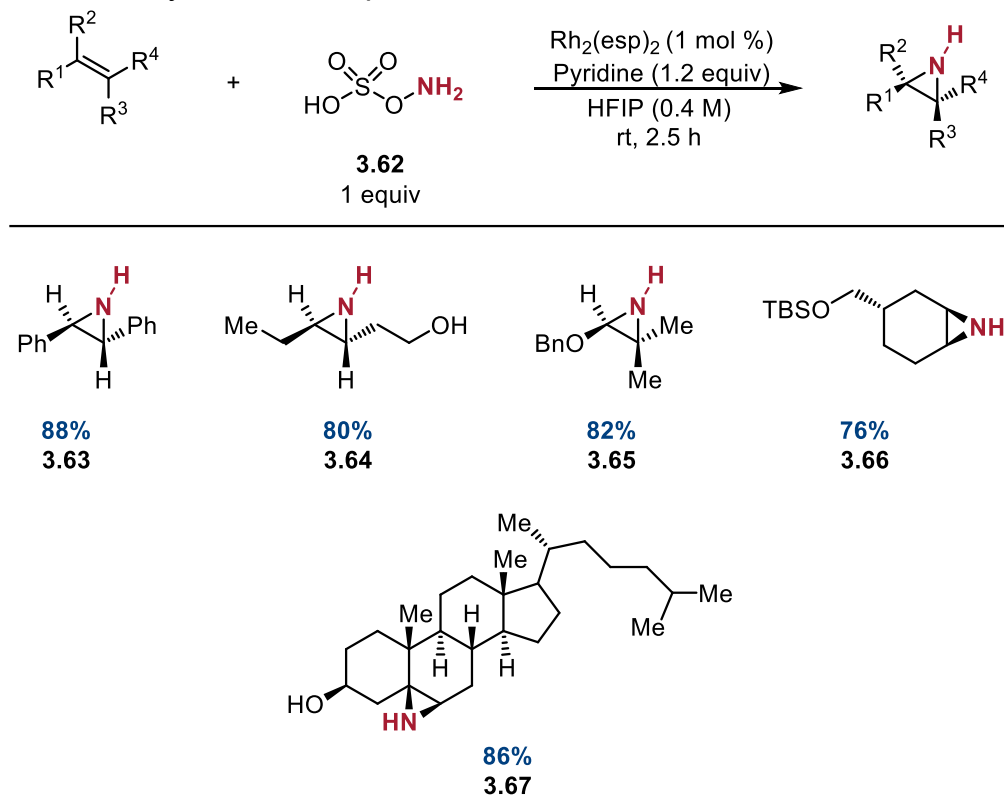
Lebel and co-workers later expanded this strategy to Rh[(S)-Br-nttl]<sub>4</sub>-catalyzed aziridinations using chiral *N*-tosyloxycarbamates, resulting in good yields and diastereoselectivities (**Scheme 3.9**).<sup>36</sup> No isomerization of the *cis* to the *trans* product was observed; thus, it was suggested that this mechanism is concerted and involves a singlet rhodium nitrene species. In addition, when using the (S)-version of the nitrene source with

the Rh(II) catalyst, the yield and diastereoselectivity of the product greatly decreased, suggesting that the nature of the chirality of these two species greatly affects their interaction to form the active Rh(II)-nitrene species.

**Scheme 3.9.** Stereoselective Rh(II)-catalyzed aziridination



Kürti and co-workers were able to catalyze the aziridination of both acyclic and cyclic olefins with  $\text{Rh}_2(\text{esp})_2$  as the catalyst and HOSA as the nitrogen source. These reactions proceeded in up to 85% yield and, in most cases, a single stereoisomer (**Figure 3.5**).<sup>37</sup> This method was also applied to more complex structures (**3.63**), showing the applicability of this procedure to natural product synthesis and medicinal chemistry.

**Figure 3.5.** Kürti's synthesis of unprotected aziridines

$\text{Rh(II)}$  catalysts have been used extensively for nitrene transfer in both intramolecular and intermolecular reactions. The low catalyst loading required is a positive aspect of this chemistry. In addition, the ability to influence reactivity by introducing changes to ligand structure can improve reactivity and lead to stereoselective reactions. We thus investigated if we could this catalysis strategy to develop a method using nitrenes as a single atom component in a [5+1] cycloaddition reaction with VCPs.

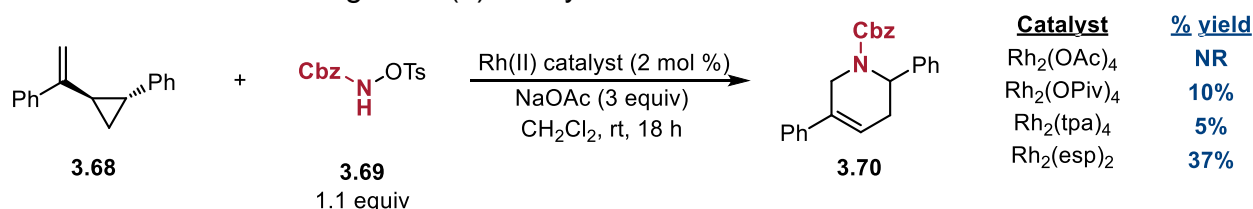
### 3.3. Investigations with 2,4-diarylvinylcyclopropanes

#### 3.3.1. Screening of $\text{Rh(II)}$ catalysts

Due to its reputation as a highly efficient nitrene transfer catalyst,  $\text{Rh}_2(\text{esp})_2$  was employed for this cycloaddition strategy. In initial investigations, we discovered that the

diphenyl-substituted VCP **3.68** was a preferred substrate for this reaction, which proceeded in 37% yield when  $\text{Rh}_2(\text{esp})_2$  was used as the catalyst and tosyloxycarbamated **3.69** as the nitrene precursor (**Scheme 3.10**). In comparison, employing  $\text{Rh}_2(\text{OAc})_4$ , which has been reported to catalyze intermolecular aziridination,<sup>31</sup> resulted in no reaction, even at an elevated temperature.  $\text{Rh}_2(\text{OPiv})_4$  and  $\text{Rh}_2(\text{tpa})_4$  – a known nitrogen transfer Rh(II) catalyst<sup>8</sup> – led to the unproductive consumption of starting material with no major products. Thus,  $\text{Rh}_2(\text{esp})_2$  was selected as the catalyst to be used for subsequent optimization studies.

**Scheme 3.10.** Screening of Rh(II) catalysts

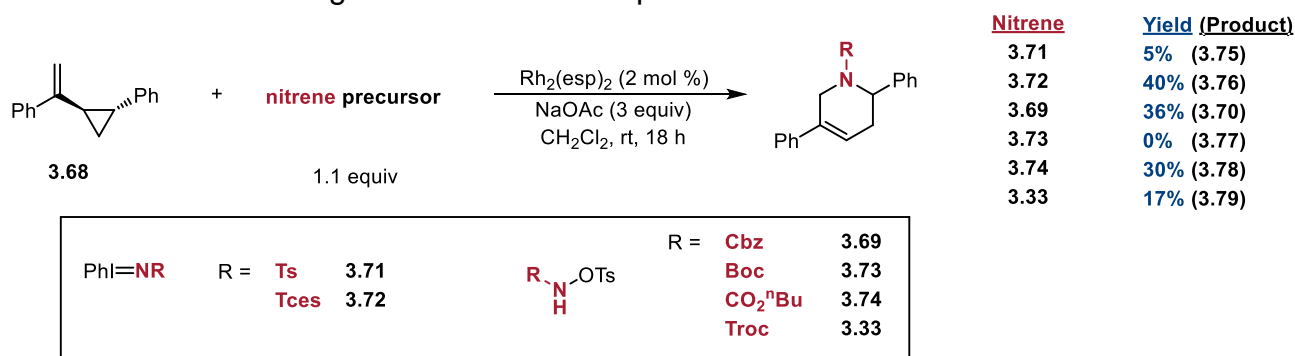


### 3.3.2. Nitrogen sources

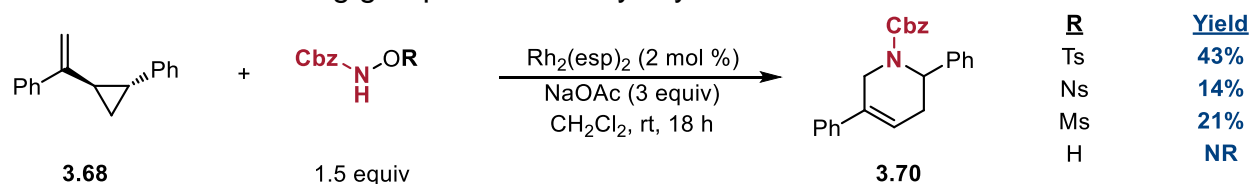
Several nitrene precursors were investigated to serve as the one-atom nitrogen component (**Scheme 3.11a**). Iminoiodinane **3.72**, which has been reported for intermolecular amination using  $\text{Rh}_2(\text{esp})_2$ ,<sup>15</sup> showed promise with a 40% yield of the desired cycloadduct. In situ formation of **3.72** from  $\text{TcesNH}_2$  and  $\text{PhI}(\text{OAc})_2$  provided none of the cyclized product. While the use of  $\text{PhINTces}$  gave the highest initial yield of the desired product, we sought to move away from iminoiodinanes due to the relatively strong reducing conditions required to deprotect the amine after product formation. *N*-tosyloxycarbamates provided a desirable alternative as the amine is easily deprotected via hydrogenolysis.

Benzyl tosyloxycarbamate **3.69** showed initial potential with providing the [5+1] product in 36% yield (**Scheme 3.11a**). The use of other protecting groups did not increase yields of the tetrahydropyridine ring (**Scheme 3.11b**). In addition, changing the nature of the leaving group from tosyl to other sulfonyl groups or an unprotected hydroxyl group also did not enhance yields. Accordingly, **3.69** was selected as the nitrene precursor for additional investigations. Further optimization showed that 1.5 equivalents of **3.69** was optimal for this [5+1] cycloaddition, providing **3.70** in 43% yield. Increasing the equivalents of the nitrene precursor proved to be detrimental to the reaction (**Scheme 3.11c**).

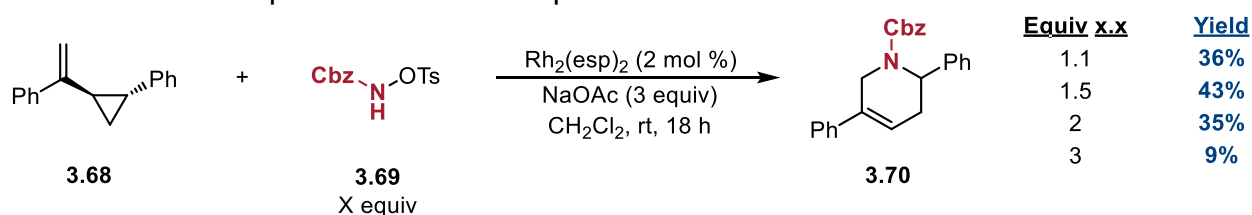
#### Scheme 3.11a. Investigations of the nitrene precursor



#### Scheme 3.11b. Leaving group on the benzyloxycarbamate



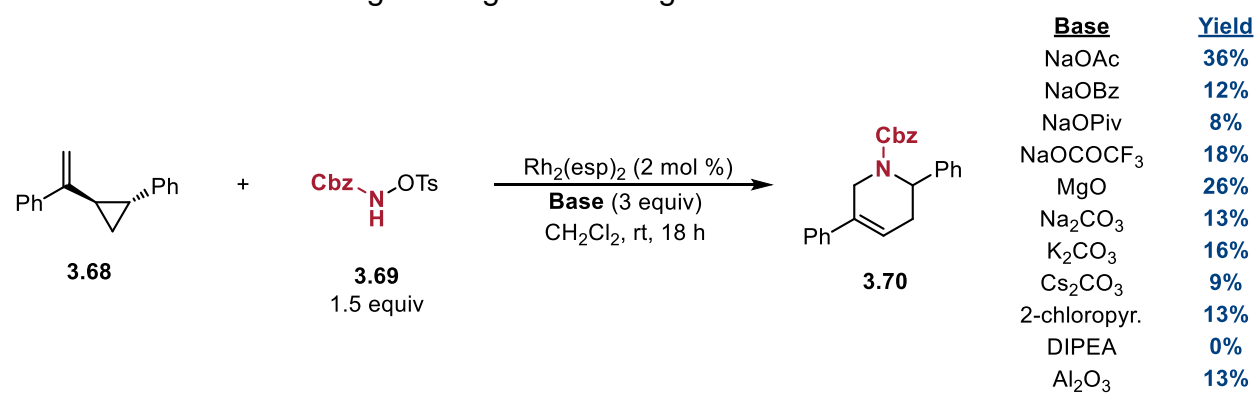
#### Scheme 3.11c. Equivalents of nitrene precursor

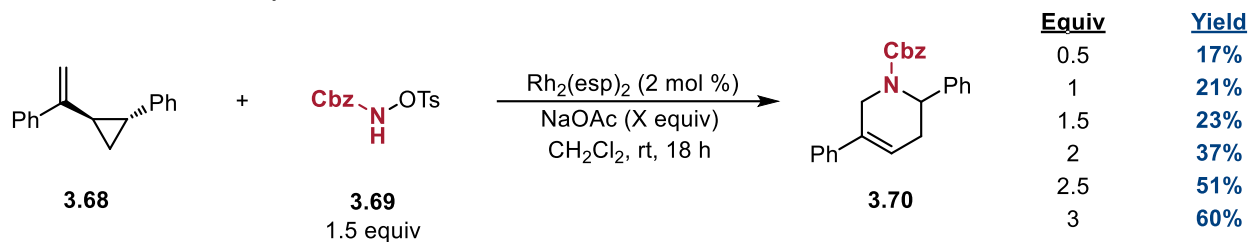


### 3.3.3. Further optimization

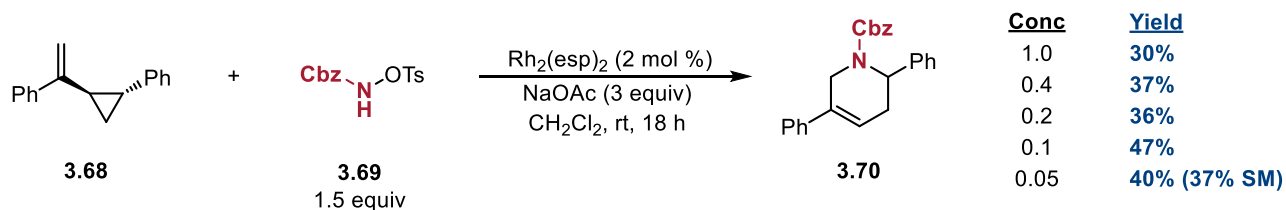
The effect of the base on the [5+1] cycloaddition was also investigated (**Scheme 3.12a**). Various inorganic and organic bases were employed. Due to the effectiveness of NaOAc, other carboxylate salts were used in this reaction, but none showed any improvements to the yield. The use of MgO, which is commonly used for the *in situ* formation of iminoiodinanes,<sup>8</sup> also failed to improve yields. In addition, carbonate bases either showed minimal or no production of the cyclized product. Organic bases such as 2-chloropyridine and Hünig's base resulted in the unproductive consumption of VCP **3.64**. The dependence on NaOAc for the Rh(II)-catalyzed cycloaddition suggests that the base plays an additional role in the reaction mechanism beyond deprotonation of benzyl tosyloxycarbamate. The potential role of the base in this reaction is further discussed in **Section 3.3.5**. Furthermore, three equivalents of base were found to be the most optimal for this reaction, providing the desired product in 60% yield (**Scheme 3.12b**).

**Scheme 3.12a.** Screening of inorganic and organic bases

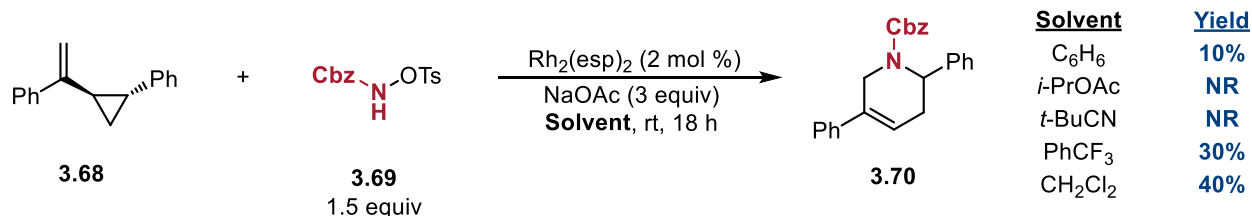


**Scheme 3.12b.** Equivalents of NaOAc

The concentration of the reaction was found to have a substantial effect on product formation (**Scheme 3.13**). Decreasing the concentration to 0.05 M resulted in a 40% yield of the desired cycloadduct along with 35% of VCP remaining, showing a somewhat control on the degradation of the VCP substrate.

**Scheme 3.13.** Effect of concentration of substrate in reaction

Solvents that have been previously used for Rh(II)-catalyzed nitrene transfer reactions were explored (**Scheme 3.14**).<sup>8,15,20,38</sup> The use of benzene resulted in a significant decrease in yields. Isopropyl acetate and pivalonitrile shut down the reaction pathway and led to no consumption of VCP **3.68**. Trifluorotoluene was not as effective as methylene chloride in the [5+1] reaction, so the latter was used in further reaction development.

**Scheme 3.14.** Solvent screening**3.3.4. Assessment of the scope**

Having optimized conditions in hand, the scope of the reaction was investigated (**Table 3.1**). With respect to the styrenyl aryl group, having an electron-donating group at the para position (e.g., **3.80** and **3.99**) led to decreased yields of the desired product. Halogens at this position were well tolerated and, in some instances, resulted in the recovery of some starting material (e.g., **3.82 – 3.84**, **3.94**, and **3.97 – 3.98**). Regarding the cyclopropyl aryl group, strong electron-withdrawing groups on the cyclopropyl aryl ring resulted in lower yields and complete consumption of the substrate (e.g., **3.87** and **3.90**). However, electron donating groups at the para position (e.g., **3.89** and **3.98**) were better tolerated. Ortho- and meta-substitution on either aryl ring were somewhat tolerated in the case of both electron-donating and withdrawing groups (e.g., **3.100 – 3.104**).

**Table 3.1.** Scope of the Rh(II)-catalyzed aza-[5+1] cycloaddition

	<b>R</b>	<b>Yield</b>
	H	60% (75%) (3.70)
	OMe	27% (3.80)
	Ph	35% (3.81)
	Cl	52% (67%) (3.82)
	Br	51% (62%) (3.83)
	I	63% (3.84)
	Cy	46% (3.85)
	<b>R</b>	<b>Yield</b>
	Me	38% (3.86)
	CF <sub>3</sub>	26% (3.87)
	Ph	42% (51%) (3.88)
	OMe	38% (3.89)
	CO <sub>2</sub> Me	22% (3.90)
	F	46% (54%) (3.91)
	Cl	40% (3.92)
	Br	43% (3.93)
	<b>R<sup>1</sup>, R<sup>2</sup></b>	<b>Yield</b>
	Cl, Me	51% (65%) (3.94)
	Me, Cl	38% (49%) (3.95)
	Me, Me	41% (3.96)
	Cl, Cl	43% (3.97)
	Cl, OMe	51% (3.98)
	MeO, Cl	27% (51%) (3.99)
		44% (3.100)
		27% (3.101)
		31% (3.102)
		20% (3.103)
		33% (3.104)
		50% (3.105)
		30% (3.106)
		40% (3.107)

brsm = based on recovered starting material

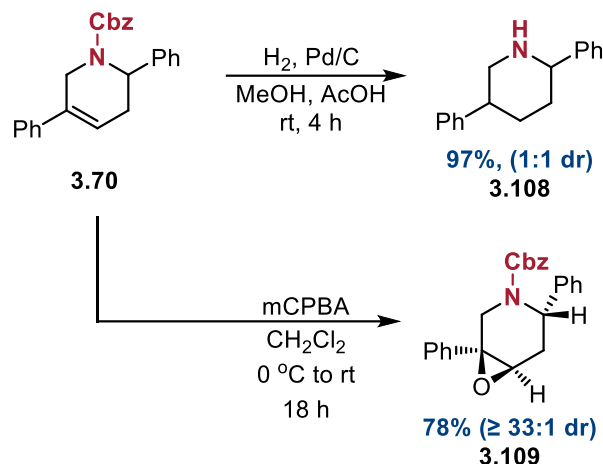
The success of synthesizing tetrahydropyridine products bearing aryl halides (e.g., **3.83**, **3.84**, **3.93**, and **3.102**) allows for further functionalization through cross-coupling

techniques. Furthermore, the ability to synthesize fluorinated products (e.g., **3.87**, **3.91**, **3.104**, and **3.105**) shows potential for this method to be used in the preparation of medicinally relevant compounds.<sup>39</sup> Successful synthesis of **3.106** allows the opportunity for further functionalization of the alkene, such as epoxidation, aziridination, or dihydroxylation. Lastly, a more complex tricyclic system (e.g., **3.107**) was able to be accessed through this method. With this method, alkyl substitution on the styrenyl or cyclopropyl side was not tolerated, resulting in none of the desired product. Furthermore, the incorporation of heterocycles, such as pyridines and thiophenes, as part of the VCP resulted in complete consumption of starting material with no formation of the desired product.

### *3.3.5. Functionalization of the tetrahydropyridine products*

To demonstrate the synthetic utility of the cyclized products, **3.70** was further derivatized (**Scheme 3.15**). Hydrogenation of **3.70** gave deprotected piperidine **3.108** in a quantitative yield. In addition, epoxidation of **3.70** with *m*-CPBA provided **3.109** in 78% yield with high diastereoselectivity.

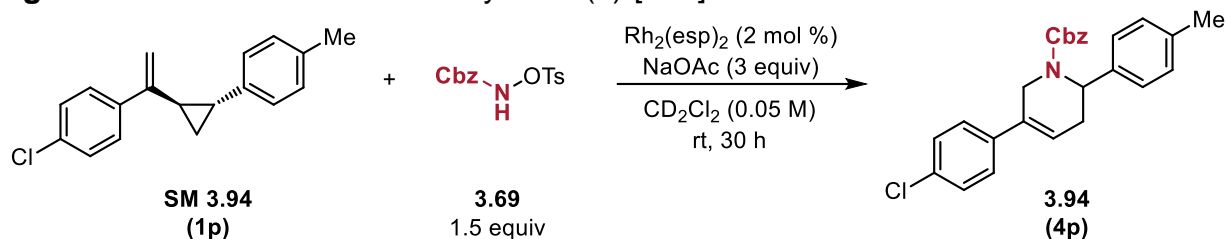
---

**Scheme 3.15.** Further functionalization of [5+1] products

**3.3.6. Mechanism of the Rh(II)-catalyzed [5+1] reaction**

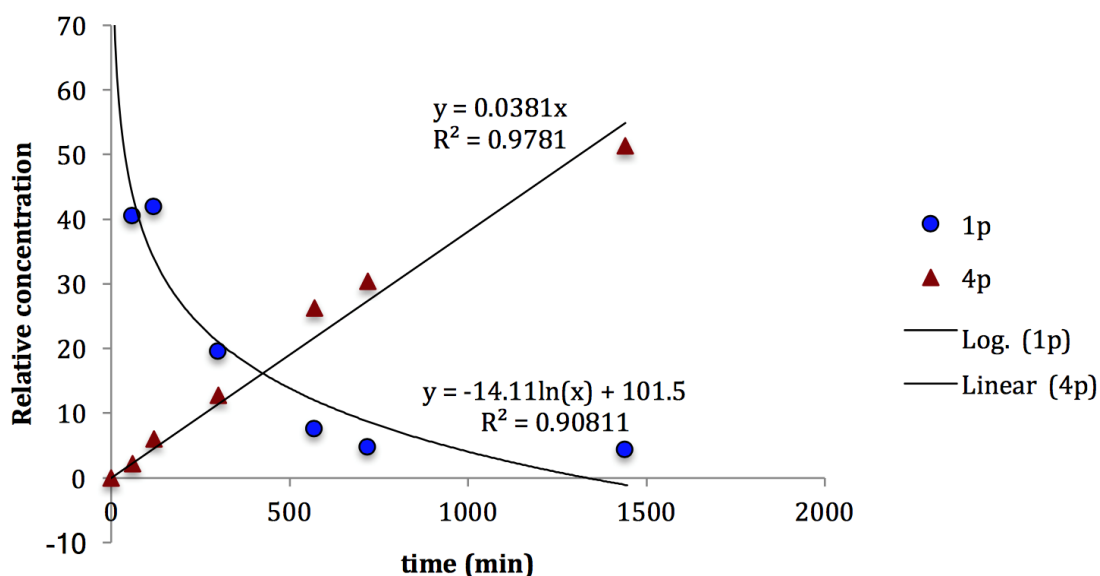
In order to investigate the mechanism of this reaction, an NMR study was conducted to identify potential intermediates (**Figure 3.6**). In this experiment, **SM 3.94** was subjected to the optimized Rh(II) [5+1] conditions with  $\text{CD}_2\text{Cl}_2$  as the reaction solvent. During the reaction period, aliquots of the reaction mixture were obtained and the relative concentrations of **SM 3.94** and product **3.94** were assessed by  $^1\text{H}$  NMR referenced to the residual solvent peak. It was found that, based on the decomposition of **SM 3.94** and the formation of product **3.94**, short-lived intermediates are being formed such as a radical or a carbocation. While they were detected by NMR, none of these species have been isolated due to instability or a low quantity of them being formed. Production formation occurred with apparent zero order kinetics while consumption of **SM 3.94** was found to be first order. These rate differences suggest that an additional mechanistic step occurs between N-insertion and ring closure, which would indicate a stepwise mechanism

involving either a carbon-centered radical or carbocation. The apparent formation of polymeric side products seems to support this as well.

**Figure 3.6.** NMR mechanistic study of Rh(II)-[5+1] reaction



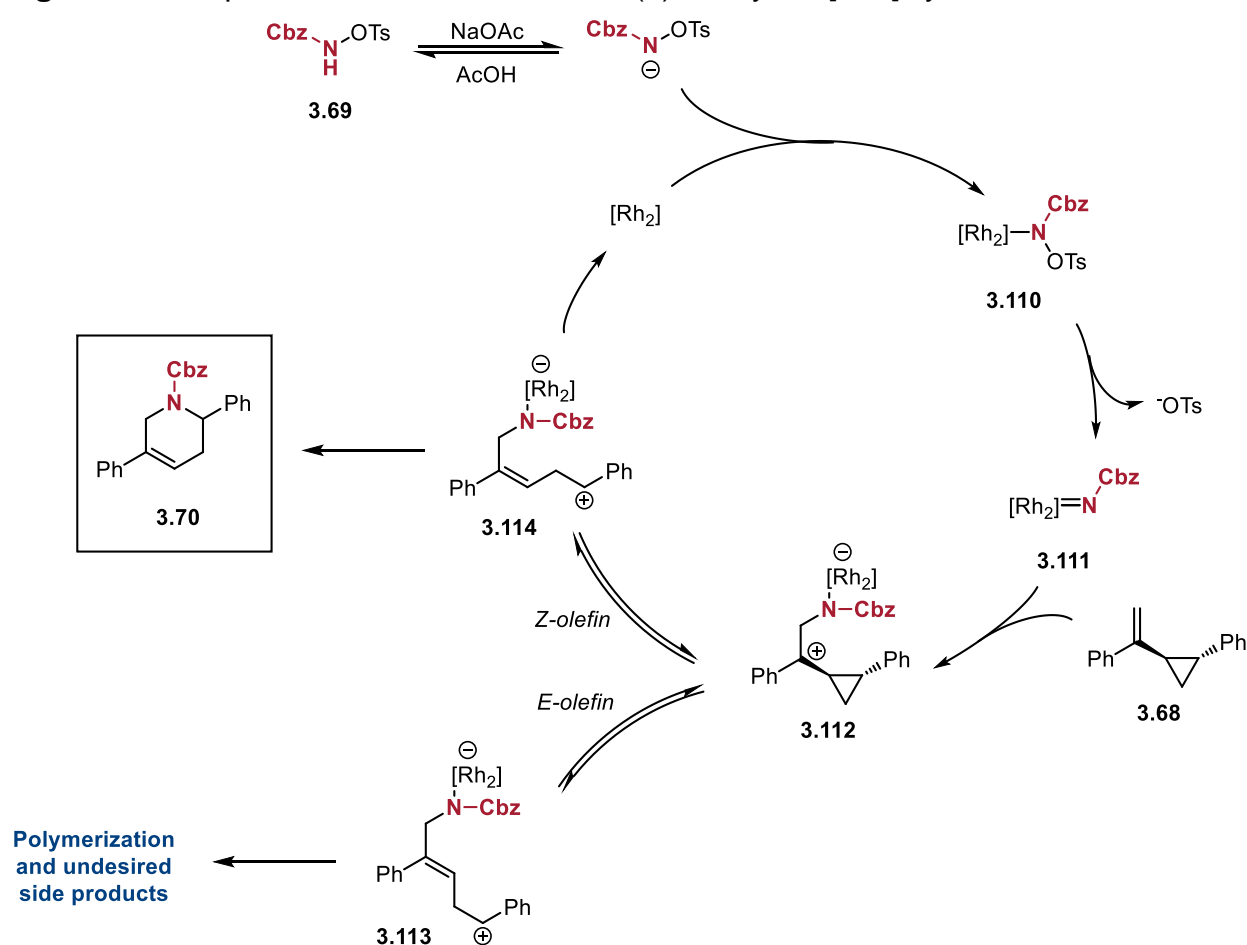
### [5+1] reaction NMR time course study



Based on this NMR study, we proposed the following mechanism (**Figure 3.7**).  $\text{NaOAc}$  deprotonates the tosyloxycarbamate that then coordinates to the dirhodium catalyst. The loss of the tosylate anion then forms the active Rh-nitrene species. The vinyl group of VCP **3.68** then, through a nucleophilic attack, attacks the nitrene to form dipolar species **3.112**. Aziridination of the vinyl group is also possible; further studies are needed to determine whether this intermediate forms. Afterwards, the cyclopropyl ring opens to either form the (*Z*) or (*E*) olefin.

If (*Z*)-olefin **3.114** is formed, the nitrogen atom attacks the carbocation and, with Rh-dissociation, forms the desired cycloadduct. However, if instead (*E*)-olefin **3.113** is formed, the geometry of the alkene does not allow for the cyclization to occur. If this species does not rearrange back to species **3.112**, this carbocation can engage in polymerization, elimination to form the corresponding dienes, or be nucleophilically attacked by either the acetate or tosylate anions in solution to form difunctionalized products. Another possible side product can come from the acyloxyamination of species **3.112**, which has been previously reported by Dauban and co-workers using a mono-substituted VCP.<sup>40</sup>

**Figure 3.7.** Proposed mechanism for the Rh(II)-catalyzed [5+1] cycloaddition

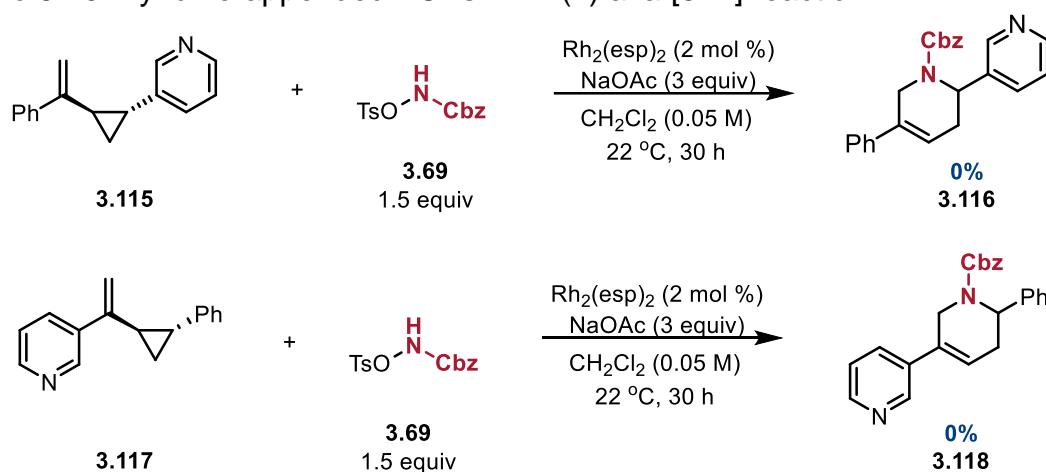


### 3.4. Expanding the Use of the Aza-[5+1] Cycloaddition

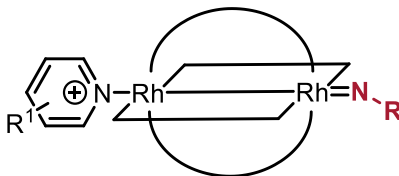
#### 3.4.1. Berry's novel $Rh_2^{II,III}$ dimer catalyst

Through our initial investigation of the scope of VCPs, we found that when a phenyl ring on either end is replaced with a pyridine ring, the reaction shuts down (**Scheme 3.16**). When the substrate is added, a vibrant red color, rather than a green color, is visible in the reaction mixture. It was hypothesized that the pyridine is coordinating to the open reactive site of the  $Rh_2(esp)_2$  catalyst, leading to catalytic arrest and therefore preventing the [5+1] reaction (**Figure 3.8**).

**Scheme 3.16.** Pyridine-appended VCPs in Rh(II) aza-[5+1] reaction



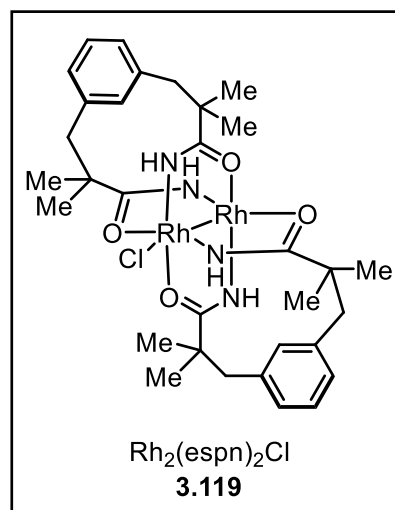
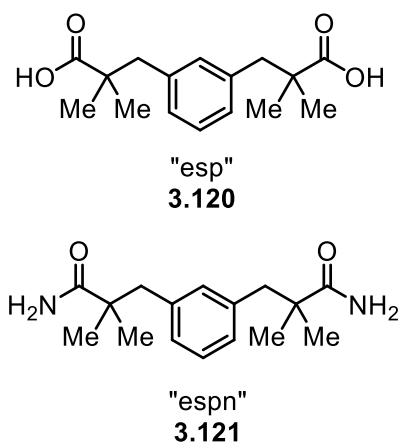
**Figure 3.8.** Pyridine-appended VCPs in Rh(II) aza-[5+1] reaction



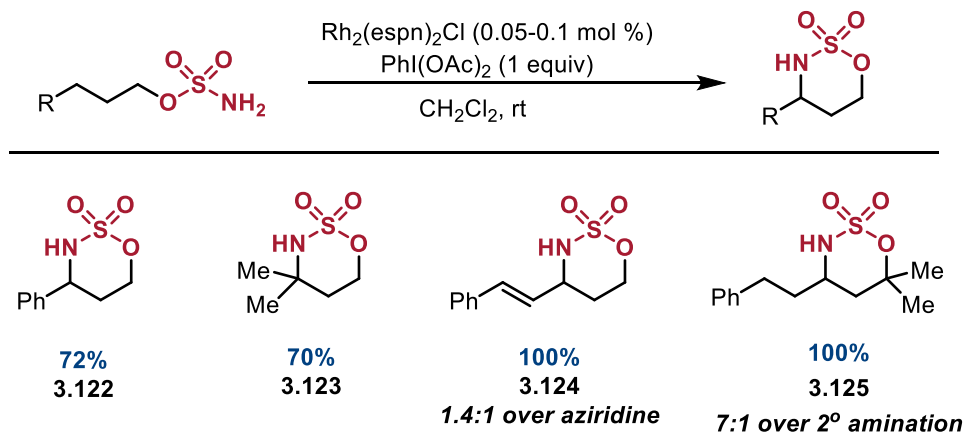
In order to reduce this interaction, we decided to initially explore this through catalyst design. We looked into a catalyst reported by the Berry group in 2011.<sup>41</sup> In prior work, it had been reported that a  $Rh_2^{II,III}$  dimer is the catalyst resting state for  $Rh_2(esp)_2$ -

catalyzed reactions.<sup>42-44</sup> In this work, they investigated the performance of a stable mixed-valent  $\text{Rh}_2^{\text{II,III}}$  dimer catalyst. The esp ligand was modified by replacing the carboxylic acids with primary amides, since it is known that N-donor ligands are able to stabilize the Rh-Rh bonds better than O-donor ligands (**Figure 3.9**).<sup>10</sup> In addition, N-chlorosuccinimide was used in the final step of catalyst synthesis to stabilize the  $\text{Rh}^{\text{III}}$  center with a chloride atom.

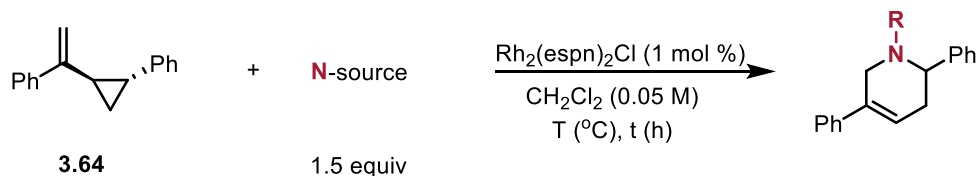
**Figure 3.9.** Berry's  $\text{Rh}_2^{\text{II,III}}$  dimer catalyst



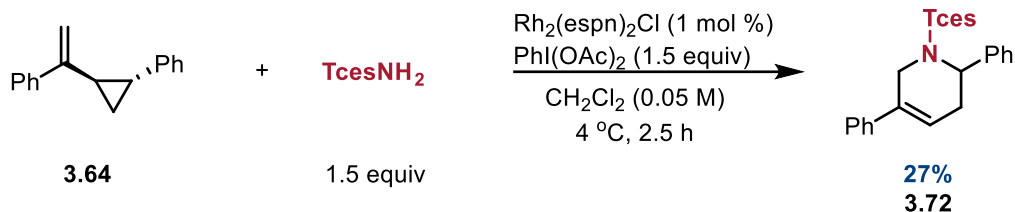
They investigated the use of this new catalyst in intramolecular amination incorporating in situ formation of the iminoiodinane (**Scheme 3.17**). The products – both aliphatic and aromatic substituted – were isolated in good to excellent yields using 0.05 to 0.1 mol% of catalyst. The higher catalytic turnover exhibited by this catalyst compared to  $\text{Rh}^{\text{II}}$  dimers supported their hypothesis. Alkenyl substrate **3.124** showed a preference for formation of the aminated product over the aziridine in a 1.4:1 ratio. Lastly, amination at the distal  $3^\circ$  position was favored over the proximal  $2^\circ$  position in a 7:1 ratio.

**Scheme 3.17.** Intramolecular amination with Berry's  $\text{Rh}_2^{\text{II,III}}$  dimer catalyst

**3.4.2. Investigation of aza-[5+1] cycloaddition with  $\text{Rh}_2^{\text{II,III}}$  dimer catalyst**

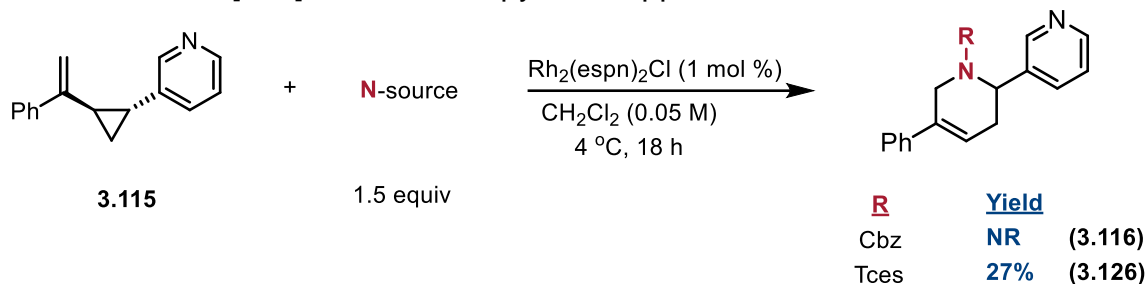
We investigated the use of the “espn” catalyst under our previously reported conditions, but observed low conversion to the cycloaddition product. In addition, we recovered close to a quantitative amount of starting material (**Scheme 3.18a**). Replacing the carbamate with PhINTs resulted in no isolation of product **3.71**, but the reaction occurred at a much faster rate. Using PhINTces as the nitrogen source also shows an accelerated reaction time but **3.72** was isolated in 41% yield. Decreasing the temperature to  $-12^\circ\text{C}$  resulted in 71% of the desired product. Not only does this method provide a higher yield of the cycloadduct but also results in a much shorter reaction time (2.5 vs 30 h). Lastly, using in situ formation of the iminoiodinane provided a 27% yield of **3.72**, showing promise to further increase the practicality of the [5+1] reaction (**Scheme 3.18b**).

**Scheme 3.18a.** Screening  $\text{Rh}_2(\text{espn})_2\text{Cl}$  for the aza-[5+1] cycloaddition


N-source	T ( $^\circ\text{C}$ )	t (h)	Product	% yield
<b>CbzNHOTs</b>	22	22	<b>3.66</b>	<b>NR</b>
PhINTs	22	2	<b>3.71</b>	<b>&lt;5</b>
PhINTces	22	2	<b>3.72</b>	<b>41</b>
PhINTces	-12	2.5	<b>3.72</b>	<b>71</b>

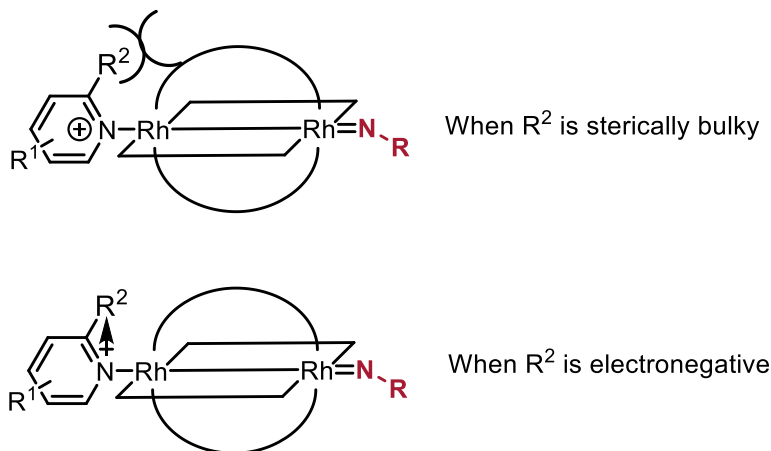
**Scheme 3.18b.** *In situ* iminoiodinane formation with Berry's catalyst


After screening conditions with the parent VCP, we wanted to study our hypothesis of pyridine coordination. If a chloride is present on the Rh atom, this would eliminate the open coordination site and therefore prevent catalyst arrest (**Figure 3.10**). As seen previously, using  $\text{Rh}_2(\text{espn})_2\text{Cl}$  with the N-tosyloxycarbamate resulted in no observable reactivity (**Scheme 3.19**). Instead, PhINTces as the nitrene source resulted in the desired cycloadduct in good yield. Further work into using this  $\text{Rh}_2^{\text{II,III}}$  dimer is ongoing as well as expanding the scope of different heterocycles that may be tolerant.

**Figure 3.10.** Simplified structure of dimer catalyst**Scheme 3.19.** Aza-[5+1] reaction with pyridine-appended VCP

### 3.4.3. The effect of 2-substitution on the pyridine VCP

In addition to studying catalyst design, we also sought out to see if sterics could be used to influence the success of [5+1] cycloadditions involving pyridine-containing VCPs (**Figure 3.11**). We hypothesized that adding a functional group at the 2-position could create a steric clash with the  $\text{Rh}_2$  catalyst ligands, preventing the pyridine group from coordinating. Furthermore, we also hypothesized that decreasing the coordination ability of the pyridine nitrogen via electronic effects would also improve reaction yields.

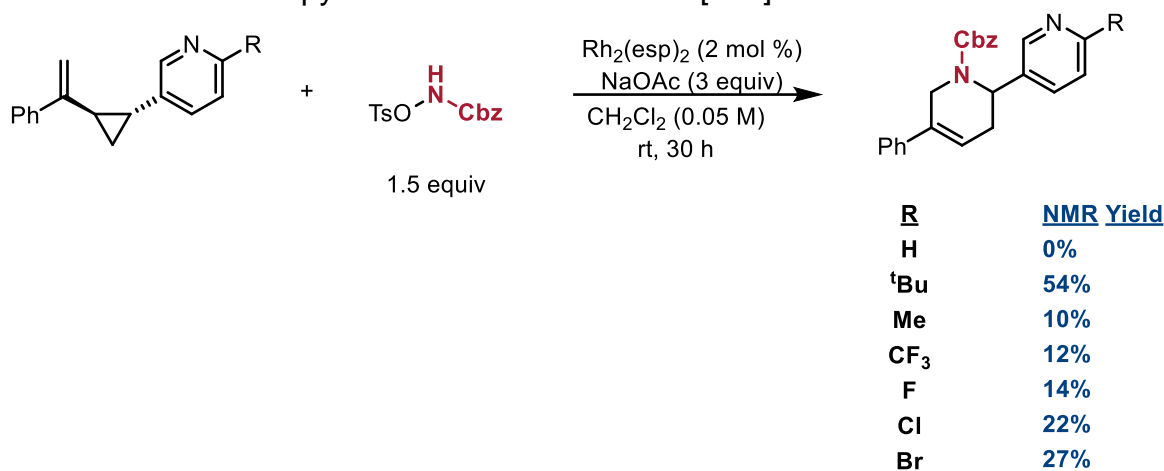
**Figure 3.11.** Modifications to pyridine ring

We investigated the use of our previously reported conditions with a variety of pyridine-substituted VCPs (**Scheme 3.20**). Using the sterically bulky  $^t\text{Bu}$  group, the desired cycloadduct was isolated in 54% yield, which is comparable to using the diphenyl VCP substrate. However, switching the group to a methyl group greatly reduced product formation to a 10% NMR yield. These results seem to align with our previous hypothesis regarding the steric interaction with the esp ligand. Moreover, we decided to use the  $^t\text{Bu}$  VCP substrate with the  $\text{Rh}_2(\text{esp})_2\text{Cl}$  catalyst and excitingly we were able to observe the cycloadduct in the crude NMR. However, difficulties with isolation made it impossible to determine the yield for this transformation. Improving the chromatography method for isolation of these products will be crucial for optimizing this technique.

The effect of electronics was then studied using both halogens as well as trifluoromethyl (**3.129 – 3.132**). Interestingly, we observed a roughly negative correlation between the electronegativity of the substituent and yields of the cycloadduct product, for example in the halogen series. These observations suggest that sterics have a larger

impact on preventing pyridine coordination, at least for 3-pyridine substituents. Further studies are needed to determine if this is applicable for 2- and 4-pyridine substitution on the cyclopropyl ring. Moreover, modifying the vinyl group with different pyridine rings is also needed to see if this same trend is seen and also to potentially provide additional insight.

**Scheme 3.20.** Effect of pyridine substitution on aza-[5+1] reaction



### 3.5. Conclusions

We have disclosed the first aza-[5+1] cycloaddition between VCPs and nitrene precursors. Using  $\text{Rh}_2(\text{esp})_2$  as our nitrene source, this method resulted in a library of 2,5-disubstituted tetrahydropyridine products, which have rarely been reported in the literature before this study. Furthermore, we showed two examples of these cycloadducts being further functionalized through hydrogenation and epoxidation, the latter occurring with a high degree of stereoselectivity. We hypothesized that this cycloaddition is proceeding via ring opening of the cyclopropyl ring to a benzyl carbocation followed by

cyclopropane C–C bond cleavage. To further improve this method, finding a way to favor formation of the (*Z*)-olefin would be an important detail to consider to favor cyclization.

Initial work has been started to improve this method in two ways: 1) through catalyst design, and 2) modifying the VCP substrates. The use of the Rh<sub>2</sub><sup>II,III</sup> dimer not only greatly increased the reaction rate but also showed promise to use VCP substrates containing pyridine and other heterocyclic rings. Furthermore, increasing the steric bulk on the pyridine ring provided evidence that this interrupts coordination of the N-atom to the open ligand site on the Rh center. Additional investigations into both of these areas are currently ongoing.

### 3.6. References

- (1) Martins, P.; Jesus, J.; Santos, S.; Raposo, L. R.; Roma-Rodrigues, C.; Viana Baptista, P.; Fernandes, A.R. *Molecules*, **2015**, *20*, 16852.
- (2) Blakemore, D. C.; Castro, L.; Churcher, I.; Rees, D. C.; Thomas, A. W.; Wilson, D. M.; Wood, A. *Nat. Chem.*, **2018**, *10*, 383.
- (3) Wu, Q.; Hu, J.; Ren, X.; Zhou, J. *Chem. Eur. J.*, **2011**, *17*, 11553.
- (4) Gilbert, Z. W.; Hue, R. J.; Tonks, I. A. *Nat. Chem.*, **2016**, *8*, 63.
- (5) Saito, A.; Kambara, Y.; Yagyu, T.; Noguchi, K.; Yoshimura, A.; Zhdankin, V. V. *Adv. Synth. Catal.*, **2015**, *357*, 667.
- (6) Matsui, K.; Shibuya, M.; Yamamoto, Y. *Communications Chemistry* **2018**, *1*, 1.
- (7) Breslow, R.; Gellman, S. H. *J. Am. Chem. Soc.* **1983**, *105*, 6729-6730
- (8) Espino, C. G.; Du Bois, J. *Angew. Chem., Int. Ed.* **2001**, *40*, 598–600.

- (9) Espino, C. G.; Wehn, P. M.; Chow, J.; Du Bois, J. *J. Am. Chem. Soc.* **2001**, *123*, 6935–6936.
- (10) Doyle, M. P.; Ren, T. *Prog. Inorg. Chem.* **2001**, *49*, 113.
- (11) Bickley, J.; Bonar-Law, R.; McGrath, T.; Singh, N.; Steiner, A. *New J. Chem.* **2004**, *28*, 425.
- (12) Lou, Y.; Horikawa, M.; Kloster, R. A.; Hawryluk, N. A.; Corey, E. J. *J. Am. Chem. Soc.* **2004**, *126*, 8916.
- (13) Espino, C. G.; Fiori, K. W.; Kim, M.; Du Bois, J. *J. Am. Chem. Soc.* **2004**, *126*, 15378–15379.
- (14) Zalatan, D. N.; Du Bois, J. *J. Am. Chem. Soc.* **2008**, *130*, 9220.
- (15) Fiori, K. W.; Du Bois, J. *J. Am. Chem. Soc.* **2007**, *129*, 562.
- (16) Liang, C.; Collet, F.; Robert-Peillard, F.; Müller, P.; Dodd, R. H.; Dauban, P. J. *Am. Chem. Soc.* **2008**, *130*, 343.
- (17) Lebel, H.; Huard, K. *Org. Lett.* **2007**, *9*, 639.
- (18) Lebel, H.; Huard, K. *Chem. Eur. J.* **2008**, *14*, 6222.
- (19) Guthikonda, K.; Du Bois, J. *J. Am. Chem. Soc.* **2002**, *124*, 13672.
- (20) Lebel, H.; Spitz, C.; Leogane, O.; Trudel, C.; Parmentier, M. *Org. Lett.* **2011**, *13*, 5460.
- (21) Liang, J. -L.; Yuan, S. -X.; Chan, P. W. H.; Che, C. -M. *Org. Lett.* **2002**, *4*, 4507.
- (22) Liang, J. -L.; Yuan, S. -X.; Chan, P. W. H.; Che, C. -M. *Tetrahedron Lett.* **2003**, *44*, 5917.
- (23) Lebel, H.; Huard, K.; Lectard, S. *J. Am. Chem. Soc.* **2005**, *127*, 14198.

- (24) Robertson, J.; Feast, G. C.; White, L. V.; Steadman, V. A.; Claridge, T. D. W. *Org. Biomol. Chem.* **2010**, *8*, 3060.
- (25) Boralsky, L. A.; Marston, D.; Grigg, R. D.; Hershberger, J. C.; Schomaker, J. M. *Org. Lett.* **2011**, *13*, 1924.
- (26) Gerstner, N. C.; Adams, C. S.; Grigg, R. D.; Tretbar, M.; Rigoli, J. W.; Schomaker, J. M. *Org. Lett.* **2016**, *18*, 284.
- (27) Gerstner, N. C.; Adams, C. S.; Tretbar, M.; Schomaker, J. M. *Angew. Chem. Int. Ed.* **2016**, *55*, 13240.
- (28) Stoll, A. H.; Blakey, S. B. *J. Am. Chem. Soc.* **2010**, *132*, 2108.
- (29) Stoll, A. H.; Blakey, S. B. *Chem. Sci.* **2011**, *2*, 112.
- (30) Mace, N.; Thornton, A. R.; Blakey, S. B. *Angew. Chem. Int. Ed.* **2013**, *52*, 5836.
- (31) Müller, P.; Baud, C.; Jacquier, Y. *Tetrahedron* **1996**, *52*, 1543.
- (32) Evans, D. A.; Faul, M. M.; Bilodeau, M. T. *J. Am. Chem. Soc.* **1994**, *116*, 2742.
- (33) Guthikonda, K.; Du Bois, J. *J. Am. Chem. Soc.* **2002**, *124*, 13672.
- (34) Fruit, C.; Robert-Peillard, F.; Bernardinelli, G.; Müller, P.; Dodd, R. H.; Dauban, P. *Asymmetry* **2005**, *16*, 3484.
- (35) Di Chenna, P.; Robert-Peillard, F.; Dauban, P.; Dodd, R. H. *Org. Lett.* **2004**, *6*, 4503.
- (36) Lebel, H.; Spitz, C.; Leogane, O.; Trudel, C.; Parmentier, M. *Org. Lett.* **2011**, *13*, 5460.
- (37) Ma, Z.; Zhou, Z.; Kürti, L. *Angew. Chem. Int. Ed.* **2017**, *56*, 9886
- (38) Chiappini, N. D.; Mack, J. B. C.; Du Bois, J. *Angew. Chem. Int. Ed.* **2018**, *57*, 4956.

- (39) Gillis, E. P.; Eastman, K. J.; Hill, M. D.; Donnelly, D. J.; Meanwell, N. A. *J. Med. Chem.* **2015**, *58*, 8315.
- (40) Ciesielski, J.; Dequierez, G.; Retailleau, P.; Gandon, V.; Dauban, P. *Chem. – Eur. J.* **2016**, *22*, 9338.
- (41) Kornecki, K. P.; Berry, J. F. *Chem. Commun.* **2012**, *48*, 12097.
- (42) Zalatan, D. N.; Du Bois, J. *J. Am. Chem. Soc.* **2009**, *131*, 7558.
- (43) Kornecki, K. P.; Berry, J. F. *Chem. Eur. J.* **2011**, *17*, 5827.
- (44) Kornecki, K. P.; Berry, J. F. *Eur. J. Inorg. Chem.* **2012**, 562.

## Chapter 4

### *Sc(OTf)<sub>3</sub>-Promoted Aza-[5+1] Cycloaddition of Vinylcyclopropanes*

#### 4.1. Introduction

Following the Rh(II)-catalyzed method, we looked to expand the scope of this [5+1] cycloaddition strategy. Cyclopropyl radicals have been used as radical clocks in order to decipher reaction mechanisms through the isolation of TEMPO-appended adducts. The non-classical nature of the cyclopropyl group has been used for rearrangements in the synthesis of cyclobutyl groups. Due to this, we envisioned that this interesting behavior could be applied to use mono-arylated vinylcyclopropanes (VCPs) through a different promoter or catalytic method. Herein, we report a follow-up study demonstrating Lewis and Brønsted acids that complete the [5+1] cycloaddition with a substrate scope complementary to the Rh(II) strategy. In this work, we used 2-aryl vinylcyclopropanes with various substitution patterns to synthesize a library of mono- and di-substituted tetrahydropyridines in the presence of an acid promoter.

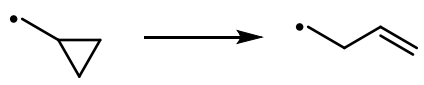
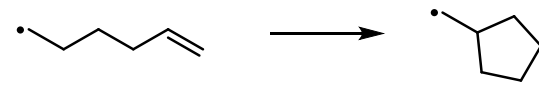
#### 4.2. Cyclopropylcarbinyl Radicals

##### *4.2.1. Introduction of cyclopropyl radical clocks*

Cyclopropyl radicals have been used as radical clocks in order to decipher radical mechanisms in reactions. Prior to these species, 5-hexenyl radicals have been used as a radical clock.<sup>1,2</sup> Following their work on using 5-hexenyl radicals, Ingold and co-workers looked towards the kinetics of the isomerization of species **4.1** and **4.3** (Table 4.1).<sup>3</sup> In this work, the rate constant for the opening of the cyclopropyl radical species was three

orders of magnitude larger than that of 5-hexenyl radical closing,<sup>2</sup> most likely due to the release of ring strain from the cyclopropane as well as better radical stability, showing promise for a better method to measure the kinetics of a radical mechanism.

**Table 4.1.** Kinetic and thermodynamic data for rearrangement of cyclopropyl rings and 5-hexenyl

Rearrangement		k (25°/s)
 <div style="display: flex; justify-content: space-around; width: 100%;"> <span>4.1</span> <span>4.2</span> </div>		$1.3 \times 10^8$
 <div style="display: flex; justify-content: space-around; width: 100%;"> <span>4.3</span> <span>4.4</span> </div>		$1.0 \times 10^5$

#### 4.2.2. Effect of substitution on cyclopropyl radicals

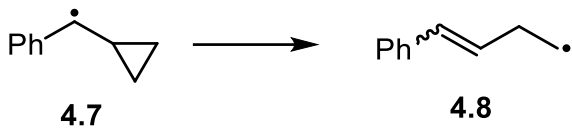
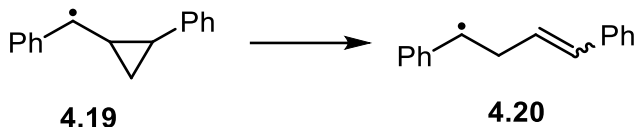
The kinetics of cyclopropylbenzyl radical clock rearrangement through pulse radiolysis of cyclopropyl benzyl benzoates was explored in 1989 (**Table 4.2**).<sup>4</sup> The substitution at the benzyl position was studied using both alkyl and phenyl groups. In general, any substitution on the radical decreased the rate constant by at least 2 orders of magnitude. Electron-rich aryl groups further decreased the rate (**4.9 – 4.12**). Lastly, a tertiary radical center showed a high rate of rearrangement. These correlations align with the Creary  $\sigma^*$  values,<sup>5</sup> which show how these radicals can be used as clocks in further competition experiments.

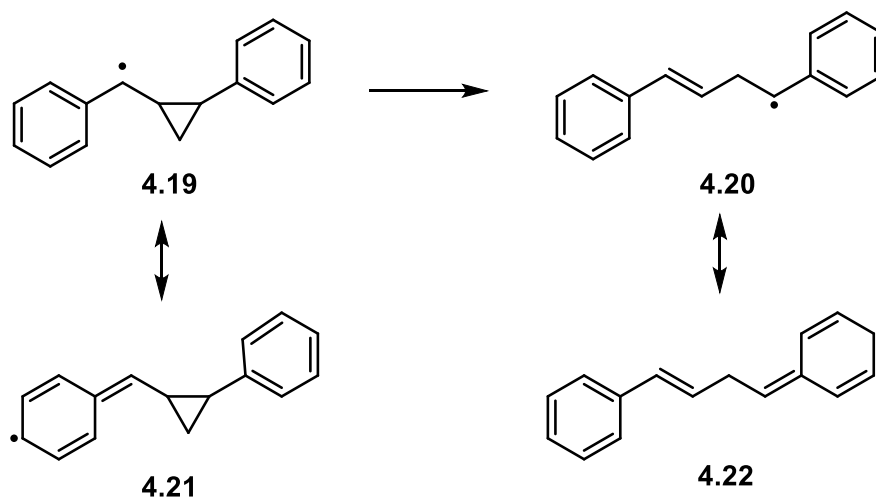
**Table 4.2.** Comparison of rate constants for differing substituted radicals

Rearrangement	R	k (25°/s)
 4.1 → 4.2	--	2.1 x 10 <sup>8</sup>
 4.5 → 4.6	--	7.0 x 10 <sup>6</sup>
 4.7 → 4.8	--	2.7 x 10 <sup>5</sup>
 4.9 - 4.12 → 4.13 - 4.16	Me Cl OMe Ph	2.1 x 10 <sup>5</sup> 2.0 x 10 <sup>5</sup> 1.4 x 10 <sup>5</sup> 0.5 x 10 <sup>5</sup>
 4.17 → 4.18	--	3.6 x 10 <sup>5</sup>

Tanko and co-workers also explored the use of phenyl groups  $\alpha$ -substituted on the cyclopropyl ring itself (**Table 4.3**).<sup>6</sup> In the case of the former, ring opening is less favorable both kinetically and thermodynamically. This has also been shown in a study by Beckwith and Bowry.<sup>7</sup> However, phenyl substituents on the cyclopropyl ring was more favorable. It was hypothesized that these differences can be rationalized through resonance stabilization (**4.21** and **4.22**). While  $\alpha$ -substitution stabilizes the closed form, substituents on the cyclopropyl ring instead stabilize the ring opened form (**Scheme 4.1**).

**Table 4.3.** Kinetic and thermodynamic data for rearrangement of  $\alpha$ -substituted vs 2-substituted cyclopropyl rings

Rearrangement		$\Delta E^\circ$ (kcal/mol)	$k$ (25°/s)
 4.7 $\longrightarrow$ 4.8		+5.8	$6.0 \times 10^4$
 4.19 $\longrightarrow$ 4.20		-5.9	$3.6 \times 10^8$

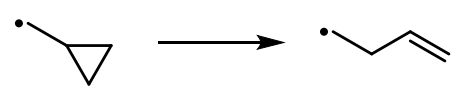
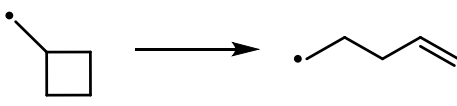
**Scheme 4.1.** Phenyl-substitution on cyclopropyl ring systems

#### 4.2.3. Kinetic and thermodynamics of cyclopropyl vs cyclobutyl ring opening

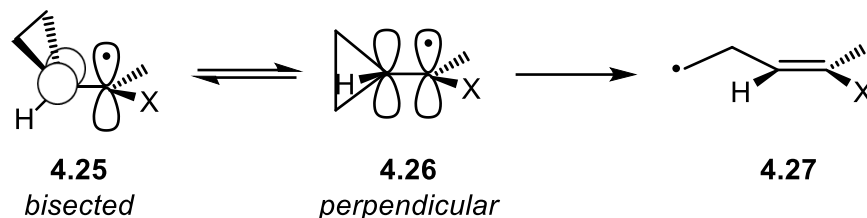
In that 2002 study by the Tanko group, the stability of cyclopropyl vs cyclobutyl ring opening was extensively studied with computational data as well as previous theory calculations (**Table 4.4**).<sup>6</sup> In the case of methyl cyclopropyl neutral radical (**4.1**), the thermodynamic driving force was almost equal to that of the cyclobutyl radical (**4.23**).

However, kinetically, the rate of cyclopropyl ring opening is five orders of magnitude faster than that of the cyclobutyl ring opening. It was concluded that the slower rates of ring-opening for the cyclobutyl ring cannot be attributed to the rate of ring strain. This is supported by previous work<sup>8</sup> that the strain energies of cyclopropane and cyclobutane are nearly the same, 27.5 vs 26.5 kcal/mol, respectively. In addition, the conjugative properties of the cyclopropyl vs the cyclobutyl groups could also play a role in the differing rates.<sup>9</sup>

**Table 4.4.** Data for rearrangement of cyclopropyl and cyclobutyl rings

Rearrangement		$\Delta E^\circ$ (kcal/mol)	k (25°/s)
		-2.3	$1.0 \times 10^8$
4.1	4.2		
		-1.6	$4.7 \times 10^3$
4.23	4.24		

The conformations for both cyclopropyl and cyclobutyl species were also examined (**Figure 4.1**).<sup>6</sup> In both systems, the bisected and perpendicular conformations are observed with the latter heavily favored due to the maximal overlap between the cycloalkyl HOMO and the radical center. According to DFT, a greater amount of spin density is transferred to the cyclopropyl group, which is reflective in the energetics. In the case of cyclopropyl, the bisected conformation is favored by 3.3 kcal/mol<sup>10</sup> while that of cyclobutyl is 1.1 kcal/mol.

**Figure 4.1.** Conformations for cyclopropyl system

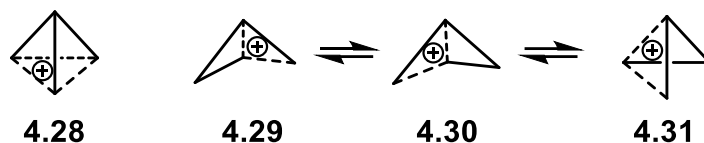
Lastly, the bond cleavage for ring opening of both species also showed that cyclopropyl ring opening was more favorable.<sup>6</sup> For the cyclobutyl ring, this bond cleavage was found to be much greater for its transition state as the lengths of the broken C-C bond and the spin density at the developing radical center are 2.04 Å and 0.398. However, for cyclopropyl ring opening, those values are 1.83 Å and 0.333. These differences indicated that the cyclopropyl ring opening undergoes a more delocalized, resonance-stabilized transition state vs cyclobutyl ring opening. This is congruent with the formation of cyclopropyl cations which undergo a non-classical carbocation transition state that adds further stabilization.

### 4.3. Cyclopropylcarbiny cations

#### 4.3.1. Seminal work with cyclopropylmethylium

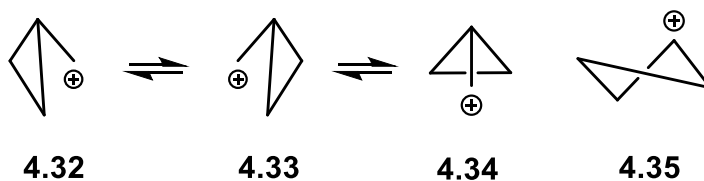
Cyclopropylcarbiny cations have been extensively studied,<sup>11</sup> though their intermediates have not been fully rationalized. The tricyclobutonium ion (**4.28**) was classified as the first “non-classical” carbocation by Roberts and co-workers due to its stability through equilibrating bicyclobutonium ion resonance structures (**Scheme 4.2**).<sup>12</sup>

---

**Scheme 4.2.** Initial reports of the “non-classical” carbocation


These intermediates were studied through solvolysis studies. In their work, Brown and co-workers observed unequal product ratios of cyclopropylcarbinyl and cyclobutyl derivatives in the methanolysis of cyclopropylcarbinyl and cyclobutyl 2-naphthalene-sulfonates, arguing the involvement of a bridged intermediate.<sup>13</sup> As a result, he proposed equilibrating cations **4.32** through **4.34** that occur through a short-lived puckered cyclobutyl cation **4.35** (**Scheme 4.3**). These fast equilibria are explained by the  $\sigma$ -conjugation involving the cyclopropyl group rather than  $\sigma$ -participation that is required for bridged structures.

---

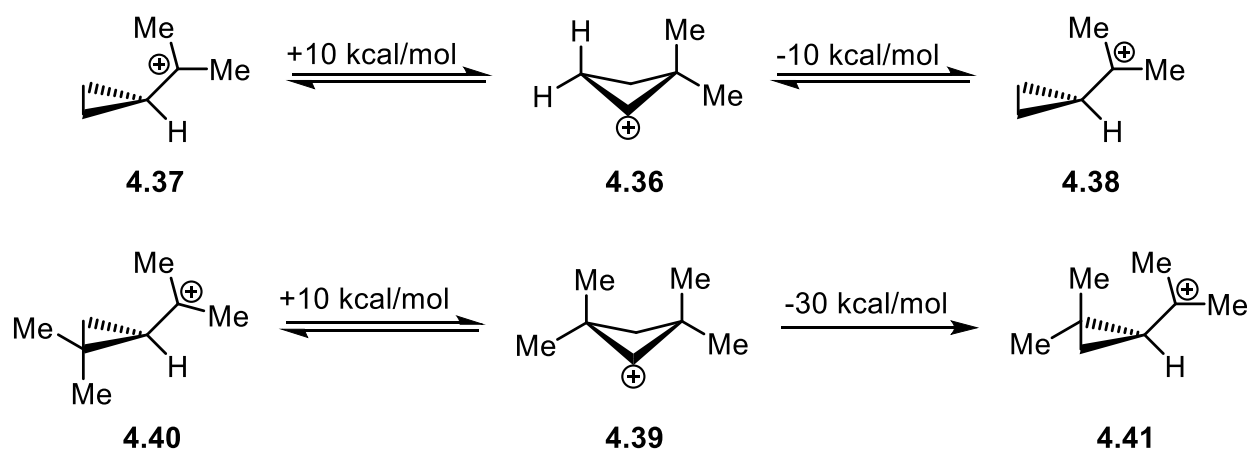
**Scheme 4.3.** Initial discoveries of VCP rearrangement


#### 4.3.2. Effect of substitution on cyclopropylcarbinyl cations

Substitution on the cation has been studied by many groups. In an early example by Hehre and Hiberty, the introduction of one or two methyl substituents on the rearrangement between cyclopropylcarbinyl tautomers compared to the unsubstituted cyclopropylcarbinyl was investigated through a combination of methyl stabilization data

as well as theoretical models (**Figure 4.2**).<sup>14</sup> For the puckered cyclobutyl cation, it was hypothesized that having the dimethyl groups on the cyclobutyl cation would not have an effect due to the location of the positive charge. However, while the unsubstituted cation has a low activation between the two cyclopropylcarbinyl-like structures, this is not seen for the dimethyl species, as the  $\Delta E$  is 30 kcal/mol below the dimethylcyclobutyl cation transition states, showing that the rearrangement is not favorable.

**Figure 4.2.** Methyl-stabilization of cyclopropylcarbinyl cation

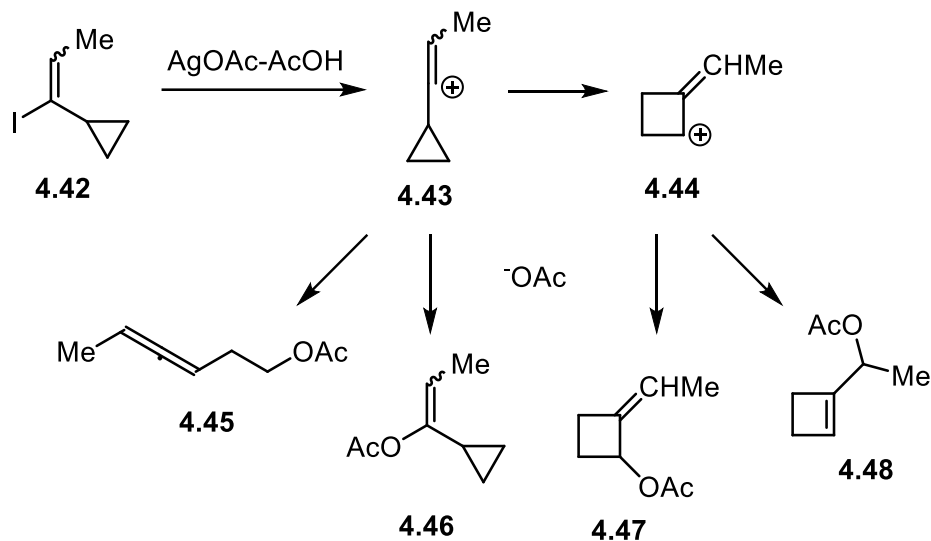


#### 4.3.3. VCP rearrangements through protonation

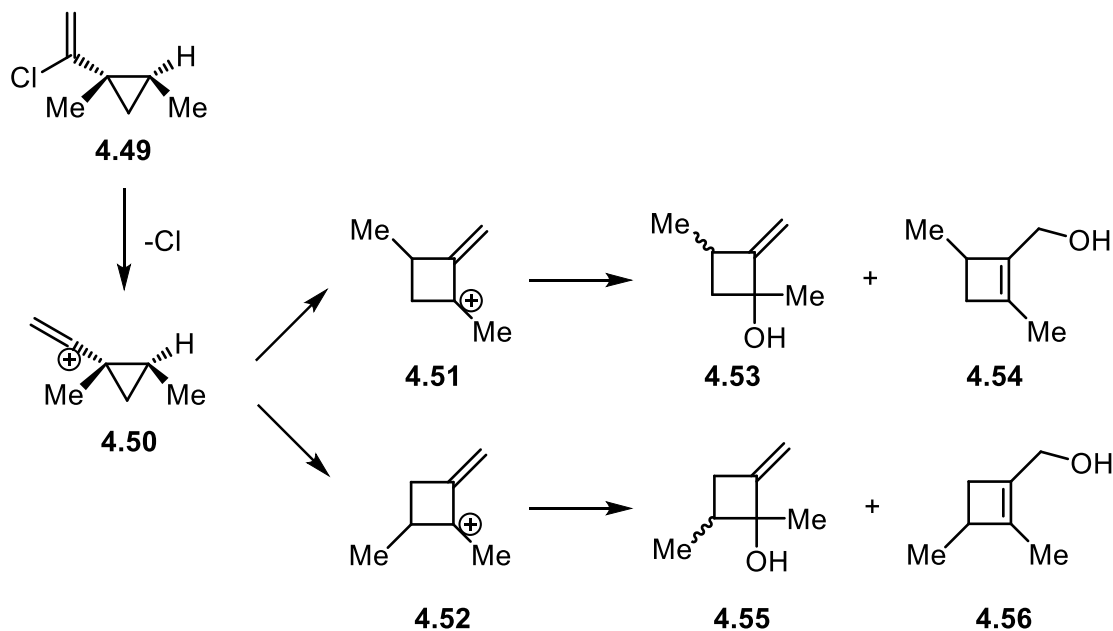
The formation of the cyclopropane-stabilized carbonium ion has been studied through protonation of a VCP. As a result, this cation may undergo several rearrangements before a deprotonation or a nucleophilic addition, usually by the solvent. 4-halogen-VCPs have shown interesting cyclopropyl-cyclobutyl rearrangements. Through solvolysis in the presence of AgOAc-AcOH is non-specific, resulting in differing acetate derivatives (**Scheme 4.4**).<sup>16</sup> The removal of the iodide anion results in species **4.43** which, if the acetate incorporates, results in allene **4.45** or VCP **4.46** in both *cis* and

*trans* isomers. However, if it rearranges to cation **4.44**, then there is a mixture of cyclobutene carbinol **4.48** and 2-methylene-cyclobutanol.

**Scheme 4.4.** Silver-initiated cyclopropyl-cyclobutyl arrangement

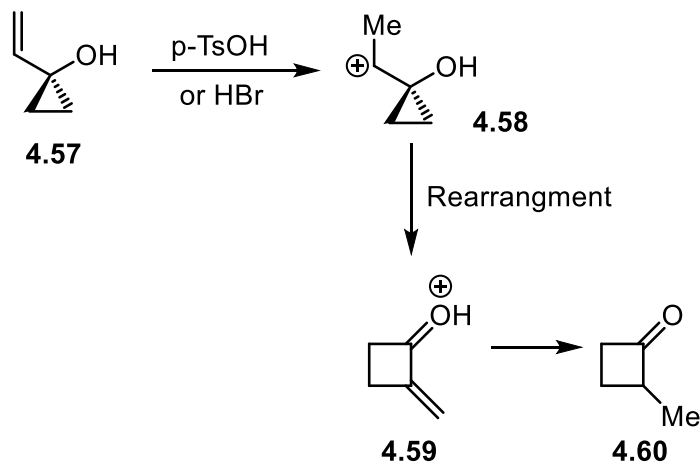


This rearrangement has also been observed from the hydrolysis of 4-chloro-VCP **4.49** (**Scheme 4.5**).<sup>17</sup> As a result of this reaction, there is a complex mixture of cyclobutanols (**4.53** – **4.56**). However, more than 84% of products (**4.53** and **4.54**) were derived from intermediate **4.51**, indicating a regioselective migration to the more substituted cyclopropane.

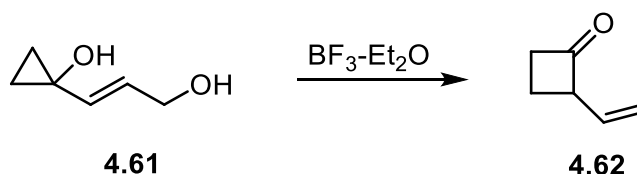
**Scheme 4.5.** Hydrolysis of 4-halogenated VCP **4.49**

This transformation has also been used with substitution at the 1-allylic position of the VCP with a hydroxyl group.<sup>18</sup> When exposed to either p-TsOH or HBr, protonation at the terminal olefin position results in intermediate **4.58** (**Scheme 4.6a**). Through a pinacol-pinacolone type of rearrangement, this leads to cyclobutanone **4.60**. This strategy was implemented by Ollivier and Salaün where, in the presence of a Lewis acid, the diol rearranges, undergoes dehydration, and results in vinylcyclobutanone **4.62** (**Scheme 4.6b**).<sup>19</sup> Silyl ethers also undergo a cyclopropylcarbinyl cation intermediate, leading to the synthesis of spiro complexes (**Scheme 4.6c**).<sup>20</sup>

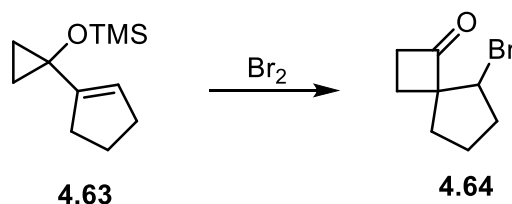
---

**Scheme 4.6a.** VCP rearrangement with Brønsted acid



---

**Scheme 4.6b.** Lewis acid-promoted VCP rearrangement



---

**Scheme 4.6c.** Silyl ether appended-VCP rearrangement



---

The rearrangement of cyclopropylcarbinyl radicals and cations have been extensively used for both syntheses and kinetic work. These transformations and mechanistic knowledge have later been applied to other motifs, in particular VCPs (see **Chapter 2**). A combination of both of these were used to further develop the [5+1] work beyond Rh(II) catalysis. In this discussion, we present a complimentary  $\text{Sc}(\text{OTf})_3$  procedure using a larger scope of VCPs that can be explained through mechanistic experiments and previous literature.

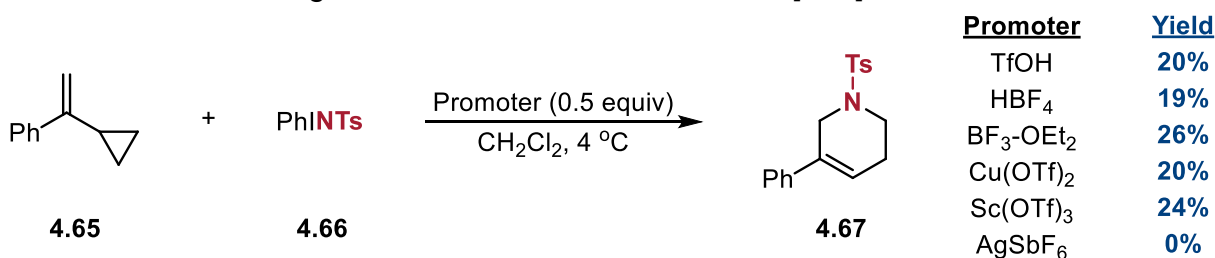
## 4.4. Investigations with 2-arylvinylcyclopropanes

### 4.4.1. Screening of Brønsted and Lewis acids

Initial screening of the [5+1] reaction was investigated using VCP **4.65**. It was found that a number of Brønsted and Lewis acids were able to initiate the cycloaddition between **4.65** and **4.66** to afford the desired cycloadduct **4.67** (**Scheme 4.7**).

Strong protic acids, such as TfOH and HBF<sub>4</sub>, were able to promote the [5+1] reaction in a sub-stoichiometric amount. In particular, triflic acid was able to synthesize **4.67** in 20% yield while increasing to 2 equivalents led to a 41% yield. Further screening with these acids, however, revealed that these acids promote oligomerization of the starting material and degradation of PhINTs even at -78°C. BF<sub>3</sub>-OEt<sub>2</sub> was also able to initiate the [5+1] reaction in comparable yields with a lower degree of consumption of the starting materials. It was found, however, that the results from these reactions were irreproducible and showed varying results, so metal triflates were instead further examined to promote this cycloaddition.

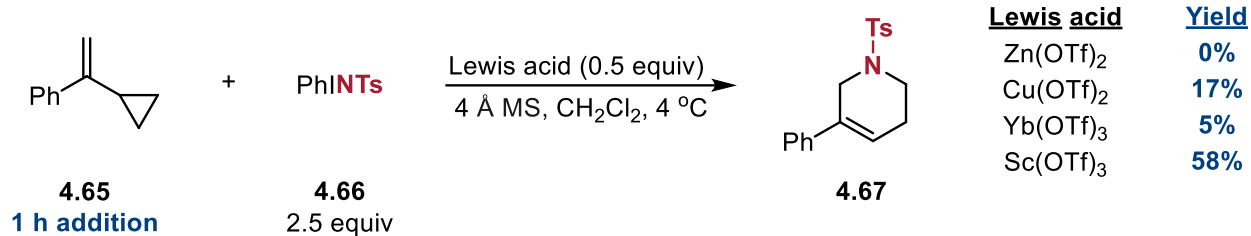
**Scheme 4.7.** Screening of Brønsted and Lewis acids for [5+1] reaction



Zn(II) and Yb(II) both had poor reactivity in this reaction with over 80% of **4.65** not being consumed even at room temperature (**Scheme 4.8**). Cu(OTf)<sub>2</sub>, which has been previously used for aziridination,<sup>21</sup> provided **4.67** in 17% yield and full VCP consumption.

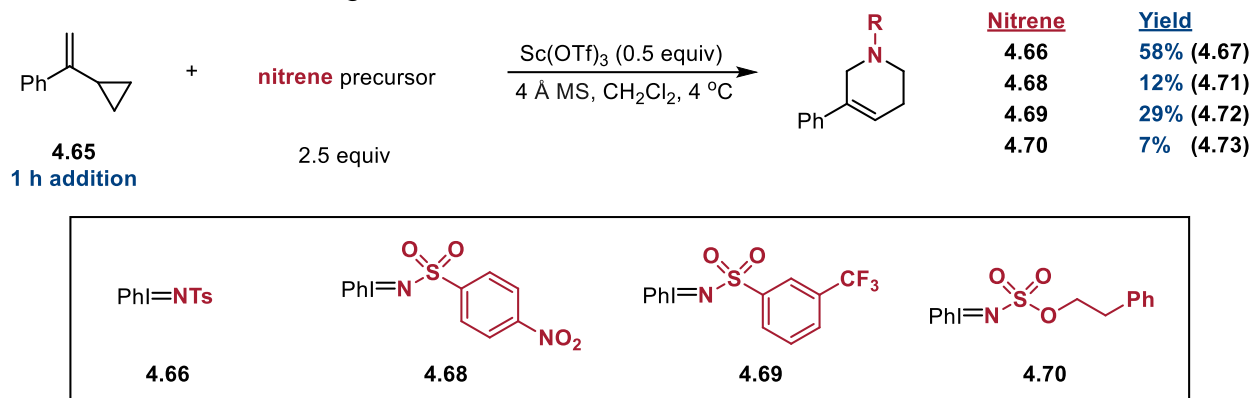
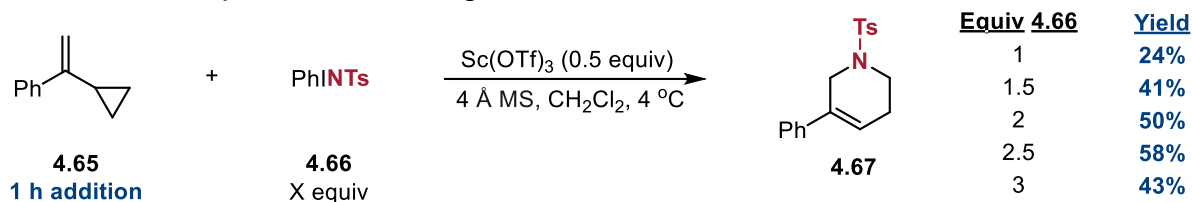
Sc(OTf)<sub>3</sub> was found to be the most effective in promoting the [5+1] cycloaddition. In order to control the unproductive polymerization of the starting material, the VCP was added dropwise as a solution in CH<sub>2</sub>Cl<sub>2</sub> in to keep the VCP concentration low and hinder the oligomerization pathway.

#### Scheme 4.8. Metal triflates screening

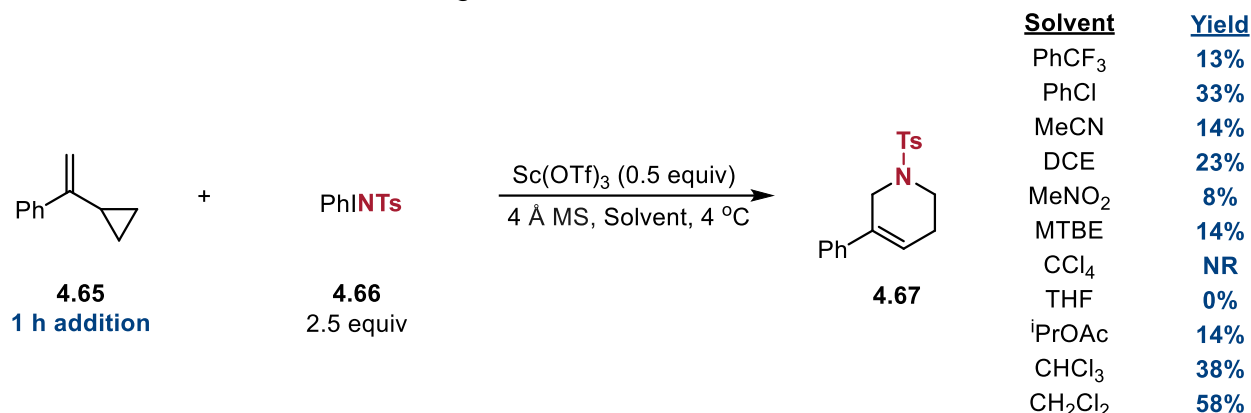


#### 4.3.2. Optimization of Sc(OTf)<sub>3</sub>-promoted conditions

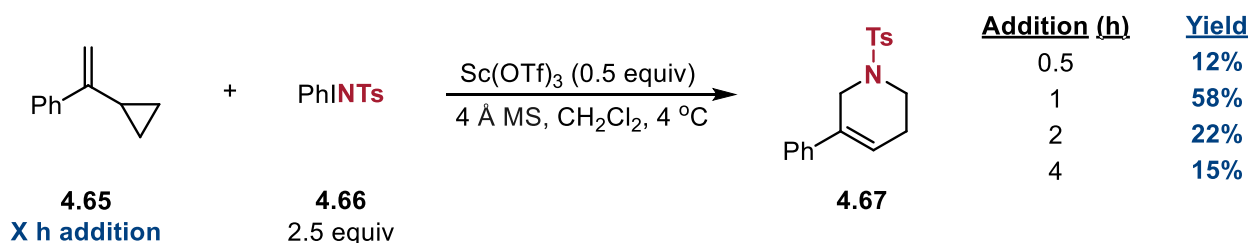
Modifying the electronics of the nitrogen source was further examined using **4.66** and **4.68** – **4.70** (Scheme 4.9a). Substituting the aryl ring with an electron deficient group (**4.68** and **4.69**) showed lower reactivity as well as decreased solubility in the reaction media. In addition, increasing the equivalents of the nitrogen source to 2.5 was found to be the most optimal (Scheme 4.9b). It was hypothesized that through the use of excess PhINTs, side reactions and degradation that may occur with the intermediate radical species can be minimized. However, further increasing the amount of PhINTs leads to a decrease in yield of the desired cycloadduct.

**Scheme 4.9a. Screening of iminoiodinanes****Scheme 4.9b. Equivalents of nitrogen source**

The effect of solvent on the [5+1] cycloaddition was investigated (**Scheme 4.10**). Chlorinated solvents, including chlorobenzene, dichloroethane, chloroform, and dichloromethane, were found to favor this cyclization. This is mainly due to the ability of these solvents to successfully solubilize  $\text{PhI}=\text{NTs}$ . In contrast, trifluorotoluene, nitromethane, and isopropyl acetate exhibited very little ability to accomplish this, leading to a lower yield of the desired cycloadduct. The use of THF and MTBE resulted in acid-catalyzed polymerization, causing a low conversion to product **4.67**.

**Scheme 4.10.** Solvent screening

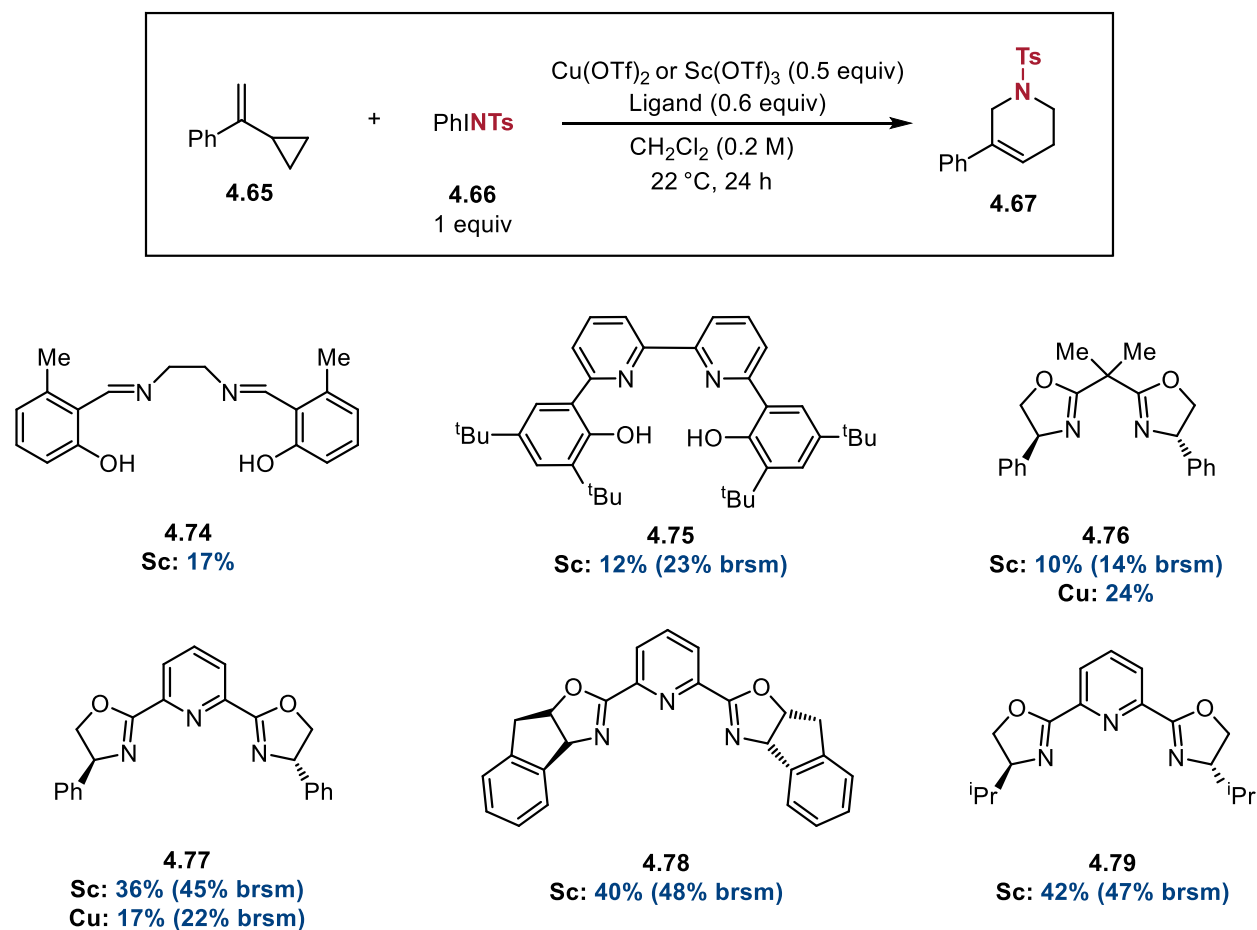
The addition time of VCP **4.65** into the reaction mixture was explored (**Scheme 4.11**). Decreasing the time led to a 12% yield of **4.67**, most likely due to the high concentration of VCP increases the likelihood of side reactions. Interestingly, there was also a drop-off in yield when longer addition times were applied. This demonstrates the sensitivity of VCP concentration in solution and the importance of limiting nonproductive side reactivity.

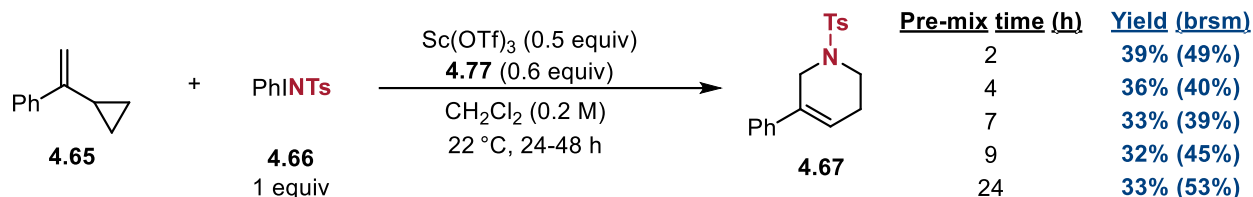
**Scheme 4.11.** Addition time of VCP **4.65**

The use of Cu(II)- and Sc(III)-ligand complexes were also examined (**Figure 4.3**). The metal triflate and ligand were stirred together for two hours to assemble the complex *in situ* before the addition of **4.65** and **4.66**. SALEN (**4.74**), bipyridine (**4.75**), and BOX ligands (**4.76**) were all found to be ineffective to form **4.67**. Using  $\text{Sc}(\text{OTf})_3$ , pyBOX ligands

(**4.77** – **4.79**) showed promise with assembling the [5+1] product up to 42% yield (47% brsm) with just one equivalence of PhINTs. As these  $\text{Sc}(\text{OTf})_3$ -pyBOX ligands have yet to be isolated in the literature, we briefly looked at extending the time of ligand and metal triflate in solution together to ensure that there was complexation (**Scheme 4.12**). Using ligand **4.77**, we saw no substantial effect on yield of **4.67**; thus,  $\text{Sc}(\text{OTf})_3$  by itself was continued to be used as the acid promoter.

**Figure 4.3.** Investigation of metal-ligand triflate complexes



**Scheme 4.12.** Pre-mixing time with Sc(OTf)<sub>3</sub> and **4.77****4.4.3. Scope of Sc(OTf)<sub>3</sub>-promoted [5+1] cycloaddition**

With the optimized conditions in hand, the scope of this aza-[5+1] reaction was assessed (**Table 4.5**). Electronic modifications to the 2-aryl group were found to have a profound effect on the reaction. Halogens in the para- (**4.80** – **4.82**) and meta- positions (**4.87** – **4.88**) were well tolerated as well as di-halogenated substrates (**4.91** – **4.92**). On the other hand, strongly electron-donating groups (**4.89**) greatly reduced yields. Tricyclic product **4.95** was obtained in 27% yield, exhibiting how this reaction can be expanded to more complex ring systems. In addition, alkyl groups at the R<sup>2</sup> were amenable to this method as **4.96** was isolated in 41% yield. However, if a cyclohexyl group is instead at the R<sup>2</sup> position, the yield dropped to 7% (not shown), suggesting that sterics at this site highly affects the cycloaddition. Lastly, substitution at the R<sup>3</sup> position was somewhat tolerated as **4.97** was obtained at 30% yield; however, methyl substitution was not.

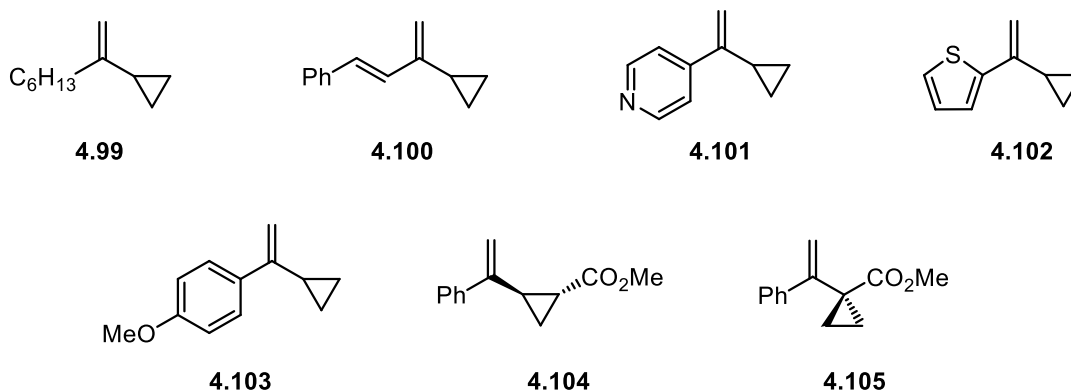
**Table 4.5.** Isolated products from the  $\text{Sc}(\text{OTf})_3$  aza-[5+1] reaction

		<b>R</b> H F Cl Br Me Ph CF <sub>3</sub> CO <sub>2</sub> Me	<b>Yield</b> <b>58% (4.67)</b> <b>21% (4.80)</b> <b>48% (4.81)</b> <b>36% (4.82)</b> <b>22% (4.83)</b> <b>26% (4.84)</b> <b>50% (4.85)</b> <b>30% (4.86)</b>
		<b>R</b> F Br OEt CN	<b>Yield</b> <b>20% (4.87)</b> <b>42% (4.88)</b> <b>12% (4.89)</b> <b>37% (4.90)</b>
<hr/>			
			<b>44%</b> <b>(4.91)</b>
			<b>27%</b> <b>(4.92)</b>
			<b>26%</b> <b>(4.93)</b>
			<b>19%</b> <b>(4.94)</b>
			<b>27%</b> <b>(4.95)</b>
			<b>41%</b> <b>(4.96)</b>
			<b>30%</b> <b>(4.97)</b>
			<b>10%</b> <b>(4.98)</b>

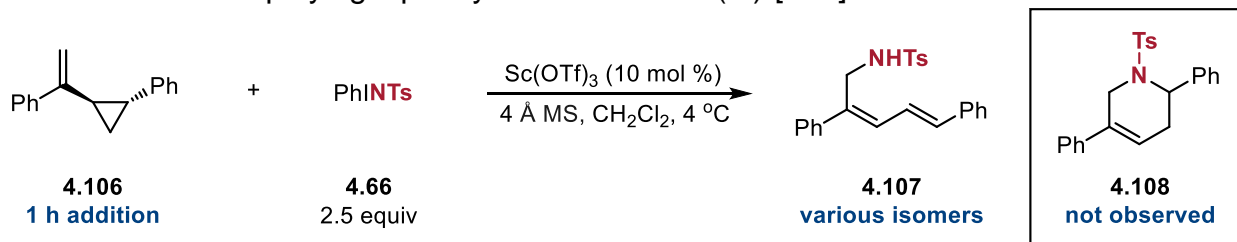
While further substitution on the VCP was moderately tolerated, an aryl group on the vinyl group was required to stabilize the ring opening of the VCP. Alkyl (**4.99**) and alkenyl (**4.100**) substitution at that position resulted in full VCP consumption and no desired tetrahydropyridine product (**Figure 4.4**). In addition, **4.101** and **4.102** weren't

amenable for this reaction due to the electron-rich atoms coordinating to the Sc(III) center, preventing activation of the iminoiodinane for the [5+1] reaction to occur. Electron-donating groups in the para- position, such as in **4.103**, resulted in rapid VCP consumption and only trace amounts of the [5+1] adduct. To demonstrate functional group tolerance on the cyclopropyl ring, substrates **4.104** and **4.105** were employed; however, even at room temperature, there was little VCP consumption and no observable products (**Scheme 4.13**). Lastly, in the case of **4.106**, exposure to the reaction conditions resulted in a mixture of diene isomers with no desired [5+1] product, even with a catalytic amount of Sc(OTf)<sub>3</sub>.

**Figure 4.4.** Incompatible substrates with the Sc(III)-promoted conditions

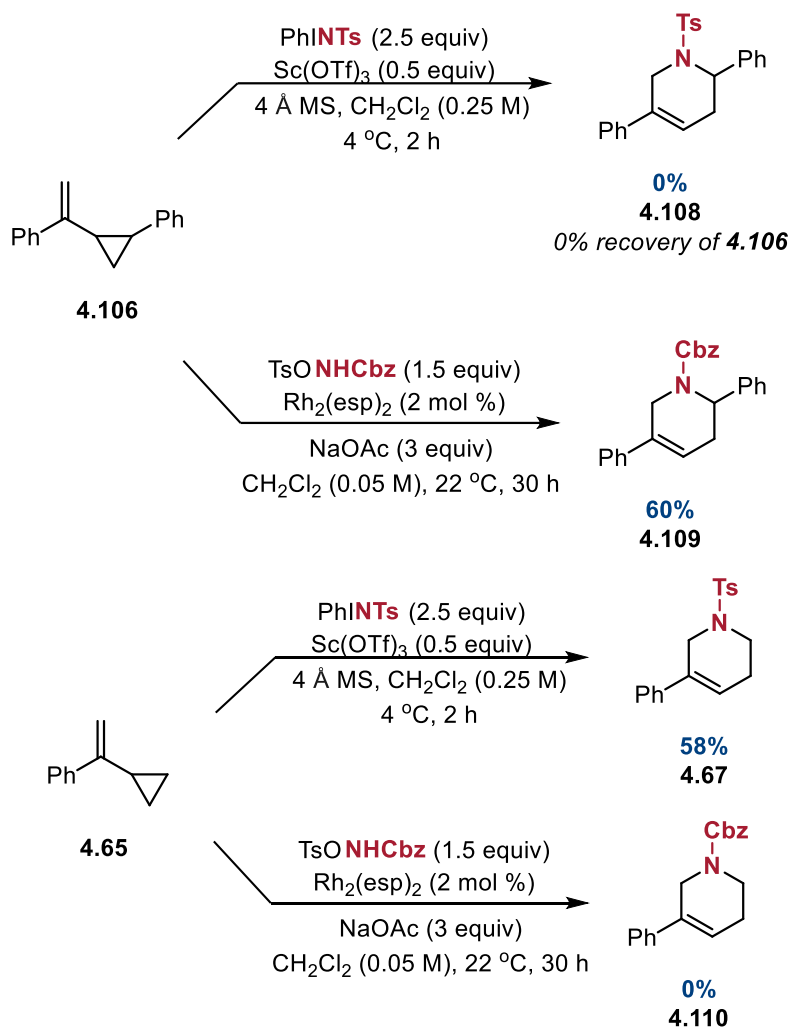


**Scheme 4.13.** Employing diphenyl substrate in Sc(III)-[5+1] reaction



#### 4.4.4. Complementarity of Rh(II) and Sc(OTf)<sub>3</sub> methods

In terms of substrate scope, that for the Sc(OTf)<sub>3</sub>-promoted method is completely different to that of our previously discussed Rh-catalyzed strategy (see **Chapter 3**). The complementarity of these methods is shown. In the case of **4.106**, the Rh(II)-catalyzed method can successfully produce **4.109** in 60% yield; however, the use of Sc(OTf)<sub>3</sub>/PhINTs as reported results in VCP degradation into a complex mixture of products, including various dialkene isomers (see **Scheme 4.14**). On the other hand, **4.65** and selected substrates **SM 4.96** and **4.97** were not amenable to the Rh<sub>2</sub>(esp)<sub>2</sub>-conditions.

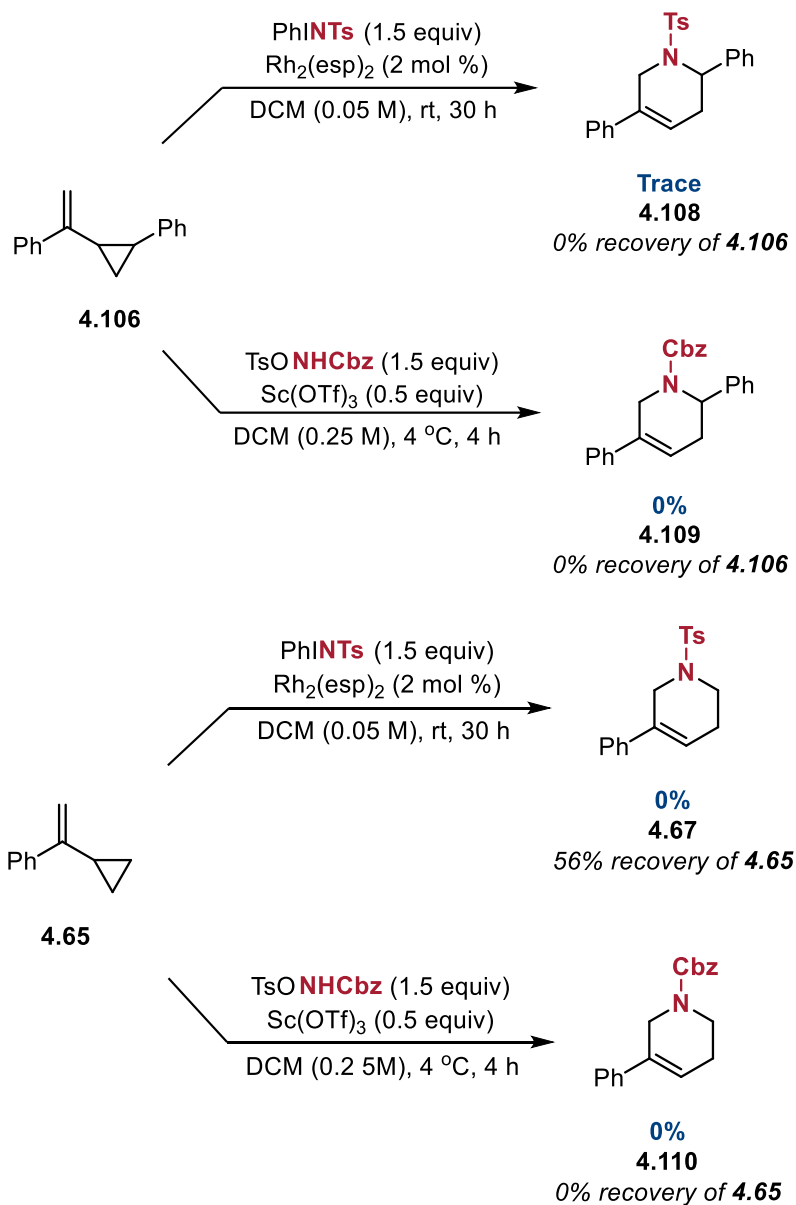
**Scheme 4.14.** Substrate dependency of Rh-catalyzed and Sc-promoted conditions

The complementarity of these different approaches was also studied through the role of the nitrene precursor as both have different reactivity (**Scheme 4.15**). In the case of all four cases using  $\text{PhINTs/Rh}_2(\text{esp})_2$  and  $\text{TsONHCbz/Sc(OTf)}_3$  reagent/catalyst conditions, no isolable amounts of the desired products were detected. In addition, in three out of the four cases, complete consumption of the starting material was consumed. These results showed that the sole choice of the nitrene precursor or catalyst is integral,

but rather the combination of both. Thus, this would seem to indicate that there are integral mechanistic differences between these two reactions.

---

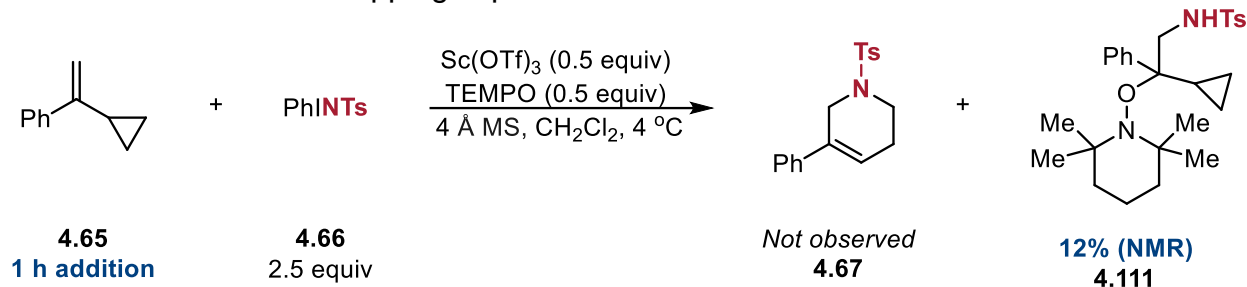
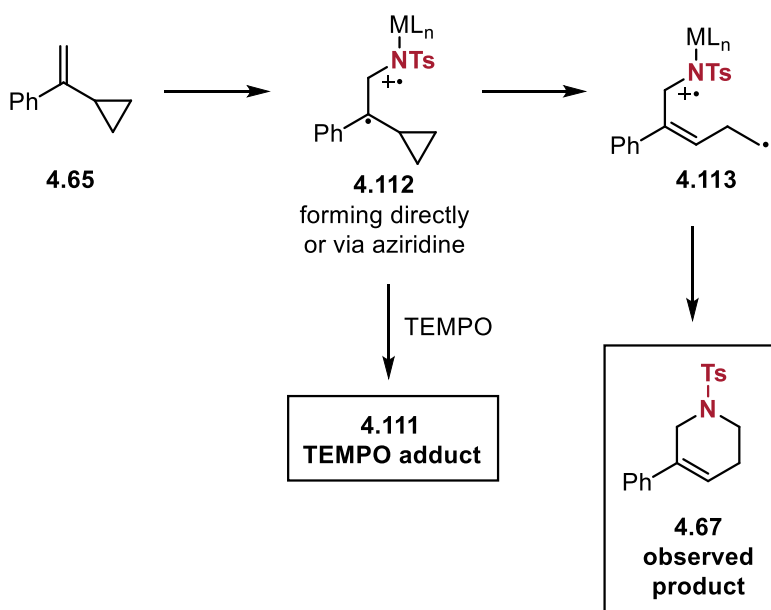
**Scheme 4.15.** Role of the nitrene precursor



#### 4.4.5. Mechanistic insight into the Sc(III)-promoted reaction

The Rh-catalyzed method is proposed to proceed through a cyclopropylcarbinylation that is formed upon nitrene transfer to the vinyl group of the VCP which then undergoes rearrangement in order to form the cycloadduct (see **Chapter 3**). Prior to this study, however, there was no prior literature for scandium-promoted nitrene transfer and, thus, no mechanistic studies on the topic. Shown in **Scheme 4.8** and **Figure 4.3**, Cu(OTf)<sub>2</sub>, which been previously used by the Evans group for aziridination,<sup>21</sup> was also capable of performing this [5+1] reaction, albeit a reduced yield. In their work, Evans and co-workers suggest that Cu-nitrenoids with styrenes undergo a non-stereospecific reaction that involves radical intermediates.

Because of the compatibility of Cu(OTf)<sub>2</sub> in this transformation, we implemented TEMPO as a radical trap (**Scheme 4.16**). With this experiment, there was no observed [5+1] product and instead, adduct **4.111** was isolated in 12% yield. The structure was later confirmed through both NMR and HRMS. With these results, it was postulated that the Sc(III)-method was undergoing a radical pathway. Scandium-promoted nitrene transfer occurs with **4.65**, providing intermediate **4.112** either directly or through an aziridine intermediate. Following cyclopropyl carbonyl rearrangement, **4.113** forms and subsequent ring closure leads to **4.67**. However, If TEMPO is introduced, the radical pathway is shut down and instead, **4.111** is observed. This mechanistic proposal is consistent with the high regioselectivity of olefin formation that is established during nitrene transfer. The R<sup>2</sup>,R<sup>5</sup> substitution of **4.96** can also be explained by the preference of C-C bond cleavage of the cyclopropyl ring to a more stable secondary radical.

**Scheme 4.16.** Radical trapping experiment with TEMPO**Figure 4.5.** Proposed mechanism in Sc(OTf)<sub>3</sub> aza-[5+1] cycloaddition**4.5. Conclusions**

We have developed a Lewis acid-promoted method to assemble tetrahydropyridines with VCPs and iminoiodinanes. These conditions were amenable for further substitution on the VCP leading to a library of differently substituted nitrogen heterocycles. This aza-[5+1] cycloaddition has been, and is currently, further developed in order to expand the substrate scope of this approach and to have this cycloaddition be done in a catalytic manner. In addition, with reflecting on the mechanistic studies with

differing substituents at the  $\alpha$ -position, perhaps tetrahydropyridines with different motifs could be synthesized using this radical technique and expand the type of tetrahydropyridine structures that can be obtained.

#### 4.6. References

- (1) Julia, M. *Pure and App. Chem.* **1967**, 15, 167; *Accounts of Chem. Res.* **1971**, 4, 386.
- (2) Lal, D.; Griller, D.; Husband, S.; Ingold, K. U. *J. Am. Chem. Soc.* **1974**, 96, 6355.
- (3) Maillard, B.; Forrest, D.; Ingold, K.U. *J. Am. Chem. Soc.* **1976**, 98, 7024.
- (4) Masnovi, J.; Samsel, E. G.; Bullock, R. M. *J. Chem. Soc., Chem. Commun.* **1989**, 15, 1044.
- (5) Creary, X. *J. Org. Chem.* **1980**, 45, 280; Creary, X.; Mehrsheikh-Mohammadi, M. E.; McDonald, S. *J. Org. Chem.* **1987**, 52, 3254.
- (6) Stevenson, J. P.; Jackson, W. F.; Tanko, J. M. *J. Am. Chem. Soc.* **2002**, 124, 4271.
- (7) Beckwith, A. L. J.; Bowry, V. W. *J. Am. Chem. Soc.* **1994**, 116, 2710.
- (8) Dewar, M. J. S. *J. Am. Chem. Soc.* **1984**, 106, 669.
- (9) Tidwell, T. T. *Conjugative and substituent properties of the cyclopropyl group*; Rappoport, Z., Ed.; John Wiley & Sons: Ltd.: New York, **1987**, 565 – 632.
- (10) Walton, J. C. *Magn. Reson. Chem.* **1987**, 25, 998.
- (11) Olah, G. H.; Reddy, P.; Surya Prakash, G. K. *Chem. Rev.* **1992**, 92, 69.

- (12) Mazur, R. H.; White, W. N.; Semenov, D. A.; Lee, C. C.; Silver, M. S.; Roberts, J. D. *J. Am. Chem. Soc.* **1959**, *81*, 4390.
- (13) Brown, H. C. *The Nonclassical Ion Problem*; Plenum Press: New York, **1997**.
- (14) Hehre, W. J.; Hibierty, P. C. *J. Am. Chem. Soc.* **1974**, *96*, 302.
- (15) Goldschmidt, Z.; Crammer, B. *Chem. Soc. Rev.* **1988**, *17*, 229.
- (16) Kelsey, D. R.; Bergman, R. G. *J. Am. Chem. Soc.* **1971**, *93*, 1941.
- (17) Santelli, M.; Bertrand, M. *Tetrahedron*, **1974**, *30*, 243.
- (18) Wasserman, H. H.; Cochoy, R. E.; Baird, M. S. *J. Am. Chem. Soc.* **1969**, *91*, 2375.
- (19) Ollivier, J.; Salaün, J. *Tet. Lett.* **1984**, *25*, 1269.
- (20) Trost, B. M.; Mao, M. K. *J. Am. Chem. Soc.* **1983**, *105*, 6753.
- (21) Evans, D. A.; Faul, M. M.; Bilodeau, M. T. *J. Am. Chem. Soc.* **1994**, *116*, 2742.

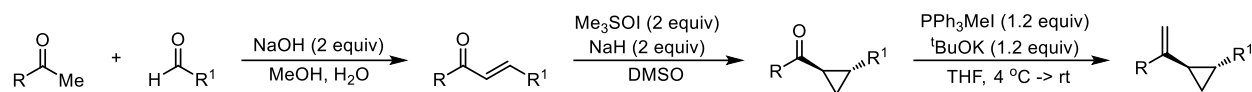
## APPENDIX 1

### Chapter 3 Experimental and Characterization

#### 1.1. General Methods

All reagents and solvents were obtained commercially in reagent grade or better quality and used without further purification. Anhydrous dichloromethane and tetrahydrofuran were obtained by degassing followed by passing through an alumina drying column before use. Anhydrous DMSO was purchased from Acros Organics and used directly. Flash column chromatography was performed using silica gel (230-400 mesh) purchased from Silicycle.  $^1\text{H}$  and  $^{13}\text{C}$  spectra were acquired at 300 K on a Bruker Avance III (600 MHz or 800 MHz) or Varian NMRS (600 MHz) spectrometer. Chemical shifts are reported in parts per million (ppm  $\delta$ ) referenced to the residual  $^1\text{H}$  resonance of the solvent. The following abbreviations are used singularly or in combination to indicate the multiplicity of signals: s - singlet, d - doublet, t - triplet, q - quartet, m - multiplet and br - broad. IR spectra were recorded on a Shimadzu IRAffinity-1S FTIR spectrophotometer with ATR attachment. High-resolution mass spectrometry was obtained from the University of Illinois at Urbana-Champaign Mass Spectrometry Lab using Waters Q-TOF ESI or Waters oa-TOF EI spectrometers.

## 1.2. General procedure for synthesis of 2,4-disubstituted vinylcyclopropanes



Sodium hydroxide (40 mmol) was dissolved in 5 ml of water. Reaction was diluted with 40 ml of MeOH and the appropriate acetophenone (20 mmol) was added. After 10 minutes, the corresponding aldehyde (20 mmol) was added and the reaction was stirred until the starting material was consumed (2 – 24 hours). If the product precipitated, it was collected via vacuum filtration and washed with water and MeOH. If not, the organic layer was added to  $\text{NH}_4\text{Cl}$  and extracted with DCM. The organic layers were combined and washed with brine and dried over  $\text{MgSO}_4$ . The desired  $\alpha$ - $\beta$  unsaturated ketone was isolated via flash silica chromatography (5-10% EtOAc in hexanes).

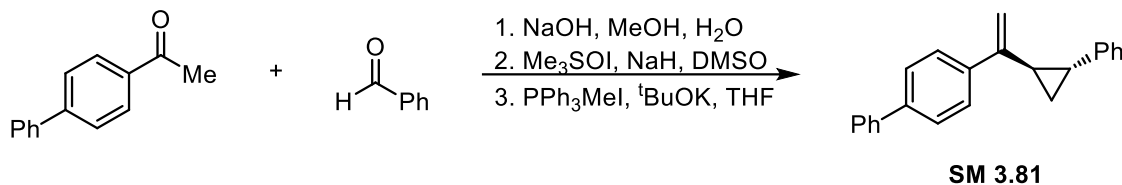
Trimethylsulfoxonium iodide (10 mmol) was dissolved in 30 mL anhydrous DMSO under inert atmosphere at ambient temperature. Sodium hydride (10 mmol) was added portionwise and the mixture was stirred 30 minutes at which time the enone (5 mmol) was added in a single portion. The reaction was stirred overnight then quenched with saturated aqueous  $\text{NH}_4\text{Cl}$  before being extracted with  $\text{Et}_2\text{O}$ . Combined organic layers were washed with aqueous  $\text{NH}_4\text{Cl}$ , then brine and dried over  $\text{Na}_2\text{SO}_4$ . The filtrate was concentrated and purified by silica gel chromatography (3-5% EtOAc in hexanes) to afford the corresponding cyclopropyl ketone.

Methyl triphenylphosphonium iodide (6 mmol) was suspended in anhydrous THF (35 mL) under inert atmosphere. After cooling to 4 °C, potassium tert-butoxide (6 mmol) was added and stirred for 30 minutes. The cyclopropyl ketone (5 mmol) was added in a single portion and the reaction mixture was allowed to warm to ambient temperature. After stirring overnight, the reaction was quenched with aqueous  $\text{NH}_4\text{Cl}$ , added to aqueous  $\text{NH}_4\text{Cl}$  (50

ml) and extracted with Et<sub>2</sub>O (50 ml x 3). The combined organic extracts were washed with aqueous NH<sub>4</sub>Cl (40 ml), brine (50 ml x 2) and dried over Na<sub>2</sub>SO<sub>4</sub>. The filtrate was concentrated and purified by silica gel chromatography (1-3% EtOAc in hexanes).

NMRs of **SM 3.70**, **3.80**, **3.82**, **3.83**, **3.86**, **3.89**, and **3.92** were in accordance with the literature.<sup>1</sup> Nitrene precursors **3.71** – **3.72**,<sup>2</sup> **3.33**, **3.69**, **3.73** – **3.74**<sup>3</sup> were synthesized according to the literature. Derivatives of the benzyl tosyloxycarbamate matched previous NMR reports.<sup>4,5</sup>

### 1.3. Characterization of new 2,4-disubstituted vinylcyclopropanes



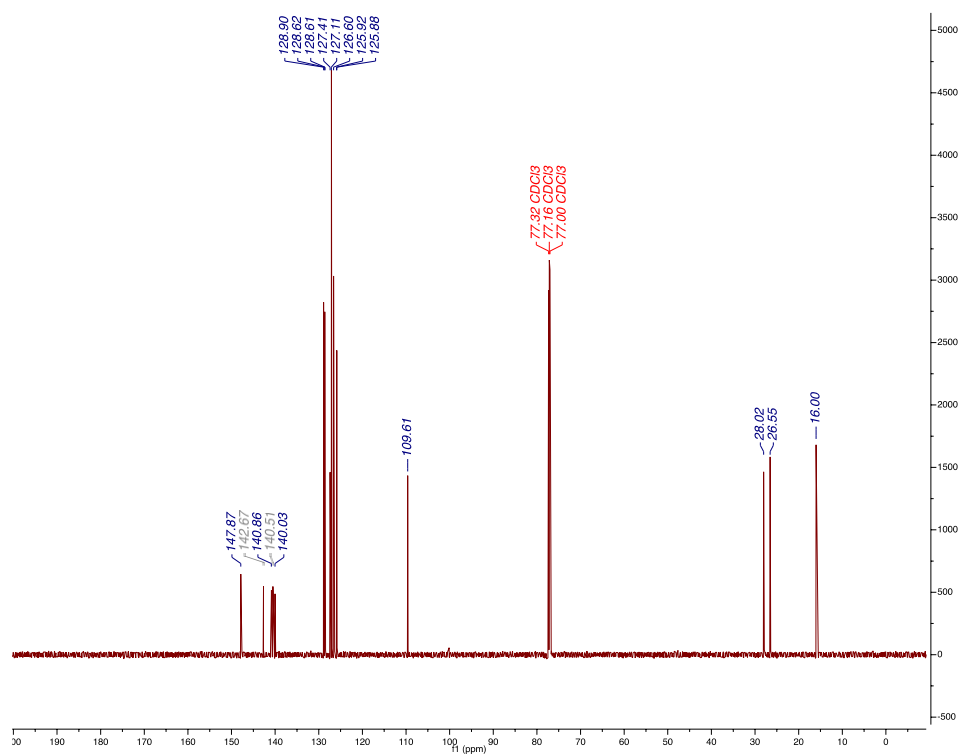
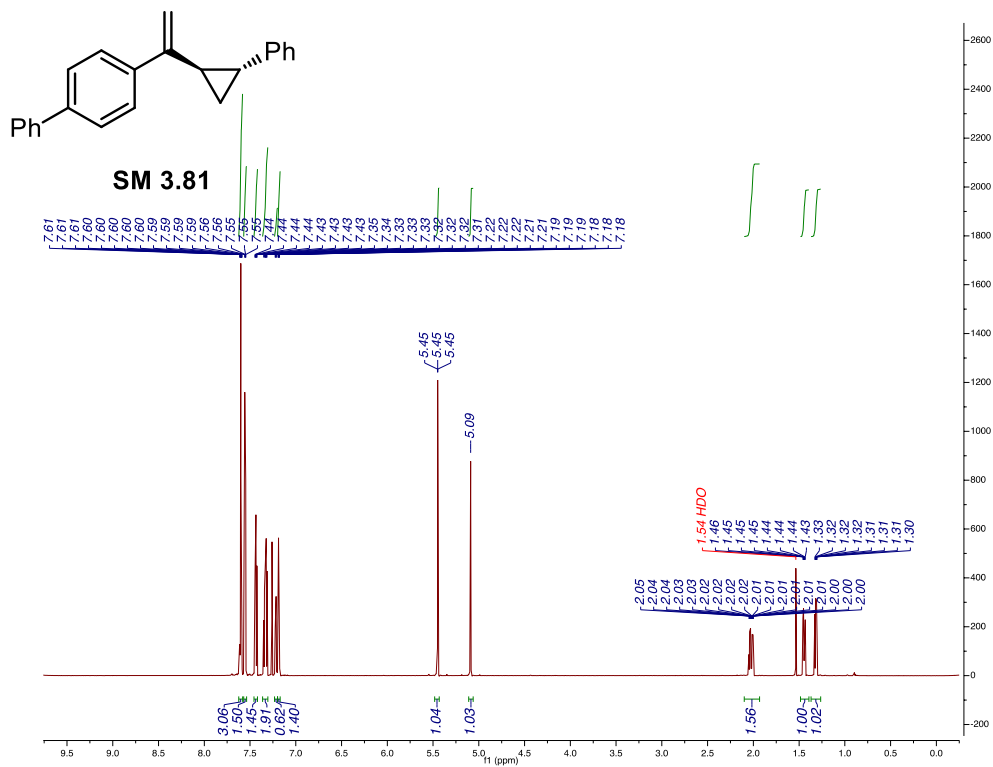
Prepared using the general procedure and purified via silica flash chromatography with 1% ethyl acetate in hexanes as a white crystalline solid.

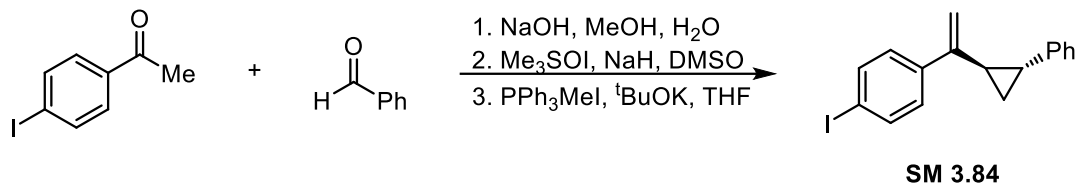
**<sup>1</sup>H NMR** (800 MHz, CDCl<sub>3</sub>) δ 7.60 (ddt, *J* = 8.3, 7.7, 0.9 Hz, 3H), 7.57 – 7.54 (m, 2H), 7.46 – 7.42 (m, 1H), 7.36 – 7.30 (m, 2H), 7.23 – 7.20 (m, 1H), 7.20 – 7.17 (m, 1H), 5.45 (t, *J* = 0.6 Hz, 1H), 5.09 (s, 1H), 2.10 – 1.93 (m, 2H), 1.45 (ddd, *J* = 8.7, 6.2, 5.0 Hz, 1H), 1.32 (ddd, *J* = 8.5, 5.7, 5.0 Hz, 1H) ppm.

**<sup>13</sup>C NMR** (201 MHz, CDCl<sub>3</sub>) δ 147.9, 142.7, 140.9, 140.5, 140.0, 128.9, 128.6, 128.6, 127.4, 127.1, 126.6, 125.9, 125.9, 109.6, 28.0, 26.6, 16.0 ppm.

**IR** (film):  $\bar{\nu}$  = 3028 (w), 2360 (w), 1602 (m), 1485 (s), 1043 (m), 846 (s), 736 (s), 692 (s) cm<sup>-1</sup>.

**HRMS** (EI): *m/z* calculated for [C<sub>23</sub>H<sub>21</sub>]<sup>+</sup>: 296.1565; found: 296.1578.





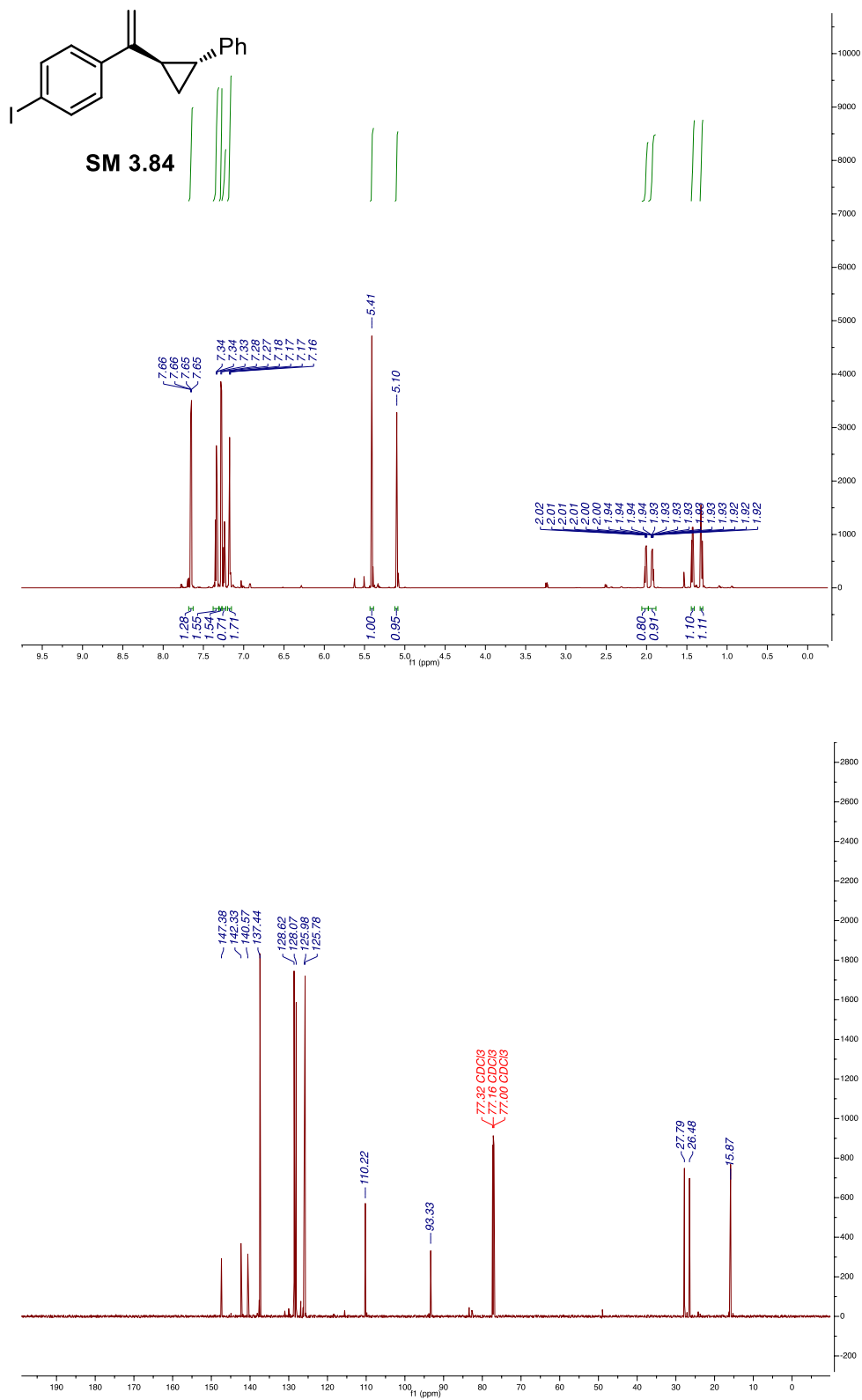
Prepared using the general procedure and purified via silica flash chromatography with 1% ethyl acetate in hexanes as a clear liquid.

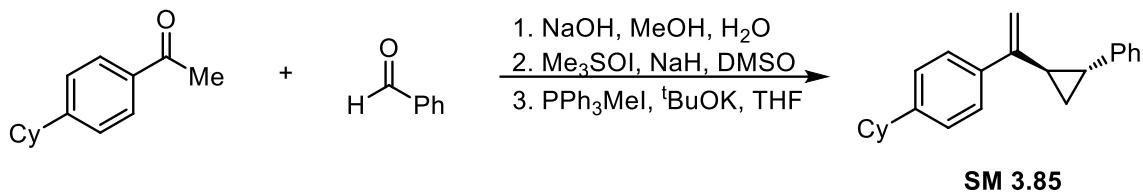
**<sup>1</sup>H NMR** (800 MHz, CDCl<sub>3</sub>) δ 7.68 – 7.63 (m, 1H), 7.38 – 7.31 (m, 2H), 7.30 – 7.27 (m, 2H), 7.24 (d, *J* = 7.4 Hz, 1H), 7.20 – 7.15 (m, 2H), 5.41 (s, 1H), 5.10 (s, 1H), 2.01 (dt, *J* = 8.9, 5.3 Hz, 1H), 1.93 (dddd, *J* = 8.6, 6.2, 4.7, 1.3 Hz, 1H), 1.44 – 1.41 (m, 1H), 1.32 (dt, *J* = 8.6, 5.4 Hz, 1H) ppm.

**<sup>13</sup>C NMR** (201 MHz, CDCl<sub>3</sub>) δ 147.4, 142.3, 140.6, 137.4, 128.6, 128.0, 126.0, 125.8, 110.2, 93.3, 27.8, 26.5, 15.9 ppm.

**IR** (film):  $\bar{\nu}$  = 3024 (w), 1793 (w), 1712 (m), 1602 (m), 1483 (s), 1002 (s) cm<sup>-1</sup>.

**HRMS** (EI): *m/z* calculated for [C<sub>17</sub>H<sub>15</sub>I]<sup>+</sup>: 346.0218; found: 346.0222.





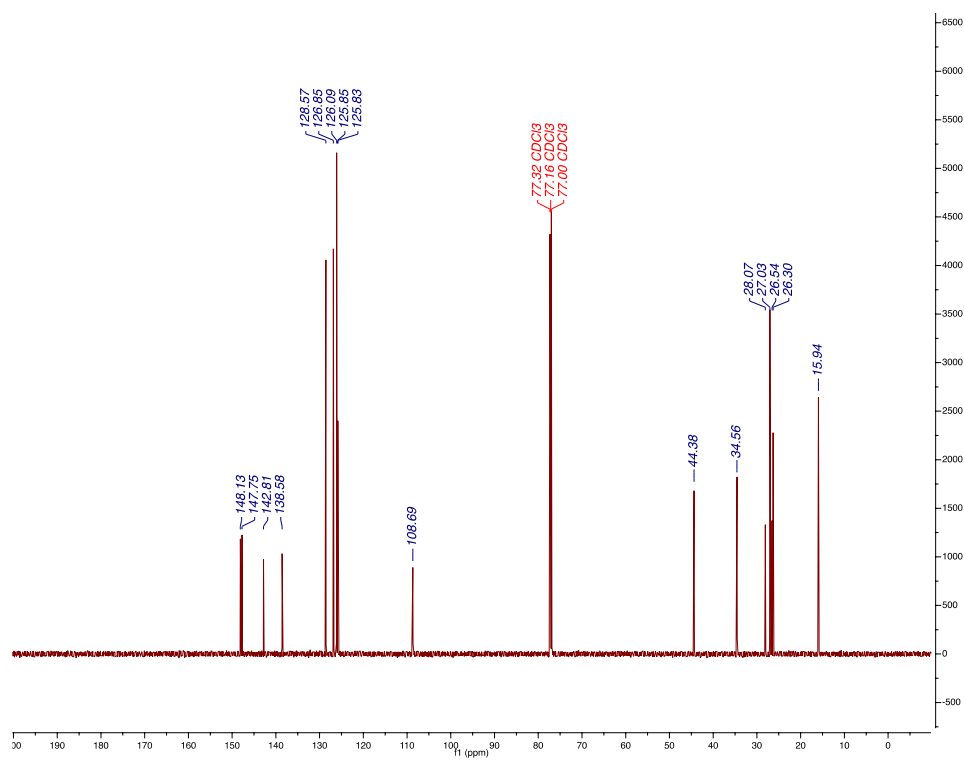
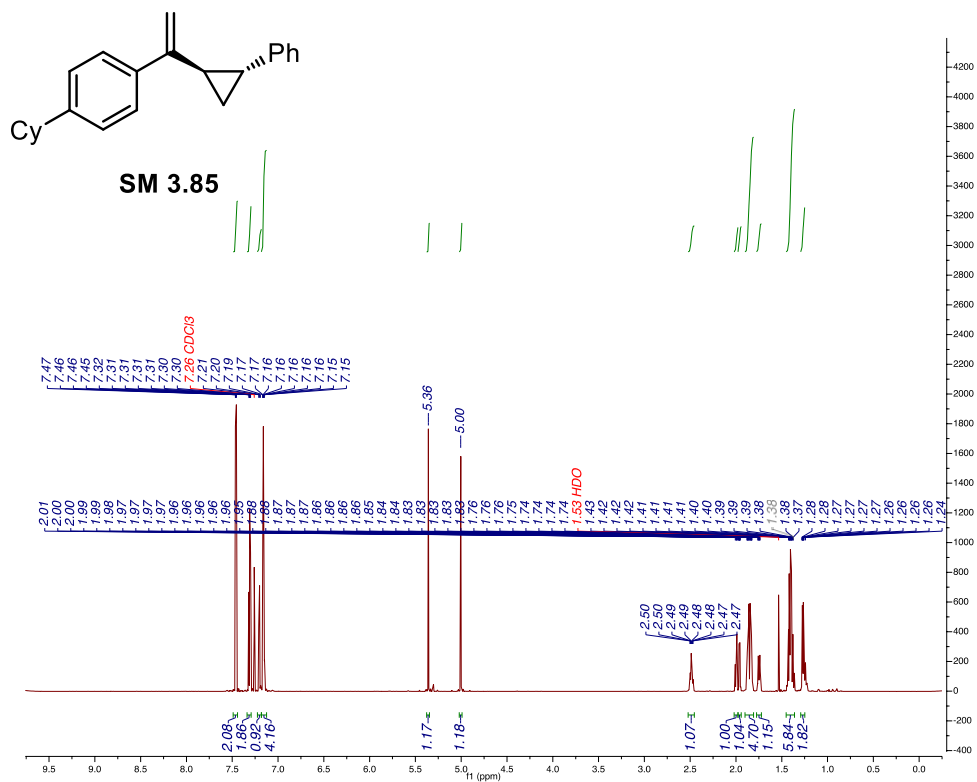
Prepared using the general procedure and purified via silica flash chromatography with 1% ethyl acetate in hexanes as a clear liquid.

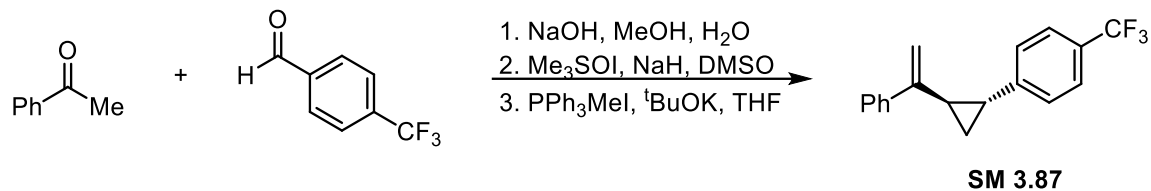
**<sup>1</sup>H NMR** (800 MHz, CDCl<sub>3</sub>) δ 7.49 – 7.44 (m, 2H), 7.34 – 7.28 (m, 2H), 7.23 – 7.17 (m, 1H), 7.19 – 7.12 (m, 4H), 5.36 (s, 1H), 5.00 (s, 1H), 2.49 (tt, *J* = 11.5, 3.5 Hz, 1H), 2.00 (dt, *J* = 8.7, 5.3 Hz, 1H), 1.96 (dddd, *J* = 8.5, 6.1, 4.8, 1.2 Hz, 1H), 1.90 – 1.81 (m, 4H), 1.75 (dq, *J* = 13.0, 3.1, 1.5 Hz, 1H), 1.46 – 1.35 (m, 6H), 1.30 – 1.24 (m, 2H) ppm.

**<sup>13</sup>C NMR** (201 MHz, CDCl<sub>3</sub>) δ 148.1, 147.8, 142.8, 138.6, 128.6, 126.9, 126.1, 125.9, 125.8, 108.7, 44.4, 34.6, 28.0, 27.0, 26.5, 26.3, 15.9 ppm.

**IR** (film):  $\bar{\nu}$  = 3680 (w), 2922 (s), 1604 (m), 1446 (m), 1053 (s) cm<sup>-1</sup>.

**HRMS** (EI): *m/z* calculated for [C<sub>23</sub>H<sub>26</sub>]<sup>+</sup>: 302.2035; found: 302.2043.





Prepared using the general procedure and purified via silica flash chromatography with 1% ethyl acetate in hexanes as a white crystalline solid.

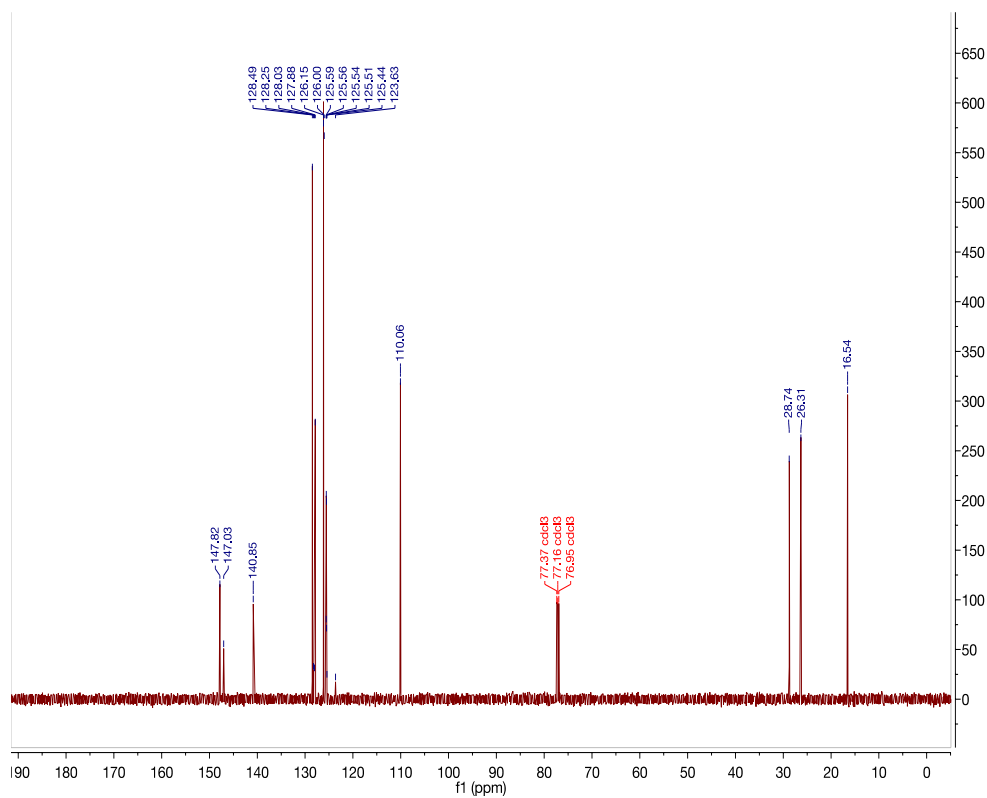
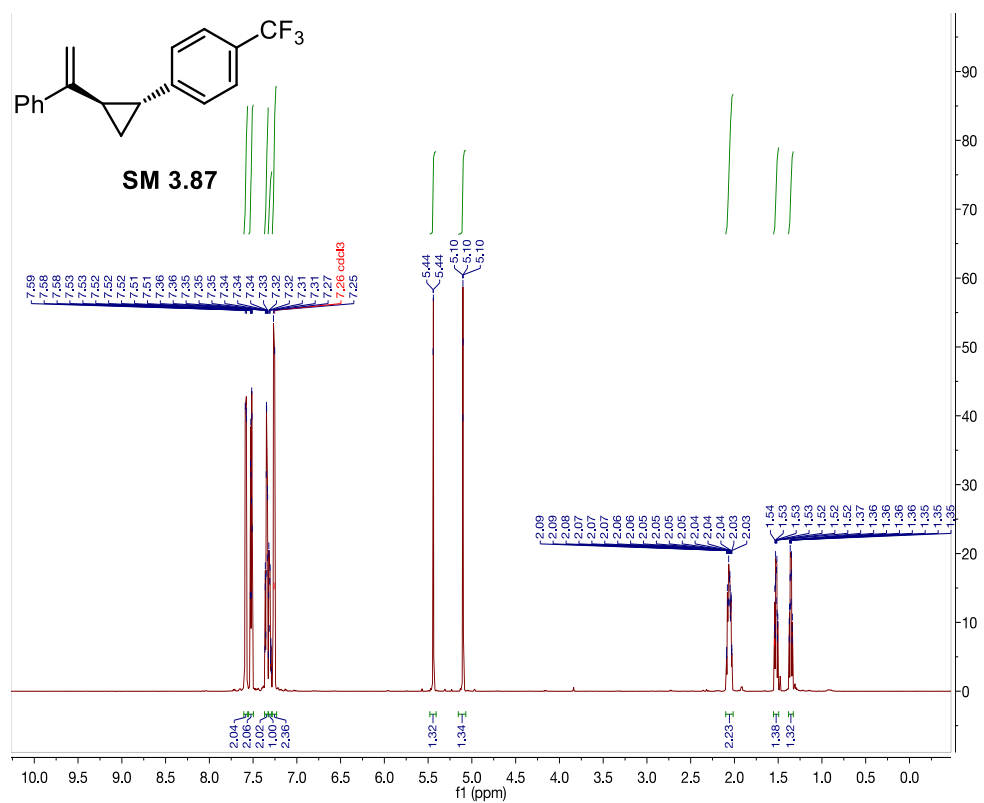
**<sup>1</sup>H NMR** (598 MHz, CDCl<sub>3</sub>) δ 7.61 – 7.56 (m, 2H), 7.52 (dq, *J* = 8.2, 1.5 Hz, 2H), 7.35 (ddt, *J* = 8.4, 5.8, 1.3 Hz, 2H), 7.33 – 7.29 (m, 1H), 7.26 (d, *J* = 8.0 Hz, 2H), 5.44 (d, *J* = 1.7 Hz, 1H), 5.16 – 5.07 (m, 1H), 2.10 – 2.02 (m, 2H), 1.55 – 1.49 (m, 1H), 1.38 – 1.33 (m, 1H) ppm.

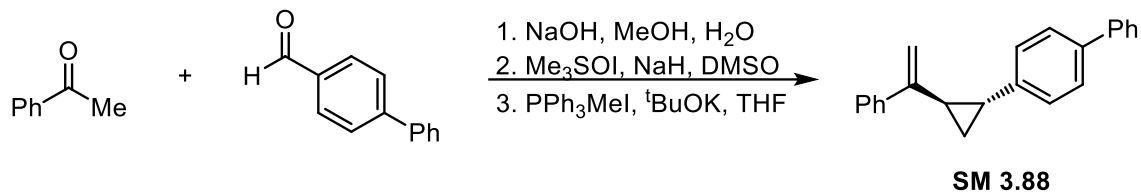
**<sup>13</sup>C NMR** (150 MHz, CDCl<sub>3</sub>) δ 147.8, 147.0, 140.9, 128.5, 128.3, 128.0, 127.9, 126.2, 126.0, 125.6, 125.6, 125.5, 125.5, 125.4, 123.6, 110.0, 28.7, 26.3, 16.5 ppm.

**<sup>19</sup>F NMR** (563 MHz, CDCl<sub>3</sub>) δ -62.23 ppm.

**IR** (film):  $\bar{\nu}$  = 3066 (w), 1618 (m), 1494 (w), 1321 (br, s), 1116 (br, s), 1066 (s), 1016 (s), 891 (br, s), 814 (s), 777 (s), 702 (s) cm<sup>-1</sup>.

**HRMS** (EI): *m/z* calculated for [C<sub>18</sub>H<sub>15</sub>F<sub>3</sub>]<sup>+</sup>: 288.1126; found: 288.1135.





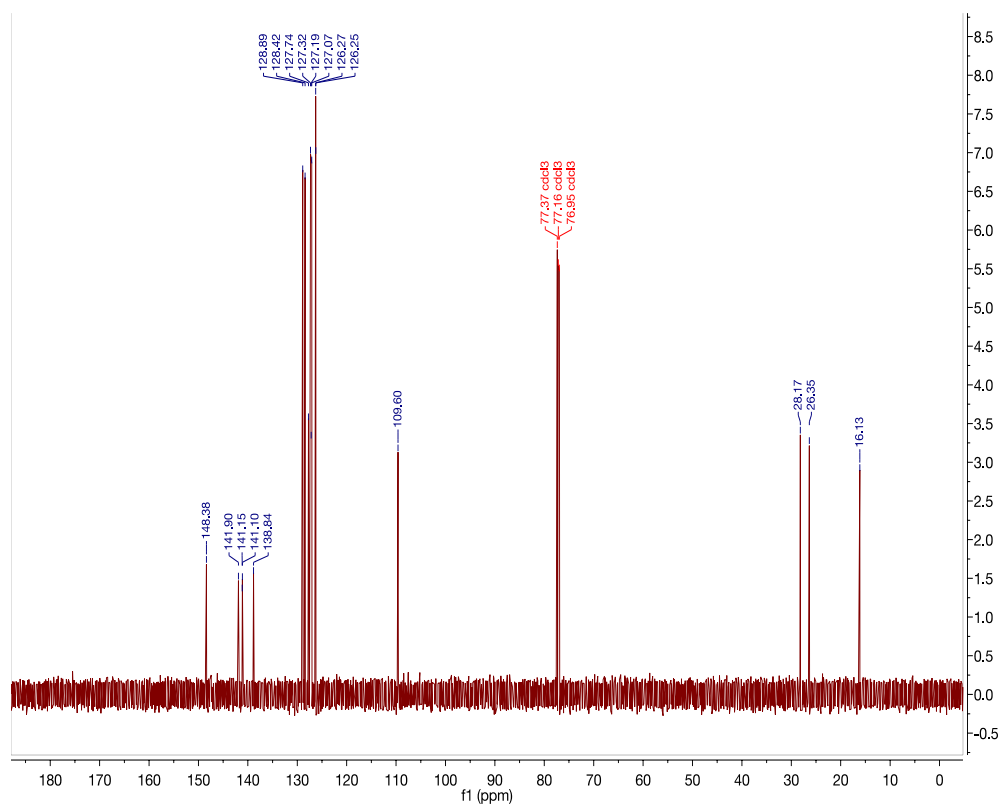
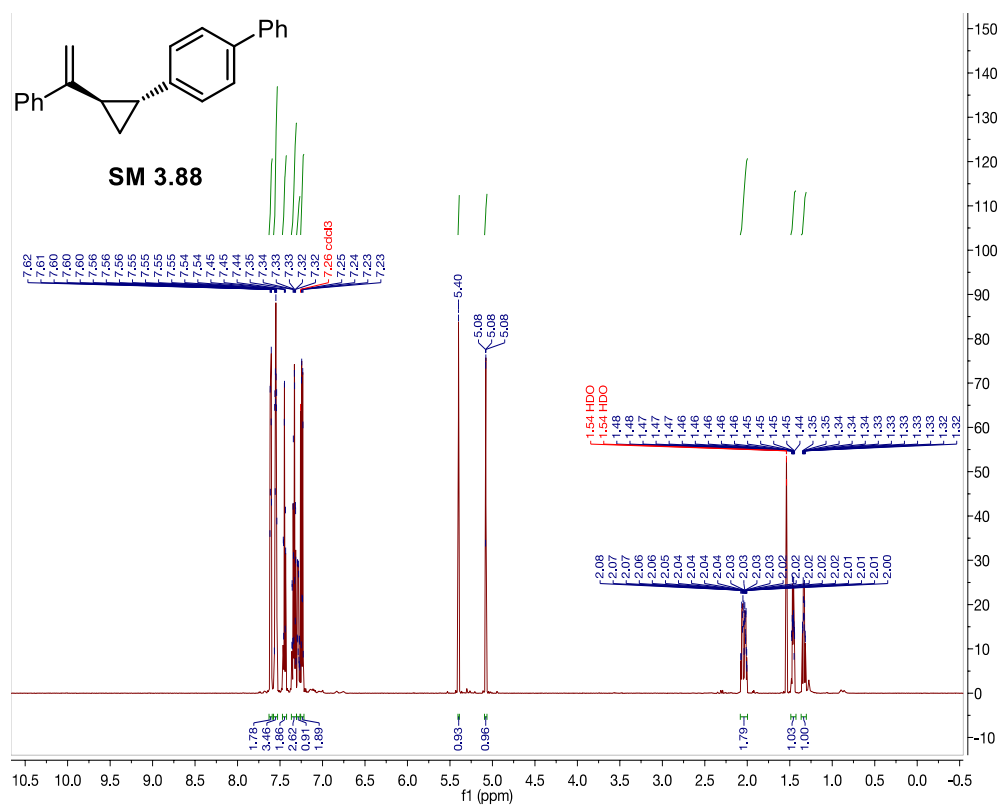
Prepared using the general procedure and purified via silica flash chromatography with 1% ethyl acetate in hexanes as a clear oil.

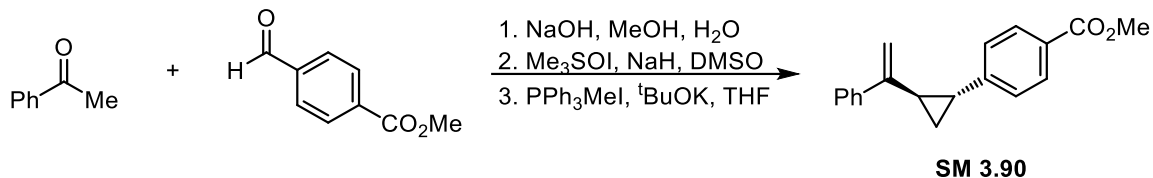
**<sup>1</sup>H NMR** (598 MHz, CDCl<sub>3</sub>) δ 7.61 (dt, *J* = 8.0, 1.3 Hz, 2H), 7.58 – 7.53 (m, 3H), 7.45 (td, *J* = 7.7, 1.4 Hz, 2H), 7.37 – 7.31 (m, 3H), 7.31 – 7.27 (m, 1H), 7.26 – 7.22 (m, 2H), 5.40 (s, 1H), 5.08 (d, *J* = 1.2 Hz, 1H), 2.08 – 2.00 (m, 2H), 1.46 (dddd, *J* = 8.7, 6.2, 4.8, 1.3 Hz, 1H), 1.33 (dtd, *J* = 8.5, 5.5, 1.2 Hz, 1H) ppm.

**<sup>13</sup>C NMR** (150 MHz, CDCl<sub>3</sub>) δ 148.4, 141.9, 141.1, 141.1, 138.8, 128.9, 128.4, 127.7, 127.3, 127.2, 127.0, 126.3, 126.3, 109.6, 28.2, 26.4, 16.1 ppm.

**IR** (film):  $\bar{\nu}$  = 3055 (w), 3026 (w), 1622 (w), 1600 (w), 1521 (w), 1487 (m), 1444 (w), 1028 (w), 891 (br, m), 819 (m), 777 (s), 763 (s), 698 (s) cm<sup>-1</sup>.

**HRMS** (EI): *m/z* calculated for [C<sub>23</sub>H<sub>20</sub>]<sup>+</sup>: 296.1565; found: 296.1576.





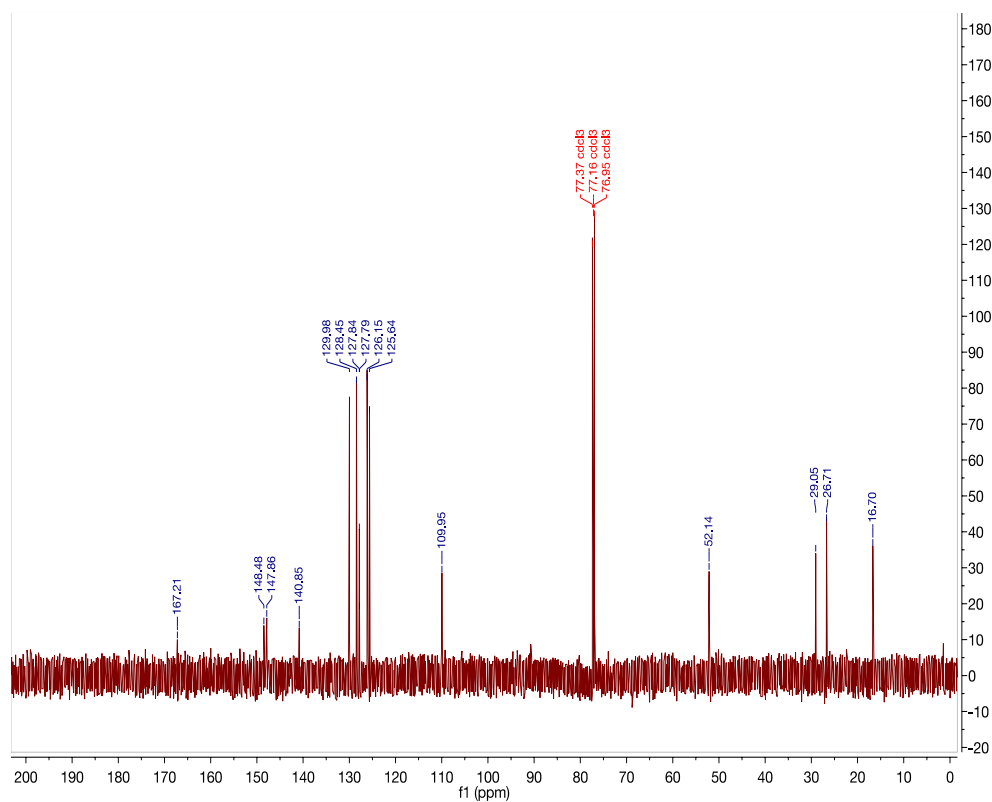
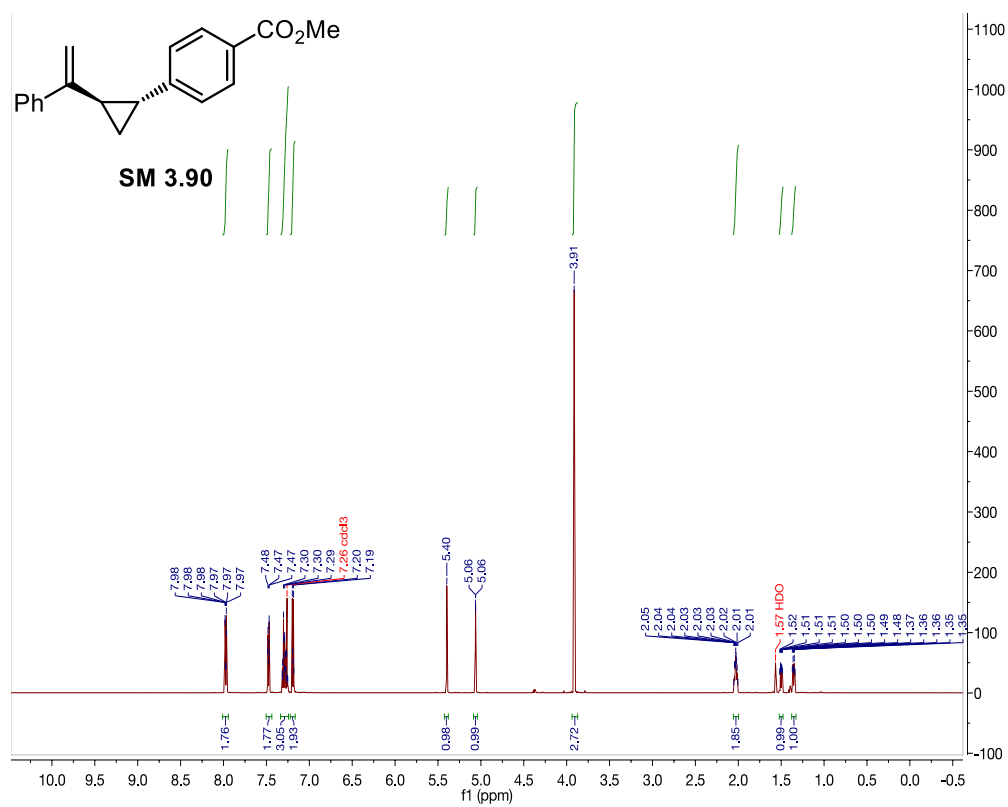
Prepared using the general procedure and purified via silica flash chromatography with 1% ethyl acetate in hexanes as a white crystalline solid.

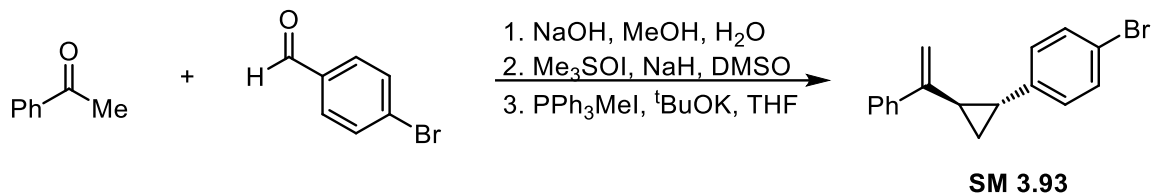
**<sup>1</sup>H NMR** (598 MHz, CDCl<sub>3</sub>) δ 8.01 – 7.94 (m, 2H), 7.50 – 7.44 (m, 2H), 7.34 – 7.24 (m, 3H), 7.22 – 7.16 (m, 2H), 5.40 (s, 1H), 5.06 (d, *J* = 1.0 Hz, 1H), 3.91 (s, 3H), 2.03 (ddd, *J* = 9.8, 8.2, 4.5 Hz, 2H), 1.52 – 1.48 (m, 1H), 1.35 (dt, *J* = 8.5, 5.5 Hz, 1H) ppm.

**<sup>13</sup>C NMR** (150 MHz, CDCl<sub>3</sub>) δ 167.2, 148.5, 147.9, 140.9, 130.0, 128.5, 127.8, 127.8, 126.2, 125.6, 110.0, 52.1, 29.0, 26.7, 16.7 ppm.

**IR (film):**  $\tilde{\nu}$  = 3089 (w), 2951 (w), 1717 (s), 1609 (m), 1497 (w), 1281 (b, s), 781 (m), 768 (s), 706 (s), 698 (s) cm<sup>-1</sup>.

**HRMS** (EI): *m/z* calculated for [C<sub>19</sub>H<sub>18</sub>O<sub>2</sub>]<sup>+</sup>: 278.1307; found: 278.1301.





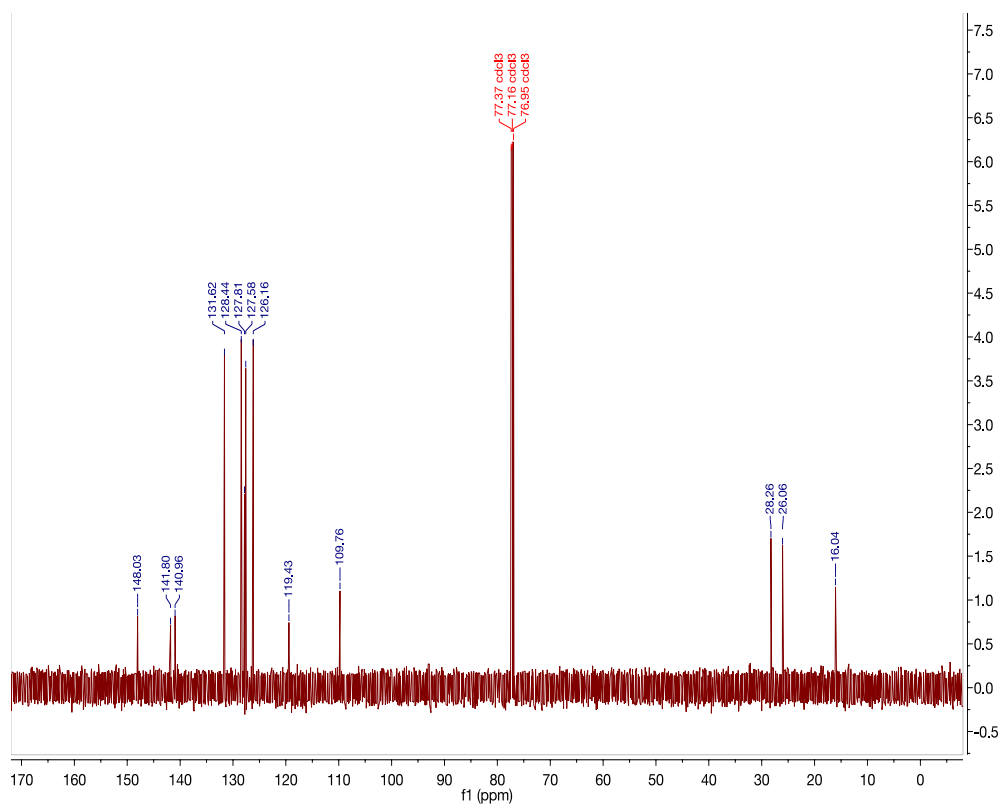
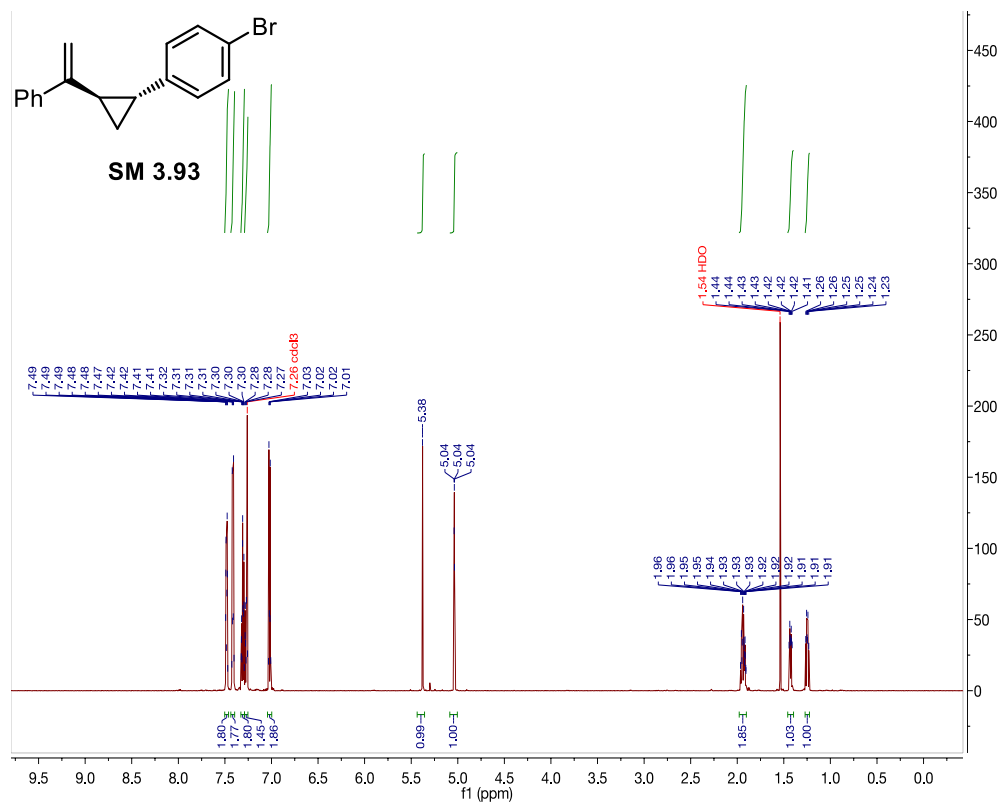
Prepared using the general procedure and purified via silica flash chromatography with 1% ethyl acetate in hexanes as a yellow liquid.

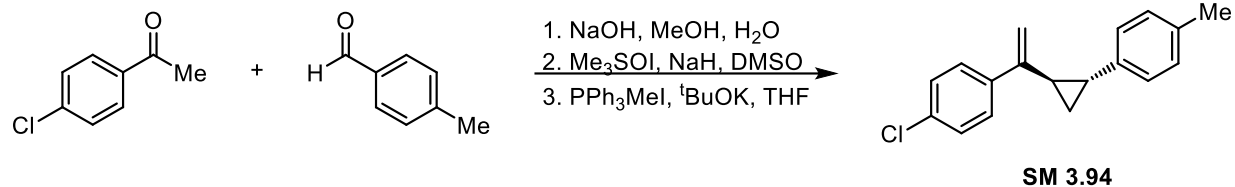
**<sup>1</sup>H NMR** (598 MHz, CDCl<sub>3</sub>) δ 7.48 (dt, *J* = 8.2, 1.1 Hz, 2H), 7.44 – 7.40 (m, 2H), 7.31 (tt, *J* = 6.6, 1.0 Hz, 2H), 7.29 – 7.25 (m, 1H), 7.04 – 7.00 (m, 2H), 5.38 (s, 1H), 5.04 (t, *J* = 1.0 Hz, 1H), 1.98 – 1.90 (m, 2H), 1.43 (ddd, *J* = 8.6, 6.3, 5.1 Hz, 1H), 1.25 (dt, *J* = 8.5, 5.4 Hz, 1H) ppm.

**<sup>13</sup>C NMR** (150 MHz, CDCl<sub>3</sub>) δ 148.0, 141.8, 141.0, 131.6, 128.4, 127.8, 127.6, 126.2, 119.4, 109.8, 28.3, 26.1, 16.0 ppm.

**IR** (film):  $\bar{\nu}$  = 3095 (w), 2995 (w), 1622 (m), 1489 (m), 1007 (m), 891 (s), 802 (s), 771 (s), 700 (s) cm<sup>-1</sup>.

**HRMS** (EI): *m/z* calculated for [C<sub>17</sub>H<sub>15</sub>Br]<sup>+</sup>: 290.0; found: 298.0356.





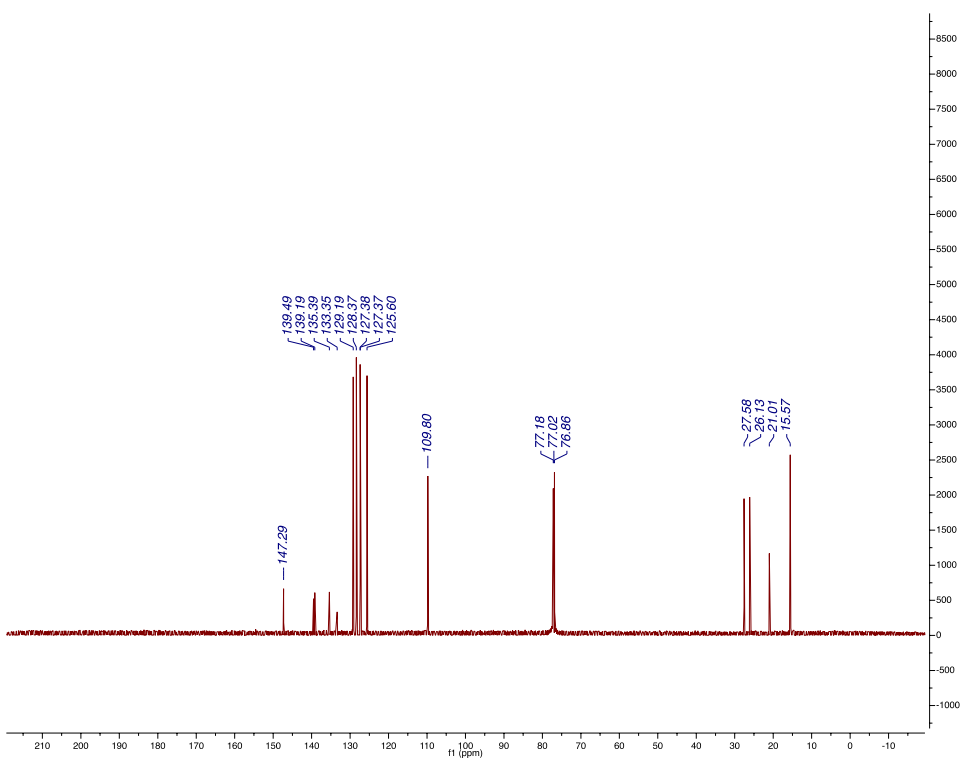
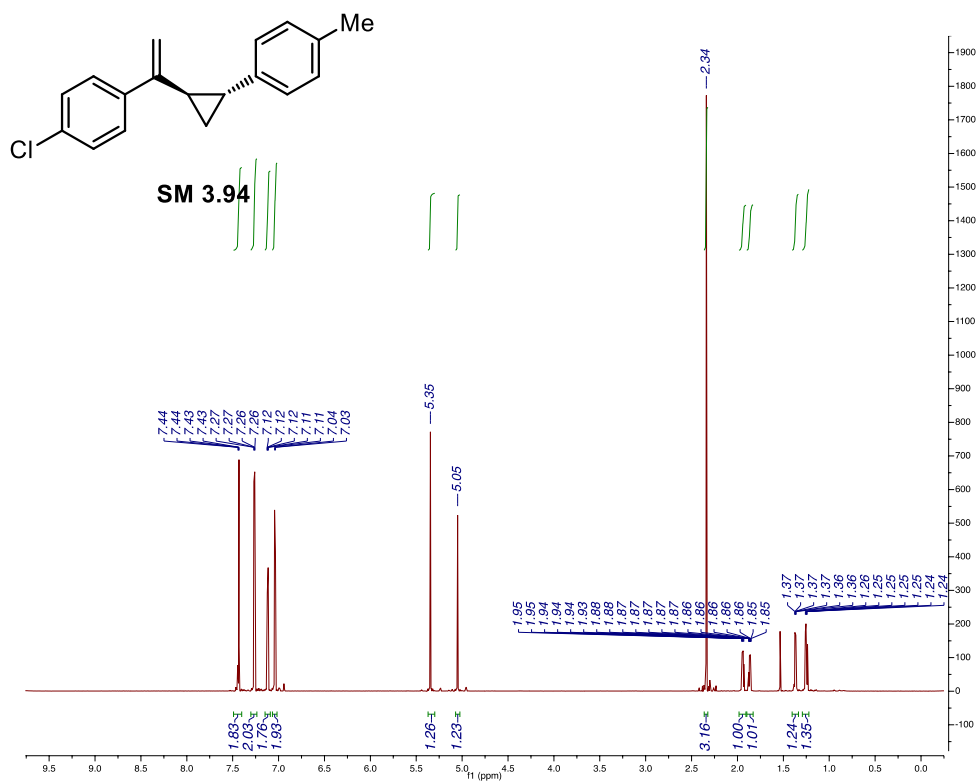
Prepared using the general procedure and purified via silica flash chromatography with 1% ethyl acetate in hexanes as a clear liquid.

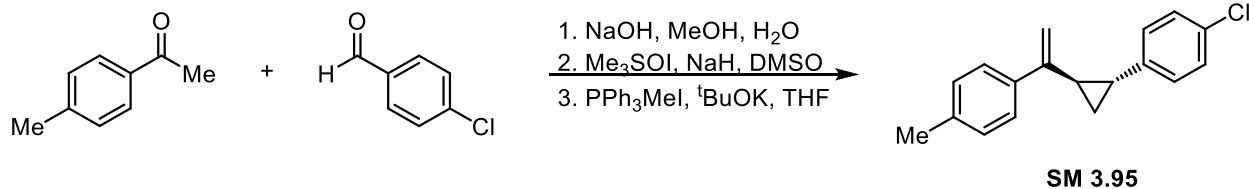
**<sup>1</sup>H NMR** (800 MHz, CDCl<sub>3</sub>) δ 7.49 – 7.40 (m, 2H), 7.30 – 7.24 (m, 2H), 7.15 – 7.09 (m, 2H), 7.04 (d, *J* = 8.1 Hz, 2H), 5.35 (s, 1H), 5.05 (s, 1H), 2.34 (s, 3H), 1.94 (dt, *J* = 8.7, 5.3 Hz, 1H), 1.86 (dddd, *J* = 8.5, 6.0, 4.8, 1.2 Hz, 1H), 1.37 (ddd, *J* = 8.8, 6.1, 5.0 Hz, 1H), 1.25 (ddd, *J* = 8.5, 5.7, 5.0 Hz, 1H) ppm.

**<sup>13</sup>C NMR** (201 MHz, CDCl<sub>3</sub>) δ 147.3, 139.5, 139.2, 135.4, 133.4, 129.2, 128.4, 127.4, 127.4, 125.6, 109.8, 27.6, 26.1, 21.0, 15.6 ppm.

**IR** (film):  $\bar{\nu}$  = 3076 (w), 2918 (w), 1618 (m), 1514 (m), 1491 (s), 1099 (s), 893 (s), 831 (s), 802 (s) cm<sup>-1</sup>.

**HRMS** (EI): *m/z* calculated for [C<sub>18</sub>H<sub>17</sub>Cl]<sup>+</sup>: 268.1020; found: 268.1022.





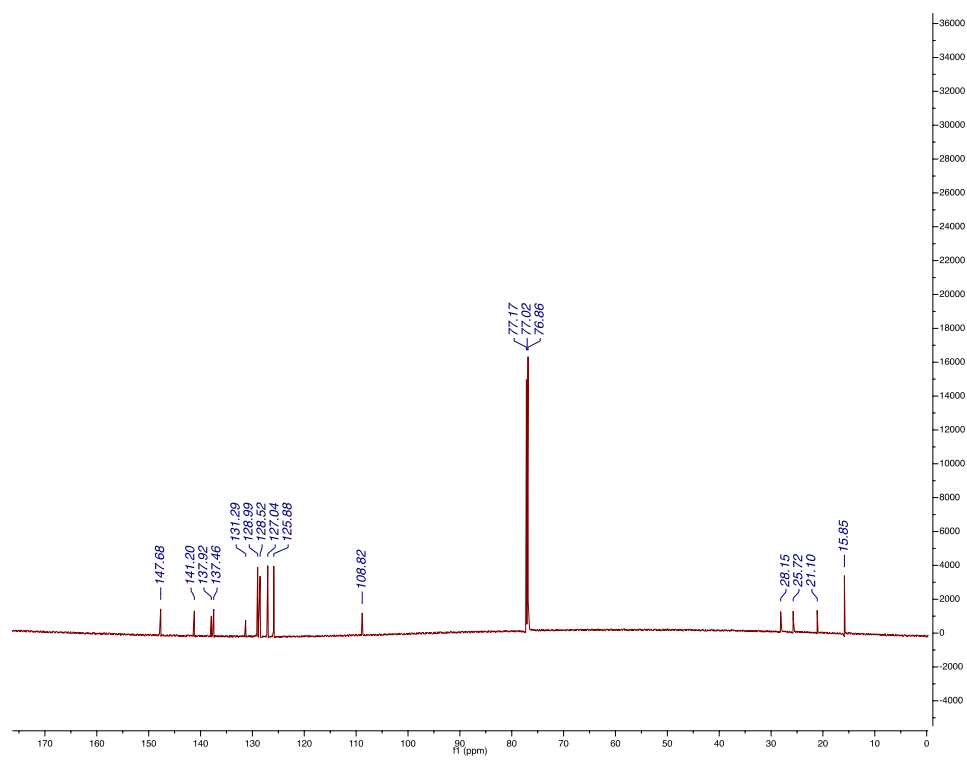
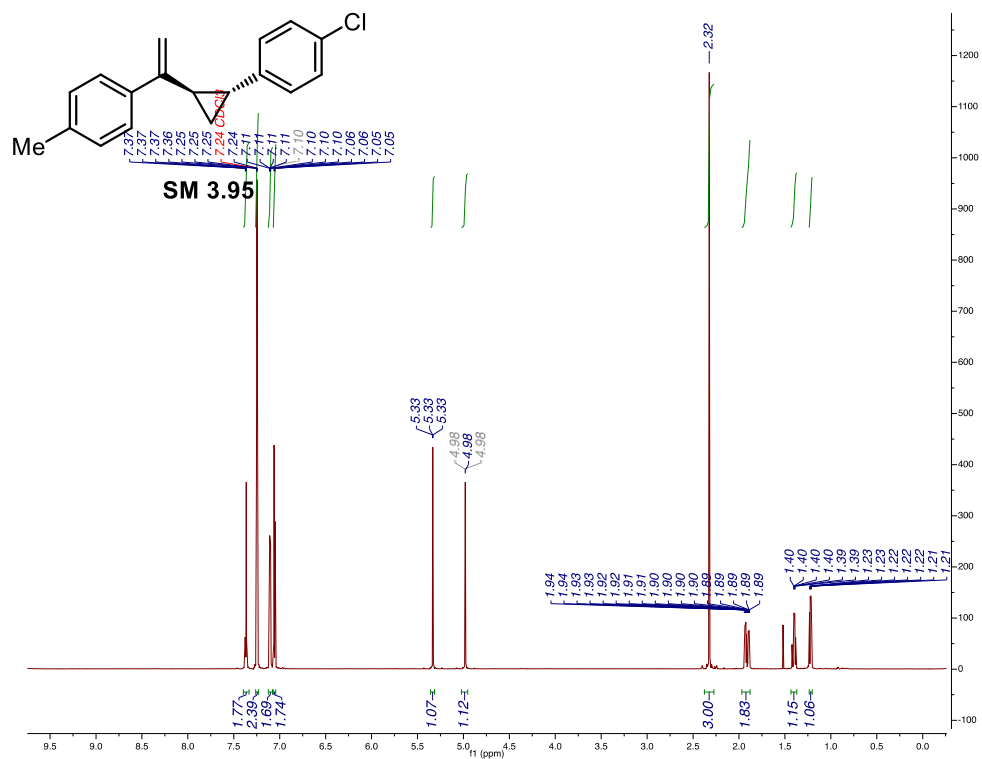
Prepared using the general procedure and purified via silica flash chromatography with 1% ethyl acetate in hexanes as a clear liquid.

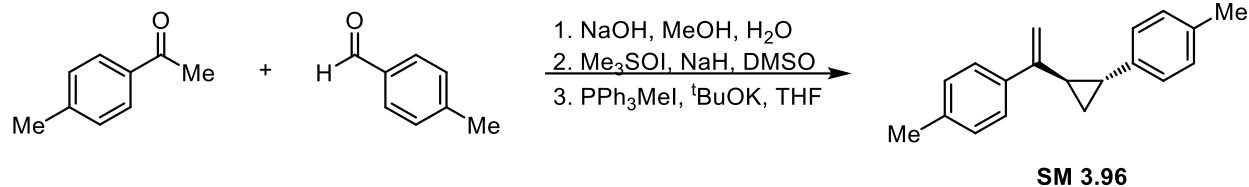
**<sup>1</sup>H NMR** (800 MHz, CDCl<sub>3</sub>) δ 7.40 – 7.33 (m, 2H), 7.26 – 7.23 (m, 2H), 7.12 – 7.08 (m, 2H), 7.07 – 7.04 (m, 2H), 5.33 (t, *J* = 0.6 Hz, 1H), 4.98 (s, 1H), 2.32 (s, 3H), 1.97 – 1.88 (m, 2H), 1.43 – 1.37 (m, 1H), 1.22 (ddd, *J* = 8.6, 5.7, 5.1 Hz, 1H) ppm.

**<sup>13</sup>C NMR** (201 MHz, CDCl<sub>3</sub>) δ 147.7, 141.2, 137.9, 137.5, 131.3, 129.0, 128.5, 127.0, 125.9, 108.8, 28.2, 25.7, 21.1, 15.9 ppm.

**IR** (film):  $\bar{\nu}$  = 2920 (w), 1618 (m), 1492 (s), 1030 (s), 1011 (m), 812 (s) cm<sup>-1</sup>.

**HRMS** (EI): *m/z* calculated for [C<sub>18</sub>H<sub>17</sub>Cl]<sup>+</sup>: 268.1019; found: 268.1022.





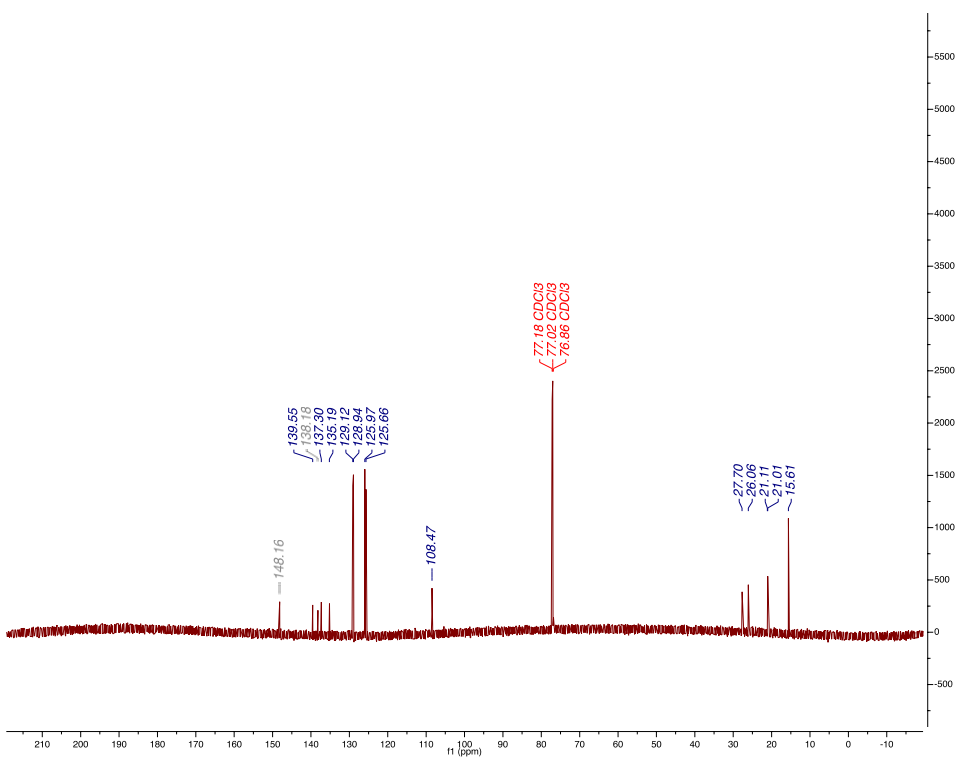
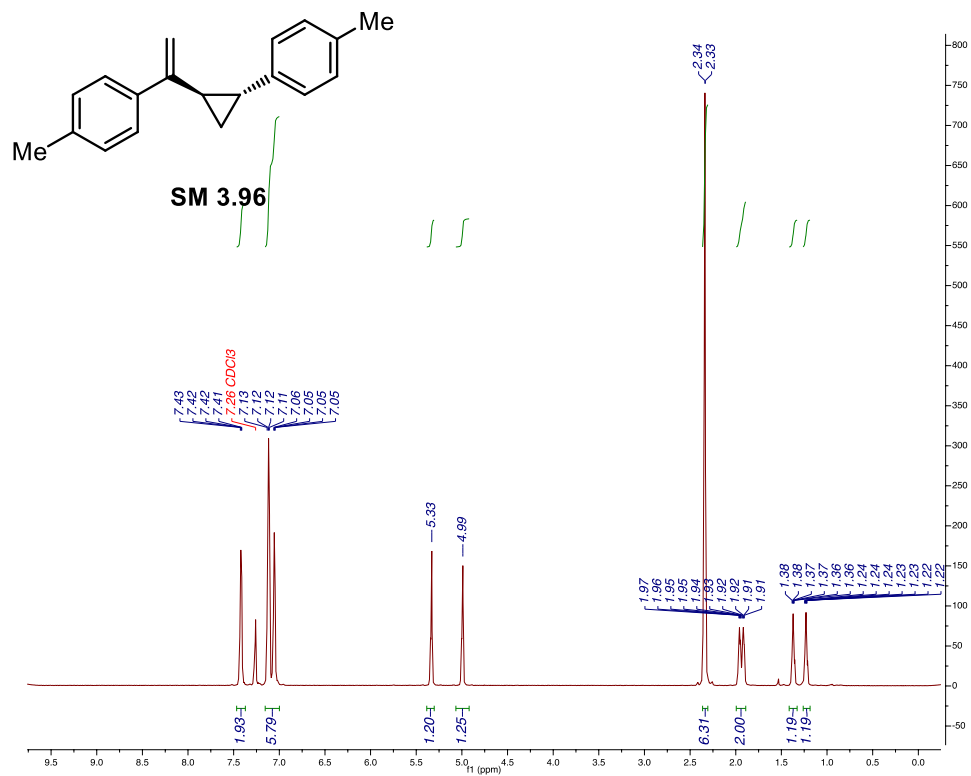
Prepared using the general procedure and purified via silica flash chromatography with 1% ethyl acetate in hexanes as a clear liquid.

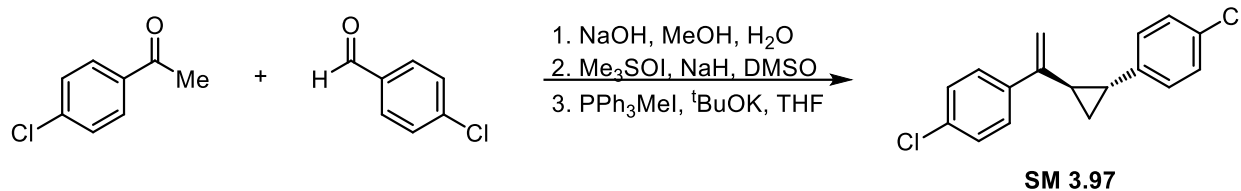
**<sup>1</sup>H NMR** (800 MHz, CDCl<sub>3</sub>) δ 7.42 (dd, *J* = 8.2, 4.1 Hz, 2H), 7.15 – 7.00 (m, 6H), 5.33 (s, 1H), 4.99 (s, 1H), 2.34 (d, *J* = 3.6 Hz, 6H), 1.94 (ddt, *J* = 28.6, 8.9, 4.9 Hz, 2H), 1.37 (ddt, *J* = 11.3, 9.0, 3.8 Hz, 1H), 1.23 (tt, *J* = 10.8, 8.8, 3.9 Hz, 1H) ppm.

**<sup>13</sup>C NMR** (201 MHz, CDCl<sub>3</sub>) δ 148.2, 139.6, 138.2, 137.3, 135.2, 129.1, 128.9, 126.0, 125.7, 108.5, 27.7, 26.1, 21.1, 21.0, 15.6 ppm.

**IR** (film):  $\bar{\nu}$  = 3001 (w), 2916 (w), 1629 (m), 1514 (s), 823 (s) cm<sup>-1</sup>.

**HRMS** (EI): *m/z* calculated for [C<sub>19</sub>H<sub>20</sub>]<sup>+</sup>: 248.1565; found: 248.1568.





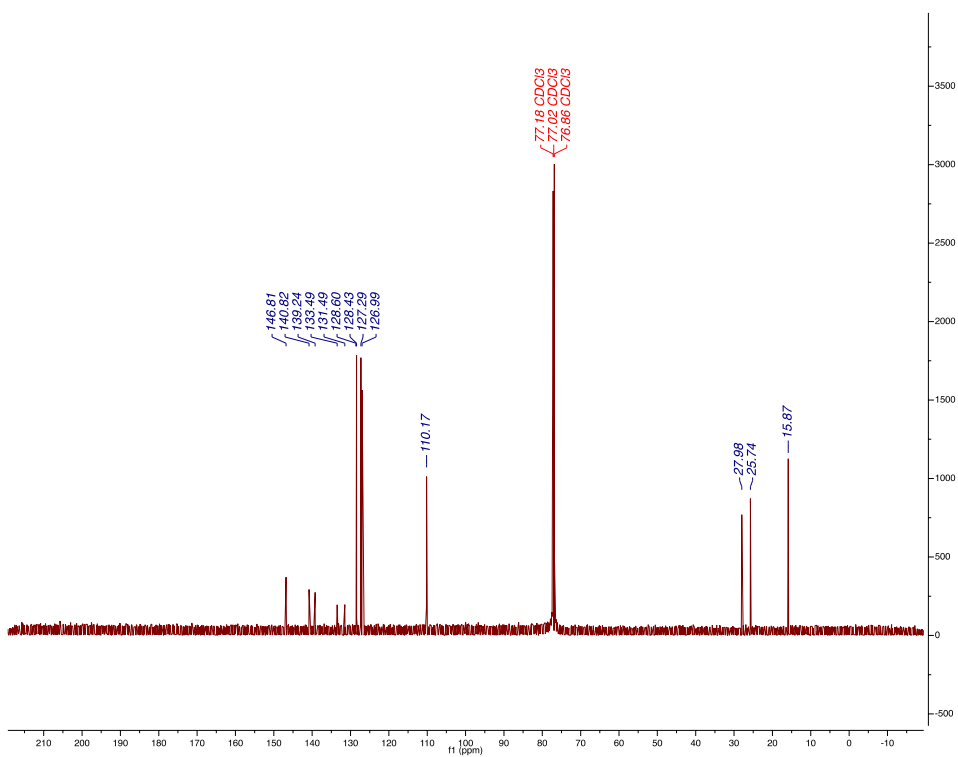
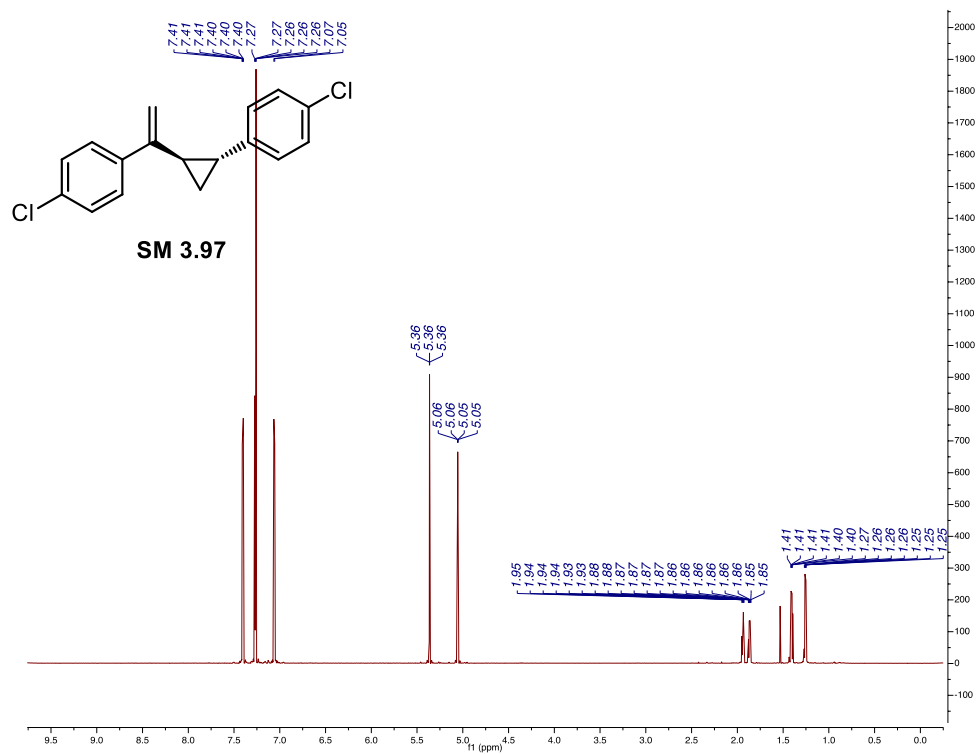
Prepared using the general procedure and purified via silica flash chromatography with 1% ethyl acetate in hexanes as a clear liquid.

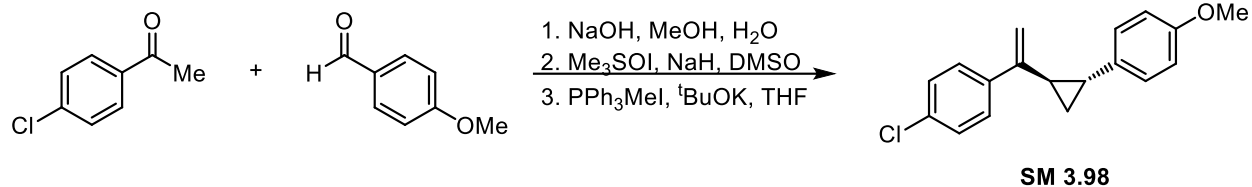
**$^1\text{H}$  NMR** (800 MHz,  $\text{CDCl}_3$ )  $\delta$  7.45 – 7.35 (m, 2H), 7.30 – 7.25 (m, 4H), 7.06 (d,  $J$  = 8.4 Hz, 2H), 5.36 (t,  $J$  = 0.6 Hz, 1H), 5.05 (dd,  $J$  = 1.3, 0.7 Hz, 1H), 1.94 (dt,  $J$  = 8.6, 5.3 Hz, 1H), 1.89 – 1.84 (m, 1H), 1.41 (ddd,  $J$  = 8.7, 6.2, 5.1 Hz, 1H), 1.26 (ddd,  $J$  = 8.6, 5.7, 5.2 Hz, 1H) ppm.

**$^{13}\text{C}$  NMR** (201 MHz,  $\text{CDCl}_3$ )  $\delta$  146.8, 140.8, 139.2, 133.5, 131.5, 128.6, 128.4, 127.3, 127.0, 110.2, 28.0, 25.7, 15.9 ppm.

**IR** (film):  $\bar{\nu}$  = 3003 (w), 2926 (w), 1897 (w), 1622 (m), 1489 (s), 1091 (s), 1010 (s), 833 (s), 810 (s)  $\text{cm}^{-1}$ .

**HRMS** (EI):  $m/z$  calculated for  $[\text{C}_{17}\text{H}_{14}\text{Cl}_2]^+$ : 288.0473; found: 288.0480.





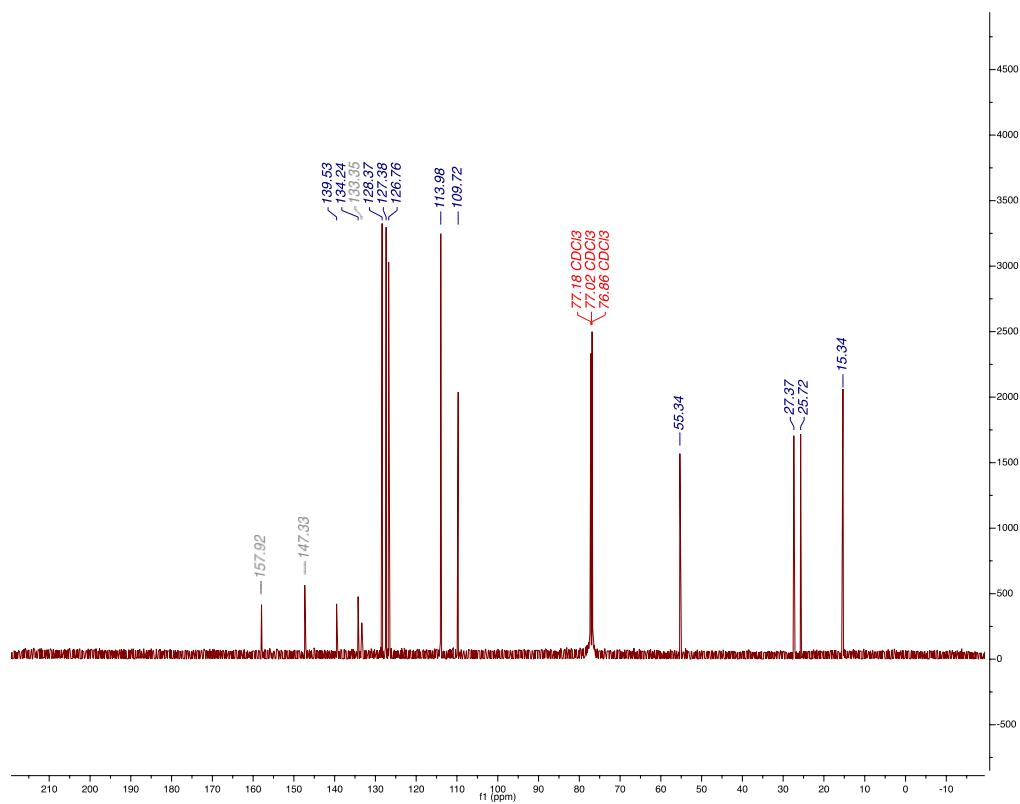
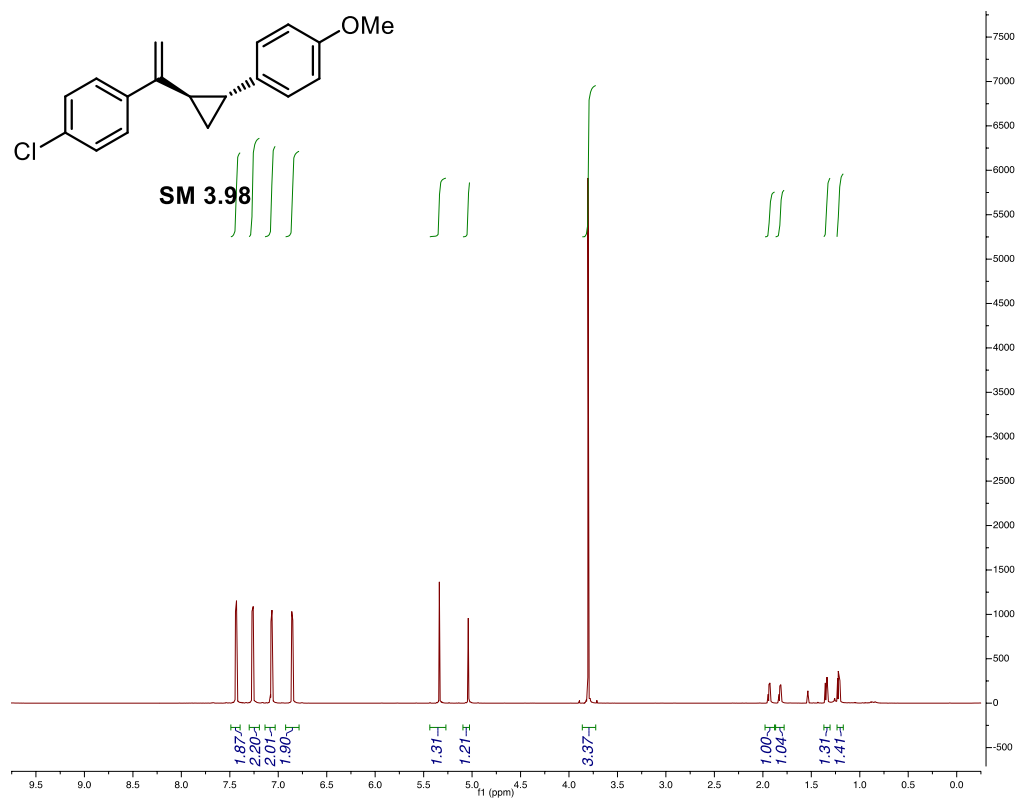
Prepared using the general procedure and purified via silica flash chromatography with 1% ethyl acetate in hexanes as a clear liquid.

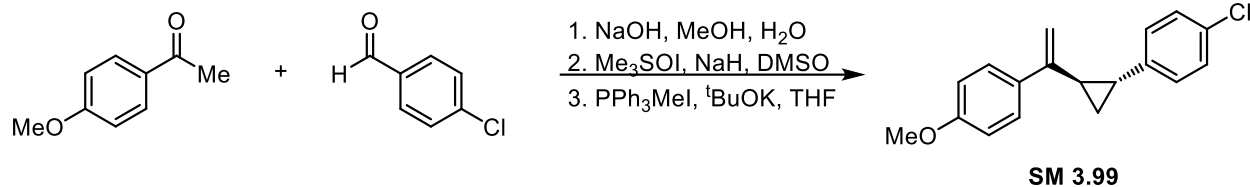
**<sup>1</sup>H NMR** (800 MHz, CDCl<sub>3</sub>) δ 7.49 – 7.39 (m, 2H), 7.30 – 7.19 (m, 2H), 7.14 – 7.03 (m, 2H), 6.92 – 6.79 (m, 2H), 5.34 (s, 1H), 5.04 (t, *J* = 1.0 Hz, 1H), 3.80 (s, 3H), 1.93 (dt, *J* = 8.8, 5.3 Hz, 1H), 1.82 (dddd, *J* = 8.5, 6.1, 4.8, 1.2 Hz, 1H), 1.34 (ddd, *J* = 8.8, 6.0, 5.0 Hz, 1H), 1.22 (ddd, *J* = 8.5, 5.7, 5.0 Hz, 1H) ppm.

**<sup>13</sup>C NMR** (201 MHz, CDCl<sub>3</sub>) δ 157.9, 147.3, 139.5, 134.2, 133.4, 128.4, 127.4, 126.8, 114.0, 109.7, 55.3, 27.4, 25.7, 15.3 ppm.

**IR** (film):  $\bar{\nu}$  = 3005 (w), 2926 (w), 1610 (m), 1512 (s), 1489 (m), 1242 (s), 1033 (m), 835 (s), 818 (s), 810 (s) cm<sup>-1</sup>.

**HRMS** (EI): *m/z* calculated for [C<sub>18</sub>H<sub>17</sub>ClO]<sup>+</sup>: 284.0968; found: 284.0962.





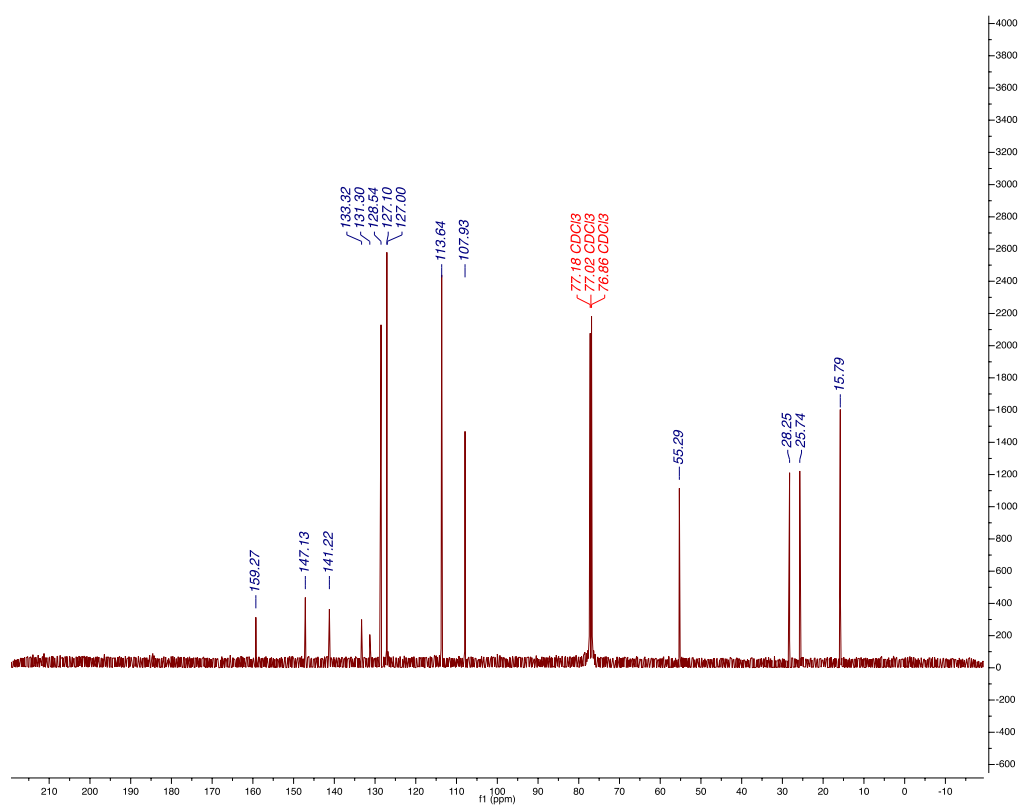
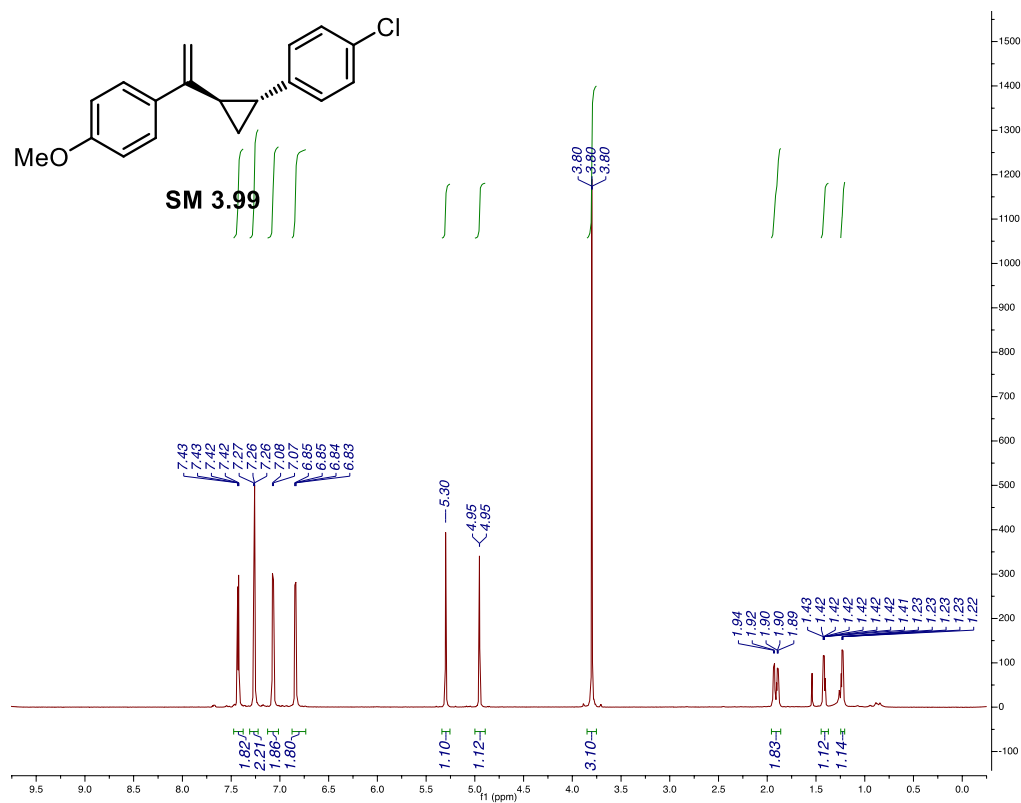
Prepared using the general procedure and purified via silica flash chromatography with 1% ethyl acetate in hexanes as a clear liquid.

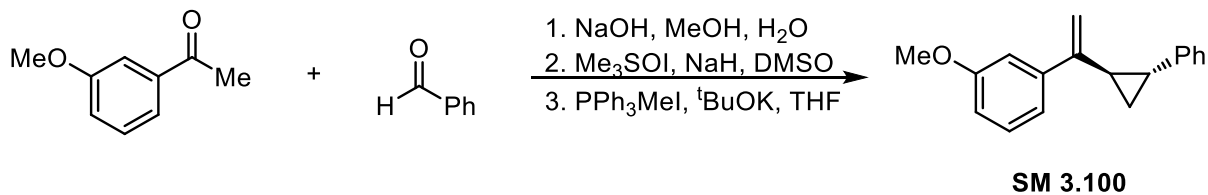
**<sup>1</sup>H NMR** (800 MHz, CDCl<sub>3</sub>) δ 7.47 – 7.38 (m, 2H), 7.31 – 7.22 (m, 2H), 7.07 (d, *J* = 8.3 Hz, 2H), 6.88 – 6.73 (m, 2H), 5.30 (s, 1H), 5.00 – 4.89 (m, 1H), 3.80 (d, *J* = 1.0 Hz, 3H), 1.91 (dd, *J* = 30.5, 8.0 Hz, 2H), 1.45 – 1.37 (m, 1H), 1.25 – 1.21 (m, 1H) ppm.

**<sup>13</sup>C NMR** (201 MHz, CDCl<sub>3</sub>) δ 159.3, 147.1, 141.2, 133.3, 131.3, 128.5, 127.1, 127.0, 113.6, 107.9, 55.3, 28.3, 25.7, 15.8 ppm.

**IR** (film):  $\bar{\nu}$  = 3003 (w), 2929 (w), 2605 (m), 1512 (s), 1493 (s), 1250 (s), 837 (m) cm<sup>-1</sup>.

**HRMS** (EI): *m/z* calculated for [C<sub>18</sub>H<sub>17</sub>ClO]<sup>+</sup>: 284.0968; found: 284.0962.





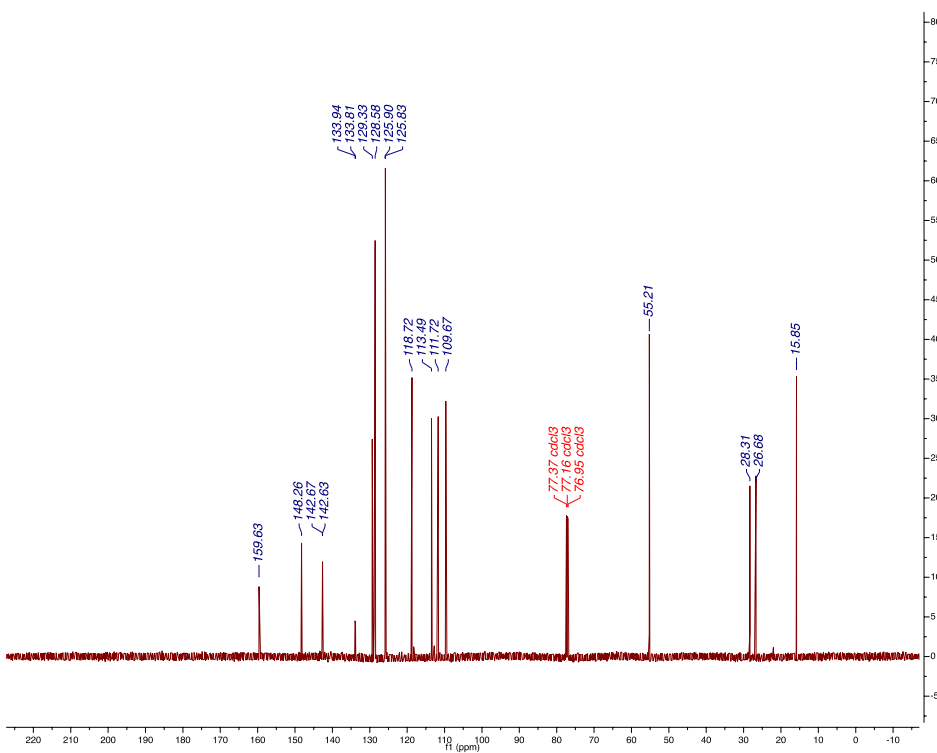
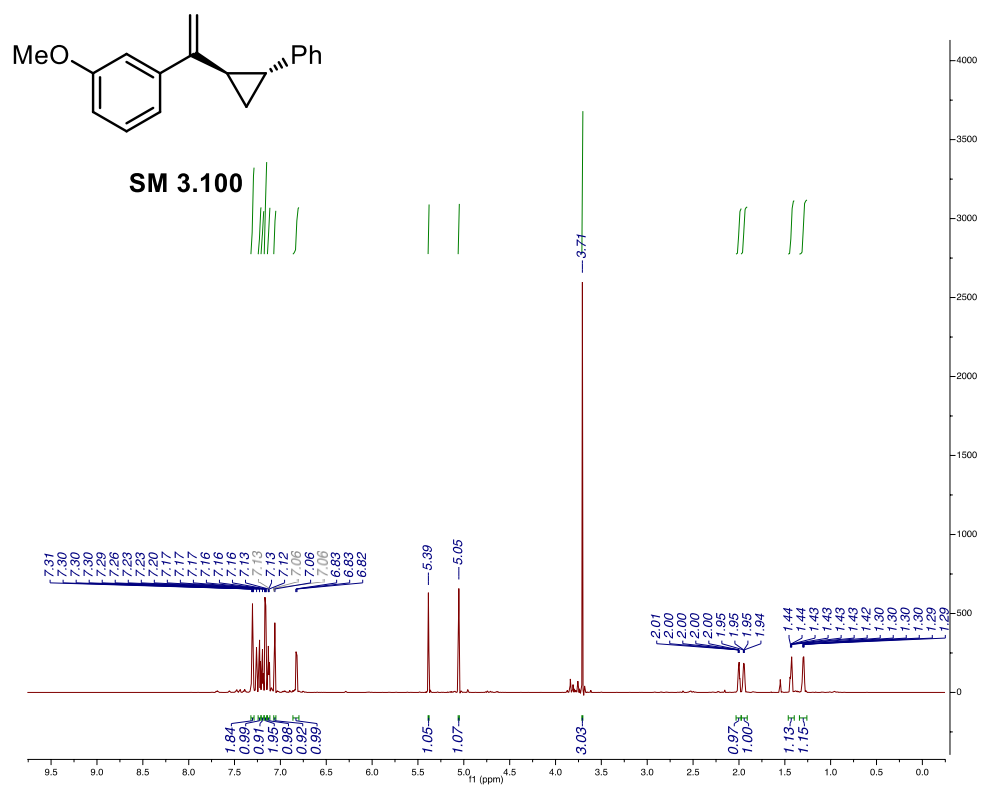
Prepared using the general procedure and purified via silica flash chromatography with 1% ethyl acetate in hexanes as a clear liquid.

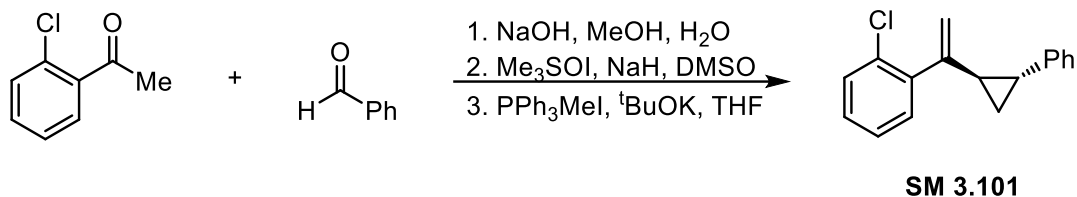
**<sup>1</sup>H NMR** (598 MHz, CDCl<sub>3</sub>) δ 7.38 – 7.05 (m, 8H), 6.84 (ddd, *J* = 8.2, 3.8, 1.8 Hz, 1H), 5.43 – 5.36 (m, 1H), 5.07 (dt, *J* = 2.1, 1.1 Hz, 1H), 3.72 (d, *J* = 2.0 Hz, 3H), 2.02 (td, *J* = 5.2, 2.9 Hz, 1H), 1.99 – 1.93 (m, 1H), 1.50 – 1.40 (m, 1H), 1.31 (td, *J* = 5.2, 2.8 Hz, 1H) ppm.

**<sup>13</sup>C NMR** (150 MHz, CDCl<sub>3</sub>) δ 159.6, 148.3, 142.7, 142.6, 133.9, 133.8, 129.3, 128.6, 125.9, 125.8, 118.7, 113.5, 111.7, 109.7, 55.2, 28.3, 26.7, 15.9 ppm.

**IR** (film):  $\bar{\nu}$  = 3001 (w), 2833 (w), 1712 (m), 1575 (s), 1489 (s), 1047 (bs) cm<sup>-1</sup>.

**HRMS** (EI): *m/z* calculated for [C<sub>18</sub>H<sub>18</sub>O]<sup>+</sup>: 250.1358; found: 250.1357.





Prepared using the general procedure and purified via silica flash chromatography with 1% ethyl acetate in hexanes as a clear liquid.

**<sup>1</sup>H NMR** (598 MHz, CDCl<sub>3</sub>) δ 7.39 (dt, *J* = 7.3, 2.0 Hz, 1H), 7.31 – 7.05 (m, 7H), 5.26 (s, 1H), 4.98 (d, *J* = 1.3 Hz, 1H), 3.56 (q, *J* = 9.4, 8.6 Hz, 0H), 1.97 (dtd, *J* = 8.6, 4.4, 2.5 Hz, 2H), 1.30 – 1.21 (m, 1H), 1.18 (td, *J* = 4.9, 2.8 Hz, 1H) ppm.

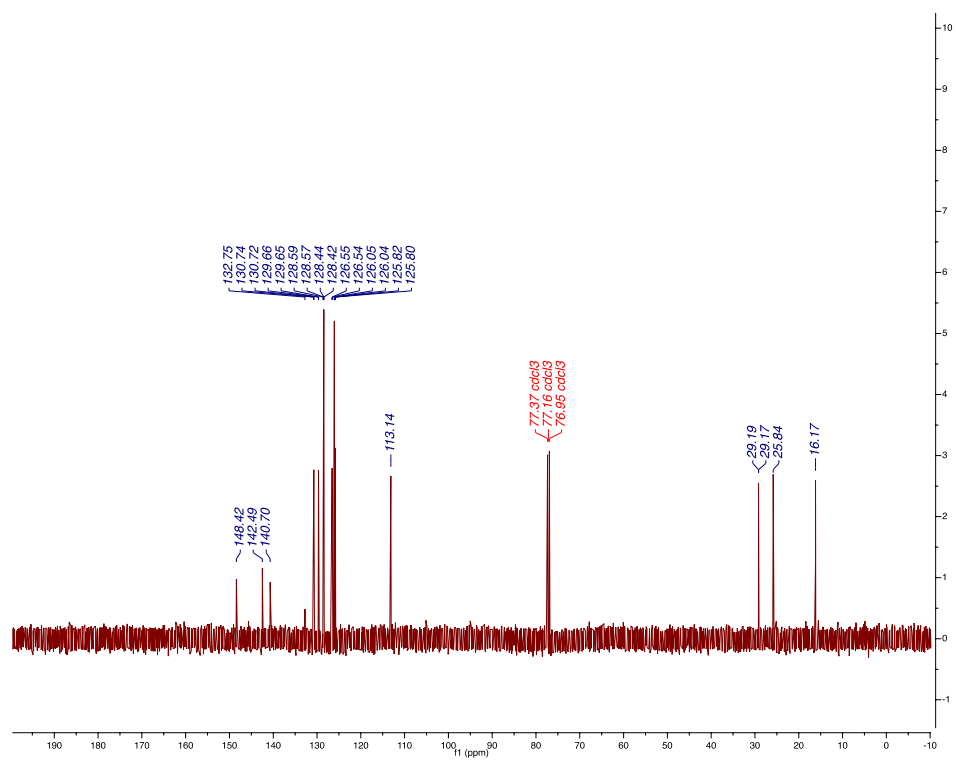
**<sup>13</sup>C NMR** (150 MHz, CDCl<sub>3</sub>) δ 148.4, 142.5, 140.7, 132.8, 130.7, 130.7, 129.7, 129.7, **1w** 128.6, 128.6, 128.4, 128.4, 126.6, 126.5, 126.1, 126.0, 125.8, 125.8, 113.1, 29.2, 29.2, 25.8, 16.2 ppm.

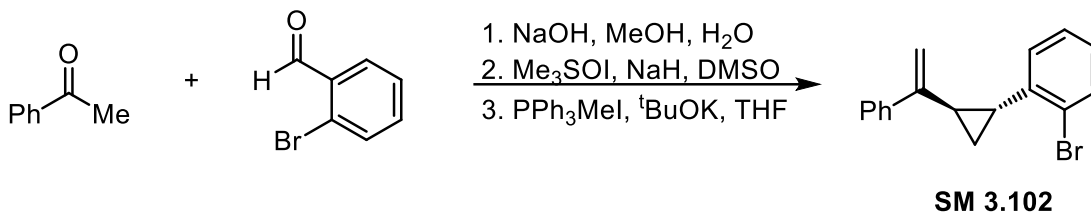
**IR** (film):  $\bar{\nu}$  = 3061 (w), 3016 (w), 1712 (m), 1622 (bs), 1494 (m), 1240 (s), 813 (m), 694 (s) cm<sup>-1</sup>.

**HRMS** (EI): *m/z* calculated for [C<sub>17</sub>H<sub>15</sub>Cl]<sup>+</sup>: 254.0862; found: 254.0873.

c1ccccc1C(=O)C2CC2c3ccccc3  
**SM 3.101**  

<sup>1</sup>H NMR spectrum (CDCl<sub>3</sub>) of SM 3.101. The spectrum shows peaks from 0 to 8 ppm. Aromatic signals are between 7.0-7.4 ppm (10H, multiplet). A cyclopropane CH is at 5.26 ppm (1H, doublet). A CH<sub>2</sub> group is at 4.98 ppm (2H, doublet). A CH group is at 2.00 ppm (1H, doublet). Aliphatic signals are between 1.1-1.3 ppm (10H, multiplet). Integration values are shown below the peaks.





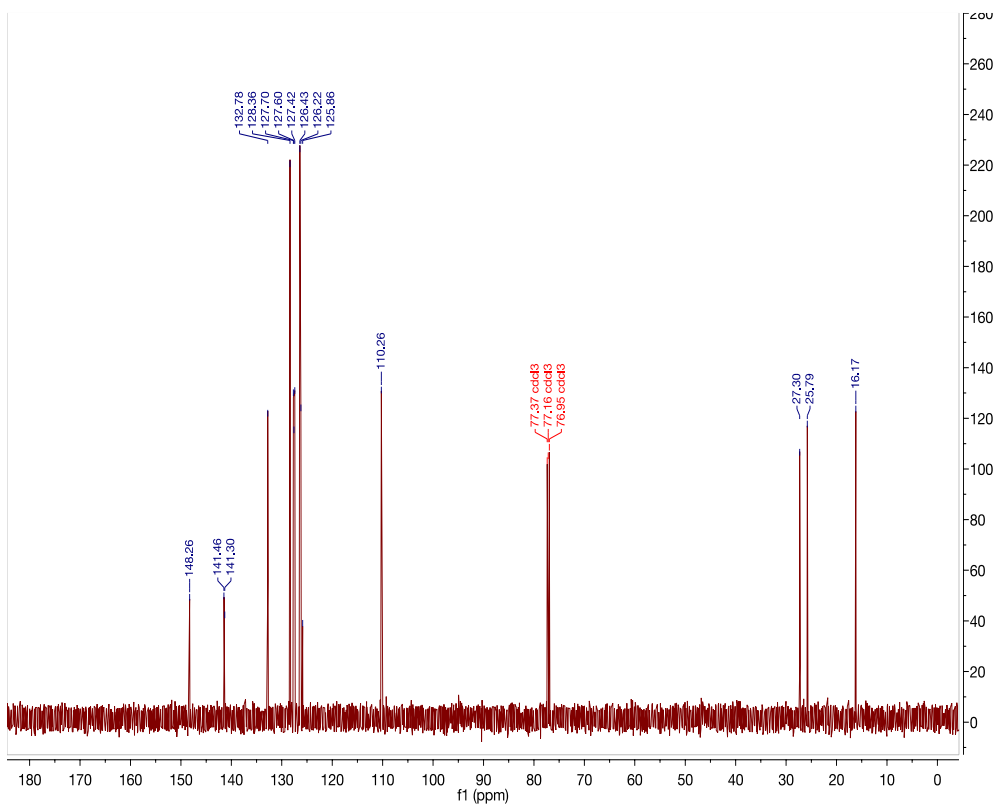
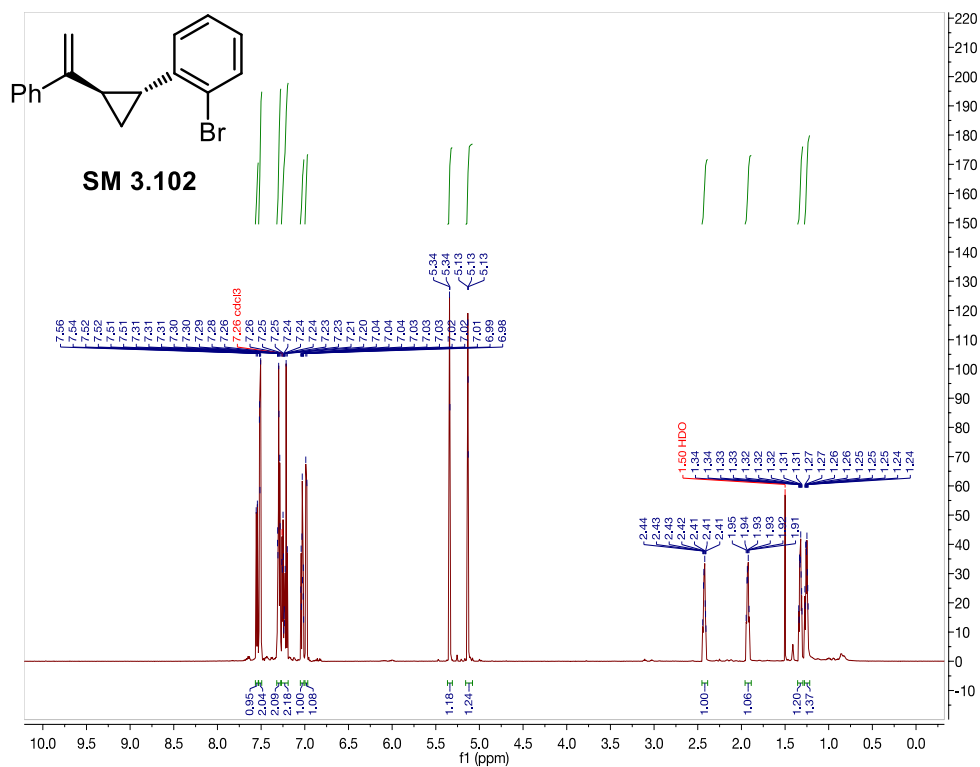
Prepared using the general procedure and purified via silica flash chromatography with 1% ethyl acetate in hexanes as a yellow liquid.

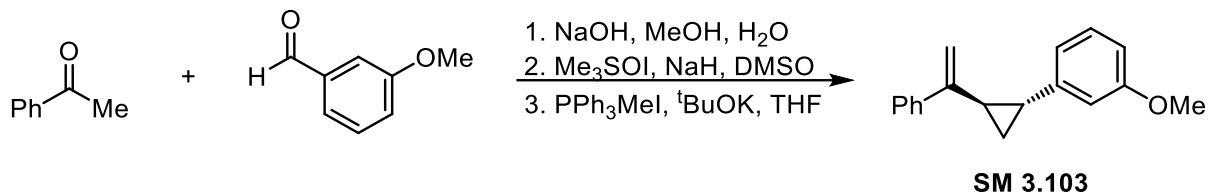
**<sup>1</sup>H NMR** (598 MHz, CDCl<sub>3</sub>) δ 7.55 (d, *J* = 7.9 Hz, 1H), 7.53 – 7.49 (m, 2H), 7.30 (td, *J* = 8.0, 1.8 Hz, 2H), 7.27 – 7.19 (m, 2H), 7.03 (td, *J* = 7.7, 1.7 Hz, 1H), 6.98 (d, *J* = 7.8 Hz, 1H), 5.34 (d, *J* = 2.6 Hz, 1H), 5.16 – 5.08 (m, 1H), 2.45 – 2.39 (m, 1H), 1.93 (dt, *J* = 8.9, 5.5 Hz, 1H), 1.36 – 1.29 (m, 1H), 1.25 (dtd, *J* = 7.8, 5.5, 2.1 Hz, 1H) ppm.

**<sup>13</sup>C NMR** (150 MHz, CDCl<sub>3</sub>) δ 225.8, 148.3, 141.5, 141.3, 132.8, 128.4, 127.7, 127.6, 127.4, 126.4, 126.2, 125.9, 110.3, 27.3, 25.8, 16.2 ppm.

**IR** (film):  $\bar{\nu}$  = 3055 (w), 1622 (w), 1495 (m), 1477 (m), 1437 (m), 1024 (m), 893 (br, m), 777 (m), 732 (s), 702 (s), 662 (m) cm<sup>-1</sup>.

**HRMS** (EI): *m/z* calculated for [C<sub>17</sub>H<sub>15</sub>Br]<sup>+</sup>: 298.0357; found: 298.0356.





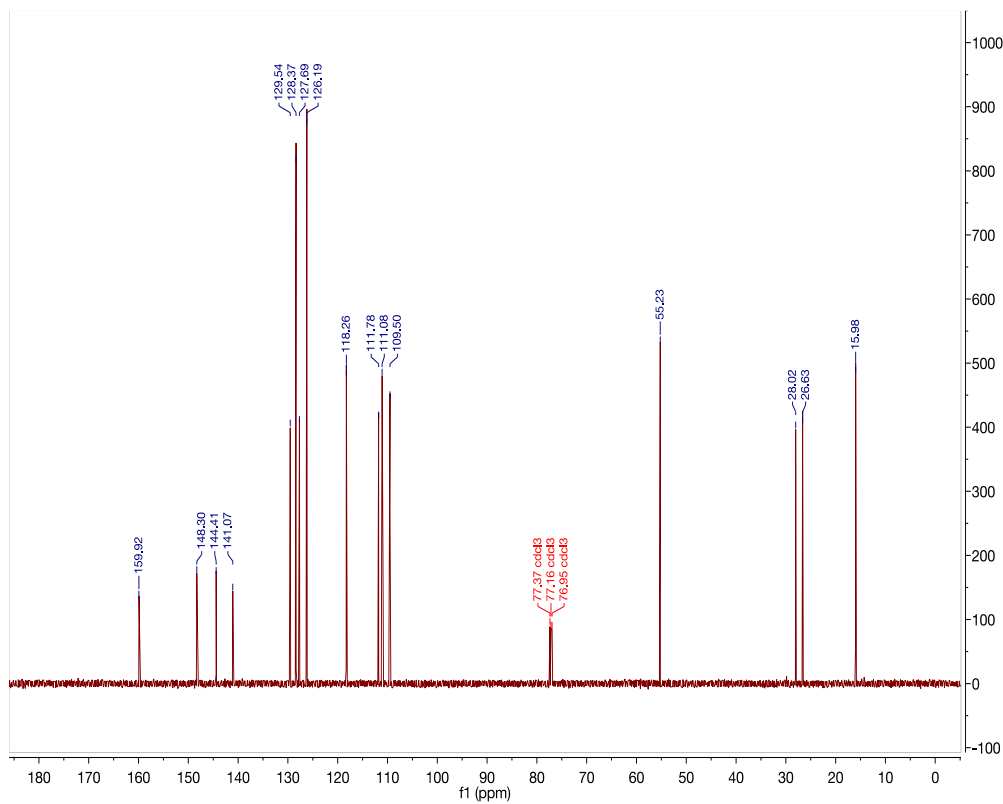
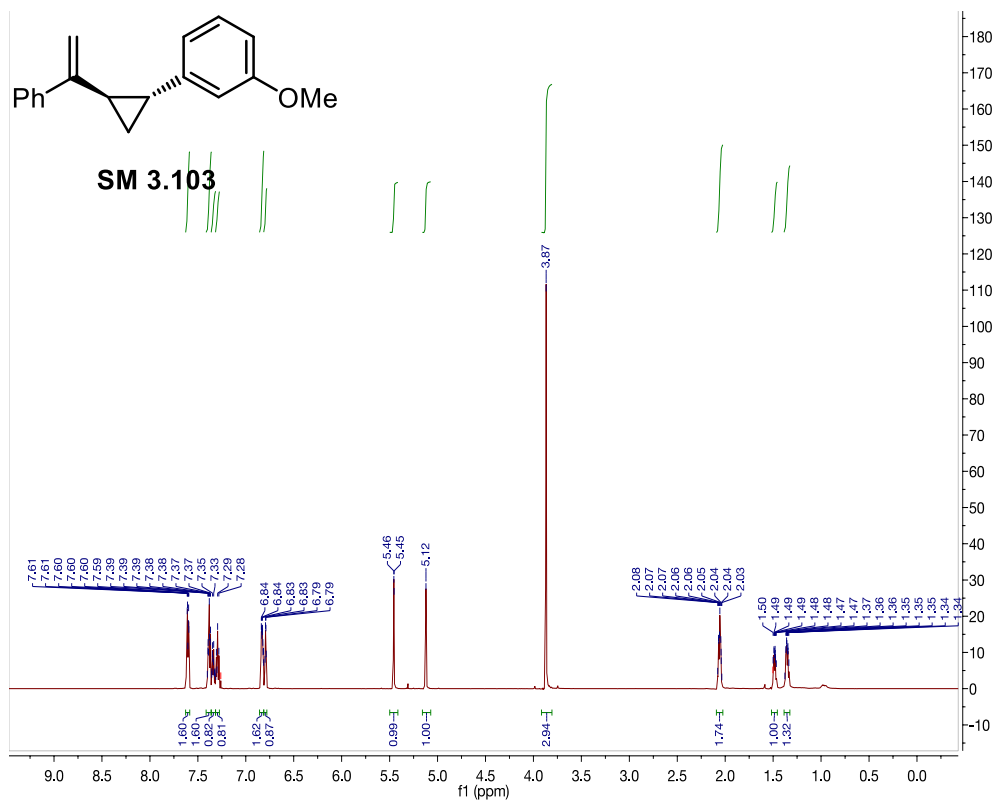
Prepared using the general procedure and purified via silica flash chromatography with 1% ethyl acetate in hexanes as a yellow liquid.

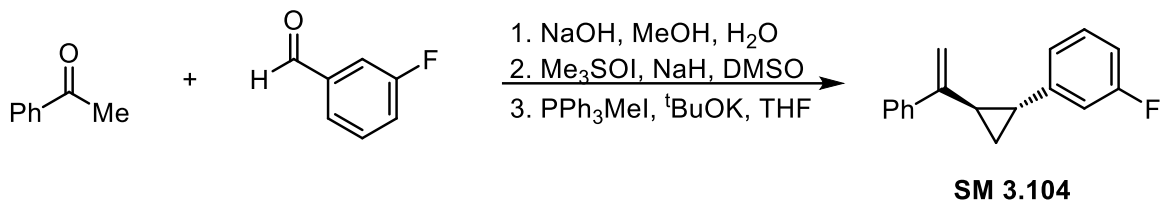
**<sup>1</sup>H NMR** (598 MHz, CDCl<sub>3</sub>) δ 7.63 – 7.58 (m, 2H), 7.41 – 7.36 (m, 2H), 7.36 – 7.32 (m, 1H), 7.29 (t, *J* = 7.8 Hz, 1H), 6.83 (ddt, *J* = 7.9, 3.3, 1.2 Hz, 2H), 6.79 (q, *J* = 2.5, 2.1 Hz, 1H), 5.45 (d, *J* = 1.1 Hz, 1H), 5.12 (s, 1H), 3.87 (s, 3H), 2.09 – 2.02 (m, 2H), 1.48 (ddd, *J* = 7.9, 6.5, 4.9 Hz, 1H), 1.35 (ddd, *J* = 8.1, 6.2, 4.9 Hz, 1H) ppm.

**<sup>13</sup>C NMR** (150 MHz, CDCl<sub>3</sub>) δ 159.9, 148.3, 144.4, 141.1, 129.5, 128.4, 127.7, 126.2, 118.3, 111.8, 111.0, 109.5, 55.2, 28.0, 26.6, 16.0 ppm.

**IR** (film):  $\bar{\nu}$  = 3053 (w), 3001 (w), 2833 (w), 1600 (m), 1581 (m), 1492 (m), 1290 (w), 1163 (m), 1049 (br, m), 891 (br, m), 775 (s), 704 (s) cm<sup>-1</sup>.

**HRMS** (EI): *m/z* calculated for [C<sub>18</sub>H<sub>18</sub>O]<sup>+</sup>: 250.1358; found: 250.1364.





Prepared using the general procedure and purified via silica flash chromatography with 1% ethyl acetate in hexanes as a clear liquid.

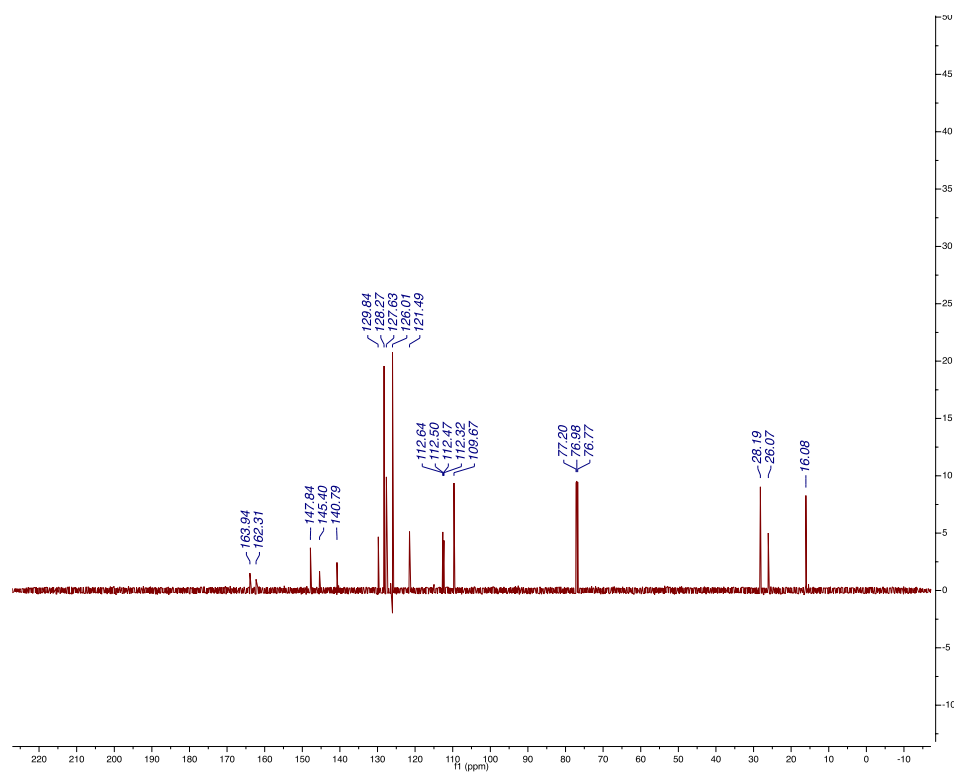
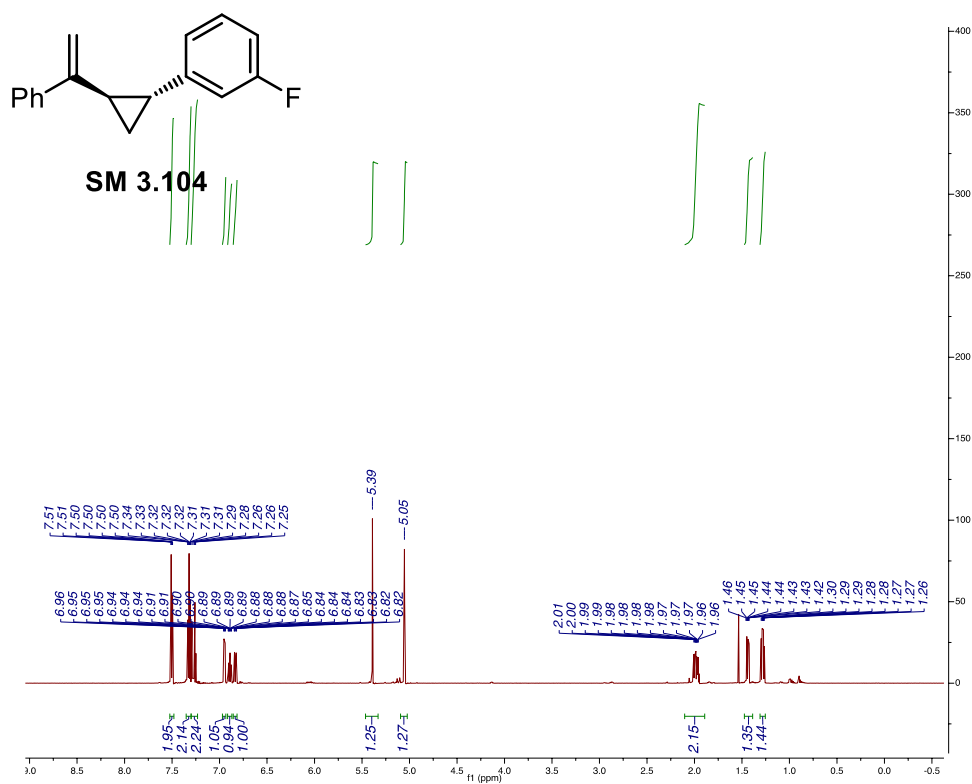
**<sup>1</sup>H NMR** (800 MHz, CDCl<sub>3</sub>) δ 7.62 – 7.55 (m, 1H), 7.46 – 7.28 (m, 3H), 7.04 (dt, *J* = 7.7, 1.3 Hz, 1H), 6.98 (dd, *J* = 2.6, 0.9 Hz, 1H), 6.92 (dd, *J* = 10.3, 0.8 Hz, 1H), 5.47 (d, *J* = 0.7 Hz, 1H), 5.14 (s, 1H), 2.12 – 2.03 (m, 1H), 1.51 (ddd, *J* = 8.7, 6.2, 5.1 Hz, 1H), 1.47 – 1.29 (m, 1H) ppm.

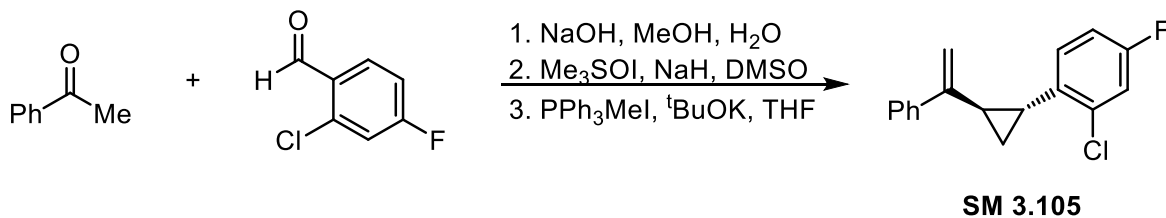
**<sup>13</sup>C NMR** (201 MHz, CDCl<sub>3</sub>) δ 163.8, 162.6, 148.0, 145.4, 145.4, 140.9, 129.8, 129.8, 128.3, 127.6, 126.0, 121.6, 112.5, 109.7, 28.1, 26.0, 26.0, 16.1, 16.1 ppm.

**<sup>19</sup>F NMR** (563 MHz, CDCl<sub>3</sub>) δ -113.68 ppm.

**IR** (film):  $\bar{\nu}$  = 3080 (w), 1614 (m), 1585 (m), 1493 (m), 1246 (m), 887 (m), 775 (s), 702 (s), 685 (s) cm<sup>-1</sup>.

**HRMS** (EI): *m/z* calculated for [C<sub>18</sub>H<sub>15</sub>F]<sup>+</sup>: 238.1158; found: 238.1165.





Prepared using the general procedure and purified via silica flash chromatography with 1% ethyl acetate in hexanes as a clear liquid.

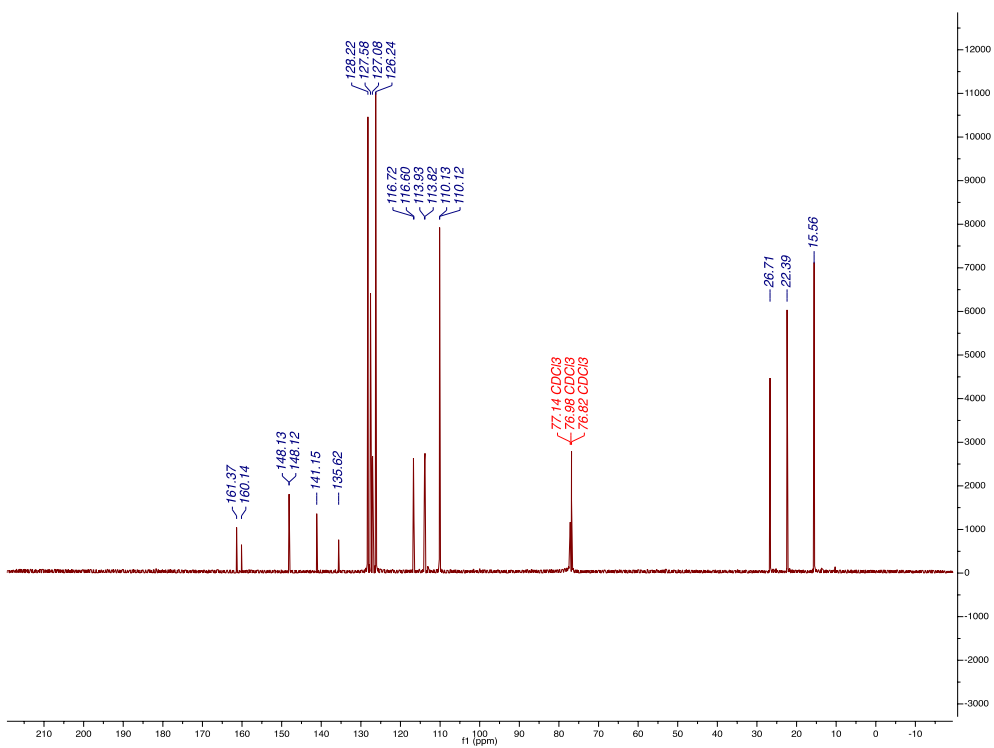
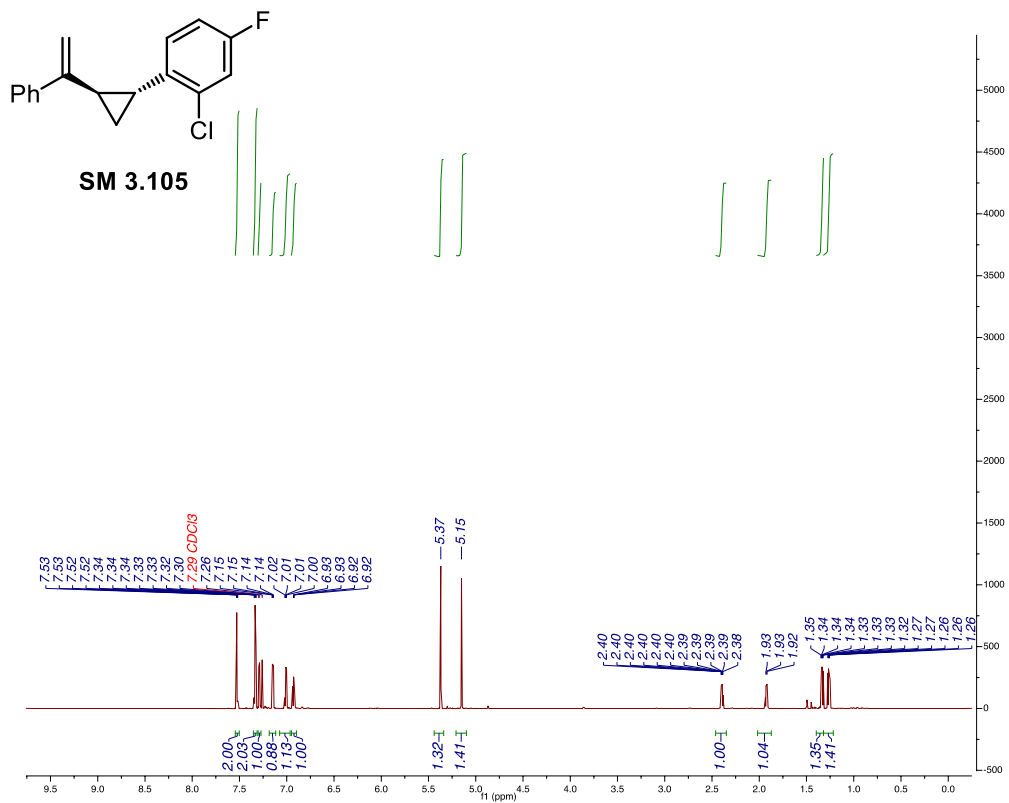
**<sup>1</sup>H NMR** (800 MHz, CDCl<sub>3</sub>) δ 7.53 (dd, *J* = 8.3, 1.2 Hz, 2H), 7.35 – 7.31 (m, 2H), 7.30 (s, 1H), 7.15 (dd, *J* = 8.5, 2.7 Hz, 1H), 7.01 (dd, *J* = 8.6, 5.9 Hz, 1H), 6.95 – 6.90 (m, 1H), 5.37 (s, 1H), 5.15 (s, 1H), 2.46 – 2.35 (m, 1H), 2.02 – 1.87 (m, 1H), 1.34 (ddd, *J* = 8.8, 6.0, 4.9 Hz, 1H), 1.26 (ddd, *J* = 8.8, 5.8, 4.9 Hz, 1H) ppm.

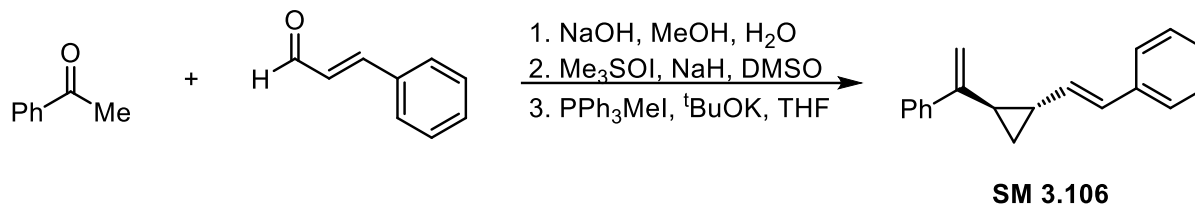
**<sup>13</sup>C NMR** (201 MHz, CDCl<sub>3</sub>) δ 161.4, 160.1, 148.1, 148.1, 141.2, 135.6, 128.2, 127.6, 127.0, 126.2, 116.7, 116.6, 113.9, 113.8, 110.1, 110.1, 26.7, 22.4, 15.6 ppm.

**<sup>19</sup>F NMR** (563 MHz, CDCl<sub>3</sub>) δ -115.28 (q, *J* = 8.3 Hz) ppm.

**IR** (film):  $\bar{\nu}$  = 3080 (w), 1600 (m), 1492 (s), 1259 (m), 1240 (m), 894 (s), 858 (s), 775 (s), 698 (s) cm<sup>-1</sup>.

**HRMS** (EI): *m/z* calculated for [C<sub>18</sub>H<sub>14</sub>ClF]<sup>+</sup>: 272.0768; found: 272.0772.





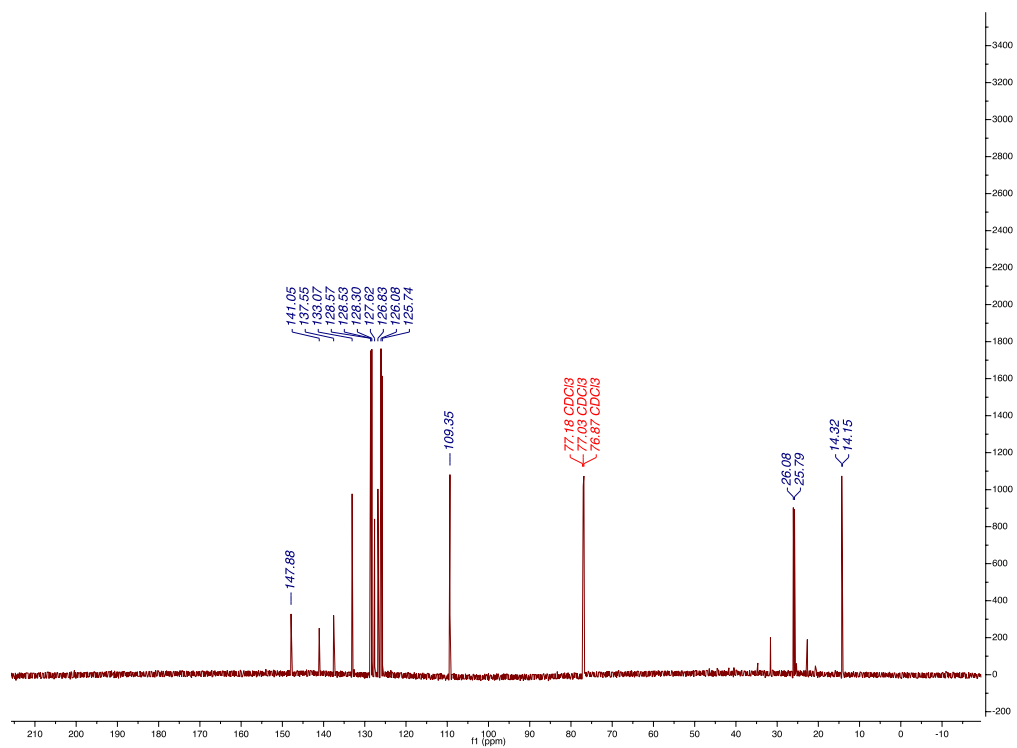
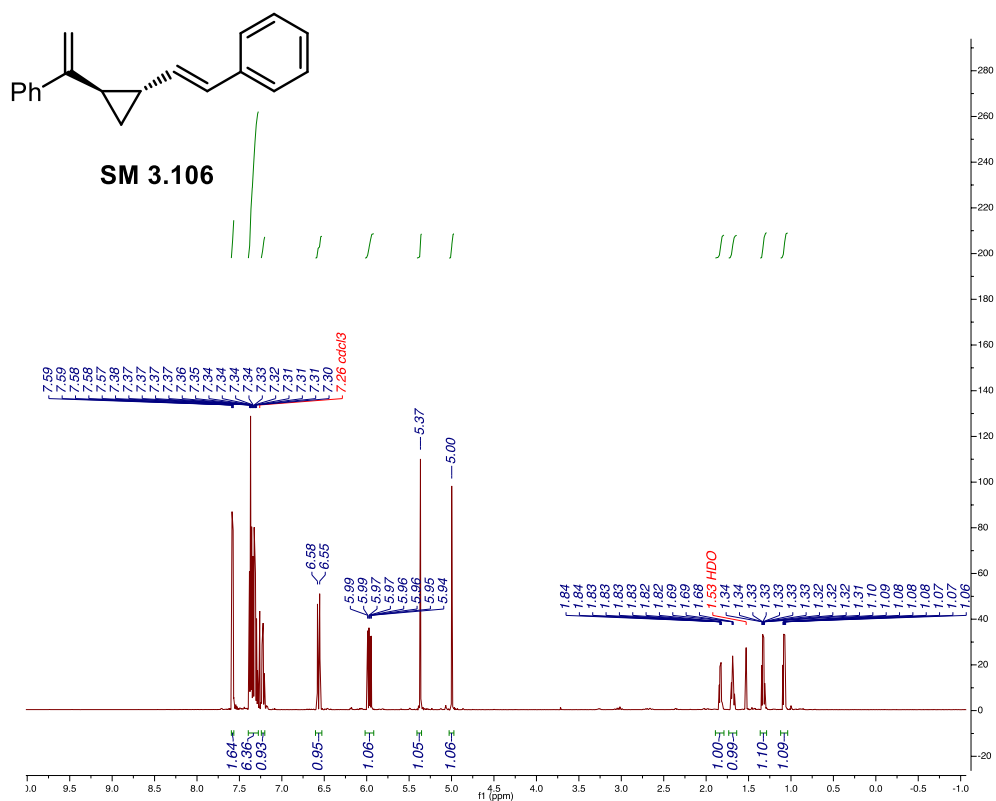
Prepared using the general procedure and purified via silica flash chromatography with 1% ethyl acetate in hexanes as a clear liquid.

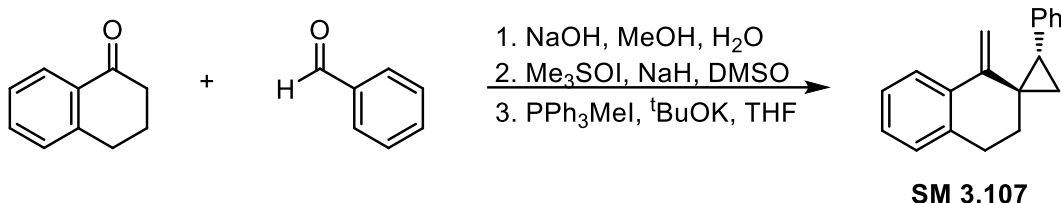
**<sup>1</sup>H NMR** (800 MHz, CDCl<sub>3</sub>) δ 7.61 – 7.54 (m, 2H), 7.40 – 7.27 (m, 7H), 7.25 – 7.18 (m, 1H), 6.56 (d, *J* = 15.7 Hz, 1H), 5.96 (dd, *J* = 15.7, 9.0 Hz, 1H), 5.35 (s, 1H), 4.98 (s, 1H), 1.85 – 1.79 (m, 1H), 1.68 (dq, *J* = 8.8, 4.6 Hz, 1H), 1.35 – 1.29 (m, 2H), 1.07 (dt, *J* = 8.7, 5.0 Hz, 2H) ppm.

**<sup>13</sup>C NMR** (201 MHz, CDCl<sub>3</sub>) δ 148.0, 141.2, 137.7, 133.2, 128.7, 128.7, 128.4, 127.8, 127.0, 126.2, 125.9, 109.5, 26.2, 25.9, 14.5 ppm.

**IR** (film):  $\bar{\nu}$  = 3082 (w), 3014 (w), 1622 (w), 1489 (m), 958 (s), 694 (s) cm<sup>-1</sup>

**HRMS** (EI): *m/z* calculated for [C<sub>19</sub>H<sub>18</sub>]<sup>+</sup>: 246.1409; found: 246.1420.





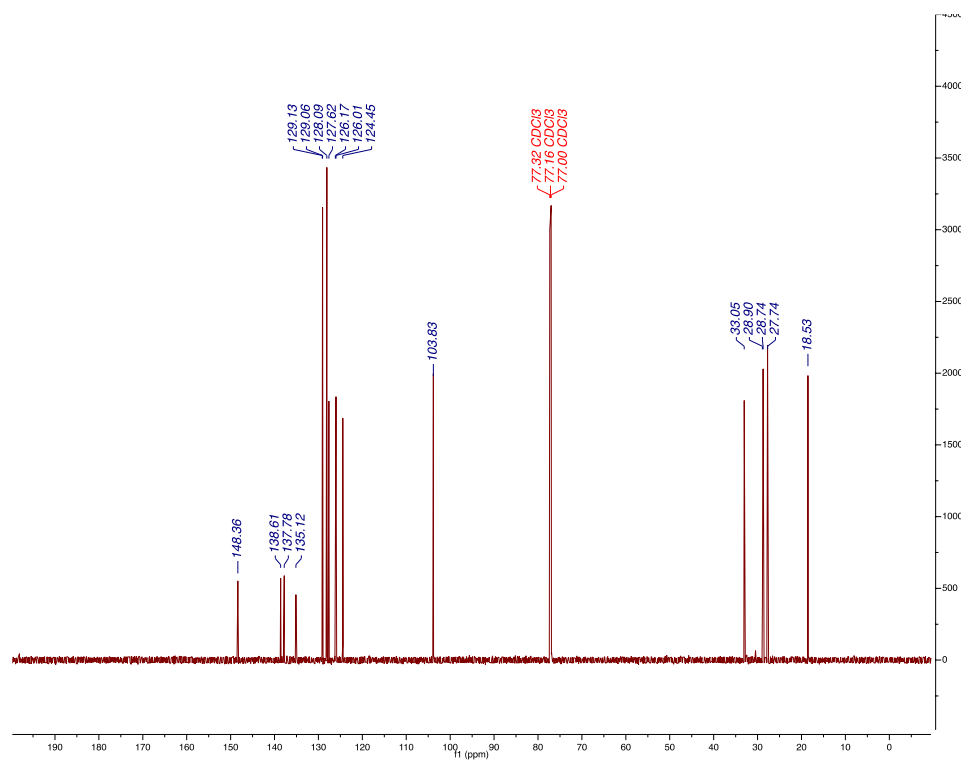
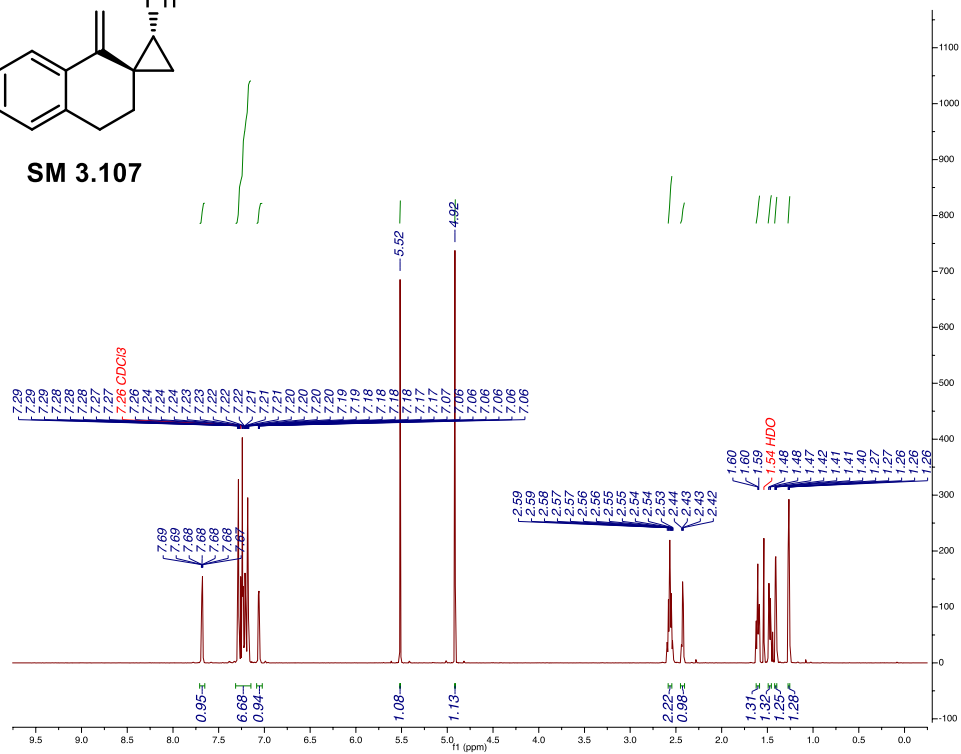
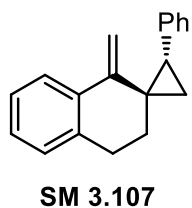
Prepared using the general procedure and purified via silica flash chromatography with 1% ethyl acetate in hexanes as a clear liquid.

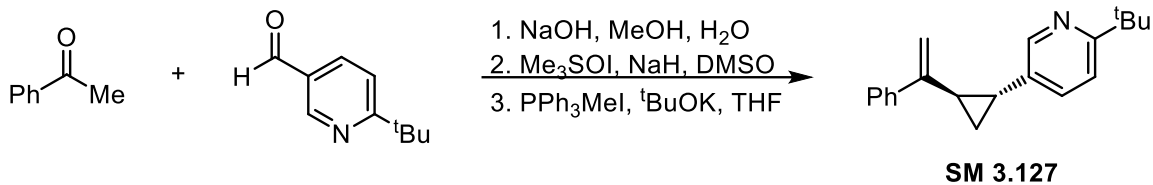
**<sup>1</sup>H NMR** (800 MHz, CDCl<sub>3</sub>) δ 7.71 – 7.65 (m, 1H), 7.31 – 7.15 (m, 7H), 7.09 – 7.02 (m, 1H), 5.52 (s, 1H), 4.92 (s, 1H), 2.58 – 2.54 (m, 2H), 2.43 (dd, *J* = 8.7, 6.6 Hz, 1H), 1.60 (ddd, *J* = 12.0, 8.5, 5.2 Hz, 1H), 1.47 (ddd, *J* = 13.6, 6.4, 4.9 Hz, 1H), 1.41 (dt, *J* = 6.9, 3.4 Hz, 1H), 1.26 (ddd, *J* = 6.8, 5.2, 1.5 Hz, 1H) ppm.

**<sup>13</sup>C NMR** (201 MHz, CDCl<sub>3</sub>) δ 148.4, 138.6, 137.8, 135.1, 129.1, 129.0, 128.1, 127.6, 126.2, 126.0, 124.5, 103.8, 33.1, 28.9, 28.7, 27.7, 18.5 ppm.

**IR** (film):  $\bar{\nu}$  = 3680 (w), 2922 (m), 2294 (w), 1602 (w), 1454 (w), 904 (s) cm<sup>-1</sup>.

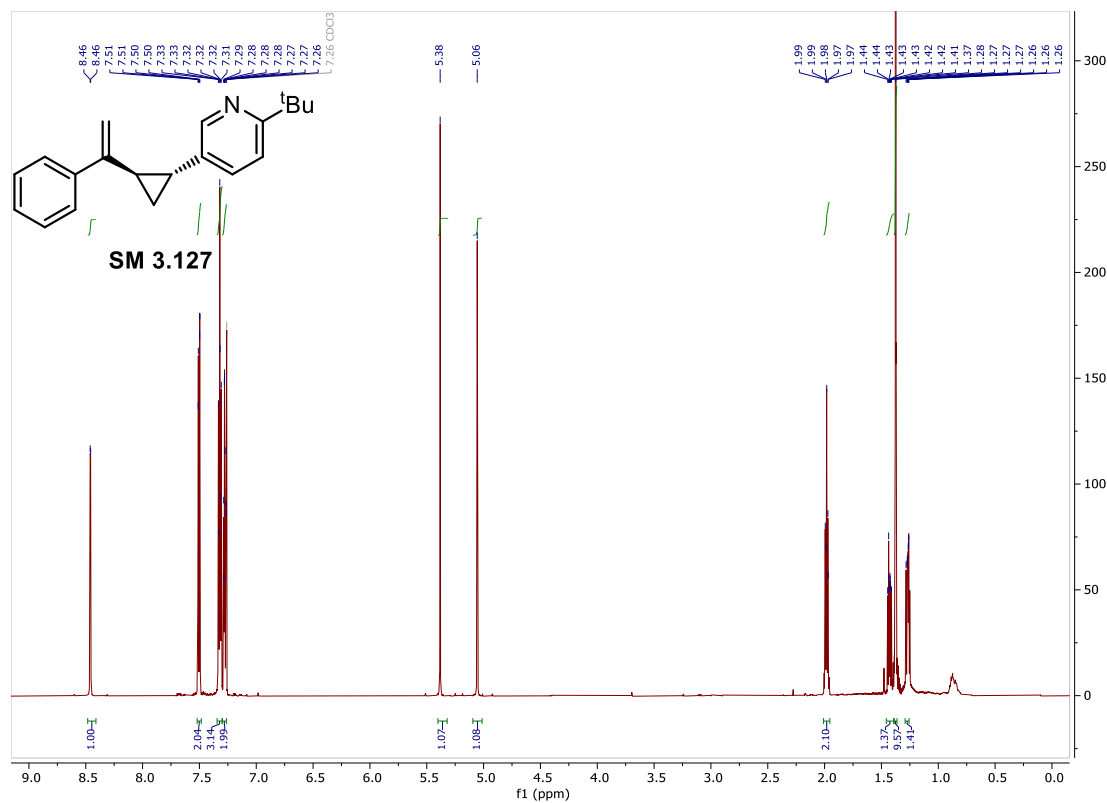
**HRMS** (EI): *m/z* calculated for [C<sub>19</sub>H<sub>18</sub>]<sup>+</sup>: 246.1409; found: 246.1419.



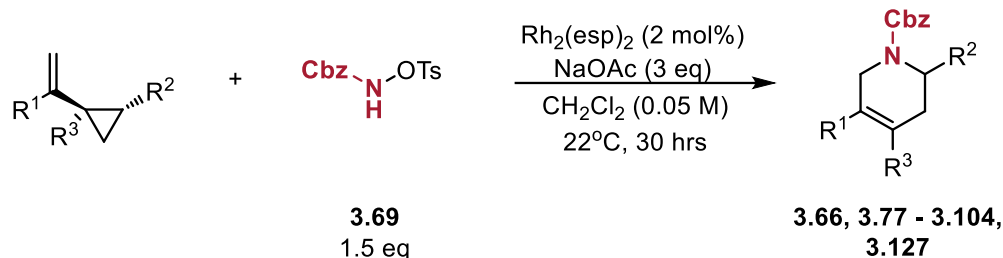


Prepared using the general procedure and purified via silica flash chromatography (deactivated with Et<sub>3</sub>N) with 3% ethyl acetate in hexanes as a white solid.

**<sup>1</sup>H NMR** (600 MHz, CDCl<sub>3</sub>) δ 8.46 (d, *J* = 2.4 Hz, 1H), 7.51 – 7.49 (m, 2H), 7.34 – 7.30 (m, 3H), 7.30 – 7.26 (m, 2H), 5.38 (s, 1H), 5.06 (s, 1H), 2.09 – 1.87 (m, 2H), 1.43 (ddd, *J* = 8.0, 6.7, 5.0 Hz, 2H), 1.37 (s, 9H), 1.27 (ddd, *J* = 8.3, 6.2, 5.1 Hz, 1H) ppm.



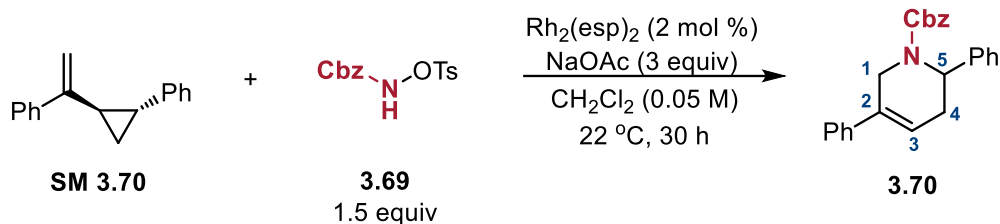
#### 1.4. General procedure for Rh(II)-catalyzed [5+1] reaction



Under inert atmosphere, 0.2 mmol of the corresponding VCP was dissolved with 0.3 mmol (96 mg) CbzNHOTs and 0.6 mmol (49 mg) NaOAc in 4 ml  $\text{CH}_2\text{Cl}_2$  at room temperature. 2 mol% (3 mg)  $\text{Rh}_2(\text{esp})_2$  was added and the reaction mixture was stirred for 30 hours. The reaction mixture was then filtered through silica with 40 ml  $\text{CH}_2\text{Cl}_2$  and concentrated. The desired tetrahydropyridine products were isolated by silica flash chromatography.

### 1.5. Characterization of products from Rh(II)-method

**Note:** The [5+1] products from this method exist as a mixture of rotamers. Due to this,  $^{19}\text{F}$  and  $^1\text{H}$  NMR spectra were obtained at 298 K and  $^{13}\text{C}$  NMR spectra were obtained at 313 K unless noted. This was done in order to coalesce rotamer peaks for better resolution. In selected cases, a mixture of rotamers is reported.



Synthesized using the general procedure, isolated via silica flash chromatography using 2% Acetone in Hexanes as a white solid (45.0 mg, 60% yield).

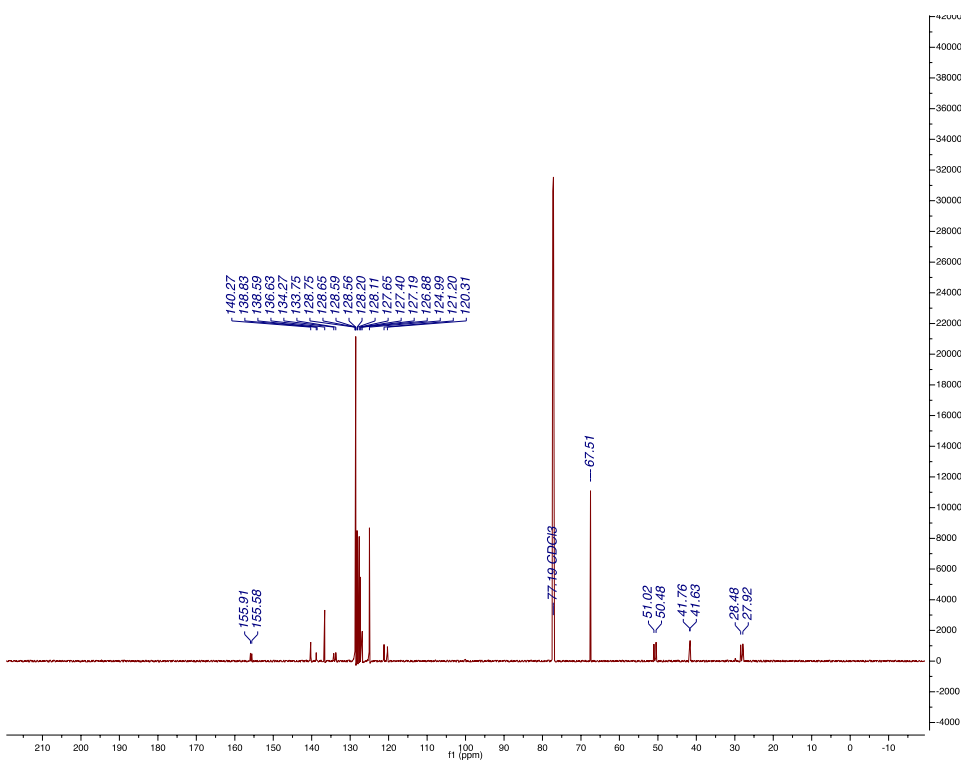
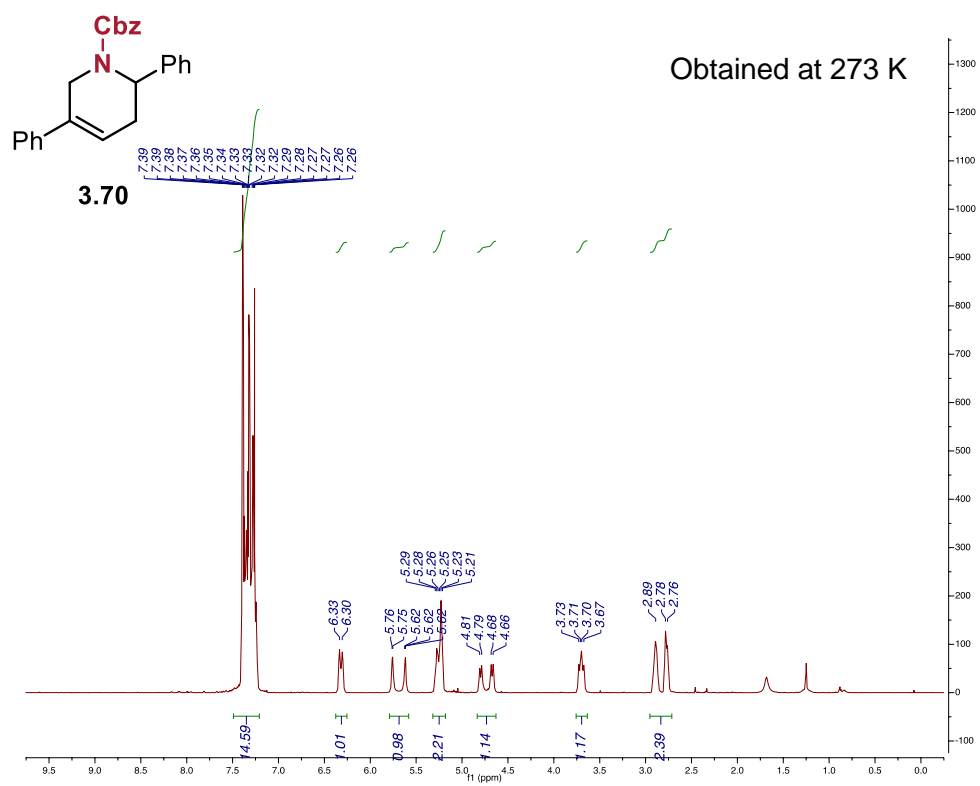
Note: NMR spectra were obtained in 4 °C.

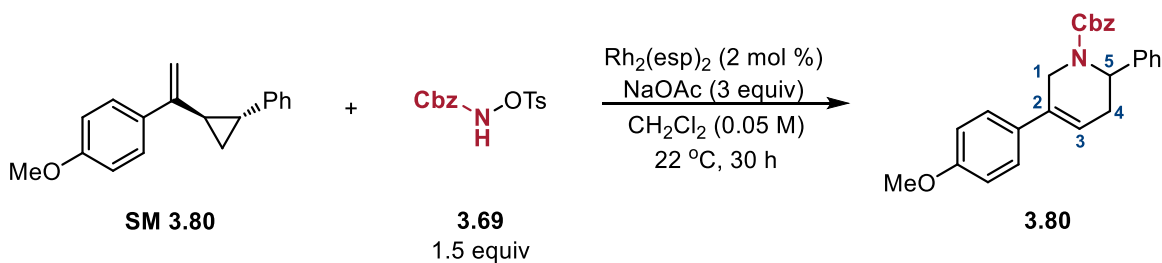
**$^1\text{H}$  NMR** (800 MHz, 290 K,  $\text{CDCl}_3$ )  $\delta$  7.47 – 7.17 (ArH, m, 15H), 6.32 ( $\text{H}^3$ , d,  $J = 23.9$  Hz, 1H), 5.80 – 5.58 ( $\text{H}^5$ , m, 1H), 5.32 – 5.17 (Cbz- $\text{CH}_2$ , m, 2H), 4.73 ( $\text{H}^1$ , dd,  $J = 99.9, 17.8$  Hz, 1H), 3.70 ( $\text{H}^1$ , dd,  $J = 27.1, 17.8$  Hz, 1H), 2.89 ( $\text{H}^4$ , s, 1H), 2.77 ( $\text{H}^4$ , d,  $J = 17.9$  Hz, 1H) ppm.

**$^{13}\text{C}$  NMR** (201 MHz, 290 K,  $\text{CDCl}_3$ )  $\delta$  155.9, 155.6, 140.3, 138.8, 138.6, 136.6, 134.3, 133.8, 128.8, 128.7, 128.6, 128.6, 128.4, 128.2, 128.1, 127.7, 127.4, 127.2, 126.9, 125.0, 121.2, 120.3, 67.5, 51.0, 50.5, 41.8, 41.6, 28.5, 27.9 ppm. (mixture of rotamers)

**IR** (film):  $\bar{\nu} = 3061$  (w), 3016 (w), 1712 (m), 1622 (s), 1446 (m), 894 (s), 694 (s)  $\text{cm}^{-1}$ .

**HRMS** (ESI):  $m/z$  calculated for  $[\text{C}_{25}\text{H}_{24}\text{NO}_2+\text{H}]^+$ : 370.1807; found: 370.1800.





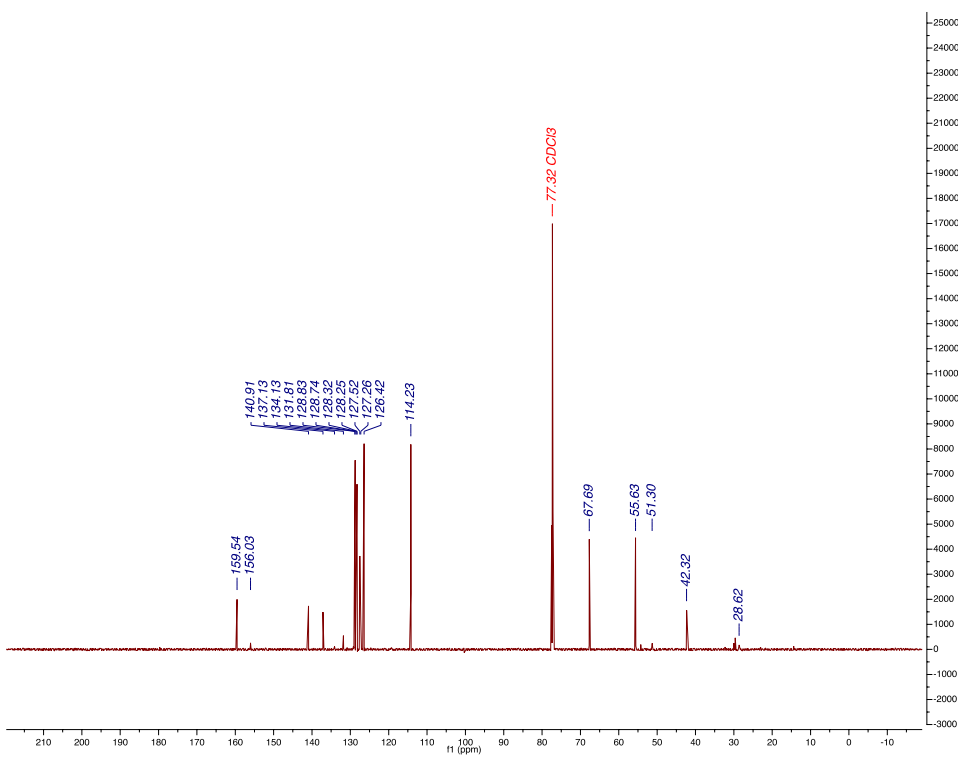
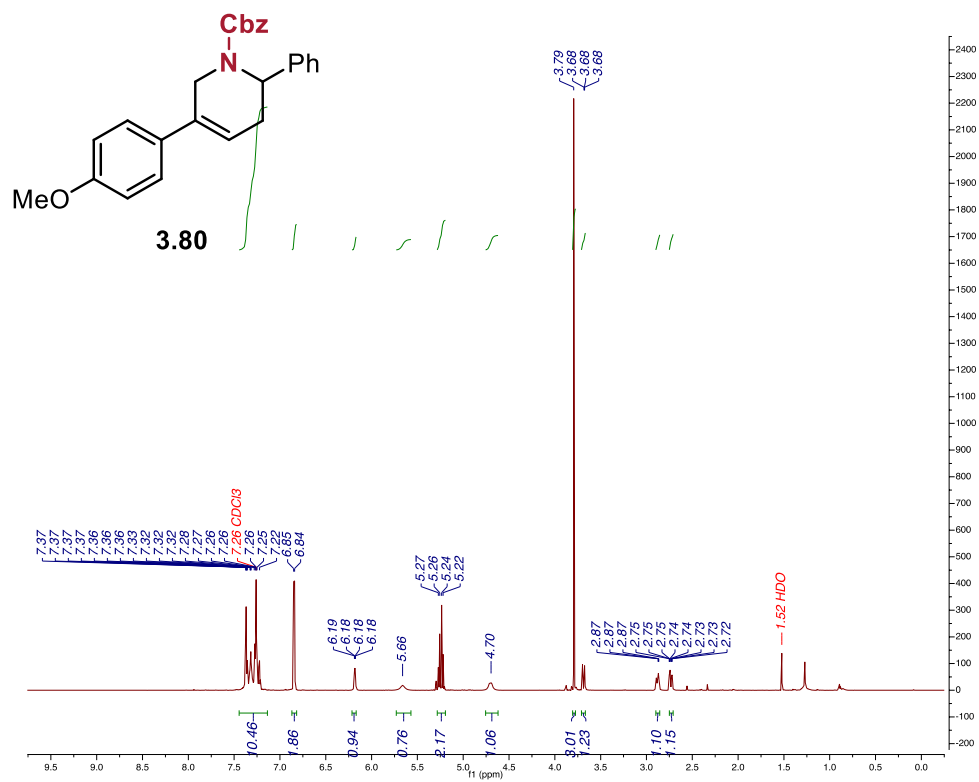
Synthesized using the general procedure, isolated via silica flash chromatography using 5% Acetone in Hexanes as a white solid (22.0 mg, 27% yield).

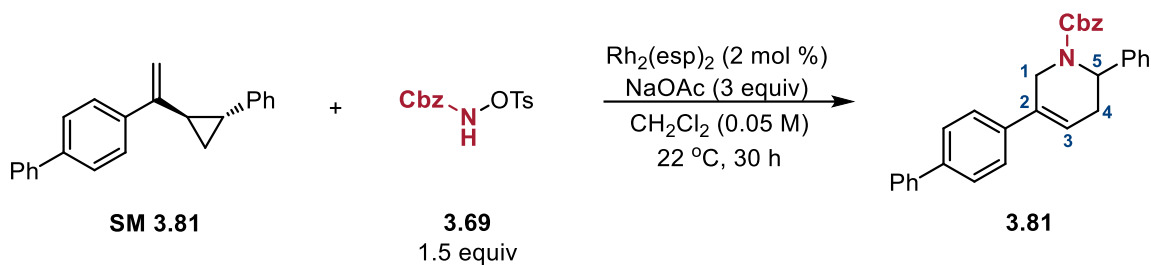
**$^1\text{H}$  NMR** (800 MHz,  $\text{CDCl}_3$ )  $\delta$  7.50 – 7.10 (ArH, m, 12H), 6.85 (ArH, d,  $J$  = 8.7 Hz, 2H), 6.18 ( $\text{H}^3$ , dd,  $J$  = 6.0, 2.6 Hz, 1H), 5.66 ( $\text{H}^5$ , s, 1H), 5.30 – 5.20 (Cbz- $\text{CH}_2$ , m, 2H), 4.70 ( $\text{H}^1$ , s, 1H), 3.79 (OMe, s, 3H), 3.74 – 3.66 ( $\text{H}^1$ , m, 1H), 2.93 – 2.85 ( $\text{H}^4$ , m, 1H), 2.73 ( $\text{H}^4$ , dd,  $J$  = 18.0, 6.2 Hz, 1H) ppm.

**$^{13}\text{C}$  NMR** (201 MHz,  $\text{CDCl}_3$ )  $\delta$  159.5, 156.0, 140.9, 137.1, 134.1, 131.8, 128.8, 128.7, 128.3, 128.3, 127.5, 127.3, 126.4, 114.2, 67.7, 55.6, 51.3, 42.3, 28.6 ppm.

**IR** (film):  $\bar{\nu}$  = 2956 (w), 2360 (w), 1689 (s), 1514 (m), 1247 (m), 903 (m), 648 (s)  $\text{cm}^{-1}$ .

**HRMS** (ESI):  $m/z$  calculated for  $[\text{C}_{26}\text{H}_{25}\text{O}_3+\text{H}]^+$ : 400.1913; found: 400.1905.





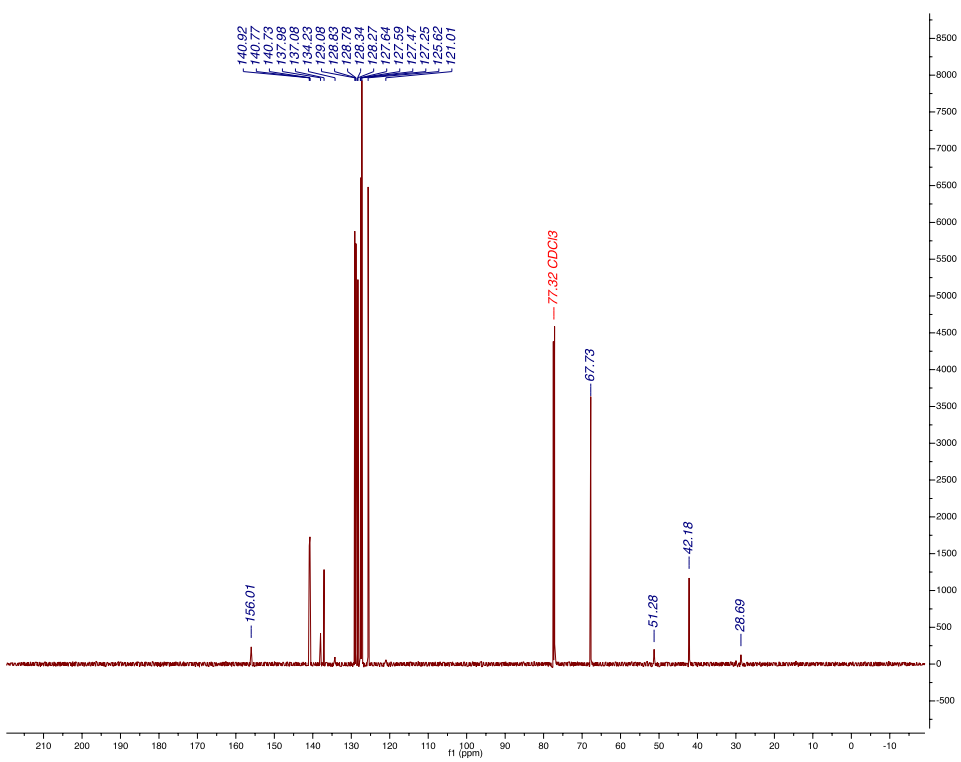
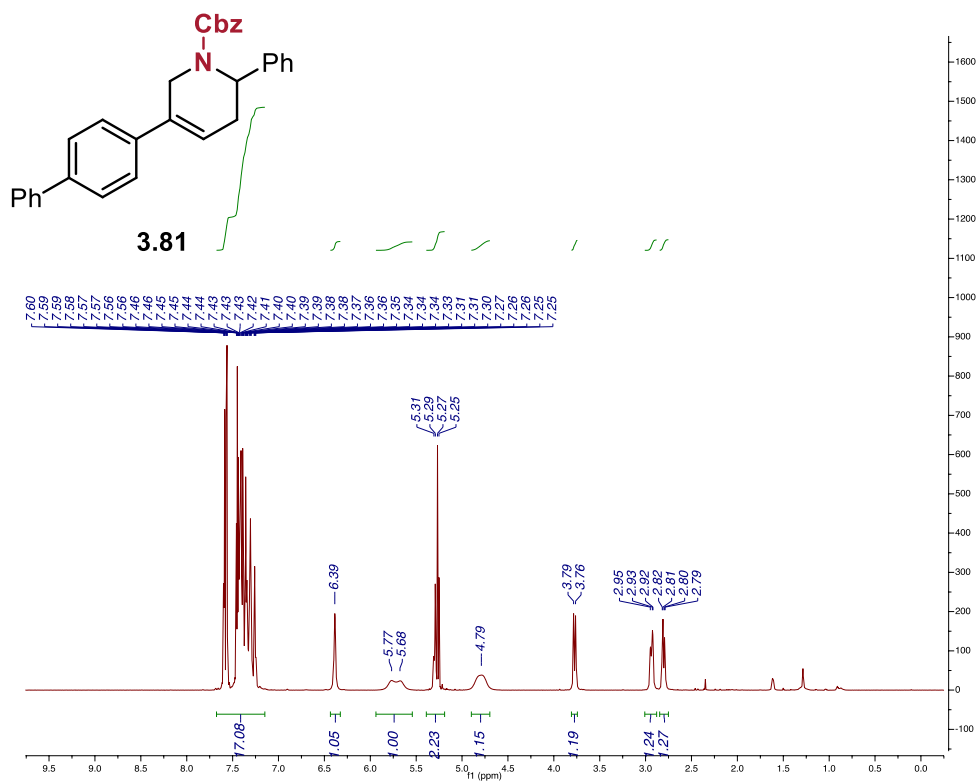
Synthesized using the general procedure, isolated via silica flash chromatography using 2% Acetone in Hexanes as a white solid (32.0 mg, 35% yield).

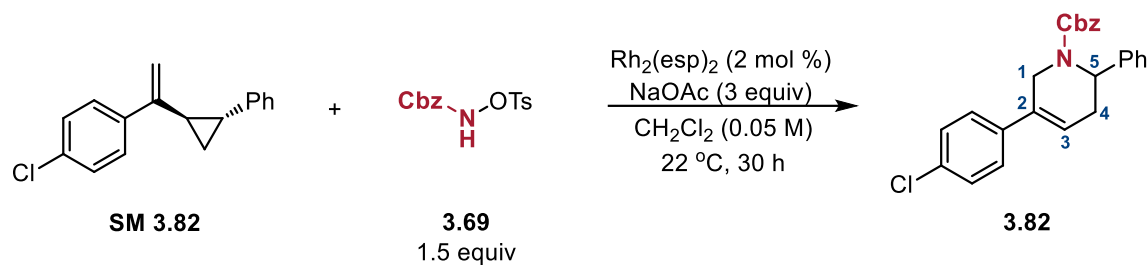
**<sup>1</sup>H NMR** (800 MHz, CDCl<sub>3</sub>) δ 7.68 – 7.15 (ArH, m, 19H), 6.39 (H<sup>3</sup>, s, 1H), 5.72 (H<sup>5</sup>, d, *J* = 73.0 Hz, 1H), 5.39 – 5.19 (Cbz–CH<sub>2</sub>, m, 2H), 4.79 (H<sup>1</sup>, s, 1H), 3.77 (H<sup>1</sup>, d, *J* = 17.6 Hz, 1H), 2.94 (H<sup>4</sup>, d, *J* = 17.2 Hz, 1H), 2.80 (H<sup>4</sup>, dd, *J* = 18.1, 6.0 Hz, 1H) ppm.

**<sup>13</sup>C NMR** (201 MHz, CDCl<sub>3</sub>) δ 156.0, 140.9, 140.8, 140.7, 138.0, 137.1, 134.2, 129.1, 128.8, 128.8, 128.3, 128.3, 127.6, 127.6, 127.5, 127.3, 125.6, 121.0, 67.7, 51.3, 42.2, 28.7 ppm.

**IR** (film):  $\bar{\nu}$  = 3032 (w), 2845 (w), 2360 (w), 1693 (s), 1417 (b), 1238 (s), 906 (m), 692 (s) cm<sup>-1</sup>.

**HRMS** (ESI): *m/z* calculated for [C<sub>31</sub>H<sub>27</sub>NO<sub>2</sub>+H]<sup>+</sup>: 446.2120; found: 446.2111.





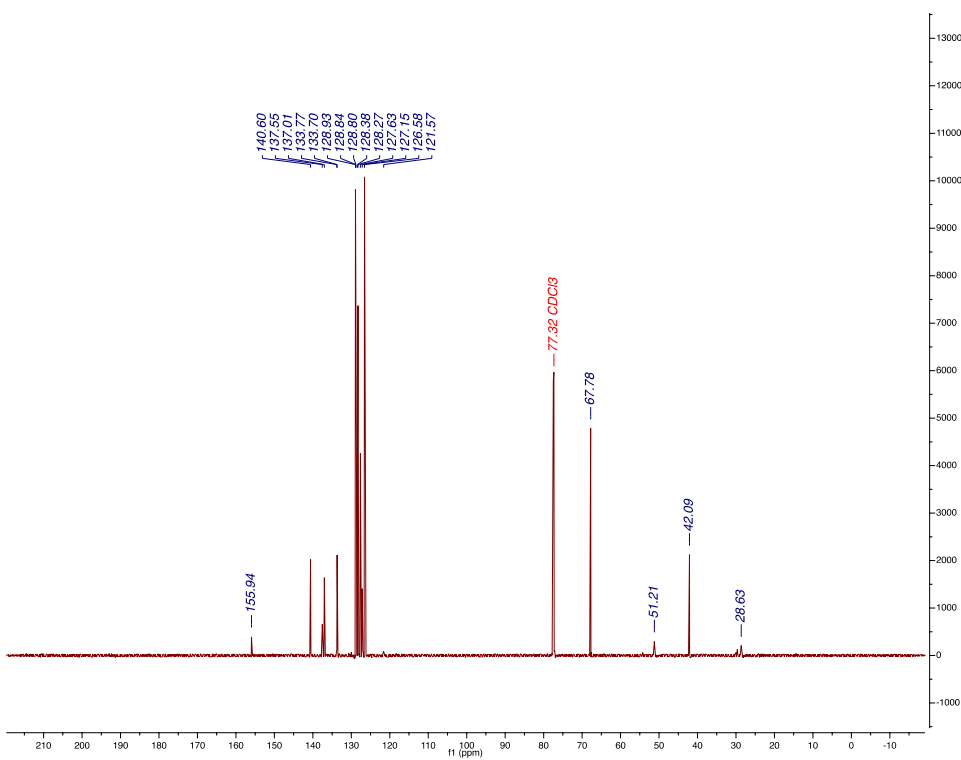
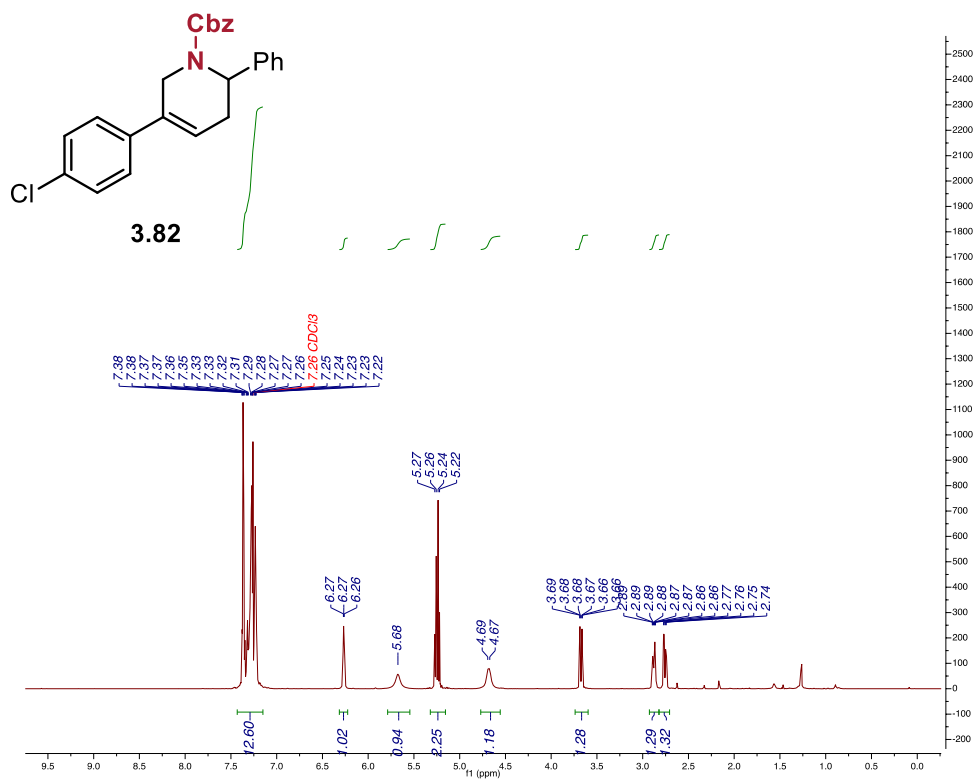
Synthesized using the general procedure, isolated via silica flash chromatography using 2% Acetone in Hexanes as a white solid (42.0 mg, 53% yield).

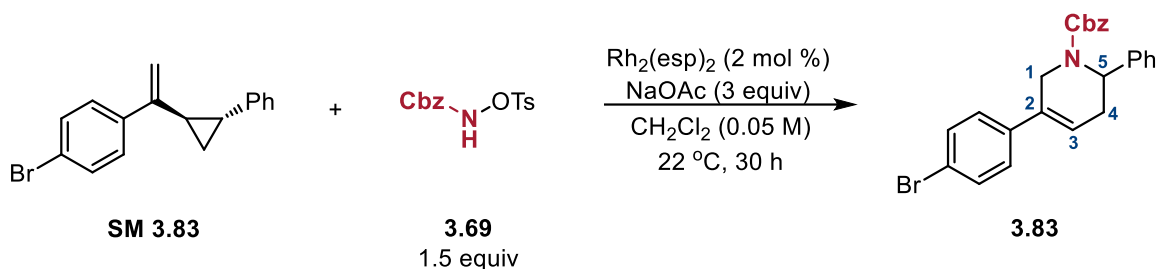
**$^1\text{H}$  NMR** (800 MHz,  $\text{CDCl}_3$ )  $\delta$  7.43 – 7.15 (ArH, m, 14H), 6.32 – 6.22 ( $\text{H}^3$ , m, 1H), 5.68 ( $\text{H}^5$ , s, 1H), 5.32 – 5.16 (Cbz- $\text{CH}_2$ , m, 2H), 4.68 ( $\text{H}^1$ , d,  $J = 17.7$  Hz, 1H), 3.68 ( $\text{H}^1$ , ddd,  $J = 17.8, 4.2, 2.1$  Hz, 1H), 2.88 ( $\text{H}^4$ , ddd,  $J = 18.1, 6.7, 3.4$  Hz, 1H), 2.76 ( $\text{H}^4$ , dd,  $J = 18.2, 6.1$  Hz, 1H) ppm.

**$^{13}\text{C}$  NMR** (201 MHz,  $\text{CDCl}_3$ )  $\delta$  155.9, 140.6, 137.6, 137.0, 133.8, 133.7, 128.9, 128.8, 128.8, 128.4, 128.3, 127.6, 127.2, 126.6, 121.6, 67.8, 51.2, 42.1, 28.6 ppm.

**IR** (film):  $\bar{\nu} = 3030$  (w), 2943 (m), 2341 (w), 1689 (bs), 1419 (m), 1240 (s), 698 (s)  $\text{cm}^{-1}$ .

**HRMS** (ESI):  $m/z$  calculated for  $[\text{C}_{25}\text{H}_{22}\text{ClINO}_2 + \text{H}]^+$ : 404.1417; found: 404.1408.





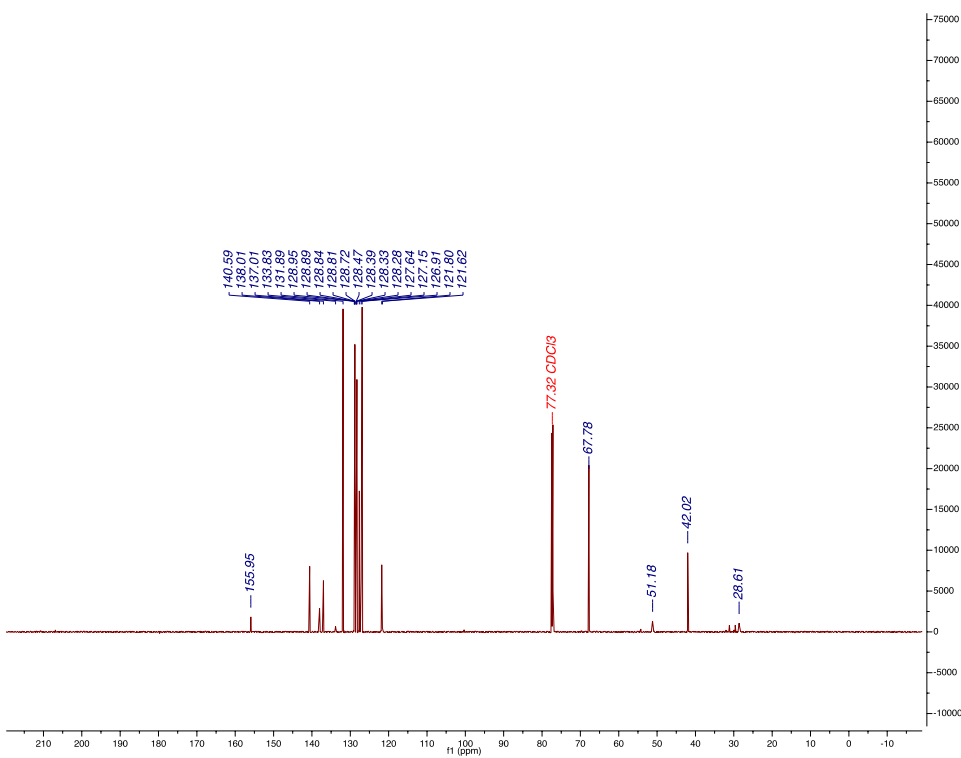
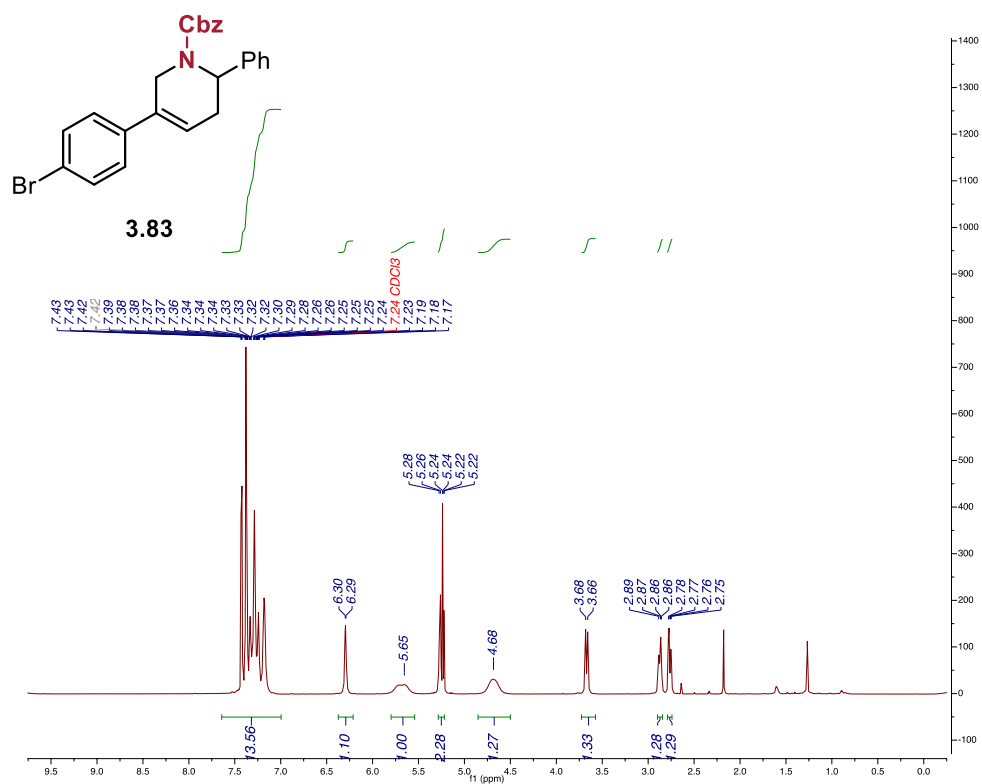
Synthesized using the general procedure, isolated via silica flash chromatography using 2% Acetone in Hexanes as a white solid (46.0 mg, 51% yield).

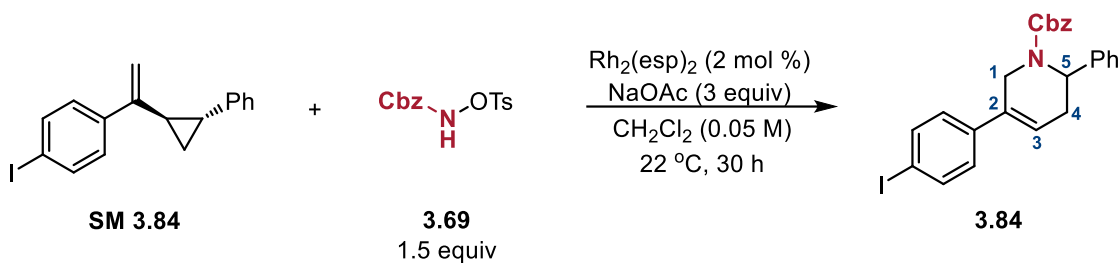
**$^1\text{H}$  NMR** (800 MHz,  $\text{CDCl}_3$ )  $\delta$  7.64 – 7.00 (ArH, m, 14H), 6.37 – 6.21 ( $\text{H}^3$ , m, 1H), 5.65 ( $\text{H}^5$ , s, 1H), 5.29 – 5.22 (Cbz- $\text{CH}_2$ , m, 2H), 4.68 ( $\text{H}^1$ , s, 1H), 3.67 ( $\text{H}^1$ , d,  $J = 17.7$  Hz, 1H), 2.87 ( $\text{H}^4$ , t,  $J = 11.8$  Hz, 1H), 2.76 ( $\text{H}^4$ , dd,  $J = 18.3, 6.1$  Hz, 1H) ppm.

**$^{13}\text{C}$  NMR** (201 MHz,  $\text{CDCl}_3$ )  $\delta$  156.0, 140.6, 138.0, 137.0, 133.8, 131.9, 129.0, 128.9, 128.8, 128.8, 128.7, 128.5, 128.4, 128.3, 128.3, 127.6, 127.2, 126.9, 121.8, 121.6, 67.8, 51.2, 42.0, 28.6 ppm.

**IR** (film):  $\bar{\nu} = 3034$  (w), 2956 (w), 2360 (w), 1691 (bs), 1415 (b), 1240 (m), 904 (m), 696 (s)  $\text{cm}^{-1}$ .

**HRMS** (EI):  $m/z$  calculated for  $[\text{C}_{25}\text{H}_{22}\text{BrNO}_2 + \text{H}]^+$ : 448.0912; found: 448.0904.





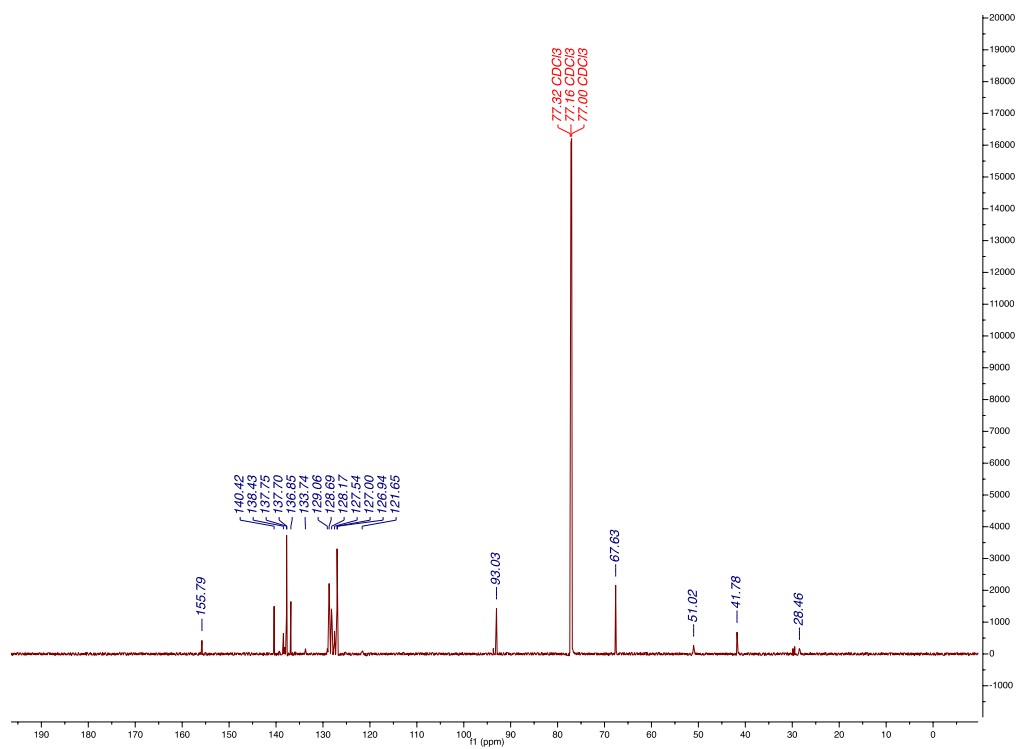
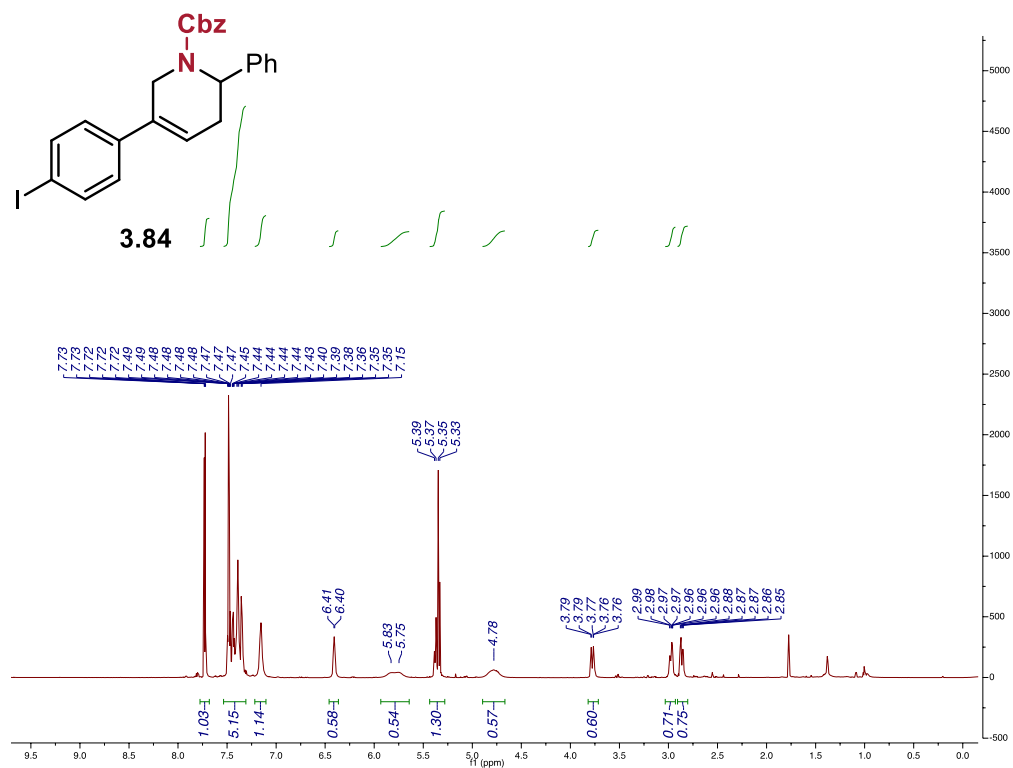
Synthesized using the general procedure, isolated via silica flash chromatography using 2% Acetone in Hexanes as a white solid (58.0 mg, 63% yield).

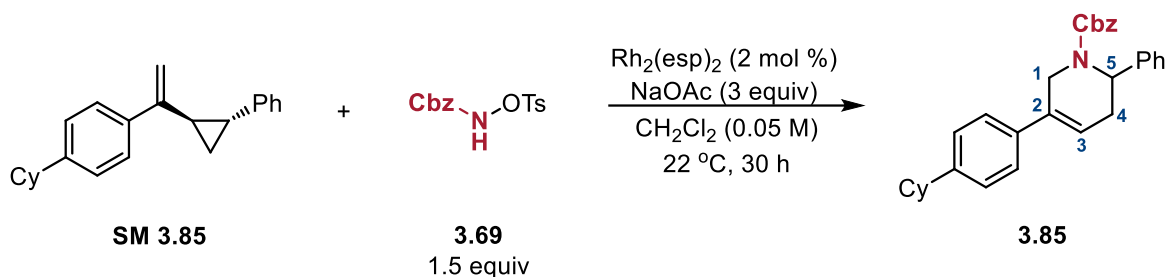
**$^1\text{H}$  NMR** (800 MHz,  $\text{CDCl}_3$ )  $\delta$  7.63 (ArH, d,  $J = 8.3$  Hz, 2H), 7.41 – 7.21 (ArH, m, 12H), 7.05 (ArH, d,  $J = 8.0$  Hz, 2H), 6.33 – 6.26 ( $\text{H}^3$ , m, 1H), 5.67 ( $\text{H}^5$ , s, 1H), 5.30 – 5.18 (Cbz- $\text{CH}_2$ , m, 2H), 4.67 ( $\text{H}^1$ , s, 1H), 3.67 ( $\text{H}^1$ , d,  $J = 18.1$  Hz, 1H), 2.91 – 2.83 ( $\text{H}^4$ , m, 1H), 2.76 ( $\text{H}^4$ , dd,  $J = 18.1, 6.2$  Hz, 1H) ppm.

**$^{13}\text{C}$  NMR** (201 MHz,  $\text{CDCl}_3$ )  $\delta$  155.8, 140.4, 138.4, 137.8, 137.7, 136.9, 133.7, 129.0, 128.7, 128.7, 128.2, 128.1, 127.5, 127.0, 126.9, 121.6, 93.0, 67.6, 51.0, 41.8, 28.5 ppm.

**IR** (film):  $\bar{\nu} = 3030$  (w), 2926 (w), 2360 (w), 1689 (bs), 1421 (m), 1240 (m), 806 (m), 694 (s)  $\text{cm}^{-1}$ .

**HRMS** (ESI):  $m/z$  calculated for  $[\text{C}_{25}\text{H}_{22}\text{INO}_2 + \text{H}]^+$ : 496.0773; found: 496.0760.





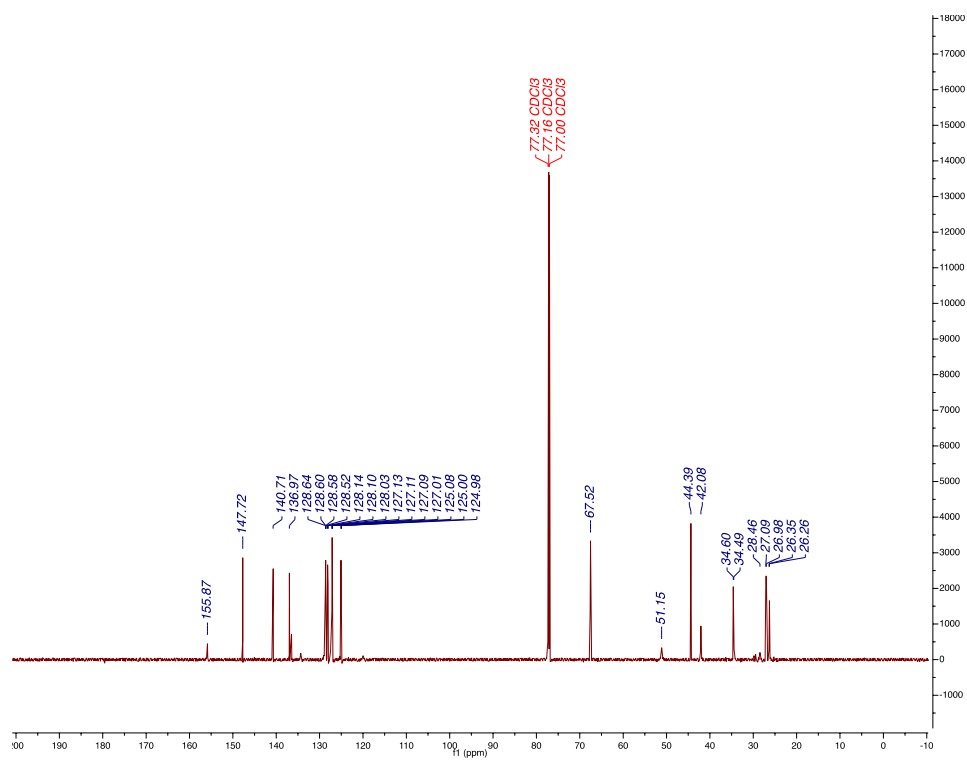
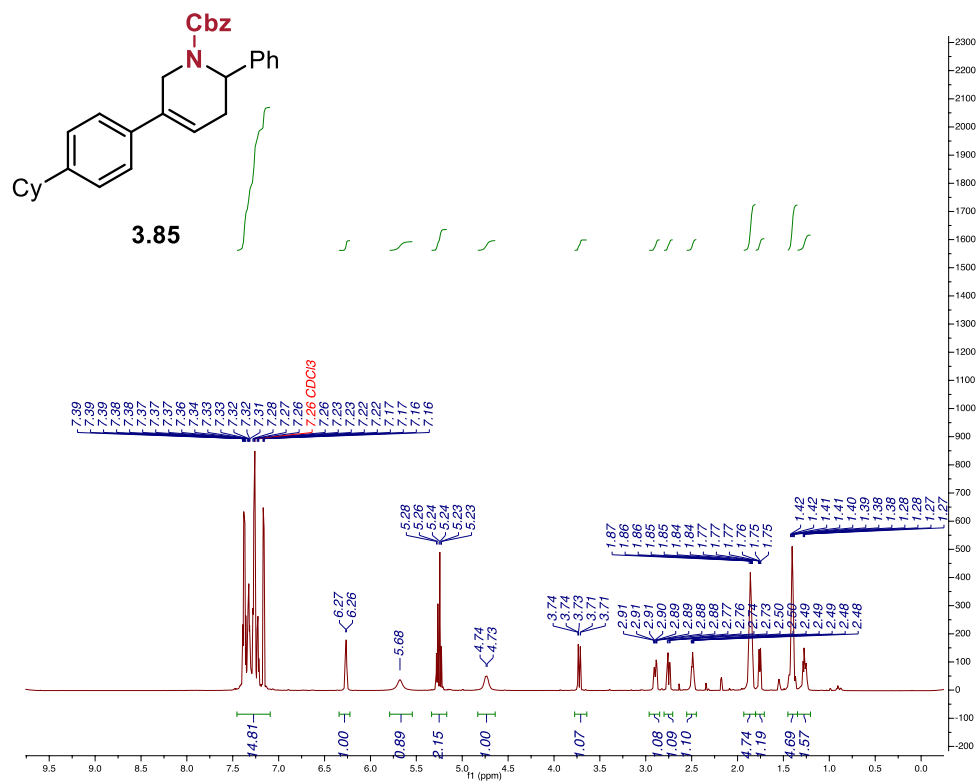
Synthesized using the general procedure, isolated via silica flash chromatography using 2% Acetone in Hexanes as a white solid (41.0 mg, 46% yield).

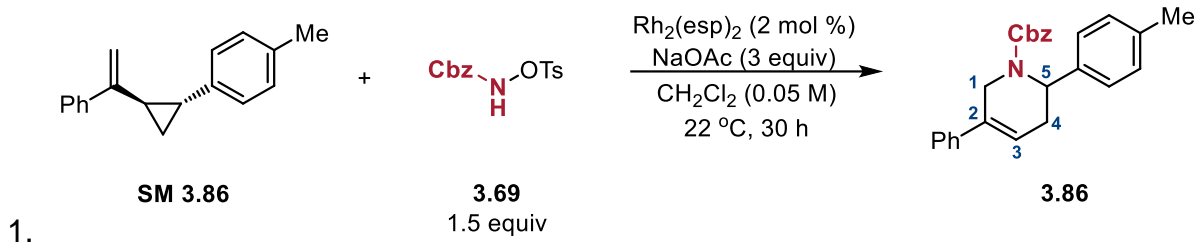
**$^1\text{H}$  NMR** (800 MHz,  $\text{CDCl}_3$ )  $\delta$  7.45 – 7.09 (ArH, m, 15H), 6.27 ( $\text{H}^3$ , d,  $J = 5.9$  Hz, 1H), 5.68 ( $\text{H}^5$ , s, 1H), 5.33 – 5.17 (Cbz- $\text{CH}_2$ , m, 2H), 4.83 – 4.64 ( $\text{H}^1$ , m, 1H), 3.77 – 3.64 ( $\text{H}^1$ , m, 1H), 2.90 ( $\text{H}^4$ , ddd,  $J = 18.1, 7.0, 3.4$  Hz, 1H), 2.75 ( $\text{H}^4$ , dd,  $J = 18.1, 6.2$  Hz, 1H), 2.49 (CyH, ddd,  $J = 11.3, 7.8, 3.5$  Hz, 1H), 1.93 – 1.80 (CyH, m, 5H), 1.80 – 1.71 (CyH m, 1H), 1.41 (CyH, qd,  $J = 12.3, 10.9, 7.3$  Hz, 5H), 1.35 – 1.20 (CyH, m, 2H) ppm.

**$^{13}\text{C}$  NMR** (201 MHz,  $\text{CDCl}_3$ )  $\delta$  155.9, 147.7, 140.7, 137.0, 136.5, 134.4, 128.7, 128.7, 128.6, 128.6, 128.6, 128.6, 128.5, 128.2, 128.1, 128.1, 128.1, 128.0, 127.4, 127.3, 127.1, 127.1, 127.1, 127.0, 127.0, 127.0, 125.1, 125.1, 125.0, 125.0, 120.0, 67.5, 51.2, 44.4, 42.1, 34.6, 34.5, 28.5, 27.1, 27.0, 26.4, 26.3 ppm. (mixture of rotamers)

**IR** (film):  $\bar{\nu} = 3030$  (w), 2922 (w), 2850 (w), 2364 (w), 1697 (s), 1413 (m), 1242 (m), 908 (m), 693 (s)  $\text{cm}^{-1}$ .

**HRMS** (ESI):  $m/z$  calculated for  $[\text{C}_{31}\text{H}_{33}\text{NO}_2 + \text{H}]^+$ : 452.2590; found: 452.2581.





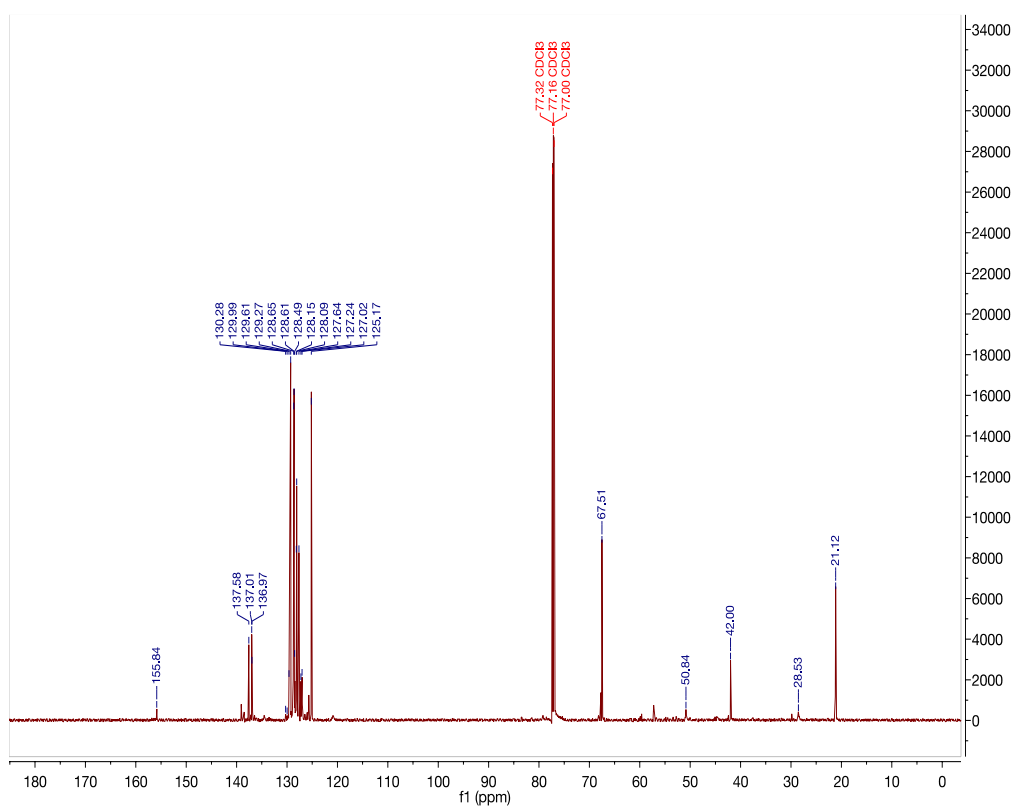
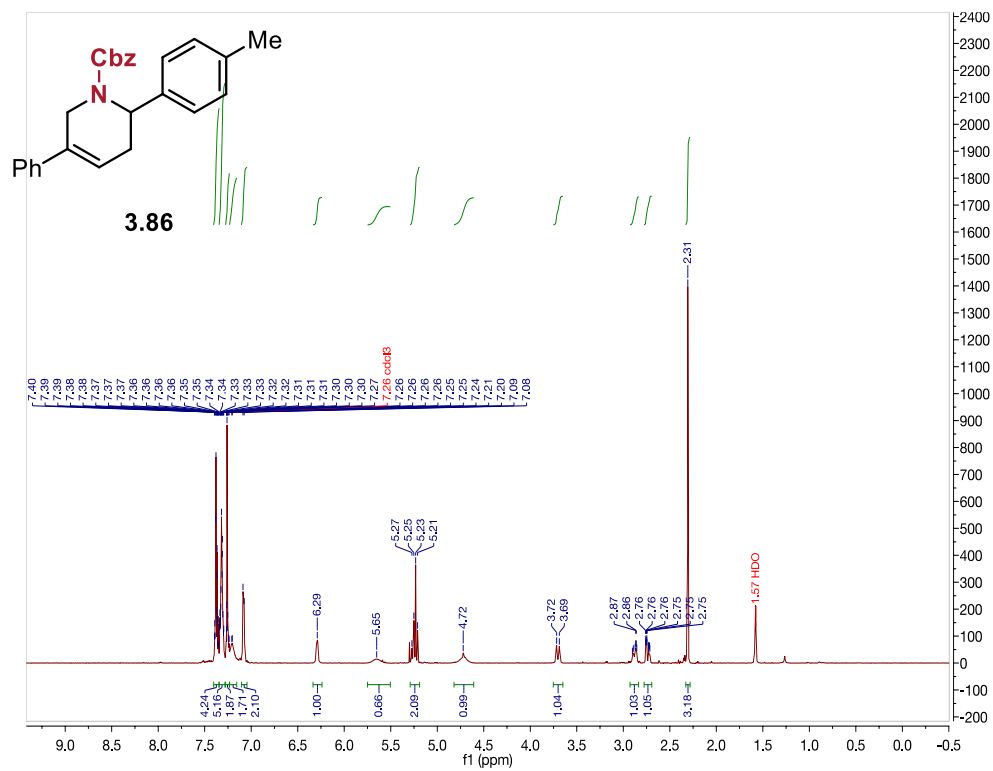
Synthesized using the general procedure, isolated via silica flash chromatography using 2% Acetone in Hexanes as a white solid (29.1 mg, 38% yield).

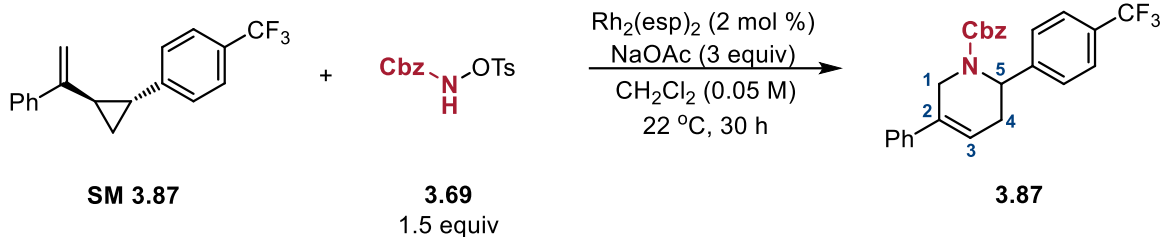
**$^1\text{H}$  NMR** (600 MHz,  $\text{CDCl}_3$ )  $\delta$  7.40 – 7.35 (ArH, m, 4H), 7.35 – 7.28 (ArH, m, 5H), 7.27 – 7.24 (ArH, m, 2H), 7.23 – 7.16 (ArH, m, 2H), 7.08 (ArH, d,  $J = 7.8$  Hz, 2H), 6.29 ( $\text{H}^3$ , s, 1H), 5.62 ( $\text{H}^5$ , d,  $J = 36.8$  Hz, 1H), 5.24 (Cbz- $\text{CH}_2$ , q,  $J = 12.4$  Hz, 2H), 4.82 – 4.61 ( $\text{H}^1$ , m, 1H), 3.70 ( $\text{H}^1$ , d,  $J = 16.9$  Hz, 1H), 2.93 – 2.84 ( $\text{H}^1$ , m, 1H), 2.78 – 2.69 ( $\text{H}^1$ , m, 1H), 2.31 (Me, s, 3H) ppm.

**$^{13}\text{C}$  NMR** (201 MHz,  $\text{CDCl}_3$ )  $\delta$  155.8, 137.6, 137.0, 137.0, 129.6, 129.3, 128.7, 128.6, 128.5, 128.2, 128.1, 127.6, 127.2, 127.0, 125.2, 67.5, 50.8, 42.0, 28.5, 21.1 ppm.

**IR** (film):  $\bar{\nu} = 3030$  (w), 2920 (w), 2850 (w), 1693 (s), 1514 (w), 1415 (m), 1325 (m), 1240 (s), 1103 (m), 979 (m), 908 (w), 750 (s), 696 (s)  $\text{cm}^{-1}$ .

**HRMS** (ESI):  $m/z$  calculated for  $[\text{C}_{26}\text{H}_{25}\text{NO}_2 + \text{H}]^+$ : 383.1964; found: 383.1958.





Synthesized using the general procedure, isolated via silica flash chromatography using 2% Acetone in Hexanes as a white solid (22.7 mg, 26% yield).

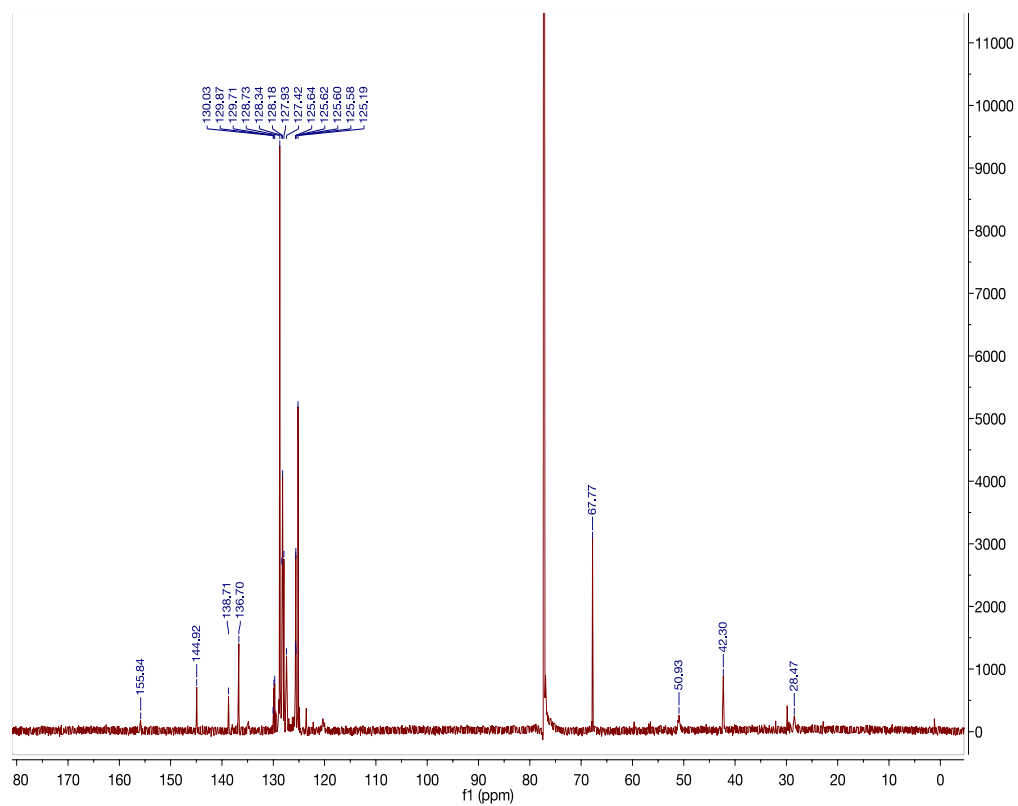
**$^1\text{H}$  NMR** (598 MHz,  $\text{CDCl}_3$ )  $\delta$  7.53 (ArH, d,  $J$  = 8.0 Hz, 2H), 7.49 – 7.24 (ArH, m, 12H), 6.32 – 6.23 ( $\text{H}^3$ , m, 1H), 5.72 ( $\text{H}^5$ , s, 1H), 5.30 – 5.17 (Cbz– $\text{CH}_2$ , m, 2H), 4.74 ( $\text{H}^1$ , s, 1H), 3.74 ( $\text{H}^1$ , ddt,  $J$  = 17.8, 4.0, 2.0 Hz, 1H), 2.93 ( $\text{H}^4$ , ddq,  $J$  = 16.5, 6.4, 3.1 Hz, 1H), 2.75 ( $\text{H}^4$ , dd,  $J$  = 18.1, 6.2 Hz, 1H) ppm.

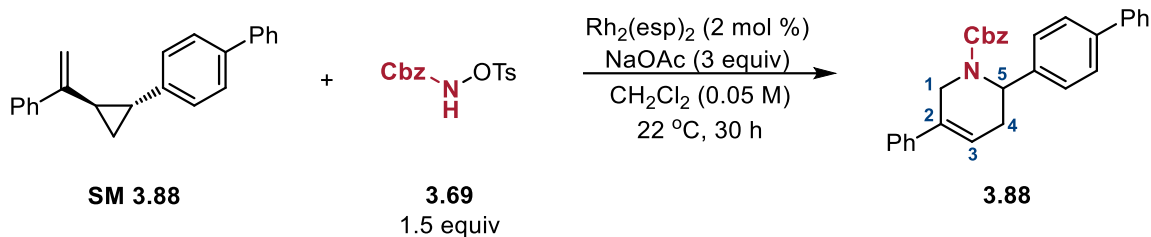
**$^{13}\text{C}$  NMR** (201 MHz,  $\text{CDCl}_3$ )  $\delta$  155.9, 144.9, 138.7, 136.7, 130.0, 129.9, 129.7, 128.7, 128.3, 128.2, 127.9, 127.4, 125.6 (q,  $J$  = 4.0 Hz), 125.2, 67.8, 42.3, 29.9 ppm.

**$^{19}\text{F}$  NMR** (563 MHz,  $\text{CDCl}_3$ )  $\delta$  -62.60 ppm.

**IR** (film):  $\bar{\nu}$  = 3055 (w), 2899 (w), 1695 (br, m), 1496 (w), 1419 (m), 1327 (s), 1265 (s), 1168 (m), 1126 (br, m), 1068 (m), 1018 (w), 910 (s), 740 (s), 700 (m), 650 (w)  $\text{cm}^{-1}$ .

**HRMS** (ESI):  $m/z$  calculated for  $[\text{C}_{26}\text{H}_{22}\text{F}_3\text{NO}_2+\text{H}]^+$ : 438.1675; found: 438.1661.





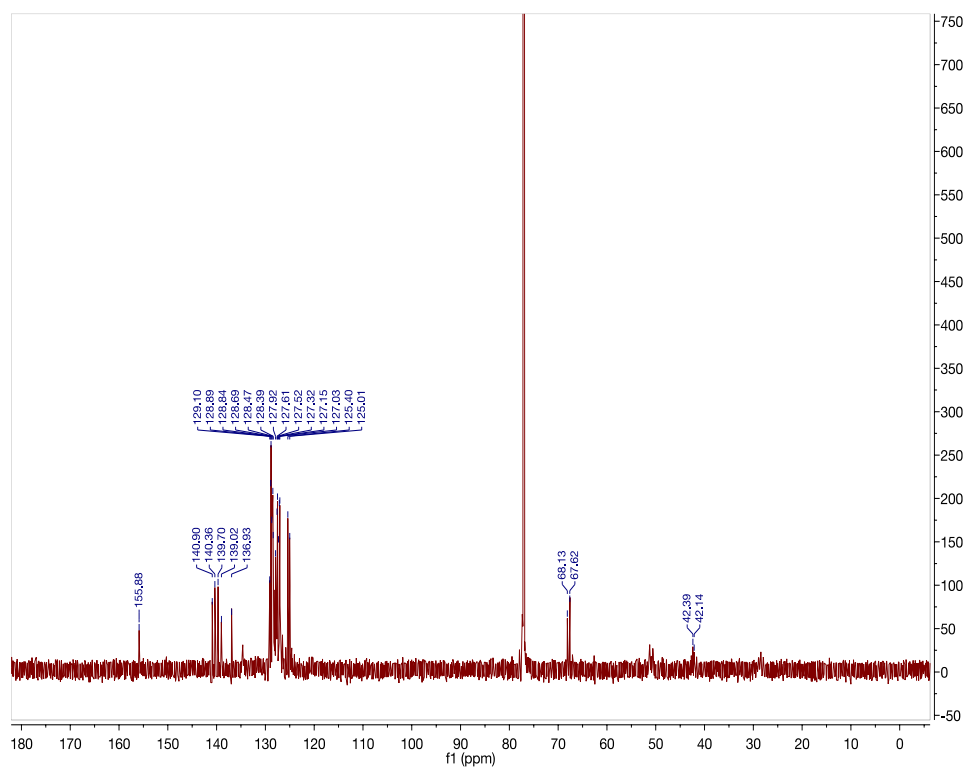
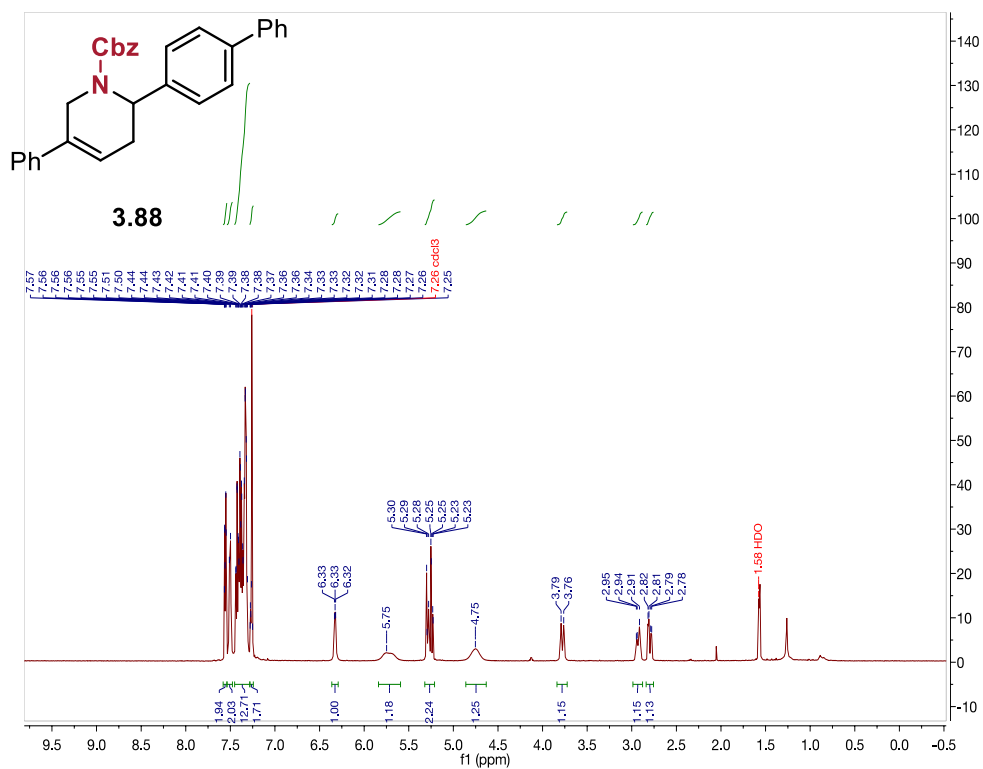
Synthesized using the general procedure, isolated via silica flash chromatography using 2% Acetone in Hexanes as a white solid (37.7 mg, 42% yield).

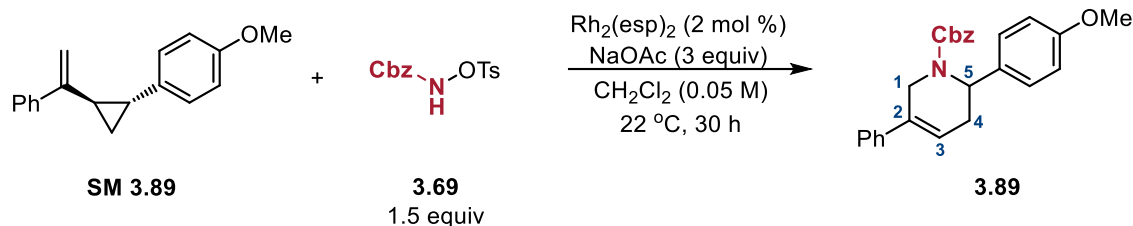
**$^1\text{H}$  NMR** (598 MHz,  $\text{CDCl}_3$ )  $\delta$  7.58 – 7.54 (ArH, m, 2H), 7.50 (ArH, d,  $J$  = 7.8 Hz, 2H), 7.45 – 7.28 (ArH, m, 13H), 7.27 (ArH, dd,  $J$  = 9.6, 5.1 Hz, 2H), 6.33 ( $\text{H}^3$ , t,  $J$  = 4.1 Hz, 1H), 5.75 ( $\text{H}^5$ , s, 1H), 5.32 – 5.21 (Cbz- $\text{CH}_2$ , m, 2H), 4.75 ( $\text{H}^1$ , s, 1H), 3.78 ( $\text{H}^1$ , d,  $J$  = 17.7 Hz, 1H), 2.93 ( $\text{H}^4$ , d,  $J$  = 15.5 Hz, 1H), 2.80 ( $\text{H}^4$ , dd,  $J$  = 18.1, 6.2 Hz, 1H) ppm.

**$^{13}\text{C}$  NMR** (201 MHz,  $\text{CDCl}_3$ )  $\delta$  155.9, 140.9, 140.4, 139.7, 139.0, 136.9, 129.1, 128.9, 128.8, 128.7, 128.5, 128.4, 127.9, 127.6, 127.5, 127.3, 127.2, 127.0, 125.4, 125.0, 68.1, 67.6, 42.4, 42.1 ppm.

**IR** (film):  $\bar{\nu}$  = 3030 (w), 2848 (w), 1691 (s), 1598 (w), 1487 (w), 1417 (br, m), 1325 (m), 1240 (s), 1103 (m), 1076 (m), 906 (s), 846 (m), 727 (s), 696 (s)  $\text{cm}^{-1}$ .

**HRMS** (ESI):  $m/z$  calculated for  $[\text{C}_{31}\text{H}_{27}\text{NO}_2 + \text{H}]^+$ : 446.2120; found: 446.2106.





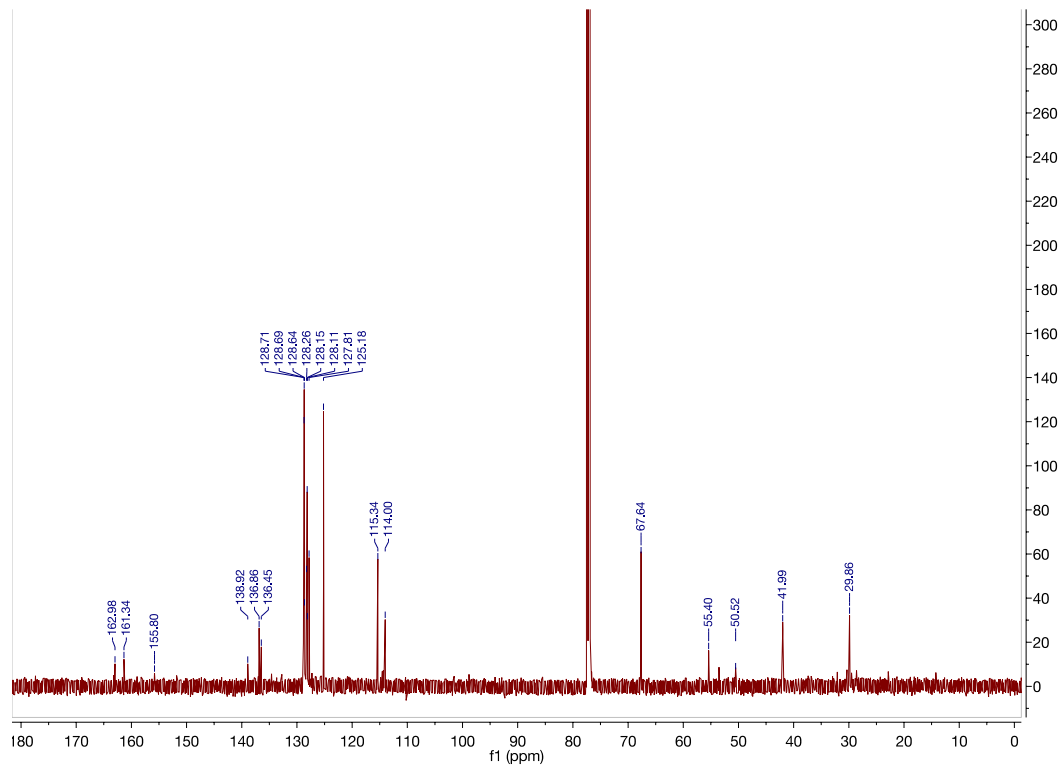
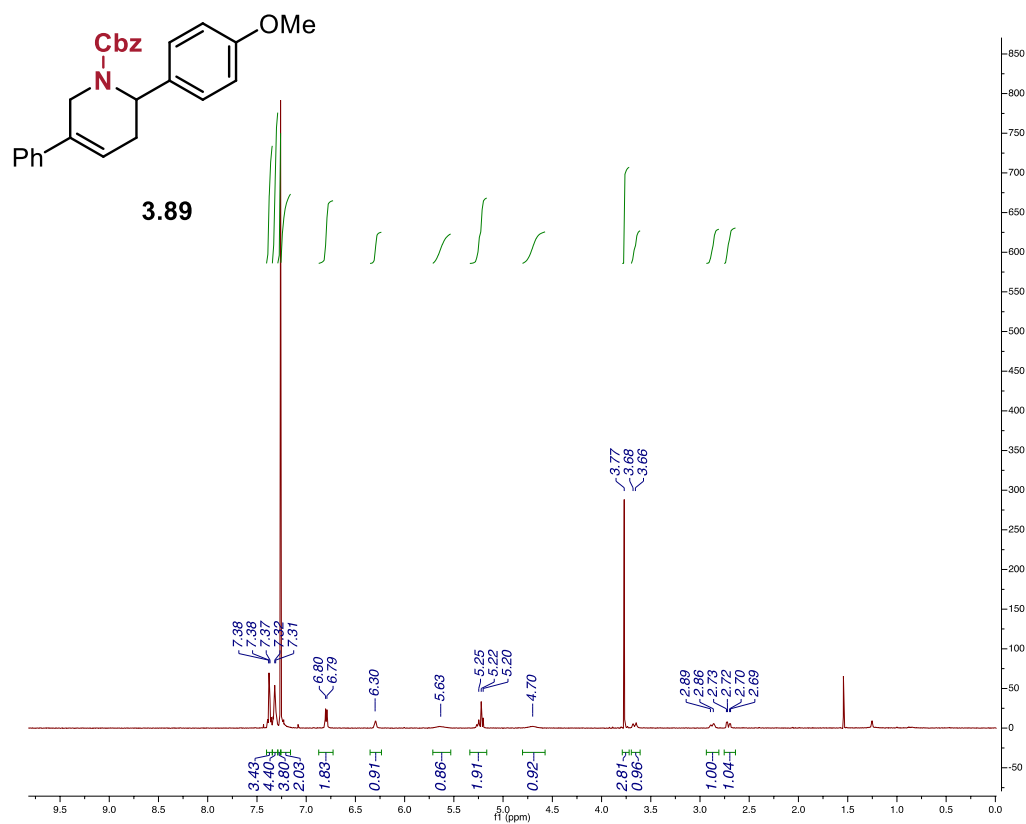
Synthesized using the general procedure, isolated via silica flash chromatography using 5% Acetone in Hexanes as a white solid (30.0 mg, 38% yield).

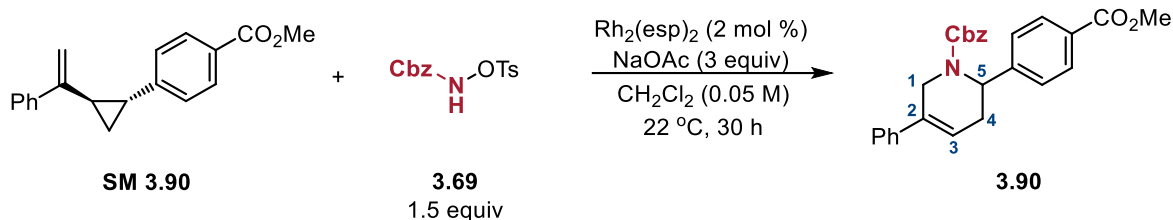
**$^1\text{H}$  NMR** (600 MHz,  $\text{CDCl}_3$ )  $\delta$  7.42 – 7.27 (ArH, m, 12H), 6.83 – 6.76 (ArH, m, 2H), 6.34 – 6.25 ( $\text{H}^3$ , m, 1H), 5.64 ( $\text{H}^5$ , s, 1H), 5.24 (Cbz- $\text{CH}_2$ , q,  $J$  = 12.6 Hz, 2H), 4.71 ( $\text{H}^1$ , s, 1H), 3.77 (OMe, s, 3H), 3.67 ( $\text{H}^1$ , d,  $J$  = 18.3 Hz, 1H), 2.92 – 2.82 ( $\text{H}^4$ , m, 1H), 2.76 – 2.67 ( $\text{H}^4$ , m, 1H) ppm.

**$^{13}\text{C}$  NMR** (151 MHz,  $\text{CDCl}_3$ )  $\delta$  162.9, 161.3, 155.8, 138.9, 136.8, 136.4, 128.7, 128.6, 128.6, 128.2, 128.1, 128.1, 127.8, 125.1, 115.3, 114.0, 67.6, 55.4, 50.5, 41.9, 29.8 ppm.

**IR** (film):  $\bar{\nu}$  = 3061 (w), 3032 (w), 2927 (w), 2837 (w), 1693 (br, s), 1608 (m), 1512 (s), 1415 (m), 1305 (m), 1242 (s), 1178 (m), 1107 (m), 1029 (m), 829 (m), 750 (s), 694 (s)  $\text{cm}^{-1}$ .

**HRMS** (ESI):  $m/z$  calculated for  $[\text{C}_{26}\text{H}_{25}\text{NO}_3 + \text{Na}]^+$ : 422.1732; found: 422.1726.





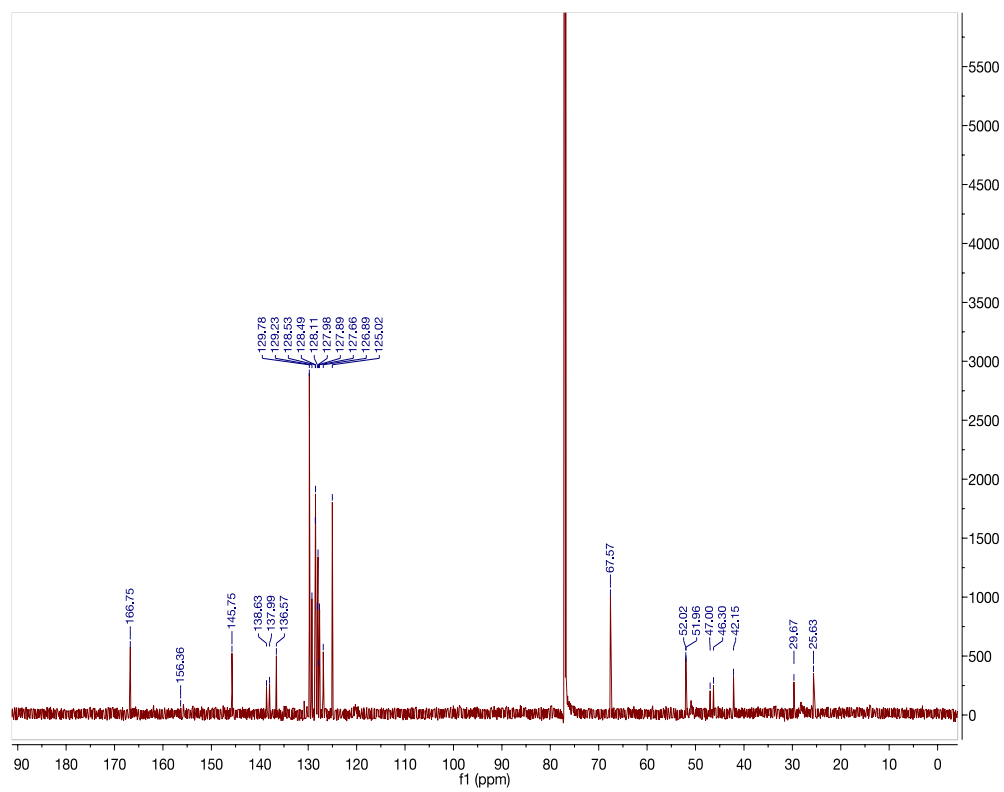
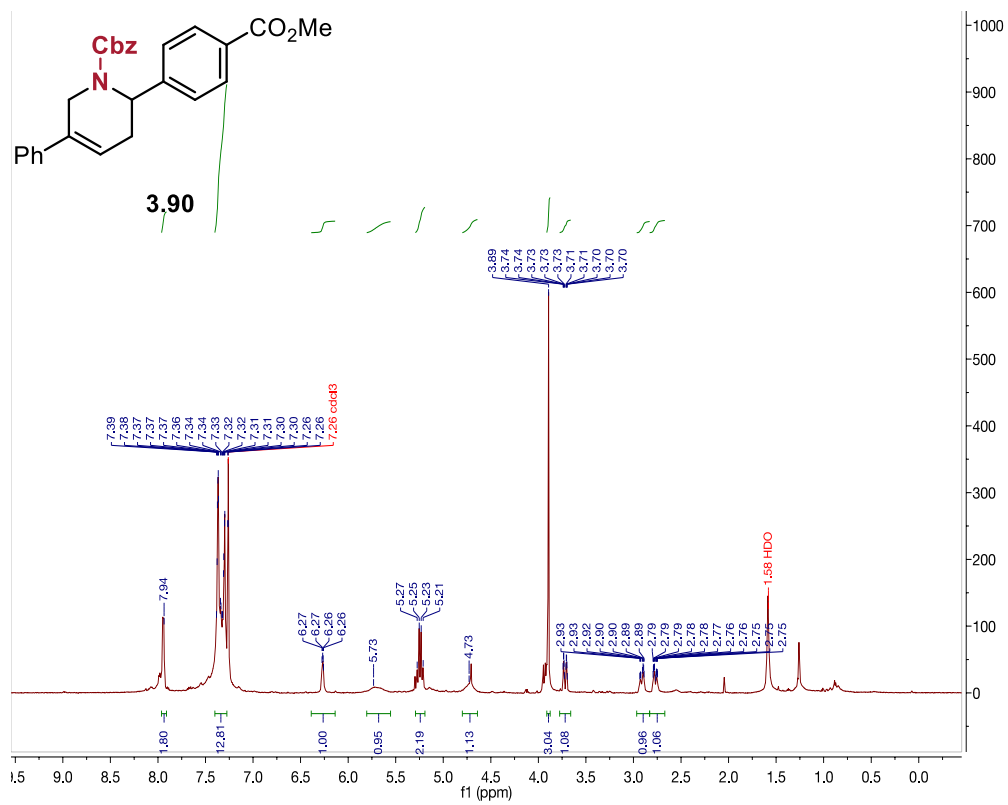
Synthesized using the general procedure, isolated via silica flash chromatography using 5% Acetone in Hexanes as a white solid (18.7 mg, 22% yield).

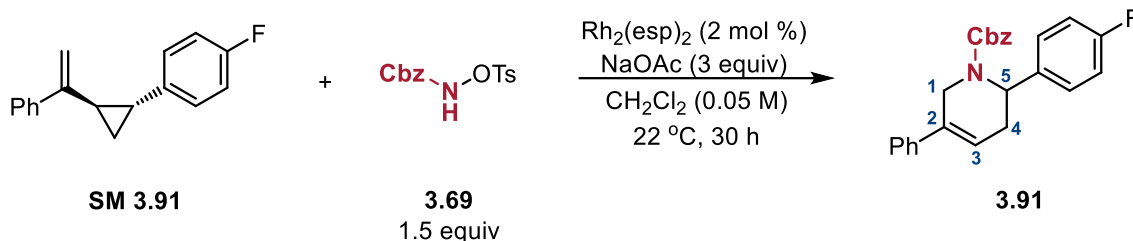
**$^1\text{H}$  NMR** (600 MHz,  $\text{CDCl}_3$ )  $\delta$  7.96 – 7.91 (ArH, m, 2H), 7.40 – 7.28 (ArH, m, 12H), 6.39 – 6.14 ( $\text{H}^3$ , m, 1H), 5.73 ( $\text{H}^5$ , s, 1H), 5.24 (Cbz- $\text{CH}_2$ , q,  $J = 12.5$  Hz, 2H), 4.73 ( $\text{H}^1$ , s, 1H), 3.89 ( $\text{CO}_2\text{Me}$ , s, 3H), 3.72 ( $\text{H}^1$ , ddt,  $J = 17.7, 4.0, 2.2$  Hz, 1H), 2.97 – 2.83 ( $\text{H}^4$ , m, 1H), 2.83 – 2.67 ( $\text{H}^4$ , m, 1H) ppm.

**$^{13}\text{C}$  NMR** (201 MHz,  $\text{CDCl}_3$ )  $\delta$  166.8, 156.4, 145.8, 138.6, 138.0, 136.6, 129.8, 129.2, 128.5, 128.5, 128.1, 128.0, 127.9, 127.7, 126.9, 125.0, 67.6, 52.0, 52.0, 47.0, 46.3, 42.2, 29.7, 25.6 ppm.

**IR** (film):  $\bar{\nu} = 3032$  (w), 2958 (w), 1689 (s), 1656 (w), 1494 (w), 1454 (m), 1409 (s), 1325 (s), 1294 (s), 1232 (s), 1180 (w), 1074 (m), 956 (m), 827 (m), 756 (m), 694 (s)  $\text{cm}^{-1}$ .

**LRMS** (ESI):  $m/z$  calculated for  $[\text{C}_{27}\text{H}_{25}\text{NO}_4 + \text{H}]^+$ : 428.2; found: 428.0.





Synthesized using the general procedure, isolated via silica flash chromatography using 2% Acetone in Hexanes as a white solid (35.6 mg, 46% yield).

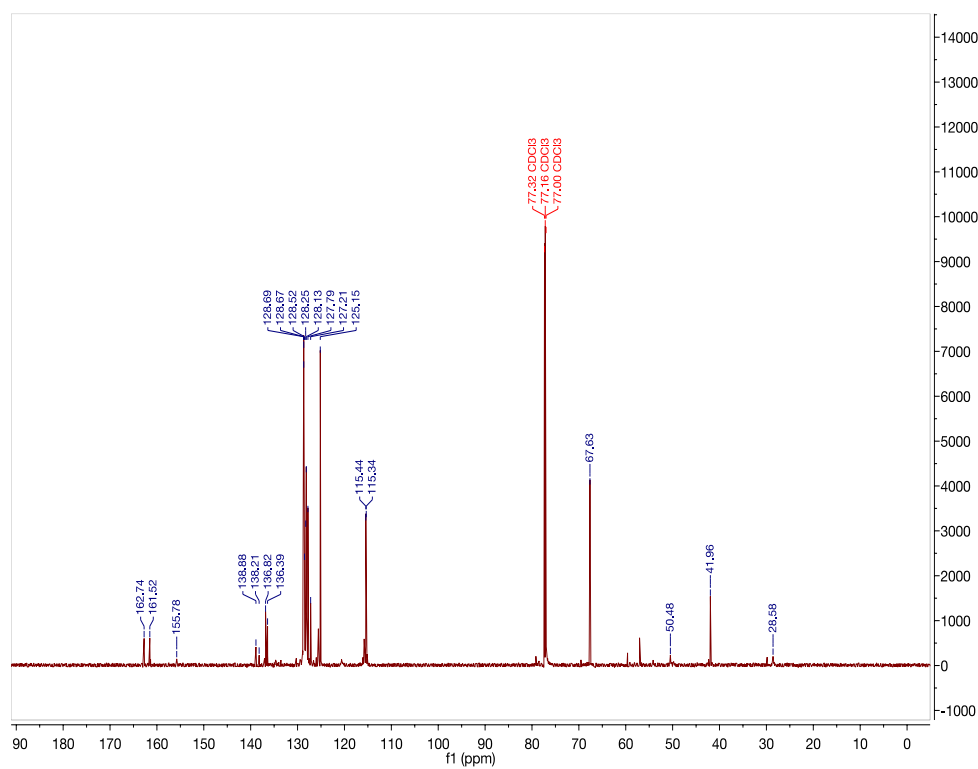
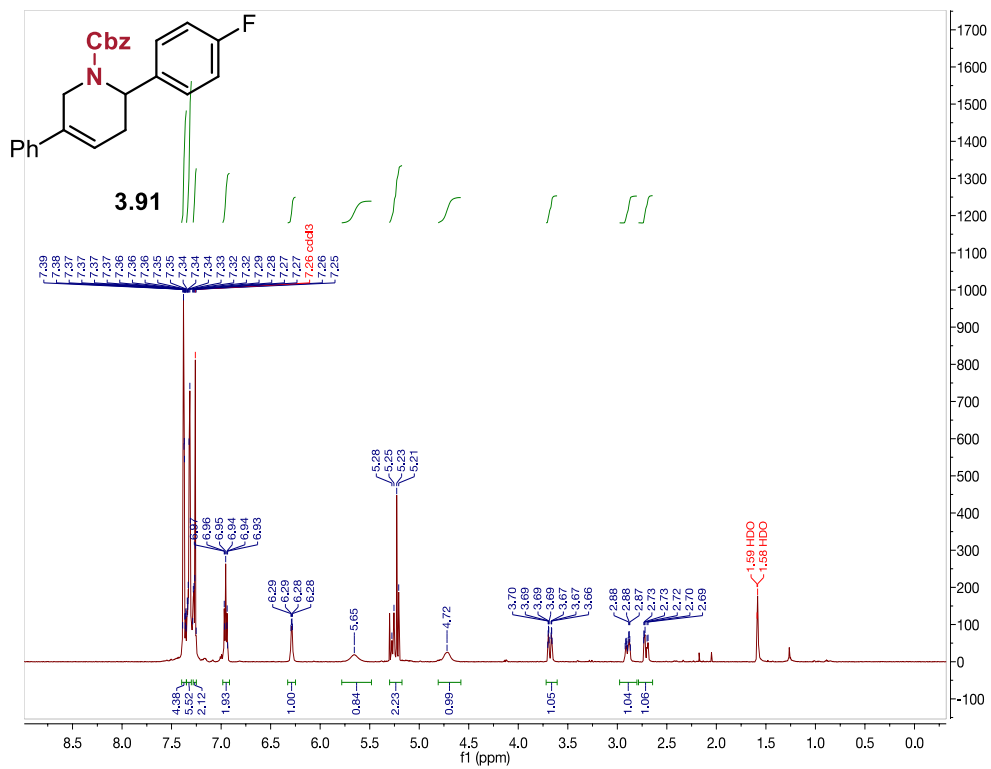
**$^1\text{H}$  NMR** (600 MHz,  $\text{CDCl}_3$ )  $\delta$  7.40 – 7.35 (ArH, m, 4H), 7.35 – 7.30 (ArH, m, 6H), 7.27 (ArH, dt,  $J$  = 8.5, 4.5 Hz, 2H), 6.95 (ArH, t,  $J$  = 8.7 Hz, 2H), 6.29 ( $\text{H}^3$ , dd,  $J$  = 6.2, 2.6 Hz, 1H), 5.65 ( $\text{H}^5$ , s, 1H), 5.30 – 5.17 (Cbz- $\text{CH}_2$ , m, 2H), 4.72 ( $\text{H}^1$ , s, 1H), 3.68 ( $\text{H}^1$ , ddd,  $J$  = 17.8, 4.2, 2.2 Hz, 1H), 2.89 ( $\text{H}^4$ , ddt,  $J$  = 16.8, 6.5, 3.2 Hz, 1H), 2.79 – 2.64 ( $\text{H}^4$ , m, 1H) ppm.

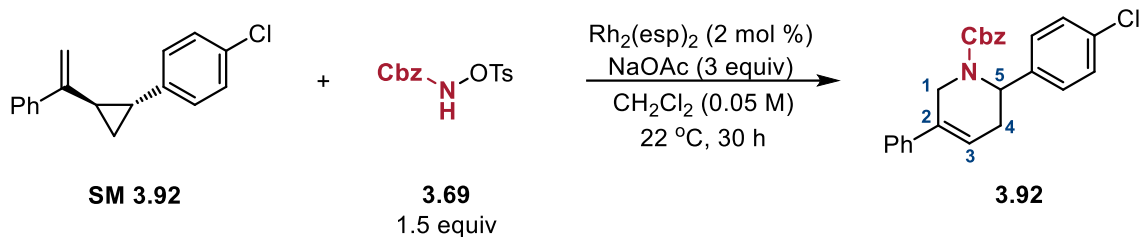
**$^{13}\text{C}$  NMR** (201 MHz,  $\text{CDCl}_3$ )  $\delta$  162.6 (d,  $J$  = 44.2 Hz), 138.9, 138.2, 136.8, 136.4, 128.7 (d,  $J$  = 1.0 Hz), 128.5, 128.3, 128.1, 127.8, 127.2, 125.2, 115.4, 115.3, 67.6, 50.5, 42.0, 28.6 ppm.

**$^{19}\text{F}$  NMR** (563 MHz,  $\text{CDCl}_3$ )  $\delta$  -115.35 ppm.

**IR** (film):  $\bar{\nu}$  = 3062 (w), 3034 (w), 2954 (w), 1693 (br, s), 1602 (m), 1508 (s), 1415 (m), 1321 (m), 1222 (s), 1159 (m), 908 (m), 835 (m), 750 (s), 732 (s), 694 (s)  $\text{cm}^{-1}$ .

**HRMS** (ESI):  $m/z$  calculated for  $[\text{C}_{25}\text{H}_{22}\text{FNO}_2 + \text{H}]^+$ : 388.1713; found: 388.1701.





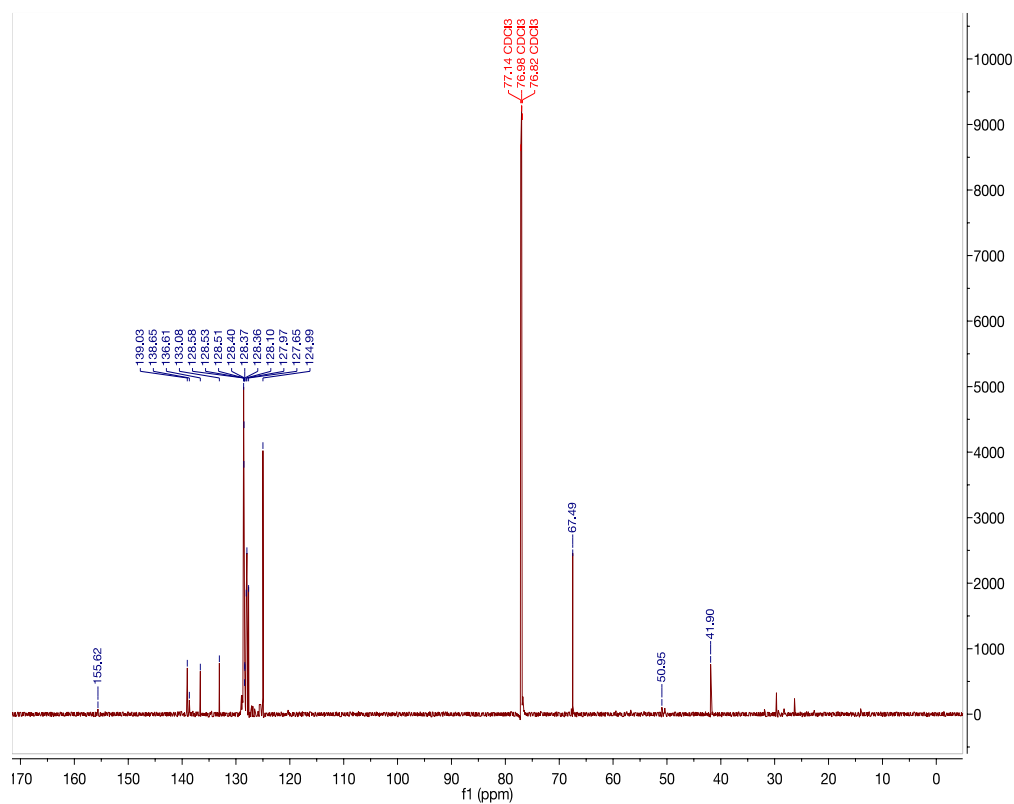
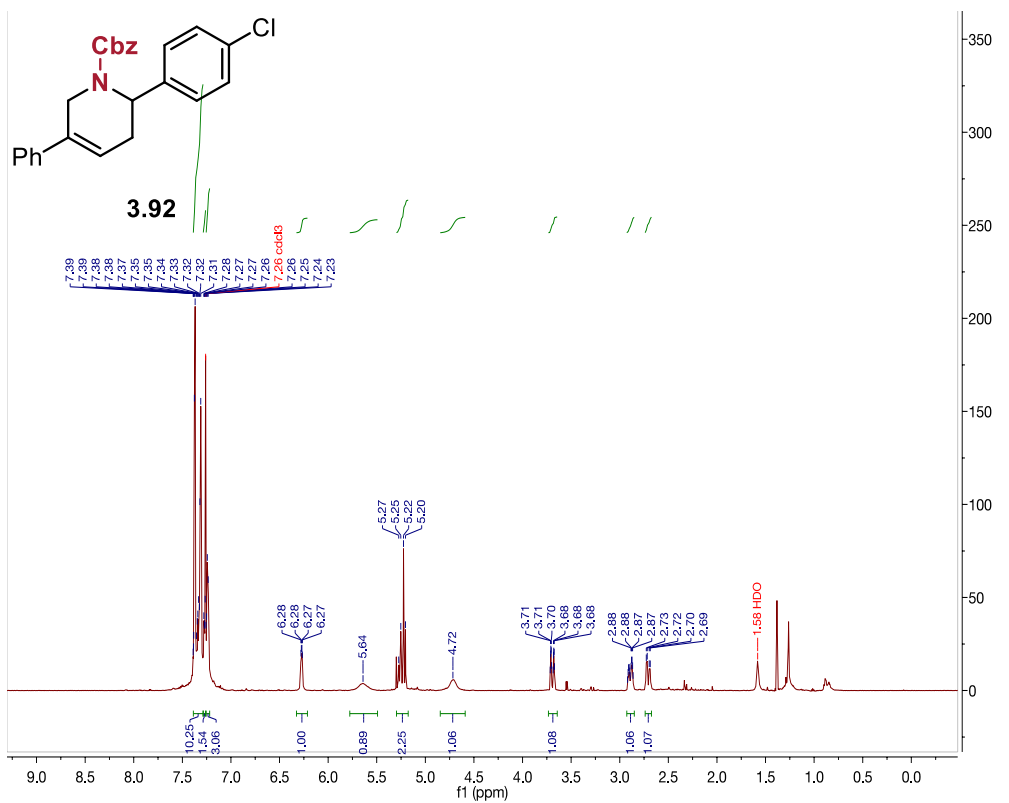
Synthesized using the general procedure, isolated via silica flash chromatography using 2% Acetone in Hexanes as a white solid (32.7 mg, 40% yield).

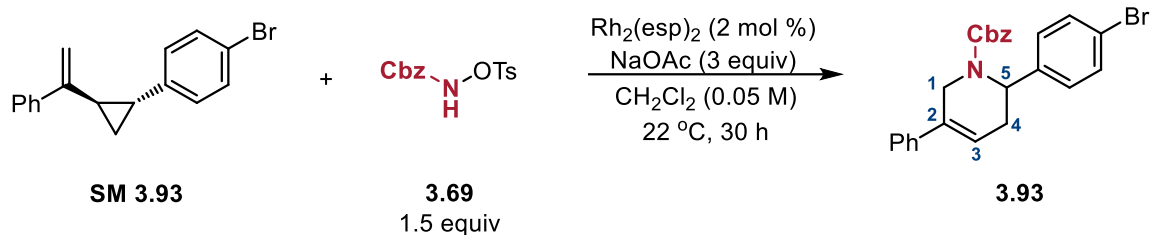
**$^1\text{H}$  NMR** (598 MHz,  $\text{CDCl}_3$ )  $\delta$  7.39 – 7.29 (ArH, m, 10H), 7.28 – 7.26 (ArH, m, 1H), 7.24 (ArH, d,  $J$  = 5.5 Hz, 3H), 6.33 – 6.21 ( $\text{H}^3$ , m, 1H), 5.64 ( $\text{H}^5$ , s, 1H), 5.30 – 5.18 (Cbz- $\text{CH}_2$ , m, 2H), 4.85 – 4.59 ( $\text{H}^1$ , m, 1H), 3.69 ( $\text{H}^1$ , ddt,  $J$  = 17.7, 4.2, 2.2 Hz, 1H), 2.89 ( $\text{H}^4$ , ddq,  $J$  = 18.0, 6.4, 3.1 Hz, 1H), 2.71 ( $\text{H}^4$ , dd,  $J$  = 18.0, 6.3 Hz, 1H) ppm.

**$^{13}\text{C}$  NMR** (201 MHz,  $\text{CDCl}_3$ )  $\delta$  155.6, 139.0, 138.7, 136.6, 133.1, 128.6, 128.5, 128.5, 128.4, 128.4, 128.4, 128.1, 128.0, 127.7, 125.0, 67.5, 51.0, 41.9 ppm.

**IR** (film):  $\bar{\nu}$  = 3061 (w), 3032 (w), 2964 (w), 2850 (w), 1693 (s), 1490 (m), 1413 (br, m), 1323 (m), 1240 (s), 1091 (s), 908 (m), 842 (m), 750 (s), 731 (s), 694 (br, s)  $\text{cm}^{-1}$ .

**HRMS** (ESI):  $m/z$  calculated for  $[\text{C}_{25}\text{H}_{22}\text{ClNO}_2 + \text{H}]^+$ : 404.1417; found: 404.1405.





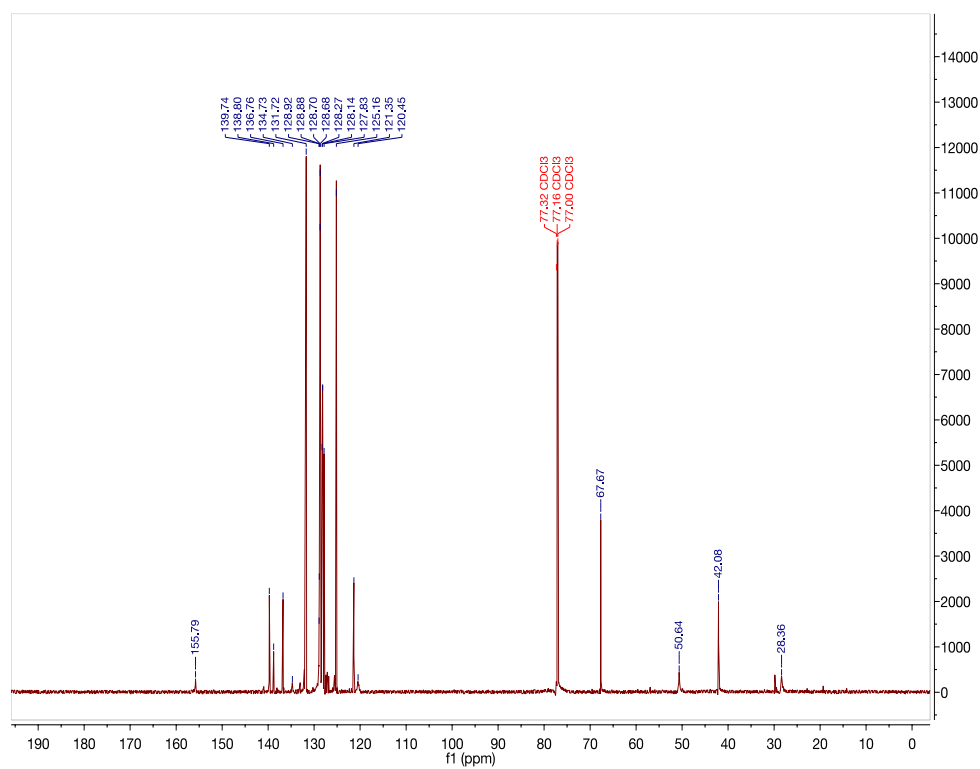
Synthesized using the general procedure, isolated via silica flash chromatography using 2% Acetone in Hexanes as a white solid (40.1 mg, 43% yield).

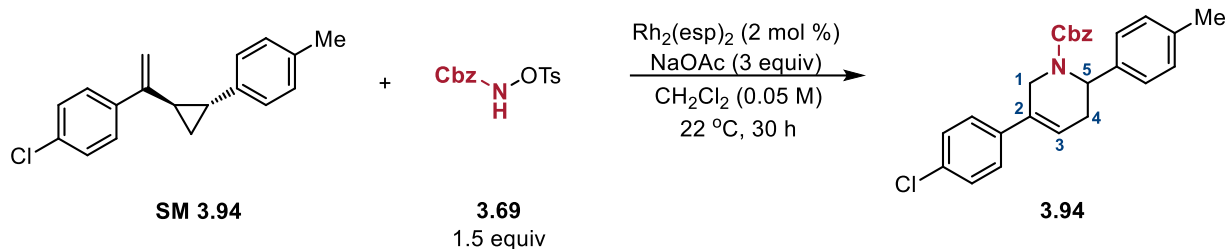
**$^1\text{H}$  NMR** (600 MHz,  $\text{CDCl}_3$ )  $\delta$  7.40 – 7.33 (ArH, m, 6H), 7.33 – 7.27 (ArH, m, 5H), 7.24 (ArH, q,  $J = 2.6$  Hz, 1H), 7.16 (ArH, s, 2H), 6.29 – 6.20 ( $\text{H}^3$ , m, 1H), 5.61 ( $\text{H}^5$ , s, 1H), 5.27 – 5.15 (Cbz- $\text{CH}_2$ , m, 2H), 4.69 ( $\text{H}^1$ , s, 1H), 3.68 ( $\text{H}^1$ , ddt,  $J = 17.7, 4.1, 2.2$  Hz, 1H), 2.87 ( $\text{H}^4$ , ddq,  $J = 16.7, 6.5, 3.1$  Hz, 1H), 2.68 ( $\text{H}^4$ , dd,  $J = 18.1, 6.2$  Hz, 1H) ppm.

**$^{13}\text{C}$  NMR** (201 MHz,  $\text{CDCl}_3$ )  $\delta$  155.8, 139.7, 138.8, 136.8, 134.7, 131.7, 128.9, 128.9, 128.7, 128.7, 128.3, 128.1, 127.8, 125.2, 121.4, 120.5, 67.7, 50.6, 42.1, 28.4 ppm.

**IR** (film):  $\bar{\nu} = 3053$  (w), 2958 (w), 2843 (w), 1689 (s), 1647 (w), 1419 (m), 1315 (m), 1253 (m), 1109 (s), 1072 (s), 962 (m), 841 (s), 767 (s), 748 (s), 702 (m), 686 (m)  $\text{cm}^{-1}$ .

**HRMS** (ESI):  $m/z$  calculated for  $[\text{C}_{25}\text{H}_{22}\text{BrNO}_2 + \text{H}]^+$ : 448.0912; found: 448.0902.





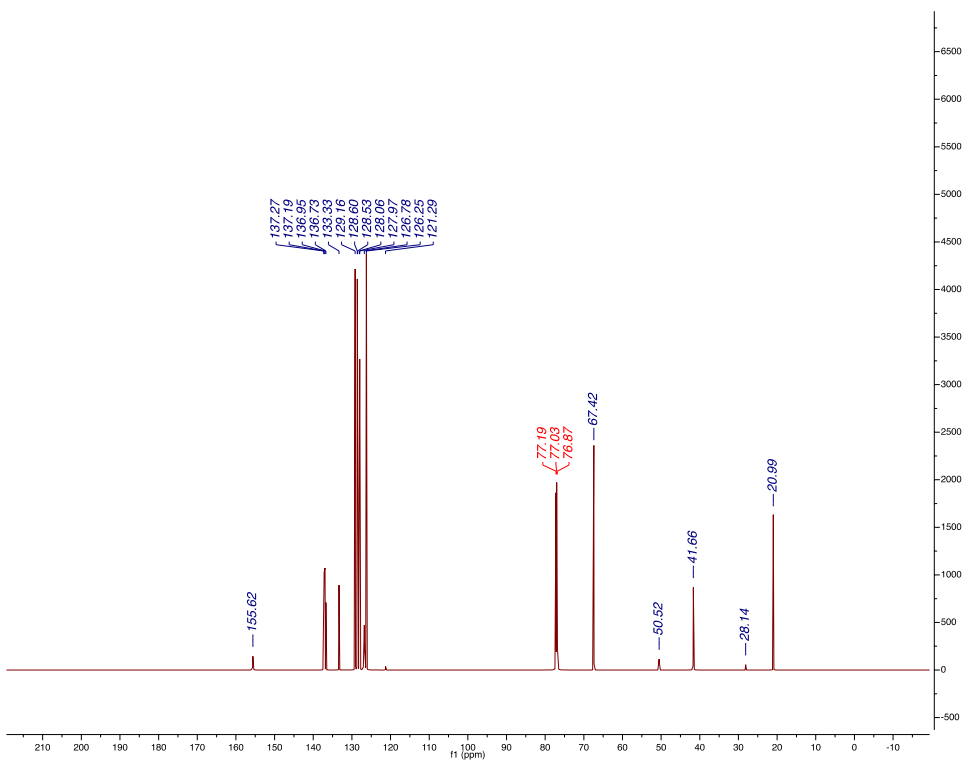
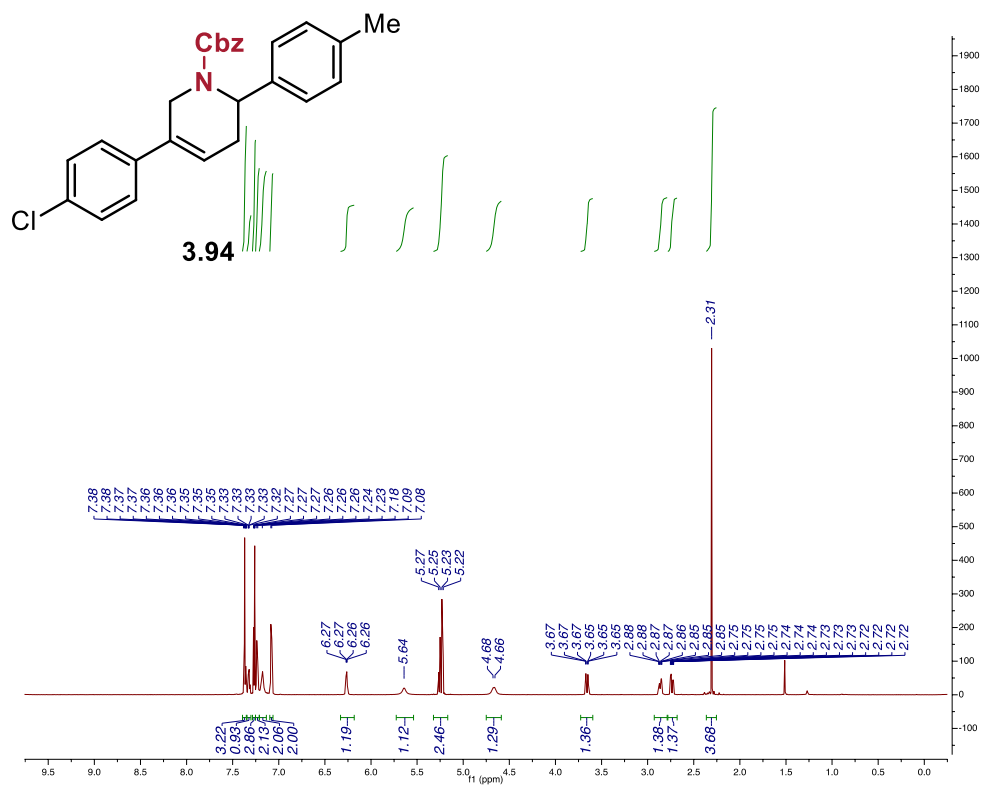
Synthesized using the general procedure, isolated via silica flash chromatography using 2% Acetone in Hexanes as a white solid (43.0 mg, 51% yield).

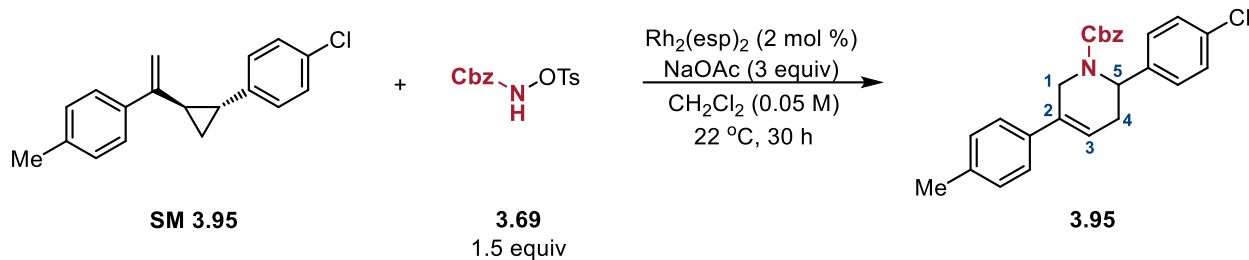
**$^1\text{H}$  NMR** (800 MHz,  $\text{CDCl}_3$ )  $\delta$  7.49 – 6.99 (ArH, m, 13H), 6.36 – 6.17 ( $\text{H}^3$ , m, 1H), 5.64 ( $\text{H}^5$ , s, 1H), 5.26 (Cbz– $\text{CH}_2$ , d,  $J = 12.6$  Hz, 1H), 5.22 (Cbz– $\text{CH}_2$ , d,  $J = 12.3$  Hz, 1H), 4.67 ( $\text{H}^1$ , s, 1H), 3.65 ( $\text{H}^1$ , d,  $J = 17.6$  Hz, 1H), 2.90 – 2.82 ( $\text{H}^4$ , m, 1H), 2.78 – 2.70 ( $\text{H}^4$ , m, 1H), 2.31 (Me, s, 3H) ppm.

**$^{13}\text{C}$  NMR** (201 MHz,  $\text{CDCl}_3$ )  $\delta$  155.6, 137.3, 137.2, 137.0, 136.7, 133.3, 129.2, 129.2, 128.6, 128.5, 128.1, 128.0, 126.8, 126.3, 121.4, 67.4, 50.6, 41.7, 21.0 ppm.

**IR** (film):  $\bar{\nu} = 3030$  (w), 2958 (w), 2841 (w), 1688 (bs), 1410 (s), 1232 (s), 694 (s)  $\text{cm}^{-1}$ .

**HRMS** (ESI):  $m/z$  calculated for  $[\text{C}_{26}\text{H}_{24}\text{ClNO}_2 + \text{H}]^+$ : 418.1574; found: 418.1558.





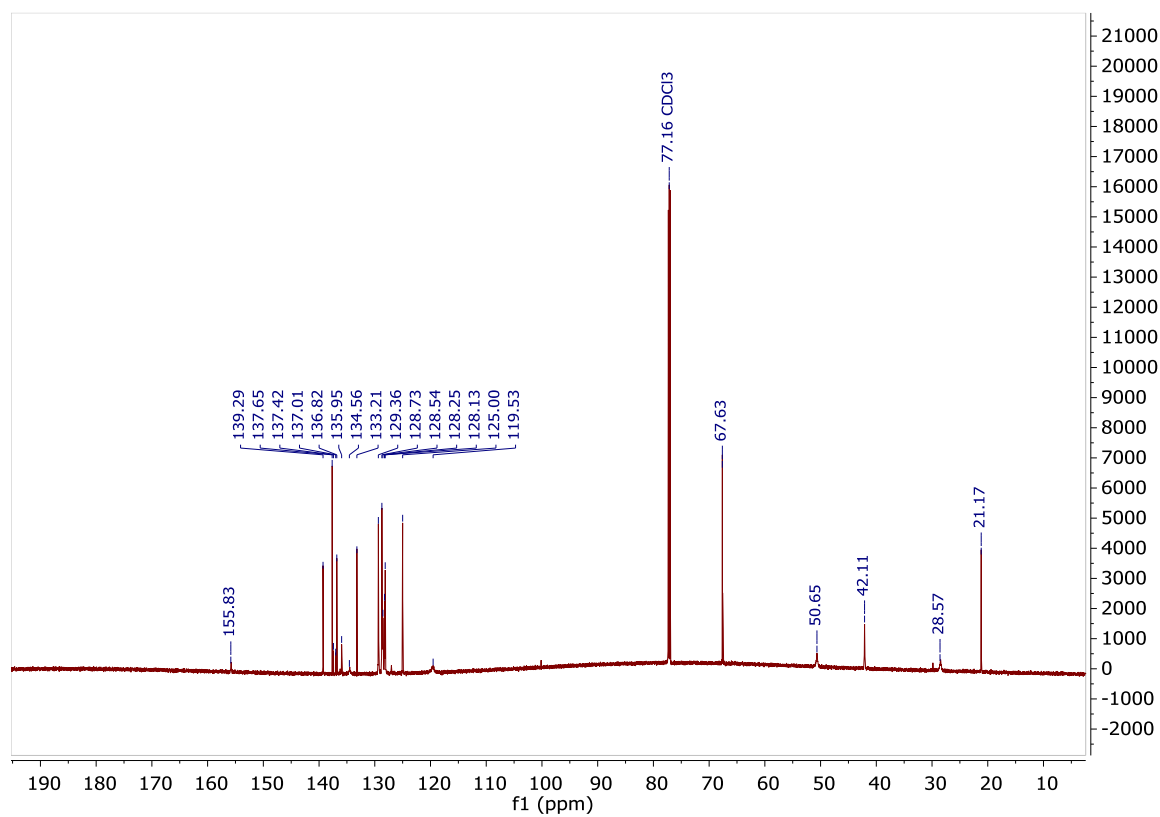
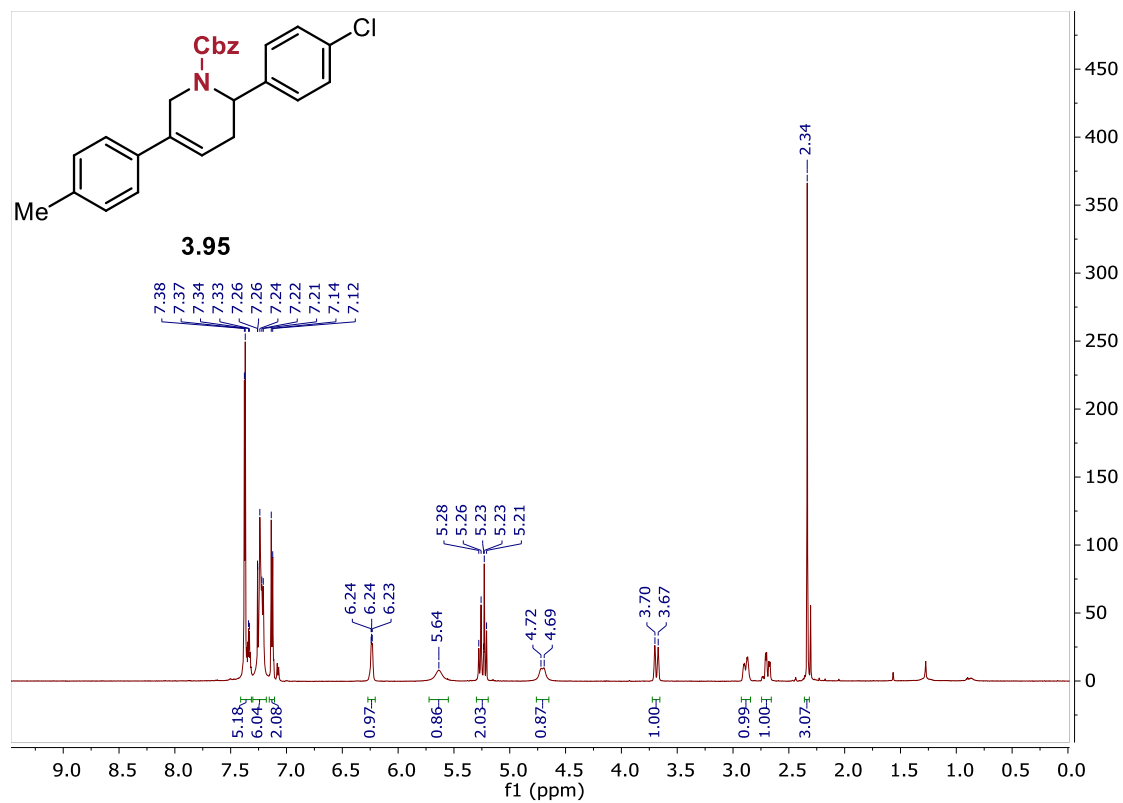
Synthesized using the general procedure, isolated via silica flash chromatography using 2% Acetone in Hexanes as a white solid (33.1 mg, 40% yield).

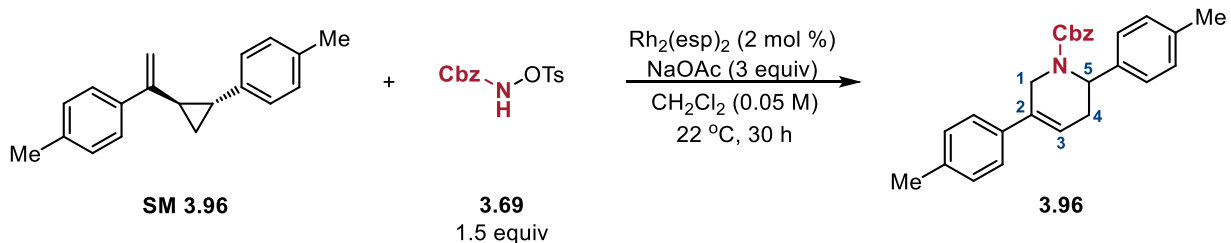
**$^1\text{H}$  NMR** (800 MHz,  $\text{CDCl}_3$ )  $\delta$  7.49 – 7.31 (ArH, m, 5H), 7.31 – 7.16 (ArH, m, 6H), 7.13 (ArH, d,  $J$  = 8.0 Hz, 2H), 6.24 ( $\text{H}^3$ , s, 1H), 5.64 ( $\text{H}^5$ , s, 1H), 5.26 (Cbz– $\text{CH}_2$ , s, 1H), 5.23 (Cbz– $\text{CH}_2$ , d,  $J$  = 12.3 Hz, 1H), 4.71 ( $\text{H}^1$ , s, 1H), 3.74 – 3.65 ( $\text{H}^1$ , m, 1H), 2.97 – 2.84 ( $\text{H}^4$ , m, 1H), 2.76 – 2.66 ( $\text{H}^4$ , m, 1H), 2.34 (Me, s, 3H) ppm.

**$^{13}\text{C}$  NMR** (201 MHz,  $\text{CDCl}_3$ )  $\delta$  155.6, 139.1, 137.5, 136.7, 135.8, 133.1, 129.2, 128.6, 128.5, 128.4, 128.1, 128.0, 124.8, 119.3, 77.2, 77.0, 76.9, 67.5, 50.5, 42.0, 29.3, 21.0 ppm.

**IR** (film):  $\bar{\nu}$  = 2949 (w), 2845 (w), 1686 (bs), 1647 (m), 1246 (s), 1105 (s), 745 (s)  $\text{cm}^{-1}$ .

**HRMS** (ESI):  $m/z$  calculated for  $[\text{C}_{26}\text{H}_{24}\text{ClNO}_2+\text{H}]^+$ : 418.1574; found: 418.1585.





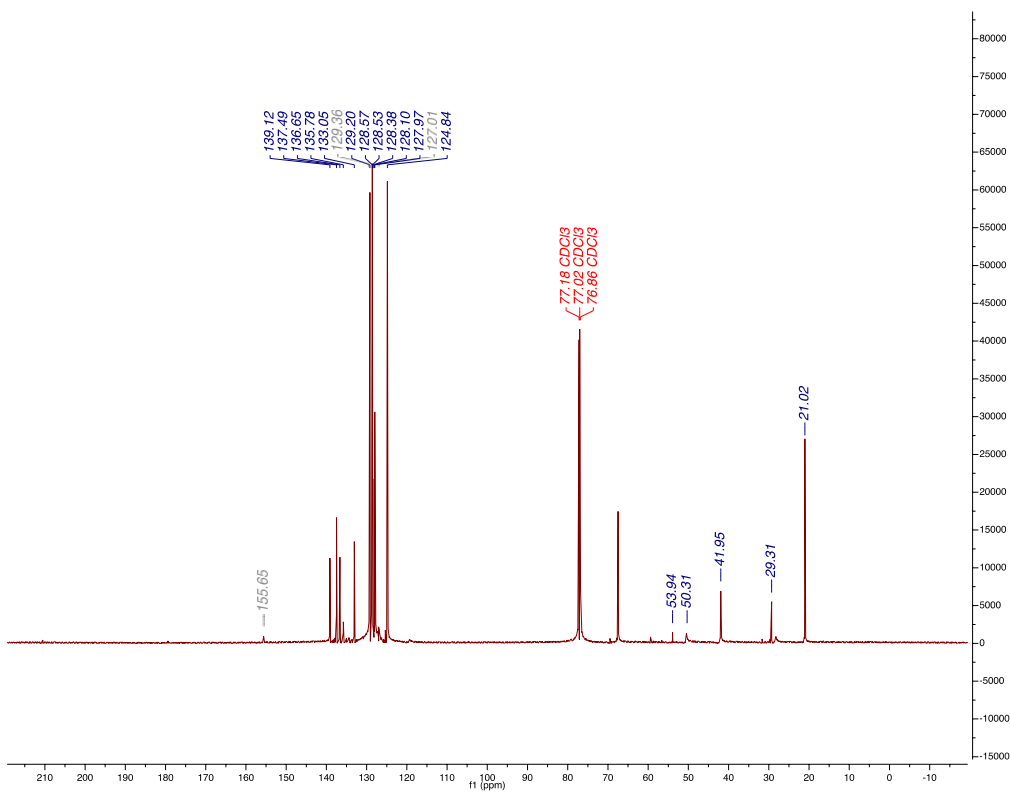
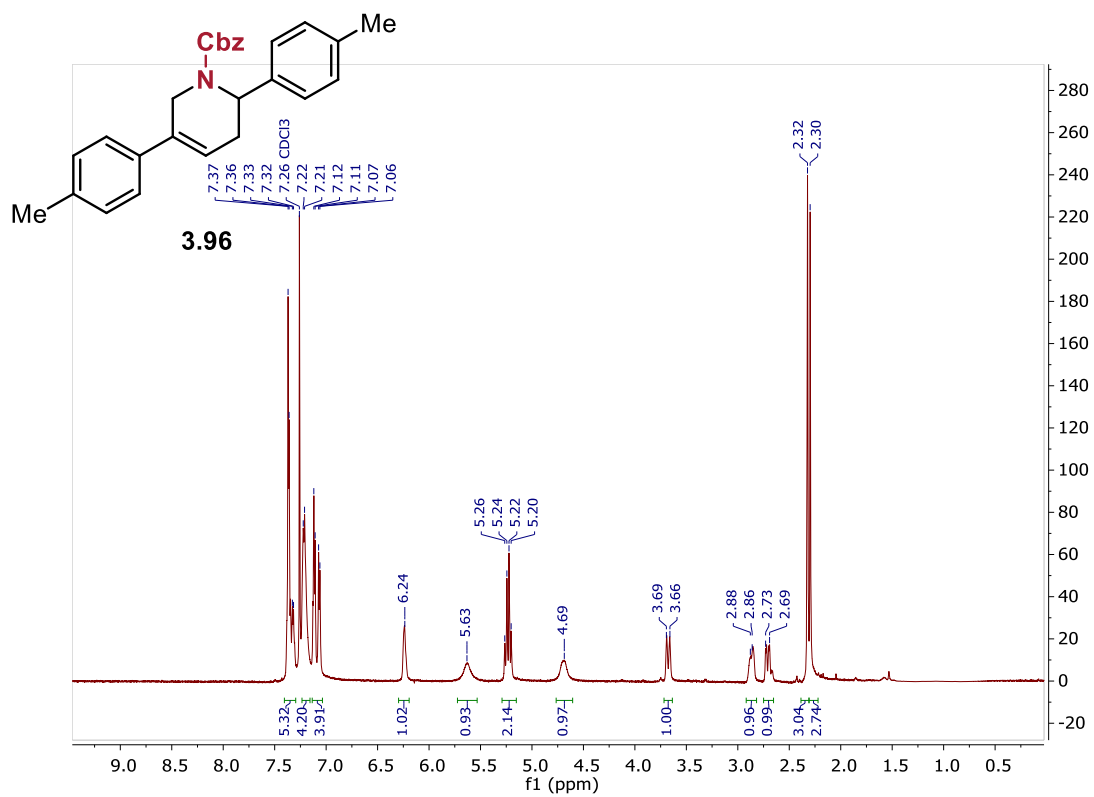
Synthesized using the general procedure, isolated via silica flash chromatography using 2% Acetone in Hexanes as a white solid (33.1 mg, 41% yield).

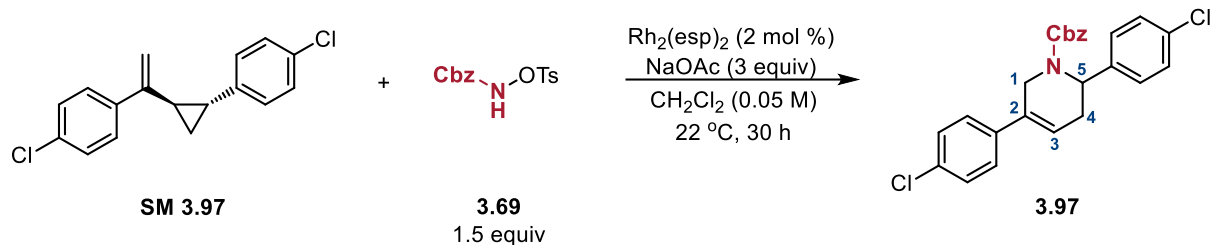
**$^1\text{H}$  NMR** (800 MHz,  $\text{CDCl}_3$ )  $\delta$  7.44 – 7.17 (ArH, m, 11H), 7.13 (ArH, d,  $J = 8.0$  Hz, 2H), 6.23 ( $\text{H}^3$ , dd,  $J = 6.1, 2.5$  Hz, 1H), 5.33 – 5.18 ( $\text{H}^5$ , Cbz- $\text{CH}_2$ , m, 3H), 4.83 – 4.61 ( $\text{H}^1$ , m, 1H), 3.70 ( $\text{H}^1$ , ddt,  $J = 17.7, 4.0, 2.1$  Hz, 1H), 2.89 ( $\text{H}^4$ , ddt,  $J = 17.1, 6.3, 3.1$  Hz, 1H), 2.76 – 2.66 ( $\text{H}^4$ , m, 1H), 2.32 (Me, s, 3H), 2.30 (Me, s, 3H) ppm.

**$^{13}\text{C}$  NMR** (201 MHz,  $\text{CDCl}_3$ )  $\delta$  155.7, 139.1, 137.5, 136.7, 135.8, 133.1, 129.4, 129.2, 128.6, 128.5, 128.4, 128.1, 128.0, 127.0, 124.8, 77.2, 77.0, 76.9, 53.9, 50.3, 42.0, 29.3, 21.0 ppm.

**IR** (film):  $\bar{\nu} = 2922$  (s), 2852 (m) 1697 (bs), 1514 (m), 1244 (s), 1103 (m), 810 (s), 690 (s)  $\text{cm}^{-1}$ .

**HRMS** (ESI):  $m/z$  calculated for  $[\text{C}_{27}\text{H}_{27}\text{NO}_2+\text{H}]^+$ : 398.2120; found: 398.2106.





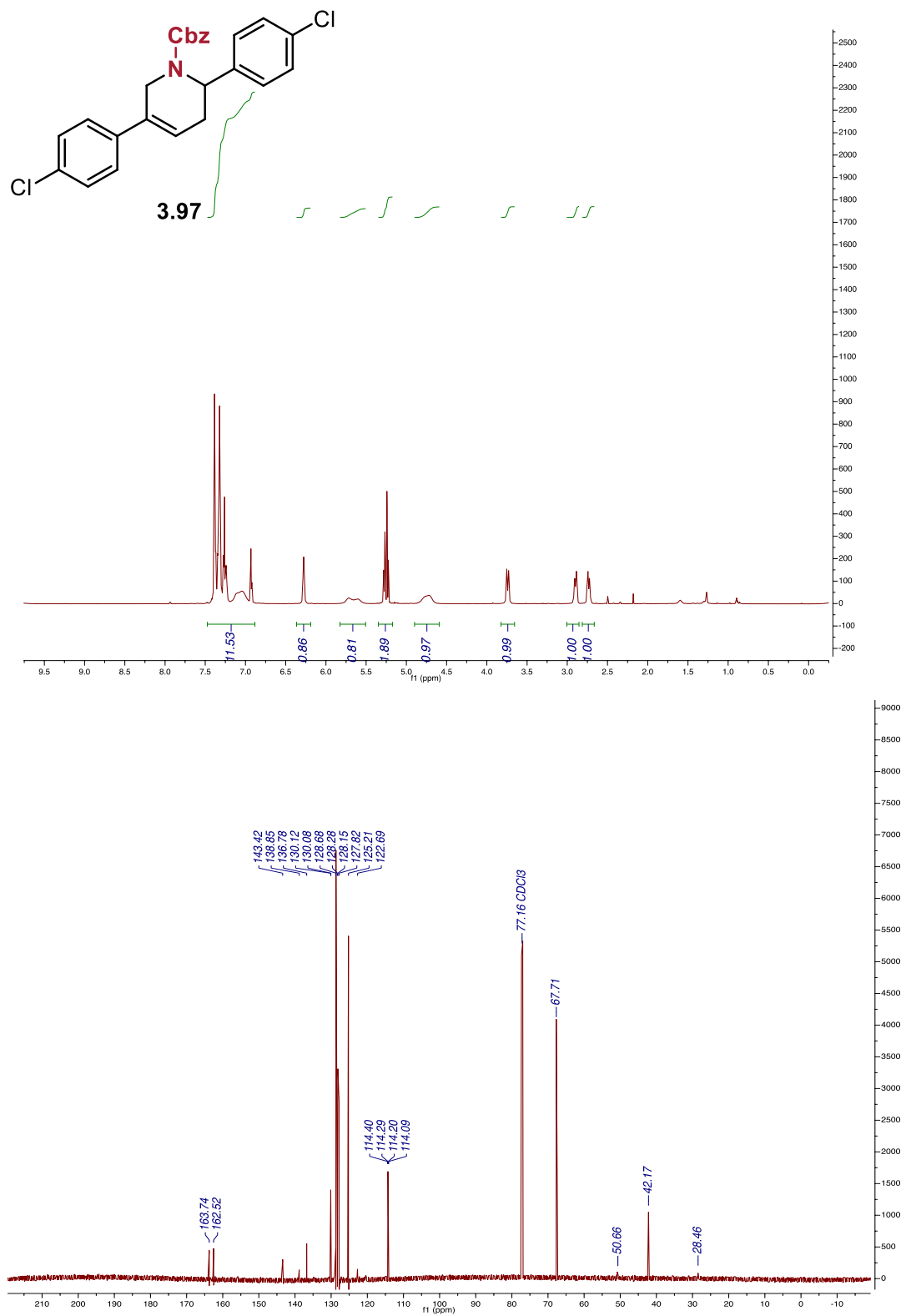
Synthesized using the general procedure, isolated via silica flash chromatography using 2% Acetone in Hexanes as a white solid (37.9 mg, 43% yield).

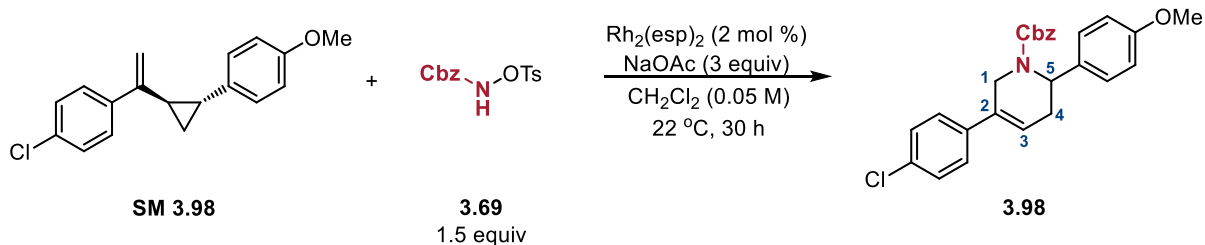
**$^1\text{H}$  NMR** (800 MHz,  $\text{CDCl}_3$ )  $\delta$  7.40 – 7.30 (ArH, m, 4H), 7.30 – 7.15 (ArH, m, 9H), 6.26 ( $\text{H}^3$ , dd,  $J = 6.1, 2.7$  Hz, 1H), 5.64 ( $\text{H}^5$ , s, 1H), 5.27 (Cbz– $\text{CH}_2$ , d,  $J = 12.3$  Hz, 1H), 5.22 (Cbz– $\text{CH}_2$ , d,  $J = 12.3$  Hz, 1H), 4.68 ( $\text{H}^1$ , s, 1H), 3.65 ( $\text{H}^1$ , d,  $J = 21.3$  Hz, 2H), 2.88 ( $\text{H}^4$ , d,  $J = 21.0$  Hz, 2H), 2.71 ( $\text{H}^4$ , d,  $J = 18.0$  Hz, 2H) ppm.

**$^{13}\text{C}$  NMR** (201 MHz,  $\text{CDCl}_3$ )  $\delta$  155.6, 138.8, 137.0, 136.5, 133.5, 133.2, 128.7, 128.7, 128.7, 128.6, 128.6, 128.3, 128.2, 128.0, 126.2, 67.6, 50.2, 41.7, 29.3 ppm.

**IR** (film):  $\bar{\nu} = 2835(\text{w}), 1692(\text{bs}), 1492(\text{m}), 1425(\text{s}), 1253(\text{s}), 1091(\text{s}), 700(\text{s}) \text{ cm}^{-1}$ .

**HRMS** (ESI):  $m/z$  calculated for  $[\text{C}_{25}\text{H}_{21}\text{Cl}_2\text{NO}_2 + \text{Na}]^+$ : 460.0847; found: 460.0850.





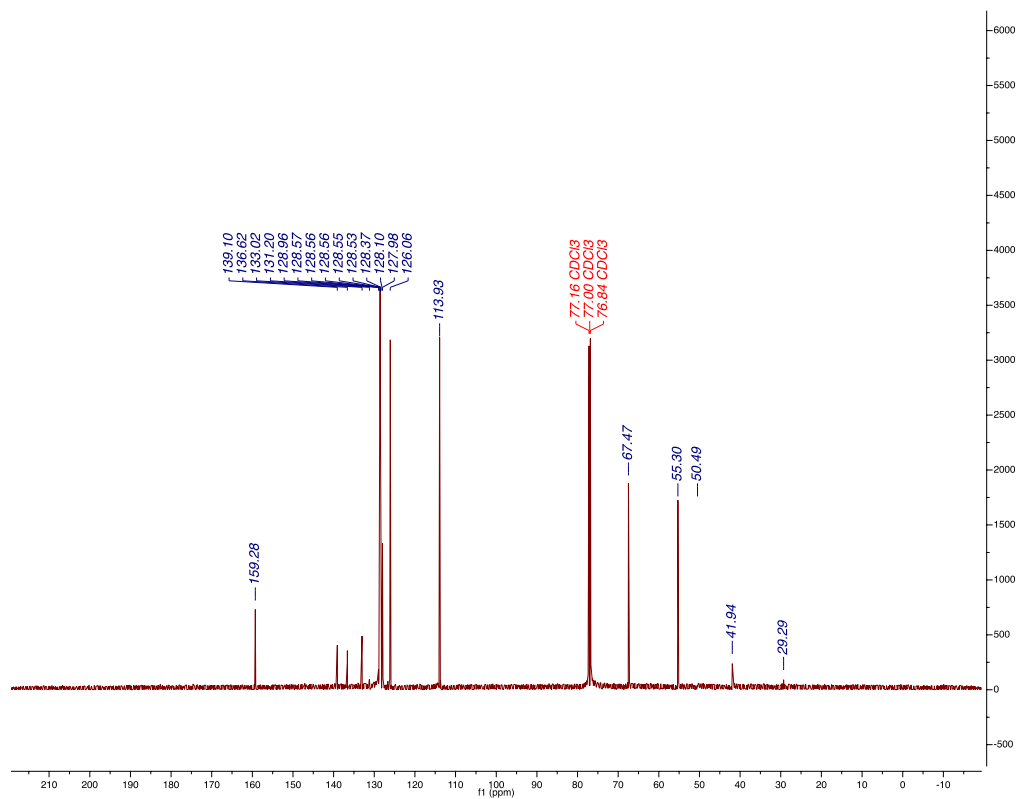
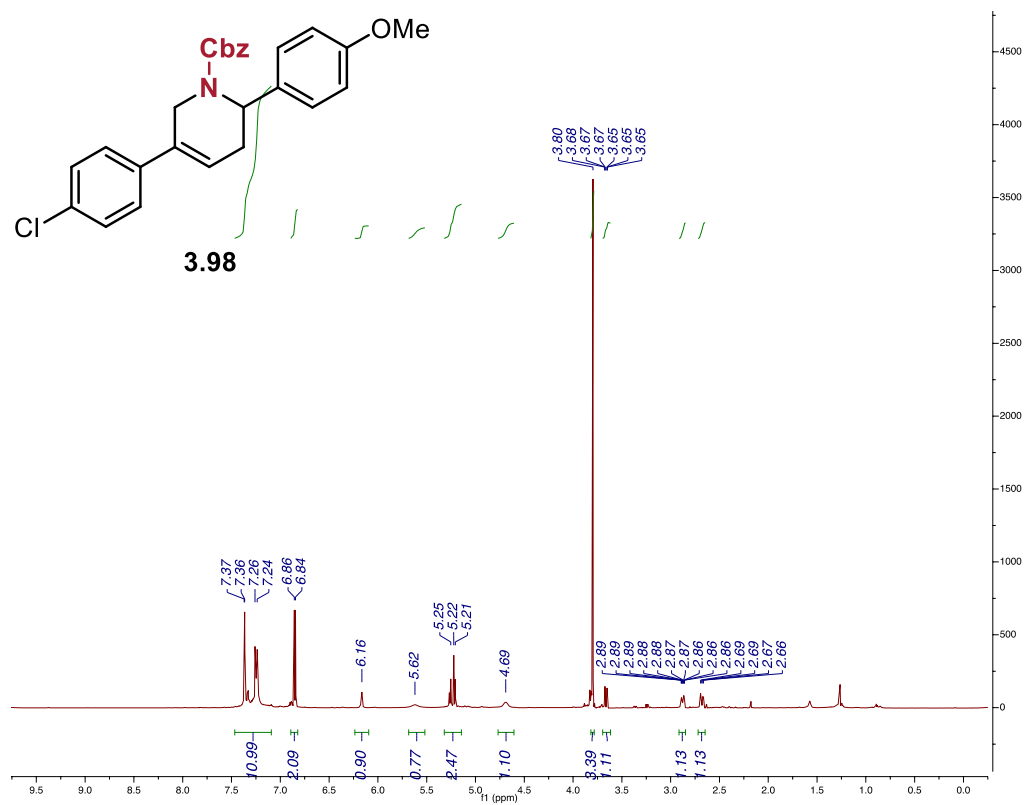
Synthesized using the general procedure, isolated via silica flash chromatography using 2% Acetone in Hexanes as a white solid (44.5 mg, 51% yield).

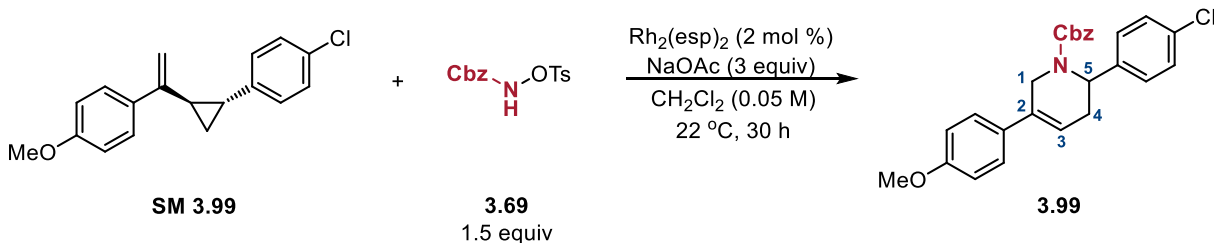
**$^1\text{H}$  NMR** (800 MHz,  $\text{CDCl}_3$ )  $\delta$  7.44 – 7.05 (ArH, m, 11H), 6.89 – 6.80 (ArH, m, 2H), 6.21 – 6.09 ( $\text{H}^5$ , m, 1H), 5.62 ( $\text{H}^5$ , s, 1H), 5.26 (Cbz- $\text{CH}_2$ , d,  $J = 12.3$  Hz, 1H), 5.21 (Cbz- $\text{CH}_2$ , d,  $J = 12.3$  Hz, 1H), 4.69 ( $\text{H}^1$ , s, 1H), 3.80 (OMe, s, 3H), 3.66 ( $\text{H}^1$ , ddt,  $J = 17.7, 4.0, 2.1$  Hz, 1H), 2.88 ( $\text{H}^4$ , ddd,  $J = 18.4, 6.6, 3.3$  Hz, 1H), 2.68 ( $\text{H}^4$ , dd,  $J = 17.9, 6.3$  Hz, 1H) ppm.

**$^{13}\text{C}$  NMR** (201 MHz,  $\text{CDCl}_3$ )  $\delta$  159.3, 139.1, 136.6, 133.0, 131.2, 129.0, 128.6, 128.5, 128.4, 128.1, 128.0, 126.5, 126.1, 113.9, 67.5, 55.3, 41.9, 29.3, 22.7 ppm.

**IR** (film):  $\bar{\nu} = 2953$  (w), 1694 (bs), 1512 (s), 1243 (s), 1091 (m), 731 (s)  $\text{cm}^{-1}$ .

**HRMS** (ESI):  $m/z$  calculated for  $[\text{C}_{26}\text{H}_{24}\text{ClNO}_3 + \text{H}]^+$ : 434.1523; found: 434.1508.





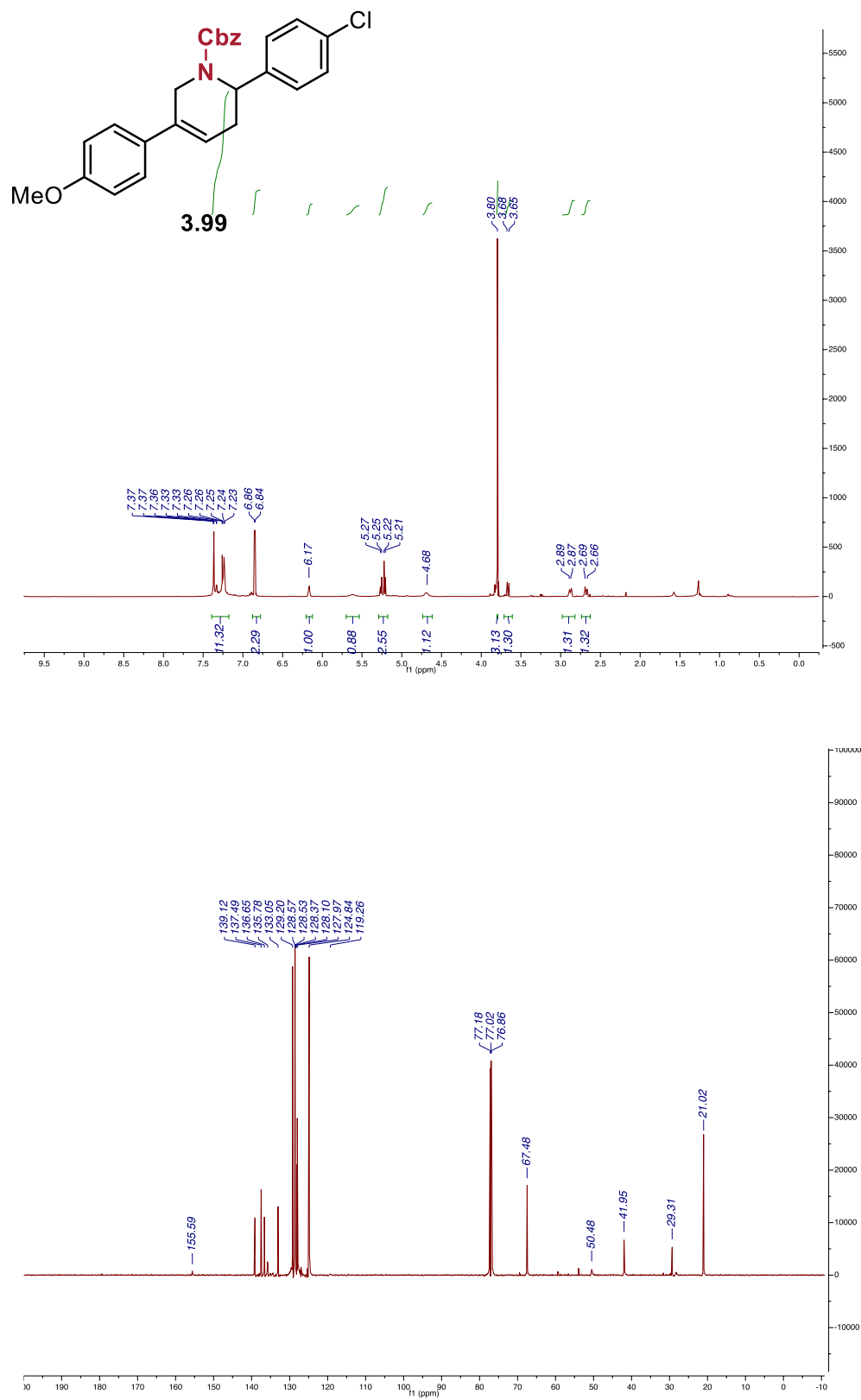
Synthesized using the general procedure, isolated via silica flash chromatography using 5% Acetone in Hexanes as a white solid (24.2 mg, 27% yield).

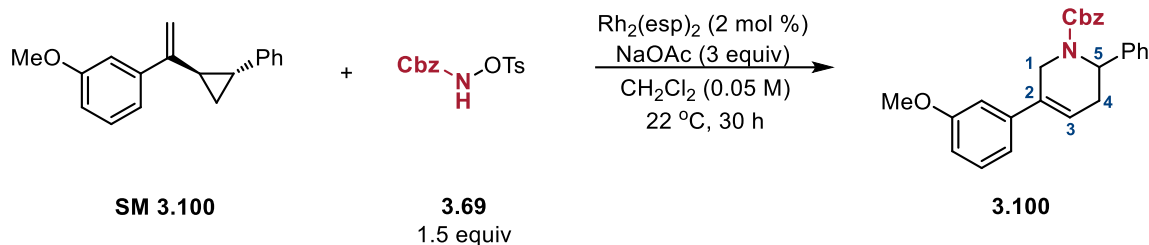
**$^1\text{H}$  NMR** (800 MHz,  $\text{CDCl}_3$ )  $\delta$  7.47 – 7.09 (ArH, m, 11H), 6.85 (ArH, d,  $J$  = 8.8 Hz, 2H), 6.16 ( $\text{H}^3$ , s, 1H), 5.62 ( $\text{H}^5$ , s, 1H), 5.32 – 5.14 (Cbz- $\text{CH}_2$ , m, 2H), 4.69 ( $\text{H}^1$ , s, 1H), 3.80 (OMe, s, 3H), 3.70 – 3.62 ( $\text{H}^1$ , m, 1H), 2.88 ( $\text{H}^4$ , ddd,  $J$  = 17.6, 6.1, 2.9 Hz, 1H), 2.68 ( $\text{H}^4$ , dd,  $J$  = 17.9, 6.3 Hz, 1H) ppm.

**$^{13}\text{C}$  NMR** (201 MHz,  $\text{CDCl}_3$ )  $\delta$  159.3, 139.1, 136.6, 133.0, 131.2, 129.0, 128.6, 128.6, 128.6, 128.6, 128.5, 128.4, 128.1, 128.0, 126.1, 113.9, 67.5, 55.3, 50.5, 41.9, 29.3 ppm.

**IR** (film):  $\bar{\nu}$  = 2927 (w), 2837 (w), 1693 (bs), 1512 (m), 1244 (s), 822 (bm), 733 (m), 696 (m)  $\text{cm}^{-1}$ .

**HRMS** (ESI):  $m/z$  calculated for  $[\text{C}_{26}\text{H}_{24}\text{ClNO}_3+\text{H}]^+$ : 434.1523; found: 434.1508.





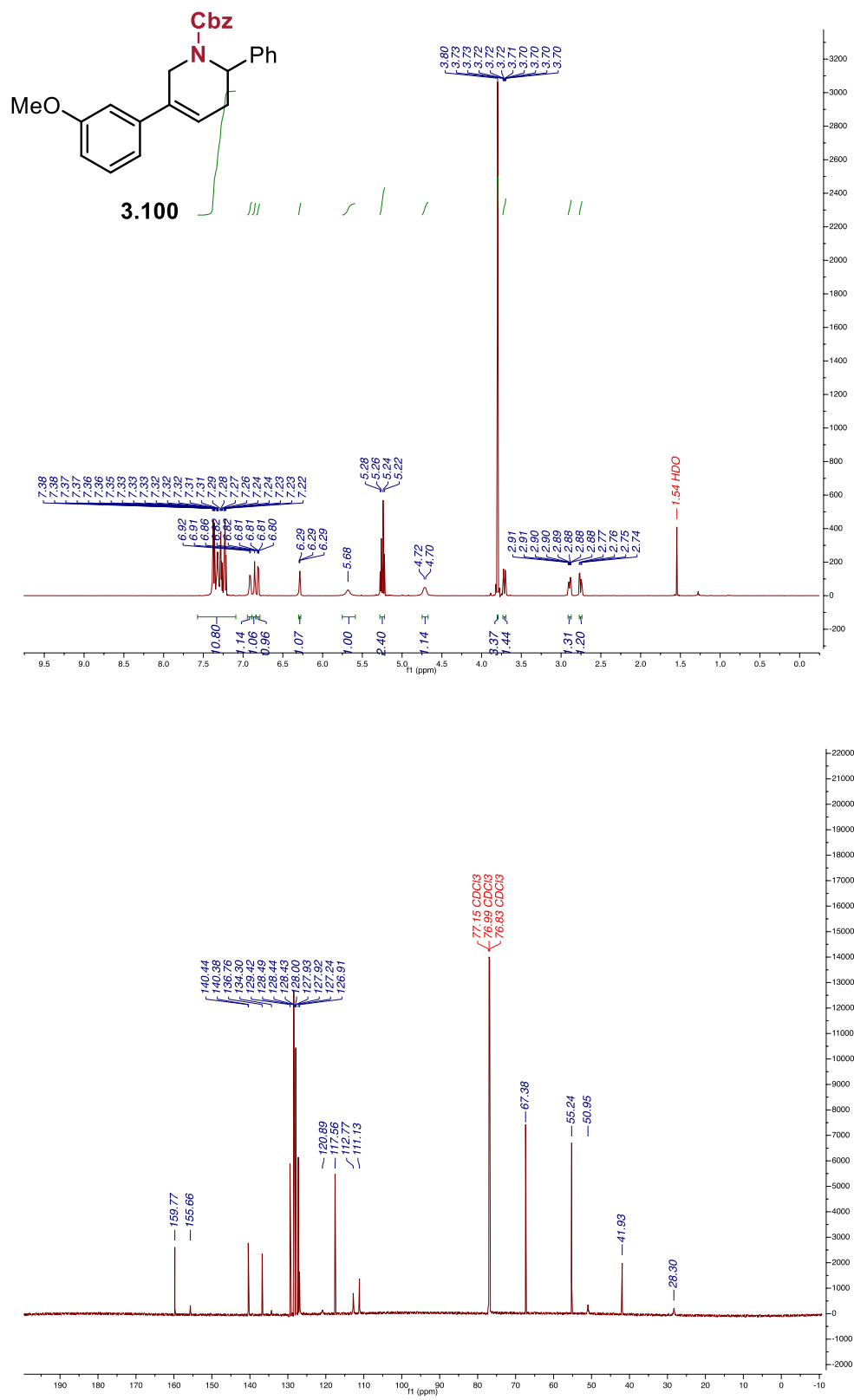
Synthesized using the general procedure, isolated via silica flash chromatography using 5% Acetone in Hexanes as a white solid (35.0 mg, 44% yield).

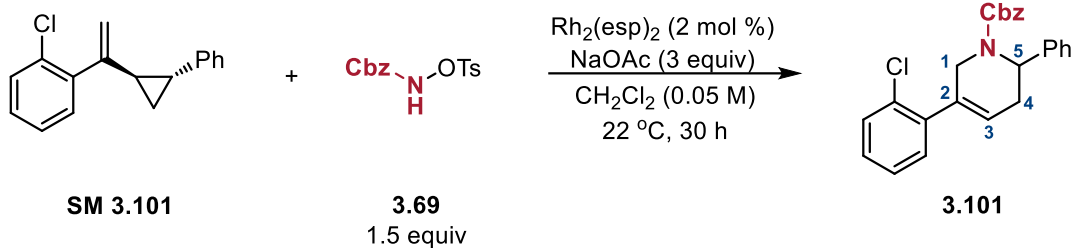
**$^1\text{H}$  NMR** (800 MHz,  $\text{CDCl}_3$ )  $\delta$  7.57 – 7.09 (ArH, m, 11H), 6.91 (ArH, d,  $J$  = 7.8 Hz, 1H), 6.86 (ArH, s, 1H), 6.81 (ArH, dt,  $J$  = 8.2, 1.6 Hz, 1H), 6.29 ( $\text{H}^3$ , dd,  $J$  = 6.3, 2.5 Hz, 1H), 5.68 ( $\text{H}^5$ , s, 1H), 5.28 – 5.22 (Cbz- $\text{CH}_2$ , m, 2H), 4.71 ( $\text{H}^1$ , d,  $J$  = 15.9 Hz, 1H), 3.80 (OMe, s, 3H), 3.71 ( $\text{H}^1$ , ddt,  $J$  = 17.7, 4.2, 2.2 Hz, 1H), 2.89 ( $\text{H}^4$ , ddd,  $J$  = 17.9, 6.7, 3.3 Hz, 1H), 2.76 ( $\text{H}^4$ , dd,  $J$  = 18.1, 6.3 Hz, 1H) ppm.

**$^{13}\text{C}$  NMR** (201 MHz,  $\text{CDCl}_3$ )  $\delta$  159.8, 155.7, 140.4, 140.4, 136.8, 134.3, 129.4, 128.5, 128.4, 128.4, 128.0, 127.9, 127.9, 127.2, 126.9, 120.9, 117.6, 112.8, 111.1, 67.4, 55.2, 51.0, 41.9, 28.3 ppm.

**IR** (film):  $\bar{\nu}$  = 3030 (w), 2953 (w), 2360 (w), 2247 (w), 1694 (s), 1417 (m), 1244 (m), 735 (s), 635 (s)  $\text{cm}^{-1}$ .

**HRMS** (ESI):  $m/z$  calculated for  $[\text{C}_{26}\text{H}_{25}\text{O}_3+\text{H}]^+$ : 400.1913; found: 400.1917.





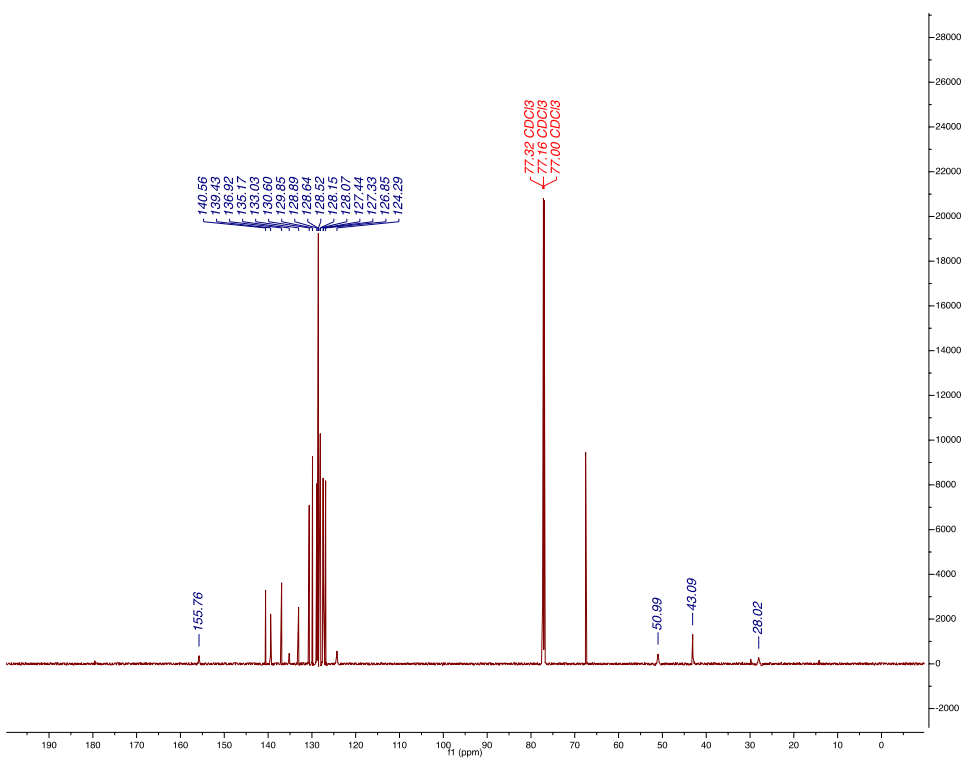
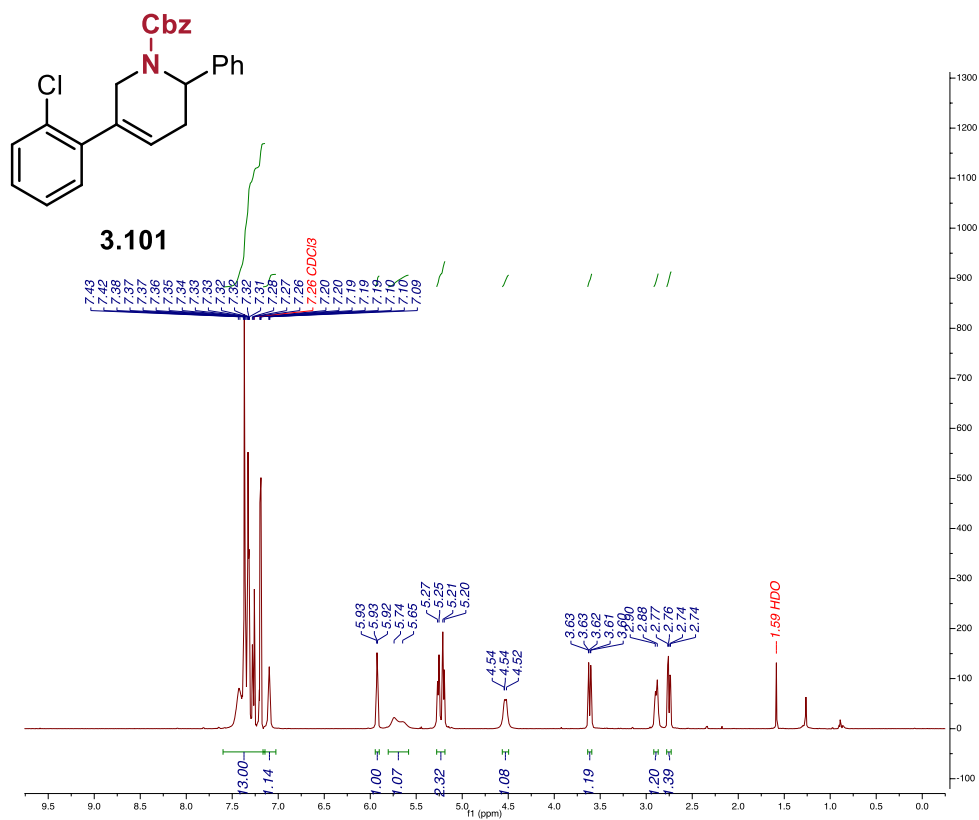
Synthesized using the general procedure, isolated via silica flash chromatography using 2% Acetone in Hexanes as a white solid (21.0 mg, 27% yield).

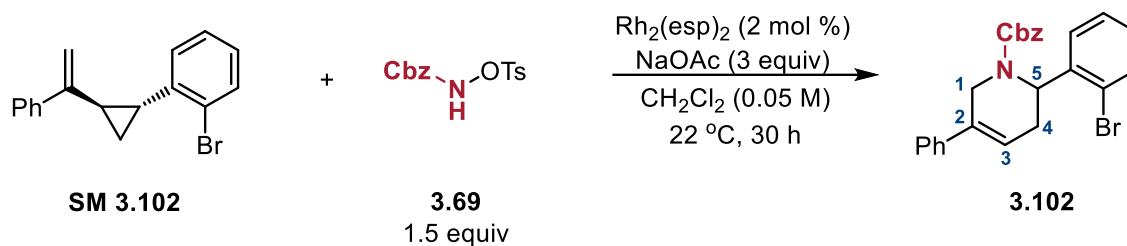
**$^1\text{H}$  NMR** (800 MHz,  $\text{CDCl}_3$ )  $\delta$  7.60 – 7.14 (ArH, m, 13H), 7.17 – 7.03 (ArH, m, 1H), 5.95 – 5.90 ( $\text{H}^3$ , m, 1H), 5.69 ( $\text{H}^5$ , d,  $J = 74.9$  Hz, 1H), 5.28 – 5.19 (Cbz- $\text{CH}_2$ , m, 2H), 4.56 – 4.50 ( $\text{H}^1$ , m, 1H), 3.64 – 3.59 ( $\text{H}^1$ , m, 1H), 2.89 ( $\text{H}^4$ , d,  $J = 17.6$  Hz, 1H), 2.75 ( $\text{H}^4$ , dd,  $J = 18.0, 6.0$  Hz, 1H) ppm.

**$^{13}\text{C}$  NMR** (201 MHz,  $\text{CDCl}_3$ )  $\delta$  155.8, 140.6, 139.4, 136.9, 135.2, 133.0, 130.6, 129.9, 128.9, 128.6, 128.5, 128.2, 128.1, 127.4, 127.3, 126.9, 124.3, 67.5, 51.0, 43.1, 28.0 ppm.

**IR** (film):  $\bar{\nu} = 3030$  (w), 2928 (w), 2247 (w), 1693 (s), 1415 (m), 1232 (m), 908 (s), 695 (s)  $\text{cm}^{-1}$ .

**HRMS** (ESI):  $m/z$  calculated for  $[\text{C}_{26}\text{H}_{25}\text{O}_3+\text{H}]^+$ : 404.1417; found: 404.1409.





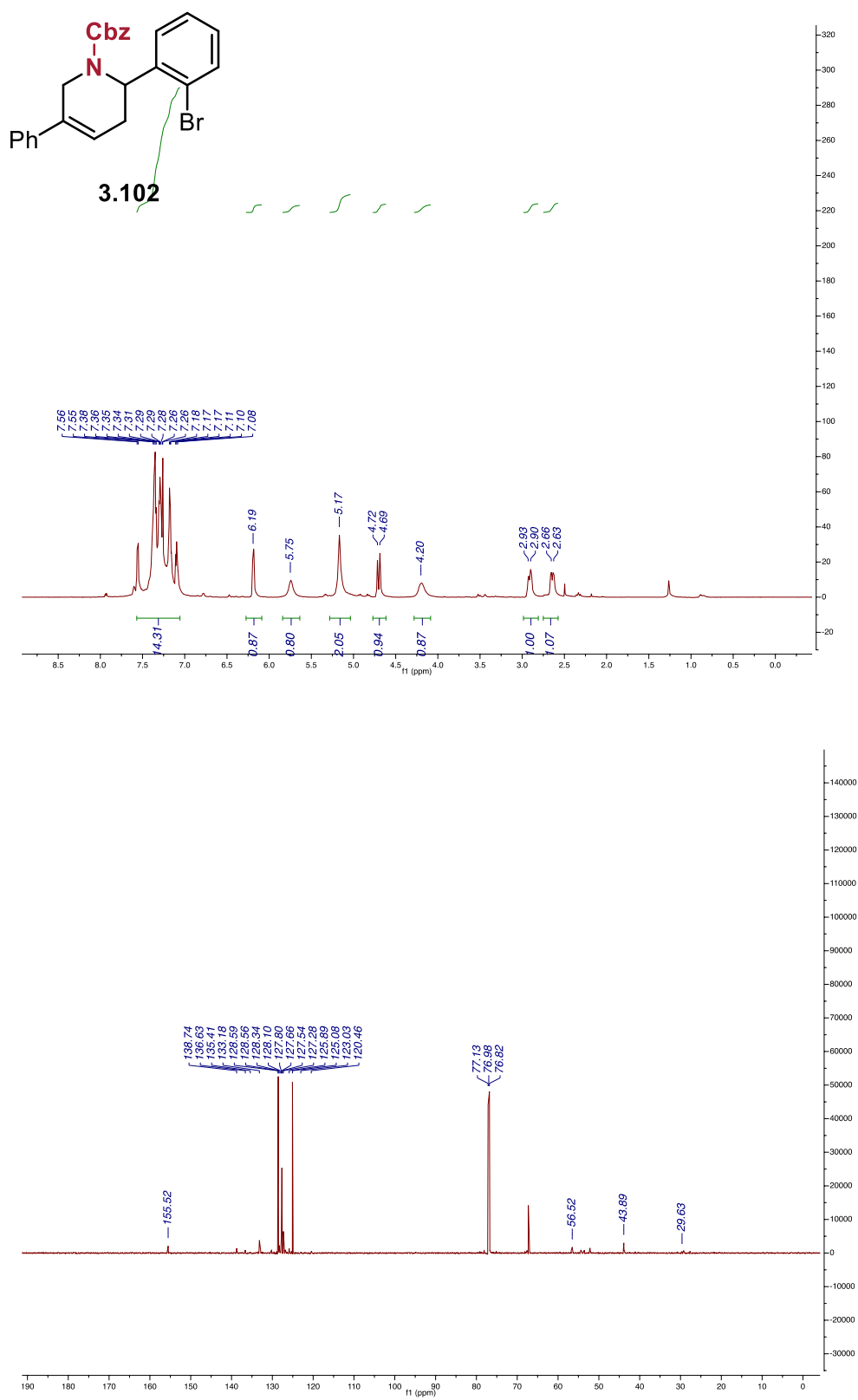
Synthesized using the general procedure, isolated via silica flash chromatography using 2% Acetone in Hexanes as a white solid (27.5 mg, 31% yield).

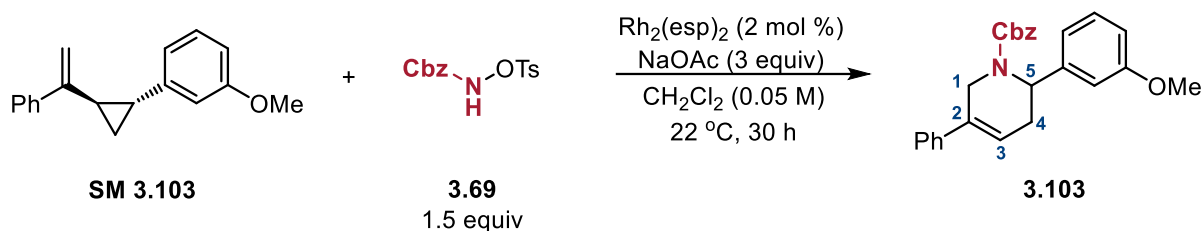
**<sup>1</sup>H NMR** (800 MHz, CDCl<sub>3</sub>) δ 7.61 – 7.04 (ArH, m, 14H), 6.18 (H<sup>3</sup>, s, 1H), 5.75 (H<sup>5</sup>, s, 1H), 5.17 (Cbz–CH<sub>2</sub>, s, 2H), 4.70 (H<sup>1</sup>, d, *J* = 17.5 Hz, 1H), 4.21 (H<sup>1</sup>, s, 1H), 2.91 (H<sup>4</sup>, d, *J* = 27.1 Hz, 1H), 2.64 (H<sup>4</sup>, d, *J* = 21.2 Hz, 1H) ppm.

**<sup>13</sup>C NMR** (201 MHz, CDCl<sub>3</sub>) δ 155.5, 138.8, 136.6, 133.2, 133.1, 128.6, 128.6, 128.5, 128.3, 128.3, 127.7, 127.6, 127.3, 127.2, 125.1, 125.0, 123.1, 120.5, 67.3, 52.1, 43.9, 29.3 ppm.

**IR** (film):  $\bar{\nu}$  = 3032 (w), 2926 (w), 1697 (bs), 1593 (w), 1496 (w), 1323 (bs), 1172 (s), 1024 (m), 748 (s), 694 (s), 654 (s) cm<sup>-1</sup>.

**HRMS** (ESI): *m/z* calculated for [C<sub>25</sub>H<sub>22</sub>BrNO<sub>2</sub>+H]<sup>+</sup>: 448.0912; found: 448.0902.





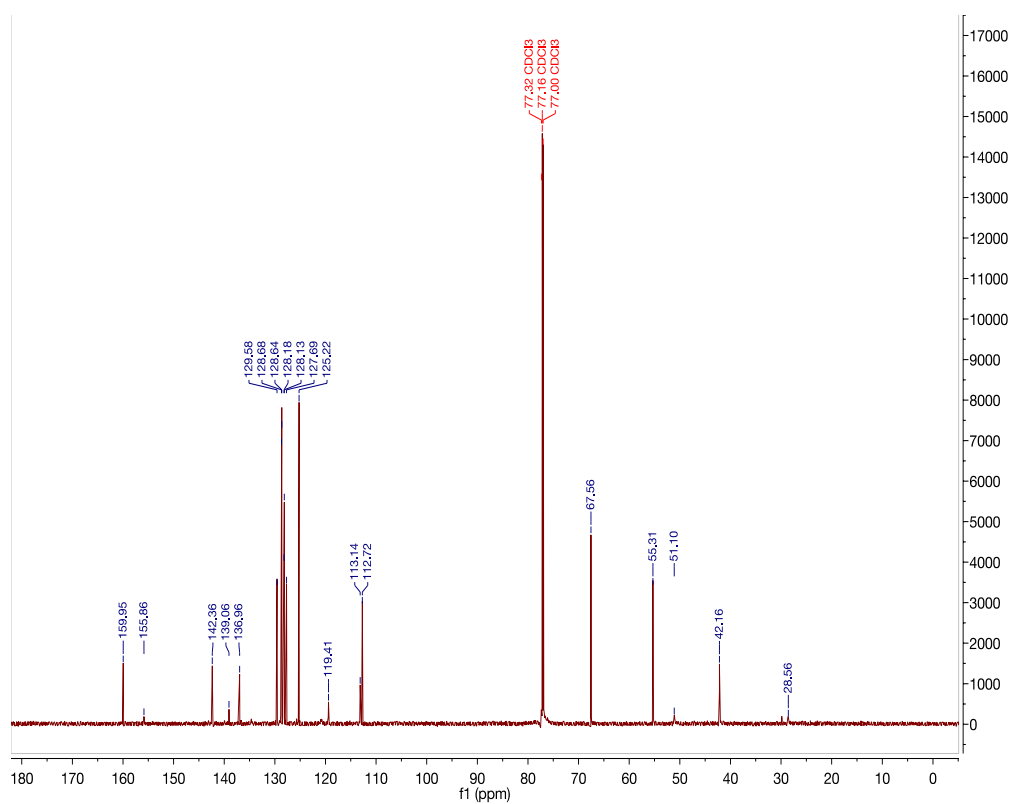
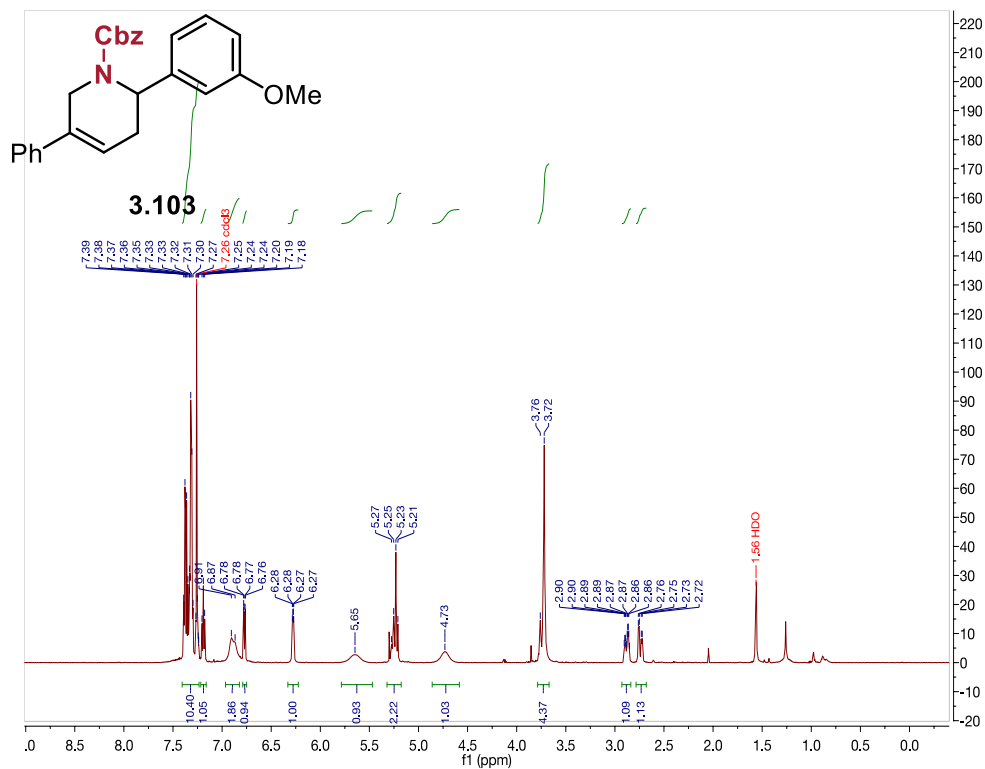
Synthesized using the general procedure, isolated via silica flash chromatography using 5% Acetone in Hexanes as a white solid (16.0 mg, 20% yield).

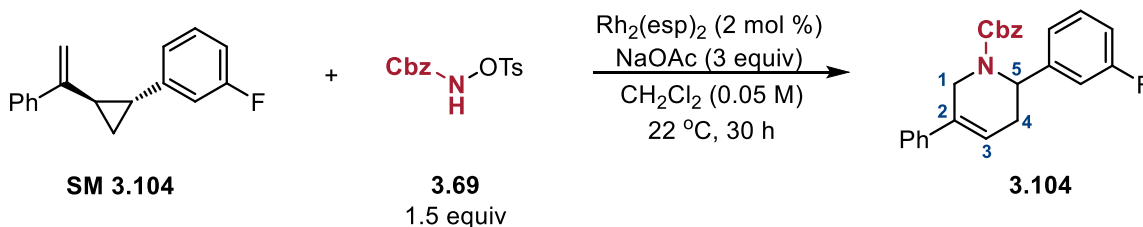
**<sup>1</sup>H NMR** (598 MHz, CDCl<sub>3</sub>) δ 7.41 – 7.28 (ArH, m, 9H), 7.25 (ArH, d, *J* = 5.4 Hz, 1H), 7.19 (ArH, t, *J* = 7.9 Hz, 1H), 6.89 (ArH, d, *J* = 23.2 Hz, 2H), 6.77 (ArH, dd, *J* = 8.3, 2.5 Hz, 1H), 6.28 (H<sup>3</sup>, dd, *J* = 5.9, 2.7 Hz, 1H), 5.65 (H<sup>5</sup>, s, 1H), 5.24 (Cbz–CH<sub>2</sub>, q, *J* = 12.5 Hz, 2H), 4.73 (H<sup>1</sup>, s, 1H), 3.74 (H<sup>1</sup>, d, *J* = 23.9 Hz, 4H), 2.88 (H<sup>4</sup>, ddq, *J* = 16.4, 6.5, 3.1 Hz, 1H), 2.74 (H<sup>4</sup>, dd, *J* = 18.2, 6.2 Hz, 1H) ppm.

**<sup>13</sup>C NMR** (201 MHz, CDCl<sub>3</sub>) δ 160.0, 142.4, 139.1, 137.0, 129.6, 128.7, 128.6, 128.2, 128.1, 127.7, 125.2, 119.4, 113.1, 112.7, 67.6, 55.3, 51.1, 42.2, 28.6 ppm.

**IR** (film):  $\bar{\nu}$  = 3032 (w), 2920 (w), 2850 (w), 1697 (br, s), 1629 (m), 1577 (s), 1406 (s), 1244 (br, s), 1049 (m), 748 (s), 694 (s) cm<sup>-1</sup>.

**HRMS** (ESI): *m/z* calculated for [C<sub>26</sub>H<sub>25</sub>O<sub>3</sub>+H]<sup>+</sup>: 400.1913; found: 400.1917.





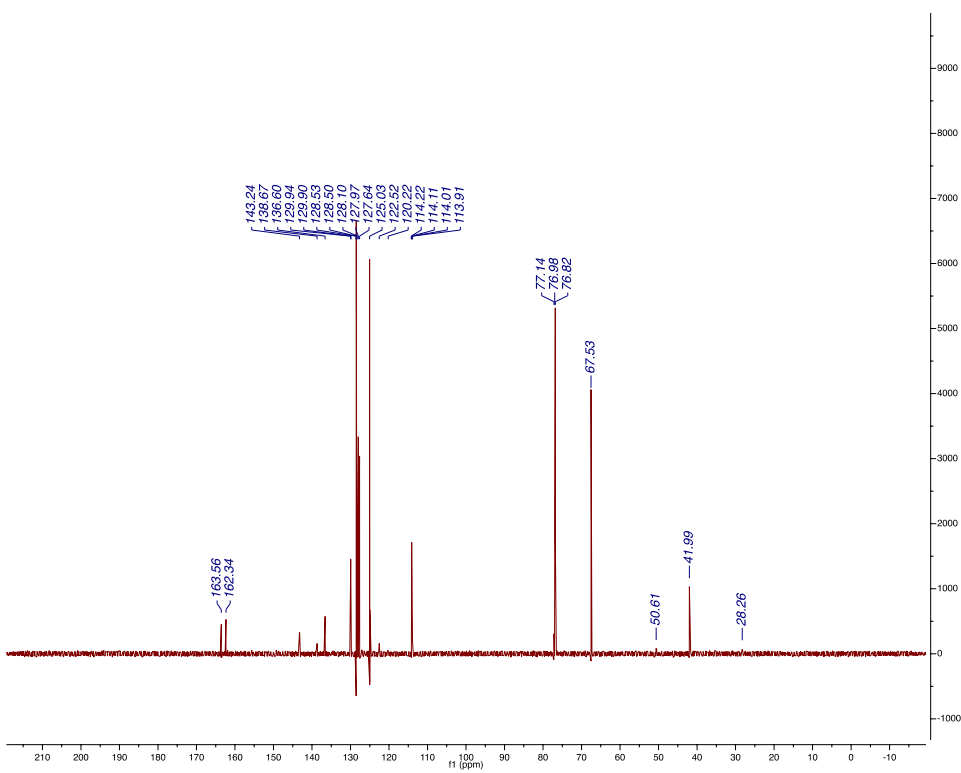
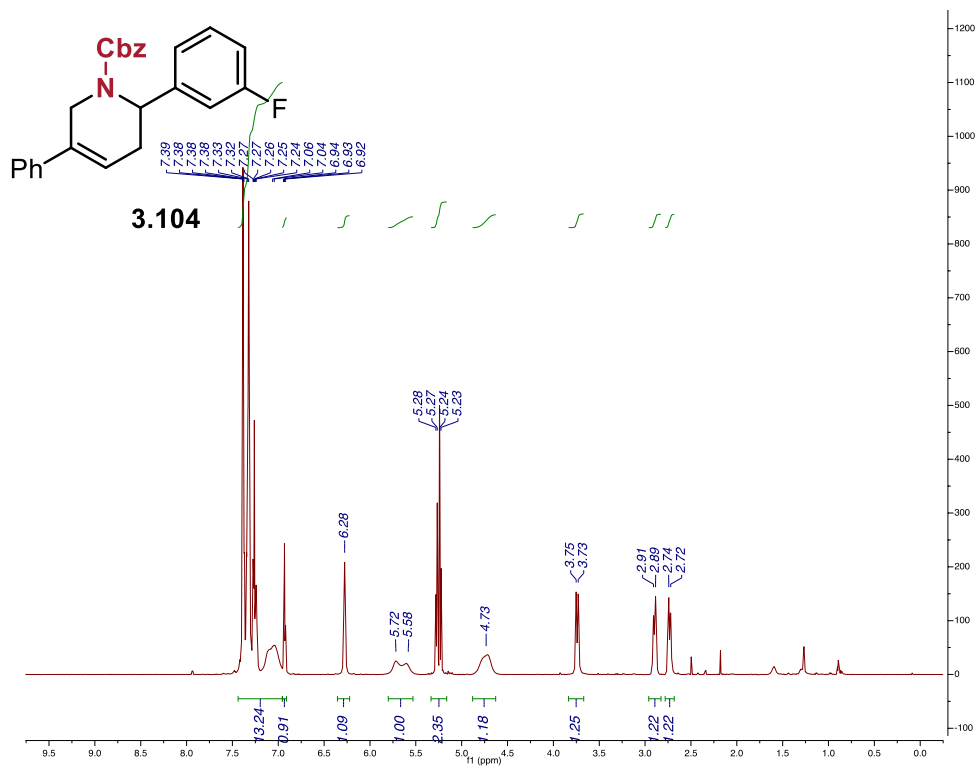
Synthesized using the general procedure, isolated via silica flash chromatography using 2% Acetone in Hexanes as a white solid (26.0 mg, 33% yield).

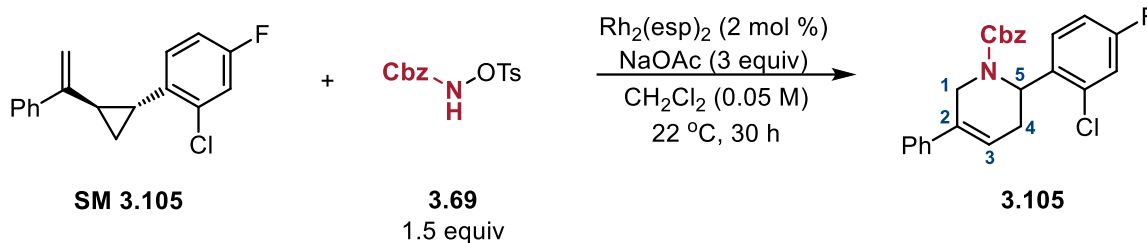
**$^1\text{H}$  NMR** (800 MHz,  $\text{CDCl}_3$ )  $\delta$  7.43 – 6.91 (ArH, m, 14H), 6.28 ( $\text{H}^3$ , d,  $J = 6.0$  Hz, 1H), 5.66 ( $\text{H}^5$ , d,  $J = 90.7$  Hz, 1H), 5.33 – 5.17 (Cbz– $\text{CH}_2$ , m, 2H), 4.72 ( $\text{H}^1$ , s, 1H), 3.74 ( $\text{H}^1$ , d,  $J = 17.8$  Hz, 1H), 2.90 ( $\text{H}^4$ , dd,  $J = 17.9, 5.8$  Hz, 1H), 2.73 ( $\text{H}^4$ , dd,  $J = 18.2, 6.0$  Hz, 1H) ppm.

**$^{13}\text{C}$  NMR** (201 MHz,  $\text{CDCl}_3$ )  $\delta$  163.6, 162.3, 143.2, 143.2, 136.6, 129.9, 129.9, 128.6, 128.5, 128.5, 128.1, 128.0, 128.0, 127.6, 127.6, 125.0, 125.0, 114.2, 114.1, 67.5, 50.6, 42.0 ppm.

**IR** (film):  $\bar{\nu} = 3036$  (w), 2857 (w), 1697 (bs), 1591 (m), 1323 (m), 1248 (m), 754 (m), 696 (s)  $\text{cm}^{-1}$ .

**HRMS** (ESI):  $m/z$  calculated for  $[\text{C}_{25}\text{H}_{22}\text{FNO}_2 + \text{H}]^+$ : 388.1713; found: 388.1708.





Synthesized using the general procedure, isolated via silica flash chromatography using 2% Acetone in Hexanes as a white solid (42.2 mg, 50% yield).

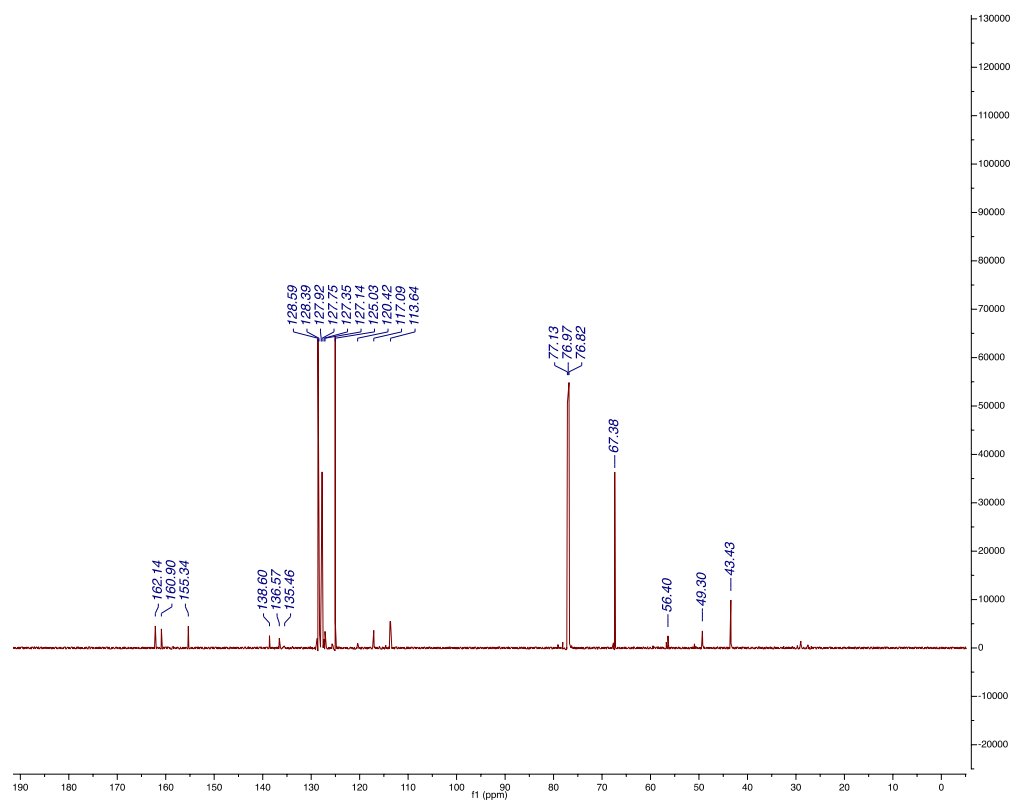
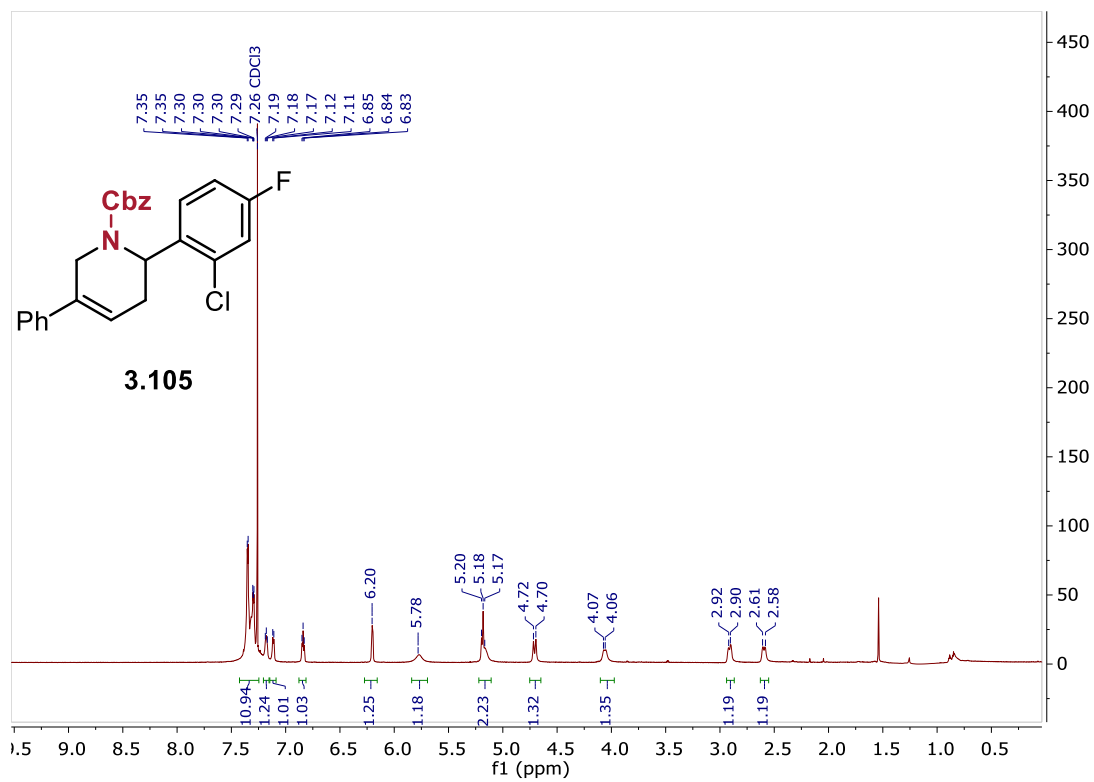
**$^1\text{H}$  NMR** (800 MHz,  $\text{CDCl}_3$ )  $\delta$  7.43 – 7.16 (ArH, m, 11H), 7.11 (ArH, dd,  $J = 8.4, 2.7$  Hz, 1H), 6.84 (ArH, ddd,  $J = 8.8, 7.9, 2.7$  Hz, 1H), 6.19 ( $\text{H}^3$ , s, 1H), 5.79 ( $\text{H}^5$ , s, 1H), 5.24 – 5.09 (Cbz- $\text{CH}_2$ , m, 2H), 4.71 ( $\text{H}^1$ , d,  $J = 17.8$  Hz, 1H), 4.08 ( $\text{H}^1$ , d,  $J = 17.6$  Hz, 1H), 2.92 ( $\text{H}^4$ , d,  $J = 27.3$  Hz, 1H), 2.60 ( $\text{H}^4$ , d,  $J = 23.5$  Hz, 1H) ppm.

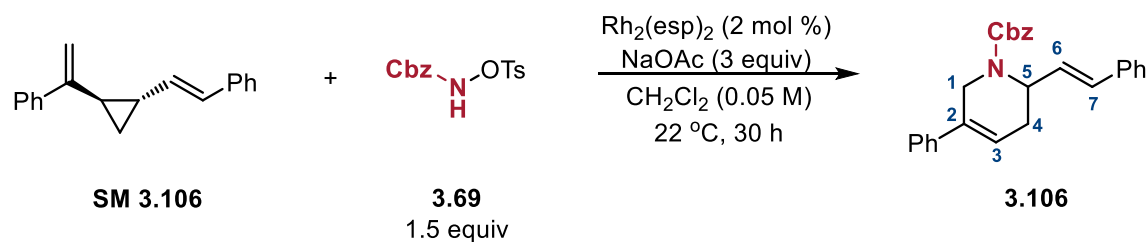
**$^{13}\text{C}$  NMR** (201 MHz,  $\text{CDCl}_3$ )  $\delta$  162.2, 160.9, 155.3, 138.6, 136.6, 128.8, 128.5, 128.5, 128.4, 128.3, 128.1, 127.9, 127.8, 127.6, 125.2, 124.9, 113.8, 113.7, 113.6, 67.4, 49.6, 49.0, 43.2 ppm.

**$^{19}\text{F}$  NMR** (563 MHz,  $\text{CDCl}_3$ )  $\delta$  -113.43 ppm.

**IR** (film):  $\bar{\nu} = 3069$  (w), 2953 (w), 1695 (bs), 1600 (m), 1489 (s), 1224 (bs), 1070 (m), 903 (m), 858 (m), 752 (m), 694 (s)  $\text{cm}^{-1}$ .

**HRMS** (ESI):  $m/z$  calculated for  $[\text{C}_{25}\text{H}_{21}\text{ClFNO}_2 + \text{H}]^+$ : 422.1323; found: 422.1317.





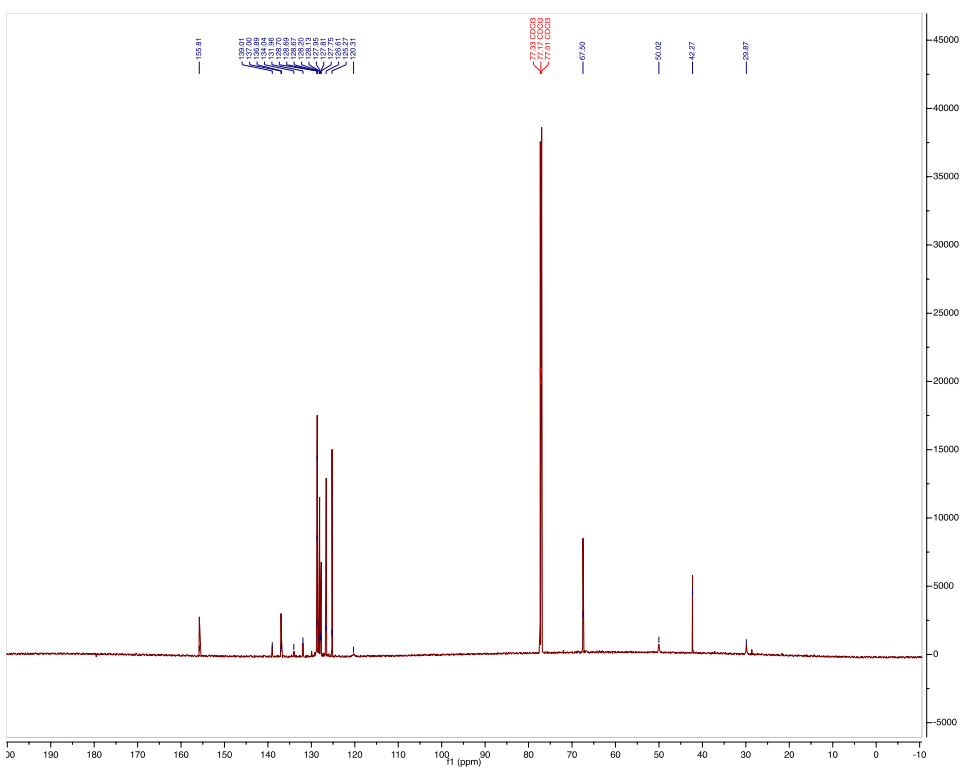
Synthesized using the general procedure, isolated via silica flash chromatography using 2% Acetone in Hexanes as a white solid (24.0 mg, 30% yield).

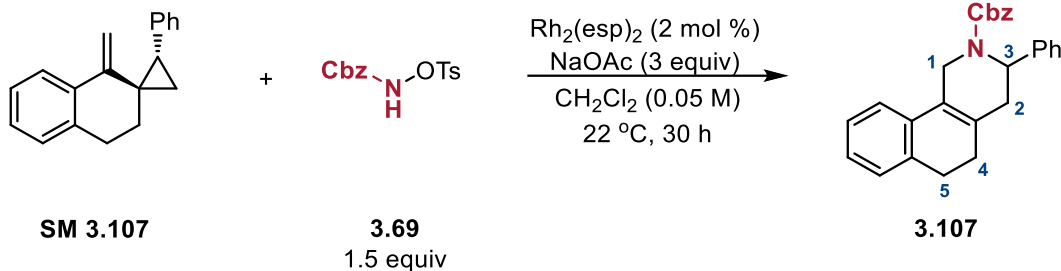
**$^1\text{H}$  NMR** (800 MHz,  $\text{CDCl}_3$ )  $\delta$  7.52 – 7.33 (ArH, m, 15H), 7.31 ( $\text{H}^7$ , d,  $J = 7.2$  Hz, 1H), 6.65 ( $\text{H}^5$ , s, 1H), 6.32 ( $\text{H}^6$ ,  $\text{H}^3$ , dd,  $J = 15.7, 5.8$  Hz, 2H), 5.36 (Cbz- $\text{CH}_2$ , d,  $J = 12.7$  Hz, 1H), 5.31 (Cbz- $\text{CH}_2$ , d,  $J = 12.1$  Hz, 1H), 4.86 – 4.73 ( $\text{H}^1$ , m, 1H), 4.12 ( $\text{H}^1$ , d,  $J = 17.8$  Hz, 1H), 2.88 – 2.84 ( $\text{H}^4$ , m, 1H), 2.51 ( $\text{H}^4$ , dd,  $J = 17.8, 6.4$  Hz, 1H) ppm.

**$^{13}\text{C}$  NMR** (201 MHz,  $\text{CDCl}_3$ )  $\delta$  155.8, 139.0, 137.0, 136.9, 134.0, 132.0, 128.7, 128.7, 128.7, 128.2, 128.1, 128.0, 127.8, 127.8, 126.6, 125.3, 120.3, 67.5, 50.0, 42.3, 29.9 ppm.

**IR** (film):  $\bar{\nu} = 3030$  (w), 2924 (w), 2364 (w), 1693 (s), 1413 (b), 1244 (s), 908 (m), 694 (s)  $\text{cm}^{-1}$ .

**HRMS** (ESI):  $m/z$  calculated for  $[\text{C}_{26}\text{H}_{25}\text{O}_3+\text{H}]^+$ : 396.1964; found: 396.1955.





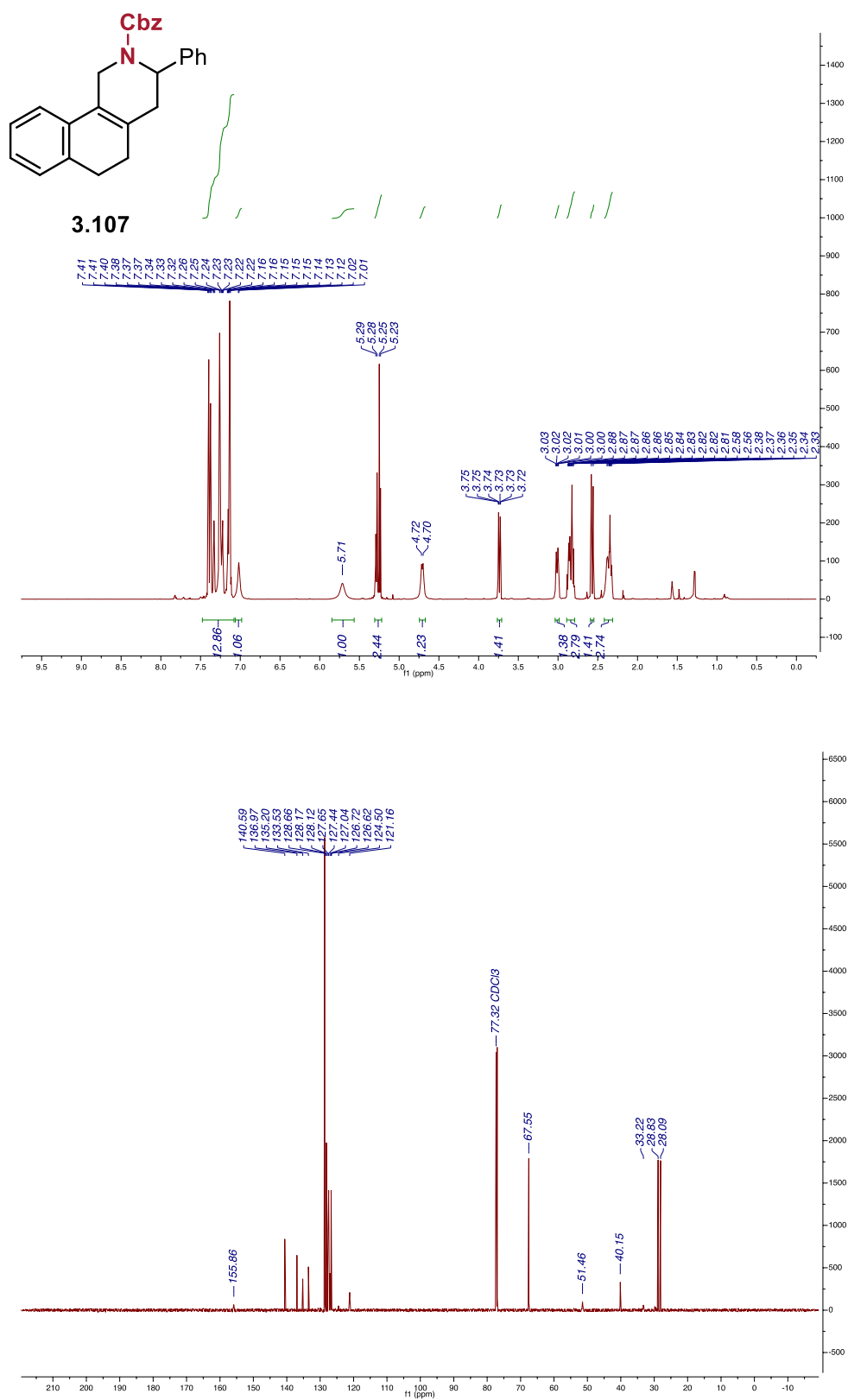
Synthesized using the general procedure, isolated via silica flash chromatography using 2% Acetone in Hexanes as a white solid (32.0 mg, 40% yield).

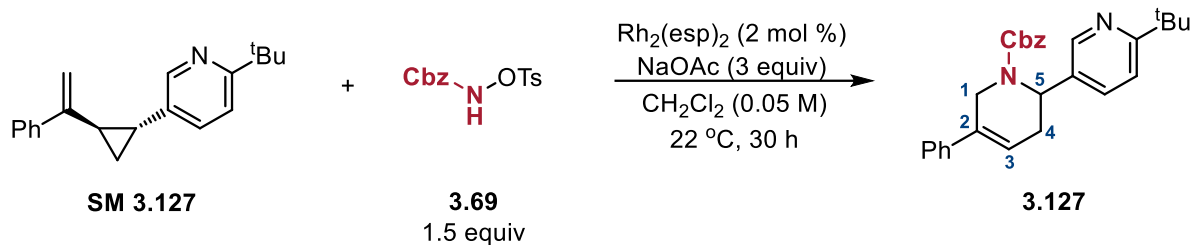
**$^1\text{H}$  NMR** (800 MHz,  $\text{CDCl}_3$ )  $\delta$  7.47 – 6.85 (ArH, m, 14H), 5.70 ( $\text{H}^3$ , s, 1H), 5.34 – 5.14 (Cbz- $\text{CH}_2$ , m, 2H), 4.69 ( $\text{H}^1$ , s, 1H), 3.77 – 3.67 ( $\text{H}^1$ , m, 1H), 2.99 ( $\text{H}^5$ , s, 1H), 2.87 – 2.77 ( $\text{H}^5$ ,  $\text{H}^2$ , m, 3H), 2.56 ( $\text{H}^4$ , d,  $J = 17.8$  Hz, 1H), 2.39 – 2.30 ( $\text{H}^4$ , m, 2H) ppm.

**$^{13}\text{C}$  NMR** (201 MHz,  $\text{CDCl}_3$ )  $\delta$  155.9, 140.6, 137.0, 135.2, 133.6, 130.6, 130.4, 128.7, 128.2, 128.1, 127.7, 127.5, 127.3, 127.1, 126.7, 126.6, 124.5, 121.2, 67.6, 51.5, 40.2, 33.2, 28.9, 28.1 ppm.

**IR** (film):  $\bar{\nu} = 3030$  (w), 2924 (m), 2341 (w), 1693 (bs), 1417 (s), 1247 (s), 692 (s)  $\text{cm}^{-1}$ .

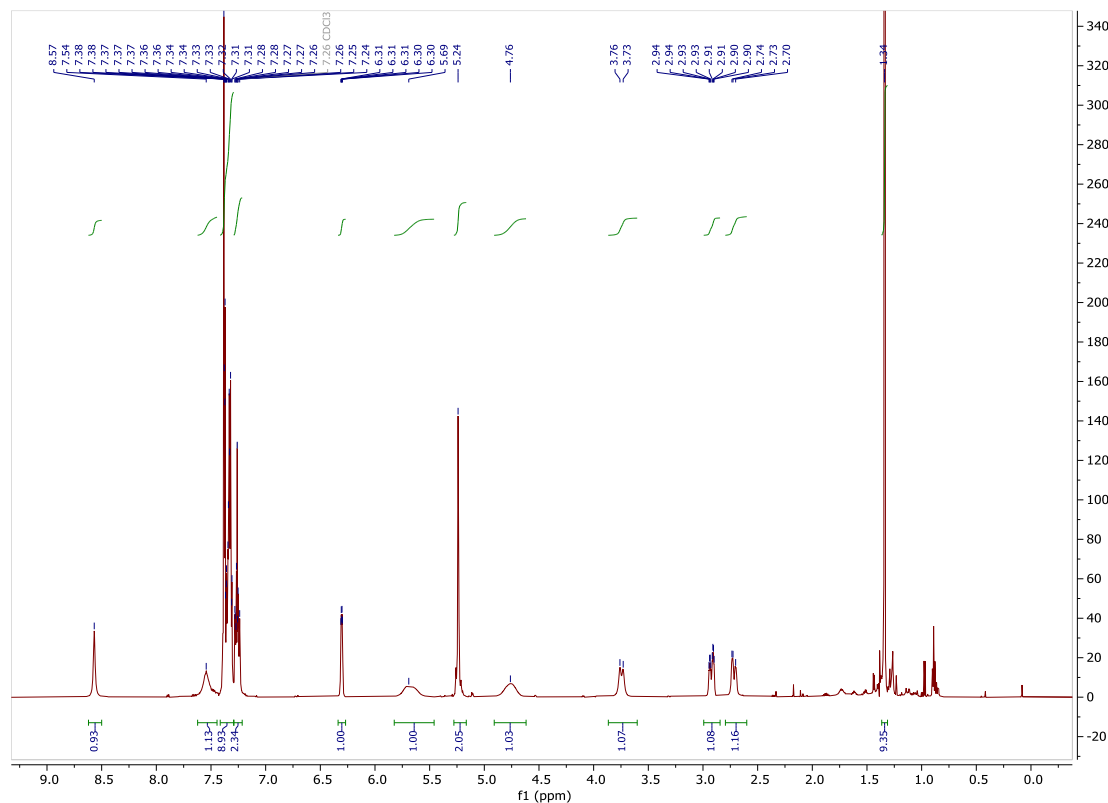
**HRMS** (ESI):  $m/z$  calculated for  $[\text{C}_{26}\text{H}_{25}\text{O}_3+\text{H}]^+$ : 396.1964; found: 396.1955.





Synthesized using the general procedure, isolated via silica flash chromatography (deactivated with Et<sub>3</sub>N) using 10% Ethyl acetate in Hexanes as a white solid (46.0 mg, 54% yield).

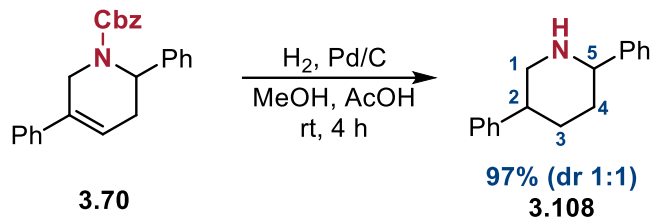
**<sup>1</sup>H NMR** (800 MHz, CDCl<sub>3</sub>) δ 8.57, (s, 1H), 7.54 (s, 1H) 7.42 – 7.30 (ArH, m, 8H), 7.29 – 7.18 (ArH, m, 2H), 6.30 (H<sup>3</sup>, d, *J* = 4.2 Hz, 1H), 5.69 (H<sup>5</sup>, s, 1H), 5.24 (Cbz–CH<sub>2</sub>, s, 2H), 4.76 (H<sup>1</sup>, m, 1H), 3.74 (H<sup>1</sup>, d, *J* = 17.9 Hz, 1H), 2.94 – 2.90 (H<sup>4</sup>, m, 1H), 2.74 – 2.70 (H<sup>4</sup>, 1H), 1.34 (s, 9H) ppm.



### 1.6. Scale-up reaction of Rh(II)-aza-[5+1] reaction

Under inert atmosphere, 1.0 mmol vinylcyclopropane **3.68** was dissolved with 1.5 mmol (480 mg) CbzNHOTs and 3.0 mmol (245 mg) NaOAc in 20 mL CH<sub>2</sub>Cl<sub>2</sub> at room temperature. To this was added 1 mol% (8 mg) Rh<sub>2</sub>(esp)<sub>2</sub> and the mixture was stirred 30 hours. The crude reaction was then filtered through a plug of silica with 60 mL CH<sub>2</sub>Cl<sub>2</sub> and immediately purified by flash chromatography to afford tetrahydropyridine **3.66** in 53% isolated yield (194.1 mg), 61% brsm yield.

### 1.7. Hydrogenation of **3.70**



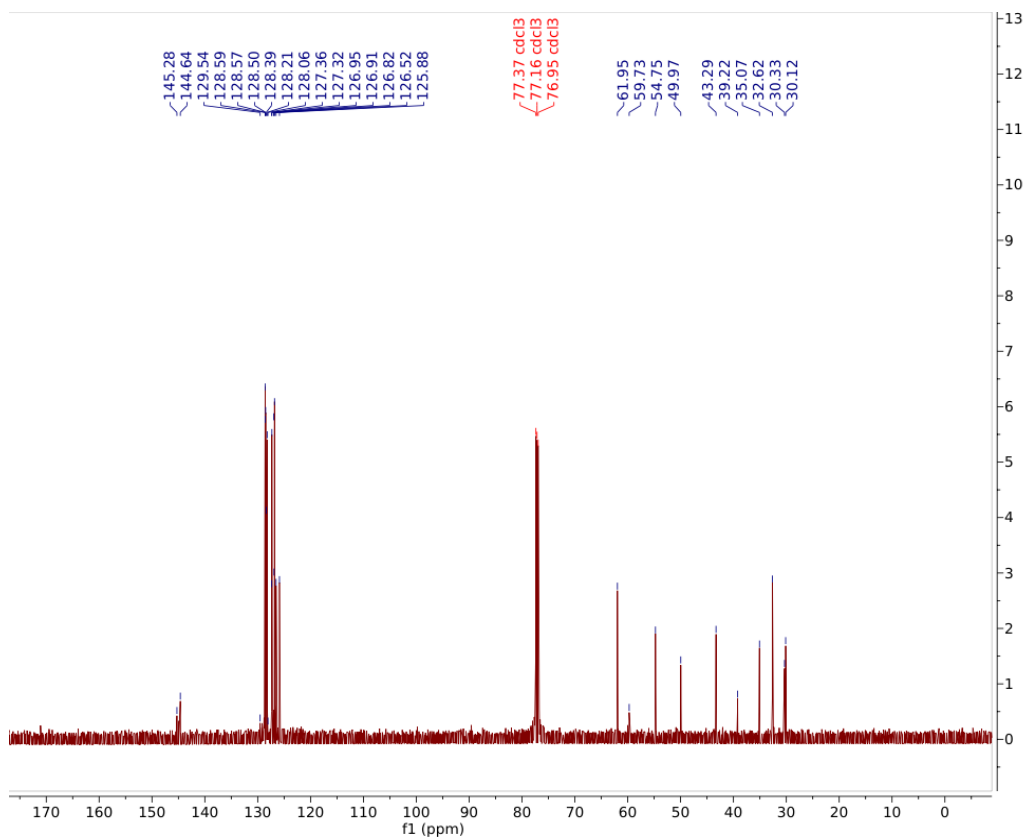
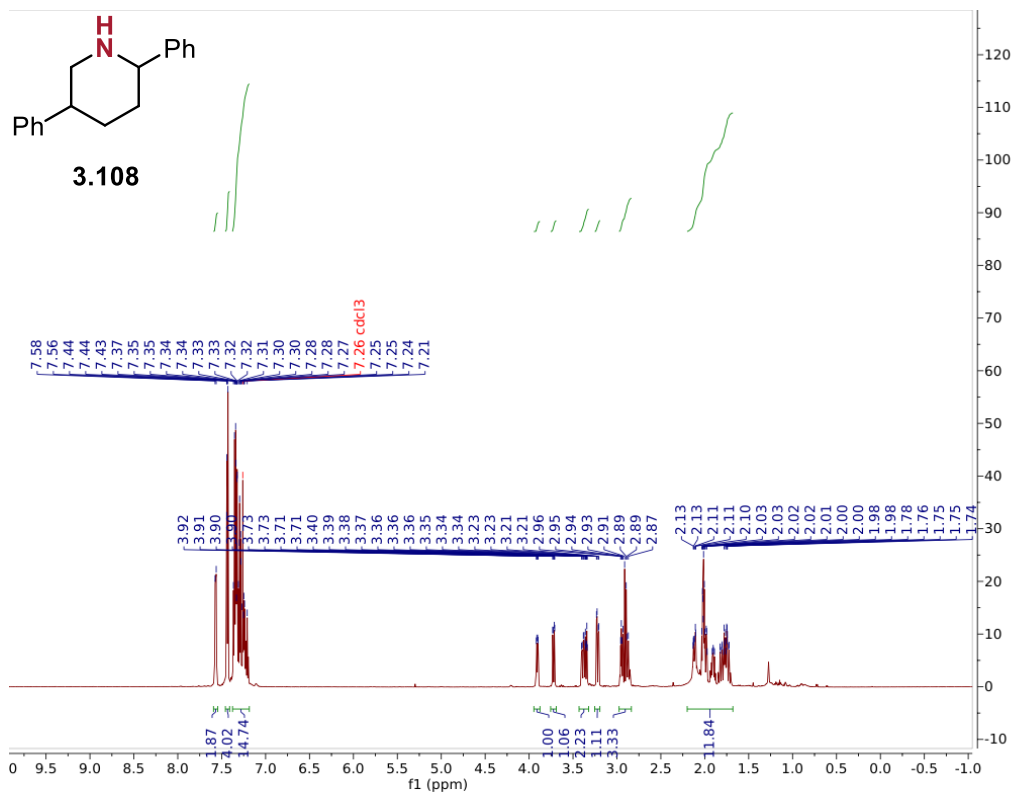
55 mg (0.15 mmol) of **3.70** was combined with 20 mg Pd/C (10% w/w) in a 25 ml round bottom flask. This flask was then evacuated under vacuum and back filled with H<sub>2</sub> gas and then 8 ml of anhydrous MeOH was added and then, subsequently, 0.75 ml of AcOH. The reaction was stirred for four hours at room temperature under a H<sub>2</sub> balloon. The mixture was then neutralized with 1 ml Et<sub>3</sub>N, diluted with Et<sub>2</sub>O, and filtered through celite to yield **3.108** (1:1 mixture of diastereomers) as a white solid (34.5 mg, 97% yield).

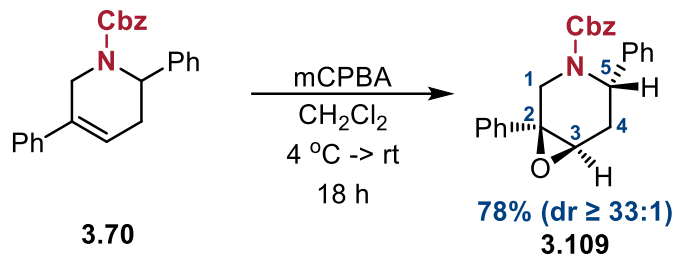
**<sup>1</sup>H NMR** (598 MHz, CDCl<sub>3</sub>) *Anti* diastereomer: δ 7.46 – 7.41 (ArH, m, 2H), 7.38 – 7.19 (ArH, m, 8H), 3.73 (H<sup>5</sup>, dd, J = 11.0, 2.6 Hz, 1H), 3.34 (H<sup>2</sup>, dt, J = 10.3, 2.8 Hz, 1H), 2.94 – 2.85 (H<sup>1</sup>, m, 2H), 2.14 – 2.09 (H<sup>4</sup>, m, 1H), 1.99 (H<sup>4</sup>, dq, J = 12.8, 3.0 Hz, 1H), 1.78 (H<sup>3</sup>, ttd, J = 23.9, 12.8, 3.4 Hz, 2H). *Syn* diastereomer: δ 7.59 – 7.52 (ArH, m, 2H), 7.39 – 7.19 (ArH, m, 8H), 3.92 (H<sup>5</sup>, dd, J = 8.3, 3.6 Hz, 1H), 3.37 (H<sup>2</sup>, dd, J = 12.2, 4.8 Hz, 1H), 3.21 (H<sup>1</sup>, dd, J = 12.3, 3.9 Hz, 1H), 2.98 – 2.93 (H<sup>1</sup>, m, 1H), 2.90 (H<sup>4</sup>, d, J = 1.4 Hz, 2H), 2.03 – 2.01 (H<sup>3</sup>, m, 1H), 1.96 – 1.88 (H<sup>3</sup>, m, 1H).

**<sup>13</sup>C NMR** (150 MHz, CDCl<sub>3</sub>) δ 144.76, 144.55, 129.57, 128.60, 128.57, 128.52, 128.36, 128.22, 127.95, 127.39, 127.32, 126.96, 126.94, 126.84, 126.54, 125.92, 77.37, 77.16, 76.95, 61.91, 59.57, 54.61, 49.84, 43.17, 39.22, 34.95, 32.58, 30.23, 30.02.

**IR** (film):  $\bar{\nu}$  = 3313 (w), 3080 (m), 3024 (m), 2937 (m), 2783 (m), 1600 (m), 1490 (s), 1452 (s), 752 (s) cm<sup>-1</sup>.

**HRMS** (ESI): *m/z* calculated for [C<sub>17</sub>H<sub>19</sub>N+H]<sup>+</sup>: 238.1596; found: 238.1599.



1.8. Epoxidation of **3.70**

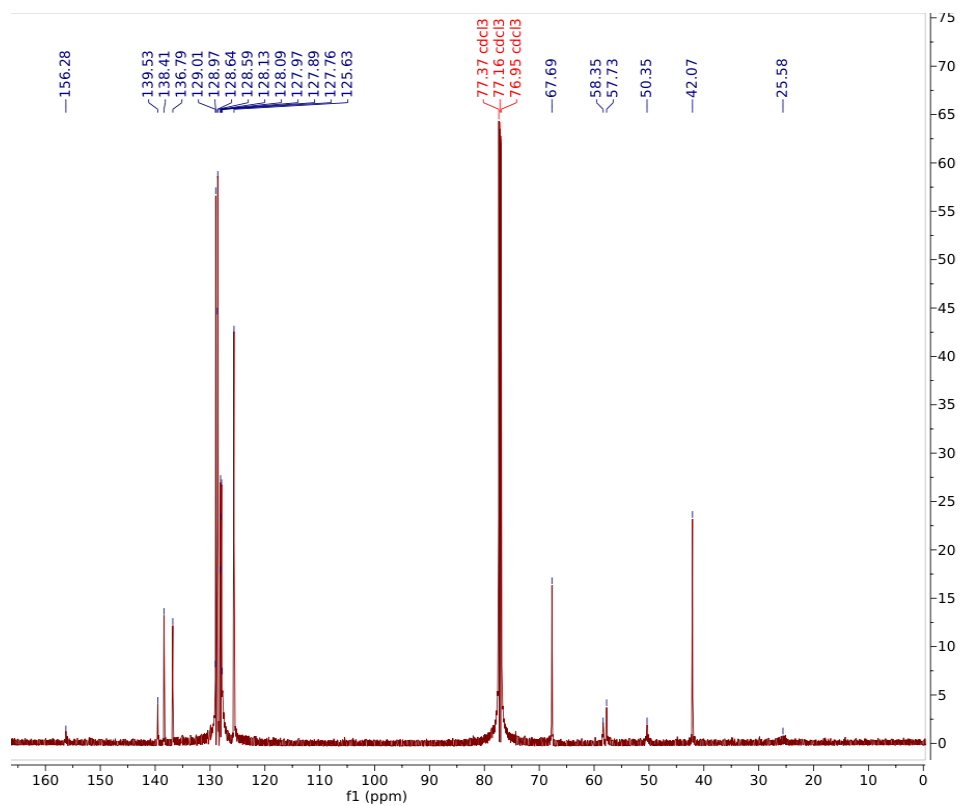
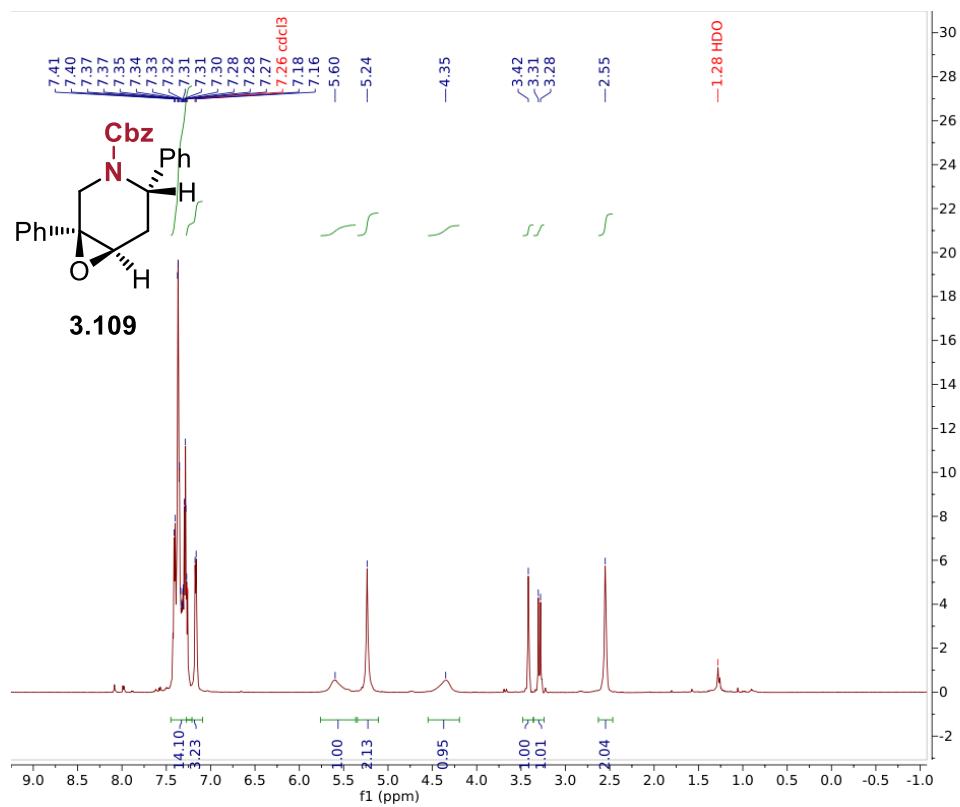
81 mg (0.22 mmol) of **3.70** was dissolved in  $\text{CH}_2\text{Cl}_2$  (10 ml) and was cooled to  $4^{\circ}\text{C}$ . *m*-CPBA (0.44 mmol, 108 mg of 70% w/w) was subsequently added and the reaction was warmed to room temperature and stirred overnight. The reaction was then diluted with 50 ml  $\text{H}_2\text{O}$  and extracted with  $\text{CH}_2\text{Cl}_2$ . The organic layers were combined and washed with  $\text{NaHCO}_3$  and brine and dried over  $\text{MgSO}_4$ . The desired epoxide **3.109** was obtained using flash silica chromatography with 5% Acetone in Hexanes as a viscous, colorless yield (67.0 mg, 78%).

**$^1\text{H}$  NMR** (598 MHz,  $\text{CDCl}_3$ )  $\delta$  7.45 – 7.21 (ArH, m, 13H), 7.17 (ArH, d,  $J$  = 7.4 Hz, 2H), 5.60 ( $\text{H}^5$ , s, 1H), 5.24 (Cbz- $\text{CH}_2$ , s, 2H), 4.35 ( $\text{H}^1$ , s, 1H), 3.42 ( $\text{H}^3$ , s, 1H), 3.29 ( $\text{H}^1$ , d,  $J$  = 15.0 Hz, 1H), 2.55 ( $\text{H}^4$ , s, 2H) ppm.

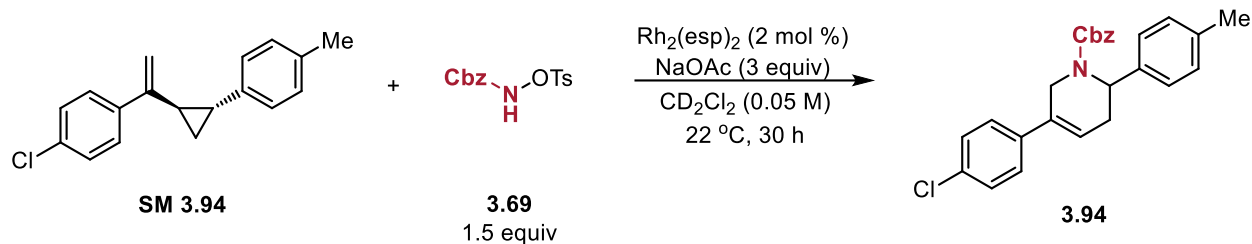
**$^{13}\text{C}$  NMR** (150 MHz,  $\text{CDCl}_3$ )  $\delta$  156.3, 139.5, 138.4, 136.8, 129.0, 129.0, 128.6, 128.6, 128.1, 128.1, 128.0, 127.9, 127.8, 125.6, 67.7, 58.4, 57.7, 50.4, 42.1, 25.6 ppm.

**IR** (film):  $\bar{\nu}$  = 3030 (w), 2929 (w), 2355 (w), 1695 (bs), 1235 (bs), 1103 (s), 736 (s), 698 (s)  $\text{cm}^{-1}$ .

**HRMS** (ESI):  $m/z$  calculated for  $[\text{C}_{26}\text{H}_{25}\text{O}_3+\text{H}]^+$ : 386.1756; found: 386.1755.



### 1.9. NMR Study of $\text{Rh}_2(\text{esp})_2$ catalyzed [5+1] reaction



Under inert atmosphere, 0.1 mmol vinylcyclopropane **SM 3.94** was dissolved with 0.15 mmol (48 mg) CbzNHOTs and 3.0 mmol (25 mg) NaOAc in 2 mL  $\text{CD}_2\text{Cl}_2$  at room temperature. To this was added 2 mol% (1.5 mg)  $\text{Rh}_2(\text{esp})_2$ . Relative concentrations of the reactant (**SM 3.94**) and desired product (**3.94**) were determined from 50  $\mu\text{L}$  aliquots of the reaction mixture, assessed by  $^1\text{H}$  NMR referenced to the residual solvent peak.

### 1.10. References

- (1) Chen, C.; Shen, X.; Chen, J.; Hong, X.; Lu, Z. *Org. Lett.* **2017**, *19*, 5422.
- (2) Combee, L. A.; Raya, B.; Wang, D.; Hilinski, M. K. *Chem. Sci.* **2018**, *9*, 935.
- (3) Masruri; A. C. Willis, M. D. McLeod, *J. Org. Chem.*, **2012**, *77*, 8480.
- (4) Ng, K. -H.; Chan, A. S. C.; Yu, W. -Y. *J. Am. Chem. Soc.* **2010**, *132*, 12862-12864.
- (5) Qin, L.; Zhou, Z.; Wei, J.; Yan, T.; Wen, H. *Syn. Commun.* **2010**, *40*, 642-646.

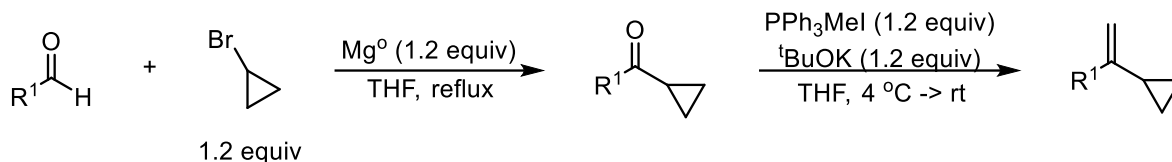
## APPENDIX 2

### Chapter 4 Experimental and Characterization

#### 2.1. General Methods

All reagents and solvents were obtained commercially in reagent grade or better quality and used without further purification. Anhydrous dichloromethane and tetrahydrofuran were obtained by degassing followed by passing through an alumina drying column before use. Anhydrous DMSO was purchased from Acros Organics and used directly. Flash column chromatography was performed using silica gel (230-400 mesh) purchased from Silicycle.  $^1\text{H}$  and  $^{13}\text{C}$  spectra were acquired at 300 K on a Bruker Avance III (600 MHz or 800 MHz) or Varian NMRS (600 MHz) spectrometer. Chemical shifts are reported in parts per million (ppm  $\delta$ ) referenced to the residual  $^1\text{H}$  resonance of the solvent. The following abbreviations are used singularly or in combination to indicate the multiplicity of signals: s - singlet, d - doublet, t - triplet, q - quartet, m - multiplet and br - broad. IR spectra were recorded on a Shimadzu IRAffinity-1S FTIR spectrophotometer with ATR attachment. High-resolution mass spectrometry was obtained from the University of Illinois at Urbana-Champaign Mass Spectrometry Lab using Waters Q-TOF ESI or Waters oa-TOF EI spectrometers.

## 2.2. General procedure for synthesis of 2-substituted vinylcyclopropanes

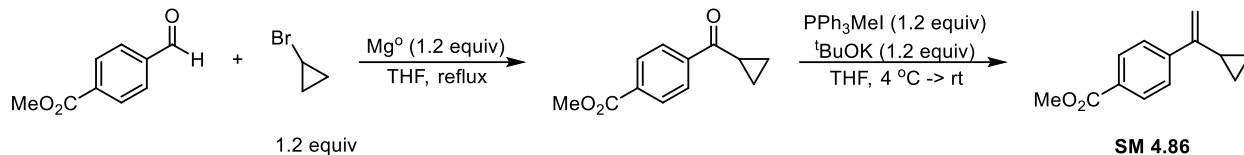


Mg<sup>0</sup> (19 mmol) and cyclopropyl bromide (19 mmol) were combined in THF (40 ml) under inert atmosphere and stirred at reflux for three hours. The reaction mixture was cooled to 4°C and the corresponding benzaldehyde was added dropwise. Following the addition, the reaction was then set to reflux and stirred until the starting material was consumed (~24 hours) by TLC. Reaction was then quenched with NH<sub>4</sub>Cl and extracted with EtOAc. Organic layer was then washed with NH<sub>4</sub>Cl, brine, and dried over magnesium sulfate. The corresponding cyclopropyl ketone was then isolated by silica gel chromatography (5% EtOAc in hexanes).

Methyl triphenylphosphonium iodide (6 mmol) was suspended in THF (30 ml) under an inert atmosphere at 4°C. <sup>t</sup>BuOK (6 mmol) was added portionwise and the suspension was stirred for 30 minutes. The corresponding cyclopropyl ketone was added and the reaction was warmed to room temperature and stirred until the starting material was consumed, monitored by TLC (1 – 24 hrs). The reaction was then quenched by NH<sub>4</sub>Cl, added to NH<sub>4</sub>Cl, and extracted with Et<sub>2</sub>O. The organic layers were then washed with NH<sub>4</sub>Cl, brine, and dried over Na<sub>2</sub>SO<sub>4</sub>. The corresponding vinylcyclopropane was isolated by silica gel chromatography (0-3% EtOAc in hexanes).

**4.65,<sup>1</sup> SM 4.80 – 4.85, SM 4.87,<sup>2</sup> SM 4.93,<sup>3</sup> SM 4.95<sup>4</sup>** were synthesized according to literature procedures.

### 2.3. Characterization of new 2-substituted vinylcyclopropanes



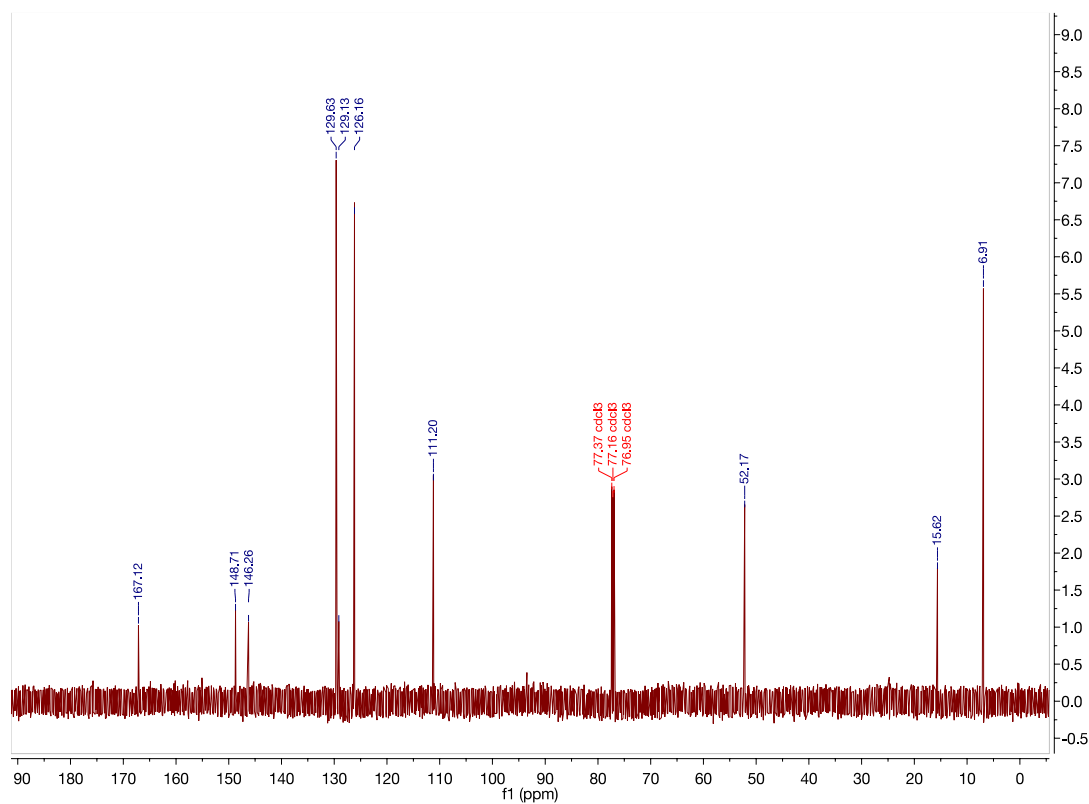
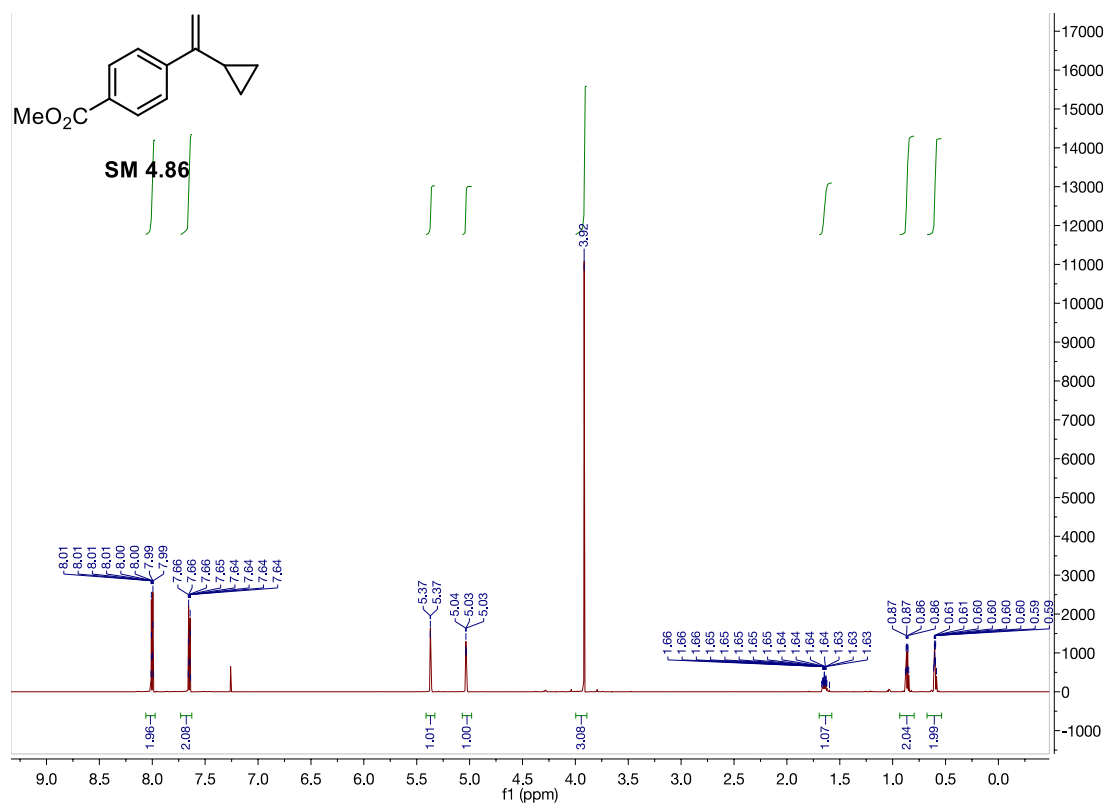
Prepared using the general procedure and purified via silica flash chromatography with 2% ethyl acetate in hexanes as a white crystalline solid (56% yield).

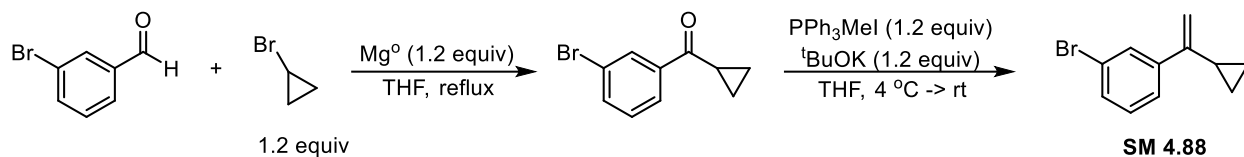
**<sup>1</sup>H NMR** (600 MHz, CDCl<sub>3</sub>) δ 8.01 – 7.99 (m, 2H), 7.65 – 7.63, (m, 2H), 5.37 (s, 1H), 5.08 (s, 1H), 3.92 (s, 3H), 1.64 (ttt, *J* = 8.3, 5.4, 1.3 Hz 1H), 0.87 – 0.84 (m, 2H), 0.61 – 0.58 (m, 2H) ppm.

**<sup>13</sup>C NMR** (151 MHz, CDCl<sub>3</sub>) δ 167.12, 148.70, 146.25, 129.63 (2C), 129.13, 126.15 (2C), 111.19, 52.17, 15.62, 6.90 (2C) ppm.

**IR** (film):  $\bar{\nu}$  = 3082 (w), 3001 (w), 2949 (w), 1813 (w), 1708 (s), 1608 (m), 1277 (m), 901 (s), 782 (s), 718 (s) cm<sup>-1</sup>.

**HRMS** (EI): *m/z* calculated for [C<sub>13</sub>H<sub>14</sub>O<sub>2</sub>]<sup>+</sup>: 202.0994; found: 202.0995.





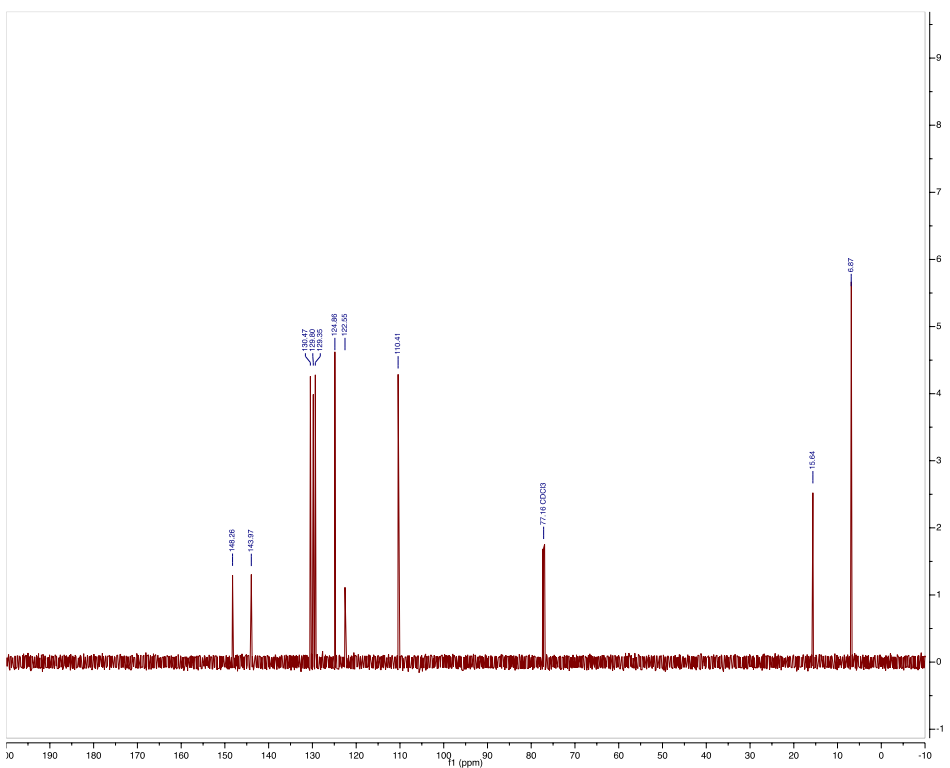
Prepared using the general procedure and purified via silica flash chromatography with 2% ethyl acetate in hexanes as clear liquid (56% yield).

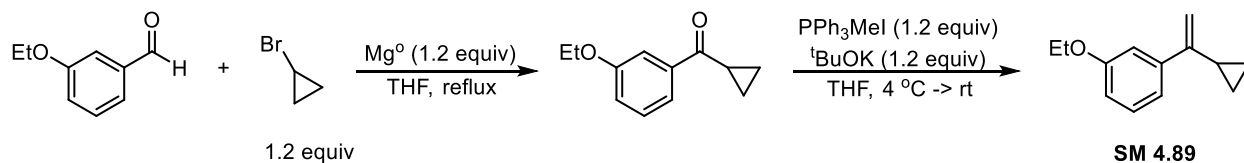
**$^1\text{H}$  NMR** (598 MHz,  $\text{CDCl}_3$ )  $\delta$  7.75 – 7.73 (m, 1H), 7.53 – 7.51 (m, 1H), 7.42-7.40 (m, 1H), 7.22 – 7.20 (m, 1H), 5.29 (s, 1H), 4.98 (d,  $J = 1.2$  Hz, 1H), 1.63 – 1.59 (m, 1H), 0.90 – 0.81 (m, 2H), 0.65 – 0.55 (m, 2H) ppm.

**$^{13}\text{C}$  NMR** (150 MHz,  $\text{CDCl}_3$ )  $\delta$  148.26, 143.96, 130.47, 129.79, 129.35, 124.86, 122.55, 110.41, 15.64, 6.86 (2C) ppm.

**IR** (film):  $\bar{\nu} = 3084$  (w), 3001 (w), 1591 (m), 1556 (s), 1257 (m), 883 (s), 785 (s)  $\text{cm}^{-1}$ .

**HRMS** (EI):  $m/z$  calculated for  $[\text{C}_{11}\text{H}_{11}\text{Br}]^+$ : 222.0044; found: 222.0046.





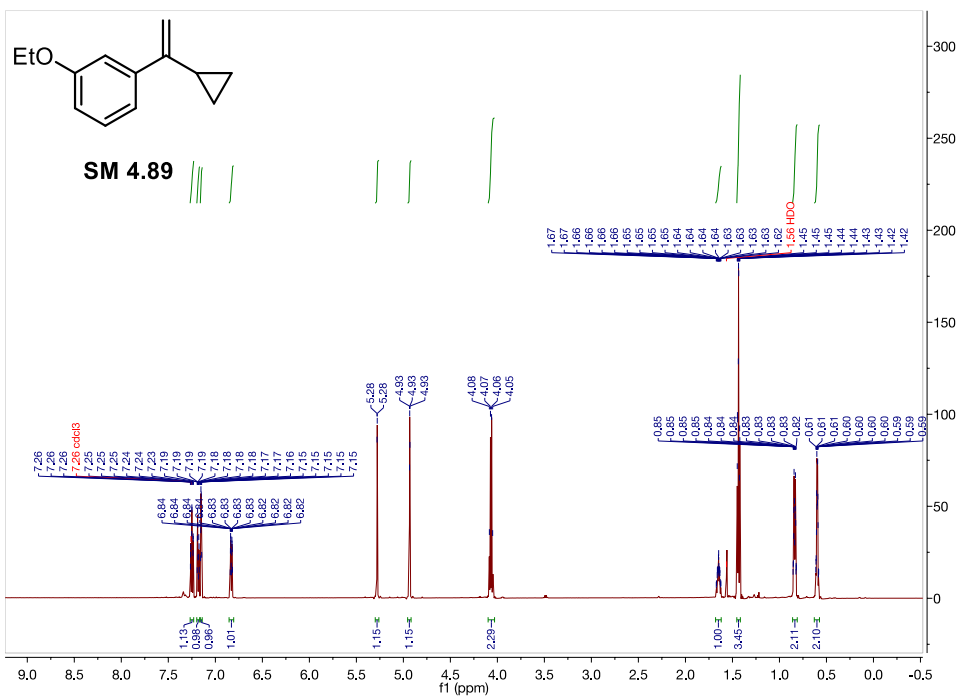
Prepared using the general procedure and purified via silica flash chromatography with 2% ethyl acetate in hexanes as a yellow liquid (40% yield).

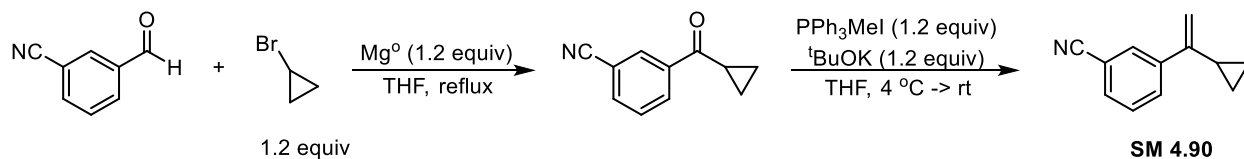
**<sup>1</sup>H NMR** (600 MHz, CDCl<sub>3</sub>) δ 7.26 – 7.23 (m, 1H), 7.19 – 7.16 (m, 1H), 7.15 – 7.14 (m, 1H) 6.84 – 6.81 (m, 1H), 5.24 (d, *J* = 1.3 Hz, 1H), 4.92 (t, *J* = 1.2 Hz, 1H), 4.06 (q, *J* = 7.0 Hz, 2H), 1.67 – 1.61 (m, 1H), 1.43 (tt, *J* = 6.9, 1.0 Hz, 3H) 0.85 – 0.82 (m, 2H), 0.61 – 0.58 (m, 2H) ppm.

**<sup>13</sup>C NMR** (151 MHz, CDCl<sub>3</sub>) δ 158.95, 149.43, 143.31, 129.17, 118.73, 113.28, 112.92, 109.30, 63.52, 15.80, 15.04, 6.85 ppm.

**IR** (film):  $\bar{\nu}$  = 3082 (w), 2980 (w), 1597 (m), 1487 (m), 1276 (m), 1049 (m), 935 (s), 879 (s), 779 (s) cm<sup>-1</sup>.

**HRMS** (EI): *m/z* calculated for [C<sub>17</sub>H<sub>15</sub>I]<sup>+</sup>: 188.1201; found: 188.1201.





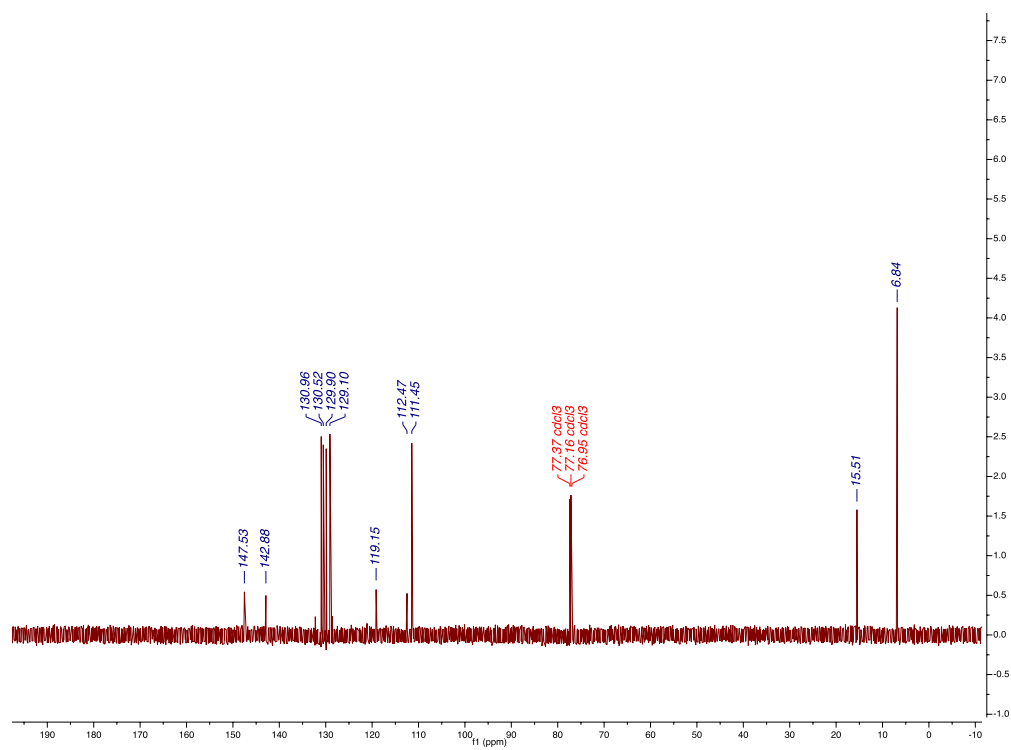
Prepared using the general procedure and purified via silica flash chromatography with 2% ethyl acetate in hexanes as a clear liquid (67% yield).

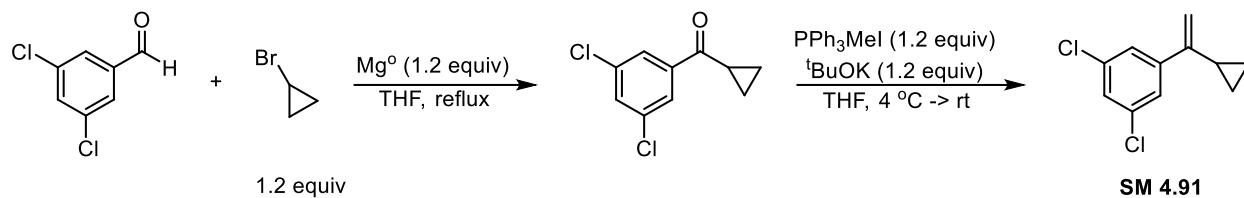
**<sup>1</sup>H NMR** (600 MHz, CDCl<sub>3</sub>) δ 7.88 – 7.86 (m, 1H), 7.83 – 7.78 (m, 1H), 7.58 – 7.54 (m, 1H), 7.44 – 7.42 (m, 1H), 5.34 (s, 1H), 5.05 (d, *J* = 1.3 Hz, 1H), 1.64 – 1.58 (m, 1H), 0.91 – 0.87 (m, 2H), 0.62 – 0.59 (m, 2H) ppm.

**<sup>13</sup>C NMR** (150 MHz, CDCl<sub>3</sub>) δ 147.53, 142.88, 130.96, 130.52, 129.90, 129.10, 119.15, 112.47, 111.45, 15.51, 6.84 (2C) ppm.

**IR** (film):  $\bar{\nu}$  = 3089 (w), 3003 (w), 2365 (w), 2229 (w), 1625 (m), 1479 (m), 896 (s), 800 (s) cm<sup>-1</sup>.

**HRMS** (EI): *m/z* calculated for [C<sub>12</sub>H<sub>11</sub>N]<sup>+</sup>: 168.0813; found: 168.0810.

[illegible]



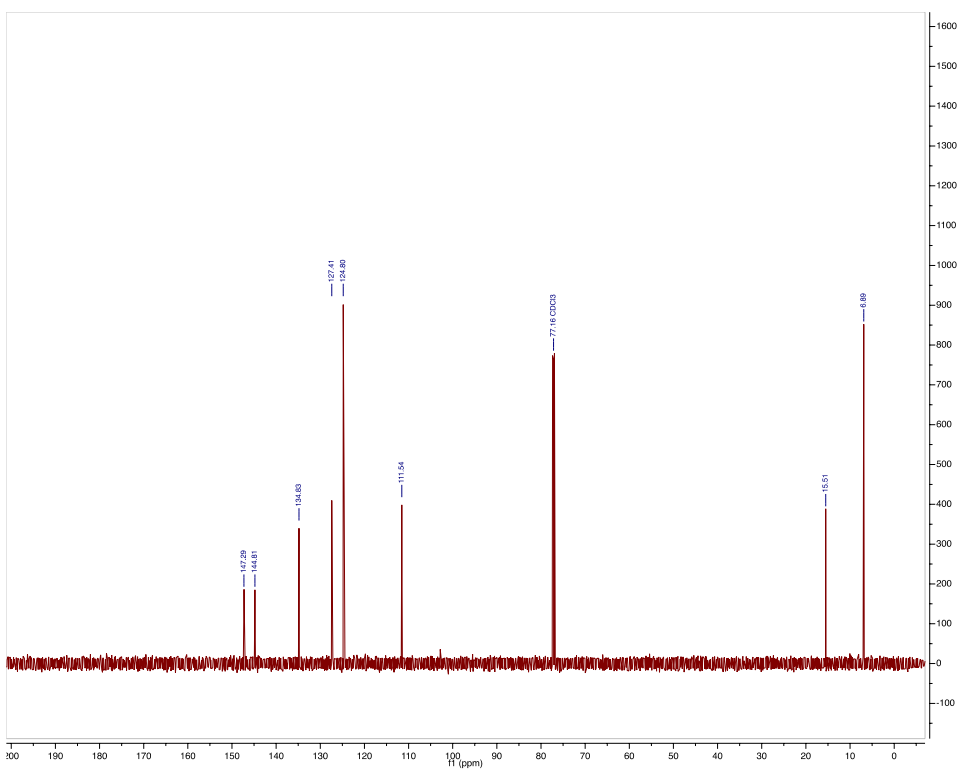
Prepared using the general procedure and purified via silica flash chromatography with 2% ethyl acetate in hexanes as a clear liquid (82% yield).

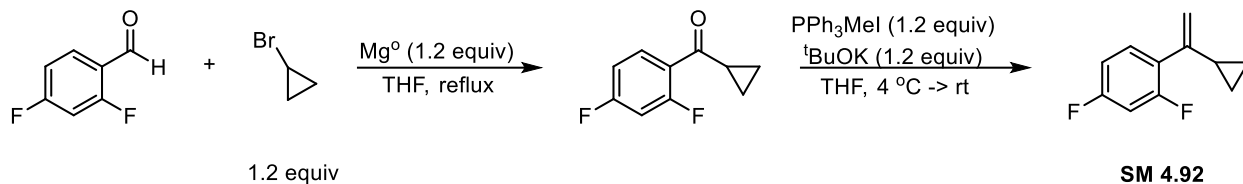
**<sup>1</sup>H NMR** (600 MHz, CDCl<sub>3</sub>) δ 7.45 (d, *J* = 1.9 Hz, 2H), 7.27 (s, 1H), 5.30 (s, 1H), 5.01 (d, *J* = 1.4 Hz, 1H), 1.60 – 1.53 (m, 1H), 0.89 – 0.83 (m, 2H), 0.61 – 0.57 (m, 2H) ppm.

**<sup>13</sup>C NMR** (151 MHz, CDCl<sub>3</sub>) δ 147.29, 144.81, 134.83 (2C), 127.41, 124.80 (2C), 111.54, 15.51, 6.89 (2C) ppm.

**IR** (film):  $\bar{\nu}$  = 3084 (w), 3005 (w), 2362 (w), 1583 (m), 1558 (s), 1379 (m), 1261 (m), 877 (s), 799 (s) cm<sup>-1</sup>.

**HRMS** (EI): *m/z* calculated for [C<sub>11</sub>H<sub>10</sub>Cl<sub>2</sub>]<sup>+</sup>: 212.0160; found: 212.0162.





Prepared using the general procedure and purified via silica flash chromatography with 2% ethyl acetate in hexanes as a clear liquid (64% yield).

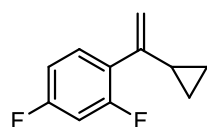
**<sup>1</sup>H NMR** (598 MHz, CDCl<sub>3</sub>) δ 7.32 (td, *J* = 8.6, 6.5 Hz, 1H), 6.86 – 6.77 (m, 2H), 5.15 (s, 1H), 5.11 (s, 1H), 1.67 – 1.61 (m, 1H), 0.79 – 0.74 (m, 2H), 0.54 – 0.49 (m, 2H) ppm.

**<sup>13</sup>C NMR** (150 MHz, CDCl<sub>3</sub>) δ 163.11 – 161.13 (m), 160.08 (dd, *J* = 250.2, 11.8 Hz), 144.79 (d, *J* = 1.7 Hz), 130.85 (dd, *J* = 9.3, 5.6 Hz), 125.99 (dd, *J* = 14.8, 3.9 Hz), 113.38 (dd, *J* = 4.1, 1.1 Hz), 110.92 (dd, *J* = 20.9, 3.7 Hz), 104.12 (dd, *J* = 27.0, 25.1 Hz), 16.77, 6.86 ppm.

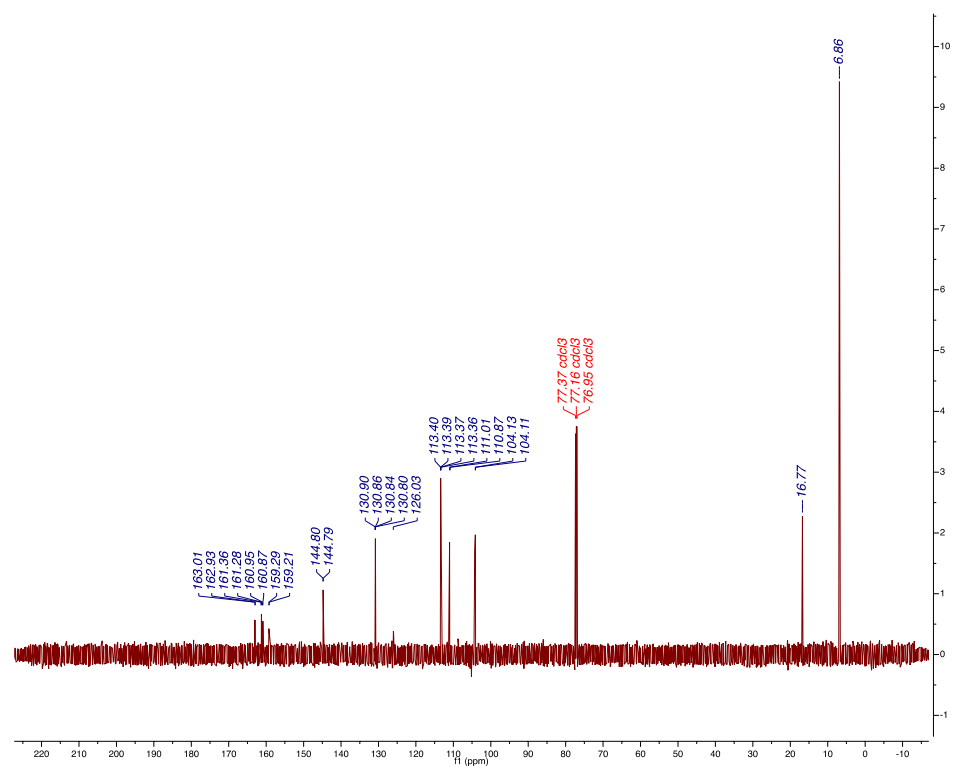
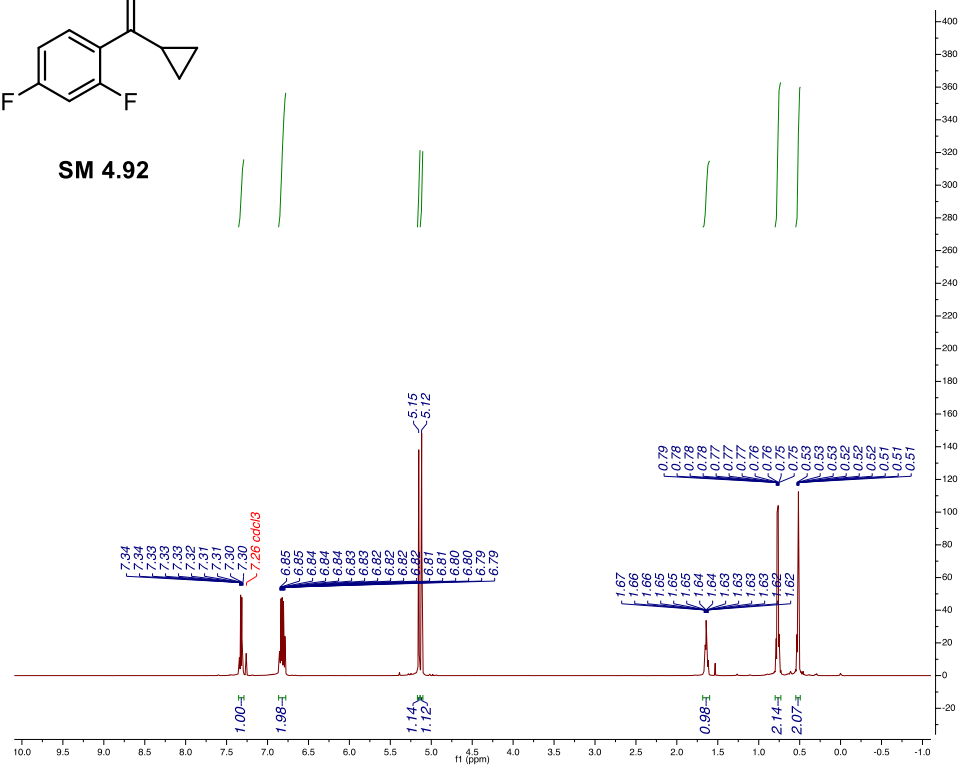
**<sup>19</sup>F NMR** (563 MHz, CDCl<sub>3</sub>) δ -110.54 (q, *J* = 8.8 Hz), -112.11 (p, *J* = 7.8 Hz).

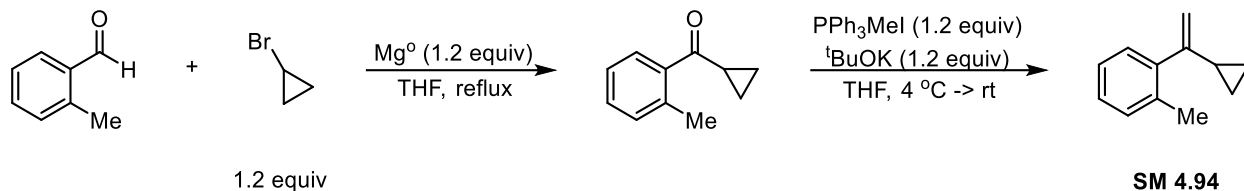
**IR** (film):  $\bar{\nu}$  = 3086 (w), 2926 (w), 2365 (w), 1608 (b), 1502 (s), 1267 (m), 1138 (m), 968 (s), 848 (s) cm<sup>-1</sup>.

**HRMS** (EI): *m/z* calculated for [C<sub>11</sub>H<sub>10</sub>F<sub>2</sub>]<sup>+</sup>: 180.0751; found: 180.0753.



SM 4.92





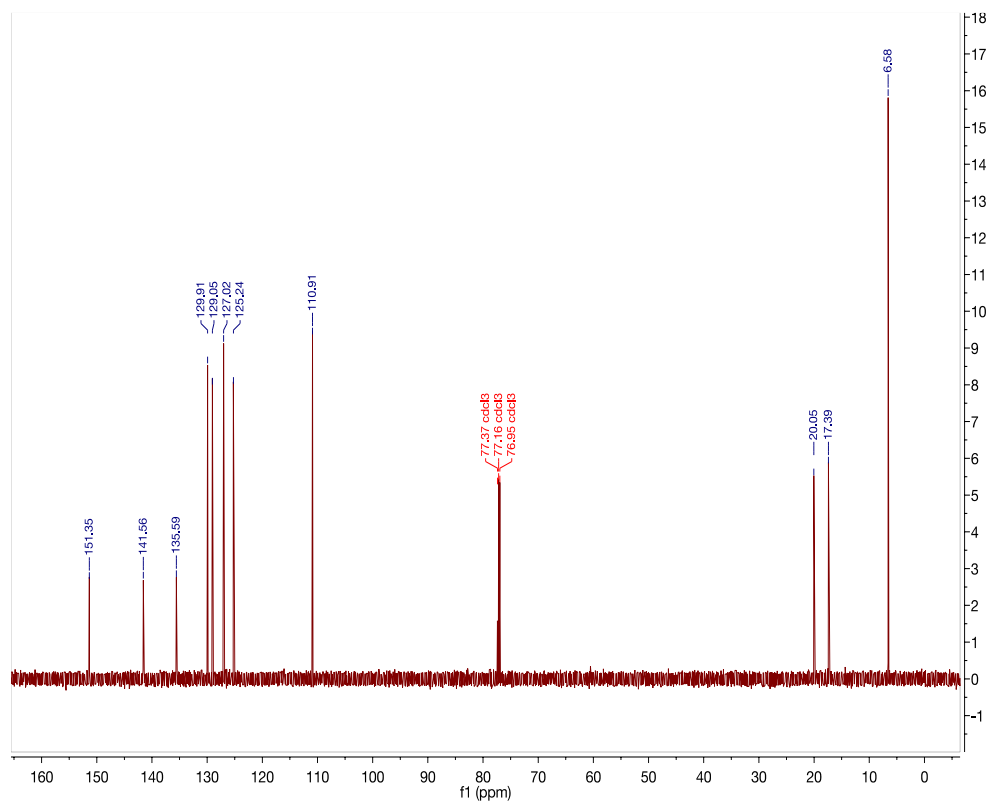
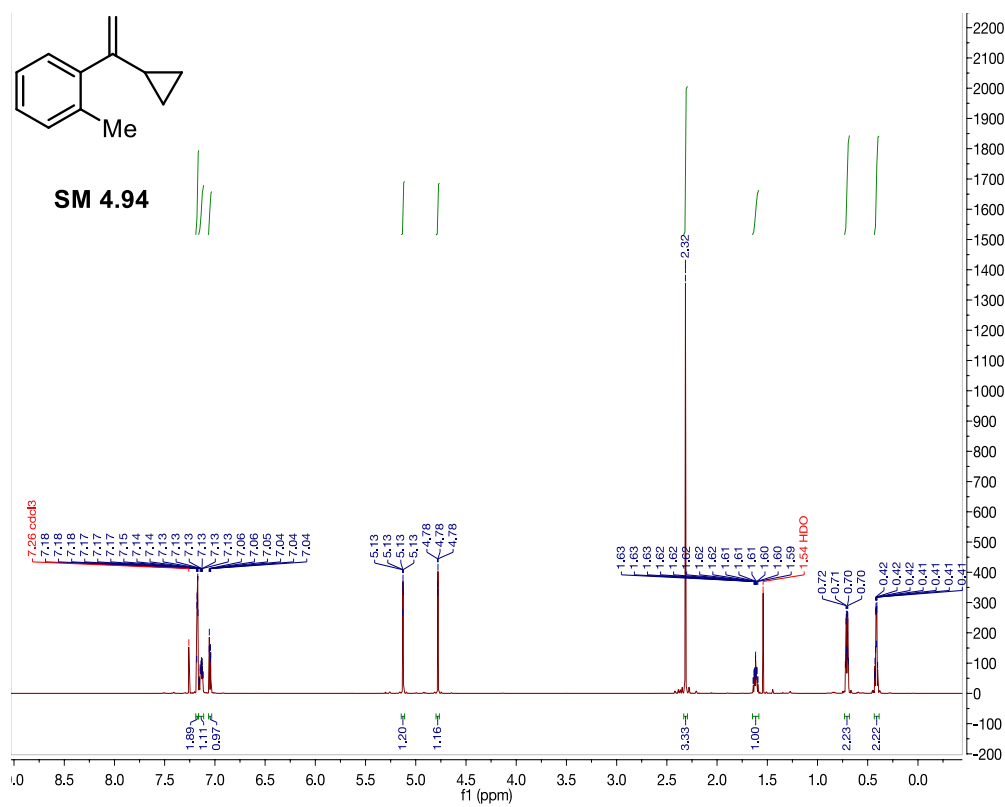
Prepared using the general procedure and purified via silica flash chromatography with 1% ethyl acetate in hexanes as a clear liquid (72% yield).

**<sup>1</sup>H NMR** (600 MHz, CDCl<sub>3</sub>) δ 7.19 – 7.17 (m, 2H), 7.16 – 7.12 (m, 1H), 7.07 – 7.04 (m, 1H), 5.14 – 5.13 (m, 1H), 4.80 – 4.78 (m, 1H), 2.32 (s, 3H), 1.65 – 1.60 (m, 1H), 0.74 – 0.69 (m, 2H), 0.44 – 0.40 (m, 2H) ppm.

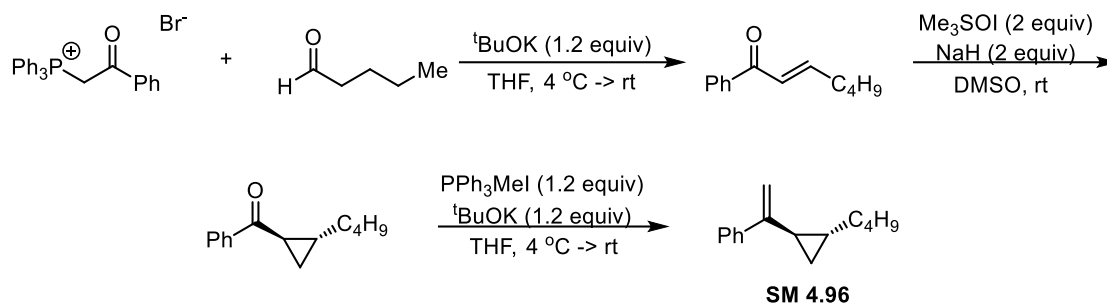
**<sup>13</sup>C NMR** (151 MHz, CDCl<sub>3</sub>) δ 151.35, 141.56, 135.59, 129.91, 129.05, 127.02, 125.24, 110.91, 20.05, 17.39, 6.58 ppm.

**IR** (film):  $\bar{\nu}$  = 3082 (w), 3010 (w), 1626 (m), 1487 (w), 939 (w), 729 (s) cm<sup>-1</sup>.

**HRMS** (EI): *m/z* calculated for [C<sub>12</sub>H<sub>14</sub>]<sup>+</sup>: 158.1096; found: 158.1094.



## 2.4. Synthesis of (1-((1*R*,2*R*)-2-butylcyclopropyl)vinyl)benzene (SM 4.96)



(2-oxo-2-phenylethyl) triphenylphosphonium bromide (12 mmol) was suspended in anhydrous THF (30 ml) under an inert atmosphere at 4°C. <sup>t</sup>BuOK (12 mmol) was added portionwise and the suspension was stirred for 30 minutes. Valeraldehyde was added and the reaction was warmed to room temperature and stirred until the starting material was consumed, monitored by TLC (24 hrs). The reaction was then quenched by NH<sub>4</sub>Cl, added to NH<sub>4</sub>Cl, and extracted with Et<sub>2</sub>O. The organic layers were then washed with NH<sub>4</sub>Cl, brine, and dried over Na<sub>2</sub>SO<sub>4</sub>. (*E*)-1-phenylhept-2-en-1-one was isolated by silica gel chromatography (3% EtOAc in hexanes) in 54% yield.

Trimethylsulfoxonium iodide (10.8 mmol) was dissolved in 25 mL anhydrous DMSO under inert atmosphere at ambient temperature. Sodium hydride (10.8 mmol) was added portionwise and the mixture was stirred 30 minutes at which time the enone (5.4 mmol) was added in a single portion. The reaction was stirred overnight then quenched with saturated aqueous NH<sub>4</sub>Cl before being extracted with Et<sub>2</sub>O. Combined organic layers were washed with aqueous NH<sub>4</sub>Cl, then brine and dried over Na<sub>2</sub>SO<sub>4</sub>. The filtrate was concentrated and purified by silica gel chromatography (3% ethyl acetate in hexanes) to afford ((1*R*,2*R*)-2-butylcyclopropyl)(phenyl)methanone as a yellow oil (42% yield).

Methyl triphenylphosphonium iodide (2.8 mmol) was suspended in anhydrous THF (20 mL) under inert atmosphere. After cooling to 4°C, potassium tert-butoxide (2.8 mmol) was

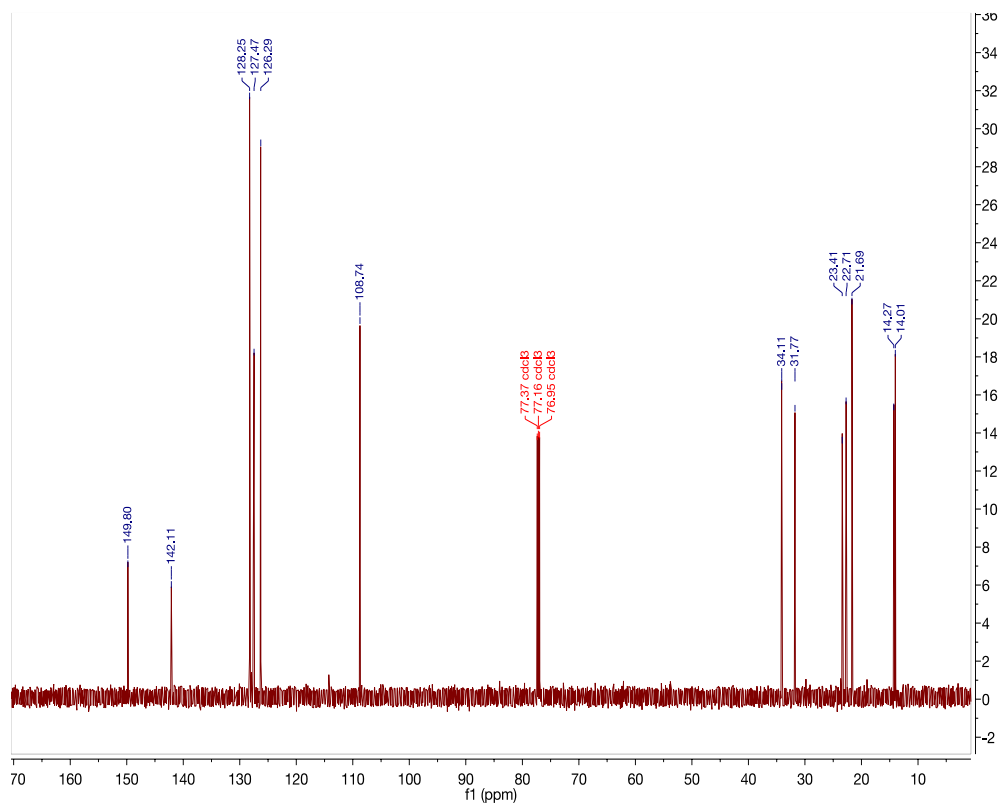
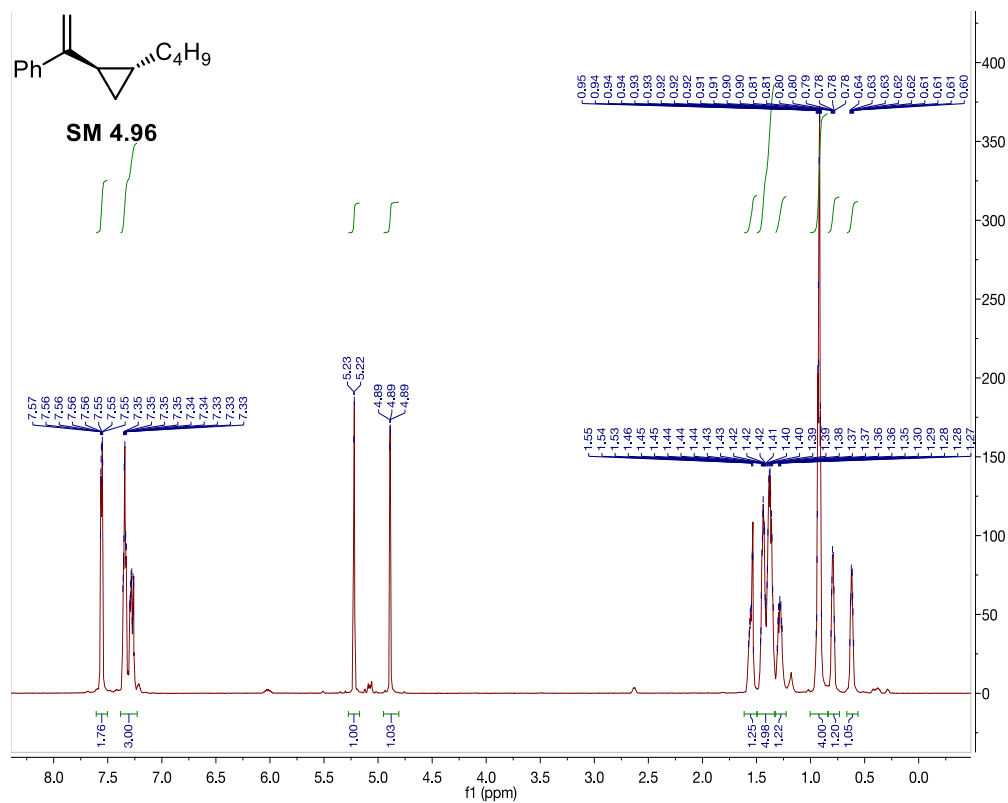
added and stirred for 30 minutes. The cyclopropyl ketone (2.3 mmol) was added in a single portion and the reaction mixture was allowed to warm to ambient temperature. After stirring overnight, the reaction was quenched with aqueous  $\text{NH}_4\text{Cl}$ , added to aqueous  $\text{NH}_4\text{Cl}$  (50 ml) and extracted with  $\text{Et}_2\text{O}$  (50 ml x 3). The combined organic extracts were washed with aqueous  $\text{NH}_4\text{Cl}$  (40 ml), brine (50 ml x 2) and dried over  $\text{Na}_2\text{SO}_4$ . The filtrate was concentrated and purified by silica gel chromatography (3% ethyl acetate in hexanes) to afford **SM 4.96** as a clear liquid (78% yield).

**$^1\text{H}$  NMR** (600 MHz,  $\text{CDCl}_3$ )  $\delta$  7.57 – 7.55 (m, 2H), 7.42 – 7.32 (m, 2H), 7.31 – 7.24 (m, 1H), 5.22 (d,  $J$  = 3.0 Hz, 1H), 4.99 – 4.63 (m, 1H), 1.70 – 1.49 (m, 1H), 1.49 – 1.25 (m, 6H), 0.95 – 0.85 (m, 4H), 0.80 – 0.77 (m, 1H), 0.64 – 0.60 (m, 1H).

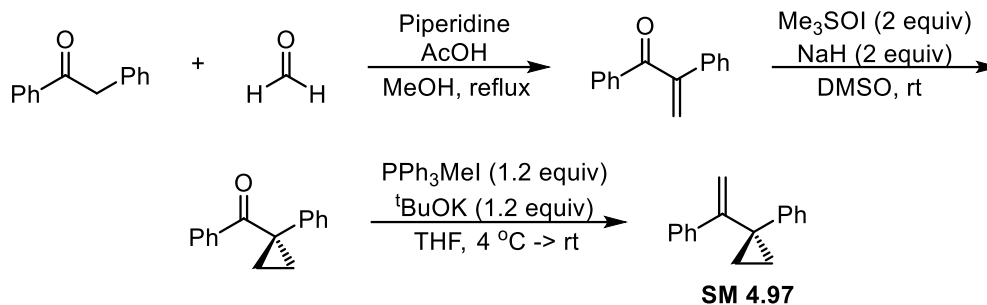
**$^{13}\text{C}$  NMR** (151 MHz,  $\text{CDCl}_3$ )  $\delta$  149.80, 142.11, 128.25 (2C), 127.47, 126.29 (2C), 108.74, 34.11, 31.77, 23.41, 22.71, 21.69, 14.27, 14.01.

**IR** (film):  $\bar{\nu}$  = 3030 (w), 1622 (w), 1494 (w), 1444 (w), 1028 (m), 889 (m), 775 (s), 702 (s)  $\text{cm}^{-1}$ .

**HRMS** (EI):  $m/z$  calculated for  $[\text{C}_{15}\text{H}_{20}]^+$ : 200.1565; found: 200.1567.



## 2.5. Synthesis of (1-(1-phenylcyclopropyl)vinyl)benzene (SM 4.97)



2-phenyl acetophenone (30 mmol) was dissolved in 100 ml of anhydrous MeOH under inert atmosphere at ambient temperature. Formaldehyde (10.6 ml), piperidine (0.4 ml) and acetic acid (0.4 ml) were subsequently added. The reaction was stirred at reflux overnight then cooled to room temperature and added to brine and extracted with EtOAc. The combined organic extracts were washed with 1M HCl, aqueous NaHCO<sub>3</sub>, brine, and dried over Na<sub>2</sub>SO<sub>4</sub>. The organic layers were concentrated and afforded 1,2-diphenylprop-2-en-1-one as a gold liquid in quantitative yield.

Trimethylsulfoxonium iodide (60 mmol) was dissolved in 100 mL anhydrous DMSO under inert atmosphere at ambient temperature. Sodium hydride (60 mmol) was added portionwise and the mixture was stirred 30 minutes at which time the vinyl ketone (30 mmol) was added in a single portion. The reaction was stirred overnight then quenched with saturated aqueous NH<sub>4</sub>Cl before being extracted with Et<sub>2</sub>O. Combined organic layers were washed with aqueous NH<sub>4</sub>Cl, then brine, and dried over Na<sub>2</sub>SO<sub>4</sub>. The organic layers were concentrated and afforded phenyl(1-phenylcyclopropyl)methanone as beige crystals (85% yield).

Methyl triphenylphosphonium iodide (12 mmol) was suspended in anhydrous THF (60 mL) under inert atmosphere. After cooling to 4 °C, potassium tert-butoxide (12 mmol) was added and stirred 30 minutes. The cyclopropyl ketone (10 mmol) was added in a single

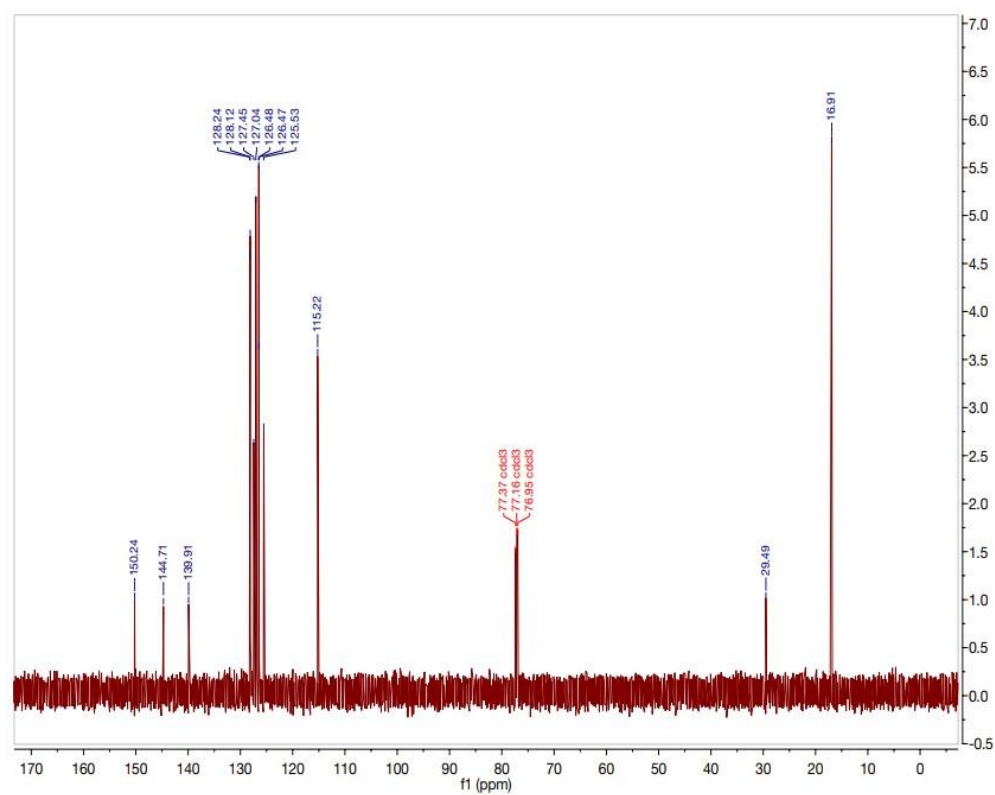
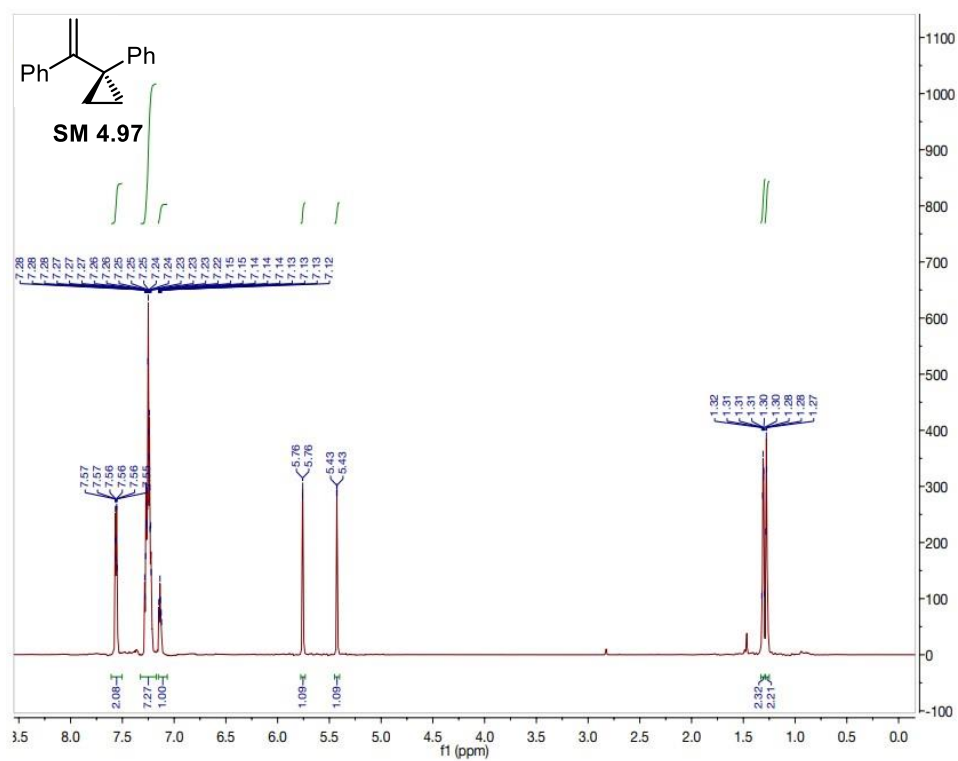
portion and the reaction mixture was allowed to warm to ambient temperature. After stirring overnight, the reaction was quenched with aqueous  $\text{NH}_4\text{Cl}$ , added to aqueous  $\text{NH}_4\text{Cl}$  and extracted with  $\text{Et}_2\text{O}$ . The combined organic extracts were washed with aqueous  $\text{NH}_4\text{Cl}$ , brine, and dried over  $\text{Na}_2\text{SO}_4$ . The filtrate was concentrated and purified by silica gel chromatography (1% ethyl acetate in hexanes) to afford **SM 4.97** as a clear liquid (82% yield).

**$^1\text{H}$  NMR** (600 MHz,  $\text{CDCl}_3$ )  $\delta$  7.58 – 7.56 (m, 2H), 7.29 – 7.22 (m, 8H), 7.15 – 7.12 (m, 1H), 5.76 (d,  $J$  = 1.5 Hz, 1H), 5.43 (d,  $J$  = 1.7 Hz, 1H), 1.34 – 1.29 (m, 2H), 1.29 – 1.27 (m, 2H).

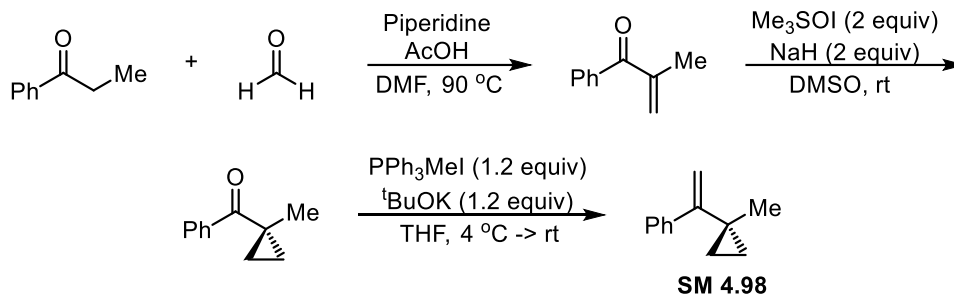
**$^{13}\text{C}$  NMR** (151 MHz,  $\text{CDCl}_3$ )  $\delta$  150.24, 144.71, 139.91, 128.24 (2C), 128.12 (2C), 127.45 (2C), 127.04 (2C), 126.48, 125.53, 115.22, 29.49, 16.91 (2C).

**IR** (film):  $\bar{\nu}$  = 3084 (w), 1600 (w), 1494 (w), 1028 (m), 904 (m), 779 (s), 756 (m), 696 (s)  $\text{cm}^{-1}$ .

**HRMS** (EI):  $m/z$  calculated for  $[\text{C}_{17}\text{H}_{16}]^+$ : 220.1252; found: 220.1257.



## 2.6. Synthesis of (1-(1-methylcyclopropyl)vinyl)benzene (SM 4.98)



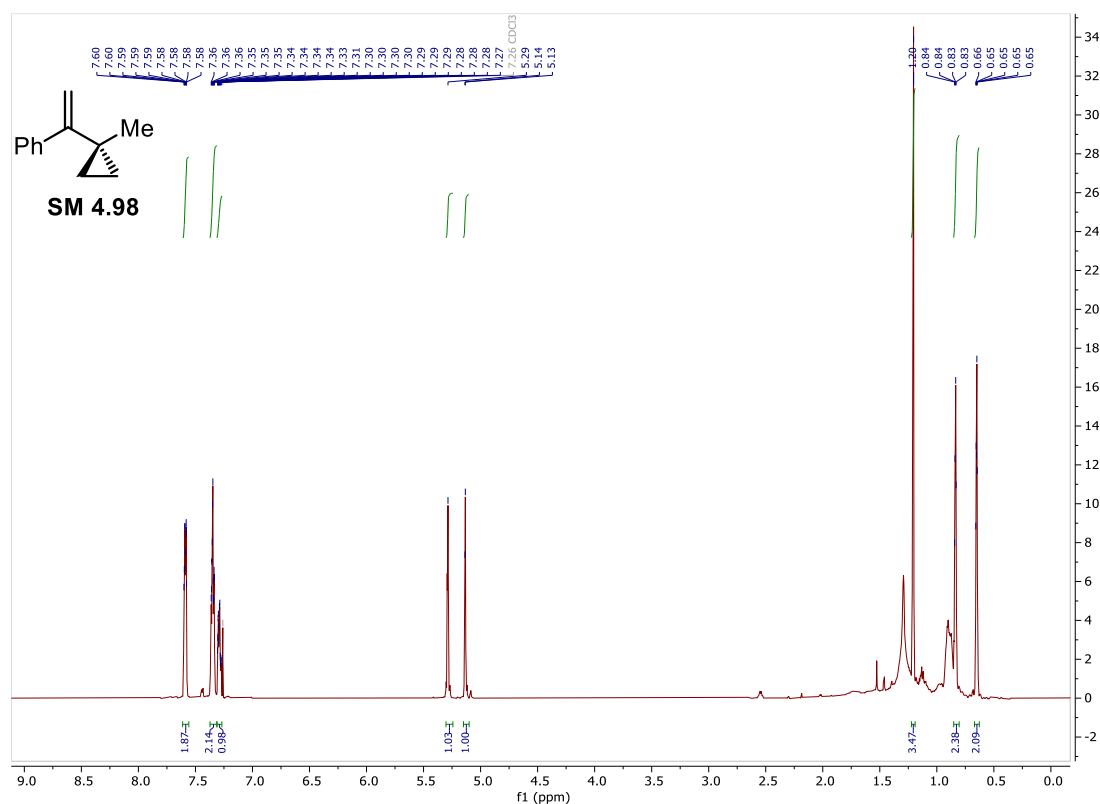
Propiophenone (15 mmol) was dissolved in 35 ml of anhydrous DMF under inert atmosphere at ambient temperature. Paraformaldehyde (90 ml), piperidine (0.19 ml) and acetic acid (0.19 ml) were subsequently added. The reaction was stirred at 90°C overnight then cooled to room temperature and added to water and extracted with Et<sub>2</sub>O. The combined organic extracts were washed with water and dried over Na<sub>2</sub>SO<sub>4</sub>. The organic layers were concentrated and afforded 2-methyl-1-phenylprop-2-en-1-one as a gold liquid without purification.

Trimethylsulfoxonium iodide (30 mmol) was dissolved in 35 mL anhydrous DMSO under inert atmosphere at ambient temperature. Sodium hydride (30 mmol) was added portionwise and the mixture was stirred 30 minutes at which time the vinyl ketone (30 mmol) was added in a single portion. The reaction was stirred overnight then quenched with saturated aqueous NH<sub>4</sub>Cl before being extracted with Et<sub>2</sub>O. Combined organic layers were washed with aqueous NH<sub>4</sub>Cl, then brine, and dried over Na<sub>2</sub>SO<sub>4</sub>. The organic layers were concentrated and afforded (1-methylcyclopropyl)(phenyl)methanone as a yellow oil without purification.

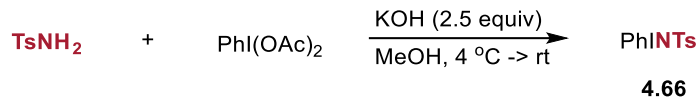
Methyl triphenylphosphonium iodide (18 mmol) was suspended in anhydrous THF (60 mL) under inert atmosphere. After cooling to 4°C, potassium tert-butoxide (18 mmol) was added and stirred 30 minutes. The cyclopropyl ketone (15 mmol) was added in a single

portion and the reaction mixture was allowed to warm to ambient temperature. After stirring overnight, the reaction was quenched with aqueous  $\text{NH}_4\text{Cl}$ , added to aqueous  $\text{NH}_4\text{Cl}$  and extracted with  $\text{Et}_2\text{O}$ . The combined organic extracts were washed with aqueous  $\text{NH}_4\text{Cl}$ , brine, and dried over  $\text{Na}_2\text{SO}_4$ . The filtrate was concentrated and purified by silica gel chromatography (1% ethyl acetate in hexanes) to afford **SM 4.98** as a clear liquid (54% yield over 3 steps).

**$^1\text{H}$  NMR** (600 MHz,  $\text{CDCl}_3$ )  $\delta$  7.60 – 7.58 (m, 2H), 7.36 – 7.33 (m, 2H), 7.31 – 7.27 (m, 1H), 5.29 (m, 1H), 5.13 (m, 1H), 1.20 (s, 3H), 0.84 – 1.82 (m, 2H), 0.66 – 0.65 (m, 2H).

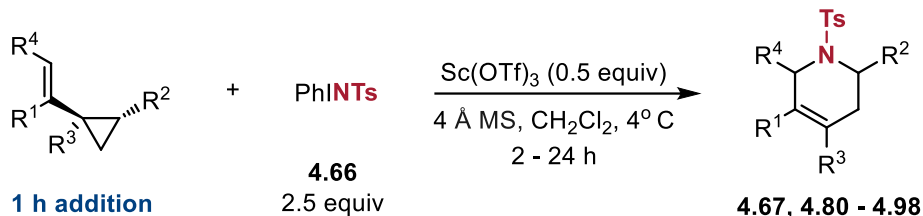


## 2.7. Synthesis of *N*-Tosylphenylimidoiodinane (PhINTs, 4.66)



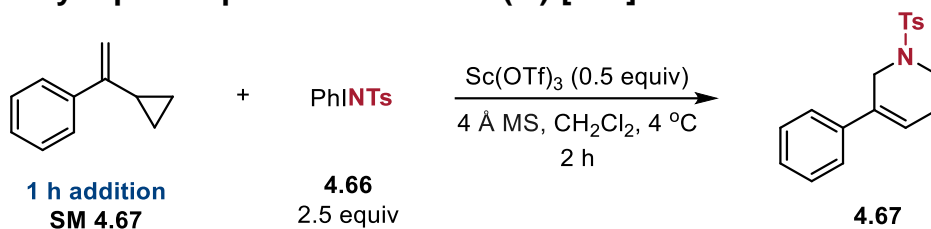
*p*-Toluenesulfonamide (20 mmol) and KOH (50 mmol) were dissolved in 80 ml of MeOH and cooled to 4°C. To the stirred solution diacetoxiodobenzene (20 mmol) was added portionwise. The yellow solution was then warmed to room temperature and stirred for 5 hours. The reaction was then cooled to 4°C, 100 ml of ice water was added, and the reaction was stirred for an additional hour at 4°C. The mixture was then filtered to collect the precipitate, which was subsequently washed with cold MeOH and cold EtOAc to afford **4.66** as a pale yellow solid (4.46 g, 65% yield). NMR data matched literature values.<sup>5</sup>

## 2.8. General procedure for the Sc(III)-promoted aza-[5+1] reaction



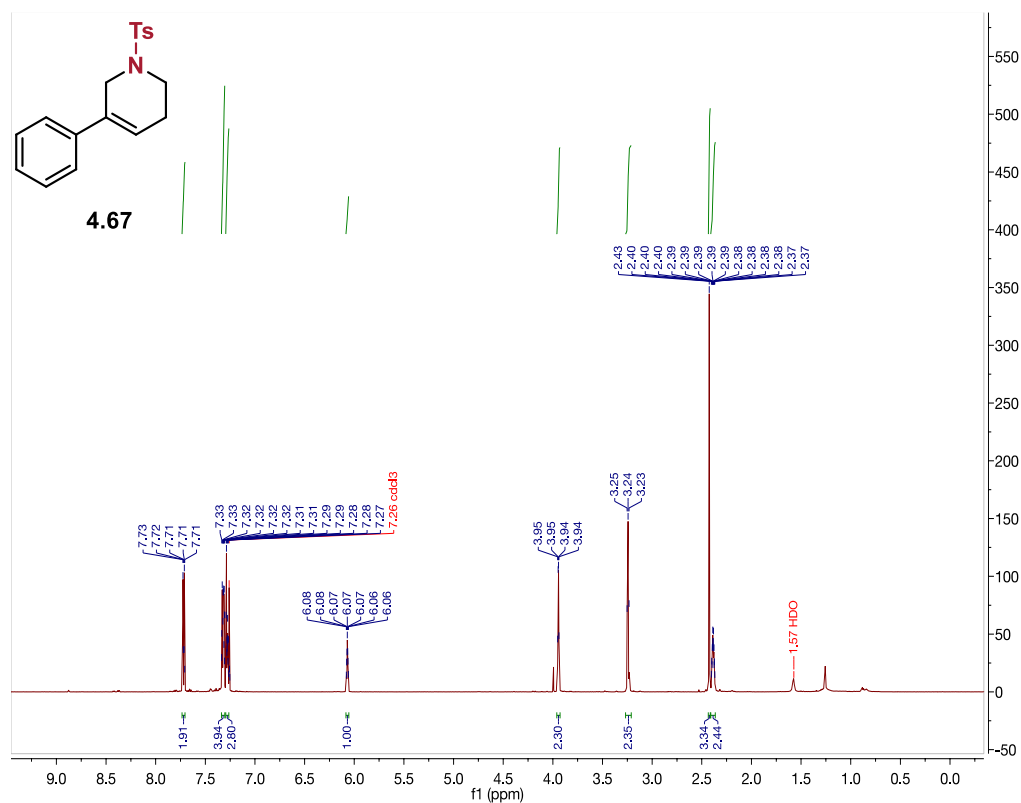
PhINTs (186 mg, 0.5 mmol), Sc(OTf)<sub>3</sub> (49 mg, 0.1 mmol), and 4 Å MS (30 mg) were combined in 600 µL of DCM under an inert atmosphere at 4°C. A solution of the corresponding vinylcyclopropane (0.2 mmol) was added to 400 µL of DCM and added dropwise over the course of an hour via syringe pump. After the starting material was consumed via TLC, the reaction was quenched with NaHCO<sub>3</sub> and extracted with DCM. The organic layers were washed with brine and dried over Na<sub>2</sub>SO<sub>4</sub>. The corresponding tetrahydropyridine products were then isolated via silica flash chromatography.

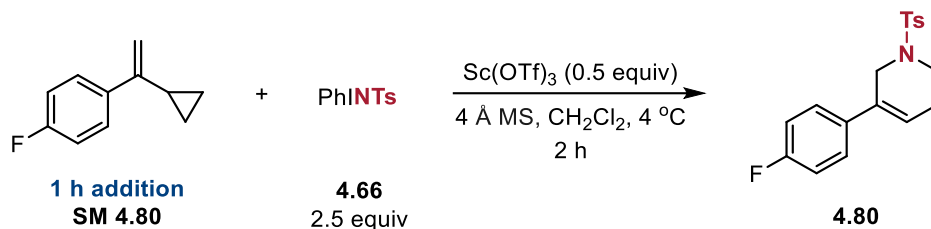
## 2.9. Previously reported products of the Sc(III)-[5+1] method



Synthesized using the general procedure, isolated via silica flash chromatography using 20:1 Hexanes/Acetone as a white solid (36.4 mg, 58% yield).

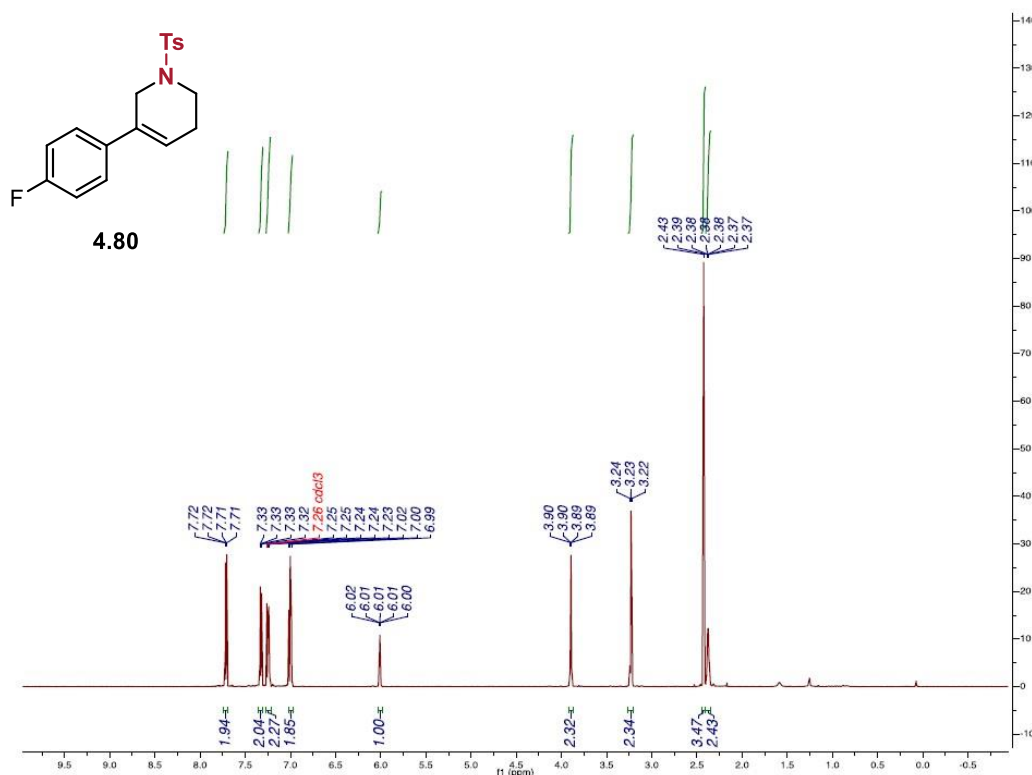
**<sup>1</sup>H NMR** (598 MHz, CDCl<sub>3</sub>) δ 7.88 – 7.62 (m, 2H), 7.37 – 7.30 (m, 4H), 7.29 – 7.27 (m, 3H), 6.07 (tt, *J* = 4.0, 1.9 Hz, 1H), 3.94 (d, *J* = 2.3 Hz, 2H), 3.24 (t, *J* = 5.8 Hz, 2H), 2.43 (s, 3H), 2.39 – 2.35 (m, 2H). Spectra consistent with previous reports.<sup>6</sup>

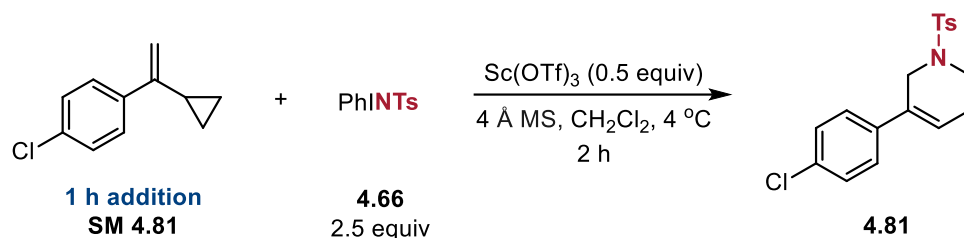




Synthesized using the general procedure, isolated via silica flash chromatography using 20:1 Hexanes/Acetone as a white solid (12.8 mg, 21% yield).

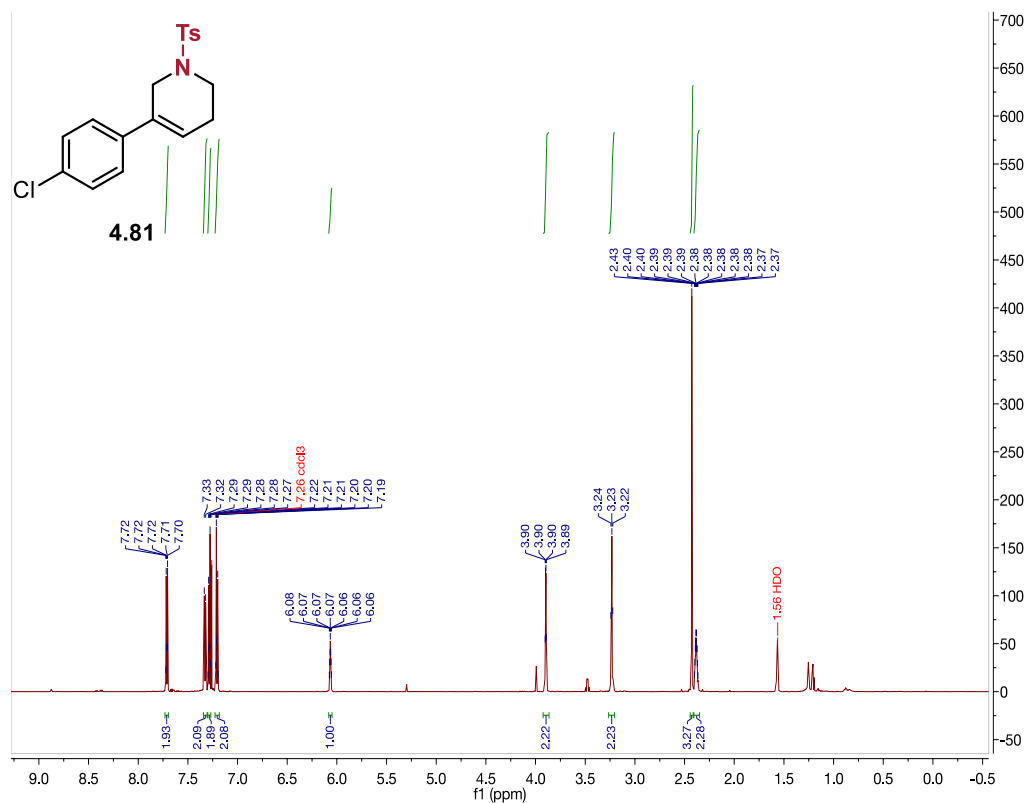
**<sup>1</sup>H NMR** (598 MHz, CDCl<sub>3</sub>) δ 7.71 (d, *J* = 8.4 Hz, 2H), 7.33 (d, *J* = 8.0 Hz, 2H), 7.25 – 7.222 (m, 2H), 7.02, (d, *J* = 8.8 Hz, 1H), 6.99 (d, *J* = 8.4 Hz, 1H), 6.02 – 6.00 (m, 1H), 3.89 (d, *J* = 2.3 Hz, 2H), 3.22 (t, *J* = 5.8 Hz, 2H), 2.43 (s, 3H), 2.41 – 2.36 (m, 2H). Spectra consistent with previous reports <sup>6</sup>

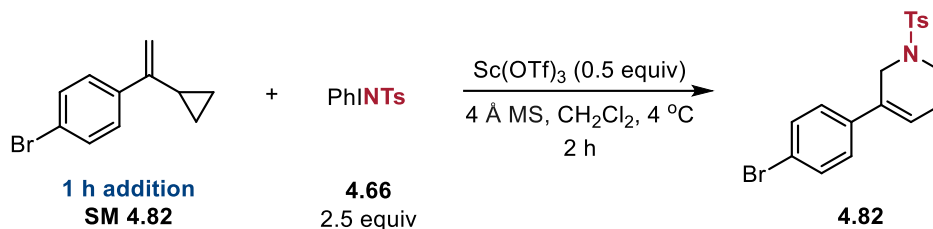




Synthesized using the general procedure, isolated via silica flash chromatography using 20:1 Hexanes/Acetone as an off-white solid (35.3 mg, 48% yield).

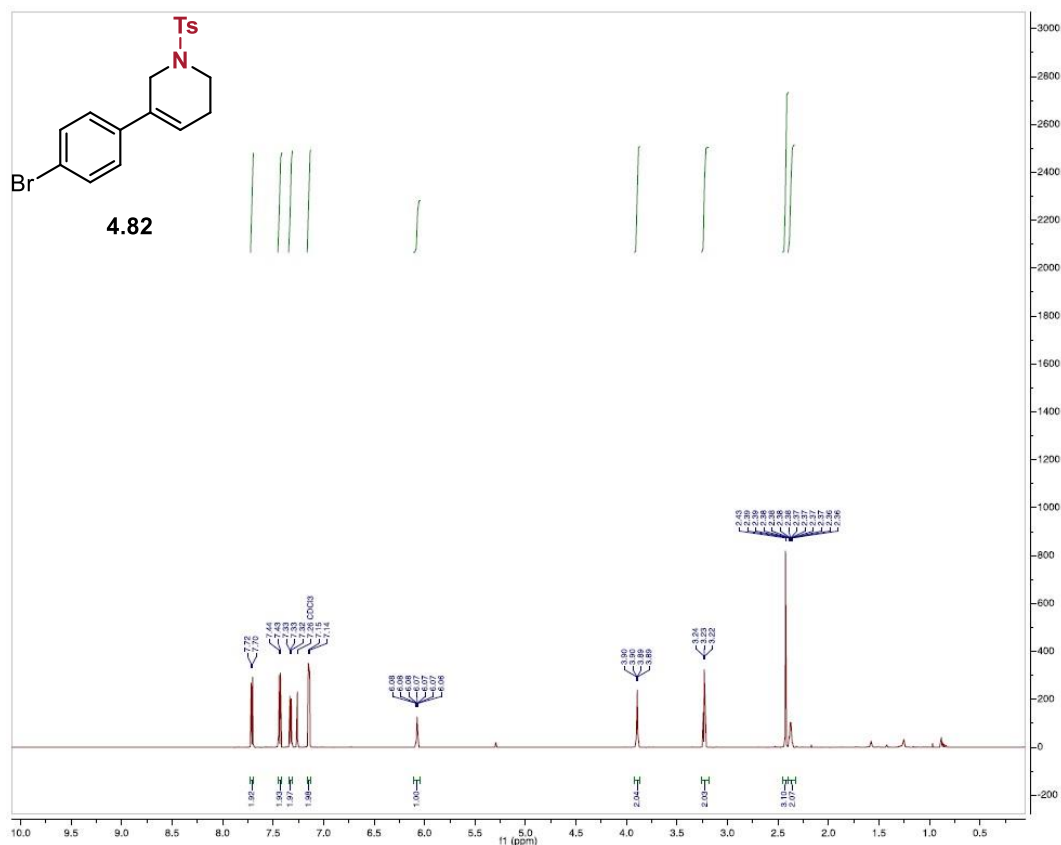
<sup>1</sup>H NMR (598 MHz, CDCl<sub>3</sub>) δ 7.77 – 7.67 (m, 2H), 7.48 – 7.31 (m, 2H), 7.30 – 7.26 (m, 2H), 7.23 – 7.17 (m, 2H), 6.07 (tt, *J* = 4.0, 1.9 Hz, 1H), 3.91-3.89 (m, 2H), 3.23 (t, *J* = 5.8 Hz, 2H), 2.43 (s, 3H), 2.40 – 2.37 (m, 2H) ppm. Matches previous reports.<sup>6</sup>

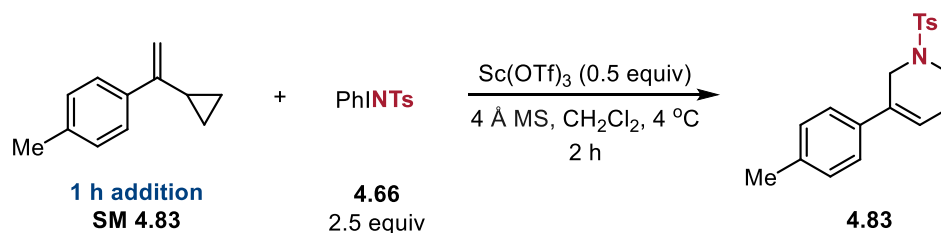




Synthesized using the general procedure, isolated via silica flash chromatography using 20:1 Hexanes/Acetone as a white solid (28.1 mg, 36% yield).

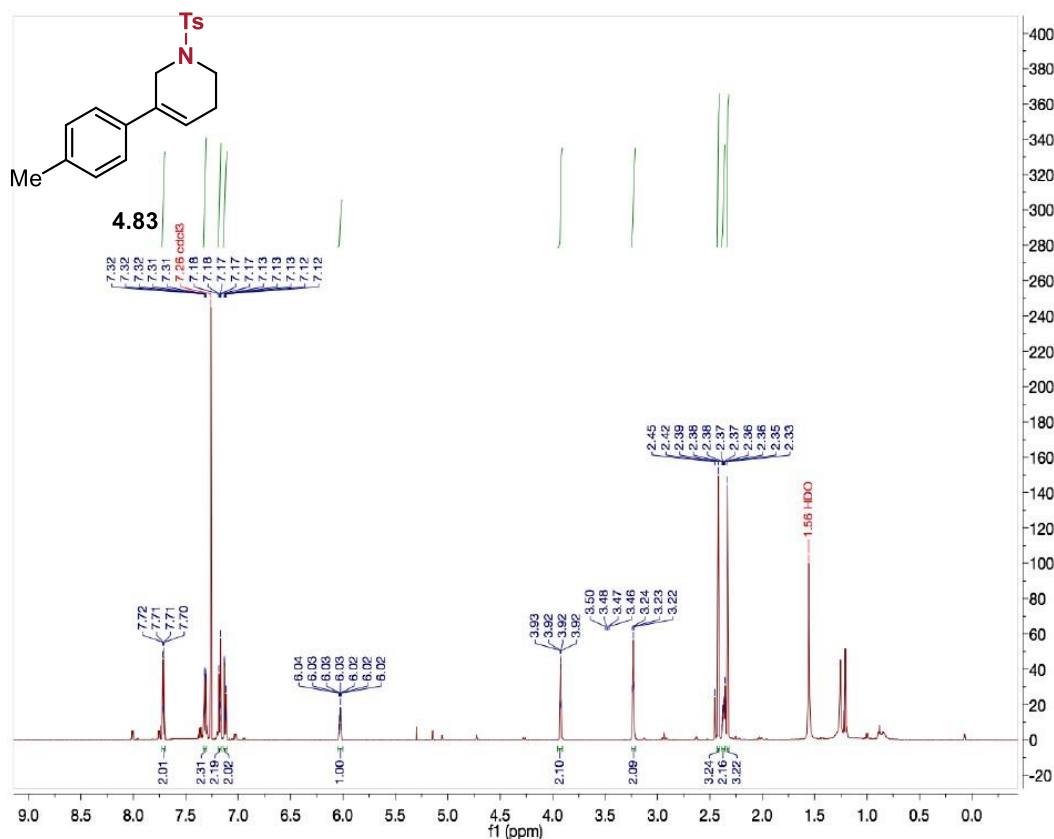
**<sup>1</sup>H NMR** (598 MHz, CDCl<sub>3</sub>) δ 7.72 (d, *J* = 8.0 Hz, 2H), 7.44 – 7.43 (m, 2H), 7.33 – 7.32 (m, 2H), 7.15 – 7.14 (m, 2H), 6.09 – 6.06 (m, 1H), 3.94 – 3.93 (m, 2H), 3.23 (t, *J* = 6.0 Hz, 2H), 2.43 (s, 3H), 2.41 – 2.37 (m, 2H) ppm. Matches previous reports.<sup>6</sup>

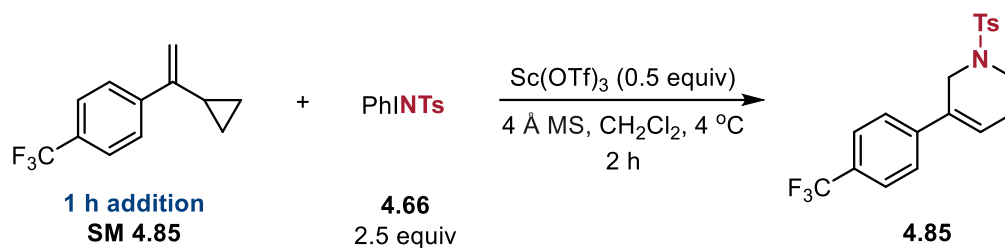




Synthesized using the general procedure, isolated via silica flash chromatography using 20:3 Hexanes/Ethyl acetate as a yellow film (14.2 mg, 22% yield).

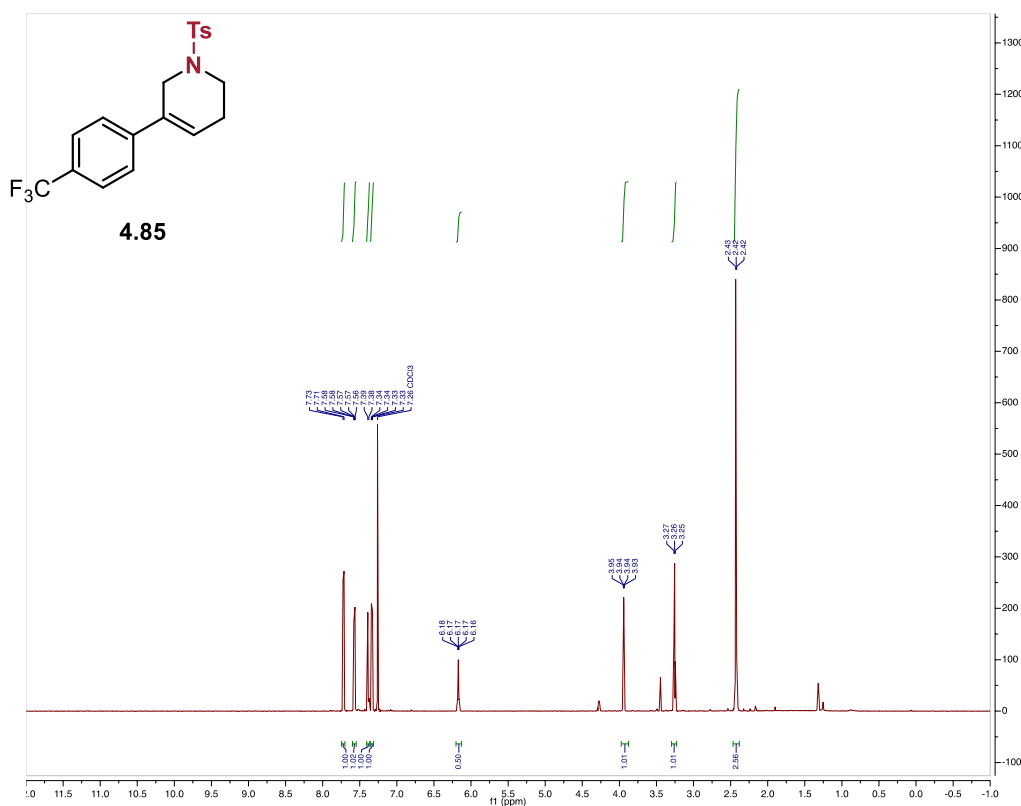
**<sup>1</sup>H NMR** (598 MHz, CDCl<sub>3</sub>) δ 7.72 – 7.70 (m, 2H), 7.32 – 7.29 (m, 2H), 7.18 – 7.16 (m, 2H), 7.15 – 7.12 (m, 2H), 6.04 – 6.02 (m, 1H), 3.93 – 3.92 (m, 2H), 3.23 (t, *J* = 5.8 Hz, 2H), 2.42 (s, 3H), 2.40 – 2.34 (m, 2H), 2.33 (s, 3H) ppm. Matches previous reports.<sup>7</sup>



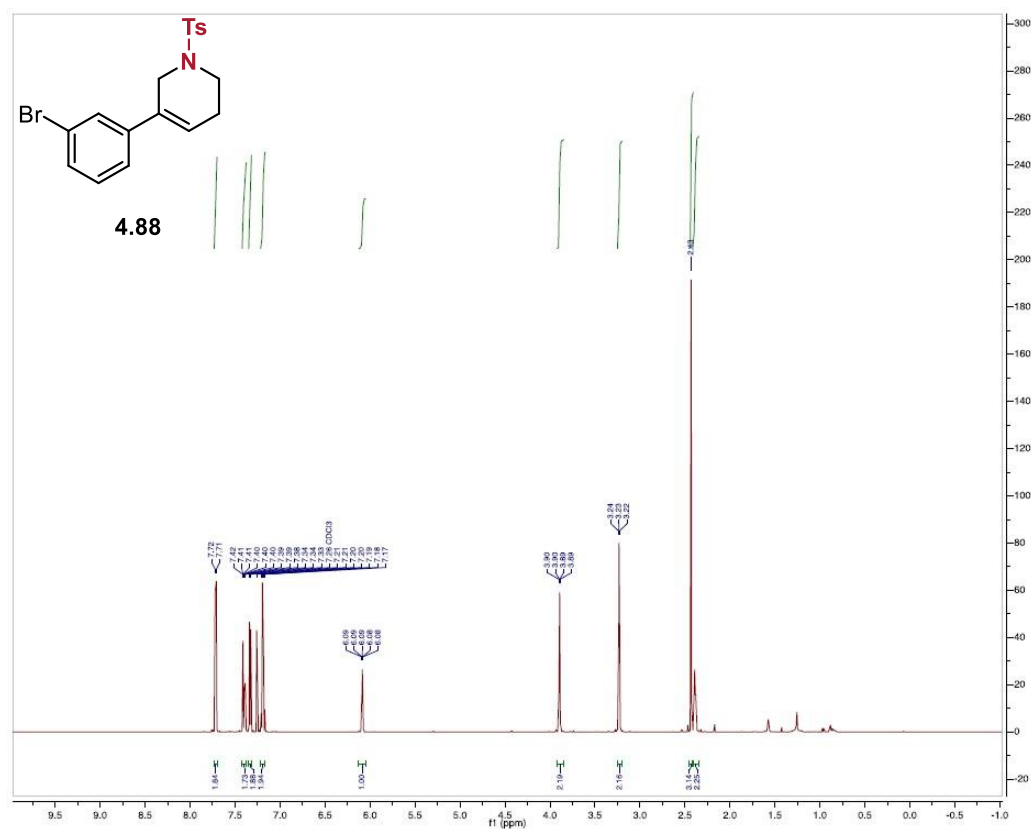


Synthesized using the general procedure, isolated via silica flash chromatography using 20:1 Hexanes/Acetone as a white solid (37.8 mg, 50% yield).

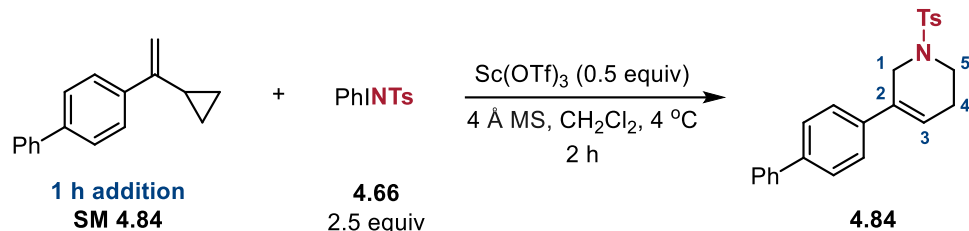
**<sup>1</sup>H NMR** (600 MHz, CDCl<sub>3</sub>) δ 7.73 – 7.70 (m, 2H), 7.57 (d, *J* = 8.1 Hz, 2H), 7.38 (d, *J* = 8.1 Hz, 2H), 7.35 – 7.31 (m, 2H), 6.19 – 6.15 (m, 1H), 3.96 – 3.92 (m, 2H), 3.26 (t, *J* = 5.8 Hz, 2H), 2.43 – 2.41 (m, 5H). Matches previous reports.<sup>7</sup>



**<sup>1</sup>H NMR** (598 MHz, CDCl<sub>3</sub>) δ 7.72 (d, *J* = 8.4 Hz, 2H), 7.42 – 7.40 (m, 2H), 7.39 – 7.34 (m, 2H), 7.21 – 7.17 (m, 2H) 6.09 – 6.08 (m, 1H), 3.90 – 3.89 (m, 2H), 3.23 (t, *J* = 5.8 Hz, 2H), 2.43 (s, 3H), 2.41 – 2.37 (m, 2H). Spectra consistent with previous reports.<sup>6</sup>



## 2.10. Characterization of new products of Sc(OTf)<sub>3</sub>-promoted method



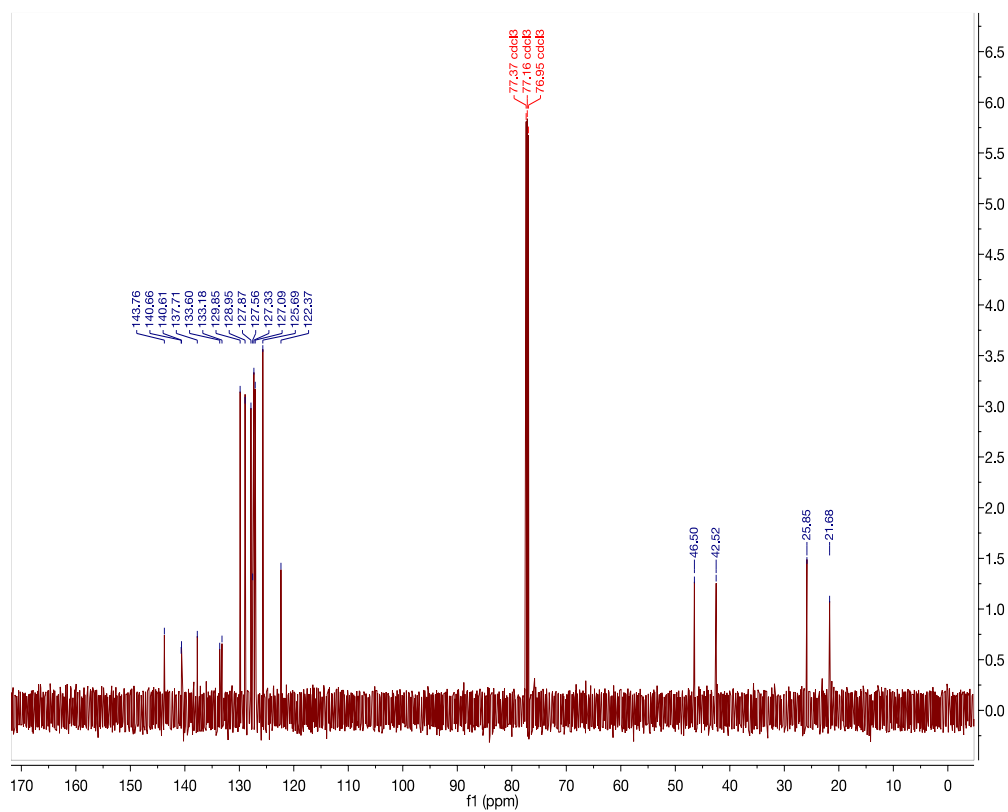
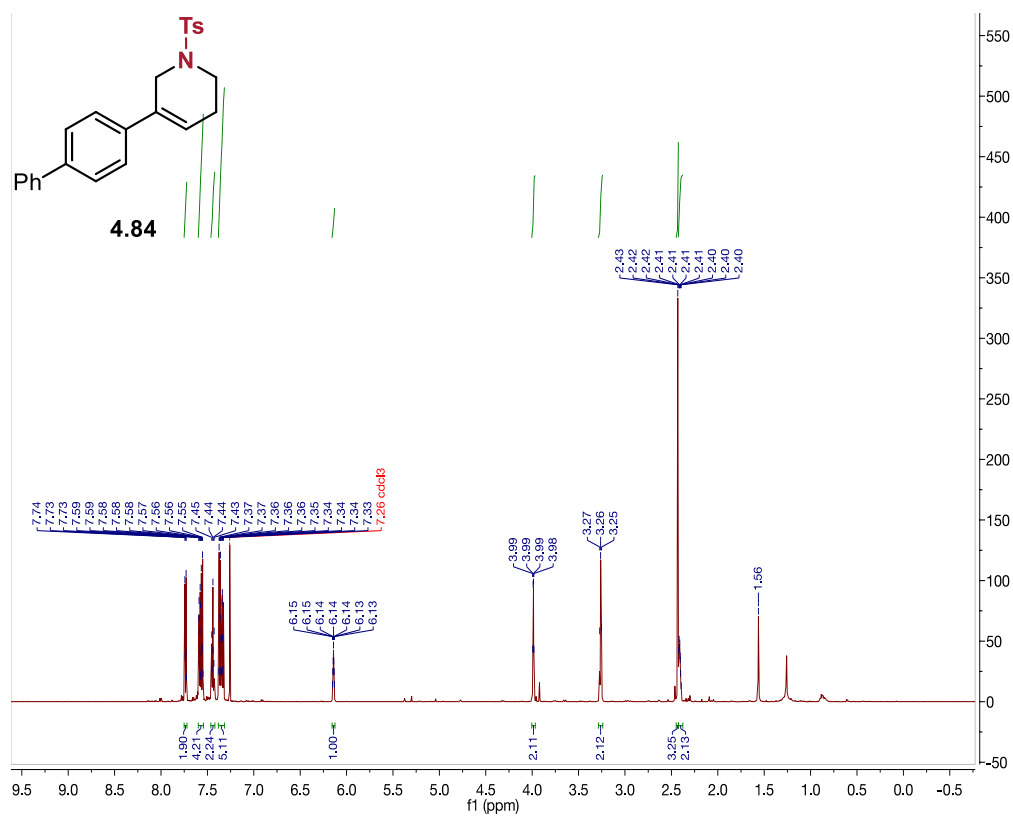
Synthesized using the general procedure, isolated via silica flash chromatography using 20:3 Hexanes/Ethyl acetate as a white solid (20.0 mg, 26% yield).

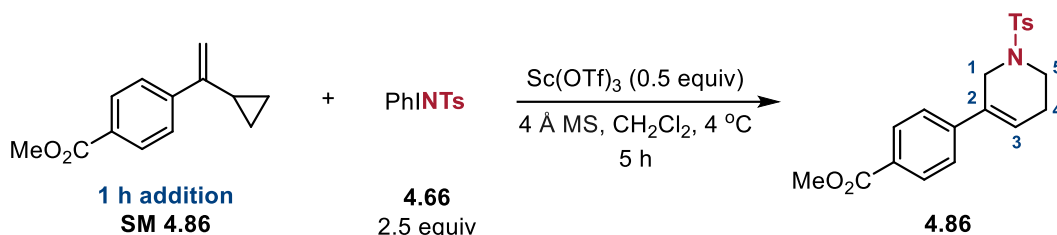
**<sup>1</sup>H NMR** (600 MHz,  $\text{CDCl}_3$ )  $\delta$  7.73 (Ts–ArH, d,  $J$  = 8.3 Hz, 2H), 7.59 – 7.55 (ArH, m, 4H), 7.44, (Ts–ArH, t,  $J$  = 7.7 Hz, 2H), 7.37 – 7.32 (ArH, m, 5H), 6.15 – 6.13 ( $\text{H}^3$ , m, 1H), 3.98 ( $\text{H}^1$ , d,  $J$  = 2.4 Hz, 2H), 3.26 ( $\text{H}^5$ , t,  $J$  = 5.8 Hz, 2H), 2.43 (Ts–  $\text{CH}_3$ , s, 3H), 2.43 – 2.39 ( $\text{H}^4$ , m, 2H) ppm.

**<sup>13</sup>C NMR** (151 MHz,  $\text{CDCl}_3$ )  $\delta$  143.76, 140.66, 140.60, 137.71, 133.59, 133.17, 129.85, 128.95, 127.86, 127.55, 127.33, 127.08, 125.69, 122.36, 46.49, 42.51, 25.85, 21.67 ppm.

**IR** (film):  $\bar{\nu}$  = 3030 (w), 2922 (w), 2851 (w), 1595 (m), 1485 (m), 1292 (s), 1161 (m), 951 (m), 766 (s)  $\text{cm}^{-1}$ .

**HRMS** (ESI):  $m/z$  calculated for  $[\text{C}_{24}\text{H}_{23}\text{NO}_2\text{S}+\text{H}]^+$ : 390.1528; found: 390.1525.





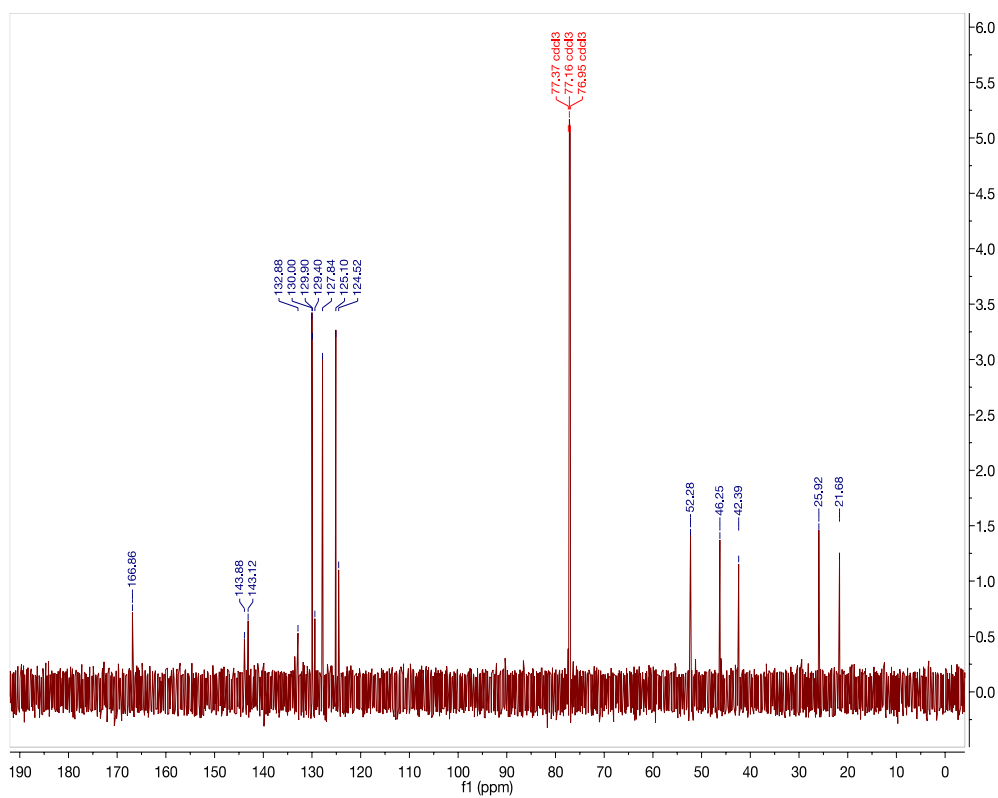
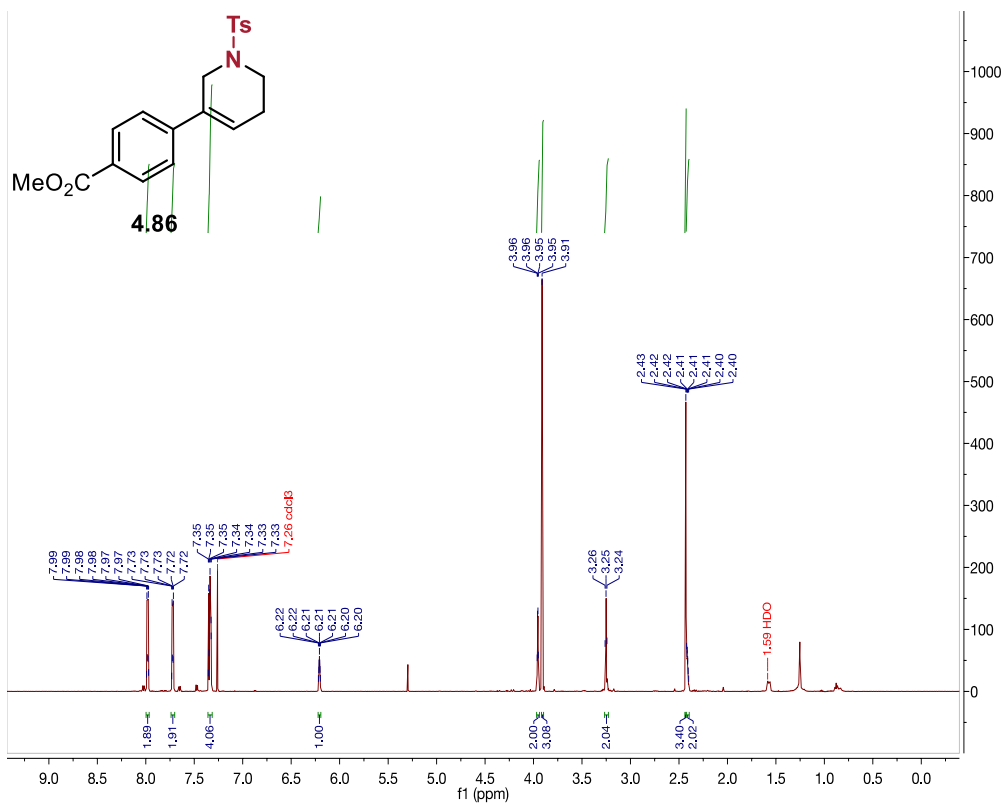
Synthesized using the general procedure, isolated via silica flash chromatography using 20:3 Hexanes/Ethyl acetate as a white solid (22.4 mg, 30% yield).

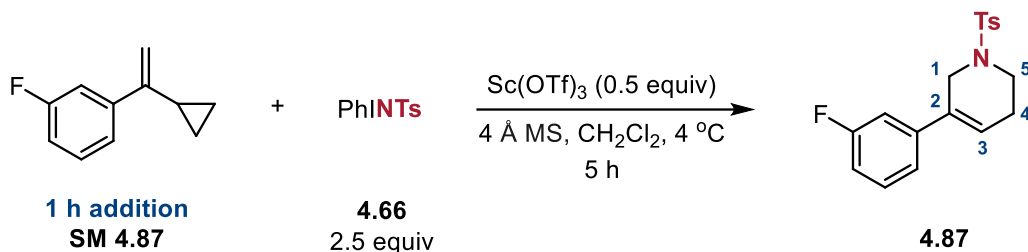
**$^1\text{H}$  NMR** (600 MHz,  $\text{CDCl}_3$ )  $\delta$  7.99 – 7.97 (Ts–ArH, m, 2H), 7.73 – 7.71 (Ts–ArH, m, 2H), 7.35 – 7.32 (ArH, m, 4H), 6.21 – 6.19 ( $\text{H}^3$ , m, 1H), 3.96 – 3.95 ( $\text{H}^1$ , m, 2H), 3.91 ( $\text{CO}_2\text{Me}$ , s, 3H), 3.25 ( $\text{H}^5$ , t,  $J = 5.8$  Hz, 2H), 2.42 (Ts– $\text{CH}_3$ , s, 3H), 2.42 – 2.39 ( $\text{H}^4$ , m, 2H) ppm.

**$^{13}\text{C}$  NMR** (151 MHz,  $\text{CDCl}_3$ )  $\delta$  166.86, 143.87, 143.11, 133.53, 132.87, 130.00 (2C), 129.90 (2C), 129.40, 127.83 (2C), 125.10 (2C), 124.51, 52.27, 46.24, 42.38, 25.91, 21.68 ppm.

**IR** (film):  $\bar{\nu} = 3045$  (w), 2918 (w), 2848 (w), 1721 (s), 1607 (m), 1436 (m), 1338 (m), 1274 (s), 1265 (s), 1161 (m), 1105 (m), 972 (m), 760 (s)  $\text{cm}^{-1}$ .

**HRMS** (ESI):  $m/z$  calculated for  $[\text{C}_{20}\text{H}_{21}\text{NO}_4\text{S}+\text{H}]^+$ : 372.1270; found: 372.1269.





Synthesized using the general procedure, isolated via silica flash chromatography using 20:1 Hexanes/Acetone as a white solid (12.8 mg, 19% yield).

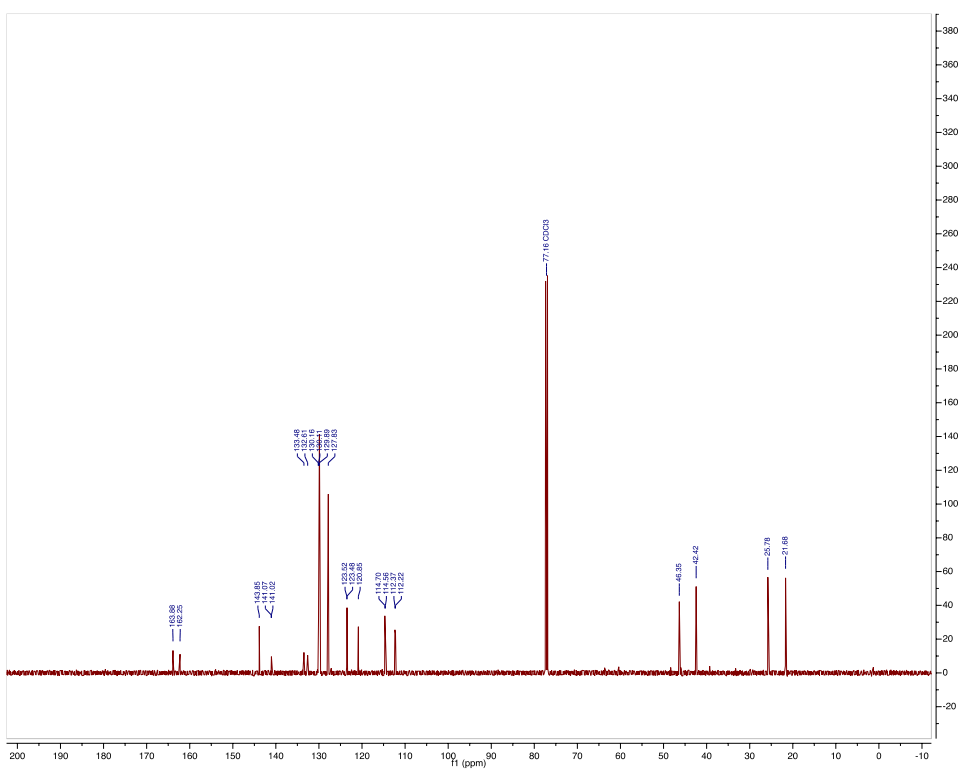
**$^1\text{H}$  NMR** (600 MHz,  $\text{CDCl}_3$ )  $\delta$  7.72 (Ts–ArH, d,  $J$  = 8.0 Hz, 2H), 7.33 (Ts–ArH, d,  $J$  = 7.9 Hz, 2H), 7.31 - 7.26 (ArH, m, 1H), 7.06 (ArH, d,  $J$  = 7.7 Hz, 1H), 6.97 (ArH, d,  $J$  = 11.4 Hz, 2H), 6.11 ( $\text{H}^3$ , s, 1H), 3.91 ( $\text{H}^1$ , d,  $J$  = 2.3 Hz, 2H), 3.24, ( $\text{H}^5$ , t,  $J$  = 5.9 Hz, 2H), 2.43 (Ts– $\text{CH}_3$ , s, 3H), 2.39 ( $\text{H}^4$ , d,  $J$  = 3.7 Hz, 2H) ppm.

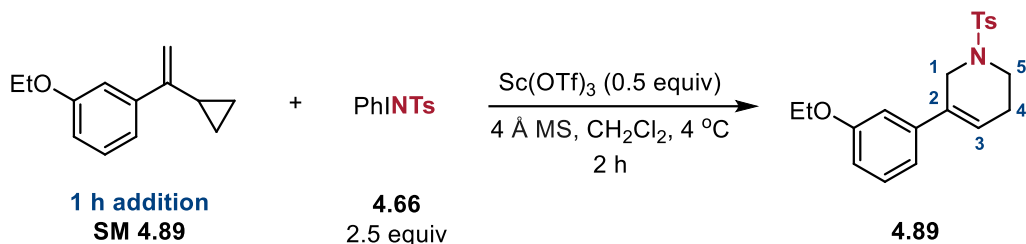
**$^{13}\text{C}$  NMR** (151 MHz,  $\text{CDCl}_3$ )  $\delta$  163.06 (d,  $J$  = 245.7 Hz), 143.85, 141.05 (d,  $J$  = 7.4 Hz), 133.48, 130.14 (d,  $J$  = 8.6 Hz), 129.89, 127.83, 123.48, 120.85, 114.63 (d,  $J$  = 21.0 Hz), 112.22, 46.35, 42.42, 25.78, 21.68 ppm.

**$^{19}\text{F}$  NMR** (564 MHz,  $\text{CDCl}_3$ )  $\delta$  -112.97 (td,  $J$  = 9.8, 6.1 Hz) ppm.

**IR** (film):  $\bar{\nu}$  = 3068 (w), 2926 (w), 2854 (w), 2420 (w), 1583 (m), 1338 (s), 1097 (m), 731 (s)  $\text{cm}^{-1}$ .

**HRMS** (ESI):  $m/z$  calculated for  $[\text{C}_{18}\text{H}_{18}\text{FNO}_2\text{S}+\text{H}]^+$ : 332.1121; found: 332.1117.





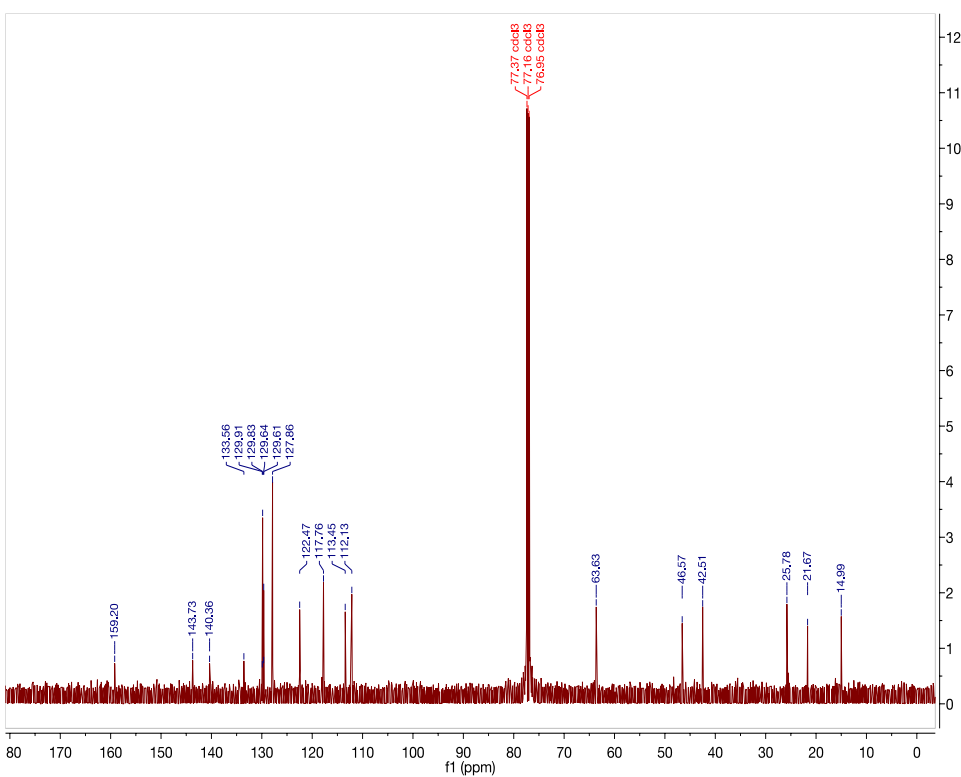
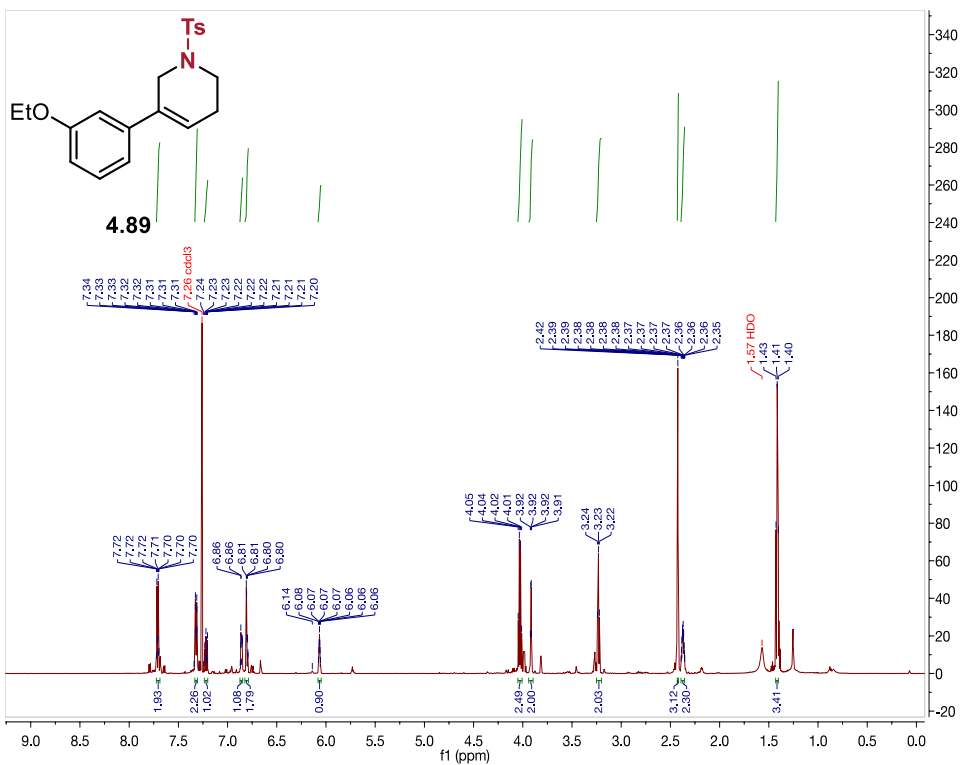
Synthesized using the general procedure, isolated via silica flash chromatography using 20:1 Hexanes/Acetone as a white solid (10.6 mg, 12% yield).

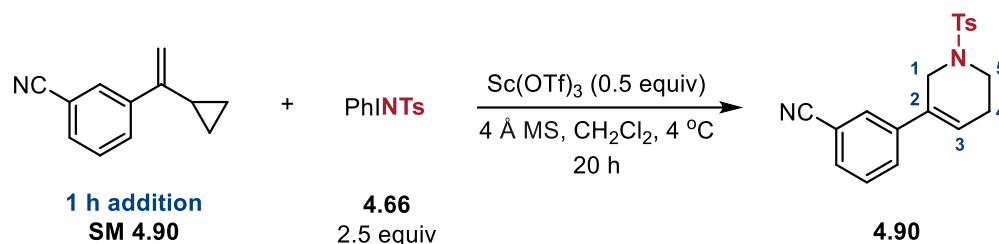
**<sup>1</sup>H NMR** (598 MHz, CDCl<sub>3</sub>) δ 7.72 – 7.69 (Ts–ArH, m, 2H), 7.33 – 7.31 (Ts–ArH, m, 2H), 7.24 – 7.20 (ArH, m, 1H), 6.87 – 6.85 (ArH, m, 1H), 6.82 – 6.79 (ArH, m, 2H), 6.07 (H<sup>3</sup>, tt, *J* = 4.1, 1.9 Hz, 1H), 4.03 (-OEt CH<sub>2</sub>, q, *J* = 6.9 Hz, 2H), 3.92 (H<sup>1</sup>, q, *J* = 2.5 Hz, 2H), 3.23 (H<sup>5</sup>, t, *J* = 5.8 Hz, 2H), 2.42 (Ts–CH<sub>3</sub>, s, 3H), 2.37 (H<sup>4</sup>, dtd, *J* = 6.9, 5.7, 2.7 Hz, 2H), 1.42 (-OEt CH<sub>3</sub>, d, *J* = 7.0 Hz, 3H).

**<sup>13</sup>C NMR** (150 MHz, CDCl<sub>3</sub>) δ 159.20, 143.73, 140.36, 133.56, 129.91, 129.83, 129.64, 129.61, 127.86, 122.47, 117.76, 113.45, 112.13, 63.63, 46.57, 42.51, 25.78, 21.67, 14.99.

**IR** (film):  $\bar{\nu}$  = 2978 (w), 2924 (w), 1597 (w), 1577 (w), 1442 (w), 1392 (w), 1338 (m), 1290 (m), 1163 (s), 1095 (m), 1049 (m), 970 (m), 908 (m), 736 (s), 667 (s).

**LRMS** (ESI): *m/z* calculated for [C<sub>20</sub>H<sub>23</sub>NO<sub>3</sub>+H]<sup>+</sup>: 358.1, found 358.0.





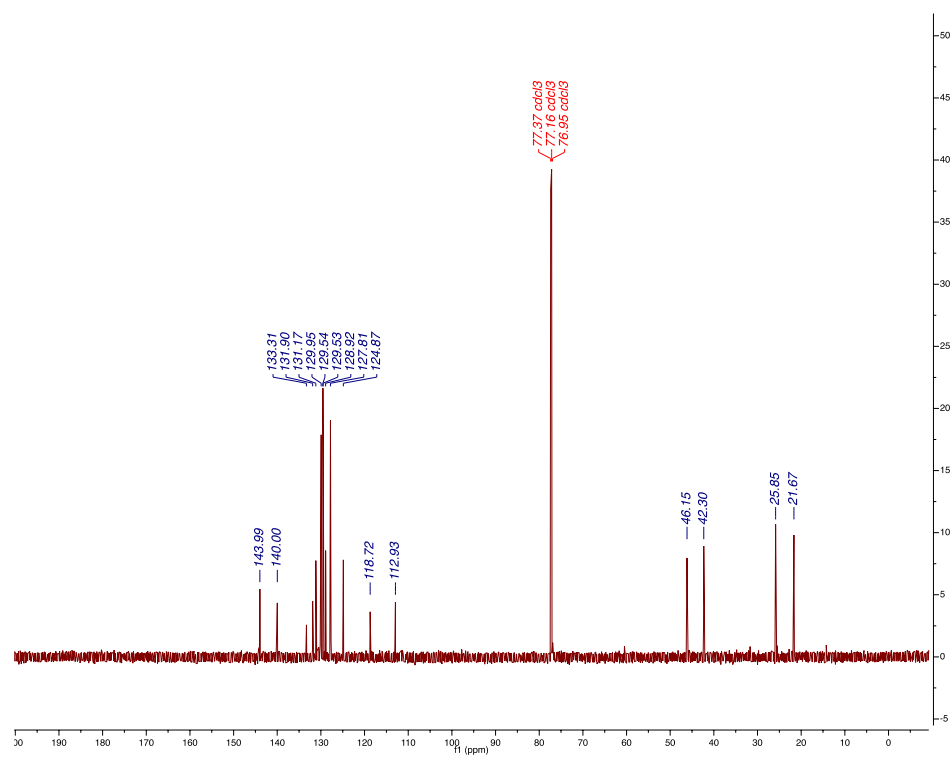
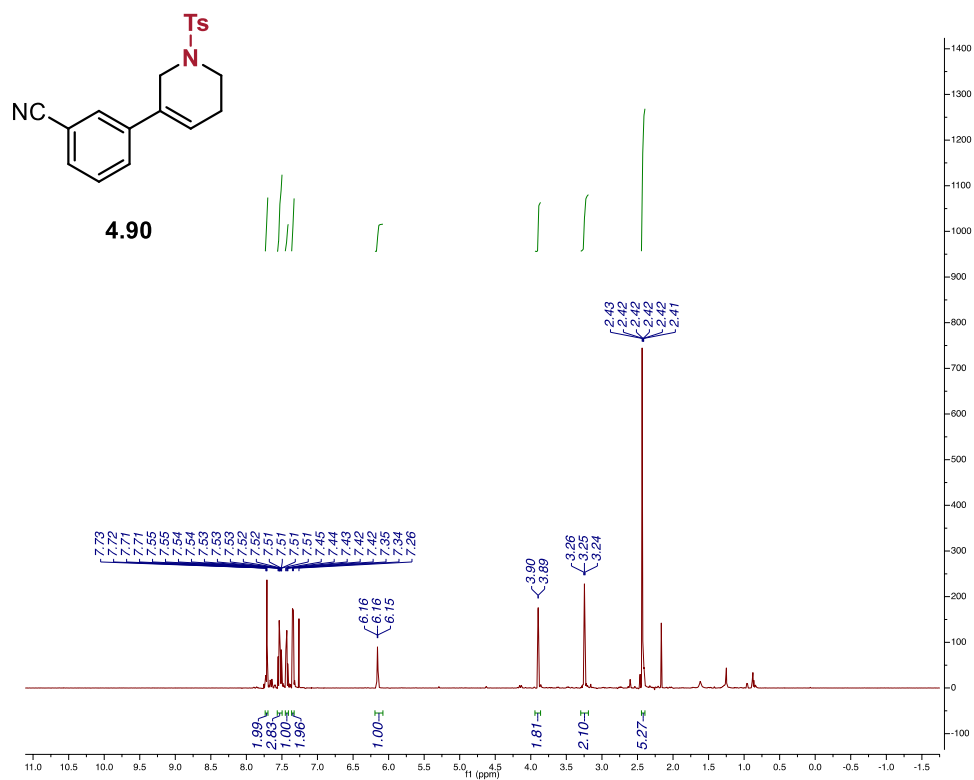
Synthesized using the general procedure, isolated via silica flash chromatography using 20:1 Hexanes/Acetone as a yellow solid (25.0 mg, 37% yield).

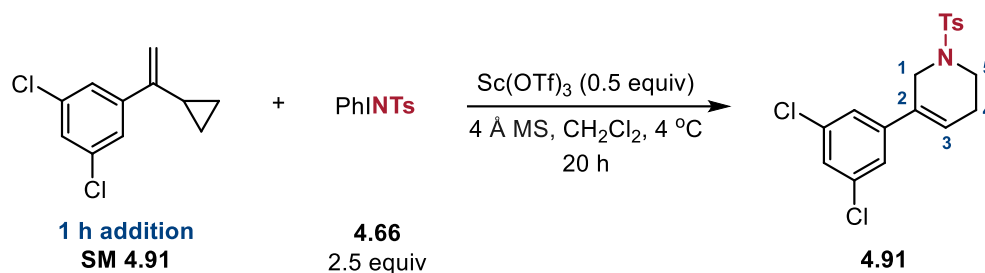
**$^1\text{H}$  NMR** (600 MHz,  $\text{CDCl}_3$ )  $\delta$  7.74 – 7.69 (Ts–ArH, m, 2H), 7.57 – 7.49 (ArH, m, 3H), 7.45 – 7.40 (ArH, m, 1H), 7.35 (Ts–ArH, d,  $J$  = 8.0 Hz, 2H), 6.17 – 6.14 ( $\text{H}^3$ , m, 1H), 3.92 – 3.88 ( $\text{H}^1$ , m, 2H), 3.25 ( $\text{H}^5$ , t,  $J$  = 5.8 Hz, 2H), 2.44 (Ts– $\text{CH}_3$ , s, 3H), 2.43 – 2.40 ( $\text{H}^4$ , m, 2H) ppm.

**$^{13}\text{C}$  NMR** (151 MHz,  $\text{CDCl}_3$ )  $\delta$  143.99, 140.00, 133.31, 131.90, 131.17, 129.95 (2C), 129.54 (2C), 128.92, 127.81 (2C), 124.87, 118.72, 112.93, 46.15, 42.30, 25.85, 21.67 ppm.

**IR** (film):  $\bar{\nu}$  = 3168 (w), 2980 (w), 2254 (m), 2233 (w), 1598 (m), 1018 (m), 972 (m), 667 (m)  $\text{cm}^{-1}$ .

**HRMS** (ESI):  $m/z$  calculated for  $[\text{C}_{19}\text{H}_{18}\text{N}_2\text{SO}_2+\text{H}]^+$ : 339.1167; found: 339.1163.





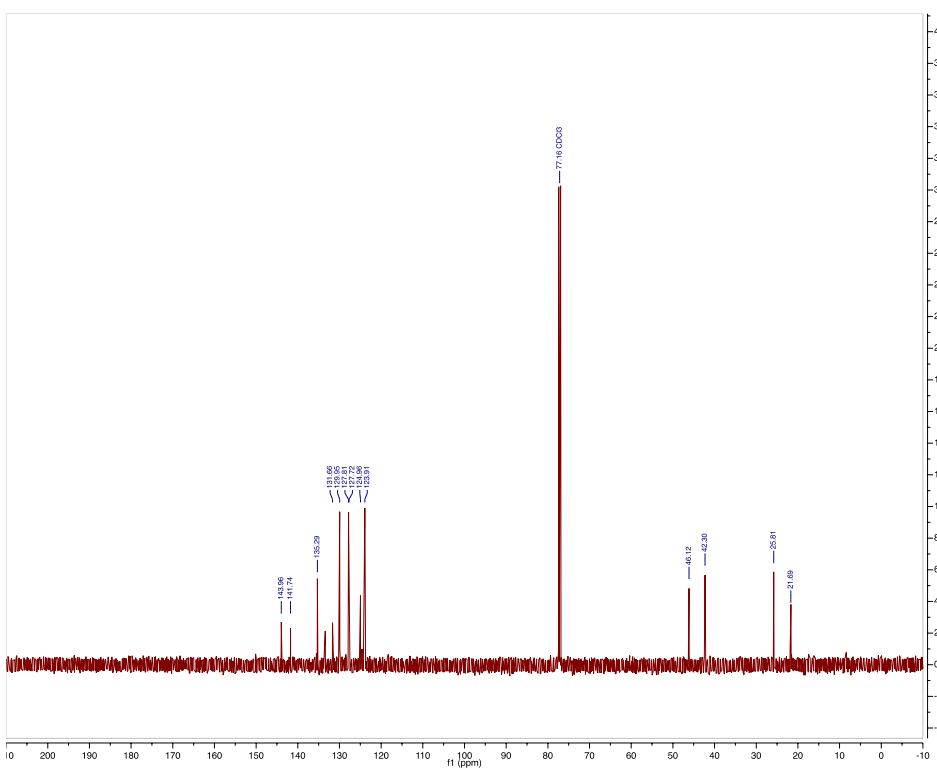
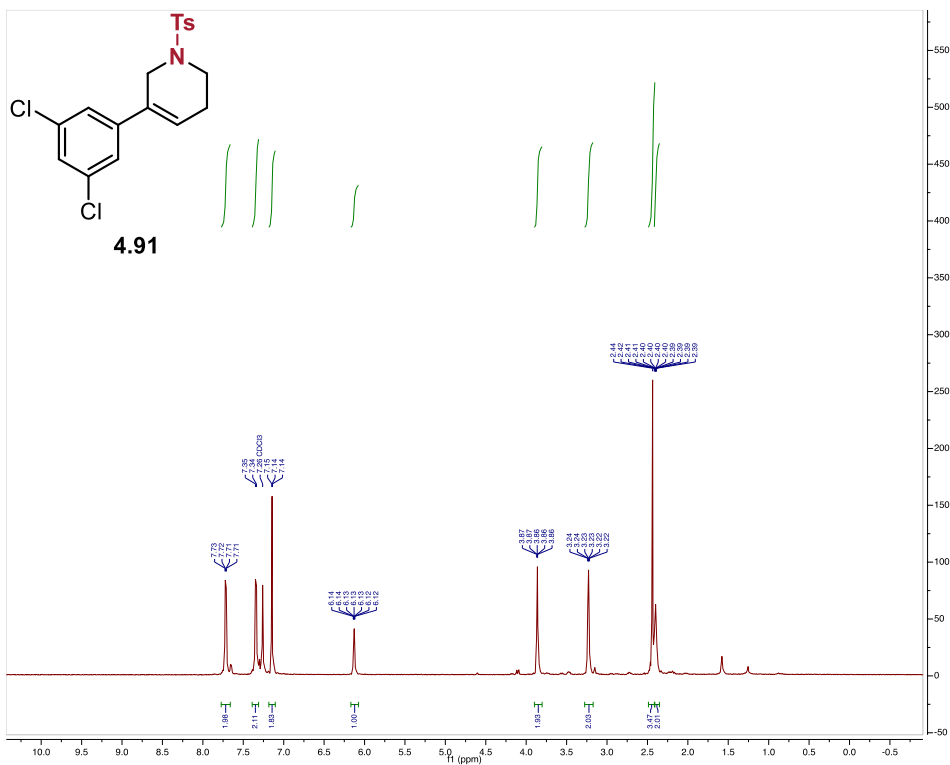
Synthesized using the general procedure, isolated via silica flash chromatography using 20:1 Hexanes/Acetone as an off-white solid (34.0 mg, 44% yield).

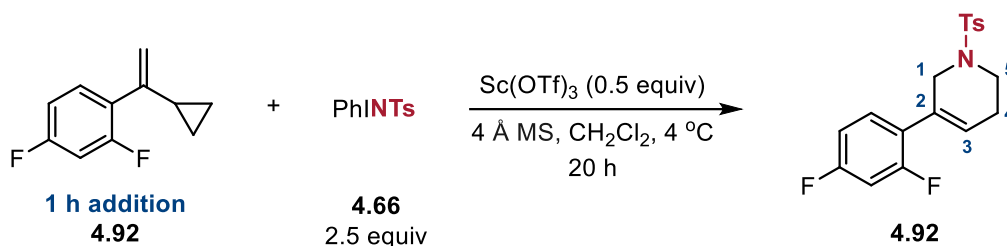
**<sup>1</sup>H NMR** (600 MHz, CDCl<sub>3</sub>)  $\delta$  7.75 – 7.69 (Ts–ArH, m, 2H), 7.38 – 7.31 (Ts–ArH, m, 2H), 7.27 – 7.25 (ArH, m, 1H), 7.15 – 7.13 (ArH, m, 2H), 6.16 – 6.10 (H<sup>3</sup>, m, 1H), 3.89 – 3.83 (H<sup>1</sup>, m, 2H), 3.23 (H<sup>5</sup>, t,  $J$  = 5.8 Hz, 2H), 2.44 (Ts–CH<sub>3</sub>, s, 3H), 2.42 – 2.36 (H<sup>1</sup>, m, 2H) ppm.

**<sup>13</sup>C NMR** (151 MHz, CDCl<sub>3</sub>)  $\delta$  143.96, 141.74, 135.29, 133.30, 131.66, 129.95 (2C), 127.81 (2C), 127.72 (2C), 124.96, 123.91 (2C), 46.12, 42.30, 25.81, 21.69 ppm.

**IR** (film):  $\bar{\nu}$  = 3061 (w), 2322 (w), 1739 (w), 1560 (m), 1271 (s), 972 (m) cm<sup>-1</sup>.

**HRMS** (ESI):  $m/z$  calculated for [C<sub>18</sub>H<sub>17</sub>Cl<sub>2</sub>NO<sub>2</sub>S+H]<sup>+</sup>: 382.0435; found: 382.0432.





Synthesized using the general procedure, isolated via silica flash chromatography using 20:1 Hexanes/Acetone as an off-white solid (18.0 mg, 27% yield).

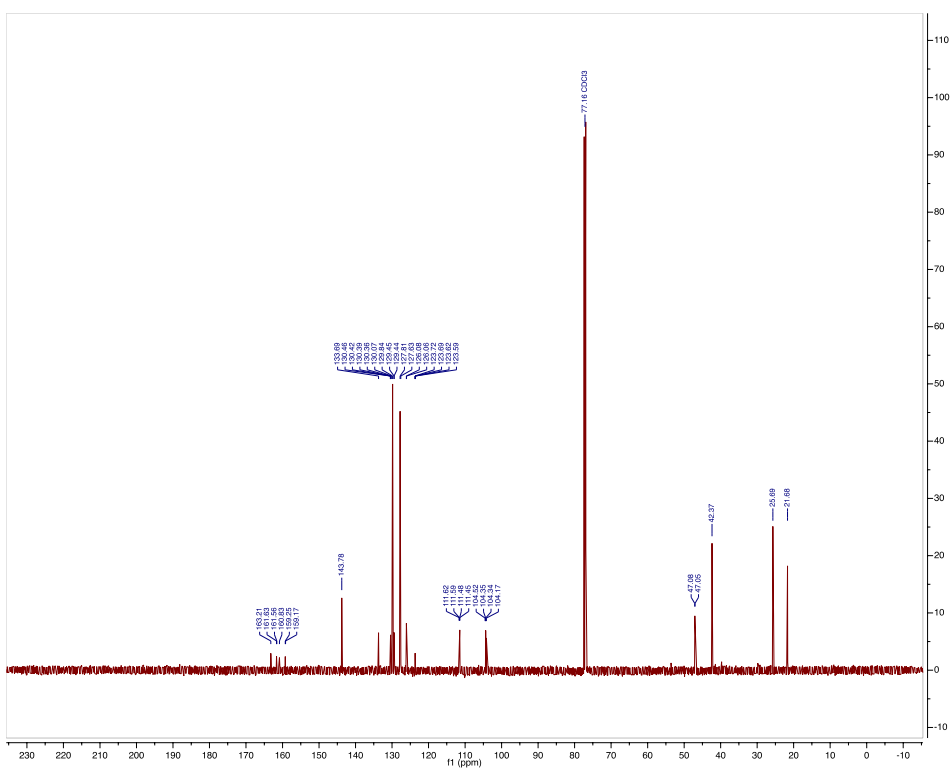
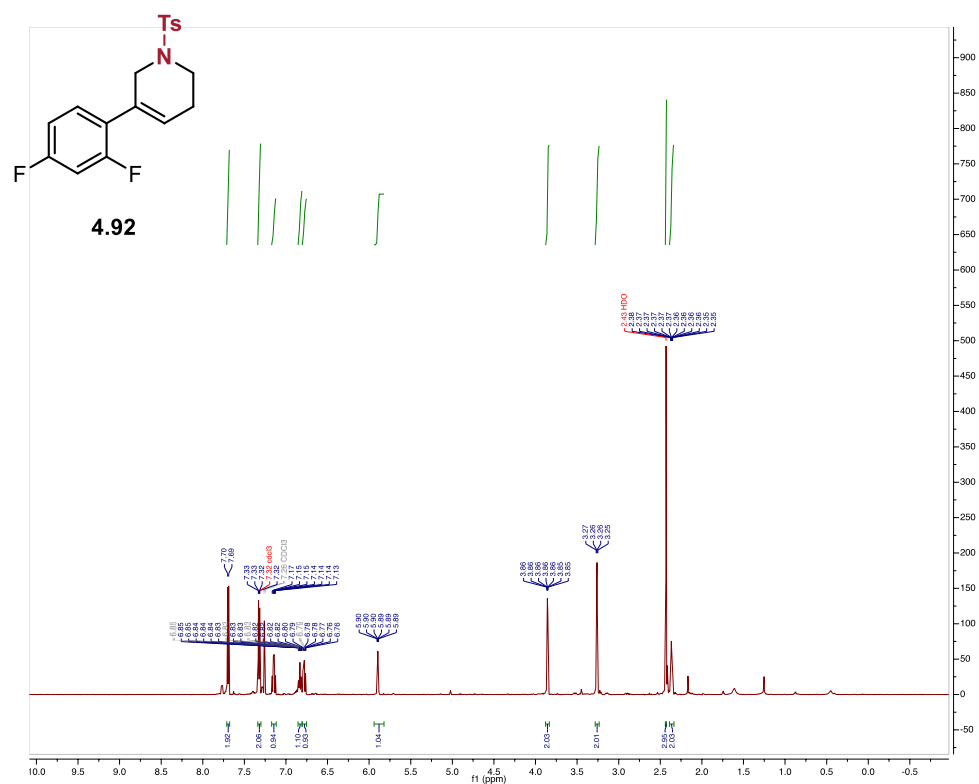
**$^1\text{H}$  NMR** (600 MHz,  $\text{CDCl}_3$ )  $\delta$  7.70 (Ts–ArH, d,  $J$  = 8.3 Hz, 2H), 7.32 (Ts–ArH, d,  $J$  = 8.0 Hz, 2H), 7.15 (ArH, td,  $J$  = 8.6, 6.4 Hz, 1H), 6.83 (ArH td,  $J$  = 8.0, 2.3 Hz, 1H), 6.78 (ArH, ddd,  $J$  = 11.0, 8.7, 2.5 Hz, 1H), 5.91 – 5.88 ( $\text{H}^3$ , m, 1H), 3.86 ( $\text{H}^1$ , d,  $J$  = 2.5 Hz, 2H), 3.26 ( $\text{H}^5$ , t,  $J$  = 5.8 Hz, 2H), 2.43 (Ts– $\text{CH}_3$ , s, 3H), 2.37 ( $\text{H}^4$ , dt,  $J$  = 6.5, 3.0 Hz, 2H) ppm.

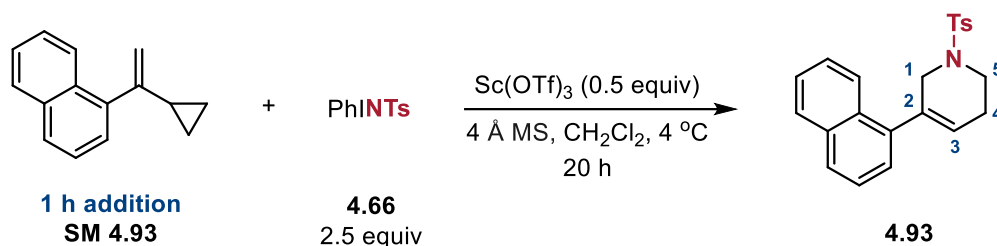
**$^{13}\text{C}$  NMR** (151 MHz,  $\text{CDCl}_3$ )  $\delta$  162.41 (dd,  $J$  = 249.0, 11.6 Hz), 160.03 (dd,  $J$  = 250.8, 12.1 Hz), 143.78, 133.68, 130.40 (dd,  $J$  = 9.3, 5.8 Hz), 129.84, 127.81, 123.65 (dd,  $J$  = 14.9, 4.0 Hz), 111.53 (dd,  $J$  = 20.9, 3.5 Hz), 104.34 (dd,  $J$  = 26.8, 25.2 Hz), 47.06 (d,  $J$  = 4.8 Hz), 42.36, 25.69, 21.67 ppm.

**$^{19}\text{F}$  NMR** (564 MHz,  $\text{CDCl}_3$ )  $\delta$  -110.66 (dt,  $J$  = 10.8, 8.1 Hz), -110.83 – -110.93 (m) ppm.

**IR** (film):  $\bar{\nu}$  = 2924 (w), 2360 (w), 1739 (m), 1595 (m), 1500 (s), 1164 (s), 958 (s), 742 (s)  $\text{cm}^{-1}$ .

**HRMS** (ESI):  $m/z$  calculated for  $[\text{C}_{18}\text{H}_{17}\text{F}_2\text{NO}_2\text{S}+\text{H}]^+$ : 350.1026; found: 350.1031.





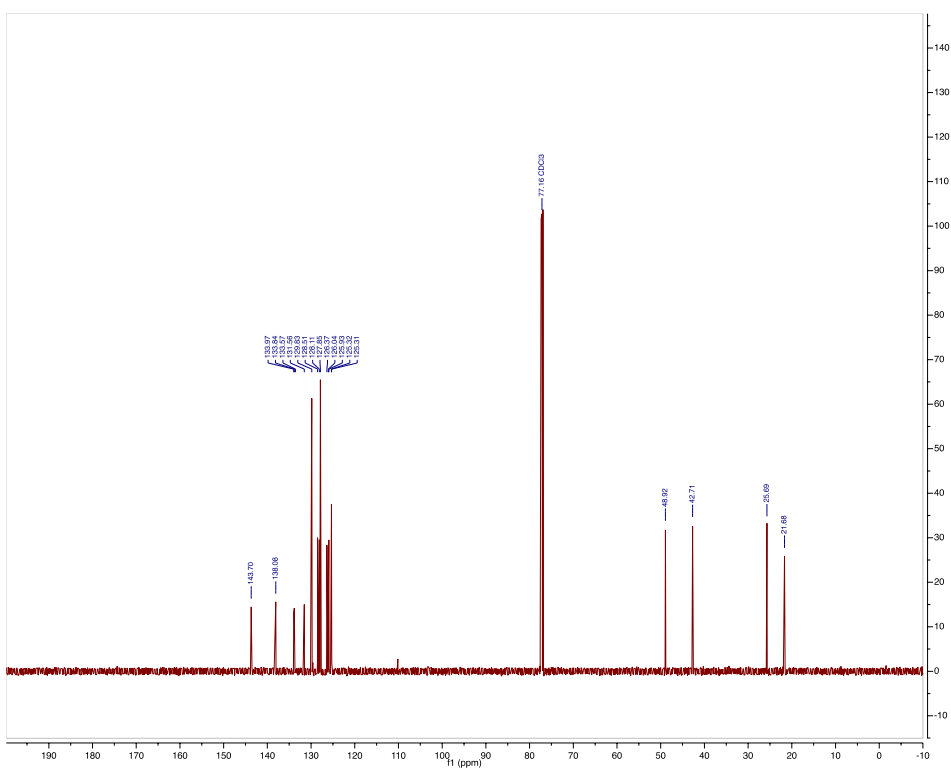
Synthesized using the general procedure, isolated via silica flash chromatography using 20:1 Hexanes/Acetone as an off-white solid (18.7 mg, 26% yield).

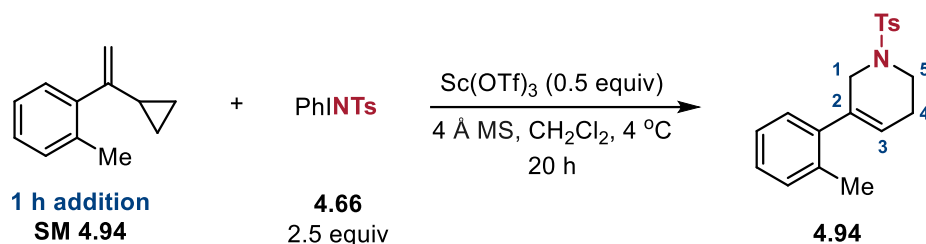
**<sup>1</sup>H NMR** (600 MHz, CDCl<sub>3</sub>) δ 7.91 – 7.87 (ArH, m, 1H), 7.85 (dd, *J* = 7.4, 1.9 Hz, 1H), 7.79 (ArH, d, *J* = 8.2 Hz, 1H), 7.70 – 7.66 (Ts–ArH, m, 2H), 7.47 (ArH, pd, *J* = 6.8, 1.6 Hz, 2H), 7.41 (ArH, dd, *J* = 8.2, 7.0 Hz, 1H), 7.31 (Ts–ArH, d, *J* = 8.0 Hz, 2H), 7.24 (ArH, dd, *J* = 7.0, 1.2 Hz, 1H), 5.83 (H<sup>3</sup>, tt, *J* = 3.9, 2.0 Hz, 1H), 3.85 (H<sup>1</sup>, q, *J* = 2.4 Hz, 2H), 3.37 (H<sup>5</sup>, t, *J* = 5.8 Hz, 2H), 2.49 (H<sup>4</sup>, tq, *J* = 5.8, 2.9 Hz, 2H), 2.43 (Ts–CH<sub>3</sub>, s, 3H) ppm.

**<sup>13</sup>C NMR** (151 MHz, CDCl<sub>3</sub>) δ 143.71, 138.09, 133.97, 133.84, 133.56, 131.56, 129.84, 128.53, 128.12, 127.87, 126.39, 126.05, 125.94, 125.34, 125.33, 125.32, 77.16, 48.93, 42.71, 25.70, 21.69 ppm.

**IR** (film):  $\bar{\nu}$  = 3043 (w), 2922 (m), 2850 (m), 2254 (w), 1597 (m), 1336 (s), 1159 (s), 777 (s), 728 (s) cm<sup>-1</sup>

**HRMS** (ESI): *m/z* calculated for [C<sub>22</sub>H<sub>21</sub>NO<sub>2</sub>S+H]<sup>+</sup>: 364.1371; found: 364.1372





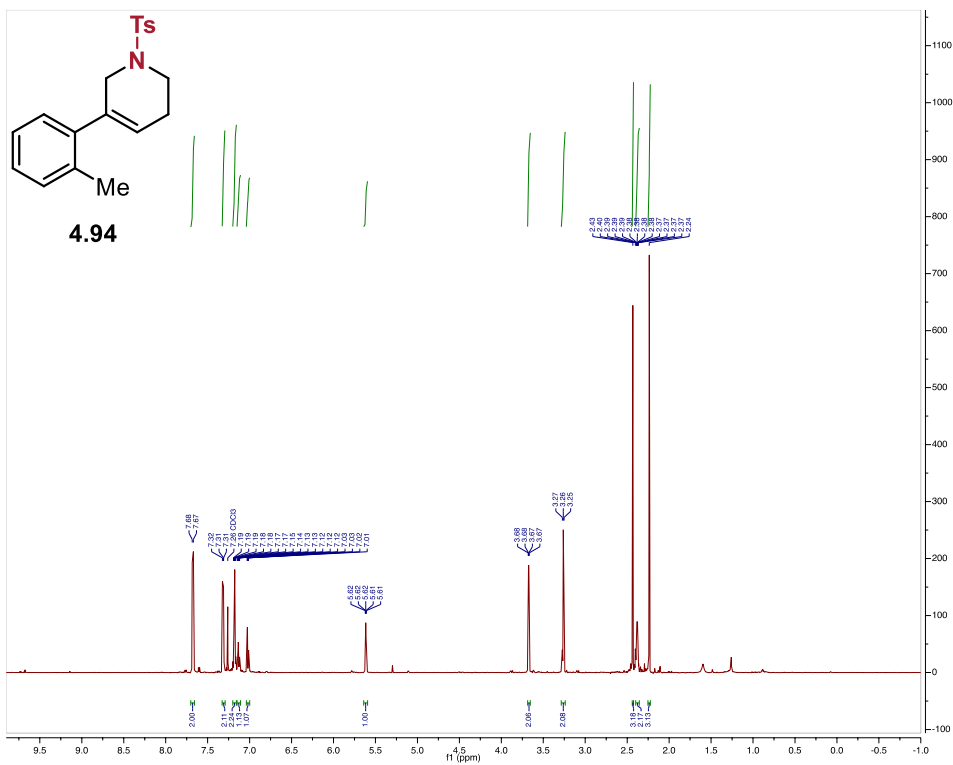
Synthesized using the general procedure, isolated via silica flash chromatography using 20:1 Hexanes/Acetone as an off-white solid (12.1 mg, 19% yield).

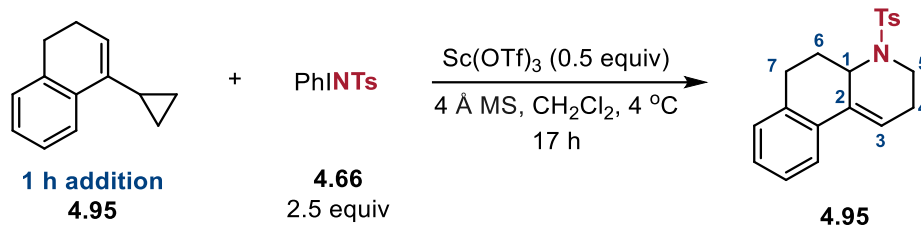
**<sup>1</sup>H NMR** (600 MHz, CDCl<sub>3</sub>) δ 7.70 – 7.65 (Ts–ArH, m, 2H), 7.33 – 7.30 (Ts–ArH, m, 2H), 7.21 – 7.16 (ArH, m, 2H), 7.13 (ArH, td, *J* = 6.9, 6.5, 2.2 Hz, 1H), 7.02 (ArH, dd, *J* = 7.3, 1.3 Hz, 1H), 5.62 (H<sup>3</sup>, tt, *J* = 3.9, 2.0 Hz, 1H), 3.67 (H<sup>1</sup>, q, *J* = 2.5 Hz, 2H), 3.26 (H<sup>5</sup>, t, *J* = 5.8 Hz, 2H), 2.43 (Ts–CH<sub>3</sub>, s, 3H), 2.38 (H<sup>4</sup>, tdd, *J* = 5.8, 4.6, 2.8 Hz, 2H), 2.24 (CH<sub>3</sub>, s, 3H) ppm.

**<sup>13</sup>C NMR** (151 MHz, CDCl<sub>3</sub>) δ 143.68, 139.84, 135.78, 135.08, 133.54, 130.41, 129.79, 128.84, 127.84, 127.73, 125.80, 123.75, 77.16, 48.21, 42.57, 25.53, 21.67, 19.81 ppm.

**IR** (film):  $\bar{\nu}$  = 2922 (m), 2850 (w), 2312 (w), 1597 (m), 1458 (m), 1336 (s), 1093 (s), 759 (s) cm<sup>-1</sup>

**HRMS** (ESI): *m/z* calculated for [C<sub>19</sub>H<sub>22</sub>NO<sub>2</sub>S+H]<sup>+</sup>: 328.1371; found: 328.1367





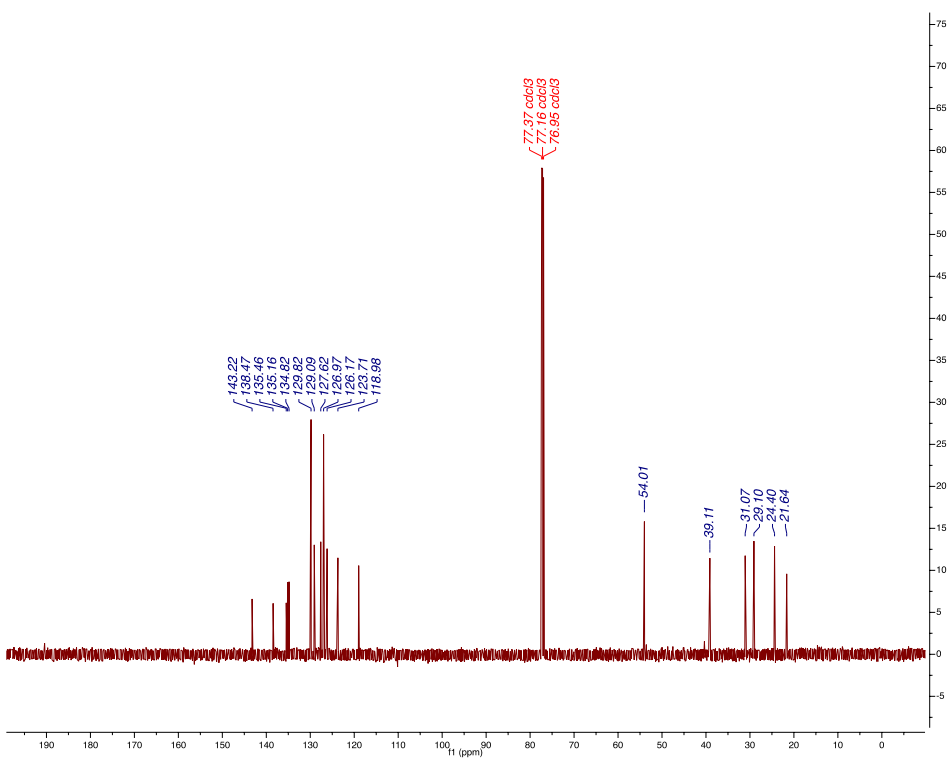
Synthesized using the general procedure, isolated via silica flash chromatography using 20:1 Hexanes/Acetone as a white solid (18.8 mg, 27% yield).

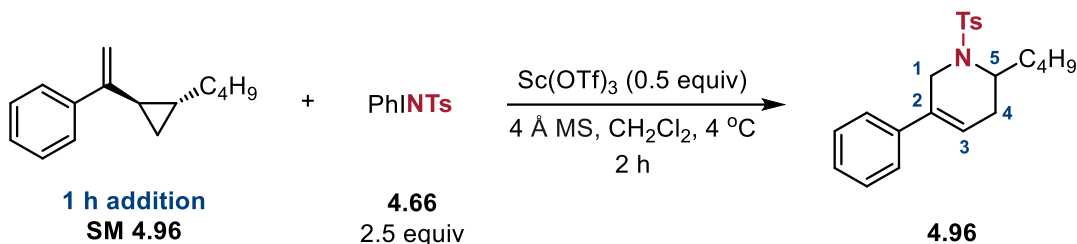
**$^1\text{H}$  NMR** (600 MHz,  $\text{CDCl}_3$ )  $\delta$  7.72 – 7.70 (Ts–ArH, m, 2H), 7.35 (ArH, dd,  $J$  = 7.9, 1.4 Hz, 1H), 7.27 – 7.21 (Ts–ArH, m, 2H), 7.18 – 7.06 (ArH, m, 3H), 6.10 ( $\text{H}^3$ , dd,  $J$  = 6.1, 3.0 Hz, 1H), 4.46 ( $\text{H}^1$ , dd,  $J$  = 12.6, 2.9 Hz, 1H), 3.87 ( $\text{H}^5$ , ddd,  $J$  = 13.9, 5.5, 1.7 Hz, 1H), 3.19 – 3.08 ( $\text{H}^7$ , m, 2H), 2.96 ( $\text{H}^5$ , dd,  $J$  = 17.4, 5.9 Hz, 1H), 2.41 (s, 3H), 2.32 – 2.25 ( $\text{H}^4$ , m, 1H), 2.11 – 1.90 ( $\text{H}^{4,6}$ , m, 3H) ppm.

**$^{13}\text{C}$  NMR** (151 MHz,  $\text{CDCl}_3$ )  $\delta$  143.22, 138.47, 135.46, 135.16, 134.82, 129.82 (2C), 129.09, 127.62, 126.97 (2C), 126.17, 123.71, 118.98, 54.01, 39.11, 31.07, 29.10, 24.40, 21.64 ppm.

**IR** (film):  $\bar{\nu}$  = 3082 (w), 2935 (m), 2360 (w), 1577 (s), 1504 (s), 1409 (m), 1006 (m), 842 (m)  $\text{cm}^{-1}$ .

**HRMS** (ESI):  $m/z$  calculated for  $[\text{C}_{20}\text{H}_{21}\text{NO}_2\text{S}+\text{H}]^+$ : 340.1371; found: 340.1372.





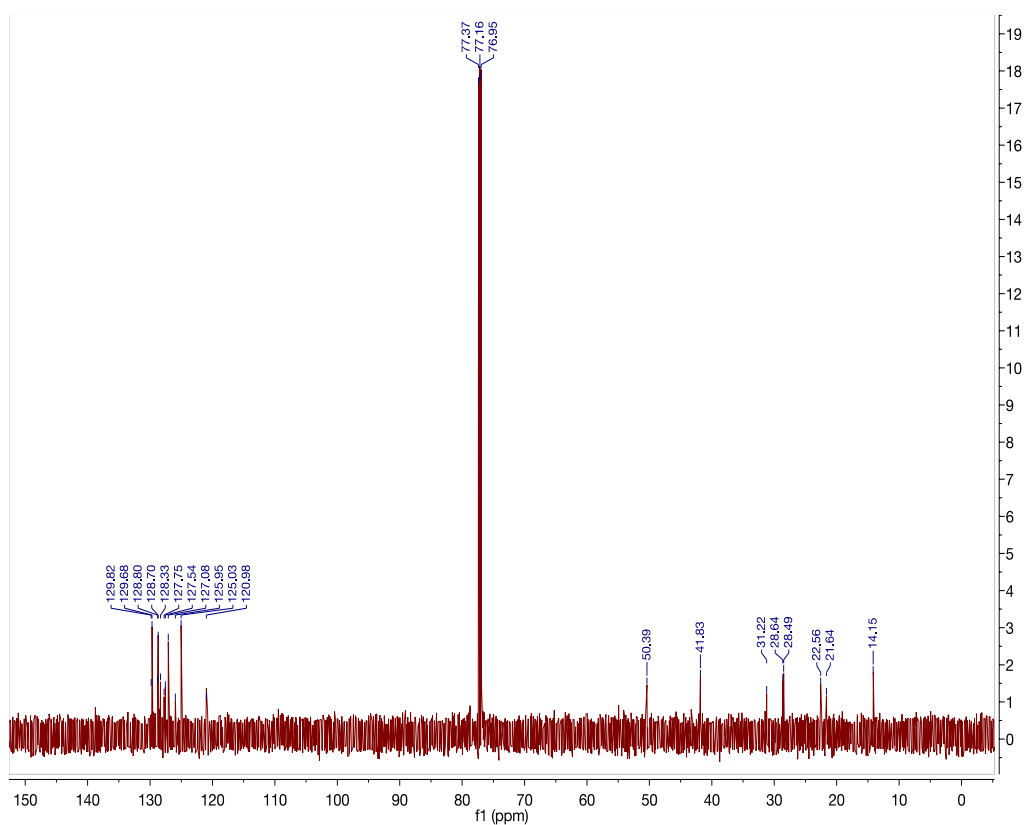
Synthesized using the general procedure, isolated via silica flash chromatography using 20:1 Hexanes/Acetone as a pale yellow solid (30.5 mg, 41% yield).

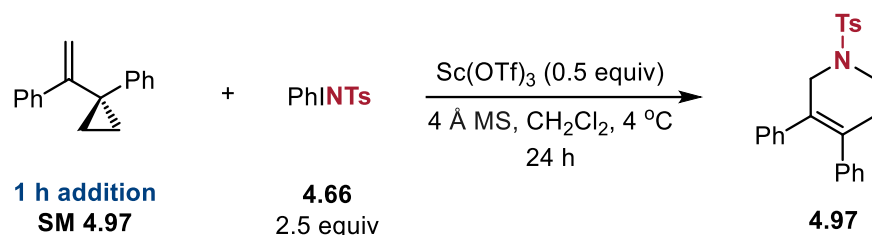
**<sup>1</sup>H NMR** (600 MHz, CDCl<sub>3</sub>) δ 7.73 – 7.68 (Ts–ArH, m, 2H), 7.37 – 7.31 (Ts–ArH, m, 2H), 7.31 – 7.26 (ArH, m, 3H), 7.24 – 7.19 (ArH, m, 2H), 5.97 – 5.81 (H<sup>3</sup>, m, 1H), 4.59 – 4.55 (H<sup>5</sup>, m, 1H), 4.13 – 4.08 (H<sup>1</sup>, m, 1H), 3.94 – 3.89 (H<sup>1</sup>, m, 1H), 2.39 (Ts–CH<sub>3</sub>, s, 3H), 2.29 – 2.13 (H<sup>4</sup>, m, 1H), 2.02 – 1.86 (H<sup>4</sup>, m, 1H), 1.43 – 1.16 (–C<sub>4</sub>H<sub>9</sub>, m, 5H), 0.92 – 0.82 (–C<sub>4</sub>H<sub>9</sub>, m, 4H) ppm.

**<sup>13</sup>C NMR** (151 MHz, CDCl<sub>3</sub>) δ 129.82, 129.68 (2C), 128.80, 128.70 (2C), 128.33, 127.54, 127.08 (2C), 125.95, 125.03 (2C), 120.98, 50.39, 41.83, 31.22, 28.64, 28.49, 22.56, 21.64, 14.15 ppm.

**IR** (film):  $\bar{\nu}$  = 2954 (w), 2927 (w), 1597 (w), 1494 (w), 1334 (m, br), 1155 (s), 1091 (m), 813 (m), 748 (s), 680 (s), 565 (s) cm<sup>–1</sup>.

**HRMS** (ESI): *m/z* calculated for [C<sub>22</sub>H<sub>27</sub>NO<sub>2</sub>S+H]<sup>+</sup>: 370.1835; found: 370.1834.





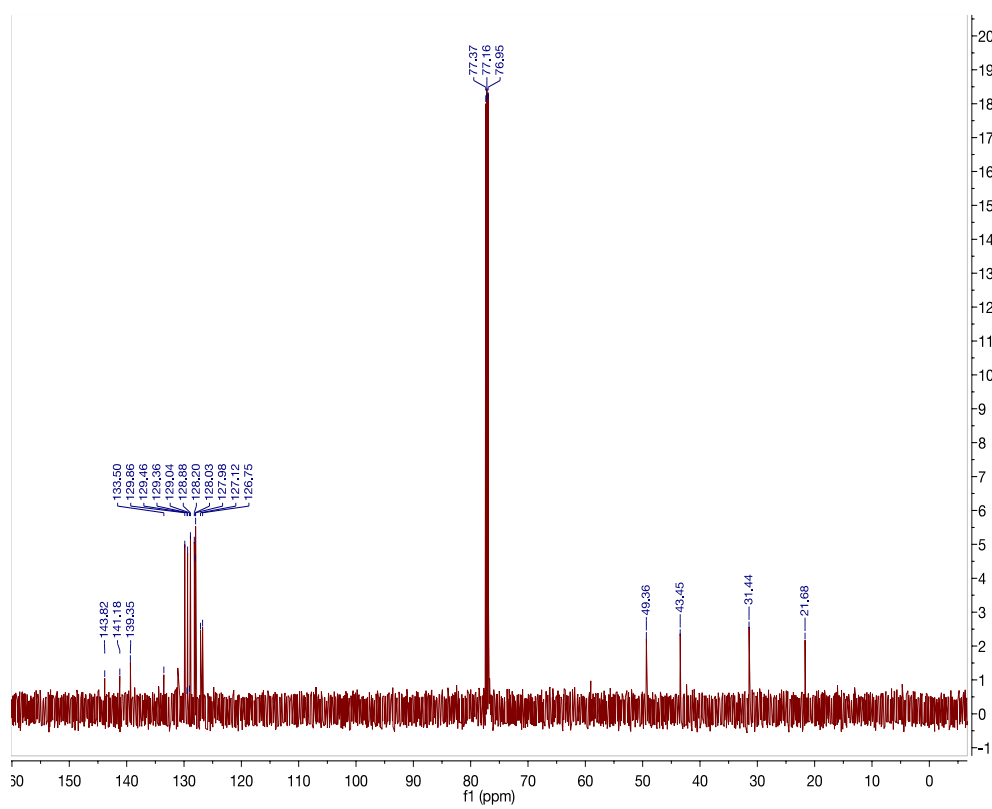
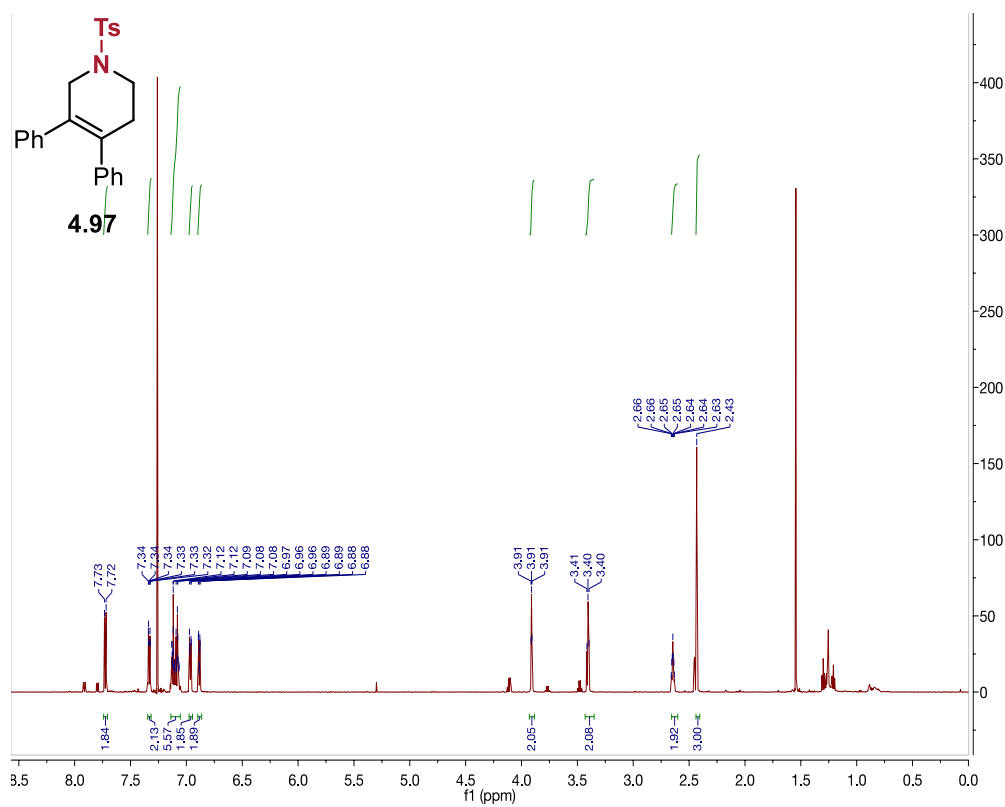
Synthesized using the general procedure, isolated via silica flash chromatography using 20:2 Hexanes/Ethyl acetate as an off-white solid (23.1 mg, 30% yield).

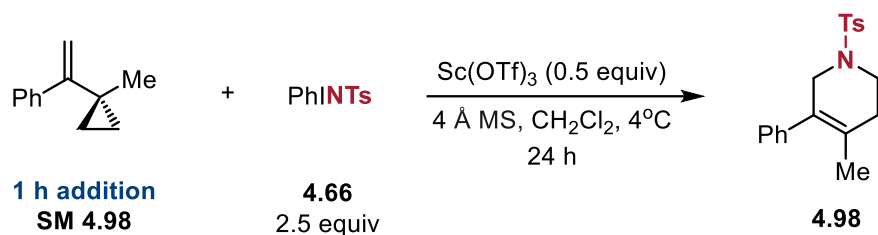
**<sup>1</sup>H NMR** (598 MHz, CDCl<sub>3</sub>) δ 7.73 – 7.71 (m, 2H), 7.35 – 7.32 (m, 2H), 7.15 – 7.04 (m, 6H), 6.97 – 6.95 (m, 2H), 6.92 – 6.88 (m, 2H), 3.91 (t, *J* = 2.5 Hz, 2H), 3.40 (t, *J* = 5.8 Hz, 2H), 2.67 – 2.63 (m, 2H), 2.43 (s, 3H) ppm.

**<sup>13</sup>C NMR** (151 MHz, CDCl<sub>3</sub>) δ 143.82, 141.18, 139.35, 133.50, 131.07, 129.86 (2C), 129.46 (2C), 129.36 (2C), 128.88 (2C), 128.20 (2C), 128.03 (2C), 127.98, 127.12, 126.75, 49.36, 43.45, 31.44, 21.68 ppm.

**IR** (film):  $\bar{\nu}$  = 3059 (w), 2922 (w), 1598 (w), 1338 (m, br), 1157 (s), 1091 (m), 759 (s), 698 (s), 665 (s) cm<sup>-1</sup>.

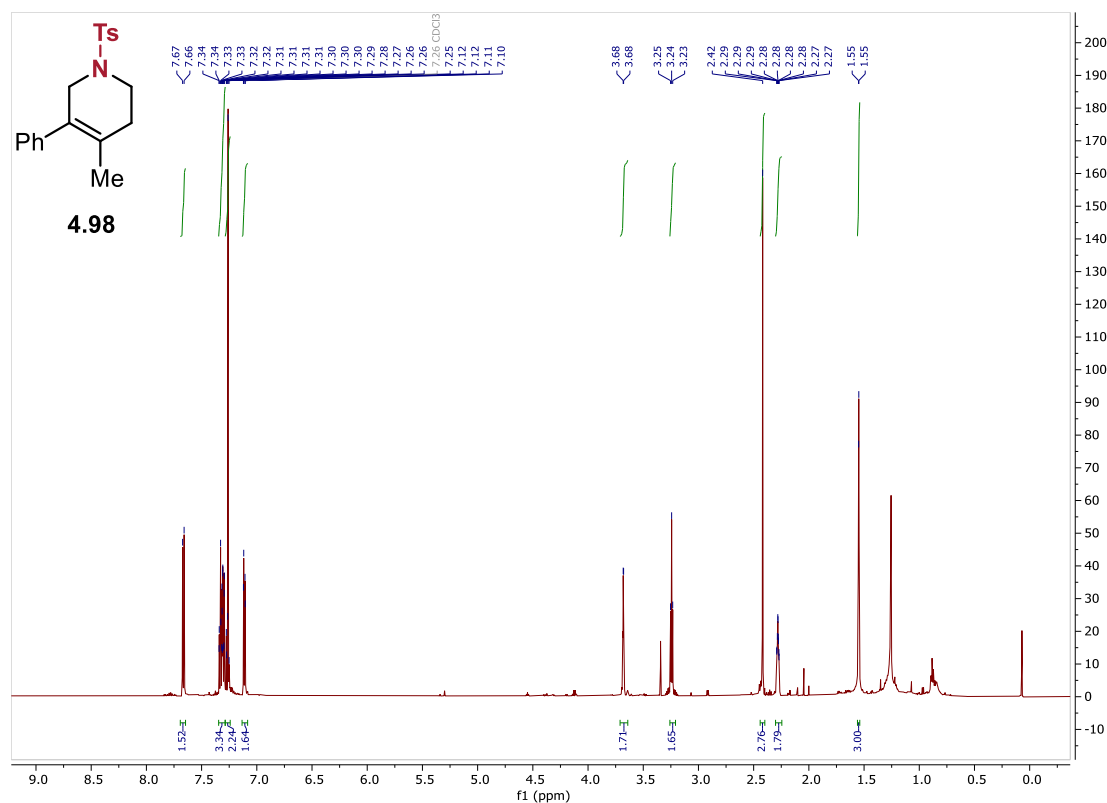
**HRMS** (ESI): *m/z* calculated for [C<sub>24</sub>H<sub>23</sub>NO<sub>2</sub>S+Na]<sup>+</sup>: 412.1342; found: 412.1342.



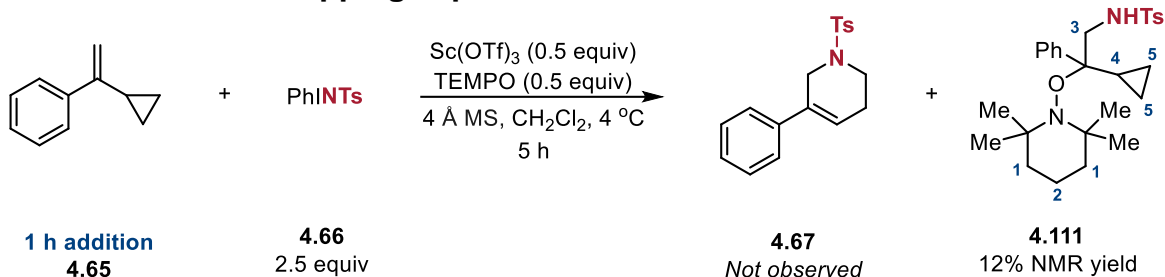


Synthesized using the general procedure, isolated via silica flash chromatography using 20:2 Hexanes/Ethyl acetate as an off-white solid (6.5 mg, 10% yield).

**<sup>1</sup>H NMR** (598 MHz, CDCl<sub>3</sub>) δ 7.67 (d, *J* = 8.2 Hz, 2H), 7.36 – 7.29 (m, 4H), 7.28 – 7.20 (m, 1H), 7.12 – 7.11 (m, 2H), 3.68 (q, *J* = 2.2 Hz, 2H), 3.24 (t, *J* = 5.9 Hz, 2H), 2.42 (s, 3H), 2.28 (m, 2.29 – 2.27), 1.55 (s, 1.55) ppm.



## 2.11. TEMPO radical trapping experiment



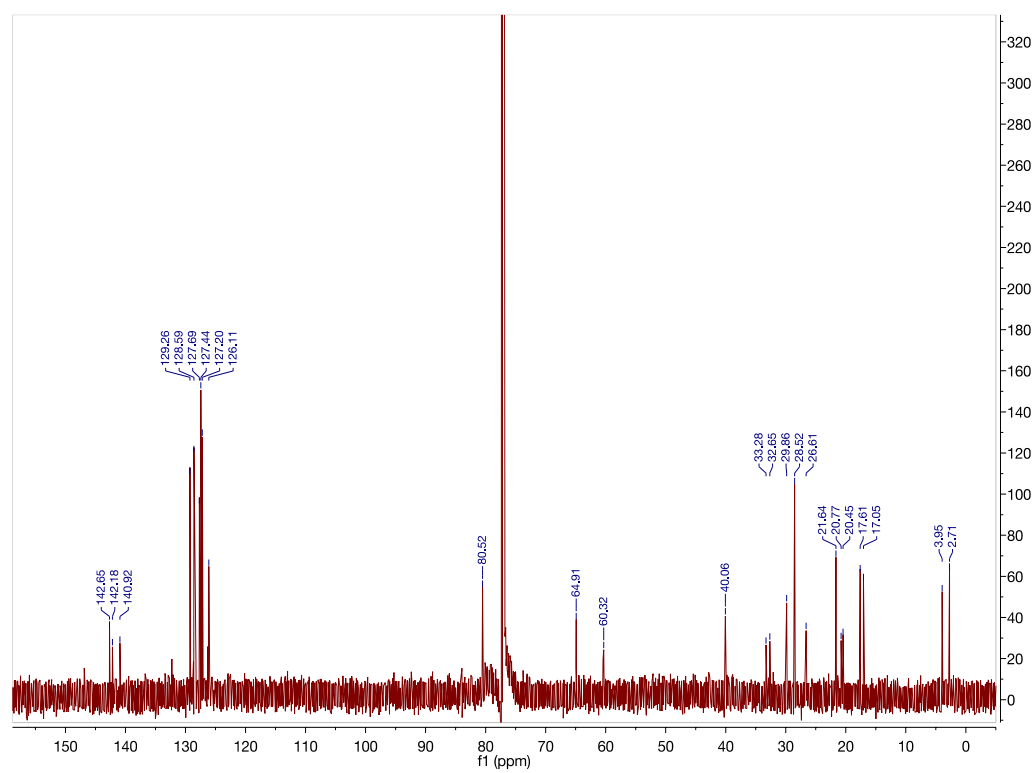
PhINTs (186 mg, 0.5 mmol), Sc(OTf)<sub>3</sub> (49 mg, 0.1 mmol), and 4 Å MS (30 mg) were combined in 600 µL of DCM under an inert atmosphere at 4°C. A solution of the vinylcyclopropane **4.65** (0.2 mmol) was added to 400 µL of DCM and added dropwise over the course of an hour via syringe pump. After the starting material was consumed via TLC, the reaction was quenched with NaHCO<sub>3</sub> and extracted with DCM. The organic layers were washed with brine and dried over Na<sub>2</sub>SO<sub>4</sub>. Product **4.111** was then isolated as an off-white solid via silica flash chromatography, eluted with 10:1 Hexanes/Ethyl acetate. Impurity co-eluted with desired product.

**<sup>1</sup>H NMR** (600 MHz, CDCl<sub>3</sub>) δ 7.67 – 7.65 (Ts–ArH, m, 2H), 7.54 – 7.52 (ArH, m, 2H), 7.25 – 7.15 (Ts–ArH, ArH, m, 6H), 5.59 (N–H, s, 1H), 3.82 (H<sup>3</sup>, d, *J* = 8.6 Hz, 1H), 3.69 (H<sup>3</sup>, d, *J* = 8.6 Hz, 1H), 2.41 (Ts–CH<sub>3</sub>, s, 3H), 1.57 – 1.53 (H<sup>1,2</sup>, m, 6H), 1.17 (CH<sub>3</sub>, s, 3H), 1.13 (CH<sub>3</sub>, s, 3H), 0.98 (CH<sub>3</sub>, s, 3H), 0.89 – 0.87 (CH<sub>3</sub>, H<sup>4</sup>, m, 3H), 0.60 – 0.51 (H<sup>5</sup>, m, 1H), 0.50 – 0.42 (H<sup>5</sup>, m, 1H), 0.36 – 0.25 (H<sup>5</sup>, m, 1H), 0.06 (H<sup>5</sup>, tt, *J* = 9.1, 5.5 Hz, 1H).

**<sup>13</sup>C NMR** (201 MHz, CDCl<sub>3</sub>) δ 142.65, 142.18, 140.92, 129.26, 128.59, 127.69, 127.44, 127.20, 126.11, 80.52, 64.91, 60.32, 40.06, 33.28, 32.65, 29.86, 28.52, 26.61, 21.64, 20.77, 20.45, 17.61, 17.05, 3.95, 2.71.

**IR** (film):  $\bar{\nu}$  = 2972 (w), 1703 (m, br), 1498 (m), 1361 (m), 1321 (m, br), 1246 (w), 1159 (s, br) 1047 (m), 1024 (m), 974 (w), 813 (m), 765 (m), 734 (m), 694 (s), 663 (s), 561 (s) cm<sup>–1</sup>.

**HRMS** (ESI):  $m/z$  calculated for  $[\text{C}_{27}\text{H}_{38}\text{N}_2\text{O}_3\text{S}+\text{H}]^+$ : 471.2686; found: 471.2673.



**A2.12. References**

- (1) Chen, C.; Shen, X.; Chen, J.; Hong, X.; Lu, Z. *Org. Lett.* **2017**, *19*, 5422.
- (2) Li, J.; Chen, J.; Jiao, W.; Wang, G.; Li, Y.; Cheng, X.; Li, G. *J. Org. Chem.* **2016**, *81*, 9992.
- (3) Shi, W-J.; Liu, Y.; Butti, P.; Togni, A. *Adv. Synth. Catal.* **2007**, *349*, 1619.
- (4) Wang, Y.; Zhang, W.; Dai, J.; Feng, Y.; Xu, H. *RSC Adv.* **2014**, *4*, 61706.
- (5) Combee, L. A.; Raya, B.; Wang, D.; Hilinski, M. K. *Chem. Sci.* **2018**, *9*, 935.
- (6) Dong, X.; Han, Y.; Yan, F.; Liu, Q.; Wang, P.; Chen, K.; Li, Y.; Zhao, Z.; Dong, Y.; Liu, H. *Org. Lett.* **2016**, *18*, 3774.
- (7) Verendel, J. J.; Zhou, T.; Li, J-Q.; Paptchikhine, A.; Lebedev, O.; Andersson, P. G. *J. Am. Chem. Soc.* **2010**, *132*, 8880.